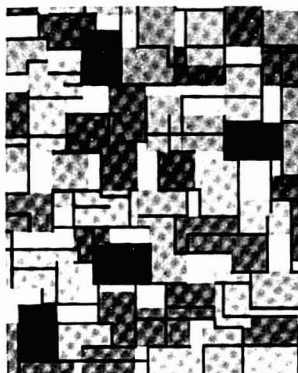


analytical chemistry

Volume 46, No. 4
April 1974

ANCHAM 46(4) 377A-482A/481-624 (1974)
ISSN 0003-2700



Our artist's conception of The Analytical Approach to problem solving, page 433 A, emphasizes the complexity and extended boundaries of problems themselves. To solve, one can focus on various smaller, sometimes overlapping, parts of the whole. The choices are manifold; the results depend not only on how the problem is defined but also on the information, including negative information, gained by the analytical choices made.

The analytical manager today has an extraordinary number of techniques at his disposal. Yet, even with the most sophisticated instrumentation at his fingertips, he cannot afford to ignore information acquired by simple observation. This type of easily gained information may have unique importance. The trained analytical chemist is acutely aware of the various facets of problem solving. This is a great part of the expertise he offers along with his specialized knowledge of certain analytical techniques in industrial, clinical, educational, research, and regulatory situations.

Our new feature, to appear at irregular intervals, should appeal particularly to the consumers of analytical methodology as well as to the developers.

Contents

REPORT

With a workload of 4.5 billion determinations per year, clinical chemistry laboratories have developed computerization concepts and approaches worthy of consideration by other analytical labs. R. H. Laessig and T. H. Schwartz of Wisconsin give an up-to-date look at "Computers in Clinical Chemistry" **398 A**

INSTRUMENTATION

R. M. Caprioli of Purdue University and W. F. Fies and M. S. Story of Finnigan Instrument Corp. demonstrate the usefulness of quadrupole mass spectrometry in direct analysis of stable isotopes **453 A**

THE ANALYTICAL APPROACH

Claude A. Lucchesi, contributing editor, introduces this new feature by showing how a chemical production problem was solved with the analytical approach **433 A**

NEWS AND VIEWS

On-Line Process Analytical Chemistry is the subject of the Summer Symposium to be held June 12-14 at Colorado State University, Fort Collins, Colo. Pattern recognition techniques relate molecular structure and anticancer drug activity **415 A**

BOOKS

Books on quantitative analysis by NMR spectroscopy, a systematic approach to chemical instrumentation, and analytical chemistry are reviewed by John A. Sogn, Gary M. Hieftje, and Robert L. Pecsok **441 A**

EDITORS' COLUMN

Contributing editor Claude A. Lucchesi describes the genesis and aims of the feature, "The Analytical Approach" **451 A**

EDITORIAL

Professor Laitinen describes *Analytical Chemistry's* efforts to broaden editorial coverage by stressing applications of analytical methodology to problem solving as well as methodology development **481**

Author Index	384 A
Briefs	389 A
Future Articles	482 A
Call for Papers	422 A
Meetings	422 A
Short Courses	424 A
New Products	469 A
Chemicals	475 A
Manufacturers' Literature	477 A

Articles

Solvatochromism of Phenol Blue in the Ethyl Acetate-Acetic Acid Solvent System. O. W. Kolling and J. L. Goodnight **482**

Spectrophotometric Analysis with the GeMSAEC Fast Analyzer—Determination of Zinc Using 4-(2-Pyridylazo)Resorcinol (PAR). Gerald Goldstein, W. L. Maddox, and M. T. Kelley **485**

Preparation, Properties, and Applications of 8-Hydroxyquinoline Immobilized Chelate. K. F. Sugawara, H. H. Weetall, and G. D. Schucker **489**

Determination of a Geometry and Dead Time Correction Factor for Neutron Activation Analysis. G. L. Hoffman, P. R. Walsh, and M. P. Doyle **492**

Determination of Phenols by Fluorine-19 Nuclear Magnetic Resonance of Hexafluoroacetone Derivatives. F. F.-L. Ho **496**

Elemental Analysis of Whole Blood Using Proton-Induced X-Ray Emission. R. C. Bearse, D. A. Close, J. J. Maloney, and C. J. Umbarger **499**

Substoichiometric Extraction of Cations with Mixtures of Hexafluoroacetylacetone and Tri-*n*-Octylphosphine Oxide in Cyclohexane. J. W. Mitchell and Roland Ganges **503**

Contents

Computer Utility for the Analytical Laboratory. J. R. DeVoe, R. W. Shidele, F. C. Ruegg, J. P. Aronson, and P. S. Shoenfeld 509

Pattern Recognition Techniques Applied to the Interpretation of Infrared Spectra. D. R. Preuss and P. C. Jurs 520

Statistical Method for the Prediction of Matching Results in Spectral File Searching. S. L. Grotch 526

Trace Determination of Beryllium Oxide in Biological Samples by Electron-Capture Gas Chromatography. G. M. Frame, R. E. Ford, W. G. Scribner, and Thomas Ctrtnicek 534

High Pressure Liquid Chromatographic Determination of Tetracyclines. Kiyoshi Tsuji, J. H. Robertson, and W. F. Beyer 539

Wide Band, Precision, DC-Coupled, Lock-In Detector and Gated Integrator for Electrochemical Measurements. A. J. Bentz, J. R. Sandifer, and R. P. Buck 542

Electroanalytical Studies of Methylmercury in Aqueous Solution. R. C. Heaton and H. A. Laitinen 547

Mixed-Potential Mechanism for the Potentiometric Response of the Sodium Tungsten Bronze Electrode to Dissolved Oxygen and in Chelometric Titrations. P. B. Hahn, D. C. Johnson, M. A. Wechter, and A. F. Voigt 553

Mechanistic Studies Using Double Potential Step Chronoamperometry: The EC, ECE, and Second-Order Dimerization Mechanisms. R. J. Lawson and J. T. Maloy 559

Recording Polarization of Fluorescence Spectrometer—A Unique Application of Piezoelectric Birefringence Modulation. J. E. Wampler and R. J. DeSa 563

Novel Mass Spectrometric Sampling Device—Hollow Fiber Probe. L. B. Westover, J. C. Tou, and J. H. Mark 568

Quantitative Dye Laser Amplified Absorption Spectrometry. R. C. Spiker, Jr., and J. S. Shirk 572

Vidicon Tube as a Detector for Multielement Flame Spectrometric Analysis. K. W. Busch, N. G. Howell, and G. H. Morrison 575

Analysis of Twelve Amino Acids in Biological Fluids by Mass Fragmentography. R. E. Summons, W. E. Pereira, W. E. Reynolds, T. C. Rindfleisch, and A. M. Duffield 582

Notes

Electrochemical Oxidation of Thin Palladium Films on Gold. S. H. Cadle 587

New Methods for the Preparation of Perchlorate Ion-Selective Electrodes. T. J. Rohm and G. G. Guilbault 590

Change in Potential of Reference Fluoride Electrode without Liquid Junction in Mixed Solvents. K. M. Stelling and S. E. Manahan 592

Quantitative Spectrometric Determination Specific for Mannose. R. W. Scott and Jesse Green 594

Application of the Carbon Rod Atomizer to the Determination of Mercury in the Gaseous Products of Oxygen Combustion of Solid Samples. Duane Siemer and Ray Woodruff 597

Graphite Braid Atomizer for Atomic Absorption and Atomic Fluorescence Spectrometry. Akbar Montaser, S. R. Goode, and S. R. Crouch 599

Double Modulation Atomic Fluorescence Flame Spectrometry. W. K. Fowler, D. O. Knapp, and J. D. Winefordner 601

Direct Mass Spectrometric Analysis of High Pressure Gasoline Streams Containing Light Ends. D. V. Rasmussen 602

© Copyright 1974
by the American Chemical Society



MANUSCRIPT REQUIREMENTS published in December 1973 issue, page 2451, outlines scope and copy requirements to be observed in preparing manuscripts for consideration. Manuscript (4 copies) should be submitted to ANALYTICAL CHEMISTRY, 1155 Sixteenth St., N.W., Washington, D.C. 20036.

The American Chemical Society assumes no responsibility for the statements and opinions advanced by contributors to its publications. Views expressed in the editorials are those of the editors and do not necessarily represent the official position of the American Chemical Society.

1974 Subscription Rates

	1 yr.	2 yr.	3 yr.
Members, domestic and foreign	\$ 5.00	\$ 9.00	\$12.00
Nonmembers, domestic and Canada	7.00	12.00	16.00
Nonmembers, foreign except Canada	15.00	27.50	40.00

Postage: Canada and Pan-American Union, \$4.00; foreign, \$5.00. Air freight rate available on request. Single copies: current, \$2.00 except Annual Reviews, \$3.00 each. Rates for back issues and volumes are available from Special Issues Sales Dept., 1155 Sixteenth St., N.W., Washington, D. C. Send all new and renewal subscriptions with payment to: Office of the Controller, 1155 Sixteenth Street, N.W., Washington, D. C. 20036. All correspondence and telephone calls regarding changes of address, claims for missing issues, subscription service, the status of

records, and accounts should be directed to: Manager, Membership and Subscription Services, American Chemical Society, P.O. Box 3337, Columbus, Ohio 43210. Telephone (614) 421-7230.

On changes of address, include both old and new addresses with ZIP code numbers, accompanied by mailing label from a recent issue. Allow four weeks for change to become effective.

Subscriptions should be renewed promptly to avoid a break in your series.

Claims for missing numbers will not be allowed (1) if received more than sixty days from date of issue plus time normally required for postal delivery of journal and claim, (2) if loss was due to failure of notice of change in address to be received before the date specified in (1), or (3) if the reason for the claim is "issue missing from files."

Those interested in joining the American Chemical Society should write to Admissions Department at the Washington Office.

Published monthly with Review issue added in April and a Laboratory Guide in August by the American Chemical Society, from 20th and Northampton Sts., Easton, Pa. 18042; Executive Offices and Editorial Headquarters, 1155 Sixteenth St., N.W., Washington, D. C. 20036; Advertising Office, 142 East Ave., Norwalk, Conn. 06851. ANALYTICAL CHEMISTRY and other ACS periodicals are available on microfilm. For information write to: MICROFILM, Special Issues Sales Dept., American Chemical Society, 1155 Sixteenth St., N.W., Washington, D. C. 20036. Second class postage paid at Washington, D. C. and at additional mailing offices.

A brief guide for selecting a precision spectrophotometer matched to your needs—from Bausch & Lomb, the optics people.



SPECTRONIC® 70

Wide 325nm-925nm wavelength range is continuous. Bandpass is narrow 8nm for excellent resolution in an extended range of applications. Accepts virtually all standard glassware—test tubes, rectangular cuvettes, cylindrical cells. Choice of quickly interchangeable sampling systems.



SPECTRONIC® 88

The Spectronic 88 has the same excellent specifications and sampling versatility as the Spectronic 70—and more. It permits you to read directly in Concentration, Linear Absorbance to 2.0A over effectively 16 inches of meter, and Transmittance. A single knob selects the operating mode. Choice of interchangeable sampling systems including semiautomatic flow-thru which permits running 300 samples per hour.



SPECTRONIC® 100

4 place digital readout displays Linear Absorbance, Concentration and Transmittance. Many interchangeable sampling options including a semi-automatic flow-thru system with self-purge, and zero error logic to eliminate cross contamination. 325nm to 925nm wavelength range, 8nm bandpass, built-in electronic check.



SPECTRONIC® 700

Low-cost, UV-visible, single beam instrument with constant 2nm bandpass over full 200-950nm range. Permits direct readings in Concentration, Linear Absorbance to 2.0A over effectively 16 inches of meter, and Transmittance. Exceptionally high resolution. Stability equal to, or better, than costlier spectrophotometers.

Write for literature to Bausch & Lomb
Analytical Systems Division, Dept. 03-04-31
820 Linden Avenue, Rochester, New York 14625.

The people who sell more
spectrophotometers than any other manufacturer.

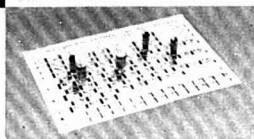
BAUSCH & LOMB 
ANALYTICAL SYSTEMS DIVISION

See us at the FASEB Booth C8-C11

CIRCLE 24 ON READER SERVICE CARD

PURE MATERIALS

With our high-purity materials we can help you eliminate one evasive variable haunting research projects: impurities. We stock a periodic chartful of elements and inorganic compounds, spectrographically analyzed.



PressuReactor®

For dissolving substances — contamination-free — in a strong acid or base with pressure and heat, this ss-encased, 35-ml-capacity Teflon crucible provides maximum safety, speed and convenience.

Spex-only features include a contact thermometer for monitoring temperature safely up to 150°C and a Teflon-coated, magnetic stirring rod to hasten reactions.



NYLON-LUCITE SIEVE SETS

Four mesh sizes in a stack as free from metallic contamination as their immaculate appearance suggests.



BORON CARBIDE MORTAR & PESTLE SETS

If you absolutely must resort to physical labor, Boron Carbide is the material for hand grinding: tough, inert, hard, mirror-finished with no bonding agents, but under more average lab circumstances outdistanced by

MIXER/MILLS®

The research literature of our field is generously sprinkled with testimonials in praise of these versatile electrical pulverizers which, in grindmanship, yield only to the

SHATTERBOX®

This laboratory grinder makes fast work of the big, hard jobs, having earned its reputation as the unexcelled work-horse. May we test grind a 100 ml sample for you, be it cement, slag, glass, minerals, fertilizer or such? No obligation, of course.

INDUSTRIES, INC. • BOX 798, METUCHEN, N.J. 08840 • (201)-549-7144

CIRCLE 235 ON READER SERVICE CARD

Contents

Semimicro Procedure for the Determination of Hydrocarbon Types in Shale-Oil Distillates. L. P. Jackson, C. S. Allbright, and H. B. Jensen 604

Improved Ion-Exchange Technique for the Concentration of Manganese from Sea Water. R. G. Smith, Jr. 607

Separation of the Tervalent Actinides from the Lanthanides by Extraction Chromatography. T. D. Filer 608

Gas Chromatographic Separation of Water from Cryogenically Collected Air Samples—Enhanced Concentration of Trace Organic Volatiles Prior to GC-MS Analyses. B. J. Tyson and G. C. Carle 610

Pyrolysis Esterification of Phosphorus-Containing Acids for Gas-Liquid Chromatographic Analysis. W. L. Clapp, R. J. Valis, S. R. Kramer, and J. W. Mercer 613

Sensitivities for Photon Activation Analysis with Thick-Target, 110-MeV Electron Bremsstrahlung. Enzo Ricci 615

Determination of Lead in Paint with Fast Neutrons from a Californium-252 Source. G. J. Lutz 618

Colorimetric Determination of N-Arylhydroxylamines with 9-Chloroacridine. R. E. Gammans, J. T. Stewart, and L. A. Sternson 620

Aids for Analytical Chemists

On the Use of a Power Divider for Thermostated Electrodeless Discharge Lamps in Atomic Fluorescence Spectrometry. D. O. Knapp, C. J. Molnar, and J. D. Winefordner 622

High Pressure Gradient Chamber for Liquid Chromatography. E. H. Pfadenhauer, T. E. Lynes, and T. V. Updyke 623

Correction. Resolution by Gas-Liquid Chromatography of Diastereomers of Five Nonprotein Amino Acids Known to Occur in the Murchison Meteorite. G. E. Pollock 614

Correction. Application of a Piezoelectric Quartz Crystal as a Partition Detector. Development of a Digital Sensor. Morteza Janghorbani and Harry Freund 621

382 A • ANALYTICAL CHEMISTRY, VOL. 46, NO. 4, APRIL 1974

At the FASEB Meeting



AMERICAN
INSTRUMENT
COMPANY

DIVISION OF TRAVENOL LABORATORIES, INC.
Silver Spring, Maryland 20910

SEE THE NEW

Fluorescence Photon Counter

A very practical new tool of great value in those applications which are sensitivity- or scatter-limited. This instrument detects fluorescence signals too weak to measure by conventional techniques; has the greater stability inherent to pulse-height discrimination; and reduces noise by observing only photo cathode impulses which are averaged.

SEE THE NEW

Oxygen Dissociation Apparatus

Generates dissociation curve by spectrophotometrically monitoring oxygen saturation of whole blood. Using less than 50 microliters of whole blood or hemoglobin solution, this dual-wavelength technique can be performed using a new filter instrument or with a new accessory for the DW-2™ UV-VIS Spectrophotometer.

SEE THE NEW

Corrected Spectra Accessory for SPF™

A third-generation corrected spectra accessory for the Aminco-Bowman Spectrophotofluorometer (SPF) which produces either quanta-corrected or energy corrected excitation and emission spectra without the use of quantum counters. The range of total energy correction is 200 to 650 nanometers for corrected excitation spectra, and 290 to 700 nanometers for corrected emission spectra.

SEE THE

Helium Glow Photometer

Determines quantities of biologically significant metals in samples of microscopic size. In principle, the vaporized sample is excited by an r.f. helium-glow discharge. The emitted radiation is sorted by interference filters and measured by two photomultiplier tubes allowing integration and simultaneous digital display of two components in a single sample. Sample volumes are often less than 10 nanoliters.

Stop at AMINCO's booths M-110 to 113 at FASEB or
contact us for further information.

FREE!!!



1974 Heath/Schlumberger electronic instruments catalog.

The new '74 Heath/Schlumberger instruments catalog is here...32 pages of high performance electronic equipment at low, direct-to-you prices. Whatever you need in test and measurement equipment for design, R&D, or teaching applications, Heath/Schlumberger has it...at much less than you planned to spend.



Our new SR-255B strip chart recorder (left) is a good example.

Four calibrated spans, 10 mV-10 V, ten accurate chart speeds from 10 in/min to 0.01 in/min. Complete remote control capability, 10 in/sec writing speed...all for just \$335*. 600 MHz frequency counter for just \$795*...110 MHz autoranging counter, just \$325*...dual trace 15 MHz scope only \$595*...the famous Malmstadt-Enke Lab Stations...power supplies...generators...digital multimeters...and dozens of other high performance, low cost instruments. To get your FREE copy of this catalog, visit your local Heathkit Electronic Center or use the coupon below.

Heath/Schlumberger Instruments		HEATH	
Dept. 831-014		Schlumberger	
Benton Harbor, Michigan 49022			
<input type="checkbox"/> Please send 1974 Electronic Instruments catalog.			
Name _____			
Title _____			
Company/Institution _____			
Address _____			
City _____		State _____	Zip _____
*Mail order prices; F.O.B. factory. EK-418			

Author Index

Allbright, C. S.	604	Maddox, W. L.	485
Aronson, J. P.	509	Malanify, J. J.	499
		Maloy, J. T.	559
Bearse, R. C.	499	Manahan, S. E.	592
Bentz, A. J.	543	Mark, J. H.	568
Beyer, W. F.	539	Mercer, J. W.	613
Buck, R. P.	543	Mitchell, J. W.	503
Busch, K. W.	575	Molnar, C. J.	622
		Montasser, A.	599
Cadle, S. H.	587	Morrison, G. H.	575
Carle, G. C.	610		
Clapp, W. L.	613	Pereira, W. E.	582
Close, D. A.	499	Pfadenhauer, E. H.	623
Crouch, S. R.	599	Preuss, D. R.	520
Ctvrtnicek, T.	534		
		Rasmussen, D. V.	602
DeSa, R. J.	563	Reynolds, W. E.	582
DeVoe, J. R.	509	Ricci, E.	615
Doyle, M. P.	492	Rindfleisch, T. C.	582
Duffield, A. M.	582	Robertson, J. H.	539
		Rohm, T. J.	590
Filer, T. D.	608	Ruegg, F. C.	509
Ford, R. E.	534		
Fowler, W. K.	601	Sandifer, J. R.	543
Frame, G. M.	534	Schucker, G. D.	489
		Scott, R. W.	594
Gammans, R. E.	620	Scribner, W. G.	534
Ganges, R.	503	Shideler, R. W.	509
Goldstein, G.	485	Shirk, J. S.	572
Goode, S. R.	599	Shoenfeld, P. S.	509
Goodnight, J. L.	482	Siemer, D.	597
Green, J.	594	Smith, R. G., Jr.	607
Grotch, S. L.	526	Spiker, R. C., Jr.	572
Guilbault, G. G.	590	Stelting, K. M.	592
		Sternson, L. A.	620
Hahn, P. B.	553	Stewart, J. T.	620
Heaton, R. C.	547	Sugawara, K. F.	489
Ho, F. F.-L.	496	Summons, R. E.	582
Hoffman, G. L.	492		
Howell, N. G.	575	Tou, J. C.	568
		Tsuji, K.	539
Jackson, L. P.	604	Tyson, B. J.	610
Jensen, H. B.	604		
Johnson, D. C.	553	Umbarger, C. J.	499
Jurs, P. C.	520	Updyke, T. V.	623
Kelley, M. T.	485	Valis, R. J.	613
Knapp, D. O.	601, 622	Voigt, A. F.	553
Kolling, O. W.	482		
Kramer, S. R.	613	Walsh, P. R.	492
		Wampler, J. E.	563
Laitinen, H. A.	547	Wechter, M. A.	553
Lawson, R. J.	559	Weetall, H. H.	489
Lutz, G. J.	618	Westover, L. B.	568
Lynes, T. E.	623	Winefordner, J. D.	601, 622
		Woodruff, R.	597

CIRCLE 118 ON READER SERVICE CARD

Briefs

Solvatochromism of Phenol Blue in the Ethyl Acetate-Acetic Acid Solvent System

The solvent-induced red-shift for the phenol blue molecule is assigned to a nearly regular perturbation from hydrogen bonding by acetic acid. The acid decolorizes the model dye, following pseudo first order kinetics.

Orland W. Kolling and Jana L. Goodnight, Chemistry Department, Southwestern College, Winfield, Kansas 67156

Anal. Chem., **46**, 482 (1974)

Spectrophotometric Analysis with the GeMSAEC Fast Analyzer—Determination of Zinc Using 4-(2-Pyridylazo)Resorcinol (PAR)

Photometric measurements with the GeMSAEC Fast Analyzer are found to be linear, accurate, and precise. From 0.2–1 ppm of Zn are determined with a relative standard deviation of 0.3–3%.

Gerald Goldstein, W. L. Maddox, and M. T. Kelley, Analytical Chemistry Division, Oak Ridge National Laboratory, Oak Ridge, Tenn. 37830

Anal. Chem., **46**, 485 (1974)

Preparation, Properties, and Applications of 8-Hydroxyquinoline Immobilized Chelate

The chelate is studied by investigating its capacity for metallic extractions at various pH. Also, desorption studies, exchange capacity, effect of complexing agents, and NaCl solutions are investigated.

K. F. Sugawara, H. H. Wetall, and G. D. Schucker, Research and Development Laboratories, Corning Glass Works, Corning, N.Y. 14830

Anal. Chem., **46**, 489 (1974)

Determination of a Geometry and Dead Time Correction Factor for Neutron Activation Analysis

The determination of a normalization constant for nondestructive neutron activation analysis which corrects for dead time and counting geometry between a standard and sample is described.

Gerald L. Hoffman, Graduate School of Oceanography, University of Rhode Island, Kingston, R.I. 02881, Paul R. Walsh, Department of Chemistry, University of Rhode Island, Kingston, R.I. 02881, and Michael P. Doyle, Rhode Island Nuclear Science Center, South Ferry Road, Narragansett, R.I. 02882

Anal. Chem., **46**, 492 (1974)

Determination of Phenols by Fluorine-19 Nuclear Magnetic Resonance of Hexafluoroacetone Derivatives

The chemical shifts of the derivatives and the equilibrium constant for derivative formation can be related to the structure of substituted phenols.

Floyd F.-L. Ho, Research Center, Hercules Incorporated, Wilmington, Del. 19899

Anal. Chem., **46**, 496 (1974)

Elemental Analysis of Whole Blood Using Proton-Induced X-Ray Emission

Proton-induced X-ray emission is shown to detect Fe, Cu, Zn, Se, and Rb to a precision of 7%, 18%, 7%, 50%, and 19%, respectively.

R. C. Bearse, D. A. Close, J. J. Malanify, and C. J. Umberger, Los Alamos Scientific Laboratory of the University of California, Los Alamos, N.M. 87544

Anal. Chem., **46**, 499 (1974)

Substoichiometric Extraction of Cations with Mixtures of Hexafluoroacetylacetone and Tri-*n*-Octylphosphine Oxide in Cyclohexane

High precision extractions of Zn^{2+} , Cu^{2+} , and Eu^{3+} are reported along with extraction curves for Mn^{2+} , Fe^{2+} , Co^{2+} , Cu^{2+} , Zn^{2+} , Fe^{3+} , Eu^{3+} , and Lu^{3+} .

J. W. Mitchell, Bell Laboratories, Murray Hill, N.J. 07974, and Roland Ganges, Stanford University, Stanford, Calif.

Anal. Chem., **46**, 503 (1974)

Computer Utility for the Analytical Laboratory

Computer control of analytical instruments is accomplished by using remote push-button-operated consoles connected to a time-shared minicomputer via standard interfaces to a high data rate party line.

James R. DeVoe, Ronald W. Shideler, Fillmer C. Ruegg, Jules P. Aronson, and Peter S. Shoenfeld, Analytical Chemistry Division, Institute for Materials Research, National Bureau of Standards, Washington, D.C. 20234

Anal. Chem., **46**, 509 (1974)

Pattern Recognition Techniques Applied to the Interpretation of Infrared Spectra

The application of pattern recognition techniques to the investigation of IR spectra of small organic molecules is presented.

D. R. Preuss and P. C. Jurs, Department of Chemistry, The Pennsylvania State University, University Park, Pa. 16802

Anal. Chem., **46**, 520 (1974)

Statistical Method for the Prediction of Matching Results in Spectral File Searching

The distribution of the mismatch criterion in the file searching of mass spectra can be accurately predicted for most codes using the theory developed.

Stanley L. Groch, Jet Propulsion Laboratory, California Institute of Technology, Pasadena, Calif. 91103

Anal. Chem., **46**, 526 (1974)

Trace Determination of Beryllium Oxide in Biological Samples by Electron-Capture Gas Chromatography

A base dissolution, chelation-gas chromatographic method for the determination of BeO in biological media is described. This method yields recoveries averaging 105% for levels of 1.0 mg BeO/ml.

George M. Frame and Roddey E. Ford, 6570th Aerospace Medical Research Laboratory, Aerospace Medical Division, Air Force Systems Command, Wright-Patterson Air Force Base, Ohio 45433, and William G. Scribner and Thomas Ctvrtnecek, Monsanto Research Corporation, Dayton, Ohio 45407

Anal. Chem., **46**, 534 (1974)

High Pressure Liquid Chromatographic Determination of Tetracyclines

A high pressure LC method is developed which separates tetracycline, anhydrotetracycline, 4-epi-anhydrotetracycline, 4-epi-tetracycline, chlorotetracycline, and doxycycline in less than 30 minutes with a relative standard deviation of 1.02%.

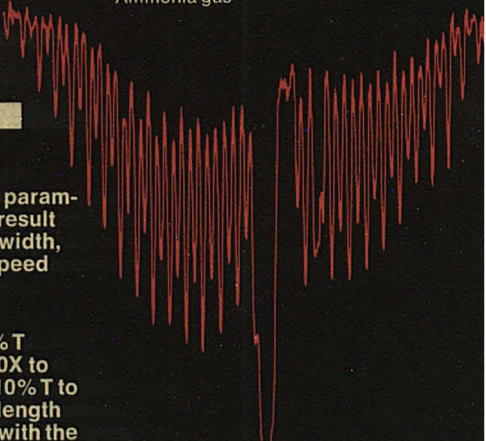
Kiyoshi Tsuji, J. H. Robertson, and W. F. Beyer, Control Analytical Research and Development, The Upjohn Company, Kalamazoo, Mich. 49001

Anal. Chem., **46**, 539 (1974)



What you set is what you get.

High resolution
Wavenumber expansion 5X
Ammonia gas



On the new SP1100 IR one control optimizes all parameters. Select the desired result and the correct gain, slit width, time constant and scan speed are automatically set.

On the new SP1100 you also get *continuous* % T expansion from 0.8X to 10X to permit expansion of *any* 10% T to full scale... and 5X wavelength expansion synchronized with the chart for unequivocal identification of band positions... repetitive scan... fast scan (6 minutes is normal).

Call Frank Hamm, Manager Spectrophotometry and Chromatography at 914-664-4500. Ask him about the price. It is about \$1000 lower than you might think.

**PHILIPS
ELECTRONIC
INSTRUMENTS**

750 South Fulton Ave.
Mount Vernon, NY 10550
A North American Philips Co.

CIRCLE 189 ON READER SERVICE CARD

Briefs

Wide-Band, Precision, DC-Coupled Lock-In Detector and Gated Integrator for Electrochemical Measurements

An instrument capable of resolving impedance (10^2 – 10^{11} ohms) or admittance data into in- and out-of-phase components is described. Precision is 1.0% when components differ by a factor of 100.

J. J. Bentz, J. R. Sandifer, and R. P. Buck, The William R. Kenan, Jr., Laboratories of Chemistry, University of North Carolina, Chapel Hill, N.C. 27514
Anal. Chem., 46, 543 (1974)

Electroanalytical Studies of Methylmercury in Aqueous Solution

The first pulse polarographic peak in the reduction of monomethylmercury compounds in aqueous solution is shown to be analytically useful at concentration levels of the order of micrograms per liter.

R. C. Heaton and H. A. Laitinen, School of Chemical Sciences, University of Illinois at Urbana-Champaign, Urbana, Ill. 61801
Anal. Chem., 46, 547 (1974)

Mixed-Potential Mechanism for the Potentiometric Response of the Sodium Tungsten Bronze Electrode to Dissolved Oxygen and in Chelometric Titrations

Potentiometric response of the Na_2WO_3 electrode to dissolved O_2 and EDTA in alkaline solution is shown to result from a mixed-potential mechanism involving spontaneous oxidation of the electrode by O_2 .

P. B. Hahn, D. C. Johnson, M. A. Wechter, and A. F. Voigt, Department of Chemistry and the Ames Laboratory—USAEC, Iowa State University, Ames, Iowa 50010
Anal. Chem., 46, 553 (1974)

Mechanistic Studies Using Double Potential Step Chronoamperometry: The EC, ECE, and Second-Order Dimerization Mechanisms

Theoretical working curves are presented showing the behavior of the current semiintegral in the potential step experiment when perturbed by homogeneous kinetic complications.

R. Joe Lawson and J. T. Maloy, Department of Chemistry, West Virginia University, Morgantown, W.Va. 26506
Anal. Chem., 46, 559 (1974)

Recording Polarization of Fluorescence Spectrometer—A Unique Application of Piezoelectric Birefringence Modulation

A spectrometer that records polarization of fluorescence is described. It uses a piezoelectric birefringence modulator as a variable retardance waveplate, a single photomultiplier, no moving parts, and can be directly computer-controlled.

John E. Wampler and Richard J. DeSa, Department of Biochemistry, University of Georgia, Athens, Ga. 30602
Anal. Chem., 46, 563 (1974)

Novel Mass Spectrometer Sampling Device—Hollow Fiber Probe

A silicone rubber hollow fiber probe is constructed for monitoring ppm levels of volatile organic compounds in aqueous solution and in air. Enrichment factors of chloroform and methanol are measured.

L. B. Westover, J. C. Tou, and J. H. Mark, Analytical Laboratories, Dow Chemical U.S.A., Midland, Mich. 48640
Anal. Chem., 46, 568 (1974)

Quantitative Dye Laser Amplified Absorption Spectrometry

The sensitivity of quantitative spectrophotometric techniques is enhanced by an intercavity absorption technique. Laser intensity is related empirically to sample concentration for Ho^{3+} and Pr^{3+} solutions in the laser cavity.

Robert C. Spiker, Jr., and James S. Shirk, Department of Chemistry, Illinois Institute of Technology, Chicago, Ill. 60616
Anal. Chem., 46, 572 (1974)

The Vidicon Tube as a Detector for Multielement Flame Spectrometric Analysis

The feasibility of performing multielement flame emission analysis is demonstrated using a silicon diode vidicon tube and optical multichannel analyzer in conjunction with a 0.5-meter monochromator.

K. W. Busch, N. G. Howell, and G. H. Morrison, Department of Chemistry, Cornell University, Ithaca, N.Y. 14850
Anal. Chem., 46, 575 (1974)

Analysis of Twelve Amino Acids in Biological Fluids by Mass Fragmentography

A GC/MS-computer method for the quantitation of amino acids at the nanogram level in biological fluids is described.

R. E. Summons, W. E. Pereira, W. E. Reynolds, T. C. Rindfleisch, and A. M. Duffield, Genetics Department, Stanford University Medical Center, Stanford, Calif. 94305
Anal. Chem., 46, 582 (1974)

Notes

Electrochemical Oxidation of Thin Palladium Films on Gold

The determination of the oxidation state of submonolayer Pd films on gold in 0.2M H_2SO_4 provides a means by which small quantities of Pd are quantitatively determined. Steven H. Cadle, Chemistry Department, Vassar College, Poughkeepsie, N.Y. 12601
Anal. Chem., 46, 587 (1974)

New Methods for the Preparation of Perchlorate Ion-Selective Electrodes

Ion-selective electrodes for perchlorate ion, however with lower selectivity coefficients than for commercial electrodes, are prepared by incorporating a commercial liquid ion exchanger in poly(vinyl chloride).

T. J. Rohm and G. G. Guilbault, Department of Chemistry, Louisiana State University in New Orleans, New Orleans, La. 70122
Anal. Chem., 46, 590 (1974)

Change in Potential of Reference Fluoride Electrode without Liquid Junction in Mixed Solvents

The shift in potential of the lanthanum fluoride membrane electrode used as a reference in acetonitrile-water solutions can be calculated from differences in solubility.

Kathleen M. Stelling and Stanley E. Manahan, Department of Chemistry, University of Missouri—Columbia, Columbia, Mo. 65201
Anal. Chem., 46, 592 (1974)

Quantitative Spectrometric Determination Specific for Mannose

By dehydration in H_2SO_4 and spectrophotometric measurement of the furan products, mannose is measured in the presence of other sugars. The standard deviation is $\pm 0.3\%$ mannose if mannose is 6% and glucose is 94%.

Ralph W. Scott and Jesse Green, Forest Products Laboratory, Forest Service, U.S. Department of Agriculture, Madison, Wis. 53705
Anal. Chem., 46, 594 (1974)

Quick relief for G.C. gas pains



Chromatrol™ Flow Controller.
Flow control down to 1 SCCM.
Dual Channel. Set and forget.
\$375.00. Volume discounts,
of course.

Dual Channel G.C. never had it so good. Our Chromatrol™ Flow Controller maintains constant, independent, pre-set flow of carrier gases to each of two columns, regardless of variations in input pressure, temperature or column back pressure. Ideal for dual column G.C.'s. And perfectly adaptable to computer or sequencer control.

What could be simpler? Hydrogen, Helium, Nitrogen, and Argon from 1 to 100 SCCM with exact repeatability of setting $\pm 0.2\%$. No tweak. No delay. No needless bulk—the Chromatrol™ Flow Controller doesn't require its own power supply. It operates on available G.C. instrument power.

The voltage program capability makes it particularly

valuable in automated systems where it's necessary to program various flows of carrier gas by computer or sequencer control.

And there's no beating the price. \$375.00. Even less in quantity. Just six weeks delivery.

Call collect for immediate requirements or write: Rod Manning, Applied Materials, Inc., 2999 San Ysidro Way, Santa Clara, California 95051, (408) 738-0600.

We make it easier for you to make it better.

applied materials



CIRCLE 3 ON READER SERVICE CARD

Briefs

Application of the Carbon Rod Atomizer to the Determination of Mercury in the Gaseous Products of Oxygen Combustion of Solid Samples

Combustion of solid samples with concentration of Hg directly onto gold plated graphite atomizer tubes is used. The relative standard deviation is about 7% on coal samples.

Duane Siemer and Ray Woodruff, Department of Chemistry, Montana State University, Bozeman, Mont. 59715

Anal. Chem., **46**, 597 (1974)

Graphite Braid Atomizer for Atomic Absorption and Atomic Fluorescence Spectrometry

The graphite braid is introduced as a new non-flame atomizer. Some of the characteristics of the atomizer are discussed and data are presented for the determination of Cu, Pb, Cd, and Zn.

Akbar Montaser, S. R. Goode, and S. R. Crouch, Department of Chemistry, Michigan State University, East Lansing, Mich. 48824

Anal. Chem., **46**, 599 (1974)

Double Modulation Atomic Fluorescence Flame Spectrometry

A double modulation 900-W continuum source atomic fluorescence flame spectrometer, with compensation for scatter, is described. Limits of detection are given.

W. K. Fowler, D. O. Knapp, and J. D. Winefordner, Department of Chemistry, University of Florida, Gainesville, Fla. 32601

Anal. Chem., **46**, 601 (1974)

Direct Mass Spectrometric Analysis of High Pressure Gasoline Streams Containing Light Ends

The method of analysis and calibration described permits the determination of hydrocarbon types present in samples containing large amounts of C_1 - C_6 hydrocarbons directly from the undepentanized mass spectrum.

Dirk V. Rasmussen, Gulf Oil Canada Limited, Research and Development Department, Sheridan Park, Ontario, Canada

Anal. Chem., **46**, 602 (1974)

Semimicro Procedure for the Determination of Hydrocarbon Types in Shale-Oil Distillates

Saturated hydrocarbons and olefins are determined as groups in shale oil distillates. Results from replicate tests deviate from average values by 1.3% or less. Aromatics are 100 minus (saturates plus olefins).

Larry P. Jackson, Charles S. Albright, and Howard B. Jensen, U.S. Department of the Interior, Bureau of Mines, Laramie Energy Research Center, Laramie, Wyo. 82070

Anal. Chem., **46**, 604 (1974)

Improved Ion-Exchange Technique for the Concentration of Manganese from Sea Water

A batch technique alleviates difficulties in the column technique caused by swelling and contraction properties of the resin. The method yields quantitative recovery with a variation in efficiency of $\pm 0.6\%$.

Ralph G. Smith, Jr., Skidaway Institute of Oceanography, P.O. Box 13687, Savannah, Ga. 31406

Anal. Chem., **46**, 607 (1974)

Separation of the Trivalent Actinides from the Lanthanides by Extraction Chromatography

An extraction chromatography procedure for the separation of trivalent actinides from trivalent lanthanides is able to recover $98 \pm 1\%$ of americium-241 with only $0.2 \pm 0.2\%$ of cerium-144 in 40 minutes of column time.

Terry D. Filer, Health Services Laboratory, U.S. Atomic Energy Commission, Idaho Falls, Idaho 83401

Anal. Chem., **46**, 608 (1974)

Gas Chromatographic Separation of Water from Cryogenically Collected Air Samples—Enhanced Concentration of Trace Organic Volatiles Prior to GC-MS Analyses

This method is shown to be useful for the analysis of a wide variety of organic compounds.

Bennett J. Tyson and Glenn C. Carle, Ames Research Center, NASA, Moffett Field, Calif. 94035

Anal. Chem., **46**, 610 (1974)

Pyrolysis Esterification of Phosphorous-Containing Acids for Gas-Liquid Chromatographic Analysis

Analysis of aqueous solutions of methylphosphonic acid and methylfluorophosphonic acid by pyrolysis esterification of their tetramethylammonium salts and GC analysis is demonstrated. Quantitative yields are obtained under controlled conditions.

William L. Clapp, Robert J. Valis, Stanley R. Kramer, and John W. Mercer, Process Technology Branch, Chemical & Plants Division, Manufacturing Technology Directorate, Edgewood Arsenal, Md. 21010

Anal. Chem., **46**, 613 (1974)

Sensitivities for Photon Activation Analysis with Thick-Target, 110-MeV Electron Bremsstrahlung

Photon-activation analysis sensitivities for a new facility of uncommon operation conditions are determined. These sensitivities are good, and agree with values for thin-target 25–30 MeV electron bremsstrahlung.

Enzo Ricci, Analytical Chemistry Division, Oak Ridge National Laboratory, Oak Ridge, Tenn. 37830

Anal. Chem., **46**, 615 (1974)

Determination of Lead in Paint with Fast Neutrons from a Californium-252 Source

Activation analysis with a ^{252}Cf source is shown to be a reliable nondestructive method for the determination of Pb in paint at levels of 1%.

George J. Lutz, Activation Analysis Section, Analytical Chemistry Division, National Bureau of Standards, Washington, D.C. 20234

Anal. Chem., **46**, 618 (1974)

Colorimetric Determination of N-Arylhydroxylamines with 9-Chloroacridine

A new colorimetric method for the determination of N-arylhydroxylamines with 9-chloroacridine is described. Concentrations of $10^{-5}M$ hydroxylamines are determined with an accuracy of 1%.

Richard E. Gammans, James T. Stewart, and Larry A. Sternson, The Bioanalytical Laboratory, Department of Medicinal Chemistry, School of Pharmacy, The University of Georgia, Athens, Ga. 30602

Anal. Chem., **46**, 620 (1974)

Aids for Analytical Chemists

On the Use of a Power Divider for Thermostated Electrodeless Discharge Lamps in Atomic Fluorescence Spectrometry

D. O. Knapp, C. J. Molnar, and J. D. Winefordner, Department of Chemistry, University of Florida, Gainesville, Fla. 32611

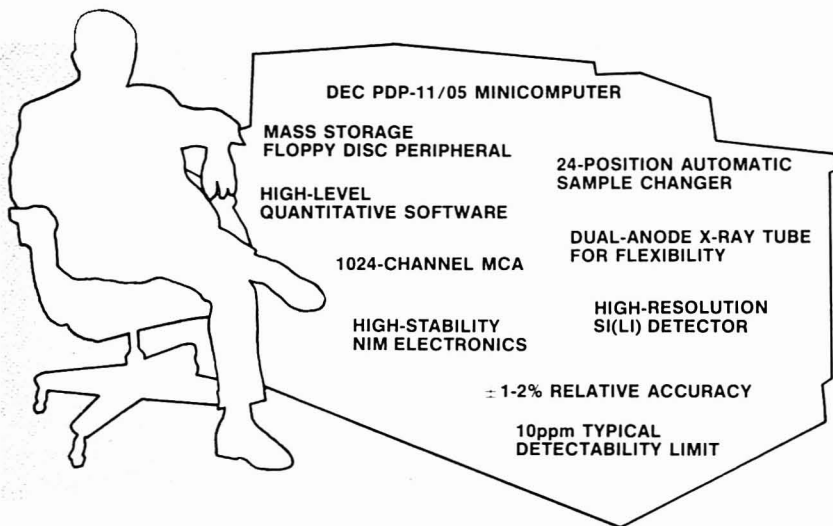
Anal. Chem., **46**, 622 (1974)

High Pressure Gradient Chamber for Liquid Chromatography

E. H. Pfadenhauer, T. E. Lynes, and T. V. Updyke, Newport Pharmaceuticals International, Inc., 1590 Monrovia Boulevard, Newport Beach, Calif., 92660

Anal. Chem., **46**, 623 (1974)

Ortec's newest x-ray fluorescence analyzer. (A sneak preview.)



We'd like to tell you something about the new 6110 TEFA (Tube-Excited Fluorescence Analyzer) Ortec is about to introduce.

You don't have to be a scientist to operate it. Just initiate the automatic program sequence and, in minutes, you'll have a computer printout of the quantitative elemental composition of up to 24 samples (powdered, granular, solid, or liquid—just about anything).

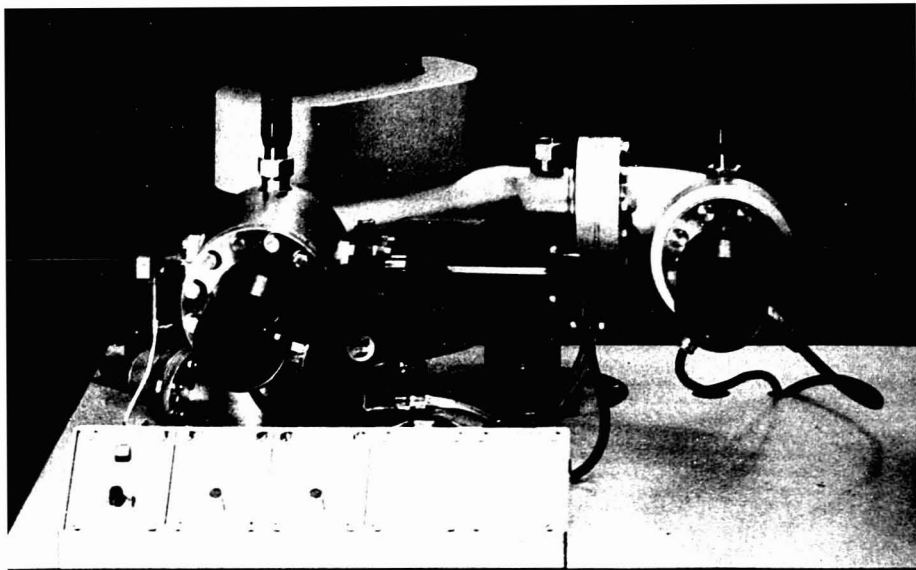
And the results you get will be consistently, dependably good. TEFA analyzes every element from sodium on up through the periodic table, and does it with $\pm 1\text{-}2\%$ relative accuracy for major elements. Total system repeatability is better than $\pm 0.025\%$. Detectability varies according to atomic number and matrix, but 10ppm is typical for elements heavier than vanadium (atomic number 23), and low parts-per-billion sensitivity can be had with sample preparation (accuracy for trace elements is limited only by the statistics of x-ray production and counting time). TEFA's dual-anode x-ray tube combined with regenerative monochromatic filters lets you optimize sample excitation (and, thereby, detectability) for the analysis at hand.

Something else to smile about: TEFA comes complete

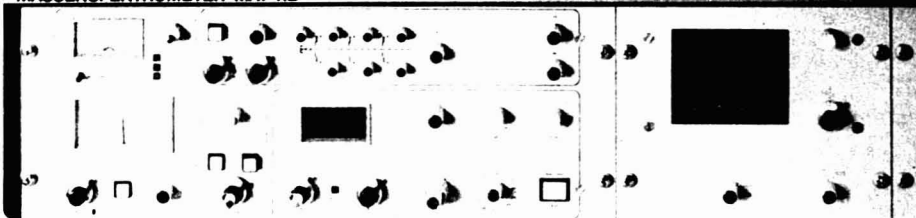
with computer programs for quantitative analysis. These programs are written in a powerful new interactive language called ORACL, which you can learn in just a couple of hours—even if you've had no exposure to software before. ORACL lets you write your own special-purpose programs and modify existing programs (such as our XRF CALC, XRF ID, and XRF QUAN) to suit both the work you're doing and your personal taste in formats and so forth. It also lets the fluorescence people at Ortec respond quickly with new programs as soon as improved analysis methods come into use.

The new TEFA will be available soon. See it demonstrated at this year's shows and meetings. Ask your nearby Ortec representative for details. Or contact Ortec Incorporated, 110 Midland Road, Oak Ridge, Tenn. 37830. Phone (615) 482-4411. In Europe: Ortec, Ltd., Dallow Road, Luton, Bedfordshire. Phone 0582 27557. Ortec GmbH, 8 München 13, Frankfurter Ring 81, West Germany. Phone (0811) 359-1001.

ORTEC
AN EG&G COMPANY



MASSENSPEKTROMETER MAT 112



Planning a new GC/MS for your lab? Ask for the brand-new model MAT 112 from Varian



You can expect a lot from your new mass spectrometer — we have anticipated your needs.

For the MAT 112 we have developed a variety of system components which provide for the versatility and high technical standard of the instrument. These include, in particular, double focusing analyzer, variable slits, efficient differential pump system with

large tube diameters and connection facility for a 600 l/s pump, direct inlet system with controllable evaporation temperature, reference inlet system, GC interface for different separator types, oscilloscope for optical spectrum display, peak matching unit for mass determinations with an accuracy of approx. 10 ppm, mass marker and digital mass display, as well as the

accessory for multi ion selection. A combined ion source for chemical ionization and electron impact ionization is available.

VARIAN MAT GmbH
28 Bremen 10/Germany
Postfach 4062

CIRCLE 239 ON READER SERVICE CARD

ANALYTICAL CHEMISTRY, VOL. 46, NO. 4, APRIL 1974 • 397 A

Computers in Clinical Chemistry

Ronald H. Laessig

State Laboratory of Hygiene and
University of Wisconsin Medical School
Madison, Wis. 53706

Thomas H. Schwartz

State Division of Health
Madison, Wis. 53706

The analytical chemist's relationship to clinical chemistry ranges from one of casual observation to enthusiastic participation. Clinical chemistry laboratories annually perform over 4.5 billion analytical determinations with direct bearing on the health of individuals. The analytical clinical chemist shares with his colleagues many unique and challenging problems. This article focuses on one—the utilization of computers in the clinical analytical laboratory. These laboratories, with their patient-oriented mission, have developed concepts and approaches to laboratory computer systems worthy of consideration by other laboratories.

This article first compares the operational philosophy of clinical and general analytical laboratories. A discussion of computerization in clinical laboratories emphasizes those techniques of general interest. Part II describes basic operational areas in clinical laboratories in the context of the potential contribution of computerization. Part III discusses significant computerization concepts developed for clinical laboratories, and Part IV briefly reviews some of the working systems. In Part V we have provided an annotated bibliography.

Part I. Analytical Vs. Clinical Laboratories: Philosophy of Operation

The analytical and clinical chemistry laboratories share a common objective—to produce chemical determinations. The emphasis in clinical labs is the ultimate objective of the analyses—the treatment and/or detection of disease. The clinical laboratory supplies the physician with data forming the basis of diagnosis and treatment. Since samples emanate from a hospital patient population, minimum turnaround time is emphasized. Benefits derived therefrom are obvious: effective therapy, reduced costs, minimum hospital

stay, and increased efficiency—all to meet increased demands on the medical care facilities. These practical considerations give impetus to the development of clinical laboratory computers.

One must also consider the nature of the clinical laboratory data. A patient's lab results are not a collection of discrete data points; they are elements in a data set characterizing the individual, his disease, the diagnosis, the therapy and its progress, and ultimately the restoration of his health. Data are used by primary and consultant physicians, nurses, and other health professionals. Records are needed for billing and workload inventory. Completed results are manipulated for quality control. Interactions with lab data are frequent, repeated, and take place at different points in time, for different purposes, and in many different ways. Often, the format and presentation of the data play a major role in determining its effectiveness at each interaction. The total operation of the clinical laboratory and the unique contribution of the computer in meeting its needs are precisely problems and solutions which we wish to emphasize.

In a casual perusal of the great array of articles, papers, and books on computerization, an obvious dichotomy of approach between the two types of laboratories becomes readily apparent. The analytical laboratory's approach to computers often views them as an adjunct or "back end" peripheral to specific analytical instruments—emphasizing the analytical instrument with the computer secondary in a role. In the clinical laboratories, the initial approach was similar. Within three years past introduction, a system-oriented computerization concept emerged—a result of the patient-oriented utilization of the information. This marked a shift in clinical laboratory computerization philosophy, a shift born of the necessity to involve all aspects of the laboratory in the information flow system.

Part II. Clinical (Hospital) Laboratory

The present stage of development for clinical laboratory computer systems is as much a product of evolution as necessity. Its understanding requires some background in clinical laboratory operation. The eight elements below enumerate interrelated areas to which computer systems must address themselves.

1. **Request/Samples.** Requests to draw samples are received randomly by the laboratory (or its computer) and must be organized into a sequence of acquisitions (draw list). Technologists (often laboratory personnel) are dispatched to obtain the specimens from the patients and check samples into the laboratory. Special provision must be made for emergency "STAT" requests and repeat or follow-up tests on the original specimen.

2. **Raw Data Acquisition.** Primary data (sensor output), instrument readings (both analog and digital), and technologist observations and commentary on specimens constitute types of raw data. Information must be assimilated, transformed into usable laboratory results, and matched to specimen identification.

3. **Intermediate Reports/Editing.** Primary test results are reviewed soon after analysis. Data are "edited," that is, modified (adjective added), discarded for analyzer or sample inadequacy, corrected for dilutions, identified as to analyst, etc., and ultimately approved for temporary filing, prior to dispersal as a finished product.

4. **Quality Control.** Quality control is involved in every stage of the laboratory operation. It is critically needed at the intermediate stage where data are accepted or rejected on the basis of control data. Multiple forms of quality control information are a necessary part of the laboratory's operating records for internal, long-term, and proficiency licensure purposes. Efficient handling, storage,

UNIVERSITY OF WISCONSIN HOSPITALS

ACCESSION NUMBER				SPEC. GRV.				PH				PROTEIN				URINALYSIS			
0	0	0	0	0	0	0	0	0	0	0	0	0	0	0	0	REDUCING SUBSTANCES			
1	1	1	1	1	1	1	1	1	1	1	1	1	1	1	1				
2	2	2	2	2	2	2	2	2	2	2	2	2	2	2	2	KETONES			
3	3	3	3	3	3	3	3	3	3	3	3	3	3	3	3				
4	4	4	4	4	4	4	4	4	4	4	4	4	4	4	4	HEMASTIX			
5	5	5	5	5	5	5	5	5	5	5	5	5	5	5	5				
6	6	6	6	6	6	6	6	6	6	6	6	6	6	6	6	BILE			
7	7	7	7	7	7	7	7	7	7	7	7	7	7	7	7				
8	8	8	8	8	8	8	8	8	8	8	8	8	8	8	8				
9	9	9	9	9	9	9	9	9	9	9	9	9	9	9	9				

UNIVERSITY OF WISCONSIN HOSPITALS

Report

Figure 1. User-controlled card input: card from University of Wisconsin Hospitals Urinalysis Laboratory

and presentation of quality control data are required.

5. Reports. Reports in many different formats which reference the data in a variety of ways are needed for different purposes. Here, the computer must be able to respond to the unique needs of the institution. An intermediate report is required at the editing stage. Other reports are required for STAT samples on a priority basis. The immediate need for telephone-requested results on a specific test from a specific patient and sample places an immense burden on the laboratory—a fast and simple means of locating the result must be available. The audit trail showing progress of all specimens is essential. Updated and complete reports must be expedited to the patient's records, an area where most systems fail or succeed. Reports are also needed for billing and for long-term patient records.

6. Inventory. Inventory includes information on samples to be drawn (test requests), the specimens available, and those scheduled to be run (in progress) and completed. It includes the status of all samples, requests, and reports in the laboratory.

7. Administration. The administrative aspects of laboratory operation include: maintenance of the patient census file, quality control records, workload data, and statistical data on parameters such as turnaround time, requests per patient, test frequency, etc. It also may include inventory data on supplies and resource utilization, cost analysis, and other operational data. The administrative aspects of computer systems will become more important as cost accounting, justification, and effective-

ness principles are applied to the laboratory.

8. Interface. The laboratory must interface the remainder of the institution. Users of the system include nonlaboratory personnel. Regardless of the effect a system has on the laboratory operation, its apparent effectiveness at many different points determines its ultimate success.

Part III. Computerization Concepts in the Clinical Laboratory

Goals. The goals of computerization in the clinical laboratory are obvious—to enable the laboratory to concentrate on producing high-quality analytical data within a time frame consistent with the ultimate use of the data. The advent of rapid, highly automated instrumentation, particularly multichannel analyzers, leaves the laboratory without a reporting system limited by its paper shuffling ability rather than its laboratory capabilities. For example, one SMA 12/60 (Technicon Corp., Tarrytown, N.Y. 10591) analyzer has a production potential of 5760 test results per 8-hr shift. Since standards and controls (comprising 20-30% input specimens) actually are part of the quality control records, they are therefore included in the total. One to two competent technologists produce this data. Expediting results to patient records, the only place where they are useful to the physician, is the critical problem. Yesterday's laboratory results, in terms of usefulness, are on a par with yesterday's newspaper.

Approaches to Computerization. The approach of clinical and analyti-

cal laboratories has been remarkably similar. Early attempts to use large, remote, or time shared systems were generally unsuccessful, largely because of the unpredictable, yet demanding use requirements of laboratory operation. Direct linkage with "outside" computers was abandoned in favor of producing data in an intermediate form which could be handled independent of laboratory operations. Card-oriented systems were by far the most common.

The development of the small (i.e., hardware cost equals \$100,000 or less) computers, such as the LINC (Laboratory Instrument Computers), was a prime mover in the evolution of today's computerized laboratory systems. Classic LINC minicomputers were initially developed under National Institutes of Health and other Federal sponsorship in the early 1960's. A commercial general-purpose computer (PDP-8) was produced by DEC (Digital Equipment Corp., Maynard, Mass. 01754) even earlier. Two groups share in the early history of the development of systems for the clinical laboratory. The BSL (Berkeley Scientific Laboratories, Hayward, Calif. 94545) as early as 1968, utilizing basically a PDP-8, was marketing a complete turnkey system. This was the initial custom-programmed system for clinical laboratories.

The G. P. Hicks group at Wisconsin (of which the principle author is not a part) incorporated the first LINC computer into the clinical laboratories before 1966 and described their system at the AACC (American Association of Clinical Chemists) meeting of that year. The approach was to automate analog signal acquisition and numerical data production

from automated laboratory instruments. These included both single-channel and multichannel analyzers. Hicks' approach, as an analytical chemist by training, thought first of the analyzer, then the laboratory, and ultimately the laboratory as a unit (with system interface to the rest of the data consumers) within the institution. This effort represented the "do-it-yourself" programming approach. The BSL initial "turnkey" approach and the early HICKS' approach of "do-it-yourself" to programming have both made significant contributions to the development of today's systems.

"Do-It-Yourself" Vs. "Turnkey"

Programming. In considering the development of one's own laboratory through computerization, most analytical chemists are faced with an immediate dilemma. Each laboratory would like to build its own computer system. The analytical chemist would like to control the lab; he feels that he alone accurately perceives its needs and goals and that the computer should be used as any other laboratory facility at his disposal. Unfortunately, laboratory computer system programs take years to develop, are often hopelessly inadequate for further expansion, and fall short of achieving real goals. On the other hand, a turnkey, custom-programmed system is not the whole answer.

Hardware/software vendors do not fully grasp the dimensions of individual (often inadequately described) laboratory problems. Systems are rigid—modification requires vendor support (in one case, flying in an expert from California to make even the smallest change in response to a change in laboratory protocol). Self-modification or additions to the system usually void any software guarantee. This dilemma has a conceptual solution which we describe as user control.

User Control Programming (Do Your Way). Clinical chemists, unlike other analytical counterparts, have virtually no standard methods or procedures. To illustrate user-controlled programming concepts, we will discuss the routine operation of the glucose AutoAnalyzer (Technicon Corp., Tarrytown, N.Y. 10591), a simple determination for which there are as many individualized protocols as there are laboratories. Variables include sample rates and times, chemical procedures, sequence of samples, use of controls, and concentration of standards. These parameters also vary within laboratories owing to changing conditions or lots of reagent, control or standard. Each laboratory has established its own criteria of acceptable AutoAnalyzer operation (i.e., quality control parameters). For

some clinical laboratory computer systems, all such variables must be software "programmed." Changes in the laboratory represent changes in software, hence reprogramming by the vendor or modification by knowledgeable do-it-yourself programmers. The former involves additional expense at a minimum, meticulously detailing modifications to allow remote software changes. The latter requires a full-time programmer on the staff and almost always jeopardizes the software performance guarantee.

For several of the clinical systems, user-controlled, do-it-yourself software modification under operating system control is provided. Changes are made by knowledgeable (of laboratory analyzer, not computer technology) bench-level analysts. The goal of user-controlled programming is to have the analyst make the system function by his criteria of optimum laboratory protocol. Two detailed applications illustrate this unique form of software and the flexibility it gives to the analytical laboratory.

Program #1, User Control Establishment of Software to Operate Single-Channel AutoAnalyzer. This general-purpose program enables analysts to specify operating parameters needed to set up and bring new instruments on line. It also allows laboratory personnel to modify operating software. Changes can be minor (modification of a standard value) or major (revision of control tolerance, acceptable base line drift criteria, or schedules of specimen sequences).

The basic program is interactive. The user is asked questions and shown the type and format of required responses. Input responses are monitors for logical errors. Once a complete set of needed operational data is obtained, it files the information for use by the operating system whenever this analyzer is run. These filed software parameters are designed for repeated and routine access by laboratory personnel—not programmers. The user-controlled system is safeguarded; it is impossible to "crash" the main system.

We have reproduced the complete text from an interactive program used to set up the single-channel analyzer. The text to the right of asterisks is the user response to the question. Note that depressing the "CR" key after an asterisk forces the program to present an explanation of the required information including the format of the input. For users familiar with the system, this step can be suppressed, speeding use. The system rejects illogical or wrong format responses. An explanatory handbook

keyed to the questions is usually used during the initial experience with the system.

For purposes of this paper, we have included in italics, comments which expand on the meaning of some of the terms encountered. For this display we consistently used the full text explanations of each response. Note that a wrong format was rejected, and the question repeated in item No. 17.

Program #2, User-Designed Card Input. Many laboratories find it convenient to use custom-designed mark sense card input for certain tests. This input form is useful for qualitative test results or particularly those which require analyst comments. Benefits include extremely flexible design and easy adaptation to unique laboratory situations. A single card reader station serves as input device for a variety of tests by use of different kinds of cards. Through internal coding, the card type is identified to the system without any other analyst action. The disadvantage to customized cards is highly personalized programming needed to implement new cards to accept changes in existing cards.

A user-controlled card input program similar to that for single-channel analyzers uses the interactive question-and-answer routine to handle a new card type. Input options include recognized programming options to a mark sense location as a qualitative result (trace or +2, etc.), a quantitative result (digit in numerical field), or modifier to either (cloudy, turbid, etc.).

The laboratory introducing a new card first designs it in an optimum format for suiting its needs. Figure 1 is a card from University of Wisconsin Hospitals Urinalysis Laboratory. It is printed in six colors corresponding to the six "CLINITEST" (Ames Co., Elkhart, Ind.) dip stick tests. Specimen accession number, results, and/or modifiers are assigned to mark sense card locations which are arranged to maximize laboratory/analyst efficiency (i.e., to correspond to the format of the CLINITEST system), not computer compatibility. The analyst simply fills in the appropriate boxes. The absence of extra locations and direct correspondence between the test and card format minimize errors. For example, boxes designated negative, small, moderate, and large are the four possible answers for ketones by this method. Likewise for pH results, values less than 5.0 are not possible (hence, the numbers 5 through 9). Since the technique is readable only to the nearest 0.5 pH unit, appropriate re-

Only one GC/MS Data System you can buy today has all the performance features you'll need tomorrow.



Real time CRT display of GC and MS data during acquisition and reduction.



User can alter any data reduction steps, even during acquisition (processing decision can be based on data acquired and displayed on CRT).



Automatic correction for mass defects. Any calibration compound can be used. Adjustable mass window for peak top search.



Real time mass fragmentography of up to four ions with automatic signal optimization and quantitation.



User can simultaneously display any two spectra, overlap them for comparison, expand any portion vertically or horizontally for close scrutiny.



Dedicated spectra library of up to 32 individual compartments and up to 20,000 library spectra per disc (most intense peak in every 14-amu segment coding).



Real time identification of ion fragments, even during acquisition.



Instant background subtraction for mass spectra with both raw and net spectra displayed.



Fully documented spectra libraries for Drugs & Drug Metabolites, and Pesticides.



Acquisition rate of up to 500 amu/second (imperative for quantitative and reproducible Capillary Column GC/MS).



Instant quantitation including background subtraction for GC peaks with or without normalization.



Access to large scale computers via standard format 9-track magnetic tape, . . . time-share access via acoustic coupler.



Acquisition capacity of about 1000 spectra with an average of 300 amu per spectra, for each disc (about 1½ hours of an average GC run).



Instant calculation and display of isotope ratios (invaluable for labelled compound analysis).



Each user can freely establish, add to, subtract or modify spectra libraries.



Acquisition and display of up to 1000-amu per spectrum.



Storage of up to 99 spectra or chromatograms for delayed hard copy output.



16-bit CPU, 8K core memory expandable to 32K. BASIC and FORTRAN packages available for use as general purpose computer.



Fully interactive data system (user can try out any number of data reduction steps and instantly observe the results on CRT).



Automatic calibration and diagraming of mass spectrometer deficiencies.



Each disc drive controller can handle up to 4 disc drives, plus cartridge tape for archival storage of large volumes of data.

The Finnigan Model 6000!

Unlike others; the capabilities of the Model 6000 GC/MS Data System are not "promises," . . . both hardware and software are complete and debugged.

And worldwide acceptance of the Model 6000 has been impressive, with more than 30 installations within 8 months of the system's introduction. Contact us for a comprehensive 24-page brochure.



finnigan

595 N. Pastoria Avenue
Sunnyvale, California 94086
408-732-0940

CIRCLE 77 ON READER SERVICE CARD

PROGRAM #1: USER CONTROLLED

CS

CS

CS

STOP

C/S BK GENERATOR 1623 HOURS 12/04/73 *

1. ENTER

2. MODIFY

3. LIST C/S BKS

4. LIST TESTS

5. TYPE SCHEDULE *

1-5 *

1-5 * 1

These are your options

*Choose a number 1-5,
we will enter a new block*

1. NAME OF C/SBK *

1-4 CHAR * GLU

2. CHANNEL # *

0-37 * 0

Analog computer channel

3. TTY # *

1-6 * 3

Output to this teletype

4. TOTAL # RESULTS/CUP *

1-15 * 1

5. # SIGNALS/CUP *

1-1 * 1

*4-6 relate to multichannel
analyzer*

6. GATED SIGNAL ? *

Y OR N * Y

7. PRINT READING PATTERNS ? *

Y OR N * Y

Check for noise, peak shape

8. CUP LAG *

1-63 * 1

*Used to collate 2 or more
analyzers to a combined
report.*

9. STD DRIFT TOL. *

0-63 * 5

*Check successive plates for
base line drift*

10. STD LINEARITY TOL. *

0-63 * 5

11. # READINGS/PEAK *

2-7 * 7

12. PEAK INTERVAL IN SECONDS *

0-255 * 60

13. PEAK SENSE? *

Y OR N * Y

14. PEAK TOL. *

0-15 * 5

15. # CUPS/PLATE *

2-255 * 10

*For this example we use
only 10 cups/plate*

16. SPECIAL CALCULATION? *

Y OR N * N

17. PREPARE SCHEDULE

CUP IDENT

1 * PAT

1 * SAX

NO SUCH CODE

1 * STD1

2 * STD2

3 * STD3

4 * MRK

5 * SAM2

7 * CTI1

8 * SAM2

10 * SAM

11 * REP

SCHEDULE COMPLETE

Typing error rejected

18. TYPE SCHEDULE? * Y

NO. OF CUPS TO PRINT * 16

*Plate and a half;
note plate numbers changing*

NUMBER BY PLATE ? * Y

GLU SCHEDULE

CUP IDENT

*Often used by routine lab as
reference during
AutoAnalyzer operation*

PLATE 1

1 STD 1 [PEAK SENSE

2 STD 2

3 STD 3

4 MRK

5 SAM

6 SAM

7 CTI 1

8 SAM

9 SAM

10 SAM

PLATE 2

1 STD 1 [PEAK SENSE

2 STD 2

3 STD 3

4 MRK

5 SAM

6 SAM

*Peak sense restarts internal
timer so that blanks may be
sensed and read in absence
of actual peak.*

STARTING RESULT TRAILER 1 OF 1

*Multichannel analyzer has
one trailer per each test*

19. WILL THIS RESULT GO INTO THE PATIENT FILE? * Y

20. RESULT NAME *

1-4 CHAR * GLU

21. # OF DEC. PLACES *

0-4 * 0

22. POWER OF TEN TO RAISE RESULTS *

0-3 * 0

23.FLAG ABNORMALS ? *
Y OR N * Y

24.LO NORMAL * 70

25.HINORMAL *
70-2047 * 110

26.EXTRAPOLATE ABOVE HI STD? *
Y OR N * N

27.EXTRAPOLATE BELOW LO STD? *
Y OR N * N

LIST DEFINITIONS ? *
Y OR N * Y

SIGNALS
SAM=0
CTL=1
STD=2
SPL=3
MRK=4

28.TREAT SAMPLE AS * SAM
0 OR 4 * 0

29.TREAT CONTROL AS *
1 OR 4 * 1

30.TREAT STD AS *
2 OR 4 * 2

31.TREAT SPECIAL CUP AS *
3-4 * 3

23-25 clinical data unique
touser lab, puts "high" or
"low" flag to call physician
attention

27, 27 management decision

"Sam" typing error, it
expected 0 or 4, and
repeated question

32. ENTER CALIBRATION STANDARDS

1 *
0-2047 * 0
2 *
0-2047 * 50
3
50-2047 * 100
4 * /

33. ENTER CONTROLS

1.NAME *
1-4 CHAR * HYLN

CONCENTRATION *
1-2047 * 130

DEVIATION *
0-130 * 5

2.NAME * /

34.CHANGES? * N

35.IS THIS C/S BLOCK OK TO FILE? *
Y OR N * Y

FILED

C/S BK GENERATOR 1630 HOURS 12/04/73 * STOP
CS DONE

33- allows lab to enter its
controls by name, value and
tolerance in usual units

sponses for fractional units are 0.0 and 0.5. In user control programming for this card, one recognizes a total of 40 columns in 12 rows. By identification of "active" locations, the computer is guided as to interpretation of the mark sense locations.

The analyst custom programming the system for input from this card first specifies six different tests. The system queries the user about each of the six tests regarding the location and nature of results, English name to be designated, etc. Note that the system "thinks" like the analyst—logically by test and modifiers, not in the serial fashion of the card reader. Once all interpretative information is assimilated, the user-controlled input program assembles it into a system subprogram. This program is able to accept input, transform it to digital data for storage, and ultimately present quantitative and qualitative results with English modifiers in patient reports (records). Cards improperly or illogically filled out are rejected. Extraneous marks, the bane of mark sense systems, are ignored.

By use of these two examples, we wish to illustrate one aspect of the sophisticated level of development of clinical laboratory systems. At the onset, user-controlled programs were specialized, i.e., for the sole use of

the single-channel AutoAnalyzer. Current user control programs, consistent with the generalized view of laboratory operation, permits programming for single channels, multiple channels (SMA 12/60, 12/30, or 6/60), and discrete analyzers such as the MARK X or HYCEL 17 through the same user-controlled program.

Application to the newer types of continuous and discrete analyzers is assumed. These instruments are significantly different in analytical concept and approach. The availability of this system flexibility in adapting the computer to a variety of instruments is judged to be a significant advantage. User control, by mark sense card manipulation, enables the laboratory to adapt the computer system to almost any new data form.

The combined instrumental and soft copy data acquisition techniques of "laboratory computerization" open the door to almost unlimited expansion. Full software guarantees for systems based on user control programming may be the means of meeting the analytical chemist's need for flexibility and adaptability in operating his own laboratory. Recently, several system vendors indicated they will have special assemblers for totally self-written programs in standard computer language which operate

within the main system. This facility is usually available in large time shared facilities built around huge computers. Their availability, along with user control in the "minis," will significantly change the chemist's concept of laboratory computerization.

Interface-Computer and/or Back End Peripheral. The most consistent approach to analytical laboratory computerization utilizes the computer as a dedicated "back end" (i.e., data acquisition and reduction) peripheral. This technique is most common in gas chromatography/mass spectrophotometry. The clinical laboratory has a counterpart to this approach. The current maxi version of one such instrument is capable of handling an SMA 18/60 (Technicon Corp., Tarrytown, N.Y. 10591) (or two SMA 12/60's in tandem). The basic system has 24K of 16-bit memory and sells for approximately $\frac{1}{2}$ to $\frac{3}{4}$ of the basic analyzer price. It is capable of programmable operations for reducing, collating, formatting, and editing data under software control. Special memory portions are allocated to quality control and laboratory operation. The instrument is highly customized for the individual laboratory under semi user-controlled programming (i.e., responses are not in

plain English but are quite understandable through use of a laboratory handbook). In contrast to the vendor concerned analytical laboratory back end peripherals (computer), these back end peripherals are capable of many of the same options available under user-controlled programming of systems. These devices are more like single-instrument computer systems. They also represent a first step for the laboratory wishing to begin computerizing with a minimal investment in hardware and systems programming.

These same systems can serve as interfaces to total (even outside) laboratory systems. They provide backup capability (a computerized data handling in the event of main system failure), an intermediate stage where editing functions can be performed without the press of the total system, and a highly specialized interface which reduces processing loads on the central system. Actual connection to the main system can be through soft linkages such as cards or paper tape or hardwired for analog or digital signals.

The generalized, user-controlled programmable back end peripheral concept seems to have been lost on developers of analytical laboratory instrumentation. The rigidly developed systems, dedicated to a single instrument, needlessly constrain the laboratory.

Integral Instrumentation. Within the last several years, the clinical laboratory has seen the development of computers inseparably integrated within the instruments. Centrifugal chemical analyzers, first described by Anderson, are integral computer systems. Their analysis processes make this a necessity rather than a convenience. The computer serves as a data acquisition device, background corrector, concentration calculator, and printer device. These are not laboratory computer systems but integral parts of analytical instruments themselves.

The SMAC (Technicon Corp., Tarrytown, N.Y. 10591) (SMA with computer) is a third generation of multi-channel analyzer but the first to use an integral computer. It is responsible for operating the instrument by controlling many of the parameters heretofore handled by the technician/operator. The computer also serves as a data handling device in addition to performing functions of laboratory computer systems such as schedule retention, calibration checks, troubleshooting, quality control, and report preparation. Private communication with the manufacturer has indicated that plans are being developed for telephone line communication of op-

erational data from the integral computer to a manufacturer's central processing facility. This is to be a part of routine troubleshooting and maintenance, lease service, etc. The low costs of computer modules and the increasing complexity of instrumentation will combine to give growth to this aspect of computerization in the future.

Part IV. Some Clinical Laboratory Systems

In one short article and without resources, we cannot hope to do what others could not do in a 550-page book. We will briefly review some current clinical laboratory computer systems. Comments are necessarily brief and cast in the context of this article and therefore not complete descriptions of all features. Systems are reviewed at three levels—the extended laboratory calculator, the true minicomputer system (not just hardware), and the large computer facilities.

Extended Calculator Systems. These acquisition, calculation, and printing systems do not organize the flow of information in the laboratory. They augment its capacity of handling data efficiently and rapidly at individual points.

Hewlett-Packard, 1501 Page Mill Road, Palo Alto Calif. 94304. Company makes a large assortment of interfaces and modular peripherals, as well as a minicomputer. These could be developed into a total system or efficient stand-alone device. At present, no claims are made for clinical applications or clinical laboratory systems.

MSI, Midwest Scientific Instruments, Inc., 1303 Willow Drive, Olathe, Kan. 66061. Computer is actually a WANG-700 type calculator. Through series of extended peripherals and special interfaces, the configuration is capable of many system-like functions in clinical laboratories.

Various. Programmable calculators and true small mini (micro) computers can perform specialized functions which greatly assist the laboratory. Examples include calculating and formatting electrophoresis data from integrator trace counts, accepting gamma counter input for calculation at T-3 or T-4 levels, etc. Some software programs are available; many are self-developed.

Clinical Laboratory Systems. These are minicomputer systems which consider approaches to the whole laboratory.

BSL-Clinidata-700, Berkeley Scientific Laboratories, 2301 Investment Blvd., Hayward, Calif. 94545. Original company in "turnkey" system

business. Early versions grouped up to three PDP-8, 12-bit computers. Current "700" maximum system uses 16-bit 8-64K system which could be expanded to include three computers in the processor. Has on-line FORTRAN programming capability. Emphasizes special-purpose terminals for input with nonnumeric results individually keyed, i.e., urinalysis—protein-trace.

LDM Laboratory Data Manager, T and T Technology, Inc., 4820 Dale Road, McFarland, Wis. 53558. Totalized vendor programmed system using customized 16-bit computer. System uses back end peripherals which allow elements of the laboratory, i.e., SMA 12/60, to operate autonomously of the main computer system. Flexibility in "programming" peripherals introduces a new concept in individualizing the system to the laboratory.

Honeywell Data Systems, 2701 Fourth Avenue South, Minneapolis, Minn. 55408. Medical management system uses 16-bit Honeywell 317 or 617 computer with 32K memory. System has unique computer-generated mark sense sheet verification and editing of results and data, including output from analyzers monitored on line. Manual test results are reported through line printer-generated mark sense forms which provide workload organization and pertinent patient information.

CLAS System, B-D Spear, Becton Dickinson Co., 123 Second Avenue, Waltham, Mass. 02154. Vendor programmed and developed system. Emphasis on support of laboratory through custom programming by vendor staff in customer's laboratory. The approach is strong in areas of billing, bookkeeping, and laboratory organization. Current CLAS 823 system built around 16-bit computer.

COM-COMP Inc., 1324 Motor Parkway, Hauppauge, Long Island, N.Y. 11787. Minimum emphasis on total laboratory system, uses small computer to acquire and organize data. Special interfaces are used to reduce the load on main processor.

LABCOM, Laboratory Computing Inc., 4915 Monona Drive, Madison, Wis. 53716. Emphasis is on total system using DEC hardware, PDP-12 with at least 12K. Most extensively developed user-controlled programming (including mark sense cards) with overall emphasis placed on computer operations in the laboratory by its own personnel. Very flexible in the use of general-purpose terminals for input and output. Vendor claims software for new installation is 95% complete but guarantees highly "customized" results by use of user.

MODULAB, Medical Data Sys-

tems, 2300 Fisher Building, Detroit, Mich. 48202. Uses trained programmers in customer's laboratory. Basic system built in four stages, starting with back end device for analyzers, expanded around basic terminals to include total laboratory. One of two vendors emphasizing phased computerization—small initial investments with an overall system design in (vendor's) mind.

DNA Diversified Numeric Applications Automated Clinical Laboratory System (UNI-LAB), 9801 Logan Ave. South, Minneapolis, Minn. 55431. Vendor programmed system also recognizing four levels of performance. Largest system is built around 16-bit computer with potential expansion of up to 8 processors (computers). Also has capabilities of interface of smallest clinical laboratory system at remote sites to total laboratory system in central laboratory.

CLINLAB 12, Digital Equipment Corp., Maynard, Mass. PDP-12 based system using some user-controlled software. Special program is by vendor. System is currently off market though support continues for users.

Time Shared Clinical Laboratory Systems. These are true laboratory systems whose main processor is not a laboratory, but rather a multiprocessor dedicated to a large objective.

Technicon Corp., Tarrytown, N.Y. Entire hospital system designed for time shared utilization by a group of users. Current installation uses redundant IBM 370 computers. This is definitely not a clinical laboratory system in the context of the article.

Clinical Laboratory Information System, IBM Corp., Armonk, N.Y. 10504. A custom-programmed system based on the IBM 1800 series computer. Many standard packages, i.e., billing, are available to buyers. Approach is strong in hardware area with a variety of peripherals and extensive interfacing capabilities. Adequately described in several bibliography references.

References

Major Concepts in Present Article

Klopfenstein, C. E., and Wilkins, C. L., Eds., "Computers in Biochemical Research," Vol 1, Academic Press, New York, N.Y., 1972. [An advanced volume written for the chemist familiar with computer applications]

Westlake, G. E., and Bennington, T. L., "Automation and Management in the Clinical Laboratory," University Park Press, Baltimore, Md., 1972. [Basic reference concerning the structure and operation of the chemical laboratory—an understanding of which is critical to computerization of the laboratory]

Ball, M. J., "Selecting a Computer for the Clinical Laboratory," Charles C. Thomas, publisher, Springfield, Ill., 1971. [A basic

text on computerization of labs—an elementary treatment of systems but with an extensive set of references]

Brittin, G. M., M.D., and Werner, Mario, M.D., Eds., "Automation and Data Processing in the Clinical Laboratory," Charles C. Thomas, publisher, Springfield, Ill., 1970. [A chemist's book, good source reference to two topics in title]

Aikawa, J. K., M.D., and Pinfield, E. R., "Computerizing a Clinical Laboratory," Charles C. Thomas, publisher, Springfield, Ill., 1973. [A good status report of development, implementation and current status (1973) of IBM 1800 system with good references. Shared experiences and thought processes should be valuable]

Jones, D., and Perone, Si., "Digital Computers in the Scientific Instrumentation—Applications," published by McGraw-Hill, 1973. [An analytical (not specifically clinical) chemist's guide to laboratory computers]

Computer Systems in Clinical Laboratories

"Clinical Laboratory Computer Systems, A Comprehensive Evaluation," L. L. Johnson and Associates—Authors, L. Lloyd Johnson Associates, Northbrook, Ill., 1971. [ASCP sponsored description (little real evaluation) of computers in clinical laboratories. Written to provide general information only]

Knight, Jr., E. M., M.D., Ed., "Mini-Computers in the Clinical Laboratory," Charles C. Thomas, publisher, Springfield, Ill., 1970. [A presentation of the concepts briefly stated in the portion of this article on programmable calculators]

Kreig, A. F., Johnson, T. J., McDonald, C., and Catlone, E., "Clinical Laboratory Computerization," University Park Press, Baltimore, Md., 1971. [Short text setting forth basic concepts of laboratory computers, includes information on how to evaluate systems]

Ball, M. J., Ball, J. C., and Magner, E. A., "A Review of Nine Clinical Laboratory Computer Systems," Lab. Management, 8 (10), 23-32 (October 1970). [Brief review of whole systems as of 1970]

Vasily, John, and Doyno, T. H., "Laboratory Cost Control Through Computers," Amer. Lab., 5, 27-34 (January 1973). [Excellent presentation of one aspect of computer use]

Linberg, D. O. B., Schroeder, J. J., and Rowland, L. R., and Saathoff, J., "Experience with a Computer Laboratory DATA System," "Multiple Laboratory Screening," Benson, E. S., and Strandjord, P. E., Eds., Academic Press, New York, N.Y., 1969. [IBM 1460 and 360/50 system with coded matrix keyboards for input of information. Discusses strengths and weaknesses of system, ideas for development of future systems. Virtual thumbnail description of the need for advanced systems of today with user control]

Lewis, J. W., "A Flexible Clinical Laboratory Computer System," Med. Electron. Data, 4, 68-71 (May-June 1973). [Emphasis of user control concepts as in present article in private hospital HICKS (LCI) LABCOM system]

Epler, R. J., "Tailoring the Software," Ind. Res., 15, 34-37 (November 12, 1973). [Develops idea of special purpose minipurpose in laboratory with custom or self-built software at heart to concept]

Premo, D. J., "A Programmable Calculator," Amer. Lab., 4, 69-71 (February 1972). [Use of WANG programmable calculators as a laboratory computer]

Computerization of Chemical Laboratories

Frazer, J. W., "Design Procedures for Chemical Automation," Amer. Lab., 5 (2), 21 (February 1973). [See below]

Perone, S. P., Ernst, K., and Frazer, J. W., "A Systematic Approach to Instrument Automation," Amer. Lab., 5 (2), 39 (February 1973).

Brubaker, T. A., "Accuracy Specifications in Chemistry Data Processing," Amer. Lab., 5 (2), 53 (February 1973).

Grey, P., "Dedicated Minicomputers in the Laboratory," Amer. Lab., 5 (2), 57 (February 1973).

Beckwith, D. C., "Computerization—A Planned Expansion," Amer. Lab., 5 (2), 67 (February 1973).

Klopfenstein, C. E., "A Planned Data System," Amer. Lab., 5 (2), 77 (February 1973). [The preceding six papers are from a symposium, "Guidelines for Defining and Implementing the Computerized Laboratory System." Published in Amer. Lab., February 1973. This excellent set of monographs, written at a sophisticated level (of computer technology), provides in one publication, an excellent source document.]

Bogle, R., Zarembo, J., Bender, A. D., "Minicomputers for R&D," Lab. Management, 58-62 (March 1973). [Article similar to the present, but dealing with costs, not systems]

Elkins, J. C., "Selecting a Computer System for Laboratory Automation," Amer. Lab., 4, 37-41 (September 1972). [Chemists' guide, not clinical systems only]

Ahuja, S., "Computer Applications in the Analytical Laboratory," Amer. Lab., 5 (9), 12-18 (September 1973). [Classic analytical chemists' view of computerization of the laboratory. Recommend for balance with present article]

Rapkin, Edward, and Rosenstingl, Emmanuel, "Simplified Computer Programming for Liquid Scintillation Counting," Amer. Lab., 5, (9), 41-45 (September 1973). [One of specialized languages which enable the laboratory (nonprogrammer) personnel to utilize the computer. This is a program writing device, not a system program]

Toren, E. C., Jr., Carey, R. N., Sherry, A. E., and Davis, J. D., "Labtran—A Language and System for Programming Chemical Experiments," Anal. Chem., 44 (2), 339 (February 1972). [Analytical chemist's version of above]

Jenning, Roger, "When a Mini is Too Much," Ind. Res., 15, 52-54 (November 12, 1973). [Makes case for calculators (programmable vs. mini computers)]

Cooper, J. W., "The Computer and Signal Averager in the Laboratory," Amer. Lab., 4, 10-21 (September 1972). [A concept utilized in most chemical analyzers with integrated computers such as SMAC]

Computers in Clinical Medicine and Laboratories

Altschuler, C. H., "Computer Selection Should be a Task for the Pathologist," Med. Lab., 9, 20 (October 1973).

Shannon, W. N., "Before You Select a Laboratory Computer," Lab. Management, 24-26 (April 1972).

Mullertz, S., "A System for Identification and Distribution of Samples and for Processing and Storage of Data in Clinical Chemistry," Scand. J. Clin. Lab. Invest., 26 (4), 407-13 (November 1970).

Schwarz, H. P., "A 'Living' Computer System for the High Volume Hospital Laboratory," *Lab. Management*, 32-42 (October 1972). [Note IBM-1800]

Shannon, W. N., "The Benefits of a Lab Computer," *Lab. Management*, 28-33, (March 1972).

Anderson, Frances, "The Chief Technologist: Hand maiden or Manager?" *Med. Lab.*, 9, 13 (October 1973).

Semba, T. T., "How the M.T. Should Orient the Computer," *Med. Lab.*, 30-33 (November 1973). [Exploitation of idea that the users must decide on how the system will look to have it fit the hospital at hand]

Madison, M. L., "What We Think of Our Blood Bank Computer," *Med. Lab.*, 9, 16-17 (October 1973).

Pollycove, Myron, "An Economic Projection of Clinical Lab Automation," *Lab. Management*, 9 (5), 16-20 (June 1971). [Cost savings due to computer billing operations]

Hoyt, R. S., Brookes, Derek, and Pribor, H. C., "Departmentalized Accounting System Shows How to Cut Costs in the Lab," *Lab. Management*, 9 (5), 22-27 (June 1973). [Cost management aspects of laboratory computer use]

Simard, E. E. (an interview with), "2-Computer Approach to Laboratory Automation," *Lab. Management*, 11, 24 (October 1973). [Uses DEC-CLINDATA-12 in Laboratory, a second computer for business]

Jacquez, J. A., M.D., Ed., "Computer Diagnosis and Diagnostic Methods," Charles C. Thomas, publisher, Springfield, Ill., 1972. [Primary asset is an indication of how physicians react to computer produced, volume quantities of data. It should be a valuable contribution to the concept of computerization of suggested diagnosis]

Altshuler, C. H., "The PALI and SLIC Systems," *CRC Critical Reviews in Clinical Laboratory Sciences*, September 1972. [C.

Altshuler is principle architect and prime mover behind development of a unique computer system which combines with the pathologist in the laboratory to significantly modify the manner in which laboratory services are utilized by staff physicians.]

Lindberg, D. A. B., "The Computer and Medical Care," Charles C. Thomas, publisher, Springfield, Ill., 1968. [Fairly detailed description of an early IBM-based system developed by Lindberg and associates]

Foley, J. P., "Clinical Lab Automation System—CLAS," *Med. Electron. Data*, 4, 61-67 (May-June 1973). [Description of B-D Spear System by company representative]

Childress, C. C., "For the Small Lab: Computerization on a Shoestring," *Lab. Management*, 9 (6), 18-21, 34-35 (July 1971). [A calculator-based system (WANG), not a computer-based system]

Computers in Analytical Laboratories

Lindberg, D. A. B., *Methods Inform. Med.*, 6, 97 (1967). [Early general description of computers in medicine, particularly laboratory]

Indman, C. M., "Why the Big Computer?" *Ind. Res.*, 15, 30-33 (November 12, 1973). [Use of large computer in R and D laboratory at Dow Chemical]

Dessy, R. E., et al., "Minicomputers: Focus of Lab Revolution," *Chem. Eng. News*, 49, 42-47 (December 20, 1971).

"Modernized Blood Bank Management System," *Lab. Management*, 24-26 (July 1972).

Brocato, L. J., "Writing Specifications for a Laboratory Automation System," *Amer. Lab.*, 5 (9), 47-51 (September 1973). [Similar to chapters in Ball and Kreig texts]

Glover, D., "Lab Automation at Low Cost," *Res./Develop.*, 22-25 (May 1973). [Minicomputer as interface device to larger system]

Dessy, R. E., and Titus, J. A., "Computer Interfacing," *Anal. Chem.*, 45 (2), 124A-136A (February 1973). [Analytical instrument interfaces are described. Most are very sophisticated. Clinical laboratory systems originally began with simple interfaces (slave potentiometers and batteries). Current versions of some are simple, others elegant. Understanding of interfaces is facilitated by utilizing concepts in this article.]

Briggs, P., Dix, D., Glover, D., and Kleinman, R., "A Multinstrument Data Acquisition System for Use with Mass Spectrometry," *Amer. Lab.*, 4, 57-65 (September 1972).

Timmer, R. B., and Malmstadt, H. V., "A Minicomputer-Controlled UV-Vis-NIR Spectrophotometer," *Amer. Lab.*, 4, 43-51 (September 1972).

Wallace, D. L., "Computer Acquisition of Chromatograph Signals," *Amer. Lab.*, 4, 67-71 (September 1972).

Beech, Graham, "Computer Treatment of Nuclear Magnetic Resonance Data," *Amer. Lab.*, 5 (9), 53-60 (September 1973).

Scott, C. D., Chilcote, D. D., and Pitt, W. W., Jr., "Method for Resolving and Measuring Overlapping Chromatographic Peaks by Use of an On-Line Computer with Limited Storage Capacity," *Clin. Chem.*, 16, 637 (1970).

Patenaude, Joseph, Bibl, Klaus, and Reinisch, Bodo W., "Direct Digital Graphics: The Display of Large Data Fields," *Amer. Lab.*, 5 (9), 95-101 (September 1973). [Interesting concept—definitely in the future for application to clinical laboratories]

Hoadley, H. W., "Micrographic Data Processing in Automated Laboratory Information Systems," *Amer. Lab.*, 4, 73-81 (September 1972). [Same as above]



Ronald H. Laessig is chief of clinical chemistry at the State Laboratory of Hygiene and associate professor of preventive medicine at the University of Wisconsin Medical School. After receiving his PhD in analytical chemistry from the University of Wisconsin in 1965, Dr. Laessig studied at Princeton University and at the Communicable Disease Center in Atlanta, Ga. His primary research interests are in the development of computers in public health and in clinical chemistry laboratories and research into the fundamental properties of automated chemical analyzers. Since October 1970, he has been assistant director of the State Laboratory of Hygiene, a part of the University of Wisconsin and official laboratory of the State Division of Health and the Department of Natural Resources. He is currently a member of the FDA Diagnostics Products Advisory Committee.



Thomas H. Schwartz received his bachelors degree from Milton College in 1965. Prior to his current position of administrator of the Wisconsin Department of Health and Social Services Multiphasic Screening Laboratory, he worked in vitamin chemistry at the Wisconsin Alumni Research Institute. His major interests are in the field of multiphasic health screening and computer applications to administration of public health programs.

More information per minute than any other analytical technique.

XES (X-ray energy spectrometry) is about the only way to analyze up to 81 elements rapidly, non-destructively, and quantitatively from ppm to 100%. Now Kevex announces a major improvement—high intensity XES. The Kevex system differs from other energy dispersive instrumentation in two key respects:

1. It uses a high-intensity (3000 watts) X-ray tube, thereby making secondary excitation practical.
2. Its secondary target emits pure characteristic X-rays with **low background**.

Here's what that means to users of the Kevex 0810 system:

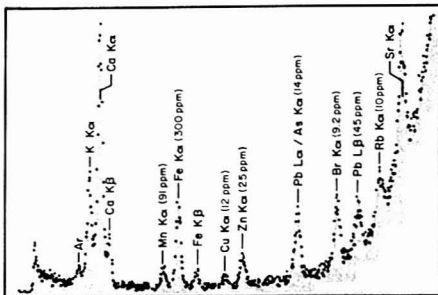
1. Spectral peaks are genuine, not system induced. Interpretation is therefore much simpler.
2. High peak-to-background (2500:1 typical with 80 mm² detector) yields early confirmation of element peaks.
3. Analytical sensitivity is enhanced by both peak-to-background ratio and high count rates.
4. Reduced costs stem from simple pushbutton operation that requires less operator time and little or no sample preparation.

Applications? The first 25 Kevex 0810 series systems are analyzing air pollution (3), lung tissue inclusions, oceanographic minerals, criminal evidence, semiconductor materials, nuclear reactor materials, exotic alloys, food and drug additives, metal ores, industrial chemicals (2), commercial laboratory samples, blood, meteorites, oil contaminants, toxic compounds, industrial waste, catalysts, cosmetics, lead in gasoline, sulfur in oil, unspecified samples in universities (2) and precious metals. Obviously the 0810 is well-adapted for research and quality control.

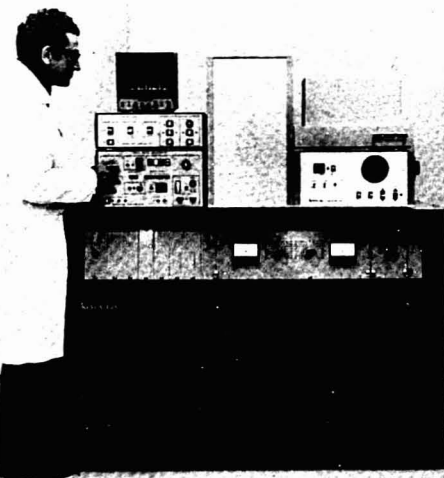
We have published a 160-page hard cover manual describing XES principles, techniques and instrumentation. Useful and plentiful graphs, tables and illustrations make "X-Ray Energy Spectrometry" an important reference handbook. —price \$7.95 plus 50 cents postage and handling. For your copy, contact us at the address below.

Low Budget. If your laboratory has a conventional X-ray wavelength spectrometer, the chances are that you can make even more efficient use of the X-ray generator and tube. You can save the entire cost of these components for XES applications. The Kevex system is especially suited to be used in conjunction with Philips, Siemens, General Electric, Rigaku Denki, Diano, Picker and Seifert generators.

New high intensity XES.



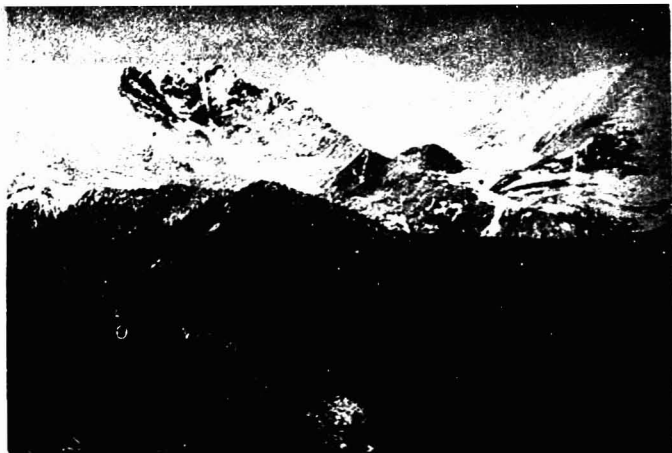
NBS #1571 Standard orchard leaf—300 second analysis, molybdenum secondary target, 35 KV, 5 mA, 1000 counts full scale using chromium target X-ray tube



Analytical Instrument Division
898 Mahler Road/Burlingame, CA 94010
Telephone (415) 697-6901

CIRCLE 148 ON READER SERVICE CARD

News and Views



Mummy Range from Trail Ridge Road, Rocky Mountain National Park

On-Line Process Analytical Chemistry

Colorado State University

Fort Collins, Colo.

June 12 to 14, 1974

Sponsors: ACS Analytical Chemistry Division and *Analytical Chemistry*

Process analytical instrumentation is the subject of the 27th Annual Summer Symposium on Analytical Chemistry to be held in Fort Collins, Colo., June 12 to 14, 1974. Technical sessions will be held in the Chemistry Building at Colorado State University. Symposium participants will be housed in Parmelee Hall.

The subject to be covered is one that, until recently, had moved away from the analyst's normal domain. While quality control, in traditional operations, brings the plant process to the laboratory, the process analyzer moves the laboratory to the plant. In the transition, the analyst has almost completely lost touch with an important segment of his discipline. While sales of this type of instrumentation have increased yearly, the reputation of the process analyzer has steadily declined. In reviewing contributing causes, cochairmen Richard A. Hagstrom and Frank W. Karasek felt that the analytical chemist must become familiar with the instrument variations required to more successfully effect the transition from the laboratory to the plant process. The

program, therefore, is designed to bring the analyst up-to-date with the present state-of-the-art. Additionally, subjects are covered with sufficient depth to encourage further analyst participation, particularly to an extent that will renew active contribution in this orphaned extension of the analytical discipline.

Colorado State University, as Colorado's land grant institution, has a tradition of excellence in higher education and research. The present enrollment of 17,000 students includes more than 2500 in the Graduate School. The Chemistry Department, located in a new building with extensive modern teaching and research facilities, has a faculty of 28, more than 20 postdoctoral fellows, and 60-70 graduate students. It is one of the few departments in the West with an unusually strong program in analytical chemistry.

Situated in Fort Collins in the foot of the Rocky Mountains, CSU provides an inspiring setting for the 27th Annual Summer Symposium. Located 60 miles north of Denver on Interstate 25, the 55,000 residents of Fort

Collins are within minutes of Roosevelt National Forest, Rocky Mountain National Park, the canyon of the Cache La Poudre River, and numerous other outdoor recreational areas. Symposium attendees planning to fly should come to Denver. Ground transportation to Fort Collins will be made available at a cost of about \$7.00, but early registration is urged to permit appropriate scheduling of this transportation.

Symposium participants wishing to stay on campus will be housed in Parmelee Hall, located one block from the Chemistry Building where the meetings will be held. The cost of a double occupancy room for Tuesday through Thursday nights is \$19.86; single occupancy cost is \$22.06; the cost for participant and spouse is \$36.39. Reduced rates are available for children, depending on age and sleeping accommodations requested. A meal package may be purchased for the Student Center Cafeteria for \$12.92 for breakfast and lunch on Wednesday, Thursday, and Friday and dinner on Thursday. The symposium mixer, followed by a barbecue,

News and Views

will be held on Wednesday. There is no additional charge for the mixer for participants; for others, the mixer fee is \$2.00. The barbecue is \$4.25 for all those attending. For those who wish, a list of motels is available, and individual meals may be purchased. Several excellent restaurants are within walking distance of the campus.

Activities are planned for accompanying ladies, including a trip to Bear Lake in the Rocky Mountain National Park on Thursday (\$10, including a box lunch). For free time, the recreational and cultural facilities of the University will be open to attendees. Visits to nearby cities, such as Cheyenne (40 miles), Laramie (65 miles), Denver, or Colorado Springs and the Air Force Academy (120 miles) may be of interest.

The complete technical program and a coupon for early registration are included below.

Richard A. Hagstrom of Olin Corp., 275 Winchester Avenue, New Haven, Conn. 06504, and Frank W. Karasek, University of Waterloo, Waterloo, Ont., Canada, are program cochairmen. Ronald K. Skogerboe, Department of Chemistry, Colorado State University, Fort Collins, Colo. 80521, is responsible for local arrangements.

PROGRAM

Wednesday Morning, June 12

General

Richard A. Hagstrom, *Presiding*

9:00 The Role of the Analytical Chemist in Process Analysis. S. Siggia, University of Massachusetts

10:00 How to Approach On-Line

Problems. R. A. Hagstrom, Olin Corp.

11:00 Process Analyzer Sample Systems. L. Fowler, Monsanto Indus. Chemical Co.

Wednesday Afternoon, June 12

Process Chromatography

John Scales, *Presiding*

1:00 Process Chromatography Instrumentation. J. Scales, Bendix Corp.

1:45 Column Selection for Process Chromatography

2:30 Process Chromatography Applications

Thursday Morning, June 13

Spectroscopic Instrumentation

William V. Dailey, *Presiding*

9:00 Infrared Instrumentation. W. V. Dailey, Mine Safety Appliances Co.

10:00 Ultraviolet Instrumentation. R. S. Saltzman, E. I. du Pont de Nemours & Co.

11:00 Automatic Chemical Analyzers. M. Du Cros, Technicon Instruments Corp.

Thursday Afternoon, June 13

Electroanalytical Instrumentation

Fred H. Zimmerli, *Presiding*

1:00 Introduction to Electroanalytical Instrumentation. F. H. Zimmerli, Rohm & Haas Co.

1:30 pH and REDOX. R. Oliver, Foxboro Co.

2:15 Use of Chemical Sensing Electrodes. J. Krueger, Orion Research Inc.

3:00 Electrolytic Moisture Analyzers. I. A. Capuano, Olin Corp.

Friday Morning, June 14

Electroanalytical Instrumentation

Fred H. Zimmerli, *Presiding*

9:00 Electrolytic Oxygen Analyzers. L. Barnes, Milton Roy/Hays

10:00 Automatic Titrators. R. Dishman, Ionics, Inc.

The Teaching of Process Analytical Instrumentation

Kenneth W. Gardiner, *Presiding*

10:45 A Rational Approach to the Teaching of Process Analytical Instrumentation. K. W. Gardiner, University of California, Riverside

Registration Form

27th Annual Summer Symposium

June 12 to 14, 1974

Division of Analytical Chemistry and Analytical Chemistry

Colorado State University, Fort Collins, Colo. 80521

Name (please print): _____

Mailing Address: _____

Professional Affiliation: _____

Registration Fee (enclosed): \$25.00 Date: _____

Campus housing from Tuesday through Thursday nights is \$19.86 per person for a double room and \$26.40 for a single room; cost for participant and spouse is \$36.39. Family rates will be provided on request. Meals from Wednesday breakfast through Friday lunch will be \$12.92 (not including the barbecue), if desired. These charges are payable upon arrival.

Please check appropriate items:

- ☐ I would like to share a double room with _____
- ☐ I will share a double room with someone you assign
- ☐ I prefer a single room
- ☐ I would like a room for myself and spouse
- ☐ I would like accommodations for myself and the following members of my family (names and ages of children)

☐ I will arrange my own housing. Please send a list of local motels

☐ I expect to attend the mixer and barbecue Wednesday evening, June 12. Please indicate number, if more than one (\$4.25 per person for barbecue; \$2.00 additional per person for mixer)

☐ I would like the meal package at the student center

☐ Please make _____ reservations for the ladies' trip to Bear Lake (\$10, including lunch)

I plan to travel by auto _____, plane _____, and will arrive in Denver on June _____

at _____; carrier and flight _____; and depart on June _____, at _____, carrier and flight _____

I would like university transportation from Denver _____

Rental cars are also available at the airport.

This form should be returned before May 24, 1974, together with the \$25 registration deposit to: Prof. Rodney K. Skogerboe, Department of Chemistry, Colorado State University, Fort Collins, Colo. 80521

Make your check payable to Colorado State University

Drugs' Molecular Structure Linked to Anticancer Activity

Pattern recognition techniques have been used to establish the relationship between therapeutic activity of anticancer drugs and details of their molecular structure. Bruce Kowalski of the University of Washington and Charles Bender of the University of California's Lawrence Livermore Laboratory have collaborated in applying this artificial computer intelligence technique to screening prospective anticancer drugs. Their work, reported in *J. Amer. Chem. Soc.*, 96, 916 (1974), dealt with purine and pyrimidine nucleoside derivatives, a class of compounds that has produced several substances of clinical interest. The pattern recognition technique proved 93.5% accurate in screening 200 of the class of drugs studied for their weight inhibition effects on solid tumors in small animals. This accuracy figure refers to the ability of the technique to place the drugs in "positive" and "negative" categories of a standard National Cancer Institute (NCI) testing system. The standard NCI test was CA 755 (adenocarcinoma), in which a drug causing a tumor weight loss of 70% or greater is considered "positive" and eligible for further testing. Since all the drugs studied had been tested previously under NCI auspices, the computer's output could be checked with actual laboratory results.

The chemists selected 50 structural characteristics of the drugs. The computer eliminated 30 as telling little or nothing about any tumor weight inhibition that had been reported in NCI tests. The remaining characteristics were then ranked according to the contribution each made toward solving the problem. First in importance was the number of sulfur atoms per number of total atoms, and second was the number of single carbon-sulfur bonds per number of carbon atoms. Based on the 20 structural characteristics alone, the screen was 94.2% accurate in placing drugs in the positive category and 92.9% accurate in placing drugs in the negative category or 93.5% accurate overall.

Although this screening method is not designed to replace laboratory testing, it should be of value in establishing priorities among the thousands of new compounds thought to have potential anticancer activity. The authors believe the technique is readily adaptable to other compounds and screening systems. It is under experimental use in screening drugs under the L 1210 (leukemia) and Walker 256 (solid tumor) systems,



Charles Bender (seated) of Lawrence Livermore Laboratory, University of California, and Bruce Kowalski of the University of Washington are shown at the Livermore computer terminal

and results of this work will soon be published. Another possible application of these techniques is in drug design where compounds might be tailor-made according to structural characteristics found to be closely linked with therapeutic activity.

1st FACSS Meeting Focuses on Energy

The theme of the first meeting of the Federation of Analytical Chemistry and Spectroscopy Societies (FACSS), to be held Nov. 18-22, 1974, at the Chalfonte-Haddon Hotel in Atlantic City, N.J., will be centered on the challenges facing the analytical community in programs to alleviate the Nation's energy problems. The first day of the meeting will be devoted to position papers on the challenge of the energy research programs to the analytical chemist and spectroscopist, the chemistry and analytical chemistry of coal, the analytical chemistry of nuclear materials, the analytical needs in coal conversion, the analytical needs in oil shale development, and the analytical instrumentation for energy sources and future energy sources.

On Tuesday through Friday, the program will be opened by plenary and award lectures. Following these, invited symposia and contributed papers will be presented.

Those who wish to present papers should submit titles by May 1 and 200-word abstracts by July 1, 1974, to James C. White, Oak Ridge National Laboratory, P.O. Box X, Oak Ridge, Tenn. 37830.

Analytical Chemistry of Pollutants

Basle, Switzerland, is the site of the 4th Annual Symposium on Recent Advances in the Analytical Chemistry of Pollutants, June 17-19, 1974. Among the sponsors of this meeting are the ACS, EPA, University of Georgia, and organizations in Switzerland, Austria, Canada, and Germany. The planned program is designed to bring together persons concerned with the application of analytical chemistry to environmental problems. The applied chemists will hear from experts in a broad range of analytical techniques. At the same time, researchers will have an opportunity to meet with those who apply the techniques they develop. The detailed technical program, all invited, appears below.

The address for the symposium is: Fourth Annual Symposium on Recent Advances in the Analytical Chemistry of Pollutants, P.O. Box 23, CH-4013 Basle, Switzerland. Those in the U.S. who want more information may contact David M. Hercules, Dept. of Chemistry, University of Georgia, Athens, Ga. 30602.

Plenary Lectures:

Eutrophication in the United States—Status and Action. A. F. Bartsch, National Environmental Research Center, EPA, Corvallis, Ore.

A Comparative Study of Analytical Techniques for Inorganic Pollutants. R. F. Coleman, Laboratory of the Government Chemist, London, England

Feel secure...



and still take a quantum jump with Perkin-Elmer's new 3920 gas chromatograph system.

As a beginning, there is the Model 3920 Gas Chromatograph. In its versatile versions, it is better than the previous world's best—the Perkin-Elmer™ Model 900—and somewhat lower in cost. In its low-cost configurations, it does not sacrifice any performance. And, as needs change, the low-cost unit can be built up to the high-versatility version at any time.

Attractive? Yes. Secure? Yes. A quantum jump? Not by itself.

The quantum jump comes from some important and exclusive extra modules, which are so interesting that we'll describe them first.

The MS-41 Capsule Sampler makes syringes obsolete for many applications. Imagine a device which can inject solids and viscous samples directly without fouling the column; which can improve sensitivity and throughput by eliminating solvents; which ends problems of sample carryover forever, and which avoids the many troubles associated with syringes. This is the MS-41. It isn't cheap, but a few minutes' calculation may convince you that you can and must afford it.

Capillary columns can give 4X better resolution, or speed, or both. It has been well known for years that capillary columns (WCOT and SCOT) can give chromatographic resolution that packed columns cannot approach. But what if you don't need the improved resolution? It's less well known that the resolution advantage can readily be traded for greater speed. Is a 4X increase in speed, with no sacrifice in quantitative accuracy, interesting to you? Then send for Application Study GCD-35, which gives all the details.

Get the new Dial-A-Flow™ module, and throw away your soap bubble meter. The measurement and setting of carrier gas flows has always ranked as a cruel (though not unusual) punishment, involving switchings, unscrews, connectings, peerings, bubble-squeezings and nomograph-consultings at a minimum, sometimes accompanied by dead volume, ignition trouble, broken columns and burned fingers.

Now, for mere money, the new Dial-A-Flow carrier gas regulator removes the whole problem. When you wish to set or change flow

rates, you turn two digital switches to the desired values in ml/min. and the Dial-A-Flow does the rest.

The Model 3920 aims high but starts low. The modular Model 3920 represents a series of gas chromatographs, with a unique new concept. It is tailor-made, at the factory, to meet the individual user's requirements.

For versatility, the Model 3920 can be equipped with all the functions of the world's premier research chromatograph, the Model 900, and will give somewhat better performance (see below), at a somewhat lower cost.

For specific purposes, the Model 3920 is simplified by the omission of unwanted components, *but there is never any substitution of cheaper equipment.*

The specific-purpose instrument delivers the same reliability, accuracy, sensitivity, and ease of operation.

What's more, you don't have to marry the instrument you initially buy. If your needs later change or increase, the extra components can then be readily installed.

All-Digital Oven Controls make complicated mechanical programmers a thing of the past. Temperatures and program rates are set directly on numerical switches.

Twin Electron Capture Detectors are available at modest cost, with new electronics which give a linear range up to 10^4 . Many government agencies are now requiring two-column ECD measurements for trace pesticides.

A New FID Amplifier can reliably measure currents as low as 10^{-15} amps, has 0.1% linearity within a range, and is so drift-free that chromatographers will look in vain for the "balance" knob.

Detector Combinations, including FID-ECD and TCD-FID, can be used simultaneously.

An interesting fact about reader service cards.

To get further information on the Model 3920 and its friends, the easiest thing to do is to circle the number on the reader service card. However, such cards can take weeks to reach the manufacturer. If you need the data faster than that, please drop a note directly to Perkin-Elmer, Department AMS, Main Avenue Norwalk, Connecticut 06856.

PERKIN-ELMER

CIRCLE 198 ON READER SERVICE CARD

carbon in water?



total organic carbon volatile organic carbon total carbon

Dohrmann's DC-50 organic analyzer makes all of these measurements accurately and rapidly. Based on proven methods, it avoids interferences and undesirable pyrolysis reactions that historically have resulted in significant errors. Here's why the DC-50 is the complete solution for the analysis of carbon in water:

DIRECT READOUT. Four-digit presentation shows carbon content directly in mg/liter or ppm. *No recorder needed!*
DIRECT MEASUREMENT. A single sample injection gives either Organic Carbon or Total Carbon content *directly, not by difference.*

INDEPENDENT MEASUREMENT. Volatile Organics are determined separately from Total Organics to aid in source identification.

RELIABLE MEASUREMENTS. Determines important, lightweight volatiles such as low molecular weight alcohols and ketones, normally lost by acidification and sparging.

FAST: 5 minutes per determination
ACCURATE: repeatability of ± 1 mg/liter or $\pm 2\%$

WIDE RANGE: 1 to 2,000 mg/liter (ppm) without dilution

PRICE: \$7,500, including start-up assistance and operator training

EPA EVALUATED: Newsletter #15
Oct. 1972 AQCL, NERC, EPA
Cincinnati, Ohio 45268

Contact: DOHRMANN Division, Envirotech Corporation, 1062 Linda Vista Ave. Mountain View, CA 94040
(415) 968-9710

ENVIROTECH



CIRCLE 60 ON READER SERVICE CARD

News and Views

Problems of Qualitative Assessment in the Environment. F. Korte, Gesellschaft für Strahlen- und Umweltforschung mbH, Munich, West Germany

Recent Evaluations of the Significance of Chemicals in Natural Aquatic Systems. G. F. Lee, Texas A&M University, College Station, Tex.

Understanding of the Complexity of the Environment; New Goals for Analytical Chemistry. W. Stumm, Federal Institute for Water Pollution Control, Zurich, Switzerland

What is the Future Role of Analytical Chemistry? W. Simon, Federal Institute of Technology, Zurich, Switzerland

Program

The Chromatographic Approach to the Environment—Potential and Perils. W. Aue, Dalhousie University, Halifax, Canada

European Intercomparison Programs and Harmonization of Techniques. A. Berlin, J. Smets, Health Protection Directorate, Luxembourg

Environmental Toxins in the Human Body and Their Detection and Characterization. H. Brandenberger, University of Zurich, Switzerland

A Computer Approach to the Identification of Pollutants. T. Clerc, Federal Institute of Technology, Zurich, Switzerland

Neutron Activation Analysis for Multielement Determination in Foodstuffs and Other Biological Samples. J. F. Diehl, Institute for Radiation Technology, Karlsruhe, West Germany

Chemical Characterization of Polluted Seawater. D. Dyrssen, University of Gothenburg, Göteborg, Sweden

Recent Experiences in the Detection of Toxic Substances in the Air by Means of Coupled GC-MS Systems. D. Ellgehausen, Sandoz Ltd., Basle, Switzerland

Methods Development in Support of Monitoring Systems. H. F. Enos, Environmental Protection Agency, Perrine, Fla.

Derivatization—High-Speed Liquid Chromatography of Organophosphorus Pesticides. R. W. Frei, Sandoz Ltd., Basle, Switzerland

A Study of Particulate Matter in Air by X-ray Fluorescence Analysis. J. Gilfrich, U.S. Naval Research Laboratory

Neutron Activation Analysis. G. Gordon, University of Maryland, College Park, Md.

Determination of Trace Organics in Drinking Water. K. Grob, University of Zurich, Switzerland

Use of Enzymes for the Detection and Decontamination of Environmental Pollutants. G. G. Guilbault, Louisiana State University, New Orleans, La.

Analysis of Pollutants in the C6-C20 Range in the Atmosphere of Paris by Chromatography. G. Guiochon, Ecole Polytechnique, Paris, France

Environmental Parameters by Remote Sensing; Evaluation of Satellite Photographs. E. B. Henson, University of Vermont, Burlington, Vt.

Recent Advances in Automation of Pesticide Residue Analysis. W. D. Hörmann, D. Eberle, Ciba-Geigy, Basle, Switzerland

High-Efficiency Liquid Chromatography of Polynuclear Hydrocarbons. J. F. K. Huber, University of Amsterdam, Holland

Reliability of Trace Analysis in Aquatic Systems. D. Hume, Massachusetts Institute of Technology, Cambridge, Mass.

Structure Elucidation of Metabolites by Mass Spectrometric Techniques. O. Hutzinger, National Research Council, Halifax, Canada

Detection of Trace Constituents on Airborne Particulate Matter by Ion Sputtering Surface Analysis. F. W. Karasek, University of Waterloo, Canada

New Possibilities in Instrumental Analysis, Especially of Traces Using the Separation Cassette Principle. R. E. Kaiser, Bad Dürkheim, West Germany

Water Analysis by X-ray Fluorescence. D. Leyden, University of Georgia, Athens, Ga.

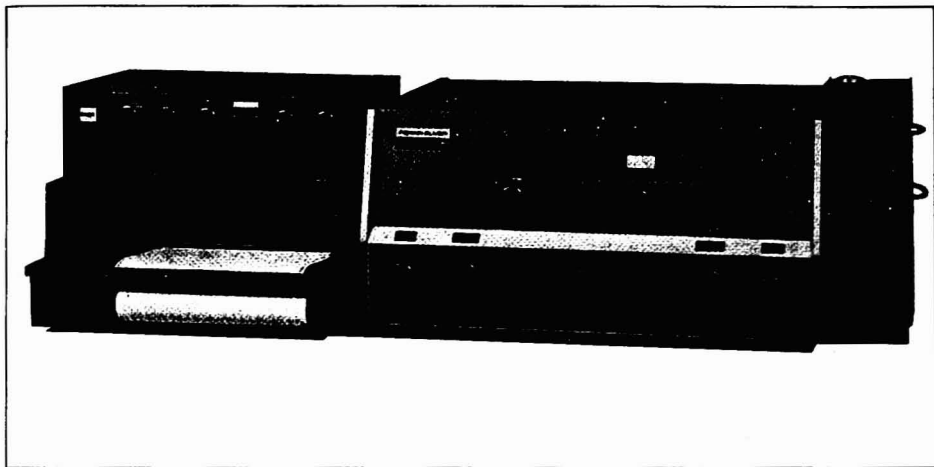
Some Aspects of Mass Spectrometry. F. McLafferty, Cornell University, Ithaca, N.Y.

Air Quality and Analytical Chemistry. H. Malissa, Institute of Technology, Vienna, Austria

Recent Developments in Isoelectric Focusing. B. J. Radola, Institute for Radiation Technology, Karlsruhe, West Germany

The Use of High-Performance Liquid Chromatography for the Analysis of Pesticide Residues. K. Ramsteiner, W. D. Hörmann, Ciba-Geigy, Basle, Switzerland

Perkin-Elmer announces the absolute in fluorescence... the Model MPF-4.



The MPF-4 extends the highly-regarded MPF series of fluorescence instruments from Perkin-Elmer. Quality is a dominant characteristic of the MPF series; the MPF-4 abounds with it! The MPF-4 is made better, performs better and does more useful functions than any other fluorescence spectrophotometer.

The MPF-4 costs a little more than "run-of-the-mill" instruments, but quality is well worth its cost. The versatility and the high-performance specifications of the MPF series will provide reliability and continue to satisfy your laboratory fluorescence needs. If you have the pleasure of owning an MPF-2A or MPF-3, you know about the high standards of reliability of these instruments and Perkin-Elmer's competent service and technical support. If you have not used an MPF-2A, or MPF-3, ask your colleagues—you will find consistently good reports.

Following are a few of the specific features and their benefits that now make the MPF-4 the quality and performance leader:

- Recording of excitation and emission spectra in relative quantum units for both fluorescence and phosphorescence. This makes it possible to record

the "true" spectral characteristics to facilitate quantum efficiency measurement, fluorescence probe studies and compound identification.

- Curved bilateral continuously adjustable slits providing better than 2A resolution and optimum bandpass for all applications.

- High efficiency gratings and monochromator design to provide the highest sensitivity/spectral bandpass available. This is especially useful for trace level measurements as in air and water pollution analysis.

- Extended wavelength range of monochromators to 1200 nm thereby increasing the applicability of luminescence measurements.

- Digital wavelength readout accurate to 3 angstroms.

- Synchronous scanning of both monochromators for absorption spectrum recording.

- Solid state electronics featuring ratio recording, automatic dynode control, optical chopping to give no more than 2% noise and less than 1% drift/hour at maximum gain.

For more information, write: Instrument Division, The Perkin-Elmer Corporation, Main Avenue, Norwalk, Conn. 06856.

PERKIN-ELMER

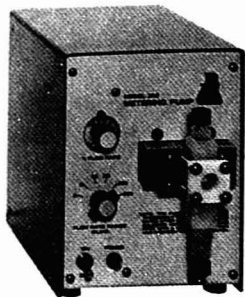
Committed to helping your samples tell you more.

CIRCLE 195 ON READER SERVICE CARD

ANALYTICAL CHEMISTRY, VOL. 48, NO. 4, APRIL 1974 • 421 A

don't be
high pressured

into buying a
low pressure
metering pump



Operating at pressures to 2000 psi, ISCO metering pumps will deliver a reproducible flow over wide dial-selected ranges, easily outperforming lower pressure peristaltic or similar variable speed pumps. Three models offer flow rates from 1.5 to 2500 ml/hr at 50 psi, to a pulseless 0.8 to 200 ml/hr at 2000 psi. No calibration is required and practically any liquid can be accommodated.



All ISCO metering and gradient pumps are described in our current catalog. Your copy is waiting for you.



BOX 5347 LINCOLN, NEBRASKA 68505
PHONE (402) 464-0231 TELEX 48-6453

CIRCLE 133 ON READER SERVICE CARD

422 A • ANALYTICAL CHEMISTRY, VOL. 46, NO. 4, APRIL 1974

News and Views

Ion-Specific Electrodes. G. Rechnitz, State University of New York, Buffalo, N.Y.

Aspects of Organic Electrochemistry. P. Zuman, Clarkson College, N.Y.

Call for Papers

1974 Pacific Conference on Chemistry and Spectroscopy

Jack Tar Hotel, San Francisco, Calif., Oct. 16-18. Sponsors: Northern California SAS and Northern California Section, ACS. Titles and authors' names due by April 2. 200-word abstracts on standard ACS abstract forms for regional meetings due by May 7. Send to (ACS): Fred Stross, Dept. of Anthropology, University of California, Berkeley, Calif. 94720, or (SAS): John W. Green, Chevron Research Co., 576 Standard Ave., Richmond, Calif. 94802. Additional information is available from W. J. Eisenlord, Public Relations Chairman, Shell Oil Co., 1660 S. Amphlett Blvd., San Mateo, Calif. 94402. 415-929-1100

23rd Annual Denver Conference on

Applications of X-ray Analysis
Brown Palace Hotel, Denver, Colo., Aug. 7-9. Emphasis on "Applications of X-ray Technology to Current Problems in Energy and Resource Development," including X-ray diagnosis of plasmas produced by lasers and electron beams; on-line X-ray monitoring and control; X-ray analysis of resource materials and pollutants; X-ray lasers. 300-word abstracts due before Apr. 15 to C. O. Ruud, Metallurgy and Materials Science Div., Denver Research Institute, University of Denver, Denver, Colo. 80210. 303-753-2621

16th Annual Rocky Mountain Spectroscopy Conference

Brown Palace Hotel, Denver Colo., Aug. 5-6. 300-word abstracts due by May 20 to Roland R. Manning, Ball Brothers Research Corp., P.O. Box 1062, Boulder, Colo. 80302.

21st Canadian Spectroscopy Symposium

Ottawa, Ontario, Oct. 7-9. Contributions are sought in the following areas: history of spectroscopy, laser spectroscopy, remote sensing of the environment, molecular spectroscopy, spec-

troscopy in the medical sciences, characterization of ultrapur materials, photochemical degradation of pollutants, energy dispersive X-ray spectroscopy, and analytical atomic spectroscopy (including new instrumentation developments). 150-word abstracts before May 15 to: A. R. Davis, Dept. of the Environment, Inland Waters Directorate, 562 Booth St., Ottawa, Ont., K1A 0E7, Canada. 613-994-9163

Meetings

1974 Meetings are listed in the January, February, and March issues. The following meetings are newly listed in Analytical Chemistry

- **Teaching Analytical Chemistry and Instrumentation Analysis.** May 16-17. Dawson College, Montreal, Canada. Contact: A. David Adley, Dawson College, 350 Silby St., Montreal, P.Q., Canada. 514-931-8731, ext. 332. Page 208 A, Feb.
- **International Exposition and Seminar on Water Resources Instrumentation (Instruments and Systems for Measuring and Monitoring Water Quantity and Quality).** June 4-6. Pick-Congress Hotel, Chicago, Ill. (previously scheduled for Feb. 25-27). Sponsor: International Water Resources Assoc. Contact: Brian J. Gallagher, Limnetics, Inc., 6132 West Fond du Lac Ave., Milwaukee, Wis. 53218. 414-461-9500
- **Conference on Analysis of Lipids and Lipoproteins.** June 12-15. Sheraton Park Hotel, Washington, D.C. Sponsor: American Oil Chemists' Society. Contact: E. G. Perkins, Dept. of Food Science, Burnside Research Laboratory, University of Illinois, Urbana, Ill. 61803
- **29th Northwest Regional ACS Meeting.** June 13-14. Eastern Washington State College, Cheney, Wash. Contact: H. W. Johnston, Chem. Dept., Whitworth College, Spokane, Wash. 99218. 509-489-3550
- **4th Annual Symposium on Recent Advances in the Analytical Chemistry of Pollutants.** June 17-19. Basle, Switzerland. Contact: D. M. Hercules, Chem. Dept., University of Georgia, Athens, Ga. 30602. 404-542-2626. Page 417 A, Apr.
- **2nd Rocky Mountain Regional ACS Meeting.** July 8-9. University of New Mexico, Albuquerque, N.M. Contact: G. Bryan, Los Alamos Scientific Lab., CMB-1, Los Alamos, N.M., 87544. 505-667-4088

New in infrared: Perkin-Elmer Model 100 Data Manipulator makes quantitative analysis a reality.

Users of infrared spectrophotometers: Would you like to use your instruments for quantitative analysis, and print out the answers in concentration, after reading them on electronic digits? Would you like to run spectra at will in transmittance or absorbance, at any desired scale expansion? Would you like to measure the depth of an ab-

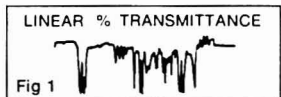


Fig 1
Polystyrene, Linear T, Spectrum Shown Actual Size.

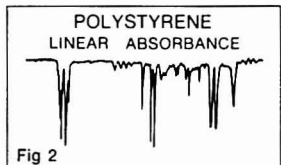


Fig 2
Polystyrene, Linear Absorbance.

sorption band automatically, with no guesswork? Would you like to set your 100% line by pushing a single button? Would you like to make single-point readings in an integrated mode, to improve the precision of repeated determinations?

If the answer to any of these questions is "Yes", meet the new Perkin-Elmer Model 100 Data Manipulator. It's easy to use, works with most instruments, and doesn't cost much.

Think of it as a little computer for people who don't have much money and don't want to know about computers.

Polystyrene Can Be Fun.

Here are two unusual views of polystyrene, run on a new Perkin-Elmer Model 735, a Model 100 Data Manipulator, and a Perkin-Elmer 056 Laboratory Recorder. Figure 1, reprinted actual size, is a little smaller than you're used to seeing. Figure 2 is recorded linearly in absorbance, over a range of 0 to 1.

Oil In Fibers Is Measured Directly. Textile people often need to know the concentration of lubricating oil in artificial fibers. The usual IR method is to make a CCl_4 extrac-

tion, draw a spectrum, convert the transmittance readings at 2930 cm^{-1} to absorbance (See Figure 3A), and compare the results to a working curve made with known concentrations. This is a whole lot faster than the gravimetric method, but is still a nuisance.

With the Data Manipulator (and, say, a Model 567) the spectra can

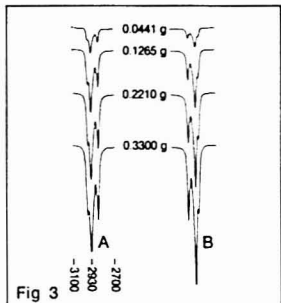


Fig 3
Oil in 5-Gram Fiber Samples. Left: Transmittance Scale. Right: Linear in Concentration.

be drawn in absorbance (with scale expansion), and the conversion step is eliminated. (See tracings in Figure 3B). In practice, you don't need to draw a spectrum at all.

You scan a sample of known concentration across the 2930 cm^{-1} band, using the Concentration and

Peak Reader modes. The digits hold the reading. You use the Concentration control to set the digits to read the known concentration. All the other samples will now read out directly in the desired units, and the results can even be printed out on the PRS-7A Printer Sequencer. Table below shows some comparative results.

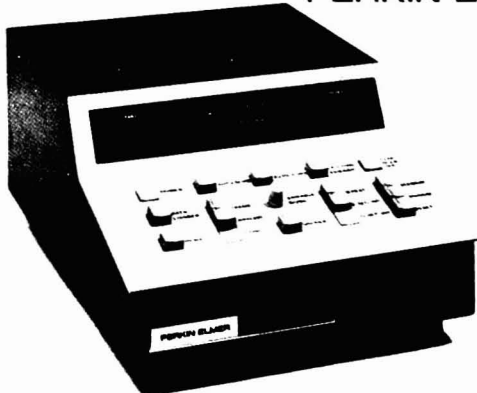
Lubricating Oil on Fiber (g of oil/5g fiber)	
Known Conc.	Measured Conc.
0.044	0.044
0.127	0.127
0.221	0.222
0.330	0.326

Models 735 and 567 Have Extended Range, Auto-Chek™ Gain.

There's also good news regarding instruments. The new Model 735 is a low-cost unit with a range extended to 400 cm^{-1} . The new medium-priced 567 has a range down to 200 cm^{-1} (50 microns). Both have a simple new way to set gain, called Auto-Chek. You press down on the gain control, and the pen should move ten recorder divisions. If it doesn't, rotate the gain control until it does. Couldn't be easier.

For more information write to the Instrument Division, Perkin-Elmer Corporation, 702 Main Avenue, Norwalk, Conn. 06856.

PERKIN-ELMER



CIRCLE 196 ON READER SERVICE CARD

Drug Analysis

at Nanogram Concentrations

As the world leader in specific G. C. detector technology, Tracor introduces the NEW Hall Electrolytic Conductivity Detector featuring:

- Selective response to nitrogen, chlorine, and sulfur with better than 0.01ng. sensitivity
- Compact single package construction
- Miniaturized rugged cell design
- Easy set up and operation

NEW HALL ELECTROLYTIC CONDUCTIVITY DETECTOR



*Be Specific, Specify
Tracor Gas Chromato-
graphs and Detectors*

Tracor Instruments

Tracor, Inc.
6500 Tracor Lane
Austin, Texas 78721
Telephone 512-926-2800

CIRCLE 226 ON READER SERVICE CARD

News and Views

- **Fourth International Conference on Thermal Analysis.** July 8-13. Budapest, Hungary. Contact: 4th ICTA Conference, c/o Hungarian Chemical Society, 1368 Budapest, P.O. Box 240, Anker köz 1, Hungary.
- **Gordon Research Conference on X-ray Photoelectron Spectroscopy.** July 15-19. Brewster Academy, Wolfeboro, N.H. Contact: A. M. Cruickshank, Pastore Chem. Lab., University of Rhode Island, Kingston, R.I. 02881. 401-783-4011
- **Gordon Research Conference on Analytical Chemistry.** Aug. 12-16. New Hampton School, N.H. Contact: A. M. Cruickshank, Pastore Chem. Lab., University of Rhode Island, Kingston, R.I. 02881. 401-783-4011
- **Gordon Research Conference on Infrared and Raman Spectroscopy.** Aug. 19-23. Kimball Union Academy, Meriden, N.H. Contact: A. M. Cruickshank, Pastore Chem. Lab., University of Rhode Island, Kingston, R.I. 02881. 401-783-4011
- **Gordon Research Conference on Separation and Purification.** Aug. 19-23. Colby College, New London, N.H. Contact: A. M. Cruickshank, Pastore Chem. Lab., University of Rhode Island, Kingston, R.I. 02881. 401-783-4011
- **International Symposium on Trace Analysis in Biological Materials.** Aug. 21-23. Dalhousie University. Contact: D. E. Ryan, Chem. Dept., Dalhousie University, Halifax, N.S., Canada. Page 326 A, Mar.
- **18th Ampere Congress on Magnetic Resonance and Related Phenomena.** Sept. 9-14. University of Nottingham, England. Contact: E. R. Andrew, Physics Dept., The University, University Park, Nottingham NG7 2RD, England
- **21st National Vacuum Symposium.** Oct. 8-11. Anaheim, Calif. Contact: L. C. Beavis, Sandia Labs Div. 2413, Albuquerque, N.M. 87115
- **26th Southeastern Regional ACS Meeting.** Oct. 23-25. Convention Center, Norfolk, Va. Contact: M. A. Kise, R&D, Virginia Chemicals, Inc., Portsmouth, Va. 27303. 703-484-5000
- **9th International Symposium on Advances in Chromatography.** Nov. 4-7. Sheraton-Lincoln Hotel, Houston, Tex. Contact: Albert Zlatkis, Chem. Dept., University of Houston, Houston, Tex. 77004. Page 326 A, Mar.

- **10th Tokyo Conference on Applied Spectroscopy.** Nov. 6-8. Tokyo, Japan. Contact: The Japan Society for Analytical Chemistry, 1-1-5 Hon-machi, Shibuyaku, Tokyo, Japan 151. Page 326 A, Mar.
- **10th Midwest Regional ACS Meeting.** Nov. 7-8. University of Iowa, Iowa City, Iowa. Contact: D. J. Pietrzyk, Chem. Dept., University of Iowa, Iowa City, Iowa 52240. 319-353-4661
- **30th Southwest Regional Meeting.** Dec. 9-11. Astroworld Hotel, Houston, Tex. Contact: J. M. Fitzgerald, Chem. Dept., University of Houston, Cullen Blvd., Houston, Tex. 77004. 713-749-2639

Short Courses

ACS Courses. For more information, contact: Department of Educational Activities, American Chemical Society, 1155 16th St., N.W., Washington, D.C. 20036. 202-872-4508

Modern Liquid Chromatography
Atlantic City, N.J. Apr. 6-7. L. Snyder, J. Kirkland. \$140

Interpretation of Infrared Spectra
New York City. Apr. 19-20. Norman Colthup. \$125

Principles of Color Technology
Boston, Mass. May 15-17. Fred Billmeyer, Jr. \$150

Laboratory Safety—Recognition and Management of Hazards
New York City. May 29-31. N. V. Steere, R. L. Olsen, Maurice Golden. \$160

Modern Liquid Chromatography
Minneapolis, Minn. June 1-2. L. R. Snyder, J. J. Kirkland. \$125

Gas Chromatography, Theory and Practice
Blacksburg, Va. June 3-7. H. M. McNair, James Miller. \$295

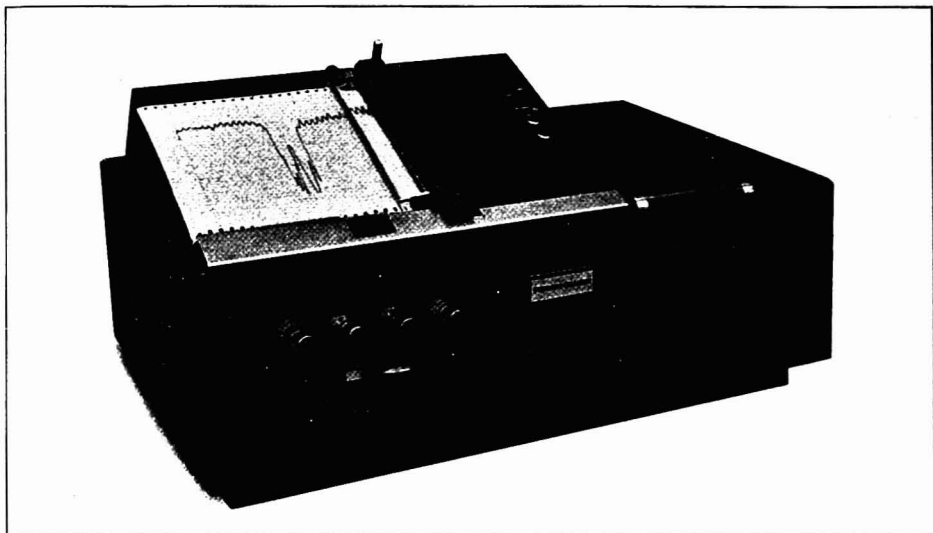
Regional Liquid Chromatography Seminars
U.S. and Canada. April and May. Half-day seminars. Contact: Waters Assoc., Maple St., Milford, Mass. 01757. 617-478-2000

Chemical Microscopy
Chicago, Ill. May 5-9. \$325. Contact: McCrone Research Institute, 2820 S. Michigan Ave., Chicago, Ill. 60616. 312-842-7105

Applied Gas Chromatography: Intermediate
Philadelphia, Pa. May 6-8. \$200. Contact: Sadtler Research Laboratories, 3316 Spring Garden St., Philadelphia, Pa. 19104. 215-382-7800

Perkin-Elmer's new Model 167 IR.

We've lowered the cost of high performance.



This new, double-beam infrared spectrophotometer is a remarkable combination of typical Perkin-Elmer performance and versatility, coupled with a very moderate cost.

By concentrating on the capabilities needed by most laboratories most of the time, we've brought high performance to the budget-conscious. In fact, in order to beat the frequency and transmittance accuracy of the Model 167, you need to pay about three times the price.

And that's not all you gain. Just look down this list of other features:

- Scans from 4000 to 600 cm^{-1} . Choice of 5-, 12-, or 48-minute scan time.
- High resolution (0.7 cm^{-1} at 1000 cm^{-1}) is available, or you can choose wide-slit programs for low-energy situations.
- Flowchart® recorder system locks chart and monochromator together, for unbeatable chart wavelength accuracy and repeatability.
- Auto-Chek™ Gain Control lets operator check gain repeatedly, even with sample in position, by simply pushing a knob.
- 5x abscissa expansion for proper presentation of high-resolution spectra.
- Ease and simplicity of operation means even the most inexperienced operator can get fast, accurate, reproducible results.

The Model 167 is compatible with all Perkin-Elmer® accessories, including our Model 100 Data Manipulator which quickly displays digital quantitative results in either concentration or absorbance units.

The new Model 167 is a lot of spectrophotometer for not so very much money. A fact we'd be glad to demonstrate in your lab. For details and descriptive booklet, write Instrument Division, Perkin-Elmer Corporation, Main Avenue, Norwalk, Conn. 06856.

PERKIN-ELMER

CIRCLE 197 ON READER SERVICE CARD

ANALYTICAL CHEMISTRY, VOL. 46, NO. 4, APRIL 1974 • 425 A

Du Pont's new ESCA helps solve surface characterization problems.

- A few examples—
- Changes responsible for degradation or poisoning of a process catalyst.
 - Surface contaminants causing poor performance of semiconductor devices.
 - Analysis of human skin composition in biomedical research.
 - Chemistry of a fluoropolymer surface treatment. Ex. Na/NH_3 .

The Du Pont 650 Electron Spectrometer provides a high-quality, analytical tool for surface analysis. By analyzing photoelectrons ejected from samples under X-ray irradiation, detailed chemical analysis can be made of the top few monolayers. All elements except hydrogen may be identified. Also measurable are oxidation state, bonding and other structural details.

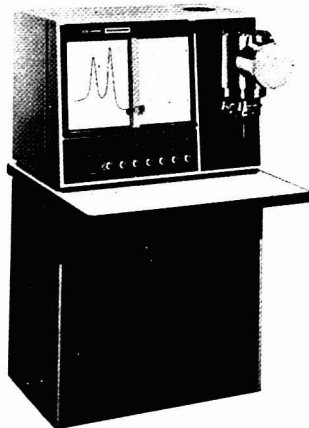
The Du Pont 650 Combines Low Cost with High Performance—uses a unique non-dispersive electron energy analyzer which provides the scientist with high sensitivity and resolution in a compact unit: 300K cps on Au $4f_{7/2}$ at 1.2 eV FWHM, in a unit requiring less than one square meter of floor space. This instrument has been designed for maximum operator convenience and efficiency. For quality-control measurements or basic research programs, the 650 offers more performance at a lower price than currently available instruments.

Other fields of study utilizing ESCA include:

- textile fiber surface characterization
- chemical structure determination
- organometallic chemistry
- surface reactions of metals

For further information on the Du Pont 650 and its applications, write Du Pont Co., Rm. 23255, Wilmington, DE 19898.

Offices in major U.S. cities and in Frankfurt (Friedberg); London (Hitchin); Milan; Paris; Mexico City; Caracas and São Paulo.



Instruments

CIRCLE 62 ON READER SERVICE CARD

News and Views

Four One-Day Programs: Competitive Protein Binding Assays and Related Techniques; Radioimmunoassay in the Clinical Lab; Improving Clinical Enzyme Analysis; Aspects of Agarose Electrophoresis

Denver, Colo., May 6-9; Seattle, Wash., May 20-23. *Contact:* Beckman Technical Education Center, 2500 Harbor Blvd., Fullerton, Calif. 92634. 714-521-3700

Electron Microprobe

Chicago, Ill. May 6-10. \$325. *Contact:* McCrone Research Institute, 2820 S. Michigan Ave., Chicago, Ill. 60616. 312-842-7105

Microscopy for Conservators

Chicago, Ill. May 13-17. \$325. *Contact:* McCrone Research Institute, 2820 S. Michigan Ave., Chicago, Ill. 60616. 312-842-7105

Practice of ESCA Workshop

Purdue University. May 20-22. *Contact:* W. E. Baitinger, Chem. Dept., Purdue University, West Lafayette, Ind. 47907

Practice of UV/VIS

Philadelphia, Pa. May 20-24. \$275. *Contact:* Sadtler Research Laboratories, 3316 Spring Garden St., Philadelphia, Pa. 19104. 215-382-7800

Nuclear Magnetic Resonance II

Philadelphia, Pa. May 20-24. \$275. *Contact:* Sadtler Research Laboratories, 3316 Spring Garden St., Philadelphia, Pa. 19104. 215-382-7800

Liquid Chromatography

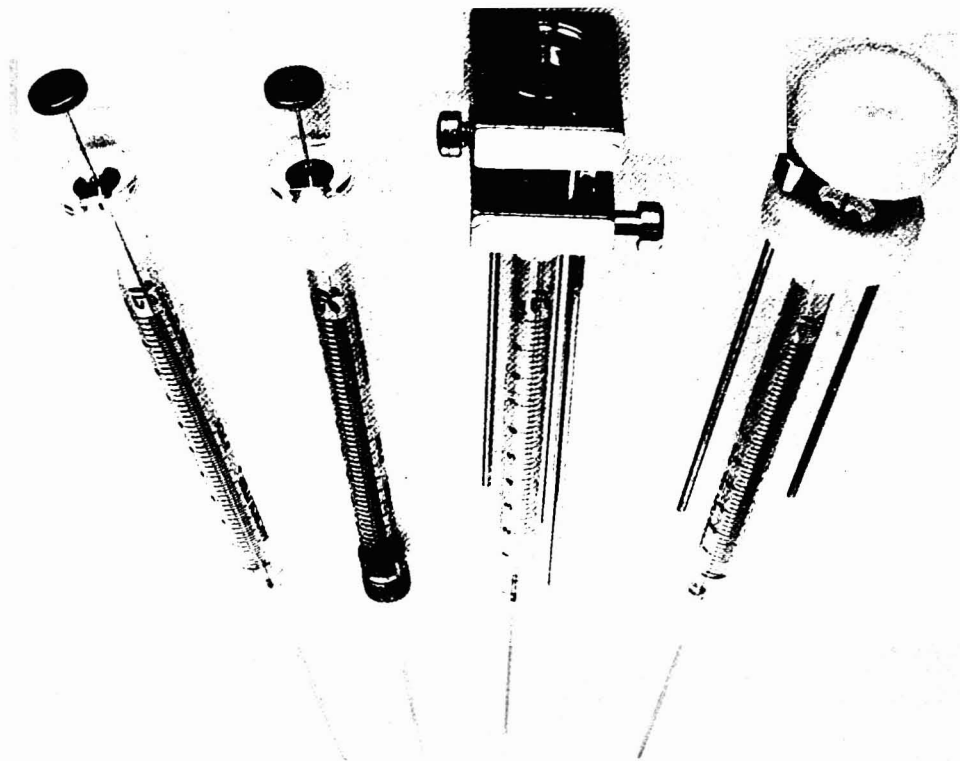
Chicago, Ill. May 22-24. *Contact:* Varian Instruments, 205 W. Touhy Ave., Park Ridge, Ill. 60068

Basic Chromatography; Liquid Chromatography; Advanced Chromatography; Gas Chromatography—Troubleshooting

LSU, New Orleans. May 24. *Contact:* Larry Mars, 312 S. Glavez St., New Orleans, La. 70119

Microscopy in the Pharmaceutical Laboratory

Chicago, Ill. May 27-31. \$325. *Contact:* McCrone Research Institute, 2820 S. Michigan Ave., Chicago, Ill. 60616. 312-842-7105



Four times as versatile

Do you know how to make a Hamilton 701N Microliter Syringe four times as versatile? You simply add attachments . . . such as a guide to inhibit bending of small diameter plungers . . . or a Chaney Adaptor that makes the 701N into a repeating dispenser. Or, you

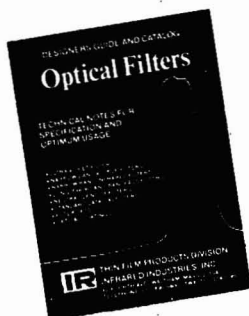
can get any one of several special needles. Or, you can get a 701 with a removable needle, designed to make it possible to replace bent or plugged needles. But no matter how versatile you make your 701N, there's no way to improve upon its quality (we guar-

antee that) or its repeatable delivery and accuracy. □ The 701N . . . versatility is only one of its virtues. Write for literature to Hamilton Company, Post Office Box 17500, Reno, Nevada 89510.

HAMILTON

CIRCLE 119 ON READER SERVICE CARD

Everything you
always wanted to
know about filters*



Thin Film Products Division of Infrared Industries, Inc. announces a new 32-page Design Guide and Catalog of Optical Filters. It provides a basic reference work for engineers and scientists involved in the specification, procurement, and use of interference filters. It includes discussions of the effects of angle of incidence and of temperature on optical properties and of rejection of wavelengths outside the passband; a discussion of mechanical construction techniques; and tables of readily attainable specifications with respect to transmission and bandwidth for filters at all wavelengths between 1950 Angstroms and 20 micrometers.

In addition, over 325 different standard filters at wavelengths between 3650 Angstroms and 10.6 micrometers, immediately available from stock, are listed along with their prices.

*And had to phone or write to ask.

Write for a catalog to:

IR
INDUSTRIES, INC.

THIN FILM PRODUCTS DIVISION
INFRARED INDUSTRIES, INC.
P.O. BOX 557
Waltham, Massachusetts 02154
Tel. (617) 890-5400

CIRCLE 134 ON READER SERVICE CARD

News and Views

Gas Chromatography
Springfield, N.J. June 5-7. *Contact:* Varian Instruments #25, Route 22, Springfield, N.J. 07081

Scanning Electron Microscopy and Electron Probe Microanalysis
Bethlehem, Pa. June 10-14. \$300. *Contact:* J. I. Goldstein, Metallurgy & Materials Science, Lehigh University, Bethlehem, Pa. 18015. 215-691-7000, ext. 627

Polymer Characterization
University of Utah. June 10-14. \$325. *Contact:* Polymer Conference Series, 2020 Merrill Engineering Bldg., The University of Utah, Salt Lake City, Utah 84112. 801-581-8431

Liquid Chromatography
New Orleans, La. June 12-14. *Contact:* Varian Instruments, Plaza Southwest, 5750 Bintliff, Suite 202, Houston, Tex. 77036

Applied Polarized Light Microscopy
Chicago, Ill. June 24-28. \$325. *Contact:* McCrone Research Institute, 2820 S. Michigan Ave., Chicago, Ill. 60616. 312-842-7105

Electrode Kinetics Seminar
Fawcett Center for Tomorrow, Ohio State University. July 7-12. \$425, includes lunch and dinner. *Contact:* Jud B. Flato, Princeton Applied Research Corp., P.O. Box 2565, Princeton, N.J. 08540. 609-452-2111

Recent Advances in NMR Spectroscopy
University of East Anglia. July 8-10. *Contact:* J. M. Usher, The Chemical Society, Burlington House, London W1V 0BN, England

Principles of Color Technology
Rensselaer Polytechnic Institute. July 8-12. \$300. *Contact:* Office of Continuing Studies, Rensselaer Polytechnic Institute, Troy, N.Y. 12181

Fiber Microscopy
Appleton, Wis. July 8-19. *Contact:* T. A. Howells, The Institute of Paper Chemistry, P.O. Box 1048, Appleton, Wis. 54911. 414-734-9251

Gas Chromatography
San Francisco, Calif. July 10-12. *Contact:* Varian Instruments, 4940 El Camino Real, Los Altos, Calif. 94022

Recent Advances in Vibrational Spectroscopy
University of East Anglia. July 11-12. *Contact:* J. M. Usher, The Chemical Society, Burlington House, London W1V 0BN, England

Applied Molecular Spectroscopy: Infrared, Raman, Ultraviolet
Arizona State University. July 22-26. \$225. *Contact:* Jacob Fuchs, Chem. Dept., Arizona State University, Tempe, Ariz. 85281

Modern Industrial Spectroscopy
Arizona State University. Aug. 5-16. \$400. *Contact:* Jacob Fuchs, Chem. Dept., Arizona State University, Tempe, Ariz. 85281

Analysis of Specks and Deposits
Appleton, Wis. Aug. 6-8. *Contact:* T. A. Howells, The Institute of Paper Chemistry, P.O. Box 1048, Appleton, Wis. 54911. 414-734-9251

Fisk Institute
Fisk University, Nashville, Tenn. Aug. 12-16. Three one-week courses: Basic Infrared and Raman Spectroscopy; Interpretation of Infrared and Raman Spectra; C. D. Craver, Norman Colthup; Gas-Liquid Chromatography, Richard Juvet, S. J. Cram, Dave Stafford. \$220. *Contact:* Nelson Fuson, Box 8, Fisk University, Nashville, Tenn. 37203. 615-329-9111, ext. 235

For Your Information

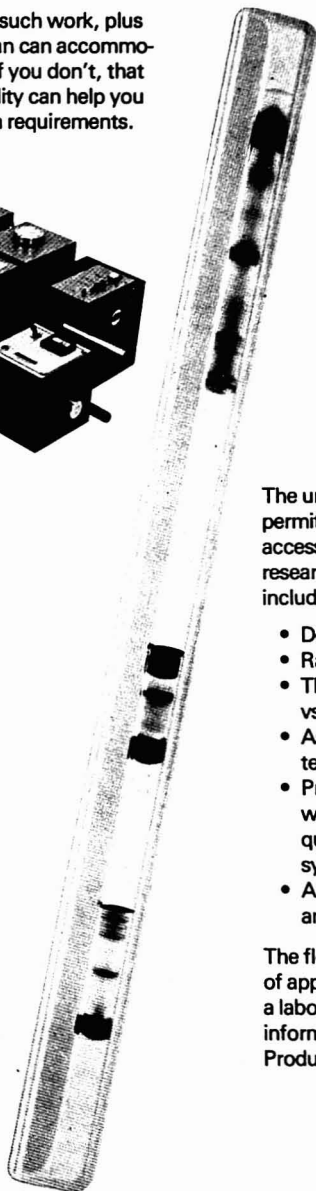
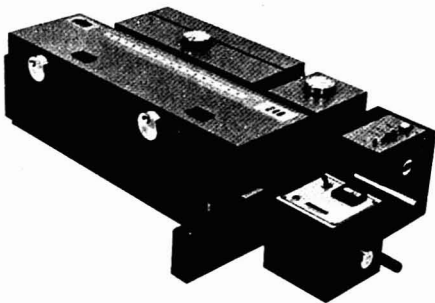
Amicon Corp. of Lexington, Mass., has formed a subsidiary, **Amicon GmbH**, in Witten, West Germany. Headquarters for Amicon's entire European operation is in Oosterhout, Holland. Amicon is a leading manufacturer of membrane filtration systems.

GCA/McPherson Instrument, 530 Main St., Acton, Mass. 01720, has acquired the complete line of **Heath/Schlumberger** spectrophotometers and will continue to honor currently held warranties and offer service for these instruments as well as its own line.

Perkin-Elmer Corp., Instrument Div., Main Ave., Norwalk, Conn. 06856, 203-762-1000, offers a new medical newsletter with articles of interest to people in clinical laboratories. The first issue of *Laboratory Medicine Newsletter*, 20 p., includes articles such as "The Analysis of Renal, Biliary, and Prostatic Calculi by Infrared Spectroscopy" and "Automation of the Indirect Fluorescent Antibody Test for Toxoplasmosis."

Do you need a 20 cm gel scanner?

If so, we have an accessory for such work, plus the only spectrophotometer than can accommodate such a sample. And even if you don't, that same instrument design versatility can help you meet your particular application requirements.



See us at FASEB,
Booths A-5, B5-6, and C5-6

The unique optical bench of our Model 240 permits the attachment of a wide variety of accessories to fulfill application needs in research, industrial, and clinical laboratories including:

- Density gradient scanning
- Rapid sampling
- Thermal programming for absorption vs $T^{\circ}C$ plots
- Aspirating thermo-cuvette for precise temperature control
- Programmed, reference compensated wavelength scanning for accurate qualitative assay as part of the basic system
- Automatic sampling system for batch analysis

The flexibility of the Model 240 for a wide variety of applications means cost savings for you. For a laboratory demonstration and additional information write or call Al Marchesi, Research Products Manager.

gilford
INSTRUMENT

Oberlin, Ohio 44074
Paris (Malakoff), France
Dusseldorf, W. Germany
Morden, Surrey, England

216 774-1041 • Cable: GILLARS

CIRCLE 95 ON READER SERVICE CARD

For accurate
results
in organic and
biochemical research,
select the reagents
with actual
analytical values
on the label

1 lb. **1-8993**

Disodium EDTA, Dihydrate Crystal

'Baker Analyzed' REAGENT

Sample Analysis of Lot No. 320245		Merck A.C.S. Specifications	
Assay $\text{C}_{10}\text{H}_{16}\text{N}_4\text{O}_{10} \cdot 2\text{H}_2\text{O}$	99.8	%	
Insoluble Matter	0.0005	%	
As of 5% Solution at 25°C	4.5	%	
Nonfluorescent Acid (HNOCOCH_3 , I, N)	0.01	%	
Heavy Metals (as Pb)	0.002	%	
(ppm)	0.005	%	
Other Impurities (in ppm):			
Ammonia (NH ₃)	0.05		
Calcium (Ca)	0.2		
Copper (Cu)	0.05		
Iron (Fe)	0.8		
Lead (Pb)	0.2		
Silver (Ag)	0.02		
Zinc (Zn)	0.4		

BAKER CHEMICAL CO., PHILLIPSBURG, N. J. 08865

You receive proof of purity with the actual lot analysis for the product in the container

You receive valuable reference point data, for today's advanced analytical techniques

You receive useful information for repetitive work, for assessment of blank values, and for reference in evaluating test results

You receive actual values for key impurities, which saves you time and money by eliminating the need to determine these values yourself

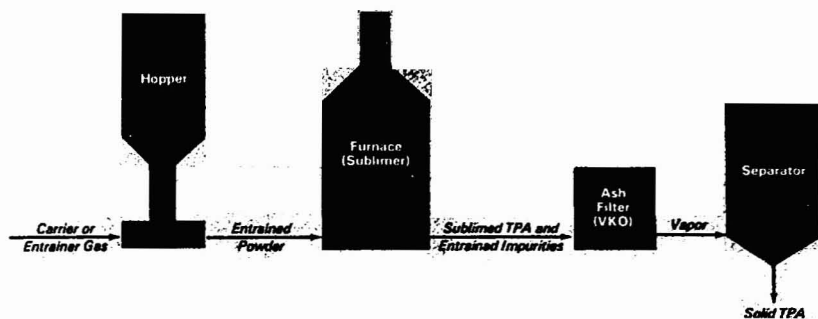


Figure 1. Terephthalic acid sublimation purification process

Urgent Production Problem Solved by Unique Capabilities of Analytical Chemists

Claude A. Lucchesi
Contributing Editor

Analytical chemists at the Mobil Chemical Co. were confronted with a challenging problem during the start-up stages of the company's terephthalic acid (TPA) pilot plant. The Mobil TPA process consisted of two parts, an oxidation section and the purification section which is illustrated in Figure 1. Dry, impure TPA powder from the oxidation section was fed into a hopper where it became entrained in a high-velocity carrier gas and passed into a furnace where substantially all of the solids were vaporized. The effluent from the furnace was passed through an ash filter where entrained solids, including catalyst residues from the oxidation section, were removed from the vaporized material. The vapor then entered a condenser for fractional condensation of the solid TPA product.

The TPA was being produced as a potential replacement for dimethyl terephthalate (DMT), then the only source of the dicarboxylic acid in many polyester films and fibers. TPA had an expected cost advantage over DMT, provided it could be produced

at an equivalent level of purity which was judged by a set of specification tests. One specification test involved the color of a 5% solution of TPA in dimethylformamide (DMF). And this is where the problem started. Its solution, in time to be of practical value to the company, required the integrated efforts of a team of specialists in IR, X-ray diffraction, X-ray spectroscopy, arc-spark spectroscopy, thermal methods, gas chromatography, and solution chemistry. In addition, a literature searcher was needed to find a synthesis procedure for the tentatively identified material to "cinch" an identification.

An early pilot plant run in Beaumont yielded TPA product which, not only failed the color test, but also did not completely dissolve in the DMF. The question was, "What is the DMF-insoluble material?" This was the question I was asked to answer when I was with Mobil Chemical as manager of the Analytical and Physical Chemistry Department. The then vice president of the Research and Development Division phoned and told me to go to Beaumont and find

out what that DMF "turbidity" was. Although the immediate question was the identity of the turbidity, the critical question was how to prevent it, whatever it was, from forming. The problem had top priority, and for several weeks most of the specialists in the department did little else. Five pounds of TPA product which failed the DMF test was requested for the Research Laboratory in Metuchen, N.J., and I went to Beaumont, Tex., to become familiar with the pilot plant operation and to obtain test samples for study.

Nondestructive Tests Used to Survey Test Samples

Because only a few milligrams of the DMF turbidity could be isolated from several pounds of TPA product, initial tests on the DMF-insoluble material were limited to the nondestructive techniques readily available in our lab: X-ray diffraction, X-ray spectroscopy, and infrared spectroscopy. The same measurements were made with the Beaumont test samples, and the material removed from the ash filter and the DMF turbidity

from the TPA product were almost identical (Figure 2). The two materials had identical infrared spectra and nearly identical X-ray diffraction patterns. Also, the X-ray fluorescence spectrographic measurements showed that the two materials contained the same metallic elements in roughly the same concentration ratios. These findings enabled us to do subsequent work with the pound or so of ash filter material rather than with the limited amount of DMF-insolubles.

Identification of Inorganic Part

The nature and concentration of the inorganic materials in the ash filter sample were established to the extent justified by the nature of the sample as illustrated in Figure 3. From all the data shown, it was estimated that about half of the inorganic material was CaSO_4 . Thus, at most, only 3 or 4% of a metal was available to form a salt or chelate with TPA. Consequently, the data on the inorganic part of the ash filter sample supported the IR conclusion that the main constituent of the ash filter sample (and the DMF insolubles) was not primarily a salt or chelate of TPA. (For example, $\text{Ca}(\text{TPA})$ contains 11% Ca.)

Cobalt, iron, and calcium were found in the DMF-insolubles by X-ray spectrography. The ratios of the three metals in the DMF-insolubles and in the ash filter sample and the concentrations in the ash filter sample suggested that less than 0.1% cobalt was in the DMF-insolubles. Consequently, the DMF-insolubles could not have been a cobalt salt or chelate. The same can be said for iron.

Identification of Organic Part

Having convinced ourselves that only a minor part of the DMF-insolubles could have been of an inorganic

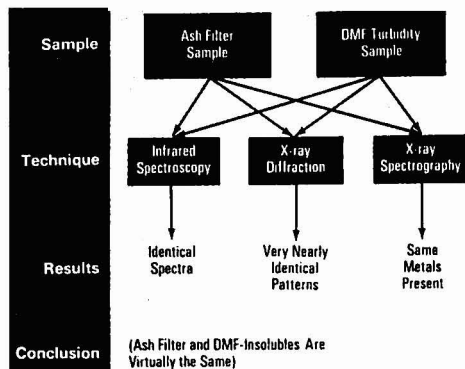


Figure 2. Nondestructive methods used to show DMF turbidity and ash filter material were virtually the same

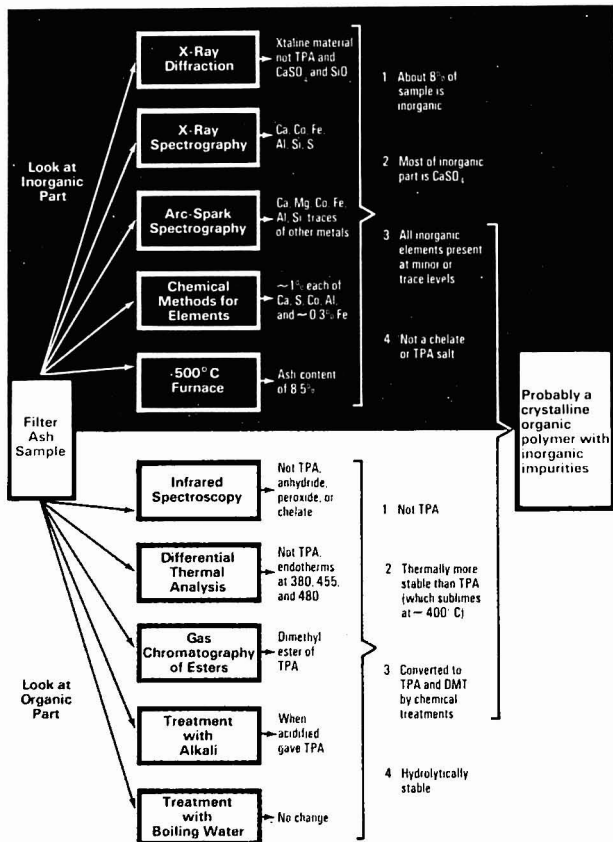


Figure 3. Techniques for inorganic and organic substances used in combination to show what material could and could not be

Carle came up with a brand-new analytical GC, so you won't have to work with a bunch of tired six-year olds.

After six or seven years, a GC gets pretty tired and cranky—no matter what it cost new. And replacing that outdated GC isn't getting any cheaper. Not if you want an instrument that does accurate quantitative analysis at a reasonable cost.

That's why Carle designed a totally new instrument: the Analytical Gas Chromatograph. We call it the AGC.

You have a choice of three models: the AGC-111 with TCD detectors; the AGC-211 with flame ionization; and the AGC-311 with both FID and TCD.

In many important ways, the performance of our AGC exceeds that of instruments costing twice as much. All in keeping with Carle's reputation for combining innovative design with cost economy.

For example, the unique AGC-111 is \$1,750 complete—and that means you get both thermistor and filament detector capability. Everybody knows



thermistors are unequalled for gas analysis, but filaments are best for high temperature work. Now you can interchange these detectors on an AGC-111 in less than five minutes.

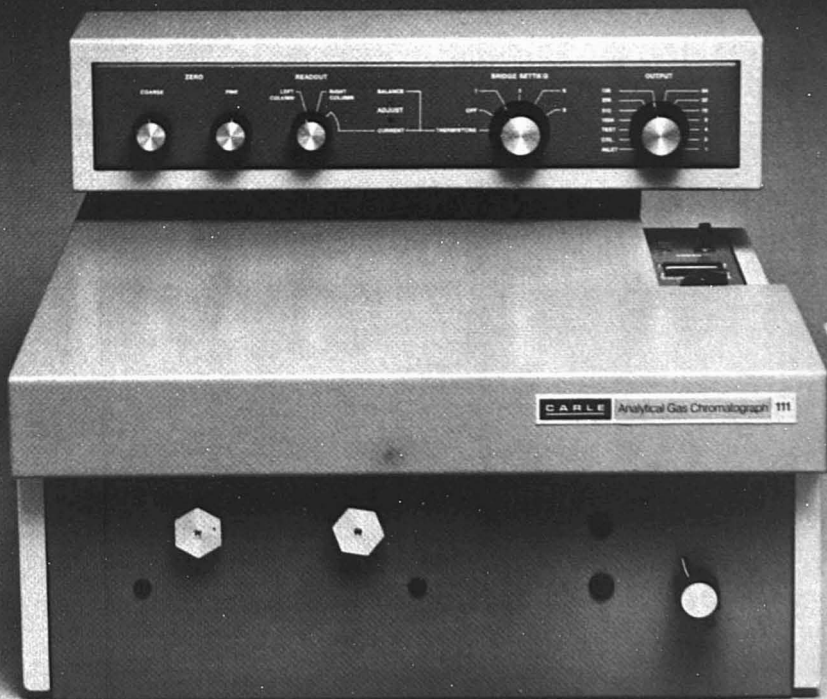
All three models have absolutely repeatable retention time, superb operational simplicity and unbeatable quantitative accuracy. That's a lot of superlatives. The AGC is a lot of chromatograph. We planned it that way, complete with ready-made round holes for dropping in round valves. An AGC doesn't have to submit to hacksaw surgery.

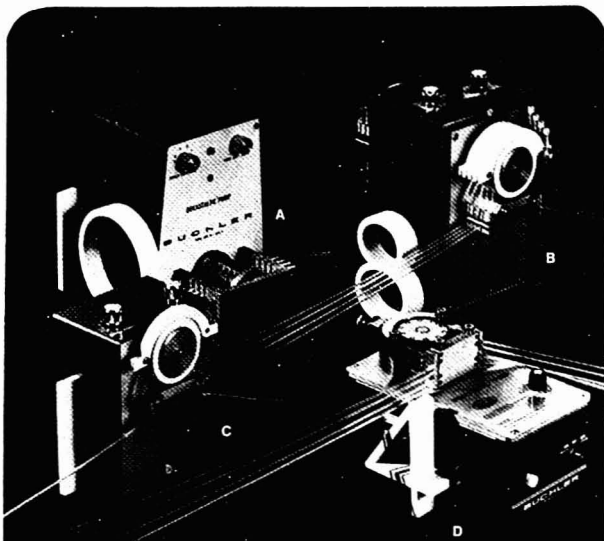
Quit struggling with a tired chromatograph. After six years, it deserves a nice long nap—you deserve an AGC. Write or call for complete specifications, performance data and descriptive material.

CARLE
INSTRUMENTS, INC.

1141 East Ash Avenue Fullerton,
California 92631 (714) 879-9900

CIRCLE 34 ON READER SERVICE CARD





Choose your channels... You'll enjoy the performance **Buchler Peristaltic Metering Pumps**

Choose from a line of multi-channel variable pumps for a wide range of applications. No matter which pump you choose, you'll find uniformly adjustable flow rates, from a few ml to a liter per hour, and settings that are reproducible in subsequent runs. These Buchler pumps are ideally suited to handling corrosive liquids, sterile solutions or biologically infectious materials since they are completely contained in chemically inert tubing. Other features include reversible flow, easy change of tubing sizes and minimum pulsation. So if you need a reliable pump for electrophoresis, chromatography, density gradients; for on-line ratio mixing in process development; with automatic analyzers... wherever a versatile, precise metering pump is essential, check out the Buchler line today.

- T.M.
A. Dekastaltic® with 10 channels
B. Multi-Staltic® with 4 or 8 channels
C. Mono-Staltic® with one channel
D. Polystaltic® with 4 channels

SEARLE Buchler Instruments

Division of Searle Analytic Inc.
1327 Sixteenth Street
Fort Lee, New Jersey 07024

nature, we concentrated on the organic part of the problem. The ash filter sample and several TPA samples were treated with methanol to produce methyl esters and other volatile substances which were extractable with chloroform and could be passed through a gas chromatograph. Although only about 20% of the sample was esterified, almost all of the material that got through the chromatograph was DMT.

Because of the gas chromatographic observation that the ash filter sample yielded only about 20% TPA ester when carried through the esterification procedure and because the IR spectrum of the residue was the same as the starting material, a hydrolysis study was made. The sample was treated with NaOH, and the insoluble residue was separated by filtration, dried, and weighed. When the filtrate was acidified, it gave a precipitate which was identified as TPA. About 62% TPA was recovered with the first treatment. After four treatments, 83% was recovered. This gave a residue of 17% which was in the ball park with the 8.5% ash figure obtained earlier.

Unfortunately, we did one more experiment that caused unnecessary confusion. We boiled the ash filter sample in water for at least 2 hr, and it remained insoluble. Nevertheless, we came to the conclusion that we had a highly crystalline polymer that was hydrolyzed with base or acid to give TPA and could be partially converted to DMT by a conventional esterification procedure.

At this point, I had a meeting with all of the specialists who worked on the problem, and we systematically decided what the DMF-insolubles could not be. The only possibilities we had left was an anhydride or a peroxide, and we concluded that the TPA more likely had formed an anhydride. But it was difficult to convince our organic chemists that TPA most likely had formed an anhydride. Consequently, one of our literature searchers went to the Chemists' Club Library in New York City and found a 1959 German article describing the synthesis of TPA anhydride. We translated the article and followed the recipe. The IR spectrum of the synthesized material matched the IR spectra of both the ash filter sample and of the DMF-insolubles. The X-ray diffraction patterns also matched.

When we were convinced that the DMF-insolubles indeed were poly-(TPA anhydride), we suggested to the engineers that steam be used as a carrier gas instead of nitrogen to prevent the formation of the anhydride. This solved the problem: no more DMF-insolubles and no more color.

CIRCLE 23 ON READER SERVICE CARD

Quantitative NMR: Good Coverage of the Literature

Quantitative Analysis by NMR Spectroscopy. F. Kasler. viii + 190 pages. Academic Press Inc., Ltd., 24-28 Oval Rd., London, NW1 7DX, England. 1973. £4.50

Reviewed by John A. Sogn, The Rockefeller University, New York, N.Y. 10021

Steady advances in instrumentation and methodology are substantially increasing the range of applications of NMR to quantitative analysis at the same time that new, relatively inexpensive spectrometers are making the technique available to a wider audience. This makes the appearance of any book on the subject timely, although this particular book is less than ideal.

The stated aims of this volume, the third in a series of monographs on the analysis of organic materials (series editors R. Belcher and D. M. W. Anderson), are twofold. The first, substantially successful aim is to collect under one cover all of the relevant literature references in what has been until now a rather diffuse application of NMR. The literature is covered through early 1972. The second, largely unsuccessful aim is to introduce this application to readers who are not yet familiar with the method.

The book is divided into four parts. Part A gives the basic theory of NMR and a discussion of instrumentation, with a table of performance criteria of commercial spectrometers. The theory is too condensed to be an acceptable introduction to NMR for someone unfamiliar with the subject, and it does not go into enough depth on subjects specifically relevant to quantitative studies. A good feature, however, is the section on lanthanide shift reagents, which are too new to be discussed in most NMR texts and

which should be useful for quantitative applications because of their ability to reduce spectral complexity in some cases. The section on instrumentation is brief but of use to newcomers to NMR, particularly because of the lucid discussion of the merits of different types of spectrometers. Spectrometer design is changing rapidly enough, however, that the list of commercial spectrometers has already become somewhat outdated.

Part B covers the most important practical considerations involved in quantitative studies by NMR, including such matters as solvent selection, sample handling, and integration techniques. It is done well with the exception of the chapter on sensitivity enhancement, which is superficial except for a detailed set of instructions for using the Varian C-1024 CAT with the Varian A-60 spectrometer, a subject of moderate but not universal interest.

Part C covers specific procedures that have appeared in the literature. The coverage is broad; yet, experimental details are included wherever they are of use. Part D briefly mentions three topics—polymers, wide line methods, and nuclei other than protons—which are in general not covered in part C.

Despite its drawbacks, this book is recommended to workers in the field, who will appreciate the collection of references. Since it is the only book devoted solely to this subject, it must also be recommended to nonexperts interested in learning about the possible applications of NMR to quantitative analysis, but only after they gain a basic understanding of the background of NMR from one of the standard introductory texts, such as "Nuclear Magnetic Resonance Spectroscopy" by Bovey.

Modular Treatment of Instrumentation

Chemical Instrumentation: A Systematic Approach. Second edition. Howard A. Strobel. xxii + 903 pages. Addison-Wesley Publishing Co., Inc., Reading, Mass. 01867. 1973. \$22.50

Reviewed by Gary M. Hieftje, Department of Chemistry, Indiana University, Bloomington, Ind. 47401

According to the author's preface, this book is designed to acquaint a student with the various spectrometric, electrometric, and other physical methods which are of importance to chemists and to develop in the student a working knowledge of the measurement process itself. With this background, the student should be able to select and perform instrumental procedures appropriate to a specific problem and to readily master unfamiliar techniques. This text is a substantially expanded revision of the earlier edition and includes a number of additional topics and chapters, two of which (on mass spectrometry and chromatography) have been contributed by other authors.

In his treatment, the author has presented a more unified approach to instrumentation than was provided in the first edition. Instrumental systems are viewed as being modular, with block diagrams extensively employed. Modules are then classified according to function, examined individually, and employed in larger systems. Accordingly, the book is organized in sections, with an initial chapter on measurement principles and "systems" design, followed by several excellent chapters on basic electronics and optics. Later sections deal with integrated modular assem-

Books

blies in the form of entire instruments, and cover spectrometric, electronic, and chromatographic techniques in detail.

This book has several strong points. Throughout, the theoretical basis of each technique is presented with a depth and clarity missing in most texts on instrumental methods. Also, the chapters on electronics and optics are well-written and unusually comprehensive. They are directed toward the practical user of these tools but are sufficiently rigorous to satisfy the better student. Wherever possible, the author has combined the discussions of several methods to emphasize their similarities. For example, the absorption of electromagnetic radiation by molecules is first discussed in a general way, with later emphasis on experimental differences to be found in each spectral region (ultraviolet, visible, infrared, and microwave). Excellent references are given at the end of each chapter and in an appendix, and frequent examples are provided within each chapter to illustrate and clarify important points. In general, the questions and problems are thought provoking and challenging, and when answers are supplied, they appear to be correct.

The primary shortcoming of the book is its attempted breadth. Even in the area of spectrochemical analysis (clearly the strongest), several topics have been omitted to maintain a manageable length. Thus, X-ray spectrometry and electron spectrometry (ESCA, etc.) are not even mentioned. More importantly, only a single chapter has been devoted to separation methods, which form such an important part of modern instrumental analysis. High-speed liquid chromatography, for example, is allotted little more than one paragraph. Other criticisms, less important than the above, could be directed at the occasional inconsistent or improper use of terms (e.g., intensity, fluorimetry) and the infrequent but confusing usage of a single symbol for several different quantities.

Because of its excellent treatment of optics and the theoretical foundation of spectrometric methods, this text can be strongly recommended for use in graduate and advanced undergraduate courses in spectrochemical analysis and instrumentation. However, the book is less suitable for two other curricular applications suggested by the author. The brief coverage

of chromatography would seriously weaken any undergraduate course in instrumental analysis, unless that material had been covered in an earlier class or could be provided in lecture by the instructor. Also, the existence of more detailed texts on electronics and instrumentation and the absence of accompanying laboratory experiments would preclude the adoption of this book for this latter kind of course.

Another Textbook

Analytical Chemistry. J. G. Dick. viii + 696 pages. McGraw-Hill Book Co., 1221 Avenue of the Americas, New York, N.Y. 10020. 1973. \$13.95

Reviewed by Robert L. Pecsok, Department of Chemistry, University of Hawaii, Honolulu, Hawaii 96822

They say you shouldn't judge a book by its cover, but this one is an exception. The cover design—a pair of crossed retorts on a black field—sets the tone for the next 500 pages. In the introductory chapter, the author reminds us that the techniques of qualitative analysis, such as in hydrogen sulfide separations, provide excellent opportunity to learn much concerning chemical reactions, and he regrets that these procedures are rarely taught or used.

After the usual overview of "fundamental" concepts in quantitative analysis (solution concentration units, chemical equations, and stoichiometry), we are treated to 50 pages on the treatment of analytical data—an overdose at this point, to say the least. Next come 124 pages on chemical equilibria including rigorous derivations and detailed examples of all types of ionic equilibria. Unfortunately, it is not clear to the reader why it is important for him to struggle through cubic equations in solving for the pH of HA or NaA solutions; or why he should be subjected to a quartic equation to get $(H^+) = \sqrt{K_1 C}$ for a solution of H_2A . Four pages are used to derive the equation for a simple buffer system. Such love of detail may please the purist, but think of the poor student who thought he was going to learn something about analysis!

The next 220 pages present detailed discussions of titration curves, including about six pages on the oxidation of organic compounds and a short chapter on nonaqueous solvents (without mentioning the "leveling" effect). An adequate chapter on gravimetric analysis includes a brief mention of the use of a thermobalance to obtain pyrolysis curves.

The chapter on electrochemistry does contain five pages on ion-selective

electrodes and discussions of coulometric titrations and polarography which resemble the material in J. J. Lingane, "Electroanalytical Chemistry," and L. Meites, "Polarographic Techniques." A fairly standard treatment of visible light absorptiometry is given. The author's devotion to equilibrium calculations is obvious in his rigorous handling of the Craig separation followed almost immediately by all of three pages on gas-liquid chromatography. The final chapter gives rather brief, cookbook style procedures for a variety of both standard and few more modern student experiments.

A few surprises are to be found. On page 15, the oxidation state of O in $NaHSO_4$ is given as -2, but its oxidation number is said to be -8. On page 86 a Greek α is used to represent both the proportionality sign and as a symbol for activity, all in the same line without definitions. HCl, HNO_3 , and $HClO_4$ are listed as "organic acids" on page 92, and Na_2A is called a "dibasic acid salt." The word "desiccator" is misspelled throughout the text.

The author's style is scholarly but pedantic. The instructor will find it difficult to teach from, and the student will find it dull. It is doubtful that many students will be turned on by the frequent pleas, "It is suggested that an appropriate student project would be the development of such exact and approximate equations." Extensive problem sets are given in each chapter, but many of these involve too much repetitive busy work.

To summarize, there is little in this text that could not be found in the texts of 30 years ago. The author has overemphasized the rigorous handling of equilibria without giving a comparable or even an adequate description of careful laboratory manipulative techniques. There is hardly an insight as to how real analyses are performed in a modern laboratory.

New Books

Undergraduate Instrumental Analysis. Second edition. James W. Robinson. xvii + 379 pages. Marcel Dekker, Inc., 95 Madison Ave., New York, N.Y. 10016. 1973. \$12.75

The object of this book, written with the nonchemistry major in mind, is to present a survey of recent innovations in analytical chemistry. For example, in the fields of spectroscopy, an attempt has been made to provide a simple approach to each development. It is not expected that

Take a fresh look at our array of instruments for measuring solution conductivity in the laboratory...

From Beckman — the leading name in solution conductivity equipment — this newly revised technical brochure provides basic theory, methods and equipment for the laboratory measurement of solution conductivity.

16 pages of information on bridges, indicators, recorders, cells, calibrating supplies and other accessories. Also, provides brief data on other types of lab test instruments and equipment from Beckman.

Send for your free catalog today

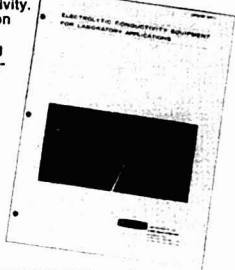
Use this publication's Reader Service Card, or write directly to:

Beckman

INSTRUMENTS, INC.
CEDAR GROVE OPERATIONS
89 COMMERCIAL ROAD
CEDAR GROVE, NEW JERSEY • 07009
(201) 239-6200 • TWX: 710-994-5781

HELPING SCIENCE AND INDUSTRY IMPROVE THE QUALITY OF LIFE

CIRCLE 26 ON THE READER SERVICE CARD
FOR A SALES ENGINEERING CALL CIRCLE 27



LET YOUR DISPOSABLES LIVE A LITTLE!

Critical situations require critical solutions. Today's supply of raw materials is creating shortages certain to result in higher prices. Finding a way to **clean and reuse** disposables has become a necessity! From the standpoint of availability and economy, ALCONOX® and LIQUI-NOX® help extend the life of your disposables... Pipettes, syringes, test tubes, emesis basins, bed pans, petri dishes, flasks, and other washable products. **The time to reuse them is now.**

DON'T EXPEND— EXTEND— WITH ALCONOX!



For Manual and Ultrasonic Cleaning.

Write for FREE SAMPLES now!



ALCONOX-POWDER DETERGENT

	Prices*
3 lb. box	\$ 3.00
Case (12 x 3 lb.)	27.00
25 lb. drum	17.50
50 lb. drum	31.50
100 lb. drum	58.00
300 lb. drum	150.00
50 pack dispenser box	3.50
Case (12 x 50 dispenser box)	28.00

LIQUI-NOX-LIQUID DETERGENT PHOSPHATE-FREE

	Prices*
1 qt. container	\$ 2.75
Case (12 x 1 qt.)	24.00
1 gal. container	8.80
Case (4 x 1 gal.)	30.00
15 gal. drum	88.00
55 gal. drum	280.00
*Slightly Higher on West Coast	

FOR MECHANICAL WASHERS,
USE ALCOJET®...The Scientific Detergent

Available from your local Hospital or Lab Supply Dealer, or write:

ALCONOX, INC.
215 Park Avenue South, New York, N.Y. 10003

HELLMA

...tomorrow's designs today!

OS QH QS OF QU QI

Hellma—the largest assortment of highest precision glass and quartz cells.
Standard • Flow-through • Constant-temperature Anaerobic • Special Designs
Also available—ULTRAVIOLET LIGHT SOURCES
Deuterium Lamps • Mercury Vapor Lamps
Hollow Cathode Lamps • Power Supplies

HELLMA
CELLS, INC.

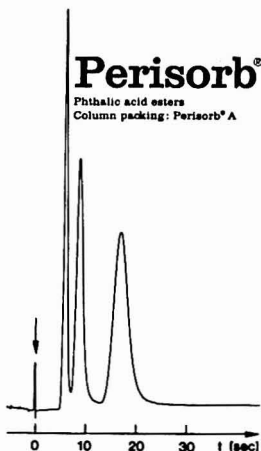
Write for literature
Box 544
Borough Hall Station
Jamaica, New York 11424
Phone (212) 544-9534

CIRCLE 116 ON READER SERVICE CARD

CIRCLE 1 ON READER SERVICE CARD

EM Reagents®

Products for High Performance Liquid Chromatography



Perisorb®

Perisorb® — these column packing materials have a chromatographically inert glass core with a coating of adsorptive silicon dioxide approximately one micron thick.

Perisorb® A: adsorption-active layer of silicon dioxide

Perisorb® RP: chemically modified support with a hydrolysis-stable, hydrophobic layer. Perisorb® KAT, shell of strong-acid cation exchanger. Particle size 30-40 µm.

LiChrosorb™

Column packing materials

LiChrosorb™ * totally porous HPLC column packings. LiChrosorb™ SI 60, LiChrosorb™ SI 100, LiChrosorb™ Alox T, LiChrosorb™ SI 60 silanized, mean particle sizes: 5 µm, 10 µm, 30 µm

*A registered trade name of
EM Laboratories, Inc.

EM Laboratories, Inc.

Associate of E. Merck, Darmstadt, Germany
500 Executive Boulevard
Elmsford, New York 10523
Phone 914/592-4660

CIRCLE 65 ON READER SERVICE CARD

Books

the student will become an expert after reading this book, but he should become aware of the principle features of the methods such as the information they provide, the difficulties involved in obtaining this information, and what information cannot be obtained from these different methods. No discussion of volumetric and gravimetric analysis is presented since the author feels that these subjects are more than adequately treated elsewhere.

Comprehensive Inorganic Chemistry.

J. C. Bailar, Jr., et al., Eds. 6000 pages. Pergamon Press, Inc., Fairview Park, Elmsford, N.Y. 10523. 1973. \$386 (five-volume set)

This reference set is designed to "fill the gap between the typical one or two volume inorganic textbooks and the existing multi-volume series which have reviewed the Periodic Table intermittently with upwards of ten volumes, often scattered over as many years."

The Analysis of Slags and Related Oxide-Type Materials—Audio Symposium.

Special Technical Publication 542. Publication Code No. 04-542000-39. Two cassettes and booklet. American Society for Testing and Materials, 1916 Race St., Philadelphia, Pa. 19103. 1973. \$12.75 (For countries other than U.S.A., Canada, and Mexico, add 5% shipping charges)

This 3-hr audio symposium contains discussions on the application of multichannel spectrometers to elemental analysis, current status of X-ray emission analysis, atomic absorption spectrophotometry, and optical emission spectrometers as used in the analysis of slags and related materials.

Guide to Modern Methods of Instrumental Analysis. T. H. Gowd, Ed. xii + 495 pages. John Wiley & Sons, Inc., 605 Third Ave., New York, N.Y. 10016. 1972. \$19.95

This "Guide" uses theoretical material as well as specific methods to describe the most widely used procedures for instrumental analysis. Its aim is to provide the reader with the information necessary "to understand the role of each technique in the solution of a particular problem, to easily

compare the different techniques, and to integrate two or more techniques for wider applications." The subjects covered are gas, high-resolution liquid, thin-layer, paper, and gel permeation chromatography; visible, ultraviolet, infrared, Raman, nuclear magnetic resonance, and electron spin resonance spectroscopy; mass spectrometry; GC/MS; electroanalytical methods; and differential thermal and thermogravimetric analysis. The book is intended as an advanced guide, and although not an exhaustive survey, it is comprehensive enough to give the reader the most important information.

Analytical Methods Developed for Application to Lunar Sample Analyses.

Special Technical Publication 539. Publication Code No. 04-539000-38. 156 pages. American Society for Testing and Materials, 1916 Race St., Philadelphia, Pa. 19103. 1973. \$15 (For countries other than U.S.A., Canada, and Mexico, add 5% shipping charges)

This publication describes the present status of advanced testing methods used in lunar sample analysis. Particular emphasis is placed on the description and evaluation of the various experimental techniques as opposed to lunar science conferences which have emphasized interpretation of the results.

Continuing Series

Annual Reports on Analytical Atomic Spectroscopy: Vol 2. D. P. Hubbard, Ed. x + 216 pages. Society for Analytical Chemistry, 9/10 Savile Row, London, W1X 1AF, England. 1973. \$13

References in the text are given to over 1100 papers which appeared in the literature or were presented at conferences, symposia, and meetings in 1972. The references are numbered in approximately chronological order. An attempt was made by the editor to be comprehensive, critical, and constructive. The contents are divided into two parts: fundamentals and instrumentation (light sources, excitation sources and atomizing systems, optics, detector systems, data processing, complete instruments, and ancillary equipment); and methodology (general techniques and applications).

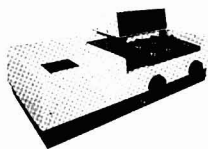
Ion Exchange and Solvent Extraction: Vol 5. Jacob A. Marinsky and Yizhak Marcus, Eds. xii + 278 pages. Marcel Dekker, Inc., 95 Madison Ave., New York, N.Y. 10016. 1973. \$19.75

Recipes to keep you out of "hot water" with the EPA...

Now, from the makers of the world's most ultra-modern UV Visible Digital Spectrophotometers, comes a "cookbook" you can't afford to pass up. And it's **FREE**.

That's right. Hitachi Scientific Instruments has compiled a new booklet that applies methods of water and waste analysis to Hitachi's Models 101, 102, 181 and 191 spectrophotometers. The booklet describes 15 spectrophotometric methods of water and waste analysis — in a concise, step-by-step "cookbook" fashion. All methods are in strictest compliance with the latest Federal Environmental Protection Agency (EPA) guidelines.

Stay out of "hot water" with the EPA the easy way with a **FREE** Hitachi water and waste analysis booklet. Address your inquiry to: Nissei Sangyo Instruments, Inc., 2672 Bayshore Frontage Road, Mountain View, CA 94040, (415) 961-4235.



Gentleman:

Thanks. I want to stay out of "hot water" with the EPA. Please send me your **FREE** Hitachi cookbook.

Name _____

Organization _____

Address _____

City _____

State/Zip _____

CIRCLE 123 ON READER SERVICE CARD

Contained in this volume are discussions of new inorganic ion exchangers, application of ion exchange to element separation and analysis, and pellicular ion-exchange resins in chromatography.

Organic Electronic Spectral Data: Vol 9. John P. Phillips, Henry Feuer, and B. S. Thyagarajan, Eds. xiii + 960 pages. John Wiley & Sons, Inc., 605 Third Ave., New York, N.Y. 10016. 1973. \$40

This series is an effort to abstract and publish in formula order all the ultraviolet-visible spectra of organic compounds presented in the journal literature. The total collection, throughout the volumes so far published, amounts to nearly 200,000 spectra. The data in this volume were abstracted from 109 journals and generally had to satisfy the following requirements: the compound had to be pure enough for satisfactory elemental analysis and for a definite empirical formula; solvent and phase had to be given (some spectra are mentioned, even if the solvent was most likely ethanol); and sufficient data to calculate molar absorptivities had to be available. Wavelength values for all maxima, shoulders, and inflections and the logarithms of the corresponding molar absorptivities are given.

Encyclopedia of Industrial Chemical Analysis: Vol 18. Foster Dee Snell and Leslie D. Ettre, Eds. xiv + 545 pages. John Wiley & Sons, Inc., 605 Third Ave., New York, N.Y. 10016. 1973. \$40 (\$35 by subscription)

This latest volume proceeds from Si, through Si organic compounds, Ag, soaps, Na, steel, Sr, styrene and its polymers, sugar, S, Ta, tea, and Ti, to thiophene.

Methods of Biochemical Analysis: Vol 21. David Glick, Ed. viii + 572 pages. John Wiley & Sons, Inc., 605 Third Ave., New York, N.Y. 10016. 1973. \$22.50

Subjects covered in this volume include techniques for the characterization of tightly bound microsomal enzymes, determination of selenium in biological materials, analysis of nucleic acid constituents at the subnanomole level by high-performance ion-exchange chromatography with narrow-bore columns, enzymic determination of D-glucose and its anomers, radiometric methods of enzyme assay, polarography and voltammetry of nucleosides and nucleotides and their parent bases, and chemical and biological applications of integrated ion-current quantitative mass spectrometric analysis.

EM Reagents®

If Plastic-backed TLC layers are your Preference, you'll prefer EM's

A major difference between EM pre-coated TLC plates and others is that EM is an associate of E. Merck, Darmstadt, Germany, a chemical company, and we make our own special TLC formulations.

Our special formulations yield plastic-backed TLC layers which are tough and stable. They possess advantages for storage, packaging and shipping which do not alter chromatographic properties.

But most important, if you now use EM's glass plates, and most everyone does, you do not have to change your system. You can transfer techniques between our different backings to pick the most suitable for any separation.

Specify EM pre-coated TLC products. Available from selected distributors throughout the country.

EM pre-coated TLC products

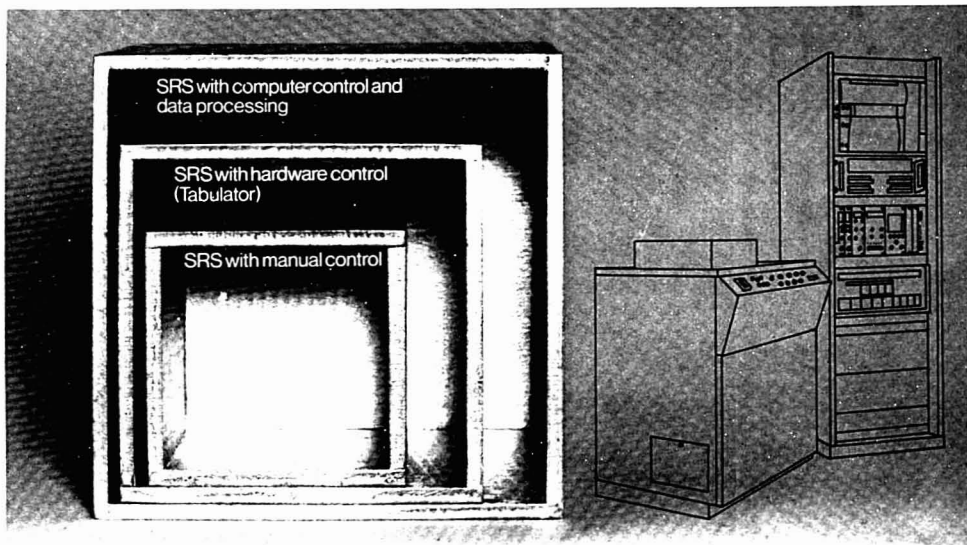
EM Laboratories, Inc.

ASSOCIATE OF E. Merck, Darmstadt, Germany
500 Executive Boulevard
Elmsford, New York 10523
Phone 914/592-4660

CIRCLE 66 ON READER SERVICE CARD

SIEMENS

The key to perfect analysis



Modular design stands for free combination and step by step extension. The sequential X-Ray Spectrometer SRS has been for years a concept of high performance analysis. Continuously modernizing technology and consistent modular block principle, make it more than ever the equipment of your choice today.

Versatile analytical problems require versatile instruments with extension capability at reasonable and economical prices. This is offered by the Siemens SRS system with its different versions. Since the several hundred installed SRS are so universal, they analyze al-

most everything: ... Glass, blood, grain, soil, meat, aluminium, oil, dust, water, coal, steel, paint, cement, milk, non-ferrous metal, plants, gasoline, pharmaceutical products, ...

Further information concerning our X-Ray Analysis Spectrometers can be obtained from the Siemens Offices or through Siemens Corporation, 186 Wood Avenue South, Iselin, New Jersey 08830.

Sequential X-Ray Spectrometer SRS

Some special features:

- 4-kW generator with equipment for simultaneous operation of two tubes (highly stabilized constant potential)
- 10 analyzer crystals available
- X-Ray tubes with Au, W, Mo, Cr, Rh-targets (assymetrical located)
- Hardware or computer control with a new evaluation program TP 88/SP 88 - powerful and flexible
- Compact electronic modules according to the NIM AEC standard

X-Ray Analytical Equipment

CIRCLE 233 ON READER SERVICE CARD

E 632/7403-101

The Analytical Approach

With this issue of the Journal, we begin a new feature entitled "The Analytical Approach." The title was inspired by an editorial by Dr. Laitinen [*Anal. Chem.*, **42**, 1121 (1970)] in which he discussed the "two equally important aspects" of analysis, research and service. It is a curious fact that even though most analytical chemists—indeed, most practitioners of any profession—spend most of their time solving problems as a service to someone else, there is no place to report the general approach taken in recognizing and solving problems. This vital role of the analytical chemist is scarcely mentioned in our journals, and it is virtually ignored in our formal training. It is the intent of the feature to illustrate how the analytical chemist solves problems via definition of the problem and choice of the most suitable method or combination of methods to arrive at a solution consistent with the urgency and priority of the problem. Stress will be placed on the generality and the novelty of the approaches presented, and a special effort will be made to point out what was *not* as well as what was done.

The feature is expected to be of particular interest to the "generalist" project leader in the industrial analytical laboratory and to the analytical manager who must keep methods in a complementary relationship so that the particular advantages and limitations of the methods are balanced for each problem. It is hoped that the articles also will be useful to teachers of analytical chemistry who may use the examples presented to show their students the scope and excitement involved in the service aspect of professional analytical practice.

A great deal of effort has gone into making this feature a reality. As early as 1967, Henry Freiser, as a member of the Editorial Advisory Board, proposed the idea of publishing a feature entitled "Casebook of Analytical Problems" to show the "problem approach counterpart to the method and technique approach of most of the Journal articles." After discus-

sions with the editors and the Advisory Board, he wrote to many industrial laboratories for contributions, but with little success. He encountered the same reluctance as I did initially in soliciting papers for the Fall 1973 ACS Symposium on "The Analytical Approach to Problem Solving" (*Chem. Eng. News*, p 21, Sept. 1973). There is a tendency to judge a possible contribution from an industrial laboratory as either too proprietary or too technically trivial to report.

In 1969, after I had given a seminar on "Analytical Problem Solving" at the University of Illinois, Dr. Laitinen asked me to see about rekindling the idea of a problem-solving column. After several attempts, I managed to put together the 1973 Chicago Symposium and from it obtained the commitments for the first four contributions to the feature which will appear at irregular intervals. The chemists and the companies that participated in the Symposium deserve our special thanks.

The 1973 Symposium was successful because the time has come for "The Analytical Approach." More and more, the analytical chemist will make his most important contribution through his problem-solving abilities. The shortening life cycle of chemical products means more frequent plant start-ups and the attendant analytical problems associated with plant debugging and with new production and sales promotion schedules. The increased activities of environmental and consumer interest groups mean more analytical problems. On the other hand, the need for specialists to support the generally diminishing synthesis programs in industry probably will decrease because of the escalating cost (health and environmental data) of bringing new compounds to market. Even the rapid changes in analytical chemistry itself mitigate against the flourishing specialists of the 1960's. Laboratories find it more difficult to support a specialist for each of the new tools now entering the analytical laboratory. For example, witness the availability of commercial analytical ser-

vices by Du Pont and Dow [*Anal. Chem.*, **44**, 649 (1972)]. More than ever, there is a need to recognize and to encourage the unique and vital role of the analytical generalist by providing a place for him to report his work. On page 433 A is my contribution to initiate "The Analytical Approach."

Claude A. Lucchesi



Claude Lucchesi is lecturer and director of analytical services for the Chemistry Department at Northwestern University. He received a BS in chemistry from the University of Illinois in 1950 and earned a PhD at Northwestern University in 1954. After serving as spectroscopy group leader at Shell Development Co., Houston, Tex., from 1954-56, he became director of the Analytical Research Department of Sherwin-Williams Co. in Chicago. In 1961 he joined Mobil Chemical Co. and was head of their Analytical and Physical Chemistry Department in the Metuchen, N.J., Research Laboratory until 1966 when he became manager of Mobil's Coatings Division laboratory. He has been at Northwestern since 1968. Dr. Lucchesi has over 30 papers in his fields of research interest of analytical chemistry, applied spectroscopy, and polymers and coatings. He is active in the Chicago ACS and SAS Sections and has recently been elected an ACS Councilor. He is also a member of the Governing Board of the recently formed Federation of Analytical Chemistry and Spectroscopy Societies (FACSS).

Now there's a REPIPET® Dispenser and Dilutor for every lab need.

The six REPIPET® Dispensers shown here are but a few of the many models Labindustries can supply you for precise repetitive measurements. Every lab reagent — even corrosives — can be used with REPIPET Dispensers except

HF. Choose from 1, 5, 10, 20 and 50 ml sizes, all with 50% lifetime guarantees. Take a moment to circle the reader number for our free new catalog "L/I REPIPETs and Dilutors."

1. Universal REPIPET Dispenser fits any container from 1/2 ml up to 5 gallons. Simply cut the TEFLON® tubing to fit. 10 ml model \$75.

2. **NEW** Low Silhouette with new 2-opening wide-mouth container. Leave the instrument in place, use the second opening to refill with reagent. This 10 ml unit \$66.50 including container.

3. **NEW** REPIPET Jr. Dispenser only \$29.50. An unbreakable plastic 0.5% precision dispenser for non-corrosive reagents. We include chemical resistance chart.

5. **NEW** AUTO-REPIPET Dispenser features air-activated foot-operated pedal — frees both of your hands for other work. The safest way possible to dispense corrosives. Model shown is \$160.

6. **NEW** MINI-REPIPET Dispensers. Especially suited for dispensing directly from diagnostic reagent containers 1/2 ml and larger with 0.1% precision. Avoid the hazards of mouth pipetting! All standard sizes \$63.50.

4. **NEW** REPIPET Dilutor. This simple, precise and low cost Dilutor now features sturdier construction and low profile container. Many models 1 to 50 ml. 10 ml model with 1 ml aspirator \$118.50.

Order from Labindustries or your distributor.

LABINDUSTRIES

1802 Second Street, Berkeley, CA 94710
Phone (415) 843-0220. Cable LABIND, Berkeley

CIRCLE 151 ON READER SERVICE CARD

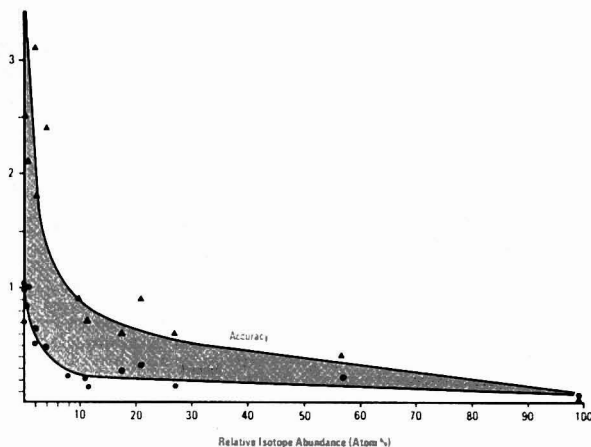


Figure 1. Percent accuracy and precision of isotope abundance measurements as functions of relative abundance on gases introduced from reservoir

Direct Analysis of Stable Isotopes with a Quadrupole Mass Spectrometer

R. M. Caprioli

Department of Chemistry
Purdue University
West Lafayette, Ind. 47907

W. F. Fies and M. S. Story

Finnigan Instrument Corp.
595 N. Pastoria Avenue
Sunnyvale, Calif. 94086

Isotope ratios can be determined with high precision by quadrupole mass spectrometry even under the dynamic conditions imposed by combined gas chromatography-mass spectrometry. Applications abound especially in chemistry, biology, and medicine

Interest in the use of stable isotopes has sharply increased in recent years in all fields of chemistry, biology, and medicine as a combined result of a decrease in the cost of stable isotopes, advances in the design and performance of magnetic resonance and mass spectrometric instrumentation, and the general concern over the hazards of radioactive isotopes. Of particular utility in isotope methodology is the emergence of mass spectrometric techniques designed to simultaneously determine the abundance of a particular isotope and also its location within the molecule. This direct analysis thus provides much structural information and has considerable advantage over other isotope techniques which require complex degradative procedures to locate the isotopic atom.

Stable isotopes have been used in a wide variety of applications, most of which involve their use as tracers either to follow the fate of a particular atom in a reaction series or an entire molecule in a complex system. For example, tracing particular atoms of a molecule is vital to the elucidation of the origin of certain atoms of cellular metabolites in biosynthetic stud-

ies (1, 2) or in the study of reaction mechanisms where the fate of one or more atoms is diagnostic of a particular mechanism (3, 4). Specific isotopic labeling is also used when the fate of the entire molecule is of interest, such as in studies of the metabolism of drugs or other compounds in living cells (5) or in isotope dilution experiments in which quantitative analyses are sought. In view of the increasing use of stable isotopes, it is becoming of critical importance to develop mass spectrometric techniques which attain better accuracy in the measurement of isotope abundances in complex molecules. In addition, the use of the technique of mass fragmentation in which samples containing mixtures are analyzed by continuous ion monitoring also requires accurate ion intensity measurements if quantitative data are to be obtained. This is of significant value in the analysis of drugs, drug metabolites, and other compounds at subnanogram levels (6).

Direct Analysis of Stable Isotopes

Direct analysis of stable isotopes involves measurement of ion intensi-

ties of the several isotopic species of a molecular or fragment ion formed in a mass spectrometer. In addition, if structural information is required, a study of fragmentation reactions through the use of normal and specifically labeled compounds may also be necessary. The alternative method for the mass spectrometric analysis of stable isotopes is indirect and involves the combustion of the sample to a gas, usually H_2 for deuterium analysis, N_2 for ^{15}N analysis, and CO_2 for ^{13}C and ^{18}O analyses, followed by measurement of the isotope ratios of these gases (7). However, this method has the disadvantages of providing no structural information; requiring relatively large amounts of sample, usually at least 1 mg; and poor accuracy as a result of the simultaneous combustion of contaminants or incomplete combustion, even though the mass spectrometric ratio measurement may have a precision as high as $\pm 0.001\%$.

Although direct analysis of stable isotopes is the method of choice in many cases, it has not become a routine tool because of the relatively poor precision obtained in isotope ratio determinations by use of magnetic mass spectrometers. To be of general utility, methods for direct analysis must be able to achieve a precision of approximately $\pm 0.1\%$ or better with microgram or nanogram quantities of sample injected into the GC inlet of a mass spectrometer. Many biomedical experiments involve the isolation of small amounts of samples containing low isotope abundances. In many cases, even high initial isotope concentrations give low abundance products owing to the enormous dilution of the isotopic compound by the system. In addition, better precision in measurement would also permit the use of isotope methodology in low enrichment experiments where, previously, the high cost of high enrichments was prohibitive.

To achieve high precision in the measurement of the intensities of two or more ions, it is desirable to measure these ions simultaneously in the manner of double collector techniques used with isotope ratio mass spectrometers. However, the fixed focus of magnetic instruments and use of a Faraday cup collector, which are essential to the high precision achieved with this method, do not lend themselves to ratio measurements on high mass and low abundance ions. The potential solution to these problems lies in the utilization or repetitive scanning techniques. Thus, Hites and Biemann (8) used continuous rapid scanning over a given mass range to measure ion intensities. Although this was an improvement over data ob-

tained from individual mass spectra, scanning a portion of the mass spectrum in this manner results in poor ion statistics since a great deal of time is spent between peaks where ions are not collected. In another approach, Sweeley et al. (9, 10), Klein et al. (11), and, more recently, Holmes et al. (12) and Watson et al. (13) used an accelerating voltage alternating (AVA) device to continuously switch the accelerating voltage in a cyclical manner so as to successively focus a series of ions at the collector. The precision of isotope ratio measurements achieved with this method was approximately $\pm 1\%$. Limitations of the AVA technique are detuning of the ion source when the accelerating voltage is changed, relatively slow switching rates demanded by the high voltages involved, and the requirement that the mass difference in ions to be compared may not be greater than about 40%.

Advantages of Quadrupoles

Quadrupole mass analyzers present some attractive features in the pursuit of higher precision isotope ratio measurements. First, the electrostatic voltages used to produce mass dispersion can be switched rapidly and measured accurately. Thus, in a high switching rate mode, each ion of an isotope series would be collected for a time on the order of milliseconds with continuous cycling over the series of ions to be measured. Such a system would approach the ideal of simultaneous collection of ions used with the double collector method. Thus, with rapid switching, only those instabilities or pressure changes comparable to the switching rate will affect the abundance measurements. Since the dead time or settling time between masses is small (~ 1 msec), almost all the time the sample is in the instrument is spent collecting the ions of interest. Thus, compounds emerging from the GC having a duration of several seconds can also be analyzed. Second, ions in a particular series may be collected for different amounts of time depending on their relative abundances, maximizing ion statistics. Third, any ions in the spectrum, no matter their mass difference, may be measured in a particular analysis and need not lie within a given percentage of the mass range.

During the past five years, the improvement of quadrupole mass spectrometer design and performance has virtually eliminated difficulties generally associated with these instruments, such as lack of high mass sensitivity and peak-tailing, and has provided capabilities which are comparable to magnetic deflection instruments in this regard. Quadrupole mass spec-

trometers, already in the forefront of GC/MS methodology, further hold the potential of becoming a primary instrument for the direct analysis of stable isotopes.

In the work described here, isotope abundances were determined on a variety of samples with a quadrupole mass spectrometer. These include some of the inert gases and ^{18}O -labeled sugars. The inert gases are ideal samples for testing both precision and accuracy of isotope abundance measurements because their abundances are known exactly and because there is a single isotopic species per mass, unlike organic compounds where there may be mixtures of carbon, hydrogen, nitrogen, and oxygen isotopes at a particular mass. In addition, the range in the relative abundances is large, being nearly 1600:1 for m/e 40: m/e 38 for argon and 1:1 for certain isotopes of krypton and xenon. Thus, in the experiments which follow, Ar, Kr, and Xe were employed as standards. Their isotope abundances were measured by use of a data system to analyze samples introduced both from a reservoir inlet in which the pressure is stable and from the GC inlet in which the pressure is constantly varying. The measurements obtained from the data system were also compared with those obtained with the programmable multiple ion monitor (PROMIM) coupled to digital integrators. A second series of experiments was performed involving measurement of isotope ratios in fragment ions of natural abundance and ^{18}O -enriched pentaacetylglucose samples introduced into the mass spectrometer via the GC inlet. This experiment was also performed with the multiple ion monitor-integrator system, and the results were compared with those obtained from the data system. The precision and accuracy of the measurement techniques are given together with a discussion of critical parameters involved in such measurements.

Experimental

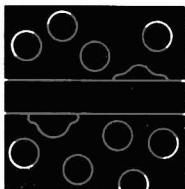
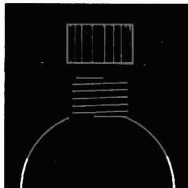
The inert gases (analyzed grade) were obtained from Matheson Gas Products. ($2\text{-}^{18}O$) and ($6\text{-}^{18}O$) pentaacetylglucose were prepared and analyzed as previously described (12).

A Finnigan Model 3100 quadrupole mass spectrometer equipped with a Model 9500 gas chromatograph and a Model 6000 data system was used for the determination of isotope abundances. For ion detection, a 14-stage beryllium-copper electron multiplier was employed. The mass spectrometer was equipped with a 1-liter reservoir inlet system for the introduction of gases. For GC studies, a 3-m \times 2-mm

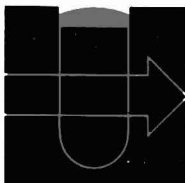
Just add sample... shake and count

**ScintiVerse™
Fisher Universal
Scintillation
Cocktail**
is specially
formulated to give
**you maximum
counting efficiency
with all types
of samples**

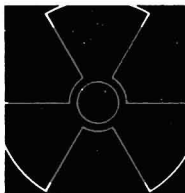
Use ScintiVerse™ Universal Cocktail right from the bottle, with any sample. No mixing. Unique formula insures maximum counting efficiency — even in the 18% water content range where some cocktails give you only partial readings or none at all.



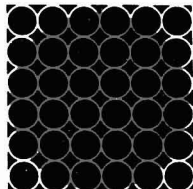
ScintiVerse is one of the most convenient and versatile liquid scintillation counting media you can buy. It's also one of the most thoroughly purified and tested.



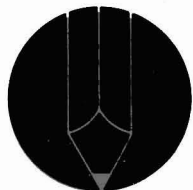
Purification eliminates contaminants that would quench energy, shift spectral absorbance, increase background, or cause chemiluminescence. Lot analysis determines purity and spectral absorbance. Pertinent information is printed on the label.



Use-testing on contemporary instrumentation insures low background, counting efficiency and quench resistance.



Depend on your nearest Fisher branch for immediate delivery of all your Scintanalyzed™ Reagents, including ready-to-use cocktails, space-saving pre-measured concentrates and dry mixes, economical primary and secondary scintillators. All are carefully tested to insure reliable results, consistently high counting efficiency, and lot to lot reproducibility.



ScintiVerse is one of the most convenient and versatile liquid scintillation counting media you can buy. It's also one of the most thoroughly purified and tested.



Fisher Scientific Company

711 Forbes Avenue
Pittsburgh, Pa. 15219

(i.d.) OV-1 column was used. A mass defect adjust device was installed in the mass calibrate circuit so that after calibration with perfluorotributylamine, the mass set point could then be moved the proper fraction of a mass unit, depending on the mass defect of the ion to be measured, to monitor the top of the mass peak. That this indeed occurred was verified by using the "diagnostic" mode of the data system which allows the operator to observe on the oscilloscope display the peaks of interest and the point on these peaks at which the instrument is calibrated.

Ion intensities for the isotope abundance determinations were obtained by using the mass fragmentography program of the data system in which, for a given mass, ions are collected through a series of sampling times, 1, 2, 4, 8, 16, 32, and 64 msec or until the analog-digital converter saturates. At this point, the computer will store the total signal intensity accumulated at the time prior to saturation and then shift to the next ion in the isotope series and repeat those operations. Thus, the time spent collecting ions of a given mass varied from 1 to 64 msec, depending upon the intensity of the ion current. After the last isotope in a series was measured, the system immediately recycled to the first, providing continuous monitoring throughout the analysis. Isotope ratios were determined by using the area under the peaks produced by the mass chromatograms, i.e., the curve produced from a plot of ion intensity vs. time for a given isotope. A total of four ions could be monitored at one time. For isotope series containing more than four ions, one ion was arbitrarily chosen as unity, and the others were calculated as a ratio of this. The abundance measurement of the ion normalized on was repeated in each set of determinations until all isotopic species were measured. The oscilloscope display of the data system allows the mass chromatogram to be observed as the data are being acquired. When this is complete, the operator can then choose the two points on the mass chromatogram through which a base line should be drawn. The two points between which the peak area is to be calculated are then chosen, and finally the peak area is obtained in arbitrary units or as a voltage, with the portion of the background under the peak subtracted. Other ions in the isotope series are then similarly measured and their relative abundances calculated.

The precision of the measurements presented in the tables which follow is given in terms of the mean deviation as a percent of the average value

calculated from four to six independent determinations of each isotopic species. The percent accuracy of the measurements is given as the percentage by which the average abundance differs from its true value.

In the experiments where the programmable multiple ion monitor (PROMIM) was used, each isotopic species was monitored on a separate channel of the unit, and the ion current measured by individual digital integrators (Autolab Model 6300). The ion monitor was modified to sweep over the top of each peak covering a range of approximately 0.25 amu, rather than remain stationary. Sampling times of 1, 10, and 100 msec could be chosen for each sweep. As before, the instrument switched from peak to peak continuously throughout the analysis.

Results

Reservoir Samples. The relative abundances measured for the inert gases are given in Table I. The gases were admitted from a 1-liter reservoir at room temperature through a molecular leak to give an indicated ion source pressure of approximately 5×10^{-7} torr. Measurements were obtained with the data system in the mass fragmentography mode, as described earlier, with a total sampling time of 5 min. Since a maximum of four ions could be monitored simultaneously, for krypton and xenon, isotope abundances were determined as ratios of m/e 82 and 129, respectively,

and then relative abundances calculated. The precision and accuracy attained as a function of isotope abundance are shown in Figure 1.

GC Samples. To make a direct comparison of the precision and accuracy possible between the reservoir gas sample where the pressure is not changing and a more dynamic case of GC samples where sample pressures are constantly changing, xenon and krypton were introduced via the GC inlet at room temperature by using a gas-tight syringe. The results are given in Table II. As a typical example, Figure 2 shows the mass chromatogram of xenon at m/e 124, the lightest and least abundant isotope, taken on continuous monitoring with the injection of four different samples. Each GC peak was of approximately 8-sec duration. The abundances of each of the four peaks shown in Figure 2 were, from left to right, 0.098%, 0.093%, 0.095%, and 0.095%, with the true value being 0.096%. The greater precision of the last two reflects the effect of better ion statistics.

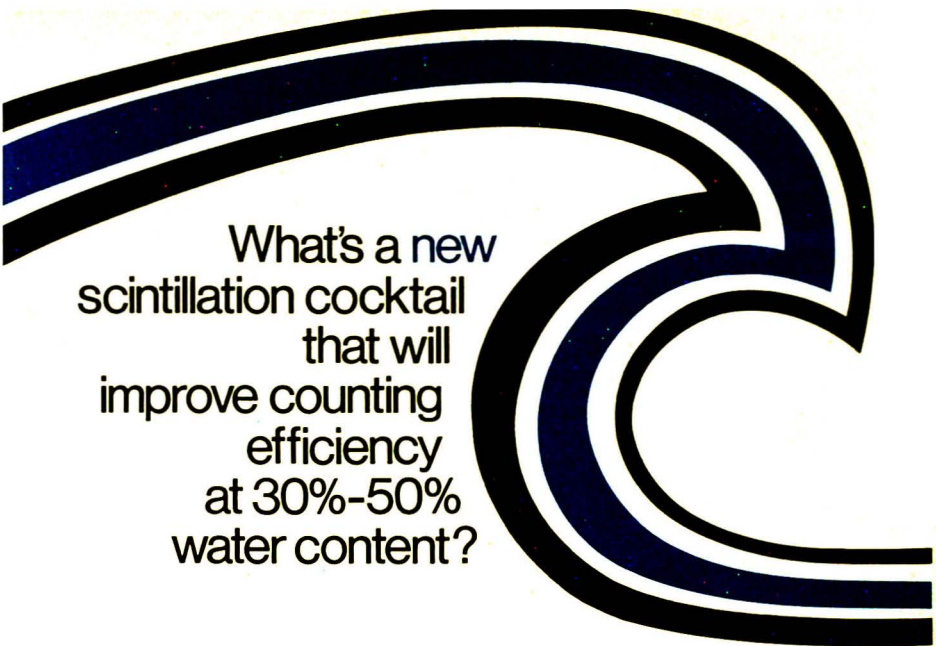
Comparison of the data given in Table II for GC analyses to that in Table I for reservoir analyses shows comparable accuracy and precision. Thus, it can be concluded that with the rapid peak-switching system used here, changes in sample pressure encountered with GC samples are sufficiently slow compared to the switching time so as to have no significant effect on abundance measurements.

Isotope abundances of fragment

Table I. Isotope Abundance Measurements on Some Inert Gases from Reservoir Sample System

Sample	m/e	Theoretical rel abundance, %	Measured rel abundance, %	Accuracy, %	Precision, %
Argon	36	0.337	0.344 ± 0.003	+2.1	± 1.0
	38	0.063	0.067 ± 0.0005	+6.0	± 0.7
	40	99.600	99.587 ± 0.003	-0.01	± 0.03
Krypton	78	0.35	0.39 ± 0.003	+11.4	± 0.83
	80	2.27	2.31 ± 0.015	+1.8	± 0.64
	82	11.56	11.51	-0.4	
	83	11.55	11.63 ± 0.015	+0.7	± 0.13
	84	56.90	56.69 ± 0.12	-0.4	± 0.22
	86	17.37	17.47 ± 0.05	+0.6	± 0.28
Xenon	124	0.096	0.098 ± 0.001	+2.1	± 1.0
	126	0.090	0.095 ± 0.001	+5.5	± 1.0
	128	1.92	1.98 ± 0.01	+3.1	± 0.50
	129	26.44	26.41	-0.1	
	130	4.08	4.18 ± 0.02	+2.4	± 0.48
	131	21.18	21.37 ± 0.07	+0.9	± 0.33
	132	26.89	27.05 ± 0.04	+0.6	± 0.14
	134	10.44	10.35 ± 0.02	-0.9	± 0.20
	136	8.87	8.53 ± 0.02	-4.0	± 0.23

* Handbook of Chemistry and Physics, 51st ed., Chemical Rubber Co., 1971. * Ion normalized on.



What's a new
scintillation cocktail
that will
improve counting
efficiency
at 30%-50%
water content?

HANDIFLUOR™

New **HANDIFLUOR™ SCINTILLAR®** is making waves. It's a complete cocktail for liquid scintillation counting that does the job you've always wanted done. **HANDIFLUOR** handles both aqueous and non-aqueous samples, forming brilliant clear solutions or firm translucent gels when you need them. And **HANDIFLUOR** really shines when you count the tough ones, like tritium at low concentrations. You need the extra 50%—100% counting efficiency that **HANDIFLUOR** can give you in these tough spots... and it works at both low and ambient temperatures.



You'll find that every lot of **HANDIFLUOR** is controlled and use-tested for freedom from quenching and minimized chemiluminescence. In short, every lot is controlled for optimum counting efficiency against stringent Mallinckrodt standards—the highest in the industry.

Compare **HANDIFLUOR** with your present cocktail. Packaged in our Safemore® gallon jug and available locally from your favorite distributor (Mallinckrodt No. 4022). Or write us for complete information.

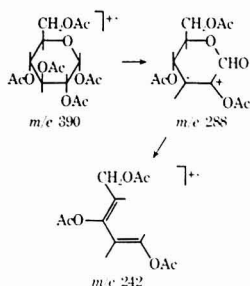
The label
you can trust

Mallinckrodt

SCIENCE PRODUCTS DIVISION
St. Louis, Missouri 63160

CIRCLE 159 ON READER SERVICE CARD

ions of organic molecules were also measured. In the mass spectrum of pentaacetylglucose, the ion of m/e 242 is derived from the molecular ion by the successive loss of acetic anhydride and formic acid (13). Thus, the



ion at m/e 242 contains the C-2, C-4, and C-6 oxygen atoms of the original glucose molecule. Samples of (2- ^{18}O) and (6- ^{18}O) pentaacetylglucose, as well as unenriched pentaacetylglucose, were dissolved in methanol to a concentration of approximately 1 $\mu\text{g}/\mu\text{l}$ and were injected into the GC inlet system at a column temperature of 220°C. The ion intensities at m/e 242 and 244 were measured, and the isotope abundances of m/e 244 are given in Table III. The mass chromatogram for unenriched pentaacetylglucose is given in Figure 3. The precision obtained with these samples was the same as that obtained from the analyses of the inert gases.

A final set of experiments was performed in which the multiple ion monitor-integrator system was used to measure isotope abundance of GC samples. Since each channel of the

Table III. Isotope Abundances of Fragment Ion m/e 244 of Labeled and Unlabeled Pentaacetylglucoses Introduced via GC Inlet

Sample	Measd rel abundance, %	Precision, %
Unlabeled	3.02 \pm 0.04	\pm 1.3
2- ^{18}O	36.27 \pm 0.03	\pm 0.08
6- ^{18}O	49.80 \pm 0.05	\pm 0.10

ion monitor was connected to a separate digital integrator, it was necessary to calibrate the integrators to obtain a valid comparison between this system and that used earlier. The calibration was performed by tuning the two channels of the ion monitor to the same mass by using a 100-msec sampling time and comparing the integrated peak areas from each channel for different amounts of sample. Figure 4 shows this calibration curve plotted as integrator units vs. the ratio of the areas. When the area of the peaks was greater than 4×10^5 units, the ratio of the areas from the two channels was constant. In the measurements which follow, sensitivity was adjusted so that the ratios fell in the linear portion of this curve. In a typical analysis, one or two sample injections are required to set the mass of each channel at the top of the proper peak and to set the sensitivity range of each channel if the approximate abundances are not known. Subsequent sample injections can then be used for the actual isotopic abundance measurements. The isotope abundances of three samples admitted via the GC were measured in this way—krypton and the two ^{18}O -enriched glucoses—and the results are given in Table IV. The precision achieved was again similar to that obtained in the earlier experiments.

Table II. Isotope Abundance Measurements on Some Inert Gases as GC Samples

Sample	m/e	Theoretical measd abundance, %	Measd rel abundance, %	Accuracy, %	Precision, %
Krypton	78	0.35	0.34 \pm 0.004	-2.9	\pm 1.2
	80	2.27	2.24 \pm 0.003	-1.3	\pm 0.14
	82	11.56	11.45	-1.0	\pm 0.1
	83	11.55	11.59 \pm 0.034	+0.3	\pm 0.29
	84	56.90	56.89 \pm 0.09	-0.02	\pm 0.16
	86	17.37	17.48 \pm 0.02	+0.6	\pm 0.11
Xenon	124	0.096	0.095 \pm 0.001	-0.1	\pm 1.1
	126	0.090	0.090 \pm 0.001	0.0	\pm 1.1
	128	1.92	1.98 \pm 0.016	+3.0	\pm 0.8
	129	26.44	26.49	+0.2	\pm 0.1
	130	4.08	4.10 \pm 0.025	+0.5	\pm 0.61
	131	21.18	21.05 \pm 0.04	-0.6	\pm 0.19
	132	26.89	26.81 \pm 0.03	-0.3	\pm 0.11
	134	10.44	10.49 \pm 0.08	+0.4	\pm 0.76
	136	8.87	8.89 \pm 0.06	+0.2	\pm 0.67

* Handbook of Chemistry and Physics, 51st ed., Chemical Rubber Co., 1971. * Ion normalized on.

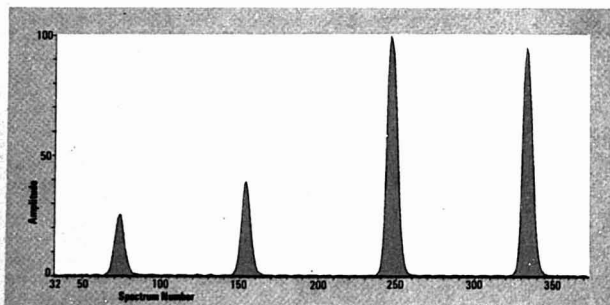
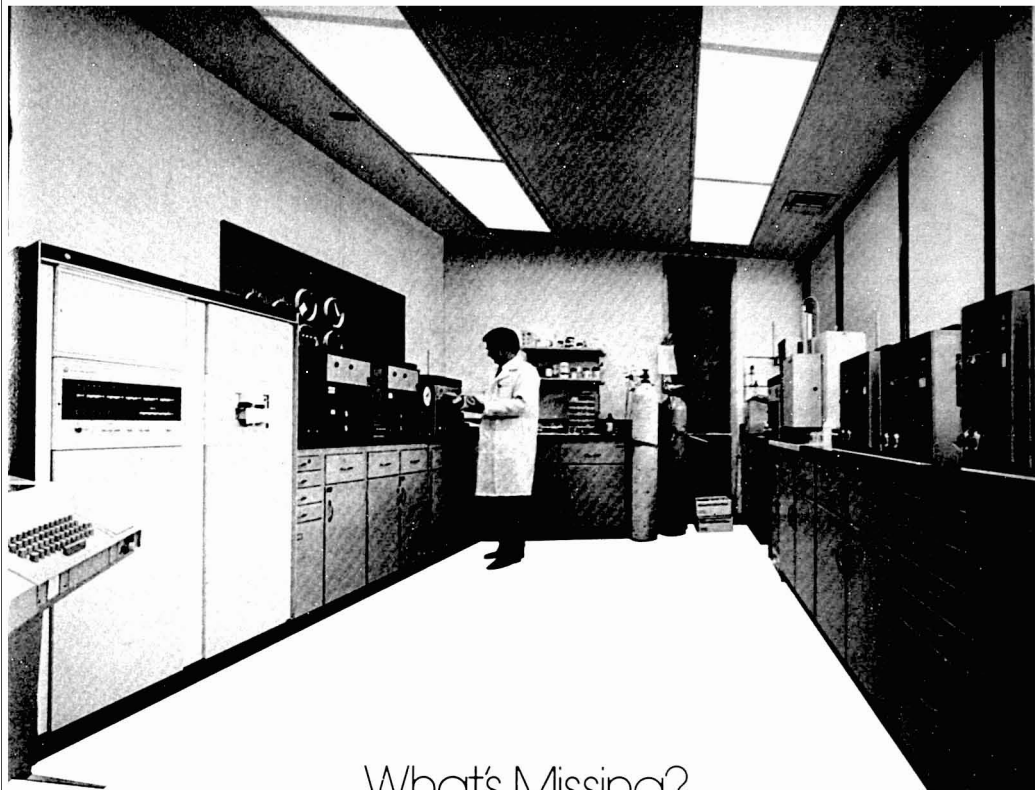


Figure 2. Mass chromatogram of xenon at m/e 124 taken on continuous monitoring of four separate sample injections. Each scan number in plot represents 1 sec

Discussion

One of the critical factors in determining isotope abundances with a mass spectrometer is peak shape. Thus, whether dealing with a magnetic or quadrupole instrument, it is important to adjust the ion source controls to give rounded tops—the closer to a flat top, the better the precision which may be obtained. However, since this type of "tuning" decreases the sensitivity of the instrument, a compromise must be made to favor one or the other depending upon the particular application. In the work reported here using a quadrupole, ion source tuning conditions for the attainment of a precision of



What's Missing?

What's missing? Wall-to-wall people. This analytical laboratory handled expansion with a Varian 200L Instrument Data System.

The mathematics were simple.

It was either hire several more people or purchase a 200L system.

The 200L would save a lot of money. And it would do a better job — automatically control all the gas and liquid chromatographs and provide complete, accurate output reports on all samples — even combine the data from multiple instruments into a single integrated report. There was no other system like it. The decision was never in doubt.

If you're planning to expand, or if your lab is overloaded, perhaps you, too, should consider a 200L Instrument Data System. We'd like to help.

For full information write or call: Varian Instrument Data Systems, 2700 Mitchell Drive, Walnut Creek, California 94598, (415) 939-2400.



varian

CIRCLE 341 ON READER SERVICE CARD

0.1–0.2% resulted in a concomitant loss of a factor of only approximately 2 in sensitivity. Since these instruments can generally obtain mass spectra from as little as 1×10^{-9} gram of sample, this loss of sensitivity is not of major significance.

Resolution also plays a significant role in isotope measurements. At maximum resolution, the peaks become extremely sharp, making it more difficult for the mass set to remain on top, since any instabilities will cause it to shift to the side of the peak. On the other hand, at low resolution the tail of one peak will add to the intensity of adjacent peaks, giving poor accuracy. Therefore, resolution was chosen to be no more than a 1–2% valley between adjacent peaks, providing a good tradeoff between resolution and accuracy.

Inspection of Figure 1 shows that for data obtained for gases sampled from the reservoir, the average precision obtained was $\pm 0.15\%$ in the abundance range 10–100 atom %, $\pm 0.4\%$ in the range 1–10 atom %, and $\pm 0.9\%$ in the range below 1 atom %. The rather sharp falloff in precision when the isotope abundance being measured is below 1–2 atom % is primarily the result of poorer ion statistics.

Also from Figure 1, the average accuracy obtained for the reservoir gases was 0.4% of the true value in the abundance range 10–100 atom %, 1.4% in the range 1–10 atom %, and 3.8% below 1 atom %. The decrease in accuracy at low abundances is the result of the combination of several factors. First, at low resolution, a small amount of cross-talk takes place between peaks and has its greatest effect when the ratio of adjacent peaks is high. Second, any background peaks present will make a larger percent contribution to the lower abundance isotopes, as also will any systematic errors in the measurements.

Figure 4. Calibration curve for multiple ion monitor–integrator system with m/e 242 of pentaacetylglucose introduced via GC inlet as a standard. Curve plots arbitrary integrator area units for each mass chromatogram vs. ratio of these area units for two channels used

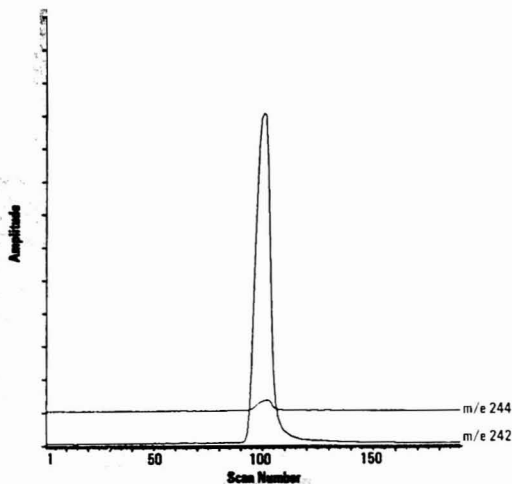
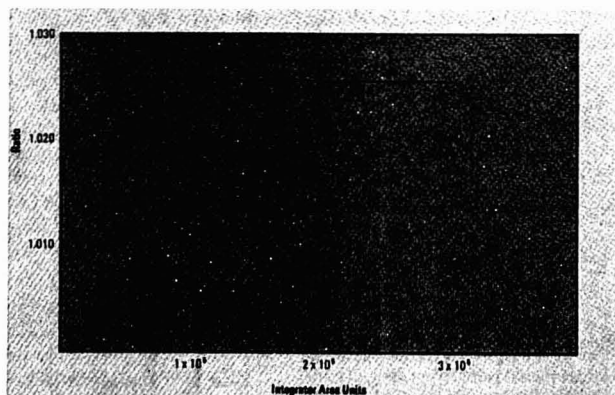


Figure 3. Mass chromatogram of m/e 242 and 244 of unenriched pentaacetylglucose. Each scan number in plot represents 1 sec

Table IV. Isotope Abundances of GC Samples with PROMIM-Integrator System

Sample	m/e	Meas'd rel abundance, %	Accuracy, %	Precision, %
Krypton	78	0.346 ± 0.003	-1.1	± 1.0
	80	2.26 ± 0.0008	-0.4	± 0.36
	82	11.54	-0.2	*
	83	11.47 ± 0.007	-0.1	± 0.06
	84	56.69 ± 0.23	-0.4	± 0.41
	86	17.70 ± 0.09	+1.9	± 0.51
(^{18}O) pentaacetylglucose	244	35.08 ± 0.04	...	± 0.11
(^{13}C) pentaacetylglucose	244	49.47 ± 0.06	...	± 0.12

* Ion normalized on.



Nine reasons why the Varian 2740 is your best buy in a research GC



1 The dual column 2740 gives you the research flexibility of two flame ionization instruments in one. You can run twice as many samples and you don't have to spend \$600 to \$800 for a second electrometer. Two electrometers are standard equipment so you can run two samples simultaneously and independently.

2 You get better chromatographic information because the 2740's electrometers are the finest — give you 1×10^{-12} A/mV sensitivity and drift less in a month ($10 \mu\text{V}$) than others do in a week.

3 Universal detector bases let you interchange detectors yourself in five minutes. You don't have to send for a serviceman.

4 You can use both flame ionization and electron capture detectors. The separate ECD power supply is standard equipment; you don't have to have it built in at \$300 to \$400 extra.

5 Automatic Linear Temperature Programmer (ALTP) provides automatic oven cooldown, reset and recycling for time and labor savings. The ALTP also gives you a greater range of program rates (eleven) to optimize your separation.

6 Big, 1090 in³ oven permits columns to be installed side by side — not convoluted — so you can adjust or remove one column without disturbing the other. Extremely important when you have a column that's working just right.

7 There's also an oven safety limit switch to prevent overheating and destroying columns.

8 Provision for installing a third injector position is particularly convenient for capillary columns.

9 Separate injector and detector temperature controls are *continuously* variable from ambient to 400°C allowing more precise adjustment for optimum performance.

The 2740 includes every standard feature expected in a research GC plus many Varian extras that help you improve your analyses.

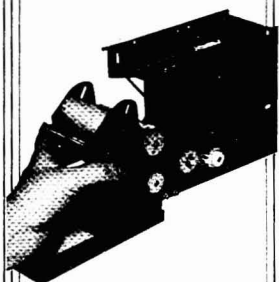
No other manufacturer matches the research performance of the 2740. Those that come anywhere close charge a higher price. For detailed information contact your Varian representative or Varian Instrument Division, 611 Hansen Way, Box D-070, Palo Alto, California 94303.



CIRCLE 242 ON READER SERVICE CARD

THE FASTEST MINI GOING

The best value
in miniature recorders
now available
from MFE.



- ☐ 5 Hz. frequency response
- ☐ Inkless thermal recording
- ☐ Continuous rectilinear trace
- ☐ Cartridge paper loading
- ☐ Chart reroll or feed out
- ☐ Basic sensitivity:
100 mV F.S.
- ☐ Quiet operation
- ☐ Rugged construction
- ☐ Compact:
5-1/2"H x 3-5/8"W x 6-1/2"D
- ☐ Light Weight - 3.5 lbs.
- ☐ Wide range of chart speeds from
1/2 in./hr. to 6 in./min.
- ☐ Portable or rack mounting
- ☐ OEM discounts available

Call or write Bill Beaulieu for details.

MFE
MFE CORPORATION
Keewardin Drive
Salem, New Hampshire 03079
Tel: 603 893 1921
TWX 710 366 1887
TELEX 94 7477

A comparison of Table I (reservoir inlet) and Table II (GC inlet) shows that although the precision of the measurements is about the same in both cases, the accuracy of the low abundance measurements is better for samples introduced via the GC inlet. This is not surprising since the data system allows a base line to be drawn for the mass chromatogram peak and background subtracted from the area of this peak to a close approximation. This could not be done for the reservoir samples, and any residual background was included in the measurements. Thus, these data show that rapid switching techniques with a quadrupole mass spectrometer can be used to analyze GC peaks for isotope abundance without sacrificing accuracy.

Perhaps a more rigorous test of the technique used here is the isotope abundance analysis of the fragment ions of normal and ^{18}O -labeled pentacetylglucoses introduced via the GC inlet. The data in Table III again show excellent precision, in agreement with that obtained with the inert gases. This, of course, provides the capability of simultaneously obtaining structural information and higher precision isotope ratio analyses, giving both the position of the isotope within the molecule and its abundance at that position.

The experiments with the multiple ion monitor-integrator system show that such a system may also be employed for high-precision isotope measurements, as shown in Table IV. This system has the main advantage of being less expensive than the data system. On the other hand, with the data system it is easier to focus the masses to be monitored. This system is also more flexible in that it has the ability to adjust for maximum integration time without prior knowledge of the isotope abundance, the capability of directly determining the ratio of areas by an "area ratio" function, and the capability of allowing the operator to visually choose the two points through which the base line is drawn. The latter is of major importance and is illustrated by the comparison of the isotope abundances of the ^{18}O -enriched glucose samples from the data system and ion monitor system. In both cases, the abundances obtained with the ion monitor are lower by 0.2 to 0.3 atom % ^{18}O than those with the data system. This was due to the presence of an impurity in the sample, giving a small peak at m/e 242 on the leading edge of the sample peak, and resulting in a base line change, but there was no corresponding peak at m/e 244. Thus, the digital integrators on the ion monitor added this shoulder into the peak

area at m/e 242, giving a lower abundance for m/e 244. The data system, on the other hand, allows visual inspection of the peak and provides the ability to go back after all the data are taken and choose the base line to a closer approximation. Thus, in the above case for the data system, this shoulder was not added to the peak area for m/e 242.

One further point dealing with isotope abundance measurements with a quadrupole mass spectrometer is worth noting and concerns mass discrimination. Of the several isotopic series studied, the accuracy attained with the low mass species was the same as that for the high mass species, within the abundance limits discussed above. Thus, no mass discrimination was observed, e.g., in Tables I and II, the relative accuracy obtained for the xenon isotopes as one proceeds from low to high mass shows no trend as a function of mass within these 12 mass units.

In conclusion, the work presented here demonstrates the capability of a quadrupole mass spectrometer for use as a high-precision instrument for the determination of isotope ratios, even under the dynamic conditions imposed by combined gas chromatography-mass spectrometry.

Acknowledgment

The authors thank Autolab Inc., for the use of two of their Model 6300 digital integrators.

References

- (1) G. Waller, R. Ryhage, and S. Meyerson, *Anal. Biochem.*, **16**, 277 (1966).
- (2) R. M. Caprioli and D. Rittenberg, *Biochemistry*, **8**, 3375 (1969).
- (3) M. Cohn, *Biochim. Biophys. Acta*, **37**, 344 (1960).
- (4) H. F. Fisher, E. E. Conn, B. Vennesland, and F. H. Westheimer, *J. Biol. Chem.*, **202**, 687 (1952).
- (5) H. Eriksson, J. A. Gustafsson, and J. Sjövall, *Eur. J. Biochem.*, **9**, 550 (1969).
- (6) C. G. Hammar, B. Holmstedt, and R. Ryhage, *Anal. Biochem.*, **25**, 532 (1968).
- (7) R. M. Caprioli, in "Biochemical Applications of Mass Spectrometry," G. Waller, Ed., p. 735, Wiley-Interscience, New York, N.Y., 1972.
- (8) R. A. Hites and K. Biemann, *Anal. Chem.*, **42**, 855 (1970).
- (9) C. C. Sweeley, W. H. Elliott, I. Fries, and R. Ryhage, *ibid.*, **38**, 1549 (1966).
- (10) J. F. Holland, C. C. Sweeley, R. E. Thrush, R. E. Teets, and M. A. Bieber, *ibid.*, **45**, 308 (1973).
- (11) P. D. Klein, J. R. Haumann, and W. J. Eisler, *ibid.*, **44**, 490 (1972).
- (12) W. F. Holmes, W. H. Holland, B. L. Shore, D. M. Bier, and W. R. Sherman, *ibid.*, **45**, 2063 (1973).
- (13) J. T. Watson, D. R. Pelster, B. J. Sweetman, J. C. Frolich, and J. A. Oates, *ibid.*, p. 2071.
- (14) R. M. Caprioli and W. E. Seifert, Jr., *Biochim. Biophys. Acta*, **297**, 213 (1973).

R. M. C. thanks the American Cancer Society for partial support.

April 1974, Vol. 46, No. 4

Editor: HERBERT A. LAITINEN

EDITORIAL HEADQUARTERS

1155 Sixteenth St., N.W.
Washington, D.C. 20036
Phone: 202-872-4600 Teletype: 710-8220151

Managing Editor: Virginia E. Stewart

Associate Editors:

Josephine M. Petrucci
Alan J. Senzel

Assistant Editor:

Andrew A. Huscovsky

PRODUCTION STAFF

Art Director: Norman W. Favin

Associate Production Managers:

Leroy L. Corcoran
Charlotte C. Bayre

Editorial Assistant: Nancy J. Oddenino

EDITORIAL PROCESSING DEPARTMENT,
EARTON, PA.

Assistant Editor: Elizabeth R. Rufe

ADVISORY BOARD: Allen J. Bard, Fred
Baumann, David F. Boltz, E. G. Brame,
Jr., Warren B. Crummett, M. A. Evenson,
Henry M. Fales, A. F. Fiesche, Kenneth
W. Gardiner, Jack M. Gill, Jeannette G.
Grasselli, H. S. Juvet, Jr., Theodore
Kuwana, Oscar Manis, Harold F. Walton

INSTRUMENTATION ADVISORY PANEL:
Jonathan W. Amy, Stanley R. Crouch,
Richard A. Durek, J. J. Kirkland, Ronald
H. Loomis, Marvin Margoshes, Harold M.
McNair, David Seligson, Howard J. Sloane

Contributing Editor: Claude A. Lucchesi
Department of Chemistry, Northwestern
University, Evanston, Ill. 60201

Published by the
AMERICAN CHEMICAL SOCIETY
1155 16th Street, N.W.
Washington, D.C. 20036

Books and Journals Division

John K. Crum Director

Ruth Reynard Assistant to the Director

Charles R. Bertsch Head, Editorial
Processing Department

D. H. Michael Bowen Head, Journals
Department

Basil Guiley Head, Graphics and
Production Department

Seldon W. Terrant Head, Research and
Development Department

Advertising Management

CENTCOM, LTD.
(for Branch Offices, see page 481 A)

A New Feature

For several years there have been discussions among the editorial staff and Advisory Board about the desirability of broadening the editorial coverage of *Analytical Chemistry* even further by some sort of feature that would stress the application of analytical methodology to the solution of problems, rather than the development of the methodology itself. The idea, while recognized as having merit, floundered for several years because of obvious problems that could be foreseen. These included the possible difficulty of obtaining the release of pertinent information from industrial laboratories where most of the examples would originate, the possible narrowness of appeal to a small group interested in a specific problem, the difficulty of maintaining quality over a period of time, and several others.

With the cooperation of the ACS Division of Analytical Chemistry, a symposium was scheduled for the Chicago ACS meeting in August 1973. The symposium was organized by Dr. Claude A. Lucchesi, who had an exceptional background in having had several years of experience in an industrial laboratory prior to his present academic appointment which involves a service as well as a teaching function at Northwestern University. Dr. Lucchesi agreed to an experimental appointment as a contributing editor in 1974, during which four articles arising from the ACS symposium will be published. Dr. Lucchesi will work with editorial staff members to prepare articles of content and style designed to appeal primarily to working analysts. The first, based on Dr. Lucchesi's own industrial experience, begins on p 433A. His account of the origins of the new feature appears in the Editors' Column, p 451A.

It is hoped that the articles will illustrate principles applicable to a variety of situations, rather than just to the specific problem at hand. It is also hoped that the articles will prove educational to students and teachers in describing actual problems confronted by the practicing analytical chemist. Finally, it is hoped that readers will give us the benefit of their opinions as to the usefulness of the experimental articles, as well as providing material for future articles so that the feature may appear more frequently in the years to come.



For submission of manuscripts, see
page 380 A

Solvatochromism of Phenol Blue in the Ethyl Acetate-Acetic Acid Solvent System

Orland W. Kolling and Jana L. Goodnight

Chemistry Department, Southwestern College, Winfield, Kansas 67156

The solvent-induced red shift for the principal absorption band of Phenol Blue was examined over the complete solvent mole fraction range in ethyl acetate-acetic acid. The influence of ethyl acetate-acetic acid upon the spectrum of the dye has some similarity to the ethyl acetate-chloroform system and is classified as regular within the mole fraction interval from 1.0 to 0.28 (EtOAc). Because of the small change in dielectric constant and index of refraction for the mixed solvent, the large red shift must be assigned almost entirely to the perturbation energy from hydrogen bonding by acetic acid. As the composition of the binary solvent approaches pure acetic acid, the medium response of Phenol Blue is irregular. The results of a restricted investigation of the kinetics of the bleaching of the dye in the same solvent pair are reported as well.

The principal electronic absorption bands of the azomethine dyes exhibit a high degree of sensitivity to changes in the solvent environment and this characteristic of the dyes has provided one experimental route to the measurement of solvent polarity (1). Phenol Blue (or *N*-(4-dimethylaminophenyl)benzoquinonemonoimine) has been the most thoroughly examined azomethine dye from both the experimental and theoretical viewpoints (2-4). The significant influences shown by minor structural changes in the dye molecule and by possible hydrogen bonding from the solvent led Figueras to conclude that solvent polarity scales based on solvatochromism can have only limited utility (3). In our preceding study, the solvent-induced red shift for Phenol Blue was measured as a function of solvent composition in binary aprotic solvents (5) and we are reporting herein an extension of that investigation to an aprotic-hydrogen bonding solvent pair.

A number of factors suggest that the cosolvents, acetic acid and ethyl acetate, are a suitable model pair for a hydrogen bond donor-acceptor system. Anhydrous acetic acid is an important nonaqueous solvent for volumetric analysis and organic syntheses, and it is a self-associated solvent. Considerable information is available on Phenol Blue in ethyl acetate, and in this solvent the transition energy for the dye conforms closely to the predictions of the McRae equation. The dielectric constants of the two pure solvents are close together: 6.20 for acetic acid and 6.02 for ethyl acetate (at 25 °C), thereby assuring only a small change in dielectric constant over the total solvent composition range. Likewise, the two solvents have nearly identical values for the index of refraction.

One disadvantage of the model cosolvent system is the destruction of the azomethine dyes by protonic acids. Ki-

netic data for the decomposition of Phenol Blue in ethyl acetate-acetic acid were obtained for the acetic acid range 0.42 to 0.94 mole fraction.

EXPERIMENTAL

Solvents and Reagents. Ethyl acetate was dried over anhydrous calcium sulfate and re-distilled as reported in the preceding work (5). Anhydrous acetic acid was prepared from reagent grade glacial acetic acid, following the method of Tappmeyer and Davidson (6). The water content of the anhydrous solvents was less than 0.001%, based upon Karl Fischer titrations.

Phenol Blue was purified by the same column chromatographic procedure as before and the melting point of the final product was 161 °C (5). Stock solutions of the dye were prepared at the $5 \times 10^{-4} M$ level in ethyl acetate only, because of the decomposition of the solute by acetic acid. Dilutions and binary solvent mixtures were made from burets protected with drying tubes.

Spectra. The spectra of Phenol Blue in each of the solvent mixtures was examined from 450 to 740 nm using the Perkin-Elmer Coleman 111 spectrophotometer, as reported previously (5). However, since the dye slowly decolorizes in the presence of acetic acid during the time required for spectral measurement, the following modification of technique was necessary.

The scan of the spectrum was made at a constant rate for increasing wavelength until the absorption peak was reached; and this scan was begun exactly two minutes after the addition of the acetic acid. Then, using an identical freshly prepared solution of the dye in the same solvent mixture, the spectrum was scanned after 2 minutes (at constant rate) in the reverse direction until the peak was reached. The value of λ_{max} was determined from the composite spectrum obtained by superimposing the forward and reverse scans and applying the graphic method outlined earlier (5).

For each solvent mixture, the absorption maximum was measured at five dye concentrations between 1.3×10^{-5} and $5 \times 10^{-6} M$. There was no statistical evidence for a concentration effect upon λ_{max} obtained in this way and the maximum experimental uncertainty in these results is ± 0.5 nm.

Dielectric-Constant Data. A Sargent-Jensen model HF titrator, having a 4.5 megacycle oscillator, was used to measure changes in dielectric cell capacitance at 25 °C. Calibration of the cell was made with the dried pure solvents, ethyl acetate and acetic acid, following procedures outlined earlier (7). The standard dielectric constant values employed were: ethyl acetate, 6.02 (8); and acetic acid, 6.198 (9). The experimental precision in the dielectric constant for each binary solvent mixture is ± 0.03 unit (std dev) based on five measurements.

Rate of Decomposition of Phenol Blue (at 25 °C). Solutions of known initial concentration (C_0) of the dye were prepared in ethyl acetate as the solvent; and, for a given solution, the desired amount of acetic acid was added rapidly with mixing. At exactly 2 minutes after the addition of the protonic solvent, absorbance measurements were begun on the 572-nm peak of Phenol Blue and monitored at regular time intervals until the dye was decomposed to at least one-half the initial amount. Upon plotting absorbance (A) vs. time (t) curves, the absorbance (A_0), corresponding to concentration (C_0) was determined by extrapolation. Then, the dye concentration (C) remaining at any experimental time was computed by simple proportion: $C = (A/A_0)C_0$.

- (1) F. Fowler, A. Katritzky, and R. Rutherford, *J. Chem. Soc. (B)*, 1971, 460.
- (2) E. G. McRae, *J. Phys. Chem.*, **61**, 562 (1957).
- (3) J. Figueras, *J. Amer. Chem. Soc.*, **93**, 3255 (1971).
- (4) J. Figueras, P. Scullard, and A. Mack, *J. Org. Chem.*, **36**, 3497 (1971).
- (5) O. Kolling and J. Goodnight, *Anal. Chem.*, **45**, 160 (1973).

- (6) W. Tappmeyer and A. Davidson, *Inorg. Chem.*, **2**, 832 (1963).
- (7) O. Kolling and C. VanArsdale, *Trans. Kans. Acad. Sci.*, **68**, 65 (1965).
- (8) J. Riddick and W. Bunger, "Organic Solvents," 3rd ed., Wiley-Interscience, New York, N.Y., 1971, p 279.
- (9) R. S. Phadke, *J. Indian Inst. Sci.*, **34**, 293 (1952).

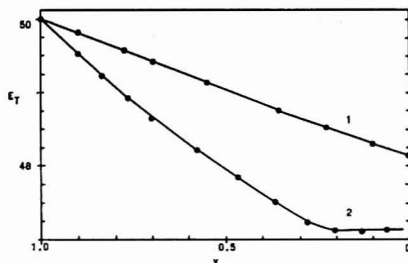


Figure 1. Experimental E_T as a function of the mole fraction (X) for ethyl acetate in the binary solvents: (1) ethyl acetate-chloroform; and (2) ethyl acetate-acetic acid

A minimum of five initial dye concentrations in the range from 1×10^{-6} to $5 \times 10^{-6} M$ were used to obtain the decomposition rate data in each EtOAc-HOAc mixture. Once absorbance measurements were begun on a given solution, that sample was not removed from the spectrophotometer until the full set of data had been collected.

RESULTS AND DISCUSSION

Polarity Measurements on the Two-Component Solvent. The general trend for the transition energy (E_T) of Phenol Blue as a function of the solvent composition is shown in Figure 1. For the purpose of comparison, the curve for the dye in the ethyl acetate-chloroform mixed solvent is included in the same figure.

If the twofold classification scheme for binary solvents which we suggested previously is now applied to the ethyl acetate-acetic acid system, the overall curve clearly indicates an irregular mixed solvent (5). By contrast, the simpler hydrogen bonding donor-acceptor pair (CHCl₃-EtOAc) exhibits a quite regular though nonlinear change in transition energy with increasing proportion of the donor solvent.

It is instructive to divide the curve for ethyl acetate-acetic acid into two parts: (a) the larger composition interval from X_{EtOAc} of 1.0 to 0.28; and (b) the higher acetic acid range from 0.28 to 0.0 mole fraction (X_{EtOAc}). In the first region (a), the shape of the curve conforms to that of a regular solvent pair and is much like the aprotic system ethyl acetate-dimethyl sulfoxide (5), although having a steeper change in slope than for the latter solvent. The magnitude of the red shift for Phenol Blue upon adding

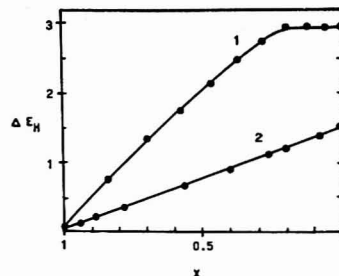


Figure 2. Perturbation energy (ΔE_H) as a function of the mole fraction (X) of ethyl acetate in the binary solvents: (1) ethyl acetate-acetic acid; and (2) ethyl acetate-chloroform

large amounts of acetic acid is greater than that for DMSO; and, as a hydrogen bond donor, the acetic acid induced shift of 35 nm is similar to *p*-cresol in DMSO or to that in the pure alcohols (3). Among the binary solvents studied to date, the limiting horizontal region (b) in Figure 1 is unique with the EtOAc-HOAc system.

Because of this general similarity between the ethyl acetate-chloroform system and the first portion (a) of the ethyl acetate-acetic acid pair, the quantitative treatment used in the preceding study was applied to the latter donor-acceptor mixed solvent. The McRae equation (Equation 1) was used to calculate the nonspecific influence of the solvent upon the ground state-excited state transition energy for the dye molecule (2). In this relationship n and D are the measured index of refraction and dielectric constant for the solvent mixture; and the McRae constants A , B , and C are -33.0, -4.4, and 57.92, respectively, when the transition energy (E_T)_M is in units of kcal/mole.

$$(E_T)_M = A \left(\frac{n^2 - 1}{2n^2 + 1} \right) + B \left(\frac{D - 1}{D + 2} - \frac{n^2 - 1}{n^2 + 2} \right) + C \quad (1)$$

A second concept applied to the donor-acceptor solvent system was the Figueras assumption (3) that the dominant perturbation energy from hydrogen bonding is independently additive, and this is stated by Equation 2.

$$\Delta E_H = (E_T)_M - E_T \quad (2)$$

Here, E_T is the transition energy computed from the measured λ_{max} and ΔE_H is the difference attributed to hydrogen bonding.

The numerical quantities needed for Equations 1 and 2 are listed in Table I, along with the calculated transition energies.

It will be noted that the ethyl acetate-acetic acid system is unusual in having a change in (E_T)_M of only 0.04 kcal/mole over the total mole fraction range of the cosolvent. Thus, the large change in the experimental transition energy upon the addition of acetic acid (Figure 1) must be attributed almost entirely to specific solvent-dye interactions (i.e., hydrogen bonding).

When the perturbation energy, ΔE_H , is plotted as a function of the solvent mole fraction (Figure 2), the regular and irregular solvent composition intervals are again visible. Over the range 1.0 to 0.28 ethyl acetate, the plot is nearly linear to within the reliability of the data, and the contribution from hydrogen bonding can now be expressed by Equation 3.

$$E_T = (E_T)_M - 3.72X_{\text{HOAc}} \quad (3)$$

Table I. Phenol Blue Absorption Maxima and Solvent Parameters in Ethyl Acetate-Acetic Acid

X_{EtOAc}	n^a	D^b	Exptl λ_{max} (nm)	E_T (kcal/mole)	(E_T) _M (kcal/mole)
1.000	1.3698	6.02	572	49.98	50.07
0.841	1.3708	6.05	581	49.21	50.06
0.701	1.3710	6.07	588	48.62	50.05
0.577	1.3704	6.09	593	48.21	50.06
0.467	1.3707	6.12	597	47.89	50.05
0.368	1.3708	6.14	602	47.48	50.04
0.280	1.3710	6.15	605	47.22	50.04
0.200	1.3706	6.16	607	47.12	50.04
0.127	1.3700	6.18	607	47.12	50.04
0.061	1.3710	6.19	606	47.16	50.03
0.000	1.3710	6.198	606.4 ^c	47.14	50.03

^a Experimental values for the refractive index at 25 °C, based upon EtOAc as the standard (ref. 8). ^b Measured dielectric constants at 25 °C determined using literature values for pure EtOAc and HOAc as standards (ref. 8, 9). ^c Extrapolated value for Phenol Blue in pure HOAc.

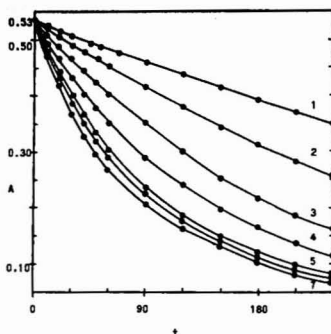


Figure 3. Representative plots for the rate of decomposition of $1.34 \times 10^{-5} M$ Phenol Blue in ethyl acetate-acetic acid as absorbance (A) vs. time (t) in minutes. Curves 1-7 correspond to increasing values for mole fraction of HOAc listed in Table II

By comparison to the ethyl acetate-chloroform system, the slope of the mole fraction term is about 2.5 times larger for the EtOAc-HOAc pair. The horizontal region of the curve in Figure 2 depicts a condition of saturation for the influence of the hydrogen bond donor upon the $\pi \rightarrow \pi^*$ transition of Phenol Blue as the solvent composition approaches pure acetic acid.

Presumably the simple acetic acid monomer is the fundamental hydrogen bond donor in the binary solvent, even though the formation constant for the dimer is of the order of 10^3 (10). However, recent information derived from factor analysis of the infrared spectrum of acetic acid as well as dipole moment data indicate that the self-association equilibrium involves two other acetic acid species in addition to the dimer and monomer (11, 12). Evidence on hydrogen bonded adducts between chloroacetic acid and dipolar aprotic bases supports the view that the primary association in such systems involves the monomeric form of the acid attached to the π -bonded oxygen of the acceptor (13). Thus, it is likely that the quinone oxygen is the acceptor site for the hydrogen bonded complex with Phenol Blue (3).

Kinetics of Decomposition of Phenol Blue. The azomethine dyes are generally unstable in acidic media and Phenol Blue is no exception. The dye has been observed to decolorize in chloroform solutions of HCl as well as in mixtures of ethyl acetate with acetic acid (14). Since there appear to be no published rate studies for the decomposition in nonaqueous media, we are reporting here the findings from a brief kinetics investigation in the model binary solvent.

Kinetics for the reactions of azomethine dyes with strongly basic anions in aqueous solutions have been thoroughly examined by Reeves and Tong (15), and we have adopted the use of their term "bleaching" for those decolorizing reactions which are not photochemical. The experimental evidence in aqueous alkaline media conforms to Equations 4 and 5 in which D_{PB} is the uncharged dye, B^- a nucleophile, and Z a complex.

- (10) G. Barrow and E. Yergler, *J. Amer. Chem. Soc.*, **76**, 5248 (1954).
- (11) H. Alfshprung, G. Findenegg, and F. Kohler, *J. Chem. Soc. (A)*, **1968**, 1364.
- (12) J. Bulmer and H. Shurvell, *J. Phys. Chem.*, **77**, 256 (1973).
- (13) D. Hadzi and J. Rajnvajn, *J. Chem. Soc., Faraday Trans. (I)*, **1973**, 151.
- (14) J. Figueras, Methods Research Division, Eastman Kodak Co., Rochester, N.Y., private communication, 1973.
- (15) R. Reeves and L. Tong, *J. Amer. Chem. Soc.*, **84**, 2050 (1962).

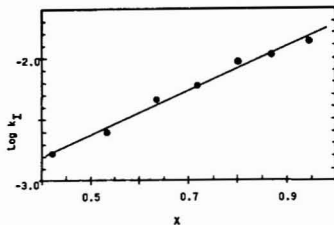
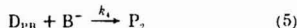


Figure 4. Trend in apparent first-order rate constant (k_1) as a function of mole fraction (X) for acetic acid

Table II. First-Order Decomposition of Phenol Blue in Ethyl Acetate-Acetic Acid at 25 °C

Mole fraction HOAc	Reaction time (min) for 1st order process ^a	Mean value k_1 (min^{-1})	Std dev
0.423	>500	0.00164	0.00014
0.533	375	0.00244	0.00026
0.632	225	0.00440	0.00040
0.720	140	0.00586	0.00052
0.800	90	0.00935	0.00021
0.873	65	0.0104	0.0003
0.939	50	0.0135	0.0002

^a Reaction time refers to the elapsed time over which the log C vs. t plot is linear.



Final colorless products (P_1 and P_2) have been identified as a *p*-phenylenediamine and a quinone (15); and essentially the same functional groups are expected as the products of the acid-catalyzed reaction (14).

The empirical rate of the bleaching reaction for Phenol Blue in the binary solvent (EtOAc-HOAc) was determined within the mole fraction range from 0.42 to 0.94 in the protonic acid. From the typical rate curves in Figure 3, it will be noted that there is a decided acceleration of the reaction with increasing acetic acid content; however, this effect diminishes at the higher mole fractions.

If the destruction of the chromophore in acidic media is analogous molecularly to either of the schemes in Equations 4 or 5, one would expect the rate of reaction to be first order with respect to the dye. Semilogarithmic plots demonstrate that the rate function is definitely linear at the lower mole fractions of HOAc over a long time interval. As the proportion of the protonic solvent increases, the time period over which the simple first-order linearity is followed becomes systematically shortened (as listed in Table II). Therefore, the rate of bleaching is a pseudo-first order process and at lower acetic acid activities it proceeds directly to a product P_2 with an apparent rate constant of k_1 . On the other hand, in mixed solvents containing acetic acid as the dominant component, the decomposition of the dye parallels the hydroxide-catalyzed reaction (Equation 4) in aqueous solutions (15). For the consecutive reactions, the same apparent rate constant k_1 can still be graphically evaluated for the faster initial reaction and this quantity is given in Table II for each of the seven solvent mixtures which were investigated. The second linear region observed in aqueous media (15) for the slower step was not found in the EtOAc-HOAc system.

In seeking to rationalize the significant increase in k_1 with increasing acetic acid content, any simple electrostatic model for the influence of the solvent upon dipole-dipole interactions must be excluded (16). The magnitude of the observed acceleration for the faster step in the bleaching reaction is inconsistent with the small increase in dielectric constant (D), and the theoretically predicted reciprocal functions in D must cover the very short interval from 0.161 to 0.164 in the solvent variable. However, most theoretical and empirical linear free energy functions share the common characteristic of expressing the reaction parameter as the logarithm of the rate constant (16). For this reason, we

(16) E. S. Amis, "Solvent Effects on Reaction Rates and Mechanisms," Academic Press, New York, N.Y., 1966, p. 59.

have correlated the log k_1 with the mole fraction of acetic acid; and in Figure 4 the empirical plot is linear within the precision of the experimental data.

ACKNOWLEDGMENT

We greatly appreciate the helpful comments of John Figueras of the Methods Research Division, Eastman Kodak Co., Rochester, N.Y., concerning the decomposition reaction of Phenol Blue.

Received for review September 17, 1973. Accepted December 5, 1973. Partial financial support for this project was supplied from a National Science Foundation grant, GP-27634.

Spectrophotometric Analysis with the GeMSAEC Fast Analyzer—Determination of Zinc Using 4-(2-Pyridylazo)Resorcinol (PAR)

Gerald Goldstein, W. L. Maddox, and M. T. Kelley

Analytical Chemistry Division, Oak Ridge National Laboratory, Oak Ridge, Tenn. 37830

The application of the GeMSAEC Fast Analyzer to conventional spectrophotometric methodology has been studied. Because the analyzer is coupled to a computer, large numbers of measurements can be rapidly averaged and relative standard deviations as small as 0.2% have been obtained. Precision is currently limited by instrument noise and unequal optical path lengths in the rotor, both of which can be improved. Instrument response is linear, and accurate results can be obtained by running standards and samples in the same rotor. As an example, a method for the determination of zinc using 4-(2-pyridylazo)resorcinol (PAR) was adapted to the analyzer. From 0.2 to 1 ppm of zinc in natural and treated water was determined with a relative standard deviation of 0.3–3%.

The GeMSAEC Fast Analyzer was developed at Oak Ridge National Laboratory (1–5) primarily for analysis of enzyme activities and enzyme substrates in physiological fluids in the clinical laboratory; commercial versions of the instrument are currently marketed for this purpose. The advantages of the instrument—versatility, high precision, and short analysis time—suggest that it should have more general applicability. For example, methods for sulfate analysis by turbidimetric measurement (6), and phosphate (7) and sulfur dioxide (8) analysis by fixed-time reaction rate methods have been described. Since straightforward spectrophotometry is still the most widely

utilized method of analysis (9, 10), particularly in routine testing laboratories, we have made a study of the characteristics of the GeMSAEC Fast Analyzer that are important in spectrophotometric applications and, as an example, have adapted a method for the determination of zinc (11) using 4-(2-pyridylazo)resorcinol (PAR) to the analyzer.

EXPERIMENTAL

Apparatus. The GeMSAEC Fast Analyzer and its operation have been described in detail elsewhere (6–8). Basically the instrument consists of: a rotor with 15 cuvettes in the rim, a transfer disk for samples and reagents, a Heath Model EU-701 monochromator, and a photomultiplier assembly; interfaced to a Digital Equipment Corporation Analog to Digital Converter and PDP-8/I Computer. A Tektronix Type 503 Oscilloscope permits visual inspection of the signal.

Reagents. All materials were Analytical Reagent Grade or better.

Cobalt Sulfate Solutions. Prepare solutions containing 1, 2, 4, 6, 8, and 10 grams of $\text{CoSO}_4 \cdot (\text{NH}_4)_2\text{SO}_4 \cdot 6\text{H}_2\text{O}$ per 100 ml of 1% (v/v) H_2SO_4 .

Potassium Dichromate Solution. Dissolve 0.500 gram of $\text{K}_2\text{Cr}_2\text{O}_7$ in 1 liter of 0.01N H_2SO_4 .

PAR Solution. Dissolve 17.64 grams of sodium citrate dihydrate, 305 mg of NaHCO_3 , and 382 mg of Na_2CO_3 in about 80 ml of water. Dissolve 8.3 mg of 4-(2-pyridylazo)resorcinol, disodium salt, dihydrate, in about 10 ml of water. Combine the two solutions and dilute to 100 ml. This solution should be freshly prepared before use.

Standard Zinc Solution, 1 mg/ml. Dissolve 500 mg of zinc metal in 8 ml of 1:1 HCl. Dilute to 500 ml with water. Prepare less concentrated solutions by appropriate dilution of this stock solution.

Procedure. Determination of Zinc. Pipet 0.2 ml of PAR solution into all 15 smaller wells in the transfer disk. In the larger wells, pipet 0.4 ml of H_2O into the first (position 0), 0.4 ml of several standards in succeeding positions, and 0.4 ml each of the samples in the remaining positions. Set the rotor speed for 600 rpm and the monochromator at 493 nm. Read the absorbances 60 seconds after rotor startup.

(9) F. W. Karasek, *Res./Develop.*, **23** (2), 30 (1972).

(10) W. N. Wham and K. S. Halaby, *Amer. Lab.*, **4** (10), 44 (1972).

(11) M. Kitano and J. Ueda, *Nippon Kagaku Zasshi*, **91**, 987 (1970).

- (1) N. G. Anderson, *Anal. Biochem.*, **28**, 545 (1969).
- (2) N. G. Anderson, *Anal. Biochem.*, **32**, 59 (1969).
- (3) N. G. Anderson, *Science*, **166**, 317 (1969).
- (4) D. N. Mashburn, R. H. Stevens, D. D. Willis, L. H. Elrod, and N. G. Anderson, *Anal. Biochem.*, **35**, 98 (1970).
- (5) C. D. Scott and C. A. Burtis, *Anal. Chem.*, **45** (3), 327A (1973).
- (6) R. L. Coleman, W. D. Shults, M. T. Kelley, and J. A. Dean, *Anal. Chem.*, **44**, 1031 (1972).
- (7) R. L. Coleman, J. A. Dean, W. D. Shults, and M. T. Kelley, *Anal. Lett.*, **4**, 169 (1972).
- (8) R. L. Coleman, W. D. Shults, M. T. Kelley, and J. A. Dean, *Anal. Lett.*, **5**, 169 (1972).

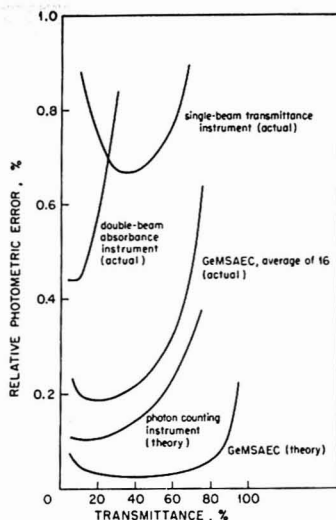


Figure 1. Relative photometric error of representative spectrophotometers of several types

RESULTS AND DISCUSSION

Transmittance Measurement. The GeMSAEC Fast Analyzer is a single-beam transmittance-reading instrument. On each revolution of the rotor (every tenth of a second at 600 rpm), the signal from the photomultiplier, as each of the 15 cuvettes passes over the light beam, is amplified, digitized, and stored as a 12-bit number in the computer. Dark current is measured when the light beam is interrupted by the body of the rotor between cuvettes at the start of each revolution. This signal is amplified, digitized, and subtracted from each of the cuvette readings. To correct for unequal transmittances caused by intrinsic optical factors (scratches, dirt, reflections, etc.) and to match the cuvettes, a calibration procedure is employed in which all the cuvettes are filled with water, and the reading obtained for each, after correction for dark current, is adjusted to equal that of cuvette 0 by multiplying by a factor—the inverse ratio of its reading to that of cuvette 0. This procedure is equivalent to adding or subtracting an appropriate absorbance to each cuvette so that its absorbance becomes zero relative to cuvette 0. This factor is retained by the computer and applied as a correction factor to every subsequent measurement on that cuvette until a new calibration is run. For analyses, the reagent blank is always placed in cuvette 0, and in our computer programs treated as a reference representing 100% transmittance. The transmittance or absorbance of any cuvette relative to the blank can then be calculated from the ratio of its corrected reading to that of cuvette 0.

Inputs of from 0–10 volts to the A-D converter generate numbers of 0 to 4096, the range of numbers that can be represented in 12 bits. To minimize the transmittance error due to the ± 1 -bit conversion error, the amplified reference (100% T) signal should ideally be 10 volts and the dark current (0% T) signal, 0 volts. The 100% T signal from cuvette 0, is displayed on the oscilloscope and can be adjusted by opening or closing the spectrophotometer slit, while the dark current can be adjusted by a bucking circuit on the photomultiplier output. Generally the instru-

Table I. Improvement in Precision by Averaging

Observations averaged per replicate, N	Rel std dev of mean, % ^a	
	Found	Theory
1	0.54	
2	0.46	0.38
4	0.26	0.27
8	0.20	0.19
16	0.14	0.14

^a 14 replicates.

ment is adjusted so that the dark current reading is about 20 and the reference cuvette reading is about 4000, a range of about 4000 numbers. Under these conditions, the transmittance range that can be measured is $1/4000$ to $3999/4000$ or 0.025% T (3.6 Absorbance) to 99.975% T (0.0001 Absorbance) in steps of 0.025% T , and the transmittance uncertainty due to A-D conversion is $\pm 0.025\%$ T .

Photometric Precision. The precision of measurements is first of all dependent on the number of independent observations (N) averaged for each measurement. If system noise is random, then the relative standard deviation is proportional to $1/\sqrt{N}$. For example, the data in Table I show typical precision data for 14 replicate measurements on the same solution in the same cuvette, a dichromate solution of absorbance 0.7, with each replicate an average of 1 to 16 observations. Computer interfaced instruments, such as the GeMSAEC analyzer, have an advantage in that large numbers of observations can be rapidly averaged with no effort on the part of the operator. We normally average 16 observations from successive revolutions of the rotor for each absorbance value, and hence our standard deviation is $1/4$ that obtained by comparing single measurements. At 600 rotor revolutions per minute, the time required for 16 observations on each of the 15 cuvettes is only 1.6 seconds.

Photometric noise and precision are related to the magnitude of the signal, and a convenient way to represent this is in the form of a plot of relative photometric error, dA/A , as a function of transmittance. Appropriate data are easily obtained by making replicate measurements of solutions of different transmittances. Furthermore, the plot is useful in evaluating the optimum transmittance range for maximum photometric precision and in ascertaining which instrumental factors limit the precision. From

$$A = -\log T \quad (1)$$

it follows that

$$dA/A = (0.434 dT)/(T \log T) \quad (2)$$

The shape of the plot and the transmittance at which dA/A is a minimum depends on the relationship between the signal, T , and the noise, dT , which is characteristically different for different types of noise. Total system noise is actually the sum of contributions from all of the components of the measurement and readout devices, a subject which has been considered in some detail by Ingle and Crouch (12), but in practice one usually deals with limiting cases in which one of the noise contributions is dominant. This plot is shown in Figure 1 for the GeMSAEC analyzer and for three other types of instruments. In presenting data for other instruments in Figure 1, it is our intent to evaluate the precision of the GeMSAEC analyzer in ordinary analytical applications by comparing it with widely used, commercially available spectrophotometers

(12) J. D. Ingle, Jr., and S. R. Crouch, *Anal. Chem.*, **44**, 1375 (1972).

operated in their normal, everyday manner. To that end, we selected representative instruments which are well known, have been studied, and for which precision data are available in the literature. GeMSAEC data are all for ensembles of 16 measurements, the normal procedure, while the data for the other instruments are for single measurements without averaging, scale expansion, or other features which may be available to improve precision. Consequently, it should be kept in mind that the curves in Figure 1 are not intrinsic properties of the particular type of instrument—other instruments of the same type may have different characteristics—and that the precision does depend on measurement conditions.

The familiar top curve in Figure 1 is taken from Cahn (13) who surveyed a large number of instruments of this type and is generally understood as a case in which the dominant error is a constant readout error of about 0.25% T on a linear readout scale. Optimum transmittance is characteristically 37% T (14). The curve for double-beam absorbance reading instruments is replotted from data collected by Slavin (15) from a survey of such instruments. In this case, photomultiplier shot noise is dominant and optimum transmittance is about 13% T (14). Although manufacturers usually do not provide this kind of information, it is probable that the majority of general purpose, inexpensive spectrophotometers on the market today have a relative error curve, for single measurements, very close to one or the other of these two. The actual curve for the GeMSAEC analyzer was obtained from measurements of cobalt sulfate solutions (group means of 16 measurements) with absorbancies ranging from 0.12 to 1.2. From the shape of the curve, with a minimum at about 20% T , it is evident that the instrument is noise limited rather than readout limited, but we have not attempted to isolate individual noise contributions. Assuming that instrumental noise could be minimized so that precision become readout limited, the limiting error would be the A-D conversion uncertainty of 0.025% T , independent of transmittance. This same error would appear three times in estimating the absorbance of a sample—measurement of dark current, 100% transmittance, and sample transmittance signals—and the bottom curve in Figure 1 was calculated by weighting and propagating these errors as described by Gridgeman (16), then reducing the relative error by a factor of 4 to reflect averaging of 16 readings. Potentially then, relative errors as small as 0.02% over a transmittance range of 20 to 70% T can be attained with the GeMSAEC analyzer. Reduction of instrument noise to this level is well within the state of the art. The National Bureau of Standards has recently achieved an average relative standard deviation on sequential transmittance measurements of 0.010% with an instrument constructed there (17). To complete the comparison, a curve for a photon counting system is also included in Figure 1, plotted from calculations by Malmstadt, Franklin, and Horlick (18) based on counting statistics. The position of this curve on the Y-axis depends on the number of counts actually taken, but assuming that the number used in the calculations (2×10^6) is reasonable and that instrument components do not contribute any significant noise, then this curve represents the precision that one might expect for single measurements.

Table II. Evaluation of GeMSAEC Cuvettes

Cuvette	Intrinsic absorbance,* Δk	Optical pathlength difference,* Δb , cm
1	-0.0054	-0.0025
2	-0.0042	-0.0016
3	-0.0064	0.0036
4	-0.0054	0.0028
5	-0.0084	0.0031
6	-0.0086	0.0011
7	-0.0086	0.0020
8	-0.0101	0.0027
9	-0.0092	0.0026
10	-0.0090	0.0035
11	-0.0096	0.0038
12	-0.0082	0.0042
13	-0.0030	0.0044
14	0.0006	0.0024

* Relative to cuvette 0.

All the previous discussion refers to replicate measurements of solutions in a single cuvette. In practice, however, we compare samples and standards in different cuvettes and, consequently, differences between cuvettes will increase the standard deviation of the results. From the manner in which the cuvettes are formed by clamping a Teflon spacer between quartz plates, one might reasonably expect small differences in the optical path length. The cuvettes were compared in the following way. It has been shown (19) that the light intensity emerging from cuvettes containing identical absorbing solutions can be expressed by:

$$I_i = I^0 10^{-(a_i b_i + k_i)} \quad (3)$$

where the subscript, i , refers to the cuvette number, k represents the intrinsic absorbance of the cuvette, and the other terms have their usual meaning. Using cuvette 0 as a reference

$$\log(I_i/I_0) = ac(b_0 - b_i) + (k_0 - k_i) \quad (4)$$

but since we have no values for b_0 and k_0 and can only evaluate differences

$$\log(I_i/I_0) = ac\Delta b + \Delta k \quad (5)$$

A plot of $\log(I_i/I_0)$ vs. c will have a slope of $a\Delta b$ and an intercept of k . We carried this test out at a wavelength of 512 nm using cobalt solutions and water with the results shown in Table II. Intrinsic absorbance can be corrected by the calibration procedure described earlier. The average Δb is 0.0023 cm with a standard deviation of 0.0020 cm. Since, as will be shown later, the average cuvette path length is close to 0.973 cm, in the rotor tested, measurements comparing solutions in different cuvettes will have a minimum relative standard deviation of about 0.21% because of optical path length differences. Each rotor is of course different. Newly-assembled rotors usually show some change in the first few weeks of use and very little change thereafter.

Photometric Linearity. Linearity was tested with solutions containing carefully weighed quantities of cobalt ammonium sulfate, at 512 nm, with the results shown in Table III. The uncertainty shown for the ratio was obtained by propagating the standard deviation of the absorbances. The instrument is linear, within the precision of the measurements, from absorbance 0.12 to 1.2, the range tested.

Photometric Accuracy. The accuracy of absorbance measurements made with the GeMSAEC Fast Analyzer (19) C. V. Banks, J. L. Spooner, and J. W. O'Laughlin, *Anal. Chem.*, **28**, 1894 (1956).

(13) L. Cahn, *J. Opt. Soc. Amer.*, **45**, 953 (1955).

(14) M. A. Ford, *Photoelect. Spectrom. Group. Bull.*, **18**, 554 (1968).

(15) W. Slavin, *Appl. Spectrosc.*, **19**, 32 (1965).

(16) N. T. Gridgeman, *Anal. Chem.*, **24**, 445 (1952).

(17) R. Mavrodineanu, *J. Res. Nat. Bur. Stand., Sect. A*, **76**, 504 (1972).

(18) H. V. Malmstadt, M. L. Franklin, and G. Horlick, *Anal. Chem.*, **44** (8), 63A (1972).

Table III. Photometric Linearity of the GeMSAEC Fast Analyzer

CoSO ₄ · (NH ₄) ₂ SO ₄ · 6H ₂ O, g/100 ml	Absorbance	Ratio
1.0000	0.1207 ± 0.0008	1.000
2.0000	0.2420 ± 0.0007	2.005 ± 0.005
4.0000	0.4835 ± 0.0010	4.006 ± 0.011
6.0000	0.7247 ± 0.0015	6.004 ± 0.017
8.0000	0.9652 ± 0.0017	7.997 ± 0.023
10.0000	1.0235 ± 0.0026	9.997 ± 0.033

Table IV. Absorbance Measurements on NBS Liquid Absorbance Standards

Standard solution	Wavelength, nm	Absorbance		Absorbance ratio, GeMSAEC/NBS
		GeMSAEC	NBS	
A	302	0.298	0.307	0.971
	395	0.295	0.304	0.970
	512	0.297	0.303	0.980
	678	0.112	0.115	0.974
B	302	0.593	0.608	0.975
	395	0.586	0.605	0.969
	512	0.591	0.606	0.975
	678	0.225	0.229	0.983
C	302	0.881	0.906	0.972
	395	0.875	0.907	0.965
	512	0.884	0.911	0.970
	678	0.337	0.345	0.977
Average				0.973
Relative standard deviation				0.51%

was tested using liquid absorbance standards (Standard Reference Material 931) from the National Bureau of Standards (20). The blank provided was placed in cuvette 0 and one of the liquid standards in all of the other cuvettes. Results are shown in Table IV. The average ratio of GeMSAEC to NBS certified absorbances is 0.973, independent of wavelength and absorbance value. Since the precision of both GeMSAEC and NBS measurements is a few tenths of a per cent, the differences are significant. Tests of the measuring circuits and A-D conversion indicated no bias, leading to the conclusion that the optical path length of cuvette 0 (all the other cuvettes having been normalized to cuvette 0) is 0.973 cm.

Determination of Zinc. We chose to study the reaction of 4-(2-pyridylazo)resorcinol (PAR) with zinc because this reagent provides a very sensitive test for many of the metals of interest in evaluating water quality. The molar absorptivity reported for the zinc complex is 8.3×10^4 (11), considerably greater than that of the dithizone and zincon methods currently recommended for water analysis (21). The method was adapted to the GeMSAEC analyzer by combining the required reagents—carbonate buffer, citrate complexing agent, and PAR reagent—in one solution such that the final concentrations after mixing 0.2 ml of the combined reagent with 0.4 ml of sample were those recommended as optimum. Preliminary tests indicated that the absorbance reading stabilized about 40 seconds after rotor startup. Color development was complete before then but turbulence in the cuvette caused poor preci-

Table V. Recovery of Zinc Spikes in Natural Water

Zinc spike, ppm		Approximate absorbance	Relative standard deviation, % ^a		
Added	Found		Individual cuvettes	Noise + optical errors	Spike recovery
0.200	0.205	0.16	0.53	0.57	3.2
0.400	0.409	0.32	0.35	0.41	0.60
0.600	0.605	0.50	0.27	0.34	0.52
0.800	0.802	0.66	0.24	0.32	0.34
1.00	0.997	0.81	0.25	0.33	0.31

^a 9 determinations.

Table VI. Determination of Zinc in Natural and Treated Water

Sample	Zinc found, ppm
Natural water	
White Oak Creek ^a	<0.05
White Oak Dam ^a	
Melton Branch ^a	
Well-water	3.68
Treated water	
Potable (tap)	<0.05-0.2
Potable (cooler)	0.2-0.4
Process water	0.4-1.2
Distilled (tap)	<0.05-0.9
Deminerlized	<0.05

^a Soluble zinc.

sion at shorter times. Absorbances were constant for at least 5 minutes thereafter and probably much longer. We chose to measure absorbances after 60 seconds. A computer program was prepared so that, after the preset 60-second delay, groups of 16 measurements were made on each cuvette at 2-second intervals, averaged, and stored as a single number. Up to 18 such groups could be accumulated, then averaged for the final result, and the relative standard deviation calculated. For analyses, five zinc standards were placed in cuvettes 1 to 5 and their concentrations entered in computer memory. After data collection and averaging, a calibration curve was constructed by a least-squares fit to the data from the standards and the zinc concentration in each of the other cuvettes calculated and printed out.

Compared to the previous measurements on stable absorbing solutions, the procedure for zinc analysis introduces the possibility for additional errors; pipetting errors in loading the transfer disk, and chemical problems such as solution instability and variable color intensities. To ascertain whether any of these are important factors, we spiked a natural water sample (containing no detectable zinc) with known quantities of zinc, determined zinc by the recommended procedure, and made a statistical analysis of the results (Table V). The precision of repetitive measurements on an individual cuvette, based on 3 groups of 16 observations, is slightly poorer than those determined previously with cobalt sulfate solutions. The difference is consistent with an estimated 0.3% pipetting uncertainty. The absorbances of the zinc-PAR complex and the reagent blank are very stable during the measurement period. In the absence of any of the other error contributions mentioned above, the relative standard deviation of the spike recoveries ought to equal the sum (root mean square) of instrument noise and pipetting error, as represented by the relative standard deviation of the individual cuvettes and the relative standard deviation of the optical path length differences. These combined errors are also shown in Table V. The relative standard deviations of the

(20) R. W. Burke, E. R. Deardorff, and O. Menis, *J. Res. Nat. Bur. Stand., Sect. A*, **76**, 469 (1972).

(21) American Public Health Association, American Water Works Association, Water Pollution Control Federation, "Standard Methods for the Examination of Water and Wastewater," Thirteenth Edition, American Public Health Association, Washington, D. C., 1971, p. 359.

spike recoveries indicate that precision in the analysis of 0.8 to 1 ppm of zinc is limited by instrumental and pipetting error. At lower concentrations it is evident that other factors are also important, most probably chemical problems. Since standards and samples were run in the same rotor, the actual optical path length is not a critical factor and recovery of spikes was quantitative. Using 0.973 cm for the path length, we calculated a molar absorptivity of 8.2×10^4 liter cm^{-1} mole $^{-1}$.

Several samples of treated and natural water from the Oak Ridge area were analyzed by the recommended procedure with the results shown in Table VI. Although this method is not specific for zinc, in many cases, particularly in treated waters, zinc is the major heavy metal contaminant due to deterioration of galvanized storage tanks and piping, and separations are unnecessary. We found the zinc content of treated water to be quite variable with time, but it never exceeded the drinking water standard of 5 ppm. Interferences in the determination of zinc by this method and techniques for eliminating them are discussed by Kitano and Ueda (11).

Preparation, Properties, and Applications of 8-Hydroxyquinoline Immobilized Chelate

K. F. Sugawara, H. H. Weetall, and G. D. Schucker

Research and Development Laboratories, Corning Glass Works, Corning, N.Y. 14830

An immobilized chelate, Controlled Pore Glass-8 Hydroxyquinoline, has been prepared by azo-linkage to an arylamine coupled to Controlled Pore Glass via γ -aminopropyltriethoxysilane. The preparation is described. This immobilized chelate was evaluated for its ability to extract metals under various conditions. The effects of pH, complexing agents, sodium chloride, and equilibrium periods on the extractions were studied. Also, exchange capacity and desorption experiments were completed. Controlled Pore Glass-8 Hydroxyquinoline was used in the analysis of distilled-deionized water for the determination of iron and copper as ultratrace contaminants. This immobilized chelate having a glass substrate extends the versatility and the scope of current available exchangers.

As a direct result of research relating to the attachment of enzymes to inorganic carriers via silane coupling agents (1, 2) forming immobilized enzymes, a unique type of new analytical reagent referred to as immobilized chelates has been developed. These immobilized chelates are capable of extracting specific cations from solutions over a definite pH range in a manner somewhat analogous to the corresponding organic ligands from which they have been prepared. The immobilized chelates were prepared from the Controlled Pore Glass-arylamine derivative described by Weetall (1, 2). Several immobilized chelates, differing only in the particular organic ligand used for coupling, were prepared. In this paper, only the preparation, properties, and applications of Controlled Pore Glass-8-Hydroxyquinoline (CPG-8-HOQ) are discussed. In a previous publication Bauman, Weetall and Weliky (3) described the preparation of diazo-coupled ligands such as dithione and hydroxyquinoline coupled to benzidine-carboxymethylcellulose. These ligand-cellulose products were used to effect recovery of trace metals from sea water. In past years, numerous types of 8-hydroxyquinoline chelating resins have also been prepared for the purpose of separating metals from solutions with varied success. Vernon and Eccles (4) have reviewed this area and reevaluated much of the published data. New methods for analyzing ultrapure water have been a matter of real concern for many years. Hughes *et al.* (5) have summarized the numerous facets of research concerning this broad and important subject.

EXPERIMENTAL

Reagents. Controlled Pore Glass (Pierce Chemical Company) 40/80 mesh, 80 m 2 /g surface area, 550-Å pore diameter was used. γ -Aminopropyltriethoxysilane (A1100, Union Carbide Corp.), triethylamine, *p*-nitrobenzoylchloride, sodium dithionite, 8-hydroxyquinoline, and Controlled Pore Glass-8 Hydroxyquinoline (Pierce Chemical) were used.

Equipment. This consisted of a Burrell Wrist Action Type Shaker.

Preparation of CPG-8 Hydroxyquinoline (CPG-8 HOQ). The arylamine derivative of the silanized Controlled Pore Glass was prepared according to the method described by Weetall (1, 2). The arylamine glass was diazotized in 2N HCl medium by adding solid sodium nitrite (0.25 gram per gram of intermediate) to the mixture in an ice bath. The reaction flask was placed in a vacuum.

(3) A. J. Bauman, H. H. Weetall, and N. Weliky, *Anal. Chem.*, **39**, 932 (1967).

(4) F. Vernon and H. Eccles, *Anal. Chim. Acta*, **63**, 403 (1973).

(5) R. C. Hughes, P. C. Murau, and Gordon Gunderson, *Anal. Chem.*, **43**, 691 (1971).

(1) H. H. Weetall, *Biochim. Biophys. Acta*, **212**, 1 (1970).

(2) H. H. Weetall, *Res./Develop.*, **22** (12), 18 (1971).

In the zinc determinations, 5 standards and 9 samples were completed, including calculations, in about 10 minutes with a 15-cuvette rotor and manual loading of the transfer disk. Rotors with as many as 42 cuvettes have been fabricated (22) and transfer disks can be loaded automatically (23), saving considerable time. We should also point out that the analyzer need not be dedicated to only one, or a few, analyses but can be used for whatever assays are required. We had no difficulty in adapting the method for zinc determination, the appropriate existing spectrophotometric methods for most elements can certainly be found.

Received for review July 31, 1973. Accepted November 30, 1973. This research was sponsored by the U.S. Atomic Energy Commission and the National Science Foundation under contract with Union Carbide Corporation.

(22) C. A. Burtis, W. F. Johnson, J. E. Attrill, C. D. Scott, N. Cho, and N. G. Anderson, *Clin. Chem.*, **17**, 686 (1971).

(23) C. A. Burtis, W. F. Johnson, J. C. Mailen, and J. E. Attrill, *Clin. Chem.*, **18**, 433 (1972).

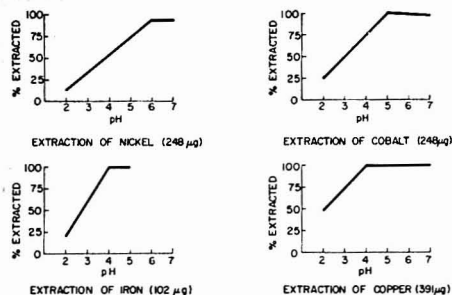


Figure 1. Batch extractions

um desiccator and evacuated. After allowing the mixture to react for approximately 30 minutes, it was filtered and washed with cold distilled water, cold 1% sulfamic acid solution, and again with cold distilled water. The diazotized glass was coupled to 8-hydroxyquinoline by adding to it a saturated solution of 8-hydroxyquinoline in 0.05M sodium carbonate. The product was filtered, washed with distilled water, and air dried. An analysis of the product indicated 4.4% carbon, 0.52% hydrogen, and 0.97% nitrogen. This composition, however, will vary somewhat from one preparation to the next. Experiments have indicated that a layering effect of the silane on the surface of the Controlled Pore Glass occurs which probably contributes toward some variability in the amount of organic present.

Batch Experiments. In separate experiments, specific amounts of different metal cations were buffered in 0.2M acetate solutions and then shaken in separatory funnels with 0.5-1.0 gram of CPG-8-HOQ for 30 minutes at definite pH intervals. The solutions were filtered to separate the CPG-8-HOQ (No. 41 Whatman) and, after washing the latter with distilled water, the filtrate was analyzed for the concentration of unextracted cations. The difference found between the micrograms of metal added to the separatory funnel and that found in the filtrate represented the amount extracted from the solution by the CPG-8-HOQ. The concentrations of the respective metals determined in the filtrate were determined spectrophotometrically as follows: a) nickel by dimethylglyoxime (6), b) cobalt by nitroso-R salt (7), c) iron by o-phenanthroline (8), d) aluminum by 8-hydroxyquinoline (9), e) zirconium by pyrocatechol violet (10), f) titanium by tiron (11), g) vanadium by *N*-benzoyl-*N*-phenylhydroxylamine (12) and h) copper by bathocuproine (13).

Column Experiments. Columns were prepared from 25-ml burets using borosilicate glass wool as support for the CPG-8-HOQ. Standard solutions of metals, buffered in 0.2M acetate solutions, were added to the columns. After washing the CPG-8-HOQ with distilled-deionized water, the metals were eluted with 1.0M hydrochloric acid solutions. The effluents were analyzed spectrophotometrically for the respective metals as with the batch experiments. The columns were prepared for subsequent runs by washing with approximately 100 ml of distilled-deionized water followed by 25 ml of 0.05M acetate buffer solution.

RESULTS AND DISCUSSION

As a new type of material, the properties of the CPG-8-HOQ proved quite interesting and experiments with standard solutions confirmed that they can be utilized to effect useful analytical separations. Inasmuch as these materials have a relatively low exchange capacity for metals, their use must be limited to separation involving either trace or low level concentrations. One such experi-

- (6) E. B. Sandell, "Colorimetric Determination of Traces of Metals," 3rd ed. Interscience Publishers, New York, N.Y., 1965, p 671.
- (7) Ref. 6, p 419.
- (8) Ref. 6, p 541.
- (9) Ref. 6, pp 234-235.
- (10) D. F. Wood and J. T. Jones, *Analyst (London)*, **90** (1068), 125 (1965).
- (11) J. H. Yee and A. R. Armstrong, *Anal. Chem.*, **19**, 100 (1947).
- (12) U. Priyadarshini and S. G. Tandon, *Anal. Chem.*, **33**, 435 (1961).
- (13) G. F. Smith and D. H. Wilkins, *Anal. Chem.*, **25**, 510 (1953).

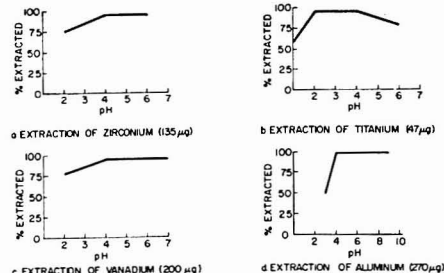


Figure 2. Batch extractions

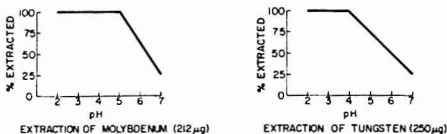


Figure 3. Batch extractions

ment was the analysis of distilled-deionized water for the ultratrace contaminants iron and copper.

Batch Experiments. Stability of CPG-8-HOQ. The stability of the CPG-8-HOQ was studied experimentally in acidic, neutral, and basic media by observing any physical changes occurring in the material. When extractions were completed in acidic and neutral media, the stability appeared to be very good. However, when extractions were extended to beyond pH 7.0 in ammoniacal medium, a slight degradation of the material was indicated by the appearance of a brownish tint imparted to the solution. On filtration, the suspended particles were removed from the solution and their appearance on the filter paper suggested that they consisted of organic particulates. Evidently, the ammoniacal medium degraded the silica substructure sufficiently to cause separation of the organic material. Later experiments showed that a CPG-8-HOQ product prepared from zirconia-coated Controlled Pore Glass exhibited improved stability in ammoniacal medium but poorer stability in strong acid. Extraction efficiency appeared approximately the same in both products.

Effect of pH. Several elements which were tested for their extractability as a function of pH using CPG-8-HOQ indicated that the general extraction pattern was similar to that obtained using 8-hydroxyquinoline-chloroform in liquid-liquid extractions. For example, the extractions of Ni(II), Co(II), Fe(III), Cu(II), Zr(IV), Ti(IV), V(V), and Al(III) gradually increased from pH 2.0 to 5.0 and then leveled off (Figures 1 and 2). The extractions of aluminum was studied from pH 3.0 to 9.0 using zirconia-coated controlled pore glass-8-hydroxyquinoline. The pH from 3.0 to 7.0 was adjusted using acetate buffer and from pH 7.0 to 9.0 using acetate buffer plus ammonium hydroxide solution. Hydrolysis of aluminum under these conditions did not present a problem at the 10-ppm concentration level used. Extraction of the remaining metals was not examined beyond pH 7.0. Since hydrolysis of titanium presented a slight problem at the 200-µg level, the amount employed for extraction was decreased to 47 µg. Complete extraction of Mo and W (Figure 3) occurred at pH 2.0 and dropped off at pH 5.0, probably caused by the formation of anionic molybdate and tungstate species. The respective curves represent extraction patterns and do not repre-

sent exact values at a particular pH. However, in instances where per cent extraction values of 100% are indicated, the accuracy is within the normal spectrophotometric range of two to three relative per cent.

Effect of Complexing Agents. To study the effect of complexing agents on the efficiency of extraction, 102 μg of Fe was extracted at pH 4.0 and 5.0 (acetate buffered) from 1% tartaric acid and 1% citric acid solutions. The results indicated that the extraction of Fe(III) by CPG-8-HOQ was effective from a tartaric acid medium but was strongly suppressed by citric acid.

Equilibrium Periods. The extraction of Fe(III) at pH 5.0 was studied under varying equilibrium periods from 1 to 10 minutes. The data indicated that after 1 minute of shaking, 84% of the Fe(III) was extracted from the solution. After only 2 minutes of shaking, 95% of the Fe(III) was extracted. Although a 30-minute equilibrium period was allowed for the batch extraction of the various metals, equilibrium was probably actually attained much more rapidly than this.

Exchange Capacity. The exchange capacity was determined by agitating an excess of acetate buffered (pH 5.0) Fe(III) solution (0.365 mg Fe) with 100 mg of CPG-8-HOQ. The buffered Fe(III) solution (approximately 35 ml) was added to the separatory funnel followed by the CPG-8-HOQ and then agitated for 30 minutes. The solution was filtered using rapid filtering filter paper and the CPG-8-HOQ washed with distilled-deionized water. The amount of Fe(III) extracted from solution was determined by the difference between the amount of Fe(III) found in the solution before and after reaction with the CPG-8-HOQ. The results indicated that the exchange capacity for this material was 0.057 mmol per gram.

Column Experiments. Elution of Fe with Dilute HCl. To determine the approximate hydrochloric acid concentration necessary to elute iron quantitatively from the column, 4080 μg of Fe(III) at pH 5.0 was added to a column of CPG-8-HOQ. A column height of 28 cm was used in a 50-ml buret. The iron was then eluted successively with 0.01, 0.10, 0.50, and 1.0M HCl. At each corresponding acid level, 100-ml volumes were used for the elution. Complete recovery was not attained until the acidity was increased to 1.0M HCl. To verify whether iron could be eluted quantitatively, the experiment was repeated by adding 1020 μg of Fe(III) to the column and eluting with 1.0M HCl. The results confirmed that the iron was completely recovered using 100 ml of 1.0M HCl.

Exchange Capacity at Column Breakthrough. The exchange capacity of 1.0 gram CPG-8-HOQ at the column breakthrough point was determined at pH 5.0 using a column prepared from a 25-ml buret. Exactly 1044 μg of Fe(III) buffered at pH 5.0 with acetate was transferred to the column and passed through. After washing the column thoroughly with distilled-deionized water until the effluent gave a negative test for Fe(III), 150 ml of 1.0M HCl was passed through the column. The amount of Fe(III) eluted by the acid was equivalent to the exchange capacity per gram at the approximate breakthrough point of the column. This amounted to 965 μg of Fe(III) or 0.017 mmol/gram. Flow rate was adjusted to about 8 ml per minute.

Effect of Sodium Chloride. The effect of sodium chloride on the elution of Fe(III) from a CPG-8-HOQ column was investigated. A solution consisting of 204 μg of Fe(III) in 0.25 M NaCl buffered with acetate to a pH of 4.0 was added to the column. The column was then eluted successively with 150 ml of 0.25M NaCl, 150 ml of 0.5M NaCl, 100 ml of 0.5M NaCl (pH 4.0), and 150 ml of 1.0M NaCl (pH 3.0). In no instance was there any iron detected in

Table I. Recovery of Trace Fe(III) and Cu(II) from One Liter of Distilled-Deionized Water

Fe, spike, μg	Fe recovery		Cu, spike, μg	Cu recovery	
	μg	%		μg	%
41.6	39.3	95	39.1	38.3	98
41.6	36.7	88	39.1	39.6	101
41.6	39.0	94	39.1	38.3	98
41.6	37.4	90	39.1	40.2	102
10.4	9.5	91	10.9	7.0	64
10.4	9.8	94	10.9	7.8	72
10.4	8.8	85	10.9	8.8	81
10.4	9.0	87	10.9	8.0	73

the effluent. The initial trace of iron eluted from the column occurred when the pH of the 1.0M NaCl solution was lowered to 2.0. The last trace of iron was eluted with a 1.0M NaCl-1.0M HCl solution. A subsequent column wash with 1.0M NaCl-2.0M HCl solution did not detect any Fe(III).

Extraction and Elution of Aluminum. By using a column prepared from a 50-ml buret with a CPG-8-HOQ height of 28 cm, 654 μg of Al(III) was extracted from a solution buffered with acetate at pH 5.0. Aluminum was eluted from the column with 150 ml of 1.0M HCl. Over 90% of the aluminum added to the column was recovered in the first 50 ml of 1.0M HCl. Additional experiments indicated that more dilute solutions of hydrochloric acid up to 0.1M HCl did not elute the aluminum completely from the column.

Recovery Experiments for Trace Amounts of Fe(III) and Cu(II). Several liters of distilled-deionized water used for chemical analysis was buffered at pH 5.0 (addition of 5 ml per liter of 1.0M acetate buffer) and purified by passing through a column prepared of CPG-8-HOQ to remove any trace cations that might be present. This purified water was then used for the blank and to conduct recovery experiments by adding trace amounts of Fe(III) and Cu(II). Three experiments were completed. The first experiment consisted of adding 42 μg of Fe(III) and 39 μg of Cu(II) to 1 liter of the purified distilled-deionized water and passing through a column of CPG-8-HOQ (25-ml buret; column height, 13 cm). The flow rate was approximately 5 ml per minute. The second experiment paralleled the first experiment; however, only 10.4 μg of Fe(III) and 10.9 μg of Cu(II) were added to 1 liter of purified distilled-deionized water prior to passage through the column. After eluting Fe(III) and Cu(II) with 50 ml of 1.0M HCl, they were determined spectrophotometrically using the bathophenanthroline (14) and bathocuproine (13) procedures, respectively. By extracting with 5.00 ml of hexanol, and measuring the absorbance of the organic phase, calibration curves from 1 to 10 μg of each element were prepared and used to determine the amount of each element in the eluate. The recovery data (Table I) show that the mean recovery for iron and copper at approximately the 40- μg level was 92 and 100%, respectively. At the lower concentration level (approximately 10 μg), the mean recovery for iron and copper was 89 and 73%, respectively. A third experiment consisted of adding a mere 4.2 μg of Fe(III) to 4 liters of purified distilled-deionized water and testing for the recovery. Duplicate determinations showed 2.9 and 3.0 μg of Fe(III) were recovered.

Analysis of Distilled-Deionized Water. By applying the same method used for the recovery experiments, the laboratory distilled-deionized water was analyzed for iron

(14) G. F. Smith, W. H. McCurdy, and H. Diehl, *Analyst* (London), **77**, 418 (1952).

and copper as ultratrace contaminants. Iron was not detectable in 4 liters of distilled-deionized water (<0.25 ppb), the absorbance being comparable to the blank (0.040). However, 1 liter of distilled-deionized water was of sufficient volume to determine copper contamination at the 8-ppb level. The source of copper contamination was probably in the metal fittings and fixtures used for the distilled water line.

SUMMARY

Because of its low exchange capacity, CPG-8-HOQ is not intended to replace ion exchange or chelating resins. Rather, its application will probably involve special areas

of research where its unique properties will make it particularly useful. Being essentially a glass product of rigid structure, shrinkage and swelling are practically non-existent. Physical properties such as pore volume and surface area are well defined. Sterile conditions are probably more easily maintained than with resins. The substrate can be altered from Controlled Pore Glass to crushed Vycor. Various organic compounds can be successfully coupled to the diazotized glass surface.

Received for review August 2, 1973. Accepted November 19, 1973.

Determination of a Geometry and Dead Time Correction Factor for Neutron Activation Analysis

Gerald L. Hoffman

Graduate School of Oceanography, University of Rhode Island, Kingston, R.I. 02881

Paul R. Walsh

Department of Chemistry, University of Rhode Island, Kingston, R.I. 02881

Michael P. Doyle

Rhode Island Nuclear Science Center, South Ferry Road, Narragansett, R.I. 02882

A method is presented for an instrumental nondestructive determination of trace metals by thermal neutron activation analysis. The method involves determining a normalizing factor which relates the geometry and dead time between standard and sample. National Bureau of Standards certified orchard leaves and bovine liver have successfully been analyzed by the method. The elements determined were Na, Mn, Cu, V, and Al.

Neutron activation analysis has been applied to trace metal determination for a number of years (1). Thermal neutron activation analysis is usually accomplished by irradiating a standard and sample simultaneously. It is generally assumed that the neutron flux and energy distribution are the same for sample and standard. If errors less than 1% are required in the analysis, accurate placement of standard and sample in the neutron flux are required to obtain reproducible results (2).

Multiple element analysis by instrumental neutron activation analysis (INAA) utilizing lithium drifted germanium [Ge(Li)] solid state detectors coupled to multichannel analyzers has greatly expanded the range of multielement analysis with each neutron activated sample. However, if INAA is used, then corrections must be made for counting geometry and counting dead time between the sample and the standard. Unless liquids are analyzed, it is often difficult to physically match the counting geometry of a standard to a sample. Dead-time losses can be taken into account by using the general equation derived by Schonfeld (3). Using Schonfeld's equation, De Wispelaere

et al. (4) developed an instrumental technique to correct for dead time with the aid of computer analysis. Heurtebise *et al.* (5, 6) developed a method to remove flux inhomogeneity, counting geometry, counter dead time, and matrix effects using one of the macro constituents in a sample as a reference standard. This technique of macro constituent correction will not work on a sample that is a complete unknown. It is a simple matter to extend the method of Heurtebise *et al.* (5, 6), such that one of the constituents in an unknown can be used to correct the activities of the other elements.

This paper describes a simple technique for the determination of a correction factor that will normalize the geometry and dead time during counting for a standard and sample. This technique is most useful for INAA of short lived isotopes (*i.e.*, $t_{1/2} < 30$ min), but it can be applied to longer lived isotopes (*i.e.*, $t_{1/2} > 30$ min). The technique developed in this work has been successfully applied to the analysis of National Bureau of Standards (NBS) certified orchard leaves and bovine liver.

PRINCIPLE OF THE METHOD

In a homogeneous matrix, the measured γ -ray activities of any two nuclides counted with a Ge(Li) detector will be in error to the same extent relative to a standard if the γ -ray attenuation is similar for both nuclides. This implies that both nuclides will have a similar normalization factor (K_n) which encompasses both the geometry and dead time corrections. If K_n can be determined for one nuclide relative to a standard, then the second nu-

- (1) "Modern Trends in Activation Analysis," J. R. DeVoe, Ed., Vol. 1 and 2, National Bureau of Standards, Washington, D.C., 1969.
- (2) E. Bruninx, *Anal. Chim. Acta*, **60**, 207 (1972).
- (3) E. Schonfeld, *Nucl. Instrum. Methods*, **95**, 13 (1971).

- (4) C. De Wispelaere, J. Op de Beeck, and J. Hoste, *Anal. Chem.*, **45**, 547 (1973).
- (5) M. Heurtebise and J. A. Lubkowitz, *Anal. Chem.*, **43**, 1218 (1971).
- (6) M. Heurtebise, F. Montoloy, and J. A. Lubkowitz, *Anal. Chem.*, **45**, 47 (1973).

clide can be determined accurately by using the same K_n value. When the standard and unknown are counted for an identical length of clock time, the corrected activity at zero time is proportional to the mass of the radioactive nuclide present. This can be expressed in two simple relationships:

$$[A_s = K_s M_s]_{\text{Ge(Li)}} \quad (1)$$

$$[A_u = K_u M_u]_{\text{Ge(Li)}} \quad (2)$$

where A_s and A_u = activity of the standard and unknown, respectively, at zero time; M_s and M_u = mass of the element present in grams for the standard and unknown, respectively; K_s and K_u = proportionality constant for the standard and unknown, respectively. K_s and K_u are not equal and are dependent upon the following variables: neutron flux, counting geometry, and counting dead time. It is not important to determine the exact proportionality constants K_s and K_u . It is only necessary to determine the normalization constant (K_n) such that:

$$\left[\frac{K_u}{K_s} \right]_{\text{Ge(Li)}} K_n = 1 \quad (3)$$

Dividing Equation 2 by Equation 1 and solving for M_u yields:

$$\left[M_u = \frac{A_u K_s}{A_s K_u} M_s \right]_{\text{Ge(Li)}} \quad (4)$$

Substituting Equation 3 into Equation 4 gives:

$$[M_u]_{\text{Ge(Li)}} = \left[\frac{A_u}{A_s} M_s \right]_{\text{Ge(Li)}} K_n \quad (5)$$

It should be noted that Equations 1, 2, 3, 4, and 5 are relative only to γ -ray activities measured for a single nuclide with a Ge(Li) detector.

If the standard and unknown are counted for an identical length of live time with a NaI(Tl) well detector, the corrected activity at zero time is proportional to the mass of the radioactive nuclide present. Like Equations 1 and 2, this can be expressed as:

$$[A_s = K_s M_s]_{\text{NaI(Tl)}} \quad (6)$$

$$[A_u = K_u M_u]_{\text{NaI(Tl)}} \quad (7)$$

Dividing Equation 7 by Equation 6 yields:

$$\left[M_u = \frac{A_u K_s}{A_s K_u} M_s \right]_{\text{NaI(Tl)}} \quad (8)$$

It should be emphasized that:

$$\left[\frac{K_s}{K_u} \right]_{\text{NaI(Tl)}} \neq \left[\frac{K_s}{K_u} \right]_{\text{Ge(Li)}} \quad (9)$$

However, under certain conditions:

$$\left[\frac{K_u}{K_s} \right]_{\text{NaI(Tl)}} \approx 1 \quad (10)$$

The conditions governing Equation 10 are the following. The neutron flux must be similar for standard and unknown; the time duration of the count must be short in relation to the half life of the nuclide determined; and the NaI(Tl) well detector must be capable of minimizing the geometry factor between standard and unknown (i.e., 4π geometry should be approximated). If the above three conditions are realized, then Equation 8 reduces to:

$$\left[M_u = \frac{A_u}{A_s} M_s \right]_{\text{NaI(Tl)}} \quad (11)$$

Dividing Equation 11 with Equation 5 yields:

Table I. Absolute Amount of Each Element Present in the Three Standards

Standard No.	Nb, μg	Cu, μg	Mn, μg	Al, μg	V, μg
I	100	20	1.0	5.0	0.2
II	...	20	1.0	5.0	0.2
III	1.0	5.0	0.2

$$\begin{aligned} [M_u]_{\text{NaI(Tl)}} &= \left[\frac{A_u}{A_s} M_s \right]_{\text{NaI(Tl)}} \\ [M_u]_{\text{Ge(Li)}} &= \left[\frac{A_u}{A_s} M_s \right]_{\text{Ge(Li)}} K_n \end{aligned} \quad (12)$$

It is obvious that:

$$M_{u\text{Ge(Li)}} = M_{u\text{NaI(Tl)}} \quad (13)$$

$$M_{s\text{Ge(Li)}} = M_{s\text{NaI(Tl)}} \quad (14)$$

Simplifying Equation 12 gives:

$$\begin{aligned} \left[\frac{A_u}{A_s} \right]_{\text{NaI(Tl)}} &= K_n \\ \left[\frac{A_u}{A_s} \right]_{\text{Ge(Li)}} & \end{aligned} \quad (15)$$

Therefore K_n can be approximated experimentally by counting the unknown and standard first with a Ge(Li) detector and then with a NaI(Tl) well detector. The K_n value can then be applied to Equation 5 to determine any other nuclide present in the unknown provided the same nuclide is present in the standard.

It is not necessary to use a NaI(Tl) well detector to determine the K_n factor. Any method of analysis that would determine any convenient element present in the γ -ray spectrum determined with the Ge(Li) detector would be satisfactory. If the normalizing element is determined by atomic absorption spectrophotometry, for example, the K_n factor will also correct for neutron flux inhomogeneity between the standard and sample. Therefore, it would not be necessary to place the standard and unknown as close together as physically possible during the thermal neutron irradiation. This is evident from the following equations:

$$[C_s = X_s K]_{\text{A.A.S.}} \quad (16)$$

$$[C_u = X_u K]_{\text{A.A.S.}} \quad (17)$$

where C_s and C_u = concentration of the dissolved standard and unknown in liters; X_s and X_u = the absorbance measured by atomic absorption analysis; and K = molar absorptivity for the element of interest.

K is equal for Equations 16 and 17 if the operating parameters of the atomic absorption unit are the same for standard and unknown. The subscript A.A.S. refers to atomic absorption spectrophotometry. Dividing Equation 17 by Equation 16 yields:

$$\left[\frac{C_u}{C_s} = \frac{X_u}{X_s} \right]_{\text{A.A.S.}} \quad (18)$$

M_s and M_u are related to C_u and C_s by a volume term:

$$C_u = \frac{M_u}{V_u} \quad (19)$$

$$C_s = \frac{M_s}{V_s} \quad (20)$$

If

$$V_u = V_s \quad (21)$$

then

$$\left[\frac{M_s}{M_u} = \frac{X_u}{X_s} \right]_{\text{A.A.S.}} \quad (22)$$

Table II. Analysis of Bovine Liver

Sample No.	Mn, $\mu\text{g/g}$		Cu, $\mu\text{g/g}$		Na, $\mu\text{g/g}$		V, $\mu\text{g/g}$		Al, $\mu\text{g/g}$	
	Method I	Method II	Method I	Method II	Method I	Method II	Method I	Method II	Method I	Method II
1	6.09 \pm 0.73	10.6 \pm 1.3	106 \pm 1.3	185 \pm 8.0	1240 \pm 67	2150 \pm 67	<0.02	<0.04	13.3 \pm 0.8	23.4 \pm 1.5
2	6.04 \pm 0.67	10.5 \pm 1.2	104 \pm 3.6	182 \pm 7.7	1310 \pm 27	2270 \pm 72	<0.02	<0.04	15.2 \pm 0.7	21.7 \pm 1.3
3	5.01 \pm 0.71	10.3 \pm 1.2	86.8 \pm 3.0	179 \pm 7.5	1090 \pm 22	2230 \pm 71	<0.02	<0.04	10.5 \pm 0.6	21.7 \pm 1.3
4	4.83 \pm 0.59	9.5 \pm 1.2	86.1 \pm 3.7	170 \pm 8.3	1100 \pm 22	2160 \pm 66	<0.02	<0.04	9.5 \pm 0.6	18.9 \pm 2.3
5	4.52 \pm 0.54	9.2 \pm 1.1	79.9 \pm 2.7	162 \pm 6.7	1020 \pm 20	2070 \pm 64	<0.02	<0.04	7.9 \pm 0.4	16.1 \pm 1.0
Mean	5.30 \pm 0.72	10.0 \pm 0.6	93 \pm 12	176 \pm 9	1152 \pm 119	2176 \pm 77	<0.02	<0.04	11.3 \pm 2.9	20.4 \pm 2.9
NBS Certified value	10.3 \pm 1.0		193 \pm 10		2430 \pm 110					

Table III. Analysis of Orchard Leaves

Sample No.	Mn, $\mu\text{g/g}$		Cu, $\mu\text{g/g}$		Na, $\mu\text{g/g}$		V, $\mu\text{g/g}$		Al, $\mu\text{g/g}$	
	Method I	Method II	Method I	Method II	Method I	Method II	Method I	Method II	Method I	Method II
1	30.8 \pm 1.7	88.8 \pm 4.9	4.9 \pm 1.3	14.2 \pm 5.0	<25	<100	0.16 \pm 0.03	0.46 \pm 0.09	142 \pm 4	419 \pm 26
2	22.1 \pm 1.1	86.2 \pm 4.4	5.2 \pm 1.3	21.5 \pm 5.5	<25	<100	0.12 \pm 0.02	0.51 \pm 0.07	101 \pm 3	418 \pm 24
3	20.1 \pm 1.0	86.8 \pm 4.3	2.6 \pm 0.8	11.6 \pm 3.5	<25	<100	0.15 \pm 0.02	0.69 \pm 0.09	88 \pm 2	398 \pm 23
4	20.8 \pm 1.1	85.1 \pm 4.2	3.0 \pm 0.8	13.0 \pm 0.8	<25	<100	0.10 \pm 0.01	0.45 \pm 0.06	91 \pm 2	397 \pm 22
5	21.5 \pm 1.1	81.3 \pm 4.0	2.3 \pm 0.8	9.7 \pm 3.5	<25	<100	0.18 \pm 0.02	0.74 \pm 0.10	95 \pm 3	402 \pm 23
Mean	23.1 \pm 1.4	85.6 \pm 2.8	3.6 \pm 1.3	14.0 \pm 4.5	<25	<100	0.14 \pm 0.03	0.57 \pm 0.14	103 \pm 22	407 \pm 11
NBS Certified value	91 \pm 4		12 \pm 1		82 \pm 6					

Again it is obvious that:

$$[M_u]_{\text{Ge(Li)}} = [M_u]_{\text{A.A.S.}} \quad (23)$$

and

$$[M_u]_{\text{Ge(Li)}} = [M_u]_{\text{A.A.S.}} \quad (24)$$

Dividing Equation 22 by Equation 5 yields:

$$\frac{[M_u]_{\text{A.A.S.}}}{[M_u]_{\text{Ge(Li)}}} = \frac{\left[\frac{X_u}{X_n} M_n\right]_{\text{A.A.S.}}}{\left[\frac{A_u}{A_n} M_n\right]_{\text{Ge(Li)}} K_n} \quad (25)$$

Simplifying Equation 25 gives:

$$\frac{\left[\frac{X_u}{X_n}\right]_{\text{A.A.S.}}}{\left[\frac{A_u}{A_n}\right]_{\text{Ge(Li)}}} = K_n \quad (26)$$

It is apparent that when K_n is determined by a second method of analysis, the neutron flux inhomogeneity never enters into the calculation. The primary disadvantage of determining K_n by a secondary method of analysis is that the sample matrix is usually destroyed.

EXPERIMENTAL

Preparing of Standards and Unknowns. Solid standards were prepared by adding 0.100 ml of a liquid standard to a polystyrene filter disk (1.27-cm diameter). The filter disks were cut from a Delbag Microsorb polystyrene filter (Type 99/97) with a polyethylene disk cutter. Delbag polystyrene filters are hydrophobic so the liquid drop does not wet the surface. The liquid drop was allowed to dry on the filter disk in a laminar flow clean bench. After drying, the metal salts were deposited as a small area (approximately 0.3-cm diameter) on the filter disk. The disk standard was then transferred to a polyethylene die specifically constructed for the standards. A second Delbag filter disk was placed on top of the standard filter disk and a polyethylene ram was pushed into the die. Hand pressure was sufficient to ensure that the two polystyrene disks are pressed together. The standard metal salts are then approximately in the center between the two polystyrene disks. The pressed disk standard was then inserted into a small polyethylene bag (3 cm \times 3 cm) and heat sealed. Standards made up in this manner are stable and do not change concentration for the elements determined in this study. Presently we make several hundred of these standards at a time and then use them as needed over a period of several months. Three standards are irradiated with each sample. The absolute mass of each element in each standard is given in Table I.

NBS (No. 1577) bovine liver and orchard leaves NBS (No. 1571) were simply weighed (100 mg) into acid cleaned 0.5-dram polyethylene vials and heat sealed. The outside of the sealed polyethylene vials were rinsed with distilled-demineralized water and inserted into a clean polyethylene bag (3 cm \times 3 cm) which was then heat sealed. It should be noted that the bovine liver and orchard leaf samples had a different geometry from the standards.

Thermal Neutron Irradiation. Irradiations were carried out at the Rhode Island Nuclear Science Center. The nuclear reactor at this facility is of the swimming pool type with a power rating of 2 megawatts. A thermal neutron flux of $\sim 4 \times 10^{12}$ n/cm²-sec is available in the pneumatic irradiation tube that is used to rapidly insert and retrieve samples from a location near the reactor core. The thermal to fast neutron flux ratio is 40 in the pneumatic irradiation tube location. The length of the irradiations for this study was exactly 5 minutes.

Data Collection and Processing. Subsequent to irradiation, the sample and standard were counted at decay times of exactly 2 minutes and 6 minutes, respectively. The duration of the count for samples and standards was exactly 200 seconds of clock time. The first counts of sample and standard were made with an Ortec 40 cm³ Ge(Li) coaxial detector (resolution of 2.3 keV for the 1332-keV gamma ray of ⁶⁰Co) coupled to a Nuclear Data 2200 4096 channel analyzer with computer compatible magnetic tape output (AMPEX TM-7) for spectrum analysis. A computer program (J. L. Fasching, personal communication) was used to process the Ge(Li) spectra acquired. Only standard I was counted on

Table IV. Analysis of Laboratory Prepared Unknowns Using the K_n Factor in the Calculations

Sample No.	Mn, μg	Cu, μg	V, μg	Al, μg
1	1.03 ± 0.04	19.4 ± 0.8	0.188 ± 0.009	4.6 ± 0.2
2	1.02 ± 0.04	20.7 ± 0.9	0.188 ± 0.009	5.0 ± 0.2
3	1.04 ± 0.04	19.8 ± 0.9	0.204 ± 0.009	5.0 ± 0.2
4	1.03 ± 0.04	20.3 ± 0.9	0.210 ± 0.010	5.0 ± 0.2
5	1.03 ± 0.04	22.7 ± 0.9	0.204 ± 0.009	5.0 ± 0.2
6	0.98 ± 0.04	21.2 ± 0.9	0.207 ± 0.010	4.9 ± 0.2
7	0.98 ± 0.04	19.5 ± 0.8	0.205 ± 0.009	4.9 ± 0.2
8	0.96 ± 0.04	20.2 ± 0.8	0.199 ± 0.009	4.9 ± 0.2
Mean	1.01 ± 0.03	20.5 ± 1.1	0.201 ± 0.008	4.9 ± 0.2
Quantity present	1.00	20.0	0.200	5.00
1	1.02 ± 0.04	5.0 ± 0.3	0.49 ± 0.02	10.2 ± 0.4
2	1.03 ± 0.04	5.1 ± 0.3	0.49 ± 0.02	9.8 ± 0.4
3	1.03 ± 0.04	4.8 ± 0.3	0.52 ± 0.02	10.2 ± 0.4
Mean	1.03 ± 0.04	5.0 ± 0.2	0.52 ± 0.02	10.0 ± 0.2
Quantity present	1.00	5.00	0.50	10.0
1	0.97 ± 0.04	10.3 ± 0.5	1.02 ± 0.04	5.2 ± 0.2
2	0.96 ± 0.04	10.0 ± 0.5	0.99 ± 0.04	5.1 ± 0.2
3	0.98 ± 0.04	10.2 ± 0.5	1.03 ± 0.04	5.2 ± 0.2
Mean	0.97 ± 0.01	10.2 ± 0.1	1.01 ± 0.02	5.1 ± 0.1
Quantity present	1.00	10.0	1.00	5.00
1	0.10 ± 0.01	5.2 ± 0.5	0.10 ± 0.01	10.0 ± 0.8
2	0.11 ± 0.01	4.3 ± 0.4	0.093 ± 0.008	9.6 ± 0.8
3	0.11 ± 0.01	5.0 ± 0.5	0.094 ± 0.008	9.5 ± 0.8
Mean	0.11 ± 0.01	4.8 ± 0.5	0.096 ± 0.004	9.7 ± 0.2
Quantity present	0.100	5.00	0.100	10.0

the Ge(Li) detector. The various γ rays used for the activity determination with the Ge(Li) detector were as follows: 1779 keV for ^{223}Rn ; 1434 keV for ^{223}Ac ; 1039 keV for ^{223}Fr ; 1039 keV for ^{223}Ac ; 1811 keV for ^{223}Ac ; and 1370 keV for ^{223}Ac . The 847-keV γ -ray of ^{56}Mn was not used since the activated bovine liver and orchard leaves contained reasonably large quantities of ^{27}Mg , which has a γ -ray of 844 keV.

The second sample and standard count was made 5 hours to 2 days after the irradiation. This count was made using a 3-in. \times 3-in. NaI(Tl) well detector (resolution of 106 keV for the 1332-keV gamma ray of ^{60}Co) coupled to a Nuclear Data 512 channel analyzer. The samples and standards were counted for 1 minute of live time. The spectrum was read out on a typewriter and hand integrated for the γ -ray of interest. Standards I, II, or III were counted with NaI(Tl) detector depending on the presence of ^{24}Na or ^{64}Cu in the sample. The γ -ray peaks used for the activity determination with the NaI(Tl) detector was one of the following: 847 keV for ^{24}Na ; 510 keV for ^{64}Cu ; or 2750 keV for ^{24}Na . It should be noted that the 847 keV γ -ray activity of ^{56}Mn could be used in the NaI(Tl) spectra since all the ^{27}Mg activity was gone 5 to 6 hours after irradiation. The 510-keV annihilation γ -ray of ^{64}Cu was used since the activity due to the 1040 keV γ -ray of ^{64}Cu was gone after 5 to 6 hours. The 2750-keV γ -ray of ^{24}Na was used since less spectral interference was encountered at the higher end of the energy spectrum, making background corrections more exact. If ^{64}Cu or ^{24}Na were used as the normalizing isotope, the samples and standards were counted several days after the irradiation to ensure that shorter lived radioactive nuclides had decayed away.

RESULTS AND DISCUSSION

The results of the NBS bovine liver and orchard leaves analysis are shown in Tables II and III, respectively. The Ge(Li) counter dead time for bovine liver and orchard leaves was approximately 40% and 30%, respectively. The Ge(Li) counter dead time for Standard I was 20%. The results of the analysis have been calculated two ways. The first method (I) compares the corrected activities of the standards and unknowns for dead time and decay time. The second method (II) was done by using Equation 5. Mn was used to determine K_n for orchard leaves and Na was used to determine K_n for bovine liver. The certified

NBS values for Mn, Cu, and Na are also given in Tables II and III. The uncertainties given for each individual analysis are a combination of the count rate uncertainties for the activities used in each metal determination. The uncertainty given for the average is the standard deviation of the mean for each set of analyses. It can be seen that the precision of Methods I and II is comparable but the accuracy is not. The agreement between Method II and NBS certified values for Na, Mn, and Cu is good. The certified values of Al and V are not available from NBS at this time. However, Maienthal (7) has reported an Al value of 347 ± 7.5 for orchard leaves. Method I values are lower than Method II values for all the elements listed by factors of 2 and 4, respectively, for bovine liver and orchard leaves. The differences are predominantly due to the lack of a geometry correction in Method I.

The Al values given in Tables II and III may be high since the Si content of bovine liver and orchard leaves is not known. ^{28}Al is produced from ^{28}Si by the n,p reaction with fast neutrons. Studies at this reactor indicate that equal concentrations of Al and Si will produce an ^{28}Al activity that is $\approx 0.5\%$ in error (e.g., 0.5% of the ^{28}Al measured will be produced from the n,p reaction with ^{28}Si). It is possible that the Si concentration could be greater than the Al concentration in bovine liver and orchard leaves. If this were true, the Al values given in Tables II, and III would have to be corrected for both Method I and II.

In order to test the concept of using a second method of analysis to determine K_n , two standards containing identical concentrations of Na (i.e., 100 μg) were irradiated simultaneously. The relative concentrations of Mn, Cu, V, and Al were varied in the standard chosen as the unknown. No attempt was made to reproduce geometry or detector dead time during counting with the Ge(Li) detector. It was then assumed that the Na concentration had been determined in the unknown by a second method

(7) E. June Maienthal, *J. Ass. Offic. Anal. Chem.*, 55, 1109 (1972).

of analysis and had a zero uncertainty. The K_n factor was then calculated. The results of the analysis are given in Table IV. It can be seen that the results are very good. The uncertainties for the individual analyses are based on count rate statistics. The uncertainties reported for the mean values are the standard deviations of the mean for each set.

It is likely that the improvement in the data presented in Table IV, relative to bovine liver and orchard leaves, is due to the elimination of the flux inhomogeneity from the calculation. Also a small uncertainty in geometry is still present in the analysis of the bovine liver and orchard leaves which is obviously not present in the laboratory prepared unknowns.

There are three primary advantages to using the K_n factor correction. Geometry and dead time corrections are simple for short lived nuclides for a nondestructive analysis. Accurate standard and sample placement during counting is not important (This means that a sample with a high dead time can be moved away from the detector without noting its location relative to the detector). The

method is fast since no special sample pretreatment is required.

We presently use this method of K_n factor correction routinely in our laboratory. Several hundred samples have been analyzed in this manner. The method is rapid (generally 20-30 samples can be analyzed per day), and has been used on atmospheric and sea water samples.

ACKNOWLEDGMENT

We are grateful to the nuclear reactor staff at the Rhode Island Nuclear Science Center for providing space and facilities for these analyses. We also wish to acknowledge James L. Fasching of the University of Rhode Island, Kingston, R.I., for making a computer program, which analyzed the gamma ray spectra, available to us.

Received for review May 29, 1973. Accepted October 26, 1973. This research was supported by the Office of the International Decade of Ocean Exploration, National Science Foundation, under NSF Grant GX33777.

Determination of Phenols by Fluorine-19 Nuclear Magnetic Resonance of Hexafluoroacetone Derivatives

Floyd F.-L. Ho

Research Center, Hercules Incorporated, Wilmington, Del. 19899

Our previous study of the application of hexafluoroacetone to the characterization and quantitative measurement of alcohols has been extended to the determination of phenols. It was found that the F-19 resonance of the hexafluoroacetone-phenolic adducts can be measured with high sensitivity and resolution. All six isomers of dimethylphenol can be determined in a mixture at low concentrations. The dominant effect on the fluorine chemical shift of the adduct is steric interaction with the ortho substituents on the phenols; electronic and resonance effects from meta and para substituents provide secondary differentiation. Equilibrium constants of adduct formation were determined for several ortho alkyl phenols. Although reaction with most phenols is quantitative, caution should be exercised in the case of phenols with bulky ortho alkyl groups or strong electron-withdrawing substituents.

The determination of hydroxyl has been reviewed generally in two recent monographs (1, 2). In analyses for phenols, by far the most common procedures are based on titration of the phenolic hydroxyl with various chemical reagents. Recently, we have demonstrated that hexafluoroacetone reacts readily and quantitatively with common primary and secondary hydroxyls of both monomeric and polymeric materials (3). Measuring the fluorine NMR signal of these hexafluoroacetone adducts has the advantages of increased sensitivity (because of the replacement of a

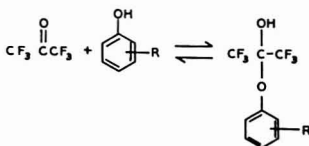
single hydroxylic proton with 6 fluorines) and much greater resolution. This report describes the extension of this technique to the characterization and quantitative measurement of phenols.

EXPERIMENTAL

The F-19 NMR spectra of the HFA adducts were obtained on a Bruker HFX-90 instrument, as described previously (3). The operating frequency for fluorine resonance is 84.67 MHz. The ambient probe temperature was 25 °C.

Hexafluoroacetone (HFA) was obtained from Pierce Chemicals, Rockford, Ill., in disposable cylinders (bp = -28 °C). Preparation of a stock reagent of HFA in ethyl acetate was described earlier (3). Phenol and substituted phenols were reagent grade material purchased from either Eastman Organic or Aldrich Chemical Co. An NMR spectrum and a gas chromatogram were taken on each phenol to check its purity. Several *o*-alkyl phenols used in this study were further purified by fractional distillation at reduced pressure. The fluorine resonance of *n*-butyl trifluoroacetate, obtained from PCR, Inc., and purified by fractional distillation, was used as an internal standard to provide a fluorine resonance signal for instrument integral calibration in quantitative measurements.

The normal procedure for sample preparation involves weighing the phenol and internal standard (to 0.0005 gram) directly into a 1.00-ml volumetric flask, followed by dilution to the mark with HFA/EA reagent. Spectra taken immediately after mixing the sample solution showed that the reaction (Equation 1) is fast and quantitative with most phenols.



(1) Stig Veibel, "The Determination of Hydroxyl Groups," Academic Press, London, 1972.

(2) "The Chemistry of the Hydroxyl Groups," S. Patai, Ed., Interscience Publishers, New York, N.Y., 1971.

(3) F. F.-L. Ho, *Anal. Chem.*, **45**, 603 (1973).

However, phenols with bulky substituents in the ortho position require longer reaction times. For example, the reaction with 2-*tert*-butylphenol requires 24 hours at room temperature to reach equilibrium. Equilibrium constants for several *o*-alkylphenols were determined (Table III), using the general expression:

$$K = \frac{c}{a \times (b_o - c)} \quad (2)$$

where *a* and *c* are molar concentrations of excess hexafluoroacetone (a sharp singlet observed at 7500 Hz from HFB) and phenolic adduct, respectively; *b_o* is the molar concentration of phenol initially weighed into the flask.

RESULTS AND DISCUSSION

Isomer Analyses. Several NMR procedures for characterizing isomeric phenols in a mixture have been described in the literature. Dietrich, Nash, and Keller (4) found that individual hydroxylic proton signals of phenols in a mixture dissolved in hexamethylphosphoramide (HMPA) can be resolved. Crutchfield, Irani, and Yoder (5) reported that characteristic patterns from the resonances of the protons on the carbon atoms in the α -position relative to the aromatic ring can yield information concerning the ortho:para ratio in alkylphenols. Lindeman and Nicksic (6) used acetate methyl resonances of the acetate derivative to determine ortho and para isomers. Konishi, Mori, and Taniguchi (7) differentiated isomers by observing the fluorine resonance of the corresponding trifluoroacetates. After comparing these methods with the one described in the present study, we believe that measurement of the fluorine resonance of the HFA derivative generally has the advantages of higher resolution, higher sensitivity, and easier correlation of chemical shift data with structural parameters.

To illustrate the excellent resolution and sensitivity obtained with the HFA derivatives, a spectrum showing all six isomers of dimethylphenol is shown in Figure 1. This spectrum was run on a solution prepared by introducing 1- to 5-milligram quantities of each dimethylphenol isomer directly into a standard NMR tube containing about 1.0 ml of reagent. Each isomer in the mixture gives a sharp and characteristic singlet. Interestingly, these isomers can be roughly grouped into 3 classes based on substitution in the ortho position. Those having no ortho substituent appear at a higher field; those having one ortho methyl appear in the center, and the one having two ortho groups is observed at a lower field. The substituents at the meta and para position provide a secondary differential.

To demonstrate further the primary influence of ortho substituents on chemical shift, a limited series of phenols with different degrees of substitution was examined. The results, summarized in Figure 2, show that the dominant effect is indeed due to the substitution at the ortho position, with the magnitude of the shift increasing with the bulk of the substituent. In general, substitution at the meta and para positions provides only a secondary influence (represented approximately by the length of the horizontal bar in Figure 2). For example, with respect to unsubstituted phenol, the *p*-nitrophenol adduct appears at only 0.05 ppm to lower field and the *p*-methoxyphenol at only 0.01 ppm to higher field. These relatively small shifts suggest that the electronic and resonance properties of the substituents on the phenolic ring have little effect on the observed fluorine chemical shift of the HFA adduct.

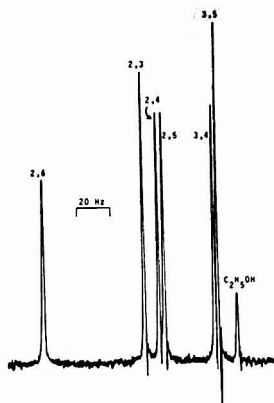


Figure 1. ^{19}F NMR spectrum of hexafluoroacetone adducts with all six dimethylphenol isomers (Field increases from left to right)

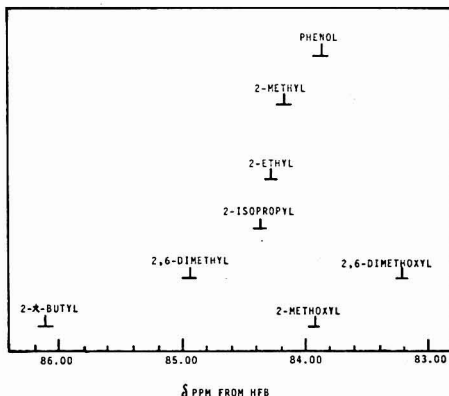


Figure 2. Summary of chemical shifts of phenols with various substituents

On the other hand, meta and para substituents can profoundly modify the reactivity of the phenolic hydroxyl group toward HFA. For instance, it was observed that the equilibrium constant of Equation 1 with *p*-nitrophenol is almost one order of magnitude smaller than that with phenol. A study of the effect of substitution at the meta and para positions on the reactivity of the hydroxyl group with HFA is in progress and will be reported elsewhere shortly. It is, nevertheless, the ortho substituents which dominate the chemical shift of the HFA adduct. The reproducible and highly resolvable chemical shifts of the HFA adducts provide a sensitive tool in analyses of phenols.

This ortho substituent effect evidently arises from steric interaction, although the detailed mechanism is not clear at present. A major contribution can perhaps be visualized as arising from the magnetic anisotropy of the aromatic ring current. The CF_3 groups in a HFA adduct can assume various positions relative to the ring, by virtue of free rotation along both of the chemical bonds in the $\text{C}-\text{O}-\text{C}_6\text{H}_5$ moiety. In ortho substituted alkylphenols, the

(4) M. W. Dietrich, J. S. Nash, and R. E. Keller, *Anal. Chem.*, **38**, 1479 (1966).

(5) M. M. Crutchfield, R. R. Irani, and J. T. Yoder, *J. Amer. Oil Chem. Soc.*, **41**, 129 (1964).

(6) L. P. Lindeman and S. W. Nicksic, *Anal. Chem.*, **36**, 2414 (1964).

(7) K. Konishi, Y. Mori, and N. Taniguchi, *Analyst (London)*, **94**, 1002 (1969).

Table I. Chemical Shifts of HFA and HMPA Derivatives of Phenols

Compound	¹⁹ F-HFA ^a	¹ H-HMPA ^b
Phenol	83.855	10.30
3,5-Dimethyl	83.820	10.02
3,4-Dimethyl	83.852	9.93
2,5-Dimethyl	84.197	...
2,4-Dimethyl	84.245	9.97
2,3-Dimethyl	84.339	10.02
2,6-Dimethyl	85.036	9.20

^a Parts per million downfield from hexafluorobenzene (HFB). ^b Obtained from Reference 4.

Table II. Comparison of Chemical Shifts of Trifluoroacetate and Hexafluoroacetone Adducts of Various Phenols

Alkylphenols	TFA ^a	HFA ^b
Methylphenol		
Ortho isomer	0.507	84.174
Para isomer	0.319	83.850
	$\Delta = 0.188$	$\Delta = 0.324$
Ethylphenol		
Ortho isomer	0.464	84.257
Para isomer	0.361	83.845
	$\Delta = 0.103$	$\Delta = 0.412$

^a From Reference 7, converted from Hz (downfield from trifluoroacetic anhydride) to ppm, using the reported instrument frequency of 66.4 MHz. ^b In ppm downfield from hexafluorobenzene.

most favorable structure is that in which the CF₃ groups occupy positions relatively far from the alkyl substituent, with the C-O bond in the C-O-C₆H₅ moiety almost in plane with the phenolic ring but on the side opposite from the alkyl group. This structure places the CF₃ groups in the deshielding region of the ring current and correlates with a downfield shift. Because of steric interaction, this structure becomes more important with increasing size or number of ortho substituent. Thus, adducts with 2,6-dimethyl- and 2-*tert*-butylphenols are observed at a progressively and substantially lower field.

Notice in Figure 2 that the fluorine resonance of the *o*-methoxyphenol adduct is found at a slightly higher field than 2-methylphenol and that the corresponding signal from 2,6-dimethoxyphenol is even at a much higher field. This again can be qualitatively accounted for by the ring current anisotropy. The hydroxyl in the adduct (see Equation 1) is more acidic and thus a good proton donor, favoring intramolecular hydrogen bonding with the electron-rich oxygen atom of the *o*-methoxyl groups. A favorable position for the formation of this seven-membered, hydrogen-bonded structure is with the C-O bond in the C-O-C₆H₅ moiety making a large angle with the phenolic plane. This position places the CF₃ groups above the plane and subject to the diamagnetic effect of the ring current, causing the adduct signal to be observed at a higher field.

The chemical shift due to the difference in ring current anisotropy between these two extreme positions—i.e., positions with the C-O bond making the smallest and largest possible angles with the phenolic plane—is estimated to be about 4 ppm using the data of Johnson and Bovey (8). The chemical shift range in Figure 2 approaches this limit.

Although the data obtained thus far appear to be consistent with an explanation based on a simple ring current model, other mechanisms which may contribute to the chemical shift in these compounds may be postulated, in-

Table III. Equilibrium Constants of HFA with *o*-Alkylphenols in EA at 25 °C

<i>o</i> -Alkylphenols	Equilibrium constant (l./mole ⁻¹)
2-Methyl	107
2-Ethyl	84
2-Isopropyl	73
2- <i>tert</i> -Butyl	5.8
2,6-Dimethyl	2.6

Table IV. Comparison of Equilibrium Constants with Other Structural Parameters of *o*-Alkylphenols

<i>o</i> -Alkylphenols	log <i>K</i>	σ_{ortho}^a	p <i>K</i> _a ^b
2-Methyl	2.03	-0.13	10.15
2-Ethyl	1.93	...	10.28
2-Isopropyl	1.87	-0.23	...
2- <i>tert</i> -Butyl	0.76	-0.52	...
2,6-Dimethyl	0.42	...	10.59

^a Apparent σ_{ortho} constants for substitution in phenols obtained from Reference 10. ^b Dissociation constants from Reference 11.

cluding the carbon-carbon bond interaction and/or short range polarization effects.

A comparison of the chemical shifts of a mixture of dimethylphenols by proton NMR in hexamethylphosphoramide (4) and the present fluorine technique is shown in Table I. The resolution between a few pairs of isomers by the fluorine technique is slightly better. Of more importance in identifying the components of isomeric mixtures, however, is the pronounced ordering of the observed shift with respect to the structural parameters, in the phenol/HFA adducts.

A comparison between two fluorine NMR techniques, that using trifluoroacetate (7) and the present one using hexafluoroacetone adduct, is shown in Table II. Although the data available for comparison are rather limited, higher resolution can clearly be obtained by using the HFA derivatives. This is perhaps due to the fact that the CF₃ group in the trifluoroacetate derivative is further from the phenol ring, and thus less affected by the ring current or other localized effects.

Equilibrium Constants. A brief study of the equilibria of Equation 1 for various phenols was undertaken to verify the applicability of the HFA technique to quantitative analyses of phenols. With water and most alcoholic hydroxyls, the equilibrium of Equation 1 normally lies far to the right (3, 9). For example, the enthalpy of hemiacetal formation of HFA with methanol in solution at 25 °C was found to be -22.7 Kcal/mole (9). The present experiment offers a practical way to study the reaction of HFA with *o*-alkylphenols because the equilibrium under normal conditions lies in a convenient region for NMR measurement. Using the expression given in the Experimental section, a set of equilibrium constants for several selected *o*-alkylphenols was obtained, and the data are shown in Table III. A gradual decrease in *K* is observed as the size of the substituents increases from methyl to isopropyl. However, the decrease in *K* is significantly greater when the substituent is *tert*-butyl or 2,6-dimethyl. With either of these two, steric interaction is severe. This dependence of *K* on

(9) F. E. Rogers and R. J. Rapiejko, *J. Amer. Chem. Soc.*, **93**, 4596 (1971).

(10) G. B. Barlin and D. D. Perrin, *Quart. Rev., Chem. Soc.*, **20**, 75 (1966).

(11) G. Kortum, W. Vogel, and K. Andrussov, *Pure Appl. Chem.*, **1**, 187 (1961).

the size of the ortho-alkyl substituents parallels changes in other constants derived from the same structural differences, as may be seen from the data in Table IV. Again, only limited comparable data are available.

As to the application of the HFA technique to quantitative analysis, it can be concluded that although it is applicable to most phenols, caution should be exercised in systems where there is a bulky ortho substituent or a strong electronegative group at the meta or para position. In such systems, the equilibrium does not lie too far to the right. This, however, can be partially overcome by the

presence of a great excess of free HFA. For example, to reach 99% reaction in a substituted phenol whose K with HFA is 100, a 1.0 molar excess of HFA should be present.

ACKNOWLEDGMENT

The author thanks George A. Ward and Robert D. Mair for many helpful discussions, and Robert R. Kohler for experimental assistance.

Received for review May 16, 1973. Accepted November 16, 1973. Hercules Research Center Contribution No. 1614.

Elemental Analysis of Whole Blood Using Proton-Induced X-Ray Emission

R. C. Bearse,¹ D. A. Close, J. J. Malanify, and C. J. Umbarger

Los Alamos Scientific Laboratory of the University of California, Los Alamos, N.M. 87544

A technique for the analysis of trace elements in whole blood has been developed using proton-induced X-ray emission. Samples of 0.1 ml whole blood from humans and mice were dried, weighed, and then ashed in a plasma asher. Targets were prepared by placing drops made from the ash and a 400-ppm Pd solution onto Formvar backings. The samples were irradiated with 2.25-MeV protons, and the X-rays analyzed in a nondispersive X-ray detector. The elements Fe, Cu, Zn, Se, and Rb were detected with a precision of 7, 18, 7, 50, and 19%, respectively, in human whole blood. The precision of the technique was determined by statistical analyses of two different sets of 27 samples. The system was shown to be linear for variations in elemental concentration. The accuracy for determination of Zn was found to be within 10% by comparison to atomic absorption spectrometry.

Although the study of trace elements in biological systems has been pursued for many years (1), the increased awareness of trace metal toxicity has created a new interest in improved measuring techniques. The recent introduction of high-resolution nondispersive X-ray detectors has spurred a great deal of activity in X-ray fluorescence trace analysis. Several groups (2-4) have reported that proton-induced X-ray emission has great potential in trace analysis because many elements can be detected simultaneously and only small samples (~100 mg) are needed. Most of these papers, however, have been of a general and exploratory nature, and few deal with the details of a specific system for making measurements of a particular sample type. Most notably, previous workers seem to have relied on counting statistics as a measure of precision, an approach that we have eschewed.

The purpose of this paper is to present details of a method of measuring trace elements in small volumes (0.1 ml) of whole blood using proton-induced X-ray emission. Blood was chosen because it is a physiologically important fluid that is easily sampled. We will discuss the basic principles of the technique, the blood sampling and preparation techniques, the apparatus used in analyzing the samples, the preparation of the proton beam, and the precision and accuracy of our final procedure.

The principles of X-ray emission are simple. A heavy-ion beam, in passing through a thin sample, removes inner shell electrons with extremely high probability. The filling of these vacancies by outer shell electrons produces X-rays whose energies are characteristic of the element in which it is produced, and the number of X-rays is proportional to the number of atoms of that element present in the sample. Since the yield of X-rays per atom is a smoothly varying function of atomic number and bombarding energy (5), and since modern X-ray detectors are capable of resolving $K\alpha$ X-rays from the elements adjacent in the periodic table (for $Z > 11$), many elements can be measured simultaneously. Because of the multiplicity of X-ray lines (e.g. $K\beta$) from each element and because of the possibility that some elements may be several orders of magnitude more prevalent than others, it may not always be possible to measure the presence of all elements without some prior chemical separation.

EXPERIMENTAL

Sample Preparation. Capillary pipets, rinsed in heparin and air-dried, were used to draw 0.1-ml samples of whole blood from the sinus cavities of mice. Human blood samples were drawn into 5-ml syringes, potassium oxalate was added, and the samples were repipetted with an Oxford 0.1-ml autopipet. The samples were pipetted directly into 1-ml borosilicate glass beakers that had been previously weighed on a Torsal balance to an accuracy of 0.2 mg. About 30 samples were processed at one time. The filled beakers were arranged on a 7.6 by 15.2-cm borosilicate glass plate on the base of a bell-jar system, and all beakers were repeatedly filled with liquid nitrogen until the blood was thoroughly frozen. With the beakers still containing liquid nitrogen, the bell jar was sealed and the system evacuated. The system was pumped for several hours, and an ultimate vacuum of about 0.06

¹ Visiting Staff Member from the University of Kansas, Lawrence, Kan. 66045.

- (1) E. J. Underwood, "Trace Elements in Human and Animal Nutrition," 3rd ed., Academic Press, New York, N.Y., 1971.
- (2) T. B. Johansson, R. Akselsson, and S. A. E. Johansson, *Nucl. Instrum. Methods*, **84**, 141 (1970).
- (3) F. C. Young, M. L. Roush, and P. G. Bergman, *Int. J. Appl. Radiat. Isotop.*, **24**, 153 (1973).
- (4) C. J. Umbarger, R. C. Bearse, D. A. Close, and J. J. Malanify, *Advan. X-Ray Anal.*, **16**, 102 (1973).

- (5) R. C. Bearse, D. A. Close, J. J. Malanify, and C. J. Umbarger, *Phys. Rev.*, **170**, 1269 (1973).

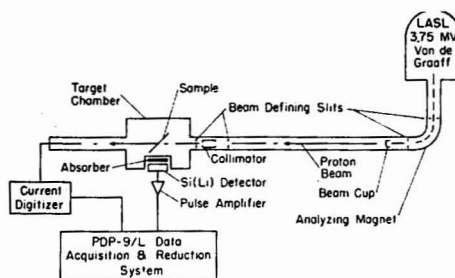


Figure 1. Equipment schematic for proton-induced X-ray emission

Torr was achieved. The beakers were then removed from the bell jar and reweighed to obtain the dry weight of the whole blood. The weight reduction from wet to dry blood was about a factor of 4.8. The samples were placed in a Tracerlab LTA-302 asher on a 7.6 by 15.2-cm borosilicate glass plate which allowed the beakers to be on the diameter of the ashing chamber. The samples were ashed for 48-72 hours at a power of 100 watts, a pressure of 0.9 Torr, and an oxygen flow of 150 cm³/min.

The purpose of ashing is to increase the concentration of the elements with $Z \geq 26$ by removal of the elements H, C, N, and O which comprise the bulk of the blood mass. Targets with a higher concentration of trace elements can then be fabricated with a much smaller total mass. This decrease in mass reduces the amount of background due to secondary electron bremsstrahlung (4), thus improving the detectability limit. It has been shown that plasma ashing is the method of choice to keep metal losses to a minimum (6).

After ashing, the samples were removed from the chamber, and 0.1 ml of a solution of 6 parts 1.8% HCl and 4 parts of 1000 ppm PdCl₂ (for normalization purposes) was added to each sample using the autopipet. A new disposable tip was used for each sample, and dissolution was effected by rapid inhalation and expiration of the solution, using the pipet. Occasionally, small black specks appeared in the solution and, so long as they were few and small, they did not seem to affect the accuracy of the analysis. A 0.02-ml autopipet was used to transfer that amount of the sample to the surface of a Formvar foil (7) on which a still wet 0.02-ml drop of 3% NH₄OH solution had been placed. The NH₄OH neutralized the acidic blood solution which would otherwise have attacked the foil. The samples dried on the foils within a diameter of 5-6 mm. They were stored and transported in a desiccator and then transferred to the Los Alamos Scientific Laboratory (LASL) trace-analysis chamber (8) which had been modified to hold six 2.5 by 5-cm aluminum frames with 1.9-cm diameter holes. Larger frame holes were used so that the target and beam area could be increased to a reasonable and practical size (governed by the size to which the liquid drops dried) without stray beam striking the frame. Even a beam 10³ times smaller than the primary beam would cause an appreciable background spectrum upon hitting the frame because of the effectively infinite thickness of the frame.

Formvar foils were used in this work because they were relatively easy to prepare in quantity, withstood the required beam intensity, and were tough enough to endure the abuse of target preparation and subsequent handling. Another important reason for using Formvar was that it can be made very thin, thus contributing insignificantly to the secondary electron bremsstrahlung continuum. A Formvar solution (7) was prepared which consisted of 16 grams of Formvar resin 15/95E (Monsanto Polymers and Petrochemicals Co.), 200 ml of methyl benzoate, 480 ml of toluene, and 320 ml of ethanol. The foils were made by placing a drop of this solution onto the surface of doubly distilled water. When the edges of the film began to wrinkle, it was picked up onto one of the aluminum frames, with care that double layers were not formed. These films were measured, by weighing and by the ener-

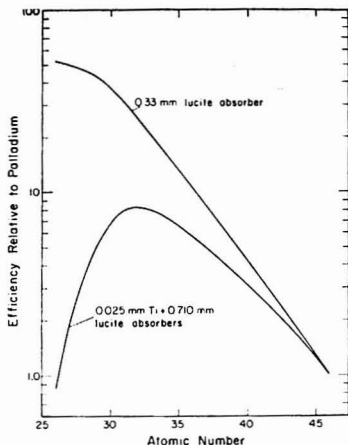


Figure 2. System detection efficiency with and without a titanium absorber

gy loss of alpha particles (9), to be about 10 $\mu\text{g}/\text{cm}^2$. The foils were prepared ahead of time, allowed to dry, and stored in a desiccator containing CaSO₄ desiccant.

Analysis Apparatus. The samples were bombarded with a 150-nA beam of protons from the LASL 3.75-MV Van de Graaff. The beam was spread over a 1-cm by 1-cm area centered on the frame hole. Beam collimation was achieved by four sets of slits and a collimator as shown in Figure 1. It is important to note that the final beam definition was performed by carbon slits only 12 cm from the target. This reduced the stray beam without the production of hard X-ray background to which the detector would be sensitive.

The X-rays were detected by an Ortec Si(Li) detector having a resolution of 175 eV at 5.9 keV. In reaching the detector the X-rays passed through a 0.013-mm Mylar foil in the X-ray chamber, a 0.025-mm sheet of Ti, a 0.71-mm Lucite absorber, and the 0.025-mm Be window of the detector. The Ti and Lucite were necessary to preferentially attenuate the large numbers of Fe X-rays produced in the whole blood samples. The efficiency of the detector relative to Pd was determined by preparing targets from known mixtures of various elements (Harleco, Inc.). The efficiency curve is shown in Figure 2.

The pulses from the detector were amplified by an Ortec 450 amplifier, set for 3- μsec shaping time, and sent to a Northern Scientific NS 624 ADC. The ADC fed the LASL A-1 PDP-9/L (10) computer system which acted as both analyzer and data reducer. Spectra of 1024 channels were accumulated such that the K β X-rays from Pd were just on scale. An example is shown in Figure 3.

The yields of X-rays were determined by a computer program which added all channels in the region of interest and performed a linear interpolation subtraction for background. This program suffers in that it is necessary to have peaks completely separated to effect accurate analysis. This was a drawback only for the Cu determinations where the K α from Cu, which is weak, was very close to the much stronger Zn K α transition. The correction to the Zn due to the Cu interference was insignificant because of the smallness of the Cu intensity.

The computer, which accepted data for a predetermined live-time, usually 500 seconds, also controlled two scalars. One recorded the beam current as measured with an Ortec 439 Current Digitizer, and the second kept real-time in hundredths of a second. The second scalar allowed easy determination of system deadtime which was typically 2-3%.

The targets were prepared in such a way that the final areal density was between 0.1 and 1 mg/cm². In this mass range, there is enough material to produce a sufficient counting rate for rapid

(6) C. E. Gleit and W. D. Holland, *Anal. Chem.*, **34**, 1454 (1962).

(7) R. J. Grader, R. W. Hill, C. W. McGoff, D. S. Salmi, and J. P. Storing, *Rev. Sci. Instrum.*, **42**, 465 (1971).

(8) E. J. Feldi and C. J. Umbarger, *Nucl. Instrum. Methods*, **103**, 341 (1972).

(9) M. C. High, University of Kansas, Lawrence, Kan., private communication, 1973.

(10) L. V. East, Proceedings of the 1973 Spring DECUS Symposium, Philadelphia, Pa.

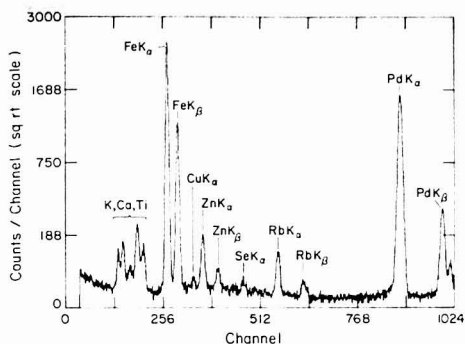


Figure 3. Typical proton-induced X-ray spectrum for mouse blood

analysis; yet the material is thin enough to make self-absorption corrections insignificant and to keep beam heating small enough to prevent target sublimation.

Beam Preparation. It was expected that since the targets were dried from solution, they would be neither uniform nor homogeneous. To investigate this point, the beam was defined to a 1-by-1-mm spot, using the final carbon slits. The target was then moved through this beam in 1-mm steps, and the emitted X-rays were analyzed. The concentration of Fe and the ratio of Fe to Zn at each point across the target are shown for one such sample in Figure 4. It can be seen that the Fe concentration of the sample varies considerably over the width of the target, while the Fe/Zn ratio is more stable.

Since the X-ray yield is proportional to the product of beam intensity and target thickness, and since the target is not uniform, it is necessary to make the beam uniform across the target area. Several schemes are available to accomplish this, and we investigated two. We attempted to homogenize the beam by passing it through a 0.0013-mm Ni foil and then accepting only part of the scattered beam on our 1-by-1-cm target area. To get sufficient target currents we had to use a primary beam of about 2 μ A, and this overheated the Ni foil, causing pinholes to develop. In addition, the amount of homogenization was not sufficient.

The method finally adopted was a simple defocusing of the beam. A 6- μ A beam was focused through the analyzing magnet and immediately intercepted in a beam cup (see Figure 1) and measured. The beam was then defocused within the accelerator so that the beam cup measured only 500 nA, the cup was removed, and the defocused beam was allowed to travel ~8 meters to reach the target chamber. Typically, of the 500 nA in the cup, 200 nA reached the target area where it passed through the target and was collected in an electrically insulated tube beyond the target chamber proper. This amount of beam is of optimum intensity, because it allows reasonable data accumulation rates without deterioration of the samples. At beam currents above 300 nA, about 50% of the samples would be destroyed by the beam.

To measure the beam profile, a 0.5-mm square Ni chip, 0.0005 mm thick, was placed on a Mylar foil in the center of the target frame. The chip was then moved through the beam in 1-mm steps, care being taken to keep the beam from hitting the frame. The number of Ni X-rays is a direct measure of the beam intensity at the Ni chip. The result of this measurement is shown in Figure 5. It can be seen that, at least in the horizontal dimension, the beam is uniform to better than 10% over the 6-mm target diameter. The result obtained with the Ni diffuser is shown for comparison. It was assumed that the vertical profiles were similar. Because of the techniques used for beam preparation, such an assumption is justified. These results, taken with the information about target nonuniformity, imply that a limit of precision of a few per cent over and above counting statistics should be attainable with the defocused beam.

Another source of variation in our results is due to the Ti absorber. The X-rays arising from target positions a few millimeters off the central axis must, because of the shallower angle of passage through the Ti, traverse more attenuating material. For our absorber, and an extreme case of 6 mm from the central axis, the absorption of Fe X-rays is 7% higher than those X-rays passing

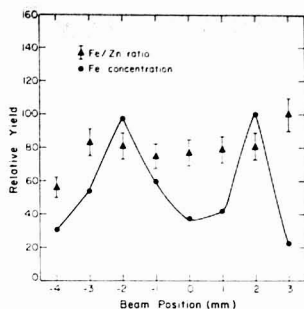


Figure 4. Blood target profile measurements showing relative Fe yield as well as Fe/Zn ratio as a function of position

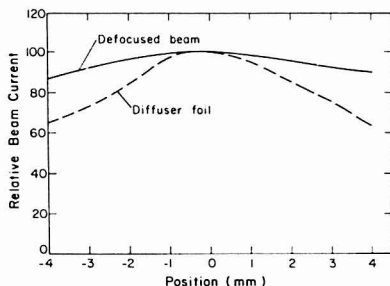


Figure 5. Beam intensity profile showing results for defocused as well as diffused beam

perpendicular to the Ti. Since no two targets are exactly alike—i.e., the mass distribution and centering are not the same—variations in the measured sample quantity of up to a few per cent can be expected to occur.

RESULTS AND DISCUSSION

To determine the precision of our method, two series of measurements were made. In the first, a 4-ml sample of oxalated whole human blood was repipetted into 27 beakers and targets were prepared as described above. The blood had 0.1 ml of potassium oxalate solution added to each 1 ml of whole blood. A subsequent measurement of the oxalate solution alone indicated a small Zn contamination which contributed less than 1% to the final Zn yield. Each sample was exposed to ~150 nA of beam for 500 seconds of analyzer lifetime. Several elements were readily seen, among them Fe, Cu, Zn, Se, and Rb, in addition to the Pd spike. Since the amount of Pd in the sample relative to the original blood weight (dry) is known, as is the efficiency of the detector system relative to Pd, it is a simple matter to determine the amount of each element present.

The ppm of each element (dry weight) is simply

$$\frac{40N}{PEW} \quad (1)$$

where E = efficiency of detection relative to Pd for X-ray of interest, W = dry weight of sample, N = number of counts in peak of interest, and P = number of counts in Pd peak.

The factor of 40 arises because 0.1 mg of the 400-ppm Pd spiking solution is used. The amount of material rela-

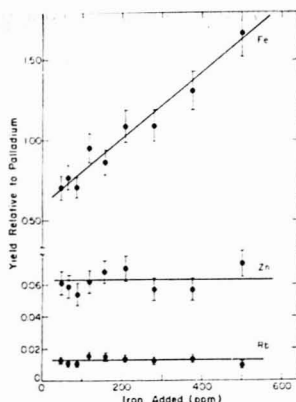


Figure 6. Detection linearity showing Fe, Zn, and Rb response as a function of iron concentration

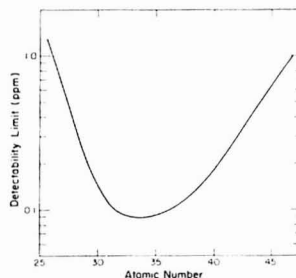


Figure 7. Proton-induced X-ray emission detectability in whole blood (wet weight) as a function of atomic number. The curve corresponds to the results for a 150-nA proton beam bombardment for 500 seconds

tive to the wet weight can be determined from the average dry weight for all the 0.1-ml samples, assuming that indeed the average of all pipettings is 0.1 ml. By making the measurements relative to Pd, it is then unnecessary to know the total mass present in the target, a difficult determination. The peaks from Ca, K, and Ti (the last due to secondary fluorescence in the absorber) were not analyzed as they were very nonreproducible.

The absolute amounts of Fe, Cu, Zn, Se, and Rb in the 27 human blood samples (wet weight) were determined and are shown in Table I. A statistical analysis was performed on these measurements, and the results are also shown in Table I. A second test was run, using samples from 27 different mice that were from a line inbred for over 60 generations. A typical spectrum from one such sample has been shown in Figure 3. The average values and the relative standard deviations of these values are included in Table I.

To determine the linearity of the technique with variation in elemental concentration, a set of nine identical blood samples was ashed and then spiked with a successively more dilute Fe-Pd solution. Targets were prepared and run in the usual way. Figure 6 shows the amount of Fe, Zn, and Rb detected as a function of the Fe concentration added to the samples. The results for Zn and Rb

Table I. Average Values and Relative Standard Deviations of Five Trace Elements Detected in Whole Blood

	Fe	Cu	Zn	Se	Rb
27 Human samples					
Av, ppm	384	1.2	6.4	0.2	0.9
Rel std dev	7%	18%	7%	50%	19%
27 Mouse samples					
Av, ppm	394	0.4	4.0	0.3	3.3
Rel std dev	5%	51%	10%	31%	14%

Table II. Comparison of the Results Obtained with Proton-Induced X-Ray Emission and with Atomic Absorption Spectrometry as well as with the Average Values of Anspaugh *et al.*^a

	Concentration in parts per million (wet weight)					
	Fe	Cu	Zn	Zn ^b	Se	Rb
Sample No. 1	434	0.77	5.9	5.1	0.09	1.2
Sample No. 2	455	0.72	5.5	5.8	0.25	1.4
Sample No. 3	453	0.59	6.8	8.4	0.25	1.6
Sample No. 4	460	0.51	6.8	7.2	<0.09	1.7
Expected ^c	390 ^c	1.00	7.4	7.4	0.18	1.5

^aAverage values from Anspaugh *et al.*, Reference 11. ^bResults from atomic absorption spectrometry, Reference 12. ^cSea level value. At altitude of 2.2 km, blood contains 10–15% more hemoglobin; hence, Fe concentration is expected to be higher.

are consistent with their fixed concentration despite a widely varying Fe concentration. The Fe results are consistent with linearity. A least squares fit to the Fe data, assuming a quadratic function, was never more than 5% different than the fit obtained assuming linearity.

The accuracy of the technique is primarily determined by the accuracy with which the Pd spiking solution is prepared and by the accuracy of the efficiency curve. The spiking solution was compared with several independently prepared Pd solutions and was at the expected strength to within 6%. The efficiency curve was measured on several occasions using different targets, and all determinations agreed to within 7%. A further error arises if the self-absorption in the blood targets is both large and significantly larger than the self-absorption in the targets used to determine the efficiency curve. Our estimates of self-absorption effects rule this out. This last effect would decrease the measured amount of material in the blood. The first two effects may be in either direction. In Table II, we compare our results with those of Anspaugh *et al.* (11). Considering that our blood samples were taken from subjects living at an altitude of 2.2 km, agreement is quite good.

As a further check on the accuracy of the technique, five aliquots of four different human blood samples were analyzed for Zn content and were compared to results obtained by atomic absorption spectrometry (AAS) (12). The results are shown in Table II. Since our expected systematic error is 10%, the agreement is reasonable.

Although we are able to see only five elements, these are normal samples, and screening for abnormalities would be an important use of the technique (screening, for instance, for Cd or other industrial health hazards). Before this work can be undertaken, we must determine if

- (11) L. R. Anspaugh, W. L. Robison, W. H. Martin, and O. A. Lowe, "Compilation of Published Information on Elemental Concentrations in Human Organs in Both Normal and Diseased States," UCRL 51013 (1971).
- (12) P. C. Stein, Los Alamos Scientific Laboratory, private communication, 1973.

toxic levels are detectable. The limit of detectability is generally assumed to be three times the standard deviation of the background. Using our results, one can infer the detectability limits as a function of atomic number, and these results are shown in Figure 7. By increasing the bombarding time by a factor of four, the detectability limit will be improved by a factor of two.

An important facet of any measuring technique is the time needed for analysis. The cleaning and weighing of the beakers (twice) takes about 1 man-hour for 30 samples. The ashing time is about 72 hours; but although we worked with 30 samples at a time, the asher would easily handle 100 samples, and larger ashers are available. Further, the asher loading time was only a few minutes. The Formvar backings could be produced quite rapidly. One man-hour per 60 foils is easily achieved. The production of targets from the ash takes about 2 minutes apiece, not counting the drying time of about 3 hours. The largest expenditure of time per sample was in the actual beam irradiation. We used bombardment times of 500 seconds. Although the beam cannot be increased without endangering the samples, decreasing the accumulation time by a factor of two would increase the relative standard deviations for Fe, Zn, and Rb to about 7, 7, and 27%, respectively. The precision of the Fe and Zn measurements are limited by target inhomogeneities and beam profile variations; the Rb results are primarily determined by counting statistics. It seems, then, that one person could perform at least 40 assays per 8-hour day under production conditions.

CONCLUSIONS

This work shows that proton-induced X-ray emission analysis of whole blood samples is capable of precision and accuracy. The spectrum is not particularly rich because of the dominance of the Fe in the spectrum and the necessity of its strong attenuation which also attenuates other heavier elements but not as severely. It is reasonable to assume that developmental efforts similar to this one for measurements on other specific samples should meet with at least equal success.

ACKNOWLEDGMENT

We are deeply indebted to a number of people whose enthusiastic cooperation made this work possible. We particularly thank Robert Keepin for his continued interest and support of this work. We thank Evan Campbell for several stimulating discussions and Pat Stein for the comparison measurements using AAS. Jean Lindsey cheerfully supplied many gallons of redistilled water. We thank Marty Holland and Jerry London for providing the mouse samples, and Joe Tafuya for providing the human blood samples. We also tender our appreciation to Colleen Burns for sample and foil preparation and to Ed Adams for his efficient Van de Graaff operation. One of us (R.C.B.) wishes to thank the staff of the Los Alamos Scientific Laboratory for their generous hospitality.

Received for review August 10, 1973. Accepted November 15, 1973. Work performed under the auspices of the U.S. Atomic Energy Commission.

Substoichiometric Extraction of Cations with Mixtures of Hexafluoroacetylacetone and Tri-*n*-Octylphosphine Oxide in Cyclohexane

J. W. Mitchell

Bell Laboratories, Murray Hill, N.J. 07974

Roland Ganges

Stanford University, Stanford, Calif.

A new method has been developed for substoichiometric extraction of cations by adduct-reactions in the presence of excess hexafluoroacetylacetone (HHFA) and of substoichiometric quantities of the neutral donor, tri-*n*-octylphosphine oxide (TOPO), in cyclohexane. The equilibria of adduct-extraction systems are discussed to show advantages over the conventional approach of reacting cations with substoichiometric amounts of chelating ligands. Distribution curves for the substoichiometric extraction of Co^{2+} , Cu^{2+} , Fe^{2+} , Mn^{2+} , Zn^{2+} , Fe^{3+} , Eu^{3+} , and Lu^{3+} have been measured, and experimental results with relative standard deviations of 0.92, 1.8, and 3.1% for the substoichiometric isolation of Zn^{2+} , Cu^{2+} , and Eu^{3+} are reported. The general utility of this extraction system for substoichiometric separation of cations following neutron activation is discussed.

Recently the utility of methods of separation in nuclear analyses has been enhanced by the development of sub-

stoichiometric methods, which extend the application of radioisotope dilution to the determination of trace elements and also make it possible to perform quantitative neutron activation analyses without measurements of radiochemical yield. Such methods have been developed rapidly and applied frequently since Ruzicka and Stary first summarized their techniques in 1968 (1). In a second review, these authors discussed methods published during the period 1968 to 1970 (2). Since this review, several additional solvent extraction methods have been reported (3-16). A general discussion of substoichiometric methods

- (1) J. Ruzicka and J. Stary, "Substoichiometry in Radiochemical Analysis," Pergamon Press, New York, N.Y., 1968.
- (2) J. Stary and J. Ruzicka, *Talanta*, **18**, 1 (1971).
- (3) F. Kukula and M. Simkova, *J. Radioanal. Chem.*, **4**, 271 (1970).
- (4) G. N. Bilimovich and N. N. Churkina, *J. Radioanal. Chem.*, **8**, 53 (1971).
- (5) U. V. Yakovlev and R. V. Stepanets, *Zh. Anal. Khim.*, **25**, 578 (1970).
- (6) R. A. Nadkarni and B. C. Haldar, *Anal. Chem.*, **44**, 1504 (1972).
- (7) B. M. Tejam and B. C. Haldar, *Radiochem. Radioanal. Lett.*, **9**, 19 (1972).

for multielemental separation by metal chelate extractions (17), a report on the selectivity of substoichiometric extraction methods (18), and a general review of the substoichiometric approach in analysis have also been published (19).

Most previous investigators have used substoichiometric quantities of chelating (1, 2) or ion-associating agents (20) to reproducibly isolate and then determine cations or anions by neutron activation (N.A.), or by radioisotope dilution (I.D.). Although numerous reagents for extraction are available (21, 22), applications for substoichiometric separations have been limited either by insufficient stability of the corresponding metal complexes or by lack of stability of the extractant at low concentrations.

The present authors report a new method, based on extraction of cations in the presence of an excess amount of a chelating ligand, hexafluoroacetylacetone (HHFA) and a substoichiometric quantity of a neutral donor, tri-*n*-octylphosphine oxide (TOPO). Particular advantages of this system are described for applications in activation analysis.

EXPERIMENTAL

Tri-*n*-octylphosphine oxide was obtained from Eastman Kodak and used without further purification. Hexafluoroacetylacetone from Peninsular Chemresearch, Inc. was freshly distilled before use. Reagent-grade cyclohexane and buffer solutions, prepared by mixing appropriate amounts of reagent-grade sodium acetate and acetic acid, were used. Except for ^{64}Cu which was prepared by irradiation of nonactive carrier with thermal neutrons at the Industrial Reactor Laboratory in Plainsboro, N.J., the radioisotopes, ^{59}Fe , ^{60}Co , ^{65}Zn , ^{54}Mn , ^{51}Cr , $^{152,154}\text{Eu}$, and ^{177}Lu were purchased from commercial suppliers. Stock solutions of the corresponding nonactive cations were prepared by dissolving either pure salts or accurately weighed amounts of the highly pure metals. Solutions prepared from salts were standardized subsequently by EDTA titrations.

Preparation of Aqueous and Organic Phases. Method I. One hundred milliliters of sodium acetate-acetic acid buffer (initial pH 6.37) was equilibrated in a separatory funnel with an equal volume of 0.07M HHFA in cyclohexane. The solution of HHFA was prepared by pipetting 1.0 ml of freshly distilled reagent (pre-equilibrated at $25 \pm 2^\circ$) into a 100-ml volumetric flask containing solvent and then diluting to volume. After the mixture was shaken for five minutes, the aqueous (pH 4.75) and organic phases were separated and used as described below. In experiments for measuring the substoichiometric distribution of cations vs. pH, a series of aqueous phases were prepared by mixing aliquots of stock cation solutions and appropriate amounts of corresponding radioisotopes and diluting to near volume (9.5 ml) in 10-ml volumetric flasks with portions of buffer solution. The pH of each solution was then adjusted to the desired value by dropwise addition of 8.0M HCl or 1.0M NH_4OH .

The resulting solution was diluted to volume by adding 0.2 to 0.4 ml of deionized H_2O . In these experiments, the amount of cation present initially in the aqueous phase was selected to approximate the concentration expected in typical activation analyses, where at least 1- to 10-mg of nonactive carrier are added during the dissolution of samples following neutron irradiation.

The organic phase was prepared by pipetting appropriate volumes of 0.1M TOPO-cyclohexane from a stock solution into a 50-ml volumetric flask and by diluting to volume with a portion of the organic phase which had previously been pre-equilibrated with the acetate buffer as described earlier. The initial concentration of TOPO in the organic phase was selected to be 25 to 50% of the amount necessary for complete extraction of carrier from the aqueous phase.

Method II. As an alternative method, organic phases were prepared as follows: 0.5 ml of HHFA, pre-equilibrated at 25° , and aliquots of 0.10M stock solution of TOPO were pipetted into a 50-ml volumetric flask and diluted to volume with cyclohexane. Corresponding aqueous phases were prepared by adding carrier and tracer and diluting to volume with a series of acetate buffers covering the desired pH region. In this case no previous equilibration of buffers with 0.07M HHFA in cyclohexane was made.

Five-ml volumes of aqueous and organic phases were transferred to 15-ml screw-cap centrifuge tubes, sealed with a polyethylene cover and capped securely. Following 30 to 60 minutes of equilibration on a wrist-action shaker, each tube was centrifuged to facilitate separation of phases. After 2- to 4-ml aliquots of the organic and aqueous phases were pipetted into polypropylene and polystyrene vials, respectively, gamma-ray activities from each phase were measured by counting in a 3-in. \times 3-in. well-type NaI detector connected to a 1024 multichannel analyzer. The equilibrium pH of the aqueous phase was then measured with a combination-electrode and meter.

Reagent Stability. Five-ml aliquots from a set of aqueous and organic phases prepared by Methods I and II were pipetted from stock solutions, transferred into centrifuge tubes, equilibrated until equilibrium was attained, and centrifuged. After this the γ -ray activity of each phase was measured. At regular intervals, the entire procedure was repeated until the original solutions had aged for several hours.

Substoichiometric Extraction of ^{64}Cu from SiO_2 . A set of 0.5-gram samples of ultrapure SiO_2 (triplicate analyses by N. A. showed 0.037, 0.059, and 0.012 ppm Cu) were irradiated independently for 20 minutes in a flux of thermal neutrons at 10^{13} n/cm 2 sec along with standard solutions of copper (0.535×10^{-6} gram Cu/ml). Following the irradiation, 1 ml of the ^{64}Cu solution was added to two platinum crucibles in which 1 mg of Cu carrier, 10 ml of HF, 1 ml of 1:1 HNO_3 , and 1 ml of HClO_4 were added. After quantitatively transferring the irradiated sample of SiO_2 to one crucible, an equal quantity of nonirradiated SiO_2 was added to the other. Both mixtures were then heated on a hot plate to dissolve SiO_2 and fumed until complete evaporation occurred. The resulting residue was dissolved in 3 ml of acetate buffer that was pre-equilibrated with HHFA-cyclohexane and the solution was transferred quantitatively to a 60-ml separatory funnel by rinsing the crucible with additional portions of the buffer solution. The pH of this aqueous phase with a total volume approximately equal to 10 ml was adjusted to a value greater than 4.8 by appropriate addition of HCl or NH_4OH . A 10-ml portion of 0.001M TOPO in cyclohexane was added and copper substoichiometrically extracted by shaking for 15 minutes on a wrist-action shaker. In some experiments, the mixture of acids and nonirradiated SiO_2 was not added. The solutions containing only Cu carrier and standard ^{64}Cu were then mixed directly with buffer and extracted with the substoichiometric reagent. In similar experiments, 0.5- μg amounts of Zn, Co, Mn, and Eu tagged with the corresponding isotopes, ^{65}Zn , ^{60}Co , ^{54}Mn , and ^{154}Eu , were added along with 10 mg of Cu carrier. In this case, a preliminary extraction with 4 ml of 0.005M TOPO-cyclohexane was performed prior to the substoichiometric extraction of ^{64}Cu with 5 ml of 0.01M TOPO-cyclohexane.

RESULTS AND DISCUSSION

The paramount importance of the stability of the chelate complex in determining the applicability of a reagent for substoichiometric separations by solvent extraction has been discussed previously (1). Although extraction

- (8) R. A. Nadkarni and B. C. Haldar, *Radiochem. Radioanal. Lett.*, **11**, 237 (1972).
- (9) W. J. Zmijewska, *J. Radioanal. Chem.*, **10**, 187 (1972).
- (10) B. M. Tejam and B. C. Haldar, *Radiochem. Radioanal. Lett.*, **9**, 77 (1972).
- (11) R. A. Nadkarni and B. C. Haldar, *J. Radioanal. Chem.*, **10**, 181 (1972).
- (12) R. A. Nadkarni and B. C. Haldar, *Radiochem. Radioanal. Lett.*, **9**, 205 (1972).
- (13) Z. K. Doctor and B. C. Haldar, *J. Radioanal. Chem.*, **9**, 19 (1971).
- (14) B. M. Tejam and B. C. Haldar, *Radiochem. Radioanal. Lett.*, **9**, 169 (1972).
- (15) R. A. Nadkarni and B. C. Haldar, *Radiochem. Radioanal. Lett.*, **8**, 341 (1971).
- (16) R. A. Nadkarni and B. C. Haldar, *J. Radioanal. Chem.*, **8**, 45 (1971).
- (17) A. Elek, J. Bogances and E. Szabo, *J. Radioanal. Chem.*, **4**, 281 (1970).
- (18) G. A. Perexhagin, *Zh. Anal. Khim.*, **25**, 1245 (1970).
- (19) N. K. Baishya, R. B. Heslop, and J. R. DeVoe, *Crit. Rev. Anal. Chem.*, **2**, 345 (1971).
- (20) I. P. Almarin and G. A. Perexhagin, *Talanta*, **14**, 109 (1967).
- (21) G. H. Morrison and H. Freiser, "Solvent Extraction in Analytical Chemistry," John Wiley and Sons, Inc., New York, N.Y., 1957.
- (22) J. Stary, "The Solvent Extraction of Metal Chelates," Pergamon Press Inc., New York, N.Y., 1964.

methods that form highly stable chelates are very satisfactory, the number of usable chelate systems are somewhat limited. However, it is well known that few cations other than Hg^{2+} , Cd^{2+} , Cu^{2+} , and Zn^{2+} (with dithizone), and Fe^{3+} (with cupferron) form primary chelates that are more stable than a ternary or adduct-complex consisting of the cation, a suitable chelating agent and a neutral donor-molecule. For example, a comparison of extraction constants of thenoyltrifluoroacetates ($\text{M}(\text{TTF})_n$) with corresponding adduct-complexes of TOPO ($\text{M}(\text{TTF})_n \cdot (\text{TOPO})_m$) shows orders of magnitude higher constants for the ternary complexes (23-28).

While available data on extraction- or formation-constants for other ternary complexes of cations with acidic, fluorinated, beta-diketones and TOPO are scarce, metal chelates (MA_n) formed by complexation with ligands more acidic than HTTA, particularly hexafluoroacetylacetones, are expected to react very strongly with TOPO (29). Chelates of hexafluoroacetylacetone, $\text{M}(\text{HFA})_n$, form more stable adducts with tri-*n*-butylphosphate (TBP) than corresponding $\text{M}(\text{TTF})_n$ chelates as indicated by adduct-constants (β_2) for $\text{Tm}(\text{HFA})_3(\text{TBP})_2$ and $\text{Tm}(\text{TTF})_3(\text{TBP})_2$ in cyclohexane; $\log \beta_2 = 10.8$ (30) and 8.2 (28), respectively. The constant for $\text{Lu}(\text{HFA})_3(\text{TOPO})_2$ in benzene is reported as $\log \beta_2 = 12.50$ (31). Adduct-reactions in cyclohexane are stronger by at least two orders of magnitude indicating a conservative estimate of $\log \beta_2 = 14.5$ in this solvent (32). Inasmuch as a variety of cations are capable of forming ternary complexes that are significantly more stable than binary-chelate species, the present investigation was conducted to develop methods for substoichiometric extractions with donor molecules.

Theory of Substoichiometric Extractions in Ternary, Adduct or Synergic Systems. The extraction of a cation of charge n , (M^{n+}), by a substoichiometric amount of a chelating ligand (HA), represented by the general reaction

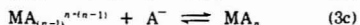
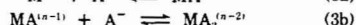


where the subscript, (o), indicates organic-phase species, has been treated by Ruzicka and Stary (7). These investigators demonstrated that the threshold pH at which the same quantity of metal can always be extracted in such systems can be calculated by substituting values for the concentration of $[\text{MA}_n]_o$, $[\text{HA}]_o$, $[\text{M}^{n+}]$ and K° at equilibrium into the expression for the extraction constant for reaction 1,

$$K^\circ = \frac{[\text{MA}_n]_o [\text{H}^+]^n}{[\text{M}^{n+}] [\text{HA}]_o^n} \quad (2)$$

For many metals, substoichiometric separations will be precluded in chelating systems if $K^\circ \leq 10^4$ since hydrolysis, precipitation, or other aqueous phase redox reactions are possible. A new approach to substoichiometric extraction, which precludes losses of minute quantities of cations from the aqueous phase via adsorption or other side reactions, is introduced in this manuscript. The present authors have used an excess amount of a ligand (HA) that

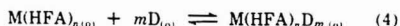
dissolves and dissociates readily in the aqueous phase to complex the cation via the stepwise reactions



If ligand, HA, is a very poor extractant, the concentration of chelate (MA_n) in the organic phase at equilibrium will be small even though excess HA is used—i.e. $[\text{MA}_n]_o \ll [\text{M}^{n+}]$. Such properties are exhibited by hexafluoroacetylacetone (HHFA), a ligand with a $\text{p}K_a$ of 4.63 and a K_D of 6.8×10^{-3} at pH ≤ 3.88 in H_2O -cyclohexane (33). The poor extraction of rare earths (33), Be^{2+} (34), and the nonextraction of Al^{3+} , Zr^{4+} , and Hf^{4+} (35) with this reagent have been reported.

If excess HHFA is present in the extraction system, the same quantity of metal (substoichiometric extraction) can always be separated from the aqueous phase by introducing a substoichiometric amount of a strong Lewis base, D, into the organic phase. As long as unreacted donor is present in the organic phase, reaction 3c proceeds in order to accommodate the subsequent formation of the ternary complex, which has a high preference for distribution into the organic phase.

To obtain reproducible substoichiometric extraction, the donor must be quantitatively reacted (99% or better) via the reaction



The reaction product, $\text{M}(\text{HFA})_n\text{D}_m$, must be completely extracted and have only one composition in the organic phase—i.e., under substoichiometric conditions all adduct-complexes in the organic phase must have the same number (m) of donor molecules. It is obvious that substoichiometric extractions require donors that have large distribution coefficients and also necessitate conditions that prevent the extraction of $\text{M}(\text{HFA})_n$ and preclude the formation of extractable species of the form, $\text{M}(\text{HFA})_n(\text{HHFA})_m$. Experimental data have been reported previously to confirm the above for tri-*n*-butylphosphate adducts of the rare earth hexafluoroacetylacetones (30).

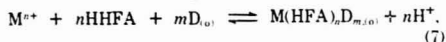
For the conditions (1) an organic phase initially 0.001M in D, (2) 99% reaction of D at equilibrium, and (3) a maximum of 1% extraction of MA_n into the organic phase, the equilibrium constant for reaction 4,

$$\beta_m = \frac{[\text{M}(\text{HFA})_n\text{D}_m]_o}{[\text{M}(\text{HFA})_n]_{ol} [\text{D}]_o^m} \quad (5)$$

$$\text{becomes} \quad \beta_m = \frac{10^2}{(0.01C_D)^m} \quad (6)$$

where C_D is the initial concentration of donor in the organic phase. The above requirements are satisfied if mono- or diadduct complexes have formation constants, β_1 and β_2 , $\geq 10^7$ and $\geq 10^{12}$, respectively.

The effect of pH must be considered to define additional requirements for substoichiometric adduct reactions. For the overall extraction process



the expression for the extraction constant (K) can be written as

$$(33) \text{ J. W. Mitchell, Ph.D. Thesis, Iowa State University, Ames, Iowa, 1970.}$$

$$(34) \text{ W. G. Scriber, M. J. Borchers and W. J. Treat, Anal. Chem., 38, 1779 (1966).}$$

$$(35) \text{ J. R. Stokely, unpublished Ph.D. thesis, University of Tennessee, Knoxville, Tenn., 1966.}$$

(23) T. V. Healy, *J. Inorg. Nucl. Chem.*, **30**, 1025 (1968).

(24) M. A. Carey and C. V. Banks, *J. Inorg. Nucl. Chem.*, **31**, 533 (1969).

(25) T. Sekine and D. Dyrssen, *J. Inorg. Nucl. Chem.*, **26**, 1727 (1964).

(26) R. J. Casey, J. M. Fordy, and W. R. Walker, *J. Inorg. Nucl. Chem.*, **29**, 1139 (1967).

(27) S. M. Wang, W. R. Walker, and N. C. Li, *J. Inorg. Nucl. Chem.*, **28**, 875 (1966).

(28) T. Sekine and D. Dyrssen, *J. Inorg. Nucl. Chem.*, **29**, 1457 (1967).

(29) O. Fernando, *Separation Sci.*, **1**, 575 (1966).

(30) J. W. Mitchell and C. V. Banks, *Talanta*, **19**, 1157 (1972).

(31) T. Honjo, *Bull. Chem. Soc. Jap.*, **42**, 995 (1969).

(32) T. V. Healy, *Nucl. Sci. Eng.*, **16**, 413 (1963).

Table I. Substoichiometric Extraction of Zn²⁺ and Mn²⁺ as a Function of the Age of HHFA-TOPO-Cyclohexane Reagent

Age of extraction system, hr		γ -Ray activity in organic phase, c/min	
Zn ²⁺ ^a	Mn ²⁺ ^b	Zn ²⁺	Mn ²⁺
0.1	0.1	89996	18050
1.0	1.0	90684	18440
2.0	2.0	89952	17800
4.3	6.0	90144	18317
24.5	11.5	81724	17659

^a Aqueous and Organic phases prepared by Method I (See Experimental Section). ^b Aqueous and Organic phases prepared by Method II.

$$K = \frac{[M(HFA)_n D_m]_o [H^+]^n}{[M^{n+}] [HHFA]^n [D]_o^m} \quad (8)$$

To achieve 50% extraction with a substoichiometric amount of D in the organic phase—i.e., $[M(HFA)_n D_m]_o / [M^{n+}] = 1$, where $[M^{n+}]$ represents all metal-containing species in the aqueous phase—the concentration of chelating anion (HFA⁻) in the aqueous phase must be sufficient for complexing at least 50% of the metal. For a cation of charge n the requirement

$$[HFA^-] \geq n \frac{1}{2} C_M \quad (9)$$

must be met.

The equilibrium concentration of ligand in the aqueous phase can be calculated by substituting appropriate values into

$$[HA] = \frac{C_{HA}}{K_{D,HA} + 1} \quad (10)$$

where C_{HA} is the total initial concentration of HA in the entire extraction system. The threshold pH required to achieve the degree of dissociation to satisfy requirement 9 can be calculated from the expression,

$$pH \geq pK_a + \log[A^-] - \log[HA] \quad (11)$$

For 50% extraction of a divalent cation ($n = 2$) present at an initial concentration of 0.002M in the aqueous phase, Equation 8 changes to

$$K = \frac{[H^+]^2}{[HA]^2 [D]_o^m} \quad (12)$$

If the initial concentration of D in the organic phase is 0.001M, 99% of D is consumed, and the diadduct is formed exclusively; at equilibrium, expression 12 becomes

$$\log \frac{[H^+]^2}{[HA]^2} = \log K + 2 \log(0.01C_0) \quad (13)$$

which simplifies further to

$$pH \geq -\frac{1}{2} \log K - \log[HA] + 5 \quad (14)$$

It is seen from expression 14 that substoichiometric adduct reactions are possible for a divalent cation when $K \geq 10^4$, $pH \geq 4$, and $[HHFA] = 0.1M$. In the presence of excess ligand, separations at higher pH can also be accomplished easily for adduct complexes with $K < 10^4$.

The system, HHFA-TOPO-cyclohexane, was selected for the following reasons: 1) Because of the weak chelating powers and poor extraction of metal chelates into organic solvents, excess amounts of the chelating agent, HHFA, can be used. 2) Weak interaction between cations and hexafluoroacetylacetone produces a chelate with strong

Lewis acidity that participates readily in further adduct reactions to form tenary complexes of high stability with TOPO, a strong Lewis base. This donor is readily available in pure form and has a low solubility in H₂O at 25°, 3.88×10^{-6} moles/liter (36, 3). Cyclohexane was selected since the greatest synergic effects have been observed in this solvent (32).

Reagent Stability. The stability of HHFA-TOPO-cyclohexane was examined by substoichiometrically extracting Zn²⁺ and Mn²⁺ following the preparation of fresh phases by Methods I and II, respectively (see Experimental). As shown by data in Table I, the extracted quantity of Zn²⁺ and Mn²⁺ did not change up to 4 and 11 hours, respectively, after preparation of the phases. Although the stability of the extraction system was sufficient in both cases, Method I was preferred since control of the equilibrium pH was facile and precipitation of hydrated HHFA from the organic phase stock solution was prevented.

Substoichiometric extractions with this system proceeded rapidly and equilibrium was reached within 15 minutes for the cations that were studied. Data for the extraction of ⁵⁴Mn²⁺ showed 16132, 17782, 18051, 18441, and 17798 counts/minute of gamma-ray activity after 5, 15, 30, 60, and 120 minutes of equilibration, respectively. In all experiments, phases were shaken a minimum of 1 hour to ensure attainment of equilibrium.

Substoichiometric Extraction of Cations. Distribution curves for several cations as a function of pH are shown in Figure 1. Substoichiometric extractions are shown in 1(a) for Eu³⁺ and Lu³⁺, respectively, at $1.4 \leq pH \leq 3.0$ and $1.5 \leq pH \leq 2.5$; in 1(b) for Zn²⁺ and Cu²⁺ at $pH \geq 4.5$ and ≥ 3.6 ; and in 1(c) for Mn²⁺ and Co²⁺ at $pH \geq 3.4$ and ≥ 7.0 . No region of constant extraction was found for Fe²⁺ or Fe³⁺ as shown in 1(d). Apparently the reaction, $Fe^{n+} + nHHFA = Fe(HFA)_{n,(n-1)} + nH^+$, is appreciable. Studies of the extraction of Cr³⁺ also showed no substoichiometric extraction of this cation. In view of the reported synergic extraction of Sc³⁺, UO₂²⁺ and Th(IV) (37), U(IV) (25), the actinides (38), and Ca²⁺ (39), it is anticipated that substoichiometric extractions of these cations with HHFA-TOPO-cyclohexane will also be possible.

Under substoichiometric conditions, the cations Mn²⁺, Zn²⁺, Cu²⁺, Co²⁺, and other divalent metals are extracted into the organic phase as $M(HFA)_2(TOPO)_m$ species where m has been reported to be 2 for the extraction of Zn(HFA)₂(TOPO)₂ (27). The composition of the Lu³⁺ adduct has been reported as Lu(HFA)₃(TOPO)₂ (31). Other lanthanides are presumed to have this same composition in the organic phase (30).

Reproducibility of Substoichiometric Separations. To perform quantitative determinations of trace elements by neutron activation, substoichiometric separations must be at least reproducible to within $\pm 5\%$ or better. Precision better than this is obtained easily when the adduct reagent is quantitatively reacted with the chelate of the cation to be separated, or is consumed to the same degree during the adduct reaction to form a species that partitions completely into the organic phase.

In addition to the requirements of thermal and photochemical stability of the substoichiometric reagent, which are very adequately met by TOPO, careful attention must be given to preventing fluctuations in the concentration of

(36) "Data Sheet on tri-*n*-octylphosphine oxide," Carlisle Chemical Works, Inc., Reading, Ohio.

(37) J. R. Ferraro and T. V. Healy, *J. Inorg. Nucl. Chem.*, **24**, 1463 (1962).

(38) T. Sekine and D. Dyrsen, *J. Inorg. Nucl. Chem.*, **29**, 1481 (1967).

(39) T. Sekine and D. Dyrsen, *Anal. Chim. Acta.*, **37**, 217 (1967).

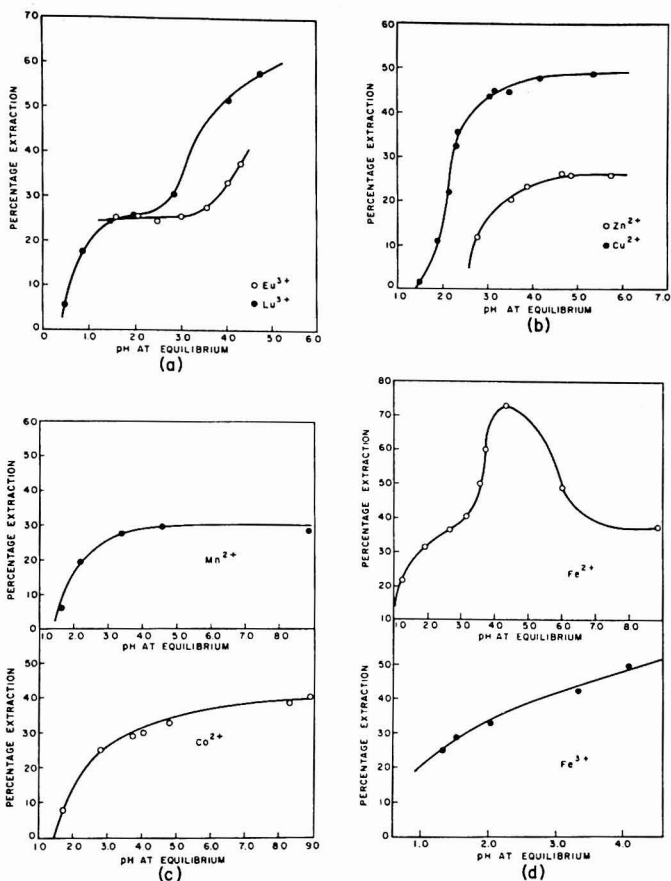


Figure 1. Substoichiometric extraction curves for (a) Eu^{3+} and Lu^{3+} , (b) Zn^{2+} and Cu^{2+} , (c) Mn^{2+} and Co^{2+} , and (d) Fe^{2+} and Fe^{3+} .

Conditions:

Concn	Cation	[HHFA]	[TOPO]
(a) Eu^{2+}	0.00189M	0.0704	0.001
Lu^{2+}	0.002M	0.0704	0.001
(b) Zn^{2+}	0.0028M	0.0704	0.001
Cu^{2+}	0.2 mg/ml	0.0704	0.0015
(c) Mn^{2+}	0.2 mg/ml	0.0704	0.002
Co^{2+}	0.2 mg/ml	0.0704	0.002

the substoichiometric reagent by variations in phase volumes, which result from evaporation, spillage or mutual miscibility.

The data reported in Table II for the extraction of Cu^{2+} , Zn^{2+} , and Eu^{3+} are representative of the precision obtained with the present method. Five replicate separations from an aqueous phase containing 0.008 mmole of Eu^{3+} indicated 23.5 ± 0.3 percentage extraction of Eu^{3+} , and $14,363 \pm 234$ counts/min of γ -activity from $^{152,154}\text{Eu}$ in the organic phases. From the series of phases in which the concentration of Eu^{3+} was varied from 0.004 to 0.016 mmole, a γ -ray activity of $14,548 \pm 582$ counts/min was found. Corresponding data for Zn^{2+} indicated 36.4 ± 0.1

Table II. Reproducibility of Substoichiometric Extractions

Cation in aqueous phase, mmole			γ -Ray activity in organic phase		
Cu^{2+}	Zn^{2+}	Eu^{3+}	^{64}Cu	^{65}Zn	^{152}Eu
0.0094	0.006	0.004	79471	27581	14072
0.0125	0.008	0.006	80560	26970	13820
0.0142	0.008	0.008	80503	27336	14319
0.0157	0.008	0.008	77040	27356	14395
0.0188	0.008	0.008	77771	27340	14143
0.0220	0.008	0.008	78760	27604	14042
...	0.010	0.008	...	26953	14914
...	0.012	0.010	...	27113	14898
...	0.016	0.012	...	28839 ^a	14938
...	...	0.016	15014
...	79017 ^b	27282 ^c	14455 ^d

^a Value rejected; ^b mean, $\sigma = 1437$; ^c mean, $\sigma = 250$; ^d mean, $\sigma = 446$.

percentage extraction and a gamma activity of $27,411 \pm 98$ C/min from ^{65}Zn in the organic phases. From the series of aqueous phases in which the Cu^{2+} and Zn^{2+} concentra-

Table III. Separation of ^{64}Cu from SiO_2 Following Neutron Activation

Gamma ray activity isolated in org., ^a c./min		
Sample	Standard	Sample/standard
67566	68617	0.985
65392	67863	0.963
65918	67987	0.969
63587	65376	0.973
62533	66336	0.943
69138	70567	0.980
69060	70525	0.979
66170 ^b	68182 ^c	0.970 ^d

^a $[\text{Cu}]_{\text{LiCl}} = 5.39 \times 10^{-2}$ gram, NaI detector, 20-min irradiation, γ of $^{64}\text{Cu} = 0.511$ MeV. ^b Mean value for separation of Cu from sample, $\sigma = 2571$. ^c Mean value for separation of Cu from standard, $\sigma = 1949$. ^d Mean value of ratio, Activity of Sample/Activity of Standard, $\sigma = 0.0141$.

tions were varied, an average organic phase activity of $27,491 \pm 535$ and 79017 ± 1334 counts/min were measured, respectively.

Practical Applications in Neutron Activation Analysis. Substoichiometric neutron activation analysis has previously been demonstrated to be useful for practical analyses of real samples. Where specific or reasonably selective extractants have been used, quantitative measurements by direct substoichiometric extractions have been achieved (1, 2). Complexation of interfering trace elements by masking agents has also been employed (1, 2, 40). When major constituents or matrix elements interfere, substoichiometric isolations have been performed following a preliminary separation of the constituent being determined. The latter two approaches are expected to be most suitable for practical applications of the system described in this paper since a large number of cations participate in adduct formation.

For the analysis of ultrapure materials this nonspecificity is not particularly damaging. The addition of nonactive carrier following irradiation of the sample allows the analyst to make the concentration of the constituent to be separated orders of magnitude larger than the total concentration of other trace impurities present in the sample. Any trace elements with adduct extraction constants $\geq K$ of the cation of interest will complex a negligible amount of the substoichiometric reagent. This is illustrated by the data reported in Table III. The first three separations of ^{64}Cu from the standard were performed after carrier only was added. These data agree closely with the remaining four standard values, obtained by separating ^{64}Cu substoichiometrically from a solution treated in the same manner as the irradiated sample. The reproducibility of the overall method and the actual precision expected for re-

sults calculated from the ratios of ^{64}Cu activity in samples to activity from corresponding standards are demonstrated to be quite adequate for quantitative trace determinations by neutron activation.

A preliminary separation of trace impurities with larger K values than the carrier cation can be performed by extracting with an organic phase containing 10% of the TOPO necessary for complete extraction of the carrier. Substoichiometric isolation of the cation of interest can then be accomplished in the presence of impurities with extraction constants less than that of the carrier. To verify this, a solution of $0.5 \mu\text{g}$ each of Eu^{3+} , Mn^{2+} , Zn^{2+} , and Co^{2+} was tagged with $^{152,154}\text{Eu}$, ^{54}Mn , ^{65}Zn , and ^{60}Co , then added to an aqueous phase that contained 10 mg of Cu carrier and 1 ml of ^{64}Cu tracer, which was prepared by irradiating a 0.107×10^{-6} gram/ml Cu solution for 30 minutes in a flux of 2×10^{13} n/cm² sec. A preliminary extraction with 4 ml of 0.005M TOPO-cyclohexane was followed by the substoichiometric extraction of Cu with 5 ml of 0.01M TOPO-cyclohexane.

The gamma ray spectrum of the preliminary extract indicated that most of the Eu and Mn were extracted. Traces of the other isotopes were extracted simultaneously with copper during the substoichiometric separation; however, no interference with the reproducibility of the isolation of copper was found by assaying the ^{64}Cu activity in the organic phase with a Ge(Li) detector. The results of five replicate substoichiometric separations of Cu by this procedure showed the following gamma ray counts due to ^{64}Cu in the organic phase: 10395, 10639, 11504, 11185, and 10756. In the absence of the impurity, isotopes 11003 counts from the 0.511 MeV gammas of ^{64}Cu were detected.

Determinations of traces of Cu, Mn, Zn, Co, and rare earths by direct substoichiometric separations with HHFA-TOPO-cyclohexane following neutron activation can be performed in the case of ultrapure reagents, and alkali salts or metals. Separations of these cations from appropriately treated samples of the semiconductor materials, silicon and silicon dioxide, should also be possible. Measurements of these traces in high purity salts of alkaline earths, in the pure metals Al, Ga, and Ge, or in other materials with matrix elements that undergo reactions with HHFA or TOPO will require preliminary separations. A description of a specific procedure for the determination of manganese in ultrapure calcium carbonate by a preliminary separation with a mixture of pyrrolidine dithiocarbamic acid and diethylammonium dithiocarbamate in CHCl_3 is forthcoming (41).

Received for review June 25, 1973. Accepted October 12, 1973.

(40) J. Stary and J. Ruzicka, *Talanta*, **11**, 697 (1964).

(41) J. W. Mitchell and R. Ganges, *Talanta*, in press.

Computer Utility for the Analytical Laboratory

James R. DeVoe, Ronald W. Shideler, Fillmer C. Ruegg, Jules P. Aronson,¹ and Peter S. Shoenfeld

Analytical Chemistry Division, Institute for Materials Research, National Bureau of Standards, Washington, D.C. 20234

The use of a parallel digital data bus as part of an elaborate teleprocessor system enables the analytical chemist to utilize computer control of his instrument in a manner which is simpler than has been previously described. The use of pushbuttons and thumbwheels with data display, plot, or print in the laboratory, coupled with interactive control of the experiment control program, provides a capability in computer control of instrumentation that approaches the concept of a computer utility. The teleprocessor and software used in a multiprogram environment are described.

At the beginning of this century, electricity was relegated to special uses most often related to scientific applications. Twenty years later it had taken on the aspect of indispensability and today as a utility, electricity has become so critically involved with our existence that much concern relates to assurance of its continued availability in the desired quantity and quality.

An analogy can be made with the electronic computer. It has yet to reach the point of being considered indispensable in the sense of its critical nationwide economic impact, but there is no doubt that it is soon (20-40 years) to become critically needed. The computer has solved important scientific and technological problems that would have been impossible otherwise. Currently, in most areas of experimental science, there is much interest in the use of computers (particularly "minicomputers") to control and acquire data from experiments. In many cases, the experiment could be performed only with computer interaction, and in other cases it relieves the tedium in operating switches, etc. on the experiment. Like electricity in its early stages, computers are cumbersome to use. Communication between the user and a computer is impaired by constraints that relate directly to the design of computers. Slowly these barriers to communication are being removed. When this reaches a level of high efficiency, computers will be looked upon as a utility. It is with this concept in mind that a computer system was designed, fabricated, and installed within the laboratories of the Analytical Chemistry Division.

An ideal computer utility for the laboratory has the following attributes: Low cost per unit of use; high capacity (for number of experiments that can be accommodated, for data storage, and for computation); rapid response time to inputs from the experiment; simple and direct communication (very easy to program and to operate); and high reliability—approaching that obtained with electricity.

As everyone knows, the state of development of computer components and software has yet to result in compatibility between all of the above items. However, like electricity, the item of major consideration, cost per unit of performance, is continually decreasing and consequently makes it more attractive to use. Ziegler *et al.* (1) have

described a system that provides for considerable multi-instrument capability, at considerable investment. Another similar system has been described by Shapiro and Schultz (2), and, of course, a variety of IBM 1800 systems have approximated a multi-instrument operation (3).

The system to be described is believed to represent a significant advancement toward the concept of a computer utility. A multi-program minicomputer with an average amount of core and fast access storage communicates to each laboratory via a bidirectional teleprocessor. A teleprocessor is a device that allows transmission of data from one place to another and provides the necessary control and synchronization functions. The user's experiment is connected to a receptacle box on the wall in the laboratory. Communication from the user to the computer is done by labeled thumbwheels and push buttons. Communication from the computer to the laboratory is done by the usual type of devices; teletypewriters, plotters, cathode ray tube, light emitting diode display, etc. Communication between the user and the computer can proceed at all times during the operation of the experiment. The paragraphs to follow describe the functional design of the entire system including software. Detailed design parameters can be obtained by writing to the authors.

TELEPROCESSOR

In providing a computer facility as a utility in a laboratory, it is a clear requirement that easy access to the computer must be made available to the users. The teleprocessor serves in this capacity. Its foremost function is that of communicating—e.g., via a bidirectional data link between an experimenter's device and the computer. The user should be able to consider the teleprocessor as a "black box" that accepts signals at the end of some wires and which connects his data device to the computer. The designer, on the other hand, must not share this view. He must consider every aspect of the user's requirements, otherwise, the desired transparency will be lost, and the presence of the teleprocessor will be felt through its inadequacies and unnecessary constraints.

The method of initiating data transfer should be simple so as to invite the experimenter to explore the new capabilities of computer interaction rather than to intimidate by ritualistic complexity of its operation. Its operation should seem natural—that is, in keeping with the usual methods of operating instruments. It should place few restrictions on the customary operation of the data device it services. In addition, it must be impervious to random or unprogrammed instructions inadvertently supplied by the experimenter.

Hardware interconnection to the teleprocessor should be natural, straightforward, and simple. Although the hardware responsibility is not strictly in the user's domain, it should not require "specials" to handle ordinary tasks. Minor modifications or additions should be easily accommodated without re-engineering. The designer must consider, as well, the interactions at the opposite end of the

¹ Present address, Institute for Computer Sciences and Technology, National Bureau of Standards, Washington, D.C., 20234.

(1) E. Ziegler, P. Henneberg, and G. Schamburg, *Anal. Chem.*, **42** (9), 51-61A (1970).

(2) M. Shapiro and A. Schultz, *Anal. Chem.*, **43**, 398 (1971).

(3) Proceedings IBM Scientific Computing Symposium on Computers in Chemistry, Thomas J. Watson Research Center, Yorktown Heights, N.Y., August 1969.

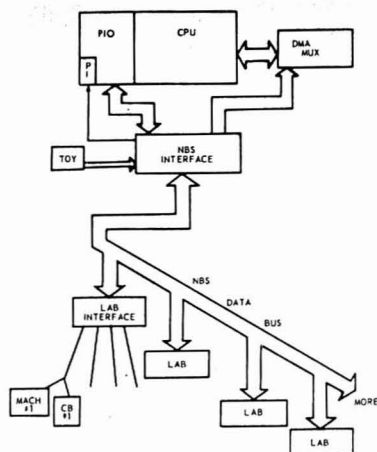


Figure 1. NBS Analytical Chemistry Teleprocessor System

teleprocessor where the computer resides. At this end of the teleprocessor, design criteria may have an even greater impact on the success of the system from the standpoint of a utility. The formatting of the data words, special control information, and status of the teleprocessor can greatly affect the speed of processing data and the ease in programming.

When data sources are from widely separated locations and from many independent sources, the decision as to whether to connect each location separately to a central distribution system *vs.* a common bus data carrier for all locations needs to be considered. Many design criteria must be evaluated before such a decision can be made. The types and number of data sources and their individual data rates combined with the very important estimate of the time averaged data transfer rate from many sources must be considered. Coupled with this is the all-important response time (minimum time for receiving a control signal from the computer after an input stimulus is sent from the experiment). Reliability of the data transmission precludes long distance transmission of analog signals. It is clear that there is no single optimal design of teleprocessor because the various tradeoffs between the requirements and resources, both financial and technical, will be different for each laboratory. Moreover, availability of electronic components which provide more capability at decreasing cost will have a profound effect on the design of future teleprocessors.

The most compelling reason for implementing the design of the teleprocessor described below resides in its universality from both a hardware and software standpoint between widely dissimilar experiments. A single data bus, common to all experiments, allows concentration on design of generalized interfacing to the experiment instead of being forced to design both the experiment and computer ends of the interface to accommodate special requirements of the experiment.

The Digital Data Bus. A digital communication bus to provide a bidirectional flow of data between individual laboratories and the computer facility was installed. It consists of fifty twisted pairs of 52-ohm line with each pair shielded in an aluminum-coated Mylar sheath, and it includes a third bare wire per pair as a ground. The bus in-

terconnects the laboratories of the building in parallel. Approximate 44-foot lengths are connected between distribution boxes in utility closets located at the side of every second laboratory module. At each of the distribution boxes, there are five 100-pin connectors. The five connectors provide for the bus incoming and outgoing and one each to ports located at the first, second, and third floors. The wiring of the boxes is done with a special printed circuit board which parallel-connects 48 of the 50 pairs. The remaining two pairs are connected in series to accommodate the intercept pulse to be described below. (See section titled Time Shared Multiplexing.)

The bus appears as a long trunk line with ports arranged periodically along its length and tied off to the individual laboratories (Figure 1). The cables to each port location are currently in place and in a connected configuration to avoid the situation of adding ports one at a time, only to find that system performance degrades with additional connections.

The computer interface is connected at the approximate center of the bus, and the system can be properly thought of as having two separate buses, center connected, and sharing line drivers and receivers.

The bulk of the signals is handled with a bimodal driving scheme. A balanced line, current-mode transmission, sends data to the computer interface since high speed movement of large amounts of acquired data is necessary.

In the reverse direction where computational results or control data outputs from the computer constitute a much smaller magnitude and speed of data flow, a voltage mode system is employed. The voltage mode signal drives both sides of the balanced line from its normally negative five-volt state to zero volts when a one is transmitted. At the laboratory logic box (LLB), or laboratory interface, the line receivers are composed of simple strobe-pulse-driven resistor-capacitor integrators. These are diode-coupled to transistors which directly drive the LLB data buffers. These receivers are highly immune to noise spikes and maintain a dc level noise immunity of at least ± 2 volts. They have practically no loading effect on the line and are highly economical.

The line transmitters are composed of a single transistor "floating switch" between the two sides of the balanced line which in the zero state have a differential voltage of 300 to 500 millivolts. A second transistor (driven electrically) isolates the switch except when in the driven state. When a "one" is transmitted, the driver turns on the floating switch to shunt the current from one line to the other. This, in effect, reduces the differential voltage seen at the high sensitivity differential line receivers of the computer interface. This method of transmission operates as a true "party line" (wired OR) system, and no current commutation or compensation is required.

The Laboratory Interface. In each laboratory where instruments are interfaced to the teleprocessor, a laboratory logic box (LLB) is situated on the wall with the data bus entering from the rear. A blower is housed in back of this box and blows air from the hallway outside of the laboratory into the LLB. The cable pass-throughs are sealed to an extent that only air flow from the LLB into the laboratory is possible. This avoids corrosions due to laboratory fumes, etc. The LLB houses all of the interfacing and bus interconnecting logic to sustain up to four separate experimental hook-ups which are connected by short cables (<100 ft). Provisions made for each experiment include inputs for: a major data source such as a pulseheight analyzer or other word-serial devices, a control panel, and six 16-bit words of ancillary data which are

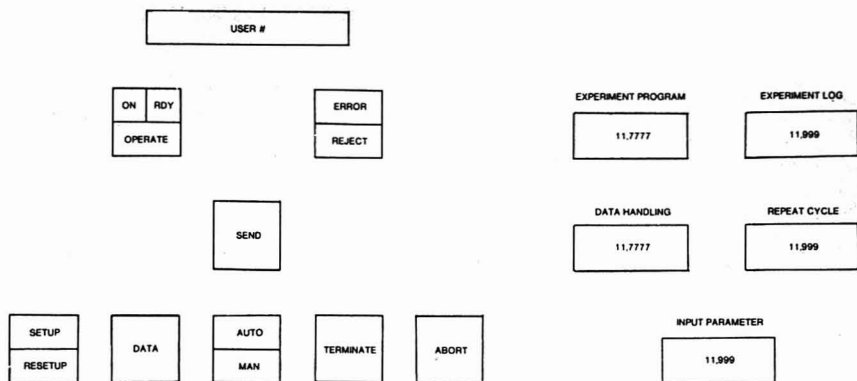


Figure 2. Layout of switches and thumbwheels on the experiment control panel (ECP)

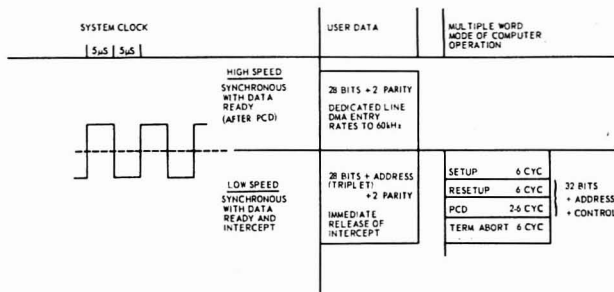


Figure 3. Diagram representing the modes of data transmission via the teleprocessor

accessible through the control panel. The major data source can accommodate up to 28 bits of data and four control lines. These lines run directly to the LLB and can handle data rates in excess of 60 kHz. The control panel (Figure 2) for each experiment has six lighted push buttons, two dual light indicators, and five sets of thumbwheel switches to give the experimenter completely independent communication to the computer for interactive control of his experiment. Communications from the computer to the laboratory are provided in eight 16-bit words of output which can be divided or shared between the experiments as needed. Standard output devices are available including: teletype, plotter, display CRT, as well as logic output for relay drivers used in experiment control.

Operation of the system begins when the experimenter inserts his identification card (see Figure 2) user number and dials in appropriate setup data using the thumbwheels on the control panel. He pushes SETUP and then SEND. Each time a pushbutton is depressed, it lights, signaling to the experimenter that the intended operation was carried out. If the computer has understood and validated all commands, the ready (RDY) light extinguishes and the OPERATE illuminates, and, in AUTO mode, the experiment proceeds under computer control. The SEND button flashes to indicate data transmission. The experimenter can terminate or abort the experiment. A resetup constitutes a capability of changing experiment control criteria as the experiment proceeds.

Communication Structure. It is necessary to provide a teleprocessor design where the data from a variety of devices in the laboratory can be processed rapidly with protection to prevent entry onto the bus at a rate greater than can be handled. A fully parallel communication bus provides part of the answer. A second part comes from dividing the bus into two time-multiplexed subsystems. A symmetric clock pulse of 5-μsec half-cycle alternately defines the high and low speed sides of the bus. A data triplet constitutes a single transmission of an 8-bit instrument address and 32 bits of data, and it occurs within a 5-μsec half-cycle. The clock signal originates at the computer interface but is routed along the data bus in the direction of the data flow to avoid a "clock skew" due to propagation time along the bus.

Based upon a survey of data rates expected, the sources are divided into two distinct categories (Figure 3). The first category is low speed data (LS) and is noncyclic and usually nonbuffered such as might be provided by a digital voltmeter. This type of data must be picked up after only a short time delay. Data in this "time volatile" category are transmitted with a worst case delay of 1 millisecond. Therefore, a maximum transmission repetition rate of 1000 per second is specified. Only one cycle containing a data triplet (two 16-bit words plus address) may be transmitted before control is relinquished to the next device on the system. This, in effect, time shares the LS side of the bus between many devices. Since most data

Table I. Types of Records Transmitted to the Computer Via the Teleprocessor

Type	Size (bits)	Use
Triplet	8 (address) 16 (data) 12 (data)	For all data received from the instrument
Precursor (PCD)	8 (address) 11 (experimenter I.D.) 4 (No. words in PCD) 48 (Time of Year) 16 (Input parameter) 128 (Special data)	Normally transmitted before a block of triplets, and it provides a means of transmitting special parameters that might need monitoring or for interactive operator control.
Setup	8 (address) 11 (experimenter I.D.) 4 (No. words in PCD) 48 (Time of Year) 16 (Experiment log No.) 16 (Input parameter) 16 (No. of High Speed Words) 16 (Nonresident program No.) 16 (Repeat Cycle No.) 16 (Data Handling Code) 48 (Special purpose)	Initiates the experiment by loading the experiment control program and setting all pertinent values.
Resetup	Same as Setup (except that control bits have been changed)	Causes a terminate of the current control program and a reload of a new one or a reload of the old program with new parameters, also used for interactive control.
Terminate	Same as Setup (except that control bits have been changed)	Initiates a terminate and can include any of the pertinent parameters needed by the terminate routine of the experiment control program.
Abort	Same as Terminate	Currently, the record is handled the same as terminate

devices coupled to the system run at much less than the 1-kHz rate, this limitation is not a burden.

The second category is high speed data (HS) and is usually generated from a buffered data device such as a multichannel analyzer. With these data, small delays of 1 or 2 seconds before the data may be transmitted are tolerable, but once the readout is begun, data can be sent at rates of 60-70 kHz. In this case, the high speed side of the line is dedicated to the transmitting device and, at the computer, data are routed into a direct memory access (DMA) channel. This form of input can handle large blocks of data, and it contributes little to the time required for executing data-handling software.

Time Shared Multiplexing. The LS side of the communication bus must be shared among each of the LS users without chance of conflict. To allow control of individual communications, a pair of data bus lines provide a circular "daisy chain" path around which a single intercept pulse circulates. This pulse is regenerated at each LLB

location in sequence. In order for a LS transmit to take place, the intercept pulse must first be received and held in the interlatch logic circuit of the requesting device. At the end of the transmit cycle, the intercept pulse is released to proceed to the next interlatch circuit.

Multiple Transmissions. While almost all data records consist of a data triplet sent in a single transmission with subsequent release of the intercept, there are other data records that are used to establish a mode of computer operation (MCO) of the experiments (See Table I).

These MCO data records have a multiword format of between two and six sequential cycles and include: SETUP, RESETUP, PRECURSOR DATA (PCD), TERMINATE, and ABORT. Each of the sequences holds the intercept pulse until its transmission is completed. The arrival of every MCO at the computer interface is detected, and "Time of Year" is automatically included in the MCO format. Any LLB ready to transmit an MCO record can hold the intercept pulse and transmit if the computer interface buffer is empty; otherwise, because these records constitute a sizable fraction of the buffer storage in the computer interface, loss of some control words would result. However, the PCD can hold the intercept even though the data buffer is not empty, but transmission is deferred until the buffer is cleared. Holding the intercept for these MCO data records does not appreciably affect the 1-millisecond response time because these types of records occur infrequently.

Each of the MCO data records (See Table I) contain the following information: the combined control word and instrument address, the experimenter ID number, the experimenter log number, the input parameter, and time of year to the nearest millisecond. The setup and resetup sequences also include: the experiment control routine number, data handling number, number of repeat cycles, number of words to be read, and four variable entry words. The PCD data record differs in that its length is hardware-programmable and can include up to six additional words of ancillary data.

Instrument Address Structure. Complete address information is required to identify all experiments or instruments on the data bus, and the address is sent in parallel with each data block. Parity of the address word is set on a fixed parity basis. The sub-address bits are wired to fixed locations of the input system control boards and identify a transmitted word by its physical location in the LLB. The output words are similarly decoded and routed to specific board locations of the output words.

Common Logic. Whenever possible the LLB makes use of logic common to all of its input-output (I/O) systems. The synchronous interaction within the communication bus is timed by a 100-kHz clock in the computer interface.

All data transmissions are synchronized to the clock by a single set of pulses for each transmit cycle. A separate generator, one for HS transmission and one for LS transmissions, produce a pulse to reset all buffer registers; a pulse, overlapping the reset pulse, to strobe data "ones" from the selected input lines into the input bus which in turn will set the appropriate buffer registers; and a transmit pulse which enables the transmit gates for the remainder of the clock cycle.

All control word sequences are synchronously initiated by the clock and produce successive LS transmit cycles. Any test word received is synchronously transmitted back to the computer (without clearing the buffer registers) on the next available clock cycle.

The relationship of the timing between the intercept and clock is under the control of the computer interface

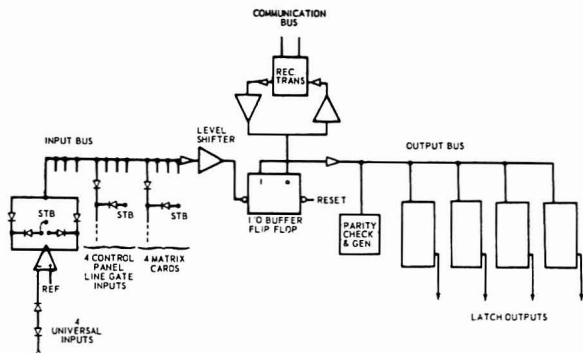


Figure 4. Diagram depicting the bus structure of laboratory logic box (LLB)

and can be used for teleprocessor reset or initialization.

State Control. Interaction between the LLB and any given data production device is controlled entirely by the state control circuit board and the control panel. The various signals from the experiment control panel, the system controls, and the output state of the readout device are combined in what is basically a sixteen-state asynchronous register. This register, comprised of 4 flip-flops, has multiple inputs so that each flip-flop can be set by one or more control signals. The register's state is decoded to provide outputs to the lamp drivers for the control panel and for control logic gating.

LLB Data Input/Output. The LLB has a data buffer common to the communications data bus that is also bus-connected to the four independent input systems and the eight words of output, Figure 4.

The input bus accommodates a data input, a control box data input, and a matrix input for each of the experiments connected.

I/O Buffer. The I/O Buffer consists of 42 flip-flops: eight for the address, 28 for data, four control bits, and two parity bits.

The I/O buffer operates as a bilateral temporary storage for data being transmitted to the computer as well as for data being received. The data contained in it are considered valid only for the duration of the given operational cycle because of its time-shared nature. In all operations, the buffer is first cleared to zero immediately followed with a write strobe. Parity check or generation occurs simultaneously.

Universal Input Card. Data outputs from a major data source are connected to inputs located within the LLB through a "Universal Input Card." Each card accepts 16 bits, 14 data lines, and two control signal lines. Used in pairs, they accommodate a seven-digit BCD input word and its control signals.

The design of this circuit eliminates the necessity for different designs to handle signals from different types of data sources. Programming by interconnection of the input connector allows positive, negative, or bipolar input signals with either a positive or negative fixed 0.7-volt zero offset. Common mode noise of up to ± 2 volts can be separated from the signal.

Input voltage levels can range from ± 2 to ± 50 volts without alteration to the card. The input impedance is high, typically drawing 200 μA from a positive 10-V signal.

The outputs of these data signals are diode-gated to the

LLB input bus with a strobe command pulse and can be chosen for either the inverted or noninverted logic sense. The control line inputs are similar to the data inputs, but they have separate gate lines provided to allow for independent selection of logic sense and control of input gating.

Control Panel Input. The control panel for each experiment connects to the LLB to provide control and indicator signals for the state control logic. It also connects to the 32-bit input and for the readout of thumbwheel data entered in MCO operations. These same data inputs provide for six words of 16-bit ancillary data input. Each of these words is strobed once during a PCD cycle and can contain information from devices such as shaft encoders or digital panel meters. Diode disconnects or line gates provide the final gating at the bus internal to the LLB to avoid the effects of cable capacity or crosstalk due to capacitive coupling.

Input Level Shifters. To permit the use of passive gating, the input bus works into level shifters which restore the DC zero and provide a high impedance input to the data buffer.

One additional feature of the input level shifters is the inclusion of power diodes connected between the bus to ground and the 5-volt supply to prevent inadvertently applied large voltages from getting further into the system. Fusible links on the circuit boards can melt if the overvoltage condition persists.

Data Outputs. The I/O buffers are bussed to eight 16-bit output card locations. When output data are received by the LLB, the output location address is selected, and the data are strobed singly or in word pairs into the output latches during the last part of the receive cycle. Standard output cards have been designed to interface up to four teletypewriters from a pair of locations and to provide two single word outputs for a plotter and CRT display scopes. A universal logic output card can "sink" currents from positive, negative, or alternating current (AC) sources.

The Computer Interface. The computer interface (CI) provides the mechanism to transfer data from the data bus to the computer. It also provides control and timing signals to the data bus. The computer interface can pass data to the computer in two ways: a priority interrupt controlled I/O channel (PIO) and a direct memory access channel (DMA). The computer interface receives the parallel data (40 bits + parity) from the data bus and multiplexes it into 16-bit computer words. The data on the bus are time multiplexed into high speed and low speed data,

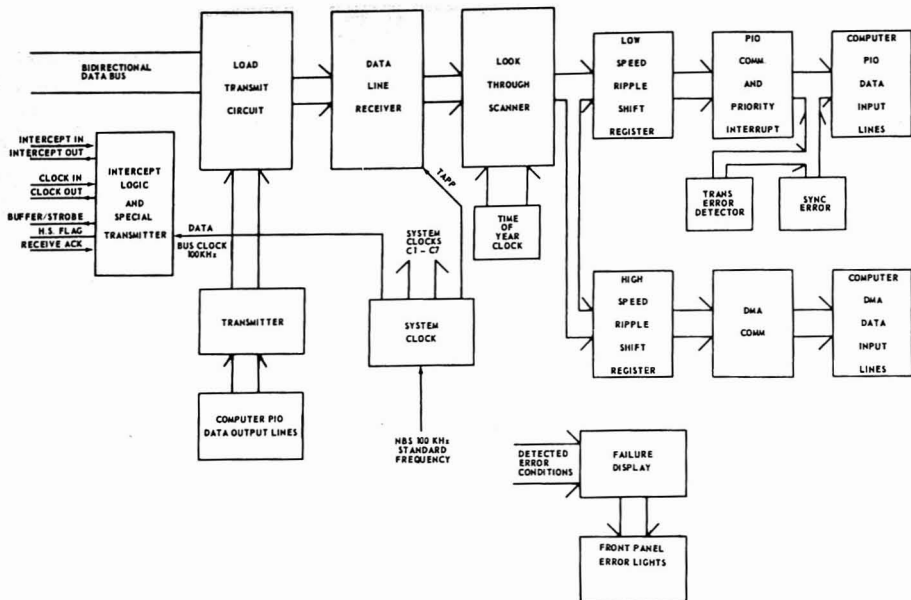


Figure 5. Diagram of the computer interface

and the CI transfers all of the low speed data to the PIO channel and the high speed data to the DMA channel. The computer interface also provides the mechanism for transferring data from the computer to the data bus.

Computer Interface Logic. Flow of Data to the Computer. The data arrive from the data bus on the data bus input cards (See Figure 5). Data pass next to the load transmit circuit boards where its direct current (DC) level is adjusted, and then to the data line receivers where the data bits are converted from low level differential signals to TTL logic levels and parity is checked. The data are next strobed under control of the lookthrough scanner (LTS) onto either the high or low speed ripple shift register (RSR) where they ripple to the home position. The LTS also provides for introduction of time of year for certain combinations of control word bits. For low speed data, a priority interrupt is generated when the data are ready to be read by the computer. For high speed data, the presence of data causes a strobe to be generated which transfers control to the computer's DMA channel.

Flow of Data from the Computer. The computer data output bus is connected to the transmitter ripple shift register (TX,RSR). The computer sends a control word which contains the LLB and port address and bits which inform the CI how many data words follow. Output transmission to the LLB can include either the first 16-bit word, the second word, both words, or a single bit (time mark) can be sent on the address word. When all of the data words have been loaded into the TX,RSR, the computer sends a transmit error terminator (TET) which causes the transmit cycle to begin. The data which are stored in the TX,RSR are strobed onto the data bus through the LTX circuit boards by the TX Gate, and transmitted to the LLB selected by the address word.

Intercept Logic and Special Transmitter. The intercept pulse is used by the LLBs as a flag to allow them to

transmit low speed data when the intercept pulse is present in the box. Each LLB serially receives and then transmits the intercept pulse.

The CI intercept logic receives the intercepts from the two buses (A and B) and retransmits them immediately unless there is a hold or a transmit inhibit. The logic sends the intercept around one bus (A) and then around the other bus (B). If, for any reason, an intercept fails to return, a new intercept is generated after a time delay, and an intercept fail condition is sent to the failure display circuit.

The special transmitter contains the control function line drivers. The control functions are: high speed flag (HSF), buffer empty/strobe (B/S), A&B clock, and A&B intercept.

Priority Interrupt Circuit. The priority interrupt circuit sends a priority interrupt (PI) to the computer when an address ripples to the home position of the RSR. It also controls the reset of the home position of the RSR. The sequence of events which occur to transfer data to the computer is: an address ripples to the home position of the RSR which generates a PI; the computer reads the address and the prescribed number (2 to 14) of data words; and the computer sends a SET and reads the parity and sync error bits. The SET turns the RSR reset on, and it remains on until another address reaches the home position. The RSR reset is used to clear the RSR of any words which might be erroneously stored.

Sync Error. The synchronize error circuit accepts inputs from the RSR, PIO COM., and the parity error (PE) circuits and checks for error conditions. The two synchronize error conditions are: the computer tried to read too many or too few words from the RSR between addresses. The synchronize error logic also controls a shift register which receives the PE bits from the RSR one at a time as the words are transmitted to the computer. When a SET is

received, the PE's (if any) are transmitted to the computer with one error bit for each word transmitted.

Direct Memory Access Communication and High Speed Flag (DMA-COMM). The DMA-COMM provides the logic necessary to interface with one of the computer's multiplexed direct memory access ports. It also provides a high speed flag to signal all of the LLBs that a DMA transfer is in progress. The computer sets up the DMA channel when it receives a high speed request. The high speed request is transmitted on a low speed PCD word by a LLB when a buffered device starts its readout. When the DMA channel is set on, there is a pulse to turn on the high speed flag which allows the LLB to start sending its high speed data.

Failure Display. The function of the failure display circuit is to indicate parity failures and to display failures that occur in the interface control functions. These are: a failure to receive an intercept pulse previously sent, failure in the clock, and no acknowledge from a transmit. Each error condition is stored by a flip-flop and the output of the flip-flop is connected to a lamp on the front panel. The failure display circuit also sounds an audible alarm whenever a parity error occurs. The addresses which are received by the interface are decoded and displayed in octal on the front panel, and when a parity error is detected, the address is latched so that the source of the data can be visually determined.

Performance of the Teleprocessor. Since there was concern about the noise immunity and data rate capability of the teleprocessor particularly relative to the digital data bus, the actual cable was installed and made operational even before the computer was delivered. The design resulted in a negligible failure rate when the transmit clock is set to 100 KHz (~ 4 megabits/sec).

A computer program is used to send test data to each LLB. Special test bits are sensed, and the test data are transmitted back to the computer. This routine can execute in a multi-programmed environment, and it can test a LLB that is in an active data transmitting state. The data from the experiment are simply held for a 10- μ sec transmit cycle. The test routine rarely detects an error. Nominally, 10^7 - 10^8 transmissions occur between failures. This means that the cable is highly immune to noise. As a result of careful design, the overall integrity of the cabling and connectors is exceptionally good because we have yet to experience a line failure three years after installation!

DESCRIPTION OF THE COMPUTER

General Description. The computer is manufactured by UNIVAC Corp. (Series 60). It is the former EMR model 6135, with 32,768 sixteen-bit words, two random access disks (data rate approximately 300 kilobits per second), each having a one-million word capacity, 80-column line printer (200 lines per minute), paper tape reader and punch, card reader, and nine-track magnetic tape (800 bits per inch, 25 inches per second), and a model 35 Teletype console.

Figure 6 shows the configuration of the system. The teleprocessor interfaces to the computer at two places; a channel of the direct-memory-access (DMA) type is used for the high speed data transmission (60 KHz), and an input to a program controlled I/O (PIO) channel is used for the low speed side. Hardware priority interrupts (high priority) are used for the PIO from the teleprocessor, magnetic tape, teleprocessor/computer transmit acknowledge, interval timer, watchdog timer, line printer, and teleprocessor DMA, in decreasing order of priority.

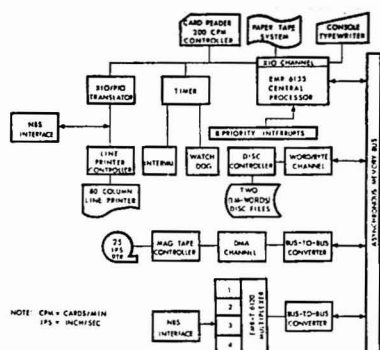


Figure 6. Configuration of the computer system

Connection with the Teleprocessor. An important aspect of this system is the fact that there are only two data input ports into the computer from the teleprocessor, the DMA and the PIO channel; and only one output port, also a PIO channel. From a hardware standpoint, the type of computer that is attached to the teleprocessor is unimportant. The major criterion is that of speed, because at present no single computer is known to be available that can process the data rate that the teleprocessor is capable of producing.

SOFTWARE

In order to provide an adequate data handling and processing capability with the teleprocessor described above, it is necessary to have fast computer hardware and to design efficient software to maximize rate of data handling and minimize response time to the instrument in the laboratory.

The computer has a fast read-write cycle (~500 nsec) and a moderately fast instruction set. The software provided by the company includes an efficient multi-programming monitor with capability for rapid handling of the teleprocessor's interrupt. (The term multi-programming refers to a computer with a single processor that allows more than one program to be in an executable condition.)

The software system consists of three parts that can be classified according to their transparency to the user. (Transparent software is that which is being used as part of the total system without active initiation by the user program.) These are (in order of decreasing transparency) executive routines of level 0 and 1 and the user programs. Figure 7 shows a block diagram of the major components. The software provided by the manufacturer is indicated by the box marked ASSET and the arrow marked OTHER I/O: everything else was done at NBS.

Level 0 Software. Level 0 software is concerned with maintaining the integrity of the operating system; such as scheduling of required tasks and input-output (I/O) operations. Much of this software called ASSET was supplied by the manufacturer. The heart of this part of the operating system is the job selector. Three main lists are kept: the interrupt stack, the job processing stack, and the memory request stack.

Control is given to ASSET when interrupts are received from user programs or peripheral hardware devices. Hardware interrupts are given the highest priority in the system and result in immediate entry into a response rou-

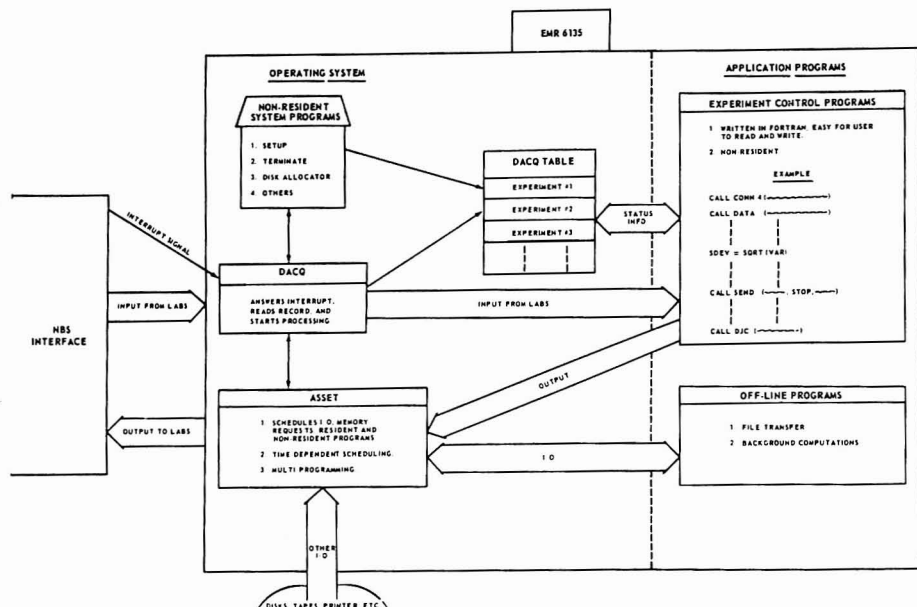


Figure 7. Block Diagram showing major components of the operating system

time. The teleprocessor input response routine called DACQ has highest priority followed by other high priority interrupt response routines for the high speed channels servicing disk, etc. Peripheral devices such as the card reader, paper tape reader-punch, and teleprocessor output are on scanned interrupts which are the next highest priority. Control may also be given to ASSET via direct calls. Input-output, scheduling, etc. can all be done by this method. The job selector checks priority among the three lists and determines which operation receives control. If tasks of equal priority exist in the different lists, the tasks are performed in the order, interrupt, job processor, and memory request lists. Tasks of equal priority in the same list are done on a first in, first out basis. I/O and memory requests are handled in quasi subprocessors with their own job lists. These also communicate with the job selector to determine the next execution. As indicated above, the system is designed to allow parallel operation of I/O drivers. For example, once an I/O operation is initiated, the operating system can continue on an alternate job until it becomes interrupted when that I/O operation is completed.

DACQ. The interrupt response routine called DACQ reads data into the computer from the teleprocessor's computer interface. The first word of the data record is read from the computer interface and its control bit is tested to determine its type. If the record is a MCO record, an appropriate branch is taken for SETUP, PCD, etc.

Table I describes the data that are transmitted from the instrument control panel to the computer. Time of year is automatically entered by the computer interface and read to the nearest millisecond. The experiment log number (thumbwheels) is used along with the instrument address and the experimenter identification number to produce a file name for the file manager. Input parameters are used

(thumbwheels) to communicate to the experiment control program. The number of high speed words is usually fixed or experimental instrument controlled (not via thumbwheels). The experiment control program number, ECP, is set (thumbwheels) to call the nonresident program. Repeat cycle (thumbwheels) is used to allow the ECP to repeat execution for the prescribed number of times. Data handling thumbwheels indicate either that a data processing routine is to be called upon completion of the ECP or that display and plotting of data in the laboratory is required.

SETUP. If the data is a setup record, control branches to a SETUP routine which obtains a buffer to store the setup record. The data are read into the buffer, and a nonresident program is scheduled to be loaded from disk and executed in order to continue processing of the setup record.

Data Handling. After using the DACQ table to look up the appropriate entry points, a check is made to determine if a buffer is allocated and if there is room for the triplet or PCD in that buffer. If not, a new buffer is obtained. The triplet or PCD is read into the buffer and the status of the computer interface is checked. This is done to determine if there were any parity or sequence errors detected by the hardware during transmission. A sequence error is either an address in the home position without a SET command being received or data in the home position when a SET command is received. If a sequence error is detected, an error is typed on the console.

Before exiting from DACQ, a check is made of the number of pending external priority interrupts. If this is too high, the interrupt stack is allowed to reduce without clearing the teleprocessor's interrupt. Control returns to DACQ and the interrupt is then cleared and control is given to ASSET.

Since an interrupt stack overflow condition can mean that data records may be lost, this condition is considered a major catastrophe. An error message is typed on the console and the cause for so many interrupts must be determined. Basically, the interrupt response routine is not the slow step in the data processing chain and, moreover, the summed data rate of all currently on-line experiments could not exceed the response time of experiment control programs.

An important level 0 program is called TEST whose execution is initiated from the console and provides for a continual check of the teleprocessor from the CPU to the experiment interface in the laboratory logic box (LLB). This program sends a prescribed bit configuration on both output words to the LLB which immediately reflects it (before real data are sent) back to the CPU. A comparison of word sent with those received is made, and any bit errors are noted on the console.

Level 1 and User Programs. The level 1 routines are callable subroutines from Fortran IV designed to interface the user's program with level 0 routines. Most of these routines have been written in assembly language. The relationship between the level of routines is illustrated by the operational sequence of instructions written for illustration in pseudo-Fortran (Table II).

The program is then compiled, assembled and loaded onto the nonresident library on disk. The user then proceeds with his experiment as follows.

He sets the proper values into the thumbwheels and pushes SETUP and SEND on the console. DACQ inputs the data and determines that a setup record is being received. DACQ processes the record as described above, and loads the nonresident user program for execution. The execution of the nonresident experiment control program begins with CONN4, a level 1 assembly language subroutine which links entry points 10 and 9000 in the program to a row labeled TAB in DACQ's table of parameters pertinent to the user program. Thereafter, incoming data cause the program to be scheduled and executed at the proper entry point. CONN4 also passes the laboratory instrument address (AD) for returning signals to the instrument.

Data are processed as described above with execution always beginning at the scheduled entry point, location 10.

The initiation of data transfer from DACQ is done by the experiment control program (ECP). Normally, the first process is to call subroutine DATA which causes the transfer of control to the experiment control program for purposes of reading of the data.

DACQ stores incoming data in fixed length (N) buffers. Only one buffer is allocated at a time for any given experiment control program. If no buffer space is available, the filled buffer is read onto disk. When DATA executes, a check is made to determine if any buffers are written onto disk. If there are, these are passed to the ECP first. A buffer of N words is passed to the ECP with M being set to the number of new words in the buffer. Disk addresses and the current location of the active buffer along with the count of new words in the buffer are stored in DACQ's table.

In order to send experiment control signals to the laboratory, the subroutine SEND is used. SEND takes the value of an experiment control word and sends it to the laboratory instrument address, AD. CONT is a control word which provides information to the teleprocessor interface regarding the number of data words, N, to be sent to the laboratory. FWD is the address of the data field to be sent out. SEND uses a program that has the attributes of

Table II. Subroutine EX (TAB)

	COMMON/STORE/A,B,C,D
	COMMON/ESTOR/IDUM
	CALL CONN4 (TAB, \$10, \$9000, AD).
	CALL RESTOR (TAB)
	CALL DJC (TAB)
10	SCHEMT
	CALL DATA (TAB, IBUF, M, N).
C	Do computation of data and/or code conversion
C	KBCDBN (IEXTR, X, Y, I)
	CALL CONV (IBUF, Y)
C	Send data to laboratory instrument
	SEND (AD, CONT, N, FWD)
	CALL OPEN (LU, STAT)
	ENCODE (N, 1000, MESS, CC) A, B, C,
1000	FORMAT (2X, 3(F5.2))
	CALL RIOS2 (0, 0, IPRI, \$20, LV, IAD, IS, NW,
	MESS)
	CALL CLOSE (LV, STAT)
	CALL SWAP (T, TAB)
	CALL ERROR (Y, TAB).
C	If end of program is reached call terminate routine
9000	SCHEMT
C	Do necessary execution before terminate
	CALL DJC (TAB)
	END

a standard system I/O driver, and in this routine resides all the communication with the teleprocessor.

After all data are read into the computer by DACQ, a sequence error terminator (SET) command is sent to the CI and it returns a status word which flags parity errors in each word of the record read into the computer. Currently, a data record containing a bad sequence results in an error message on the computer console and a rejection of the data record. The usual procedure for a missing type of data record then occurs when the experiment control program begins execution. If the ECP is of the "forgiving" type, it sends out a "restart" and tries to receive a proper retransmission of the record.

The experimenter may interact with the experiment control program (ECP) at any time by adjusting various thumbwheel switches. Values of labeled switches or thumbwheels are transferred with the next transmission of data (on the precursor data record), and the operating parameters of the ECP can change or a particular branch in the program can be executed. An entirely new ECP can be initiated at any time by the experimenter by pushing RESETUP and SEND. This causes a terminate of the existing program and a load of the new program with an entirely new set of pertinent setup parameters. ERROR is a level 1 routine for alerting the console operator of ill conditions existing in the experiment control program.

Execution time of an experiment control program is considerably reduced via the use of a spooling routine for a teletypewriter or plotter. The output is spooled onto disk, and a file is initiated by OPEN and terminated by CLOSE which then begins transmission to the output device.

A very useful level 1 routine provides the display of X-Y data on a CRT or plotter. The software package provides for region of interest display using upper and lower limits, sign and exponent of both X and Y values. This routine can be operated from the laboratory. Automatic display of collected data can be done via Fortran from the experiment control program.

Design of the system software has been dictated primarily by the desire to protect the users from interacting with each other and the system. In addition, one desires to maximize the number of experiments that can be run.

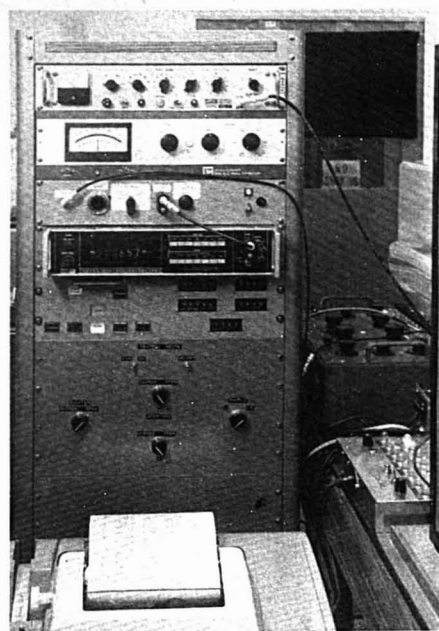


Figure 8. Photograph of instrument panel for the high accuracy spectrophotometer

This can be done by utilizing level one routines which reduce the time-average occupancy of core per user. The subroutine called SWAP is one of these, because it provides for removal of the ECP for specified time periods, *T*. The assembly language subroutine SWAP calls a Fortran subroutine SAVE which writes variables that must be saved onto disk.

Other difficulties must be considered. For example, what happens to the experiment using SWAP, if the instrument is inoperative after scheduling the program for execution after a predetermined time? The answer is that after the experiment control program is loaded, it begins execution by sending a data enable signal to the instrument, and it then waits for a response that never comes. To remedy this a level 1 subroutine has been written that performs in a similar manner to SWAP, except that the program is scheduled for load and execution only upon the arrival of data from the experiment. This routine performs the same functions as SWAP except that the timing for execution comes from the experiment itself. If the experiment fails to send data, no problem occurs because the program is not loaded into core.

The logical opposite of the above condition is failure of the instrument to respond to a stop data transmission signal. The user program must be written to accommodate such a situation, for example, by sending out more than one stop signal. However, if this fails, little recourse is left but to sound a very loud alarm and force a terminate!

The user may terminate his program from the laboratory by pushing the covered TERMINATE button and SEND. Termination of a program must be handled carefully. If the experimenter wishes to terminate his pro-

gram, the user program (ECP) must be informed of this fact before termination is executed. This allows the program to complete any I/O or other activity. A terminate can also be initiated from the user program. Upon a normal completion of program execution, a direct call can bring about a terminate.

File Handling and Processing. A file manager has been implemented which consists of a series of re-entrant subroutine calls from Fortran to open, close, reopen, delete, etc. files. Files are named by the user in the laboratory and redundancy checks are made on this name. Data files are retained on a general backup tape daily and may be saved on archive tapes identified by the user. The important considerations in managing files, are that the user know the name of his file at file generation time, and that there be no duplicate names of files. Disk backup tapes which will contain files generated during any given day will be saved for a period of time so that a user who notes that a particular file is not in his archive, can request that it be transferred from these backup tapes to his personal archive tape.

Data files may be processed automatically after collection, if the computation is not lengthy, by scheduling another nonresident routine from the experiment control program. Small amounts of result computation or small data files can be transmitted to the laboratory for plotting or CRT display.

Program Protective Features of the System. A multiprogramming system can be subject to errors in one program that could cause the entire system to fail. A desirable feature of any operating system is protecting one sub-process from errors in another. Especially desirable is the protection of the level 0 software against errors.

This computer system has a hardware protection scheme based on a division of core storage into protected and nonprotected words by the setting of a bit associated with each word. The operating system and the user non-resident programs function in a protected portion (so-called foreground area) while the batch processor functions in unprotected portions of core. Thus, errors in batch do not affect the operating system because protection circuits generate an interrupt whenever an unprotected instruction attempts to write into or transfer control to a protected location.

Unfortunately, an error in an ECP which executes in the protected area may cause the system to fail. After final compilation on the batch processor, our policy is to thoroughly evaluate such programs and to test them during inactive periods in the protected mode before allowing free use of that program. Our experience is such that fatal errors can be detected off line, and the chances of a catastrophic system crash is reduced but not entirely eliminated.

DESCRIPTION OF TYPICAL ANALYTICAL INSTRUMENTS CONNECTED TO THE SYSTEM

The following paragraphs describe briefly a number of the experiments that have been connected to the system. They are characterized by either low data rates or low volume high rates. Response time for instrument control is on the order of seconds and the degree of using instrument control is still relatively undeveloped. All of the experiments on the system can run at any time, and the user feels that he has sole use of the computer.

High Accuracy Spectrophotometer. This system provides for the indexing under computer control of samples into the path of a light beam. A programmable number of light intensity readings separated by approximately 40

msec are taken and per cent absorbance values are calculated and printed on a teletypewriter in the laboratory immediately after collection. The use of the computer has improved precision, and it has provided a significant increase in throughput (See Figure 8).

Constant Temperature Readings of Electrochemical Cells. This system uses the computer to set the temperature of a water bath, to check the stability, and to read temperature and the EMF of cells immersed in the bath every 5 to 10 minutes as determined by the program. Running time performed manually required constant attention over a 32-hour period. Precision of the measurement was improved and the tedium and human error resulting from manual control were avoided.

High Accuracy Mass Spectrometer. This system measures the ion current at two mass positions and computes appropriate intensity ratios. The computer changes the mass position and determines the proper range for the measurement which incorporates a vibrating reed electrometer with its voltage digitized by a voltage to frequency converter-scaler combination. Timing is critical in this system if maximum precision is to be obtained, and significant improvement in precision has been observed.

Electron Probe Microanalyzer. The computer sets the electron beam position and the system collects up to six scalars of fluorescent X-ray data (one for each element) for each electron beam position on a sample. After data collection, a series of routines display the data by element on a contour plot or as intensity *vs.* position superimposed upon the electron scatter display provided by the instrument. This allows the analyst to display his data in many different ways as well as to provide a data bank for subsequent detailed computation.

Multi-Channel Analyzers. The system provides an automatic dump of data from a multichannel analyzer to disk at a time interval determined by the experiment. These data are displayed in the laboratory by region of interest determined by the user and plotted when desired. All interaction occurs via use of the experiment control panels. These analyzers are connected to gamma-ray spectrometers, Mossbauer spectrometers, and an ESCA (electron spectrometer for chemical analysis) spectrometer.

SUMMARY

Performance. Time in full operation without catastrophic failure of the operating system constitutes a major performance criterion regarding integrity of software modules and their interaction. Our experience has been that an average of about one system software failure per seven days occurs. The rate of "crashes" has been decreasing as a result of painstakingly eliminating "bugs" as they appear.

The system is now supporting 20 instruments including special devices in a time-shared environment. However, we have yet to experience more than three programs in core at any one time. Of the three in core, one of these is our teleprocessor test routine which is scheduled on second intervals, and one other is scheduled on 1-minute intervals. Consequently, with projected data rates of instruments currently attached to the system, it can be expected that at least 50 instruments can be serviced.

With the experiment currently connected to the system, control signals need not be returned on an exceedingly short time scale. However, signal returns within 50 milliseconds are routine. Most of the simple calculations, averaging, standard deviations, etc. are done immediately upon receipt of the data, and the results are transmitted to the laboratory at that time.

Success of the Utility Concept. The concept of a computer utility is beginning to show signs of greater viability due to improvement in the ease of remote access to computers resulting from progress in teleprocessor design. This system utilizes a mode of remote communication that is designed to implement simplified structure of communication. For the user, it has proved beneficial to push buttons rather than type in tedious system "book-keeping" information. The result of this concept has presented some interesting ramifications.

Since there are only two types of input and one type of output, the complexity of I/O has been greatly reduced. Communication between the computer and all instruments is done in a common manner. This factor has deep implications, because it becomes readily apparent that software can be modularized in such a way that only a few modules are required to service a wide variety of instruments. For example, a single program written in Fortran using the subroutines as indicated above can be used virtually without modification for such diverse experiments as a constant velocity Mossbauer spectrometer, an ESCA photoelectron spectrometer, or a fluorescence spectrophotometer.

Future Plans for the System. The decrease in the cost of computer memory will continue to have a profound impact upon the utilization of minicomputers. The cost of mass storage devices is also decreasing and, as a result of both of these, rather highly user oriented systems can be connected to a single instrument. Enough memory can be made available to provide for high level languages in these computers. The cost of peripheral devices such as line printers, cathode ray displays, and plotters still keeps the total dedicated system cost between \$15,000-20,000, and these have been known to expand quickly to the \$50,000 category.

A serious problem with the time-shared computer system is that software development costs tend to be excessive, and a degree of inflexibility exists in transferring to another more advanced computer because a significant portion of the software related to the teleprocessor would have to be rewritten.

On the other hand, the existence of minicomputers on each instrument represents a different type of inflexibility. If the programming of the computers is done by the laboratory scientist, considerable time and effort must be spent on factors other than, *e.g.*, the subject of analytical chemistry.

Our effort will gradually shift to laboratory-centered computer systems, but support for these systems will come from the central group responsible for the time-shared system.

The time-shared system then becomes a part of an hierarchical system which allows access to large file storage and reasonably elaborate computational capability.

With such a system of standardized interfacing and software modules, the term "high level language" could take on new meaning and the concept of a computer utility as defined in the introductory paragraphs can be more closely approached.

Until such capabilities become readily available to all experimenters, the use of the computer system described herein satisfies many of the requirements for an ideal computer utility in the analytical laboratory.

ACKNOWLEDGMENT

The assistance of John F. Barkley, Advile A. Bell, and Lawrence J. Kaetzel of the Technical Services Group, Analytical Chemistry Division, is most gratefully acknowl-

edged. Advice during the early stages of the project regarding the specifications for procurement of the computer, the initial design of the interrupt response routine, and the functional aspects of the system from Roy G. Saltman, Institute for Computer Services and Technology, NBS, was sincerely appreciated. Also the assistance of Richard N. Freemire, Institute for Basic Standards, is appreciated. Permission to use the photograph in Figure 8

was granted by Radu Mavrodineanu, Analytical Chemistry Division, NBS.

Received for review, July 12, 1973. Accepted, November 28, 1973. In no case does the identification of trade names imply recommendation or endorsement by the National Bureau of Standards, nor does it imply that the material or equipment identified is necessarily the best available for the purpose.

Pattern Recognition Techniques Applied to the Interpretation of Infrared Spectra

D. R. Preuss and P. C. Jurs

Department of Chemistry, The Pennsylvania State University, University Park, Pa. 16802

Pattern recognition techniques can be usefully employed for the interpretation of chemical data. An investigation into the classification of infrared spectra is reported. A new training routine utilizing a new thickness parameter for the decision surface is introduced. The thickness is then used in developing a new effective feature selection routine. This routine is successfully applied to a number of well-characterized synthetic infrared data sets and plots of the resulting weight vectors are presented. The techniques are finally applied to three chemical classes—carboxylic acids, esters, and primary amines—and the resultant weight vectors are plotted and discussed.

The interpretation of infrared spectral data to be used in the classification and identification of unknown compounds depends to some extent on the theory which describes the vibrational motion of atoms in molecules, characterized by atomic masses, and vibrational force constants. To an even greater extent, particularly in the study of complex organic molecules, the interpretation of infrared spectra depends upon empirical and semi-empirical rules which have been developed by analyzing the spectra of large numbers of compounds for which the structures have been previously determined. It is this semi-empirical method which closely parallels the pattern recognition technique.

Pattern recognition comprises the detection, perception, and recognition of invariant properties among sets of measurements on objects or events. The purpose of pattern recognition is generally to categorize a sample of observed data as a member of the class to which it belongs. This general approach has been applied to problems from a great number of diverse fields (1). There is now a growing literature reporting applications of pattern recognition to chemical problems (2-7).

The pattern recognition method used in this study is a binary classification technique employing an error correc-

tion feedback algorithm for development. Information concerning the application of pattern recognition techniques to the interpretation of infrared spectral data has appeared previously (8, 9). The work by these authors has demonstrated that infrared data can in general be quite successfully treated by pattern recognition techniques.

DATA SETS

For this study, two data sets were prepared. The first data set consisted of 500 infrared spectra of simple organic compounds, which fit the general formula: $C_{3-10}H_{2-22}O_{0-3}N_{0-2}$. The first 500 solution infrared spectra listed in the Sadler tables, which satisfied this criterion were selected for the data set. Each spectrum was digitized at 0.1-micron intervals, from 2.0 to 14.7 microns, giving a total of 128 descriptors. The transmittances were read as accurately as possible to the nearest per cent. If the strongest absorption in the spectrum was greater than 5% transmittance—i.e., the absorption was weaker than one which would give 5% transmittance—the spectrum was normalized, using Beer's law, so that the strongest absorption was equal to 5% transmittance. Finally, all descriptors were scaled as integers ranging from 0 (complete absorption) through 31 (no absorption) for convenience.

The second data set was randomly calculated in an effort to simulate real infrared data. Each synthesized spectrum consisted of 128 descriptors. In preparing a single spectrum, all of the descriptors were initially set equal to 100% transmittance. Next, a specified number of Gaussian shaped absorption peaks were coded onto the spectrum according to Beer's law. Each peak was centered about a randomly selected wavelength. The intensity of each peak and the full width at half maximum were randomly selected within specified ranges. The data set consisted of 500 spectra each containing 20 randomly placed Gaussian peaks with intensities between 40 and 80% and full widths at half maximum randomly chosen between 0.1 and 0.4 microns. These parameters were selected in order to simulate real infrared spectra. The simulated IR spectra appear remarkably similar to real spectra when plotted.

The spectra in the synthesized data set actually represent a collection of random backgrounds on which various

- (1) George Nagy, *Proc. IEEE*, **56**, 838 (1968).
- (2) T. L. Isenhour and P. C. Jurs, *Anal. Chem.*, **43** (10), 20A (1971).
- (3) B. R. Kowalski and C. F. Bender, *J. Amer. Chem. Soc.*, **94**, 5632 (1972).
- (4) L. B. Sybrandt and S. P. Perone, *Anal. Chem.*, **44**, 2331 (1972).
- (5) D. D. Turniciff and P. A. Wadsworth, *Anal. Chem.*, **45**, 12 (1973).
- (6) Joseph Schechter and P. C. Jurs, *Appl. Spectrosc.*, **27**, 30 (1973).
- (7) K.-L. Ting, R. C. T. Lee, G. W. A. Milne, M. Shapiro, and A. M. Guarino, *Science*, **180**, 417 (1973).
- (8) B. R. Kowalski, P. C. Jurs, T. L. Isenhour, and C. N. Reilly, *Anal. Chem.*, **41**, 1945 (1969).
- (9) R. W. Liddell III and P. C. Jurs, *Appl. Spectrosc.*, **27**, 371 (1973).

features can be added in order to test the effectiveness of various training procedures. The advantage of such a data set, over a real data set, is that the user can create a carefully controlled training problem, in which he knows in advance which descriptors are the important ones, and what kind of information they contain.

TRAINING WITH A NORMALIZED WEIGHT VECTOR

One way in which to interpret a binary pattern classifier is to consider each spectrum in the data set as a single point or vector, X , in an N -dimensional hyperspace, where N is the number of descriptors being used to characterize each spectrum. A hyperspace of N dimensions can be divided into two regions by an $N - 1$ dimensional hyperplane. The training routine attempts to define a planar decision surface, such that all the data points belonging to a particular class are on one side of the surface, and all the data points not belonging to the class are on the other side of the surface. Usually, an extra dimension is added to both the space and the plane to ensure that the plane passes through the origin.

A plane can be unambiguously represented by a vector normal to the plane, and a point lying in the plane. Since the plane of interest is assumed to contain the origin, the normal vector alone, W (called the weight vector), will suffice. From vector algebra, one has:

$$W \cdot X = |W||X| \cos \theta \quad (1)$$

where θ is the angle between W and X . The sign of the cosine term, and thus the sign of the dot product, determines on which side of the decision surface the point X lies.

Ordinarily, the training procedure is continued until a weight vector, W , is found for which all points of the training set are on the appropriate side of the decision surface. A common technique which has been found to provide a weight vector with improved predictive abilities, is to give the decision surface a finite thickness, $2t$, and then to continue the training procedure until all points in the training set are not only on the appropriate side of the infinitesimally thin decision surface, but so that no point lies inside of the finitely thick decision surface.

Introducing surface thickness to the problem has conventionally been accomplished by specifying a threshold value, Z , and requiring that the magnitude of the dot product, $W \cdot X$, exceed this value before X is considered to be properly classified. This procedure would define a surface thickness as follows:

$$Z < |W \cdot X| \quad (2)$$

$$Z < |W||X| \cos \theta \quad (3)$$

But $|X| \cos \theta$ is just the normal distance from X to the surface, or the half surface thickness, t . Rearranging yields

$$t = Z/|W| \quad (4)$$

These relationships are illustrated in Figure 1.

The user specifies the value, t , by defining Z and by initializing the weight vector. The problem encountered is that t is related to Z through the magnitude of W . W is changed as a result of corrective feedbacks, and as its magnitude changes, so does the value of t . Consequently, although a specific value of t may have been used prior to training, the user has no control over its final value. If W were normalized to a specified value after each feedback, t would remain constant throughout the training procedure.

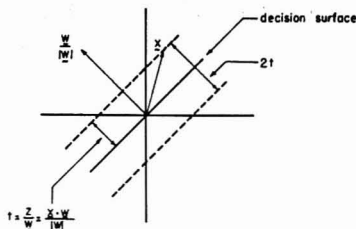


Figure 1. The relationship between Z and t . If X is the data point nearest to the surface, then $t = (X \cdot W)/|W| = Z/|W|$

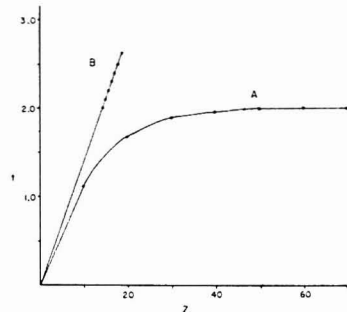


Figure 2. t vs. Z for unnormalized (A) and normalized (B) weight vectors

A training routine which employed a normalized weight vector was prepared and tested. The results obtained with this training routine are presented in the following paragraphs.

To test the normalized weight vector training routine, a training set of 200 spectra was taken from the previously described synthesized data set. To half of the spectra was added a peak of 30% intensity, 0.4-micron FWHM, at 4.4 microns. Of course, a fraction of the other synthesized spectra would also contain peaks in this region. In order to reduce the amount of calculation only the first 50 descriptors were used (wavelengths between 2.0 and 6.9 microns). Weight vectors were then developed which could discriminate between those spectra to which the 4.4-micron peak was added and those without such an addition.

The first run used unnormalized weight vector training, with each weight vector component initialized to 1, and with various values of Z . The results are shown as curve A in Figure 2. Clearly, increasing Z beyond 40 or 50 in this example served only to increase the magnitude of W , while t approached a limiting value of two.

The same training set was then used in conjunction with a training routine which effectively normalized W after each feedback in order to keep $|W|$ and therefore t constant. (Actually, the value of Z was corrected after each feedback instead of $|W|$ since it is a more convenient calculation.) The results are shown as curve B in Figure 2. These data must necessarily lie on a straight line. The line terminates at $t = 2.63$, the largest value of t for which convergence could be obtained. Thus, the normalized training routine could obtain a solution with $t = 2.63$, while the unnormalized routine asymptotically approached a solution with $t \approx 2.00$.

Table I. Results of Feature Selection

Pass number	t_{initial}	Descriptors eliminated this pass	Descriptors remaining	Per cent prediction
0	2.63		50	98.51%
1	2.63	23	27	97.55%
2	1.31	11	16	97.23%
3	1.31	1	15	97.24%
4	1.31	1	14	97.90%
5	1.31	1	13	97.89%
6	1.31	1	12	97.61%
7	1.31	1	11	98.59%
8	0.66	1	10	97.24%
9	0.66	1	9	97.25%
10	0.66	1	8	96.25%
11	0.66	1	7	96.92%
12	0.66	0	7	

In theory, if in the unnormalized case, a solution W_0 exists for some value of Z_0 then a solution, W , can be found for any value, Z , by setting $W = (Z/Z_0)W_0$. However, there should exist some optimum value of t , t_{opt} , such that for any $t > t_{\text{opt}}$, no solution could be found with any number of feedbacks. The object of the normalized training routine is to achieve a value of t as close to t_{opt} as possible, using a reasonable number of feedbacks. The disadvantage of this method is quickly realized, in that prior to performing any calculations, the user has no idea whether his choice of $t = Z/|W|$ will be greater than t_{opt} so that convergence is impossible, or whether it will be so far below t_{opt} that a comparable solution could have been obtained more easily with the unnormalized training routine.

One solution to this problem is to first use the unnormalized training routine to obtain a solution near the asymptote and then to use the normalized training routine for successive increments of t , until convergence is no longer achieved. Calculations can be reduced considerably if instead of initializing the weight vector for each trial, it is left alone so that the final weight vector from the previous trial is used as the initial weight vector for the following trial.

FEATURE SELECTION

Efficient and effective methods for the elimination of extraneous descriptors from a data set are desirable for a number of reasons. The dimensionality of the data being handled can be lowered to the point where the cost of implementing the discriminant functions is decreased. For some discriminant function training methods—e.g., least squares—systems of linear equations must be solved, and it is therefore imperative that the number of dimensions be reduced as much as possible. A useful new feature extraction algorithm using t has been developed and is described in the following paragraphs.

Given a solution for a particular training set, each data point, X_i , in the set is characterized by a normal distance, d_i , from the decision surface. For a point on the proper side of the surface, this distance is given a positive sense, and for a point on the improper side of the surface, the distance is given a negative sense. The value of the surface half-thickness can now be defined as the minimum value of d_i occurring in the training set.

$$d_i = \pm |W \cdot X_i|/|W| \quad (5)$$

$$t = \text{minimum}(d_i) \quad (6)$$

The value of t defined in this manner is the largest value which can be applied to the given decision surface, and still represent a convergent solution—i.e., all members of the training set are correctly classified.

In order to test the importance of a given descriptor, the feature selection routine temporarily omits it from the data set. Then values are obtained for all the d_i 's and t is determined. It is predicted here that the removal of an important descriptor would cause a considerable reduction in the value of t , whereas the removal of an extraneous descriptor would cause only a small variation in t . This procedure is repeated for each descriptor in the data set, and the resulting t 's are compared. The algorithm assumes that the largest value of t corresponds to that descriptor which could most easily be eliminated, and it drops that descriptor from the data set. This procedure could then be repeated over and over, eliminating descriptors one at a time. However, it has been found that superior performance is obtained if the weight vector is retrained periodically during the feature selection process.

A test of the algorithm was performed using the synthesized data set with peaks added to half the spectra at 4.4 microns as described above.

The criteria used to decide when to call the training routine to retrain the weight vector were as follows: first, t_{initial} was set equal to the value of t before the feature selection algorithm was called for the first time. On the first pass, the algorithm was used repeatedly until t became negative. Then the training routine was called with t set equal to t_{initial} . If convergence was obtained, the next pass was begun. If convergence was not reached, t_{initial} was set to $\frac{1}{2} \times t_{\text{initial}}$, and the training routine was called again. Again, if convergence was obtained, the next pass was begun. If not, the training routine was called with t set equal to zero. If convergence was not reached here, calculations were terminated. Before each pass, the predictive ability of the decision surface was tested on a prediction set of 300 members (150 positive and 150 negative). The results are given in Table I.

Passes 1 and 2 eliminated about two thirds of the descriptors quite easily. Subsequent passes could eliminate only one descriptor at a time. Initially, many components of the weight vector have values close to zero, but eliminating descriptors is equivalent to setting the corresponding component of the weight vector to zero, so dropping such a component would have little effect on the dot products and would not alter the decision surface significantly. After the first two passes have eliminated 34 descriptors, the remaining descriptors, although not bearing any predictive significance—i.e., they are not near the 25th descriptor—still have considerable magnitudes, and their removal would alter the surface enough to require the retraining of the weight vector.

At the end of the eighth pass, there remain 10 descriptors, and the predictive ability is 97.2%. The remaining descriptors are as follows: 2.0 (+), 2.2 (−), 3.0 (−), 4.0 (−), 4.3 (+), 4.4 (+), 4.5 (+), 5.4 (−), 5.6 (+), 6.2 (−), where the sign in parenthesis shows whether the particular micron interval correlated with the presence of the added peak at 4.4 microns or not.

There are many criteria, or sets of criteria which could be used in conjunction with the feature selection routine in determining when to call the training routine, what values of t to train for, and when to terminate the procedure. This is a good example of a time when not knowing t_{opt} is a considerable disadvantage. One possible way to overcome this problem would be to define Z in order to obtain an asymptotic solution using the unnormalized

Table II. Training and Prediction for a Number of Synthesized Data Sets

	Intensity, transmittance	FWHM, microns	Wavelength, microns	t	Per cent prediction
a	30%	0.4	4.4	2.63	98.51%
b	25%	0.4	4.2 to 4.6	0.73	89.80%
c	40%	0.4	3.4 and 5.4	2.94	99.64%
d	25%	0.4	3.4 or 5.4	0.0094	82.88%
e	40%	0.8	4.4	3.87	97.04%
f	40%	0.8	4.4	2.44	97.82%

training routine, and then to end calculations as soon as convergence could not be obtained in some specified number of feedbacks.

A second version of the feature selection routine was also employed in which two descriptors were eliminated at a time before checking whether $t < 0$ required retraining. The results were comparable to those of Table I; however, a considerable savings in computer time was realized. The pairwise feature selection routine was able to reduce the number of descriptors down to 8 with four passes. With only 8 descriptors, the predictive ability was 96.3%. The remaining descriptors were: 2.4 microns (-), 4.0 (-), 4.3(+), 4.4 (+), 4.5 (+), 5.4 (-), 5.8 (+), and 6.2 (-). These correlations are quite similar to those obtained above.

Finally, a feature selection routine which has been reported previously was applied to this data set for comparison. This routine involves training two weight vectors, one with all components initialized to +1 and the other with all components initialized to -1. After training, the signs of the individual components are compared, and those components for which the signs are different are dropped. The procedure is repeated until no further descriptors can be dropped. For the present problem, the results obtained were that only 12 out of the 50 descriptors could be eliminated, but predictive ability stayed high with a value of 97.8% for 38 descriptors remaining.

WEIGHT VECTOR MAPS FOR SIMPLE TRAINING SETS

The next aspect which was investigated was what a map of the weight vector looks like after various training situations. Again, synthesized data were used. The backgrounds were the same as those described previously. Various peaks, or combinations of peaks, were coded onto the random backgrounds in order to simulate different training problems. The intensities of the coded peaks were varied slightly in order to give the different training situations similar degrees of difficulty. Six situations were considered. Solutions were obtained with $t \approx t_{opt}$, and were tested with a prediction set of 300 spectra (150 positive and 150 negative). The results are given in Table II and Figures 3a through 3f. The weight vector maps are plotted in the inverted orientation commonly used for IR spectra and are arbitrarily normalized.

In the case where a single peak was added to each spectrum in the positive half of the data set at 4.4 microns, the form of the weight vector was quite distinct (Figure 3a). The component of the weight vector corresponding to 4.4 microns had the greatest magnitude, favoring a positive dot product, in the case where an absorption peak was present. On either side of 4.4 microns, the magnitudes of the weight vector components decreased rapidly, until they changed sign, and began to favor the absence of a peak at their corresponding wavelengths (a few tenths of a micron away from 4.4 microns). The overall result had the general appearance of a peak in the map of W .

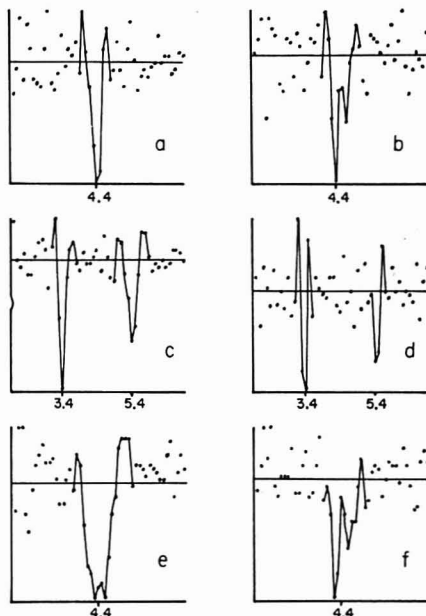


Figure 3. Weight vector maps for six synthesized data sets

In a real infrared data set, the absorption corresponding to a ketone, for example, will vary somewhat in wavelength, depending on the mixture of the normal modes. To simulate this, the second training situation had a peak coded which was centered about a wavelength which was randomly selected between 4.2 and 4.6 microns. The result (Figure 3b) was interesting in that W was peaked on either side of 4.4 microns, and at 4.4 microns it showed a relative minimum. This can be partially understood if one considers that an absorption peak centered at 4.4 microns would still have moderate absorption levels 0.1 to 0.2 micron to either side of the 4.4 descriptor, where W is peaked. This would still favor a positive dot product as well as a peak centered at either 4.2 or 4.6 microns. Based on this result, one would not expect, in real infrared data, to see such a well formed peak in the map of W , as was seen for case a. Also, in light of the fact that in spite of the increased peak intensity compared to case a, the predictive ability and t were both lower in case b, one would expect to encounter greater difficulty in obtaining good convergence and prediction percentages with real infrared data.

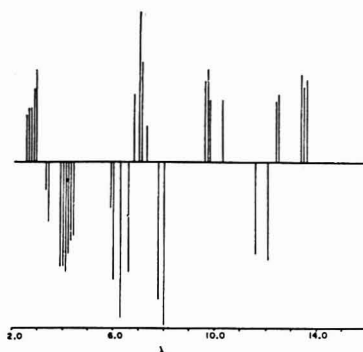


Figure 4. Carboxylic acids weight vector map

For real infrared data, a given type of compound may have two or more characteristic peaks. This situation was simulated in case *c* where the data set was coded with two absorption peaks, one at 3.4 and one at 5.4 microns (Figure 3c). As one would expect, convergence and predictive ability increased markedly over case *a*, even though smaller peak intensities were used. The weight vector was peaked in the regions of both 3.4 and 5.4 microns. However, these peaks in the map of *W* were not of equal intensity or width even though identical absorption peaks were coded on the original spectra.

If one were to try to classify two types of compounds together such as alcohols and phenols, the former would have a hydroxyl absorption around 2.8 microns, and the latter at about 3.2 microns. In this case, each positive member of the data set would have one of two absorption peaks. To simulate this situation, in case *d* (Figure 3d) a peak was coded either at 3.4 or 5.4 microns. The result was that, in spite of the greater peak intensities used, poor convergence and poor predictability were obtained, indicating the undesirability of such a training situation. Except for the fact that the peaks in *W* were relatively smaller, *W* itself appeared similar to the result from case *c*, where both absorptions were added to each spectrum.

The fifth case considered was the coding of a broad absorption peak (on a linear wavelength scale), similar perhaps to the hydrogen out of plane bending associated with aromatic compounds. The expected result was a peak in *W* similar to the one obtained in case *a*, with the exception that it would be broader. This was nearly what was observed, except that at the center of the peaked region was a depression similar to the one obtained in case *b* (Figure 3b). The depression was small enough to have questionable significance, so for case *f*, the spectra were coded exactly the same as in case *e*, except that a completely new set of random backgrounds were used. The result of this second trial was even more marked than the first (Figure 3f), giving the impression that for classification purposes, it is better to think of a broad peak as being two separate peaks (as in case *c*) located right next to each other.

In using real data, the classification of some types of compounds may depend on one or more intense absorptions, along with some weaker ones. It was observed in this section that if a single peak were the only basis for discrimination between two classes, it would have to be quite an intense peak with a fairly stable wavelength in order to give convergence for the training set. (In case *a*, a

Table III. Training and Feature Selection with Carboxylic Acids

Number of descriptors	Number of feedbacks	Percentage prediction
128	753	95.9
34	272	95.6
22	487	93.5
18	409	94.5
16	1143	91.7
14	2049	90.7
12	1508	91.2
10	1842	92.6
8	2838	88.5
6

peak of greater intensity than 40% transmittance was required, where the background peak intensities only ranged from 40 to 80% transmittance. Recall that a peak of 80% transmittance is a weaker peak than one of 40% transmittance.) In most real cases, the peaks would shift somewhat from compound to compound, so one would not expect to see any of the distinct forms in the weight vector like those seen in Figures 3a through 3f.

WEIGHT VECTOR MAPS FOR CHEMICAL CLASSES

The data set of 500 real infrared spectra described above was used to develop weight vector maps for compounds of several chemical classes. In each case, the following method was used to break down the data set. The number of positive members of the entire data set of 500 was determined. Two thirds of the positive members were put in the training set along with twice as many randomly chosen negative members. The remaining spectra were all put into the prediction set.

For each chemical class, the following procedure was followed. The unnormalized training routine was used with *Z* selected to assure a solution on the asymptotic part of the curve of Figure 1. The feature selection routine described above was called repeatedly to eliminate pairs of descriptors. Whenever *t* became negative, *W* was retained, and the predictive ability was determined. Three chemical classes were investigated: carboxylic acids, esters, and primary amines.

Carboxylic Acids. The training set consisted of 40 positive members and 80 negative members; the prediction set was split 21 (+) and 359 (-). The results of training and feature selection are summarized in Table III. The predictive ability remains high at 94.5% when only 18 descriptors remain, but declines thereafter. With six descriptors, convergence was not obtained and the routine was terminated.

Figure 4 shows a plot of the carboxylic acid weight vector of 34 components. As before, the weight vector components have been scaled arbitrarily and are plotted in the same orientation as for IR absorption spectra. Several regions are of interest, working from left to right.

There is a definite negative correlation between carboxylic acids and the region between 2.4-2.8 microns. This is where free hydroxyl stretching would be found. However, in undissociated acids, the hydroxyls are usually hydrogen bonded which shifts the absorption to longer wavelengths. Thus, this group of descriptors could be interpreted as ensuring that free hydroxyl groups are not classified as acids.

Eight descriptors, 3.2, 3.3, and 3.8-4.3, all correlate positively with carboxylic acids. It has been observed by spectroscopists that carboxylic acids generally exhibit a

Table IV. Training and Feature Selection with Esters

Number of descriptors	Number of feedbacks	Percentage prediction
128	720	96.6
36	458	95.5
24	604	94.4
14	541	93.5
12	419	93.2
10	516	91.5
8

Table V. Training and Feature Selection with Primary Amines

Number of descriptors	Number of feedbacks	Percentage prediction
128	598	95.2
32	686	95.5
24	432	96.0
18	366	95.1
12	3560	92.3
10	3991	92.6
8

broad absorption peak in this region due to hydrogen bonded hydroxyl stretching. Since such an absorption peak is relatively unique to carboxylic acids, this information was easily incorporated in the training of the binary pattern classifier.

Positive correlations are found for the 5.8- and 5.9-micron descriptors. This is the carbonyl stretching region.

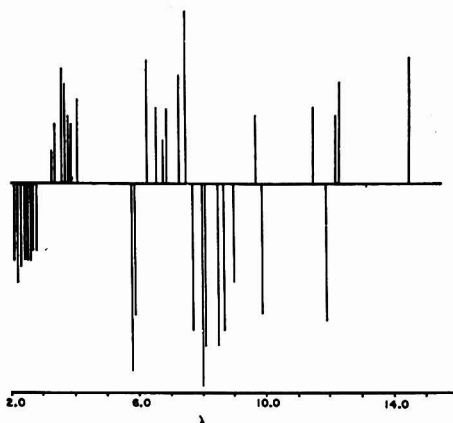
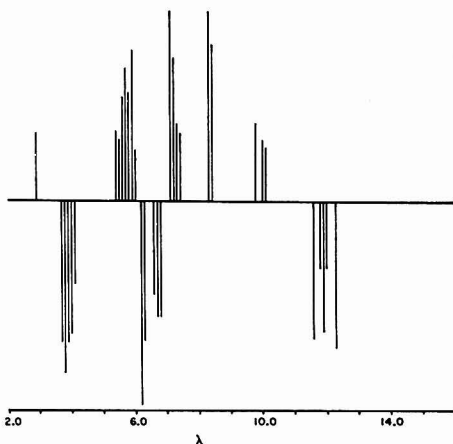
The remainder of the descriptors have values which do not obviously correlate with some particular feature of carboxylic acids or are negatively correlated with carboxylic acids. These latter descriptors' values are thought to be largely due to the particular negative members of the training set. Examination of the weight vector when it has only 18 components shows essentially the same correlations as those mentioned here.

Esters. The training set contained 40 (+) and 80 (-) and the prediction set contained 20 (+) and 360 (-). The results obtained are summarized in Table IV. The predictive ability falls slowly but steadily until no convergence could be obtained with eight descriptors remaining.

Figure 5 shows a plot of the ester weight vector with 36 descriptors. The positive correlations between esters and the descriptors for the 5.7, 5.8, 7.9, 8.0, 8.4, 8.6, and 8.9-micron regions are understandable, due to the standard ester stretch. The negative correlation for the descriptors 3.1, 3.2, 3.5-3.8 may be due to the fact that these would be especially useful in discriminating against C-H stretching vibrations of aldehydes and possibly the hydrogen bonded hydroxyl stretching of carboxylic acids. The strong correlation between esters and the 2.0-2.7 micron descriptors is difficult to explain; it could be an instrumental artifact.

Primary Amines. The training set contained 38 (+) and 76 (-) and the prediction set contained 20 (+) and 366 (-). The results obtained are summarized in Table V. The predictive ability remained steady with as few as 18 descriptors before falling.

Figure 6 shows a plot of the primary amine weight vector with 32 descriptors. A cluster of descriptors in the

**Figure 5. Esters weight vector map****Figure 6. Primary amines weight vector map**

3.6-4.0 micron region give positive correlations with primary amines which are difficult to explain. They could be due to NH_4^+ modes which could be present if there were water in the samples. A group of descriptors in the 5.3-5.9 micron range are training against characteristics of other classes of compounds. The 6.1 and 6.2 micron descriptors correlate with the N-H bending modes of primary amines. The positively correlated descriptors at longer wavelengths may correlate with known broad amine peaks in these ranges.

Received for review August 7, 1973. Accepted October 24, 1973. The financial support of the National Science Foundation is gratefully acknowledged.

Statistical Method for the Prediction of Matching Results in Spectral File Searching

Stanley L. Grotch

Jet Propulsion Laboratory, California Institute of Technology, Pasadena, Calif. 91103

In file search techniques, the distribution of mismatches quantitatively measures the fit of a particular unknown against a given library. A simple theoretical method is developed to predict, *a priori*, this distribution. With this procedure, for any unknown code and library, the mean number of mismatches can be calculated exactly. For a given library and coding scheme, the mismatch distribution for most unknown codes closely follows a common curve which is easily calculated from statistical properties of the library. When this common curve is normalized to a constant mean, the observed matching behavior is well predicted. The theory should permit the user to more clearly assess the effects of errors on file search performance and suggest techniques by which recognition performance may be optimized.

Primarily because of the need to handle the ever-increasing data rates of analytical instruments, the digital computer is becoming common-place in the chemical laboratory. Since these computers are often available to fulfill other functions in addition to conventional data processing, much attention has been directed toward applications to relieve the chemist of routine, tedious, but nevertheless, essential tasks. Among these has been the use of computers in interpreting chemical spectra (primarily infrared and low resolution mass spectra).

Undoubtedly, the most widely used technique in computerized spectral interpretation is "file searching." Here an unknown spectral code is compared against a larger known file or library of similarly coded spectra. Those known spectra which "best fit" the unknown code by some criterion are assumed to be the correct answers. A review of the mass spectral applications of file searching to about 1968 is given by Fennessey (1), and a more detailed comparison of a number of methods is given by Ridley (2).

Primarily because of economic considerations, work has focused on improving file searching in three areas: reducing the amount of storage required to express the spectrum, increasing the speed of the search, and improving the accuracy of identification.

In the mass spectral area, techniques such as "abbreviation" (3, 4) have reduced storage requirements by an order of magnitude without an appreciable degradation in identification reliability. More sophisticated coding schemes have further reduced the storage needed (5). Generally, decreased storage has been reflected in at least

a proportionate increase in search speeds (6). The "state of the art" is such that spectral codes of the order of 100 bits will produce reliable identifications (>90%) at effective search speeds of about 1000 spectra/sec (IBM-360/44).

It is in the area of improving the reliability of identification that much work remains to be done. Generally, most workers using file searching have developed different algorithms for measuring "goodness of fit" and tested these using a limited number of "unknowns." These algorithms are usually "fine-tuned" so that the reliability of identification improves for the unknowns and library considered.

While this approach is obviously pragmatic, it provides little theoretical framework for understanding the matching process in a quantitative manner. The purpose of this paper is to provide such a framework.

In the file searching of unknown codes against known libraries, the distribution of the mismatch criterion selected is central to the efficacy of identification. It will be shown here, first for simple coding schemes, and then for more complex matching criteria, how this distribution may be accurately estimated for any unknown code *without performing the matching*. The change in this matching distribution due to coding errors will also be considered and it will be seen that certain types of errors are more likely to cause difficulties than others.

With the theory derived here, it becomes possible for the user to quantitatively compare different techniques in terms of their potential efficacy of identification in at least a semiquantitative manner. The effects of coding errors on the identification become clearer, and the outlines of procedures to improve matching algorithms become more apparent.

FILE SEARCHING WITH ONE-BIT CODING

The use of one-bit coding provides a simple introduction to the proposed theory, and as will be seen, the concepts derived here are readily generalizable to the more complex case. Additionally, this form of coding is a practical search method in its own right (7).

In one-bit coding, a spectrum is expressed as a binary string of zeroes and ones. The transformation from the original spectrum to this binary code may be performed in many different ways. In the case of mass spectra, each bit in the coded spectrum generally represents an integral mass position. A "1" might designate a peak intensity above a threshold value, a "0" no peak above threshold (7). The "1's" in the code could also designate the positions of the N most intense peaks in the spectrum (2) or the positions of the most intense peaks in a given mass range [as in the "abbreviated" spectrum (5)].

Of course, analogous coding concepts apply for different types of chemical spectra. With infrared spectra, for example, the positions of the "1's" in the binary pattern

- (1) P. V. Fennessey, in "Mass Spectrometry: Techniques and Applications," G. W. A. Milne, Ed., Wiley-Interscience, New York, N.Y., 1971.
- (2) R. G. Ridley, in "Biomedical Applications of Mass Spectrometry," G. R. Waller, Ed., Wiley, New York, N.Y., Chap. 6, 1972.
- (3) B. A. Knock, I. C. Smith, D. W. Wright, W. Kelley, and R. G. Ridley, *Anal. Chem.*, **42**, 1516 (1970).
- (4) H. S. Hertz, R. A. Hiles, and K. Biemann, *Anal. Chem.*, **43**, 681 (1971).
- (5) S. L. Grotch, *Anal. Chem.*, **45**, 2 (1973).

- (6) S. L. Grotch, *Anal. Chem.*, **43**, 1362 (1971).
- (7) S. L. Grotch, *Anal. Chem.*, **42**, 1214 (1970).

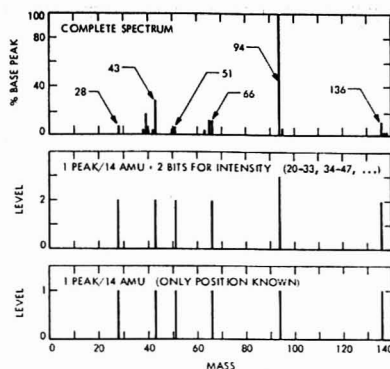


Figure 1. Spectral compression (phenyl acetate)

generally signify the location of absorption bands, such as in the ASTM or Sadtler codes (8). Obviously, other forms of sharp, resonant-like spectra (NMR, GC, etc.) will also fit naturally within this coding framework. In the following discussion, attention will be focused on low resolution mass spectra, but it should be clear that the results obtained may also be applicable to other cases. (Recent work using the ASTM infrared file has, in fact, shown that the same techniques are directly applicable in the infrared case.)

With one-bit encoding, a binary code representing a particular unknown is compared against a larger file of similar known codes using some form of "best fit" criterion. Several matching criteria for binary codes were discussed in previous work (7). Attention here is focused on the logical "exclusive or" operator (XOR). In comparing two codes in a single channel, $XOR = 0$ when the codes are the same (both "0", or both "1"), and $XOR = 1$ otherwise. In effect, when summed over all channels, this operator measures the total number of channel disagreements when two codes are compared.

In the parlance of communication theory, XOR is the "distance" between two codes. Since XOR measures mismatches, the library codes which "best" fit the unknown are those minimizing XOR. Note that the XOR operator is the equivalent of least squares when peak intensities are expressed to only two levels.

The logical "AND" operator may also be used as a matching criterion (7). If, for example, the "1's" in a code designate the positions of the N most intense peaks, those library spectra closest to a particular unknown would be those for which the sum of "1's" in AND is maximized (2).

Hybrid criteria using a linear function of XOR and AND have also been applied to the file searching of mass spectra (5, 7, 9). Tests have shown that these more complex criteria generally yield somewhat more reliable identifications than either XOR or AND alone.

To focus attention on a specific example, consider the identification of the "unknown" low resolution mass spectrum of phenyl acetate (Ref. 10, p 217). Assume that for this spectrum, only the masses of the most intense peak per 14 amu window, starting at mass 20 are encoded (e.g., window 1 covers the mass range 20-33; window 2, the

- (8) "Codes and Instructions for Wyandotte-ASTM Punched Cards Indexing Spectral Absorption Data," ASTM, Philadelphia, Pa., 1964.
- (9) F. Ertl and J. T. Clerc, *Helv. Chim. Acta*, **55**, 489 (1972).
- (10) R. M. Silverstein and G. C. Bassler, "Spectrometric Identification of Organic Compounds," 2nd ed., Wiley, New York, N.Y., 1967.

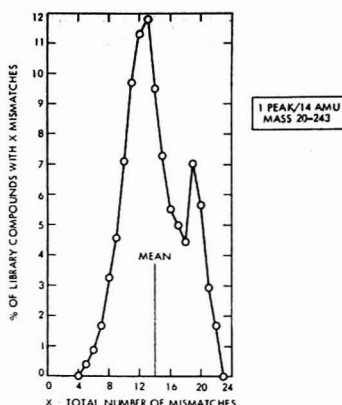


Figure 2. Matching histogram for phenyl acetate (1 peak/14 amu, mass 20-243)

range 34-47, etc.) (see Figure 1). If binary encoding using 1 bit/amu is adopted, a maximum of 1 bit in every group of 14 will be set to "1." For a binary representation of this spectrum, all bits would be coded as "0's" except for the 6 bit positions corresponding to masses 28, 43, 51, 66, 94, and 136 which would be coded as "1's". A library of 6880 known spectra (7) was also coded in the same manner covering the mass range 20-243 (16 windows each of 14 amu).

If the unknown phenyl acetate code is compared with this library, the distribution of mismatches (XOR) shown in Figure 2 is obtained. In this frequency distribution, or "matching histogram," are plotted the percentage of library spectral codes which have a given number of mismatches (X) when a specific unknown code is compared with the library. The matching histogram is analogous to the probability distribution in statistics in that the normalized area between two values of X represents the probability that a library spectrum will yield X between these limits. This distribution will, in general, be different for each unknown code and each library file of codes.

The features of this distribution are important in understanding the spectral identification problem, particularly in assessing the significance of errors leading to misidentification. Since a mismatch criterion (XOR) is used, those spectra closest to $X = 0$ are of importance in the identification. If, for example, the unknown were encoded identically to its true counterpart in the library, that match would yield $X = 0$.

In qualitative terms, as can be seen in Figure 2, relatively few codes in the library exist very close to any given code (i.e., near $X = 0$). For each code, above a certain threshold of mismatches, a very large number of library members arise with a given value X . (In Figure 2, this threshold is $X = 4$.) In terms of identification, this implies that if the number of errors between the unknown code and its true counterpart in the library lies below this threshold, then the unknown code will be correctly identified with little ambiguity. If, on the other hand, the number of errors exceeds this threshold, then the identification will be confused by the many library members which agree with the unknown code as well as or better than the correct answer.

A key, therefore, to a quantitative understanding of the matching process lies in the matching histogram. If, for

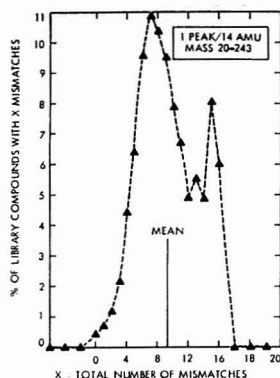


Figure 3. Matching histogram for all-zero unknown (1 peak/14 amu, mass 20-243)

any unknown, the lower threshold of this histogram can be predicted, then the number of tolerable errors before misidentification occurs can be determined, *a priori*. Using the formulation described below, it will be shown that this threshold can, in fact, be estimated, without performing the matching, given only the unknown code and some simple statistics of the library. It will be shown that a completely analogous predictive method also applies to the more general case in which peak intensities are expressed using more than two levels.

MEAN OF THE MATCHING HISTOGRAM

In order to predict the matching histogram for a particular unknown, the expected value or mean of this distribution will be calculated. For the XOR criterion, the mean is simply the average number of channels which disagree when a specified code is compared with a given library. It will be seen that this mean value is easily calculated and that the predicted value is exact. Additionally, it will be shown that the prediction of the mean is crucial to, ascertaining the final description of the histogram for any unknown in both the binary case as well as the more general case of multilevel coding.

In the comparison of a specific binary coded unknown against a specific library member, let the subscript i denote the bit position or channel in both codes. For the unknown, let v_i = value encoded in the i th channel (for binary codes, v_i = 0, 1 only). Similarly, for the library member, let l_i = value encoded in the i th channel (l_i = 0, 1). For the XOR criterion, let x_i denote the value of the XOR operator for the i th channel. (Remember that for the logical XOR, x_i = 1, if and only if l_i and v_i differ; and x_i = 0, otherwise.) Expressed arithmetically:

$$x_i = l_i + v_i - 2l_i v_i \quad (1)$$

If N bit positions (channels or mass range) are considered in establishing the disagreement criterion:

$$X_N = \sum_{i=1}^N (l_i + v_i - 2l_i v_i) \quad (2)$$

The matching histogram is defined here as the distribution of X_N when a specific unknown is compared against all members of a particular library. Let the symbols $E[X_N]$ or μ_X denote the expected value of X_N . Since the expected value of a sum is the sum of the expected values:

$$\mu_X = \sum E[l_i] + \sum E[v_i] - 2 \sum E[l_i v_i] \quad (3)$$

For a given library, $E[l_i]$ or p_i is defined as the probability of obtaining a "1" in a channel i . Since for a specific unknown code, the v_i are constants independent of the library:

$$\mu_X = \sum p_i + \sum v_i - 2 \sum p_i v_i \quad (4)$$

Note that Equation 4 is exact and requires no assumptions regarding the correlation between channels. In Equation 4, the influence of the library enters through the p_i , and the unknown through the v_i .

For a given library, the p_i are easily obtained in a one-time calculation by determining for each channel i , the number of spectra containing a "1" in that channel and dividing by the total number of spectra in the library. To compute μ_X for any unknown code over N channels, only the N -vector for the library: $p_1, p_2, p_3, \dots, p_N$ need be available.

Note that in Equation 4, the term $\sum p_i$ is a constant which is independent of the unknown and is the average number of ones encoded in the library in N channels. Similarly, $\sum v_i$ is independent of the library, and is the total number of "1's" coded in the particular unknown considered.

Equation 4 expresses the mean number of mismatches when a specific unknown code is compared against a library. Consider now this unknown to be the "average" library member and calculate the mean number of mismatches. The situation in which each member of the library is compared in turn against the remaining library was considered in earlier work (7) and the result is given by the expression:

$$\text{Mean of } X_N \text{ for the entire library} = \sum 2p_i(1 - p_i) \quad (5)$$

This expression permits one to calculate the mean number of mismatches for the "average" or typical library compound when compared with the entire library. It is, therefore, the average distance between compound codes in the library file.

APPROXIMATE SHAPE OF THE MATCHING HISTOGRAM

Although the mean of the matching distribution can be calculated exactly, the complete distribution is more difficult to estimate in general. To this end, consider as an "unknown" a binary code which contains only "0's" in all N channels. When this code is compared against the library, the distribution of XOR which is found will be identical to the distribution of "1's" coded in the library. This result follows immediately since when compared against an all-zero unknown, each library member will disagree in only those channels containing "1's."

For the library coded as described above, the resultant matching distribution for the all-zero unknown is given in Figure 3. The mean of this distribution (μ_0) is the average number of "1's" coded for the library (here, $\mu_0 = 9.3$). This follows from Equation 4 since all the $v_i = 0$, and hence $\mu_0 = \sum p_i$ or the average number of "1's" encoded in the library. Thus, for an all-zero code, the complete matching distribution may be predicted, *a priori*, exactly since it is equivalent to the known distribution of "1's" coded in the library.

Consider now what happens to the matching histogram when a single channel ($i = k$) in the all-zero unknown is changed from a "0" to a "1". If μ_0 is the mean of the matching distribution for the all-zero unknown, and μ_1 is the mean for the unknown with a single "1" in channel k , then from Equation 4:

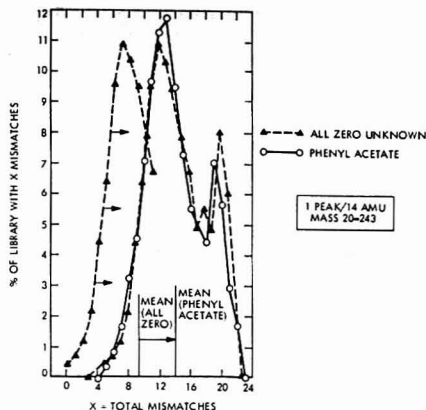


Figure 4. Matching histogram for phenyl acetate obtained by shifting all-zero unknown to match means

$$\mu_k - \mu_0 = 1 - 2p_k \quad (0 \leq p_k \leq 1) \quad (6)$$

Consider the limiting cases of $p_k = 0$ and $p_k = 1$. If $p_k = 0$, the single "1" in the unknown was added to a channel in which no library member had a "1." In this case, since every library member will now disagree in one more channel than when compared with the all-zero unknown, the matching distribution merely shifts upward by one unit along the X axis without any change in its shape. In this case, the entire matching distribution can be again predicted exactly knowing only the distribution of "1's" in the library.

Similarly, if $p_k = 1$, the "1" was added to a channel in which all library members had a "1" and, hence, when compared with the all-zero histogram, the new histogram shifts downward by one unit (again, without any change in shape).

These limiting cases suggest an approximate method for determining the complete shape of the matching histogram for any unknown.

Assume that as more and more "1's" are added to an all-zero unknown to finally yield the particular unknown code of interest, that the shape of the all-zero histogram remains unchanged, but that its mean shifts as each "1" is added. Since the mean of the matching distribution for any code may be predicted exactly from Equation 4, if only a shift occurs, the entire matching distribution may be determined by merely shifting the known all-zero histogram so that its mean matches the predicted mean for the given unknown. In effect, we have a "bootstrap" procedure which starts with a simply predicted histogram (e.g., the all-zero unknown) and evolves it by adding "1's" until the code of interest is obtained.

This procedure was followed for the distribution observed for phenyl acetate and the results are presented in Figure 4. The dashed curve is the all-zero distribution of Figure 3 shifted so that its mean matches the predicted mean for phenyl acetate, and the solid curve is the actual matching distribution observed for phenyl acetate (Figure 2). It can be seen that although the prediction is no longer exact, it is nevertheless a good approximation to the observed result.

If the above method for determining the matching histogram is valid, the implication is that all matching distributions for all codes will be the same for a given coding

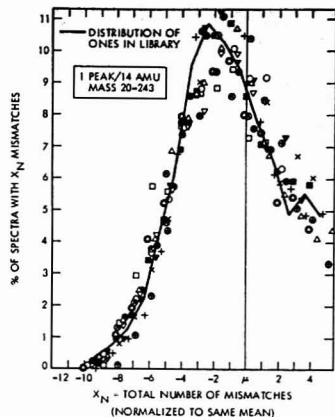


Figure 5. Distribution of mismatches for 12 different unknowns (normalized to the same mean)

scheme and library when normalized to the same mean value. This common distribution will be the known distribution of "1's" coded in the library.

To investigate this conjecture, twelve different binary codes were compared against the 6880 spectral codes in the library and the matching results are summarized in Figure 5. The solid curve is the distribution of "1's" coded in this library, and the points are observed matching distributions shifted so that the predicted mean value from Equation 4 for each unknown matches the mean value for the all-zero unknown. While the results do show some scatter, a good approximation to a single distribution is observed. It should be noted that for the codes displayed in Figure 5, the mean number of mismatches varied between 11.1 and 22.6.

The same procedure was applied to each of 125 unknown codes used in earlier studies (5) (molecular weight range 57-256, average 121) and excellent agreement was found in most cases. Additional tests using a variety of library members as "unknowns" indicate that the predictive method is widely applicable. A more quantitative comparison of these results as well as a discussion of when this procedure is likely to be accurate will be given later in this paper.

To examine the generality of these results with another binary coding procedure, calculations were also made using the coding scheme proposed by Robertson *et al.*, (11). Here the maximum intensity peak/7 amu window is encoded (rather than the 14-amu range used above). Although the distributions found in the matching were obviously different, the conclusions reached above were the same. The mean disagreements were still predicted exactly with Equation 4, and the shifting operation using the distribution of "1's" coded also yielded an excellent approximation to the observed matching behavior.

The shift in the mean, $\Delta\mu$, given by Equation 6 is a special case of a more general result involving any change in value encoded in any channel k for any binary code. Assume that the mean value for a specific code is μ and that this code is modified in a single channel k yielding a new

(11) D. H. Robertson, J. Cavagnaro, J. B. Holz, and C. Merritt, Jr., 20th Annual Conference on Mass Spectrometry and Allied Topics, Dallas, Texas, June 1972.

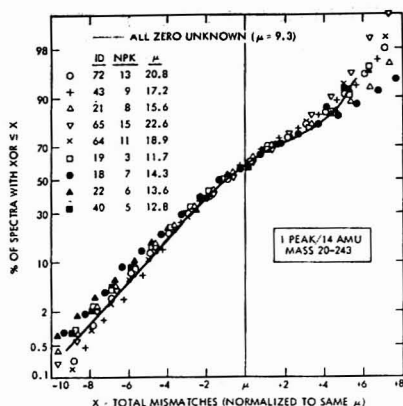


Figure 6. Cumulative distribution of disagreements (normalized to same mean)

mean μ^* . If $\Delta\mu_k$ is the change in channel k ($\Delta\mu_k = +1$ if "0" \rightarrow "1", and $\Delta\mu_k = -1$ if "1" \rightarrow "0"), from Equation 4 it follows that:

$$\mu^* - \mu = (1 - 2p_k)\Delta\mu_k \quad (7)$$

Thus, if all $p_k < 1/2$ (as is the case here), the shift in mean will be upward for any "0" to "1" change and downward for any "1" to "0" change. Therefore, in starting with an all-zero unknown and adding "1"s to generate the code of interest, if all $p_k < 1/2$, each additional "1" will produce an increase in the observed mean. Thus, in this case, the all-zero unknown will have the minimum mean value of X_N of all possible binary codes.

Note also that if all possible binary codes occur in the library, i.e., all $p_i = 1/2$, according to Equation 7, the mean will not shift as peaks are added or removed. This is, in fact, the case for in this instance, all codes give identically the same matching distribution.

THE CUMULATIVE MATCHING DISTRIBUTION

If a matching distribution such as that given in Figure 2 is integrated, the cumulative distribution of mismatches is obtained (Figure 6). Here, for a particular unknown code, the percentage (or total number) of library compounds having fewer than a specified number of mismatches is plotted vs. the number of mismatches. When normalized to the same mean, a single distribution is again observed for the unknowns presented in Figure 7. [Since the original normalized histograms (Figure 5) were nearly the same, the cumulative normalized distributions must, of course, be also the same.]

The cumulative distribution is particularly relevant for identification purposes, since it can be used directly to determine the total number of library compounds which would be expected to disagree with a particular code in fewer than a specified number of channels. With the library here, for example, 1% of the file (~70 spectra) would have a value of the disagreement criterion which is less than the mean number of mismatches minus 8.5.

In most file search procedures, the M closest library members are displayed, where M is typically of the order of 10 different compounds. If the same normalized cumulative distribution holds for all unknown codes when compared with the library, it is possible to predict the number

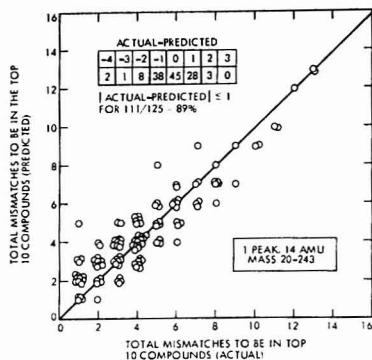


Figure 7. Mismatches to be within the top 10 compounds predicted by shifting all-zero unknown to match means (1 peak/14 amu, mass 20-243)

of mismatches which can occur before M reaches any specified value.

This has been done for $M = 10$ with the 125 different unknown codes discussed above, and the results are presented in Figure 7. Shown here are the predicted vs. actual values of the disagreement criterion for a library code to be within the top 10 compounds for a given unknown. The actual values were obtained by matching each code against the library and determining the maximum value of X_N below which there were 10 or fewer compounds in the library. The predicted value is obtained by observing in Figure 6 that for 10/6880 = 0.15% of the library, the disagreement criterion must be less than or equal to $\mu - 9.3$ to be in the top 10 compounds. In Figure 6, it can be seen that for 111 of the 125 codes examined (89%), the predicted threshold for the top 10 is within ± 1 of the actual value.

As would be anticipated from the nature of the dispersion in the data of Figure 6, the prediction of X_N to be within the top 100 compounds should be somewhat better than that for the top 10. For the top 100 case, the predicted value of X_N is within ± 1 of the actual value for 121 of the 125 codes (97%). Using this predictive method, additional tests using randomly drawn library members as "unknowns" also gave excellent agreement.

From these results, it can be seen that the lower threshold of X_N before confusion in identification occurs can be predicted with this procedure for most unknown codes. Similar results were also found using the 1 peak/7 amu encoding.

IMPLICATIONS OF RESULTS ON SPECTRAL MISIDENTIFICATION

How can these results be used to assess the effects of errors on the matching process?

Assume that binary codes are used and that for a given library and encoding method, the matching histograms for all unknown codes retain the same shape but differ only in their means as calculated from Equation 4. If this is the case, it is possible, using a cumulative distribution such as Figure 6, to determine exactly, for any code, without performing the matching, what value of the disagreement criterion X_N can be tolerated before a specified number of library members arise with values below this threshold.

If the true counterpart to the unknown spectrum ap-

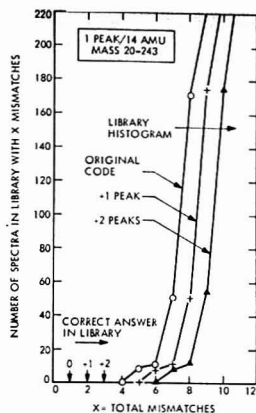


Figure 8. Effect of adding coded peaks to unknown of benzyl acetate (1 peak/14 amu)

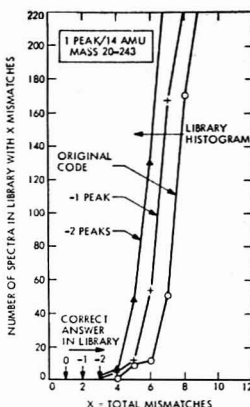


Figure 9. Effect of removing coded peaks from unknown of benzyl acetate (1 peak/14 amu)

peaks identically coded in the library, it will, of course, be found with $X_N = 0$. As spurious "1's" are added or removed (due, for example, to instrumental differences), as long as X_N remains below the predicted threshold beyond which many library codes arise, misidentification will not occur. Once this threshold is exceeded, however, a large number of library codes will fit the unknown as well as or better than the correct answer and confusion will occur in the identification.

Consider as an actual example the unknown code of benzyl acetate (Ref. 10, p 173) as peaks are added to or removed from the binary code. In this instance, the library code for benzyl acetate differs initially from that of reference 10 in a single channel and hence here, $X_N = 1$.

Assume now that an additional "1" is added to the unknown code in channel k (i.e., $v_k = 0$ becomes $v_k = 1$). When this altered code is compared with the library, the mean of the matching distribution relative to the initial unknown code will shift according to Equation 7. Since for the library considered, the values of p_k are typically <0.1 (maximum $p_k = 0.3$), the mean of the matching distribution will shift upward by approximately +1 unit. If the shape of the distribution remains unchanged, the lower threshold of X_N before confusion arises will also shift upward by one unit. In the case of benzyl acetate, the actual matching results are shown in Figure 8 and they substantiate this prediction.

Consider now what happens when this altered code is compared with its true counterpart in the library file. If the "1" is added to a channel in which the true library code had a "0", X_N will also increase by +1 for this match. If, on the other hand, the "1" were added to a channel in which the library had a "1," relative to the original unknown code, X_N would decrease by one unit. In this case, therefore, the separation between the true code and the threshold above which confusion results will either remain unchanged or increase when a "1" is added to the unknown.

If the assumptions given above are satisfied, this conclusion implies that the addition of "1's" to an unknown code should have little effect on identification since the separation between the true answer and the bulk of the library will remain substantially unchanged as "1's" are added. Naturally, the fit between the unknown and cor-

rect library answer will be poorer as spurious "1's" are added, but if the M closest fits are displayed, the correct answer will still appear in the same position in the M -best list.

This behavior was noted empirically in earlier work (7) using one-bit coded spectra where a "1" in the code designated a peak appearing above a threshold, and a "0" no peak above the threshold. It was found here that adding spurious peaks to an unknown either randomly or by the addition of impurities had relatively little effect on the identification of these codes. As in the examples shown, in these earlier cases the separation between the true answer and the bulk of the library remained essentially unchanged as spurious peaks were added.

Consider now the situation when peaks are removed from the unknown code. Here, following the same arguments as above, for each unknown peak removed, the matching histogram will shift downward by 1 unit. For the same benzyl acetate code, the actual matching results are presented in Figure 9, and the predicted downward shift is observed as peaks are removed.

When the altered code is compared with the true library code, if the "1" is removed from a channel containing a "1" in the library, X_N will increase by +1 unit. If the "1" is removed from a channel containing a "0" in the library, X_N will decrease by 1 unit. Thus, the separation between the correct answer and the threshold of misidentification will decrease by 2 units in the first instance and remain unchanged in the second. For the benzyl acetate code, the actual matching results (Figure 9) show that the separation does in fact decrease by 2 units with the removal of each peak.

If the assumption is made that the correct library code is initially identical to the unknown code, then these results imply that the removal of "1's" is more likely to have an adverse effect on identification than will the addition of "1's." If this reasoning is correct, a simple coding maxim is suggested: "When in doubt, code a peak."

It must be emphasized that the analysis presented above is predicted on several assumptions which may not always be satisfied in practice. Most important of these is that the shape of the matching histogram remains unchanged as peaks are added or removed. As can be seen in Figure 5, slight distortions do occur, particularly in the

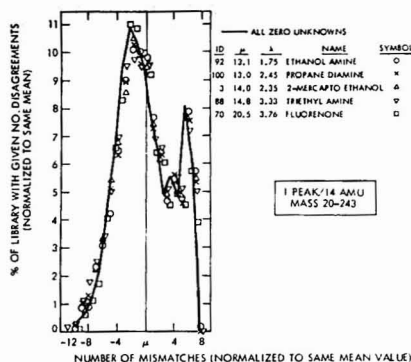


Figure 10. Shift unknowns to match means (small λ)

region of the lower threshold. A more accurate predictive method for this lower threshold may be required in certain cases.

Although the shift in the mean can be calculated exactly for all cases using Equation 7, the direction of the shift will depend upon whether $p_k < \frac{1}{2}$ or $p_k > \frac{1}{2}$ for the channels in which the "1's" are altered. In the libraries considered here, the p_k are typically close to zero. In other coding situations and with other libraries, if the p_k are close to 1, the reverse conclusions prevail. Here, a change of "0" to a "1" is more likely to cause confusion than the reverse situation.

It is interesting to speculate how these arguments might be used to select a matching criterion, *a priori*, which might be different for each code and which would tend to maintain the separation between the true answer and the bulk of the library in the presence of likely errors. Preliminary studies to this end have considered a linear mismatch criterion, disagreements minus weighted agreements, which was observed empirically to yield significantly improved identifications in earlier studies (5, 7, 9). These calculations have corroborated the empirically observed result that such a criterion is most effective when the agreements are weighted twice as heavily as the disagreements.

ESTIMATING THE ACCURACY OF THE PREDICTION PROCEDURES

While the assumption of a constant shape for the matching distribution yields a good approximation in many instances, there are situations where it may not suffice for the prediction of matching behavior. For example, it may be seen in Figure 6 that particularly near the lower threshold there is scatter in the data. Clearly, it would be useful to have a predictive method available which would indicate when these procedures are likely to be in error.

One simple technique which appears to work in practice is to consider the ratio of the third term in Equation 4 to the first two terms. Define:

$$\lambda = 100 \left[\frac{2 \sum p_i v_i}{\sum p_i + \sum v_i} \right] \quad (8)$$

Since the p_i are easily obtained for any library, and the v_i are known for any unknown code, λ may be calculated, *a priori*. λ is the normalized cross correlation between the unknown and the library.

It appears empirically for the codes examined that when λ is small ($\lambda < \sim 10$), the assumption of small distortion

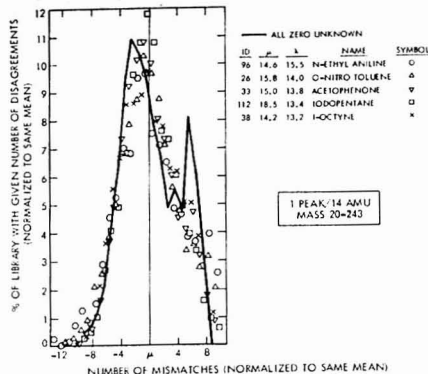


Figure 11. Shift unknowns to match means (large λ)

in the matching histogram is usually correct. When λ is large, the histogram may distort, but not necessarily. In Figure 10, for example, are presented the normalized matching histograms for five different unknowns with $\lambda < 4$, and in Figure 11, the results for five different unknowns with $\lambda > 13$. It can be seen that the results for small λ more closely fit the normalized all-zero matching distribution. However, even for large λ , in some instances, the fit is still very good.

In the prediction of the X_N to be in the top 10 compounds (Figure 7), it was found for all 42 unknown codes with $\lambda < 7$, all are predicted correctly within ± 1 unit. (When all 125 codes are considered, 14 are predicted with $X_N > \pm 1$.)

The distribution of λ for the library as a whole was determined and it was found that approximately 60% of the library codes have a value of $\lambda < 10$, and only about 10% have $\lambda > 13$. This indicates that if the unknown spectral codes are typified by the library codes, the predictive procedure described above for the matching histogram should be a good approximation in most cases.

It will be shown later in this work that the same form of λ applies in the more general multilevel situation. It will be seen that more apparent differences result between codes with large and small values of λ .

GENERALIZATION TO MULTIPLE LEVELS—PREDICTION OF THE MEAN

The results derived above will now be generalized to the situation in which peak intensities are known to more than just two levels. Again, let the subscript i be the index on channel or mass, and let l_i and v_i be the values coded in the i th channel for a particular library member and a specific unknown. The spectral codes for the N channels are thus vectors with N components (e.g., v_1, v_2, \dots, v_N for each unknown). Assume that the criterion of best fit is a non-weighted least squares. If X_N again denotes the degree of mismatch for N channels in the comparison of a particular unknown with a particular library member:

$$X_N = \sum_{i=1}^N (l_i - v_i)^2 \quad (9)$$

Once again, the library codes best fitting the unknown code are those which minimize X_N . (The minimum value $X_N = 0$, occurs only for a perfect match between unknown and library code.)

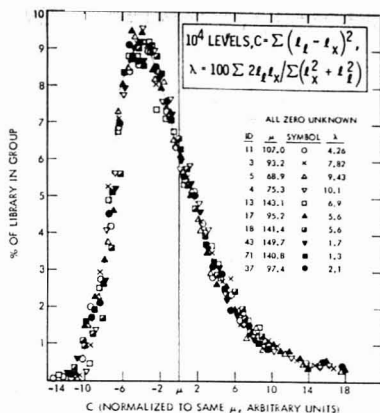


Figure 12. Matching results for 10 unknowns with small λ (10^4 levels)

Let us calculate the mean of X_N ($= \mu$) when a particular unknown is compared against the entire file. Expanding Equation 9 yields:

$$\mu_N = \Sigma E[l_i^2] + \Sigma E[v_i^2] - 2\Sigma E[l_i v_i] \quad (10)$$

For a given library over a fixed range of N channels, $\Sigma E[l_i^2]$ is a constant which is independent of the unknown code. Similarly, the term $\Sigma E[v_i^2]$ is independent of the library and only a function of the unknown. (Hence, $\Sigma E(v_i^2) = \Sigma v_i^2$). Also, since the v_i are independent of the library, the third term becomes:

$$2\Sigma E[l_i v_i] = 2\Sigma v_i E[l_i] = 2\Sigma v_i \bar{l}_i \quad (11)$$

Here, \bar{l}_i is the average level encoded for the library in the i th channel. If $\bar{l}_i^2 = E[l_i^2]$, Equation 10 can be rewritten as:

$$\mu = \Sigma \bar{l}_i^2 + \Sigma v_i^2 - 2\Sigma v_i \bar{l}_i \quad (12)$$

Note that Equation 4 derived earlier for binary codes is a special case of Equation 12. This must, of course, be the case since the XOR operator is the binary equivalent of least squares.

Given a library of codes, the terms entering in Equation 12 are easily determined in a one-time calculation. Therefore, the mean value of the square difference in levels for any unknown code can be determined exactly, *a priori*, using Equation 12.

Two methods of multilevel coding were used to corroborate Equation 12 and to further investigate the detailed matching histograms:

1. The maximum peak/14 amu window was coded as in the binary case over the mass range 20-243 but with peak intensities expressed using 4 levels or 2 bits. In earlier work (5), this form of coding was shown to be highly effective for identification purposes using an extremely compact code. In this case, in Equation 12, the l_i and v_i can assume only the values 0, 1, 2, 3.

2. The full intensity range given in the library, 0.01-100% base peak, or 10^4 levels was also used. This encoding utilizes the known library to its maximum reported dynamic range since here the v_i and l_i can assume any of 10^4 values.

When both coding procedures were used, for all "unknowns" coded appropriately, Equation 12 was found to exactly predict the mean number of mismatches which

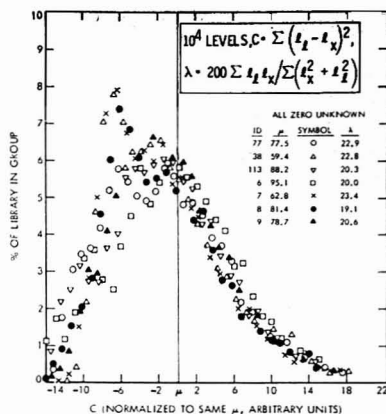


Figure 13. Matching results for 10 unknowns with large λ (10^4 levels)

were actually observed in matching. This must, of course, be the case since Equation 12 requires no assumptions regarding library correlations. In fact, since the actual mean can easily be calculated in any search procedure, Equation 12 serves as a useful check on the correctness of the computer software for a file search program.

SHAPE OF THE MATCHING HISTOGRAM FOR MULTIPLE LEVELS

By analogy with the binary case discussed earlier, all unknown codes compared against a given library should yield a universal matching distribution which is shifted only along the X_N axis with the mean calculated from Equation 12. This distribution should be identical to the distribution of levels squared for the library as a whole which is known, *a priori*.

Consider the case in which peak intensity is expressed to its full dynamic range (10^4 levels). (Peak intensities for each spectrum are normalized here in terms of % total ion current rather than the more common % base peak.) For the all-zero unknown (all $v_i = 0$), the distribution of X_N is the distribution of levels squared for the library. The distribution of intensities for mass spectra was found in earlier work (12) to be log-normal (e.g., the logarithm of the intensity is distributed normally). Thus, the matching distribution for an all-zero unknown should be log²-normal. For the library considered, the all-zero matching histogram represented by the solid line in Figure 12, is found to follow a log²-normal distribution.

The peak intensities of each of the 125 unknowns used above were coded to 10^4 levels and compared to a library of 6880 spectra using a square difference criterion. If these data are smoothed (by grouping levels of X_N) and normalized so that all means are at the same position, Figure 12 is obtained. In this figure, the solid curve is the all-zero distribution for an all-zero unknown should be log²-normal. For the library considered, the all-zero matching histogram represented by the solid line in Figure 12, is found to follow a log²-normal distribution.

(12) S. L. Grotch, Eighteenth Annual Conference on Mass Spectrometry and Allied Topics, San Francisco, Calif., June 1970.

Again, by analogy with the binary case, a semiquantitative, *a priori*, prediction can be made of the accuracy of these results. In Equation 12, the ratio of the cross product term to the sum of the first two is defined as λ :

$$\lambda = 100 \left[\frac{2\sum v_i^2}{\sum v_i^2 + \sum v_i^2} \right] \quad (13)$$

In Figure 12, all unknowns plotted have $\lambda < 11$ and the fit to the universal curve is excellent. In Figure 13, on the other hand, the unknowns were chosen with large $\lambda > 19$. Here the fit is noticeably poorer, but still acceptable in many instances.

Once again, λ can be calculated for all library members and its distribution determined. For the 6880 spectral library, this cumulative distribution indicates that approximately 60% of the spectra in this library have $\lambda < 12$. As can be seen in Figure 13, some codes with $\lambda > 15$ are well approximated by the universal distribution. As can be seen from these results, λ , as defined, is not a true quantitative measure of the applicability of these procedures. A better predictive measure is still required.

Calculations using the 1 peak/14 amu code with intensities expressed using 2 bits also agree very well with the predictions made above. The same result was also found using a completely different spectral library of 589 biologically-related compounds (also coding 1 peak/14 amu + 2 bits for intensity). Apparently, these procedures should be widely applicable to mass spectral libraries.

CONCLUSIONS

Techniques are developed to predict, *a priori*, the matching behavior of unknown codes against a library

using a least square difference criterion. It is shown that the mean square difference is *exactly* predicted for all codes using simply obtained statistical properties of the library.

The detailed matching behavior of many codes is well predicted by a common distribution shifted only in its mean value. This distribution is merely the distribution of mean squared levels for the library. The predictions of the theory were checked using a variety of codes and several different encoding procedures. A semiquantitative measure is derived permitting *a priori* estimation of when these techniques will be most accurate.

The effect of coding errors on spectral misidentification is also discussed in terms of the threshold of the matching histogram. Since this threshold can be approximately predicted, it is possible to determine the magnitude of the error which can be tolerated before misidentification is likely to occur. The theory should permit a better quantitative assessment of these errors on performance and a better optimization of reliability of these techniques.

Received for review June 15, 1973. Accepted November 16, 1973. This paper presents the results of one phase of research carried out at the Jet Propulsion Laboratory, California Institute of Technology, under Contract No. NAS 7-100 sponsored by the National Aeronautics and Space Administration. Additional support was provided by the US Army Natick Laboratories, Natick, Mass. A summary of this work was presented at the 21st Annual Conference on Mass Spectrometry and Allied Topics, San Francisco, Calif., May 1973.

Trace Determination of Beryllium Oxide in Biological Samples by Electron-Capture Gas Chromatography

George M. Frame¹ and Roddey E. Ford²

6570th Aerospace Medical Research Laboratory, Aerospace Medical Division, Air Force Systems Command, Wright-Patterson Air Force Base, Ohio 45433

William G. Scribner and Thomas Ctvrtnecek

Monsanto Research Corporation, Dayton, Ohio 45407

Two preparations of beryllium oxide labeled with ⁷Be were synthesized by calcining at 500 °C or 1600 °C. Comparative radiochemical and gas chromatographic analyses of these oxides were made using two procedures. Direct dissolution-chelation of the oxides with concentrated trifluoroacetylacetone in ampoules followed by electron-capture gas chromatography of the resultant beryllium chelate suffered from interference by a trifluoroacetylacetone reaction product. A second method employed the dissolution of the oxides in dog blood and rat liver homogenate media by a hot 75% sodium hydroxide procedure. The beryllium from the dissolved oxide was then chelated by a low temperature reaction with trifluoroacetylacetone without forming an interfering product. Subsequent gas chromatographic analysis yielded recoveries averaging 105%; standard deviation = ±7%. The samples tested were limited to the 1.0-mg BeO/ml level

by radioactivity, but the gas chromatographic base-line noise level was low enough to permit analyses of submicrogram quantities.

The toxicity of some forms of beryllium is well established (1, 2), but the mechanism of action in various biological systems is still the subject of research. Because certain beryllium compounds can cause toxic effects at trace levels in the body, analytical procedures for monitoring beryllium in biological fluids and tissues must be as sensitive as possible. Inhalation of respirable size particles

¹ Present address, 28 Highland Rd., So. Portland, Me. 04106.

² Author to whom correspondence should be addressed.

- (1) "Beryllium, Its Industrial Hygiene Aspects," H. E. Stokinger, Ed., Academic Press, New York, N.Y., 1966.
- (2) L. B. Tepper, H. L. Hardy, and R. I. Chamberlin, "Toxicity of Beryllium Compounds," Elsevier Publishing Co., New York, N.Y., 1961.

(1-5 micrometers) of beryllium oxide is especially dangerous since accumulation of some forms of this compound in the lungs can lead to the chronic form of berylliosis. The solid exhaust products of beryllium metal doped solid fuel rocket motors are largely BeO, and it would be desirable to have an analytical method capable of determining all forms of this material in biological and environmental samples.

Spencer *et al.* (3) have conducted toxicity and physicochemical studies on several forms of synthetically produced beryllium oxides. They found that the biological activity of different preparations of BeO varied greatly. Furthermore, they discovered that various motor exhaust products contain relatively large quantities of water soluble beryllium and vary in toxicity. Similar studies (4) showed that "low-fired" BeO (calcined at 500 °C) exhibited greater carcinogenic effects and more substantial translocation from the lungs to the other organs than "high-fired" BeO (calcined at 1600 °C). Nevertheless, the exhaust product from an actual beryllium rocket motor (which had physical properties more closely resembling high-fired BeO) did show sufficient tumorigenicity than translocation to warrant further attention. Therefore, an analytical method capable of trace analysis of this refractory and difficultly soluble material was desired for use in situations involving exposure to an exhaust product.

A simple and efficient method for some trace metal analyses is the gas chromatography of fluorinated beta-diketone chelates of the metal using electron-capture detection (5). This approach is especially successful with beryllium (6). It has been applied to the determination of beryllium in biological fluids and tissues (7-9) and in air samples (8, 10). A recent paper (11) describes refinements of sample preparation techniques to improve the detection limit for beryllium in a wide variety of sample media.

The possibility that this method of analysis could be applied to oxide samples without preliminary fusion or dissolution steps was raised by the observation (12) that 1,1,1,2,2,3,3-heptafluoro-7,7-dimethyl-4,6-octanedione, H(fod), could quantitatively dissolve BeO in 2 hours at 170 °C. Analytical procedures of some complexity have been published for the chelation-gas chromatography of beryllium in terrestrial, meteoric, and lunar rocks and in beryllium oxide rocket exhaust (13). Fluorinated beta-diketones have also been used for the chelation of oxides and minerals of zirconium prior to mass spectrographic analysis (14). Since high-fired BeO is a refractory ceramic ma-

terial which is impervious to mineral acids and room temperature alkaline dissolution, as well as being difficult to dissolve by ordinary fusions (13), it was surprising to find that it can be dissolved by the fluorinated beta-diketone chelating agents. This reactivity raised the possibility of developing a one-step process for the analysis of BeO employing 1,1,1-trifluoro-2,4-pentanedione, H(tfa).

Attempts to prepare accurately microgram-level samples of BeO in aqueous, blood, and tissue media by dilutions of suspensions of the accurately weighed oxide proved to be extremely difficult. The particles of oxide in the suspension tended to adsorb on the pipets and flasks which were used, and this caused substantial differences between the amounts of BeO actually present and those calculated in extensively diluted samples. To obviate this problem, ⁷Be-labeled BeO was prepared and the amount present in samples was determined by radiochemistry. This allowed monitoring the recovery of beryllium at various steps in the processes employed and permitted a direct comparison of the concentrations of Be(tfa)₂ in the chelated sample as found by radiochemistry and gas chromatography. Because of limitations in the amount of radioactivity which could be handled, such experiments could be performed only on samples which had a BeO content (10-500 micrograms) several orders of magnitude higher than the potential sensitivity of the gas chromatographic method. Hence, the work to be reported here will demonstrate how well such a method will perform on BeO-containing samples, but it does not indicate the lower level of sensitivity which might be attained without substantial modification of the technique. The verification of the accuracy of the method at lower levels might require use of carrier-free ⁷BeO which can be prepared in weighable quantities only with great difficulty.

This report describes the experiments performed to determine if both high-fired and low-fired BeO can be dissolved and chelated by trifluoroacetylacetone, and if suitable conditions could be found to make a beryllium chelate which can be determined gas chromatographically without interference. As a consequence of the unsatisfactory results of these investigations, a modified method employing a preliminary dissolution of the oxides by hot, strong base is described; analyses of samples of both high-fired and low-fired BeO at the 100-microgram level in dog blood and rat liver homogenate media are presented.

For brevity in this report, the formula ⁷BeO is used to designate oxide containing radioactive beryllium oxide.

EXPERIMENTAL

Apparatus and Chromatographic Conditions. Radiochemical gamma ray counting was done with a Nuclear Measurements well-type scintillation counter employing a US-1B well and a DS-1B scaler.

High-fired BeO was prepared in a Lucifer Furnace Inc. Model 6030-4P high temperature furnace, especially modified to contain five super Kanthal molybdenum disilicide heating elements to permit sustained operation in a normal atmosphere at 1600 °C.

Low-fired BeO was prepared in a Lindberg furnace, Type B-6.

A Varian 2100 gas chromatograph was used with a standard dc mode electron-capture detector employing a 250-millicurie titanium tritide foil ionizing source. Injections were made on the column through Supelco Teflon coated septa into 6-ft x 2-mm i.d. glass U-tubes packed with 5% SE-52 silicone gum on 60/80 mesh Gas Chrome Z (Applied Science Laboratories, Inc.). Unless otherwise specified, chromatographic conditions were: temperature: injector, 140 °C; detector, 180 °C; column, 110 °C; carrier gas (pre-purified nitrogen, J. T. Baker supplied by Matheson, Coleman and Bell) flow = 100 cm³/min.

Reagents. Chemicals used were reagent grade unless otherwise specified. All aqueous solutions were prepared with glass-distilled water. Benzene was ACS quality, thiophene free (Matheson,

- (3) H. C. Spencer, R. H. Hook, J. A. Blumenstine, S. B. McCollister, S. E. Sadek, and J. C. Jones, "Toxicological Studies on Beryllium Oxides and Beryllium-Containing Exhaust Products," *AMRL-TR-59-148* (AD 852 993), Aerospace Medical Research Laboratories, Wright-Patterson Air Force Base, Ohio, December 1958.
- (4) H. C. Spencer, S. B. McCollister, R. J. Kociba, C. G. Humiston, and G. L. Sparschu, "Toxicological Evaluation of a Beryllium Motor Rocket Exhaust Product," *AMRL-TR-72-118* (AD 756 531), Aerospace Medical Research Laboratory, Wright-Patterson Air Force Base, Ohio, December 1972.
- (5) R. W. Mosher and R. E. Sievers, "Gas Chromatography of Metal Chelates," Pergamon Press, Oxford, 1965.
- (6) W. D. Ross and R. E. Sievers, *Talanta*, **15**, 87 (1968).
- (7) M. L. Taylor, E. L. Arnold, and R. E. Sievers, *Anal. Lett.*, **1**, 735 (1968).
- (8) M. H. Noweir and J. Cholak, *Environ. Sci. Technol.*, **3**, 927 (1969).
- (9) M. L. Taylor and E. L. Arnold, *Anal. Chem.*, **43**, 1328 (1971).
- (10) W. D. Ross and R. E. Sievers, *Environ. Sci. Technol.*, **6**, 155 (1972).
- (11) G. Kaiser, E. Grallath, P. Tschopel, and G. Tolg, *Z. Anal. Chem.*, **259**, 257 (1972).
- (12) R. E. Sievers, J. W. Connolly, and W. D. Ross, *J. Gas Chromatogr.*, **5**, 241 (1967).
- (13) K. J. Eisenbraut, D. J. Griest, and R. E. Sievers, *Anal. Chem.*, **43**, 2003 (1971).
- (14) S. Tsuge, J. J. Leary, and T. L. Isenhour, *Anal. Chem.*, **45**, 198 (1973).

Coleman and Bell). Trifluoroacetylacetone, $H(tfa)$, (Pierce Chemical Co.) was distilled (bp 105.5–106.0 °C at 750-mm pressure) and stored in a Teflon bottle at -18 °C. A solution of 1% $H(tfa)$ (by volume) in benzene was prepared by dilution of this stock solution and also stored in a Teflon bottle. Beryllium trifluoroacetylacetone, $Be(tfa)_2$, was prepared by reacting 200-mesh beryllium metal powder (Alfa Inorganics, Inc.) with excess $H(tfa)$ under reflux for 15 hours. It was purified by filtration and recrystallization from benzene followed by two successive sublimations and a further recrystallization from benzene to yield a product melting at 114–114.5 °C. Glassware used with $Be(tfa)_2$ and chromatographic columns were silanized with a 10% (by volume) solution of hexamethyldisilazane in chloroform. Stock $Be(tfa)_2$ standard solutions in benzene were prepared at regular 2-week intervals by dissolving ~5-mg quantities of $Be(tfa)_2$ in 100 ml of benzene. Weighings were made on a Cahn microbalance. More dilute standards were prepared weekly or daily from this stock.

Chelation and Gas Chromatography Procedure. Direct Analysis in Ampoules. Aqueous suspensions of ^{70}Be were pipetted into ampoules (prepared as described by Taylor *et al.* (7, 9)) and dried overnight in a forced air circulation oven at 95 °C. This was required since aqueous suspensions did not react well with strong $H(tfa)$ solutions. The amount of BeO present was determined by radiochemistry. Volumes ranging from 0.025 to 0.200 ml of neat $H(tfa)$ or of 25%–50% $H(tfa)$ solutions in benzene were added, and the ampoules were heated at constant temperatures between 100 °C and 175 °C and for periods ranging from 0.33 to 17 hours. Excess unreacted $H(tfa)$ was removed by two different procedures.

In the method of choice, the ampoules were opened and their contents were washed into 25-ml volumetric flasks and made up to volume with benzene. One-milliliter aliquots of these diluted samples were shaken with 1.0 ml of 2.8% aqueous NH_4OH in a glass-stoppered centrifuge tube for 10 seconds. This was followed by brief centrifugation of the mixture and injection of 1 microliter of the benzene layer into the gas chromatograph.

In the more realistic case of much lower BeO concentrations (for which sufficiently active ^{70}Be was not available for radiochemical measurement), such dilution of the sample should be avoided. Moreover, if the NH_4OH procedure was used to analyze undiluted samples, the large amounts of unreacted $H(tfa)$ to be extracted would cause so much $NH_4(tfa)$ precipitate to form in an ammonia backwash step that the benzene layer would be inaccessible. To avoid this problem, $H(tfa)$ could be separated from $Be(tfa)_2$ when the former was present in high concentrations (even neat $H(tfa)$) by passing the sample over a column prepared using the following method. Soak Sephadex G-10 gel filtration resin (Pharmacia Fine Chemicals, Inc.) in 1.0M NaOH and allow a layer 5.0 cm high of this preparation to settle on a glass wool plug in a Pasteur pipet (diSPO, Scientific Products). Force benzene to flow through the column under pressure until a flow of about 1 ml/min occurs under gravity only. Finally, pass 0.300 ml of sample through the column thus formed, followed by three 0.300-ml washes of benzene, and inject 1 microliter of the effluent after swirling to mix well. The column can be used for four or five diluted $Be(tfa)_2$ samples but only once with a sample in neat $H(tfa)$.

Base Dissolution of BeO and Chelation. A volume of 0.2 ml of an aqueous suspension of BeO , of BeO -spiked dog blood, or of BeO -spiked rat liver homogenate was pipetted into a borosilicate glass test tube, which was cut off at the top to fit into the well counter, and the amount delivered was measured radiochemically. Six pellets (~0.6 gram) of NaOH were added, and the mixture was carefully dissolved by heating on a sand bath (250–300 °C). When the mixture became completely fluid, it was allowed to boil with swirling for exactly 2 minutes, set aside to cool on a wooden block, and just before refreezing was carefully dissolved with distilled water. It was then transferred to a 25-ml volumetric flask with subsequent washings of concentrated HNO_3 and diluted to the mark. A 5-ml aliquot of this aqueous solution was counted to check the efficiency of the dissolution step. The reaction tubes were counted and no significant radioactivity was detected.

Three 5-ml aliquots of the base dissolution preparation were placed in 1-oz narrow mouth screw-top polyethylene bottles. The solutions were neutralized with 0.5M NaOH to a phenolphthalein end point, and 2.0 ml of 0.05M Na_2EDTA and 2.0 ml of 1.0M sodium acetate-acetic acid buffer (pH 5) were added. The contents were shaken 5 minutes, heated to 95 °C in a water bath 5 minutes, and, after cooling to room temperature, 10.00 ml of 1% (by

volume) $H(tfa)$ in benzene (0.082M) was added. The mixtures were shaken on a high-speed shaker for 15 minutes. Finally, 1-ml aliquots of the benzene layer were backwashed with 2.8% NH_4OH and injected into the gas chromatograph as described previously; the $Be(tfa)_2$ content of the benzene layers was checked by radiochemical counting of a 5.00-ml aliquot. A 5.00-ml aliquot of the aqueous phase was also counted.

Gas Chromatographic Measurements. $Be(tfa)_2$ peaks appeared 1.6 minutes after injection. A series of $Be(tfa)_2$ standards was run one or more times each day, and unknowns were determined by comparing peak heights with those of standards of similar concentration. Because the response of the detector to a given concentration of $Be(tfa)_2$ tended to decrease 20–30% over the course of a day's injections, standards were injected before and after each sample chromatogram.

The minimum amount of beryllium which could be detected was 1×10^{-12} gram. This level is not due to the detector sensitivity limit but rather to interfering impurities in the benzene used. Although this caused no problem at the concentrations of $Be(tfa)_2$ encountered in the work reported here, with much lower beryllium levels found in naturally occurring samples, the substitution of "Nanograde" benzene (Mallinckrodt Chemical Works) should be considered mandatory.

Synthesis of ^{70}Be -Labeled BeO . In an attempt to parallel the procedure and conditions used by Spencer *et al.* (3), ^{70}Be -labeled $Be(OH)_2$ was prepared from solutions of 15 grams of $Be(NO_3)_2 \cdot 3H_2O$ (Fisher Purified Reagent) and 3 mCi of $^{70}BeCl_2$ (New England Nuclear) in 75 ml of distilled water by adjusting the pH to 11.5 with 10% NaOH. The filtered and washed (hot and cold water) precipitate was air-dried on a platinum dish at 42 °C. Radioactive counting of the filtrate indicated essentially quantitative precipitation.

Low-Fired ^{70}BeO . The dried $^{70}Be(OH)_2$ was calcined on the dish for 10 hours at 500 °C in a preheated Lindberg furnace and allowed to cool in the furnace for 13 hours. The oxide was then ground in an ethanol slurry with a Diamond mortar and pestle for 30 minutes, and the resulting paste was passed through a 20-micrometer sieve. The material was subjected to light microscopic examination and was reground in the same fashion until inspection showed the majority of it to be in the 1–5 micrometer (respirable) range. The particles appeared as amorphous flakes with a very rough complex surface.

High-Fired ^{70}BeO . A platinum dish containing a portion of the dried $^{70}Be(OH)_2$ was placed in the preheated Lindberg furnace, and the material was calcined for 1 hour at 500 °C. The oxide thus formed was removed, cooled, transferred to an alumina crucible, and placed in the Lucifer furnace at 482 °C. The temperature was raised to 1582 °C, and the oxide was allowed to reside for 10 hours at a temperature between 1580 °C and 1590 °C. The oxide was sieved and ground as described above. Because it was much more resistant than the low-fired oxide, in some instances it was necessary to resort to a Stoke's law gravity separation in a column of ethanol to obtain a product of the desired 1–5 micrometer size range. Under the light microscope, the particles appeared compact and highly crystalline with a surface exhibiting a glass-like fracture which was entirely different from the low-fired preparation.

These preparations were repeated as necessary during the course of the investigation to provide samples at the desired specific activity level.

Preparation of Blood and Tissue. *Blood.* Whole blood drawn from beagle dogs, using a syringe which contained Na_2EDTA to prevent coagulation, was stored in a refrigerator until used. It was spiked with ^{70}BeO by addition of several drops of a concentrated aqueous suspension of the radioactive oxide.

Liver Homogenate. Three sections (~1 gram) of liver from a freshly killed white laboratory rat (male Wistar strain) were homogenized in a hand-held Ten Broeck homogenizer using 1.3 ml of 1.0M sodium acetate and 0.2 ml of saturated Na_2EDTA for every 500 mg of liver. Stock suspensions of these combined homogenates were stored in a refrigerator until used, and ^{70}BeO -spiked samples were prepared in the same manner as that previously described for blood.

RESULTS AND DISCUSSION

Dissolution of ^{70}BeO by $H(tfa)$. Since high-fired BeO is the more difficultly soluble form of the oxide, samples of high-fired ^{70}BeO (approximately 1 mg) were placed in ampoules, and amounts ranging from 0.05 to 0.2 ml of neat

Table I. Recovery of High-Fired ^{70}BeO Suspension in Dog Blood

Sample No.	$\mu\text{g } ^{70}\text{BeO per ml benzene extract}$		% Recovery, GC vs R	% Recovery of method ^d
	R ^b	GC ^c		
1 ^a				
A	1.79	1.92	107	112
B	1.73	1.94	112	113
C	1.79	1.73	97	101
2				
A	2.22	2.21	99	103
B	2.15	2.11	98	98
C	2.27	2.01	89	94
3				
A	1.54	1.64	106	ND ^e
B	1.57	1.68	107	ND
C	1.57	1.41	90	ND
4				
A	1.63	1.59	98	101
B	1.59	1.41	89	89
C	1.58	1.59	101	101
5				
A	2.08	2.06	99	97
B	2.08	2.08	100	98
C	2.06	2.03	99	96
		Mean	99.4	100.2
		SD ^f	6.7	6.8

^a A, B, and C are 5-ml aliquots of the same suspension of ^{70}BeO . ^b Radiochemical value. ^c Gas chromatographic value. ^d Based on radiochemical measurement of the prepared oxide suspension vs. the gas chromatographic measurement of the analyzed sample. ^e Not done. ^f Standard deviation.

Table II. Recovery of High-Fired ^{70}BeO Suspension in Rat Liver Homogenate

Sample No.	$\mu\text{g } ^{70}\text{BeO per ml Benzene extract}$		% Recovery GC vs. R	% Recovery of method ^d
	R ^b	GC ^c		
1 ^a				
A	4.39	4.42	101	99
B	4.42	4.40	100	99
C	4.30	4.54	106	102
2				
A	4.08	4.50	110	109
B	4.09	4.56	112	111
C	4.12	4.84	118	118
3				
A	4.11	4.59	112	110
B	4.18	4.50	108	108
C	4.06	4.23	104	101
4				
A	2.12	2.24	106	90
B	2.10	2.25	107	90
C	2.11	2.38	113	95
5				
A	3.13	3.44	110	126
B	3.12	3.30	106	121
C	3.14	3.42	109	125
		Mean	108.1	106.9
		SD ^f	4.7	11.8

^a A, B, and C are 5-ml aliquots of the same suspension of ^{70}BeO . ^b Radiochemical value. ^c Gas chromatographic value. ^d Based on radiochemical measurement of the prepared oxide suspension vs. the gas chromatographic measurement of the analyzed sample. ^e Not done. ^f Standard deviation.

H(tfa) were added. The ampoules were then flame-sealed and placed in the counter for determination of ^{70}BeO . After being heated in an oven for periods ranging from 0.5 to 16 hours and over constant temperatures ranging from 100 °C to 175 °C, the ampoules were cooled, opened, and centrifuged for 5 minutes. The liquid phase was pipetted into a counting vial; this was followed by three successive washings with benzene and centrifugations of the remaining slurry. The ampoules and the liquid phases were counted, and the percentages of the original beryllium level in each were calculated. Recoveries ranging from 5% to 81% were observed in the liquid fraction for temperatures below 150 °C or for times less than 4 hours. For heating periods of 16 hours at temperatures of 150 °C and 175 °C, the dissolution recovery as determined radiochemically was between 99.5% and 99.8% in all cases.

To verify that the beryllium from the dissolved oxide was present as $\text{Be}(\text{tfa})_2$, samples of high-fired ^{70}BeO were placed in ampoules and treated in the same manner as those described previously in this section. (They were heated in an oven for 16 hours at a temperature of 175 °C.) When the products of these preparations were analyzed by gas chromatography, they exhibited the same gas chromatographic properties as the products formed synthetically from beryllium and H(tfa). This indicated that the beryllium from the dissolved oxide was, in fact, present as $\text{Be}(\text{tfa})_2$.

The two methods of extraction of excess H(tfa) were performed and compared. The per cent recoveries of the chromatographic analysis vs. the radiochemical determinations indicated that chelation was essentially complete when the NH_4OH method was used. The recoveries of the Sephadex-column method reflected losses occurring during the use of that technique. Nevertheless, if the use of an undiluted sample containing a high H(tfa) concentration had been required, only the column extraction would have been practical.

Interference of H(tfa) Reaction Product. When high concentrations of H(tfa) were heated in ampoules at the high temperatures and long times required to effect the complete chelation of high-fired ^{70}BeO , a gas chromatographic peak with a retention time of about 10 seconds less than that of $\text{Be}(\text{tfa})_2$ was formed. That this was a product of some reaction of H(tfa) not involving beryllium was indicated by heating H(tfa) in the absence of beryllium in the ampoules and observing that the amount of interference peak formed was proportional to the amount and concentration of H(tfa) present, and to the length and temperature of heating. The peak was not removed by backwashing with NH_4OH nor by passing the benzene phase over the Sephadex-base column. At the levels desired for detection of BeO by gas chromatography, the amount of interference peak present would obscure the $\text{Be}(\text{tfa})_2$ peak even though it posed no problem in the measurements just described. Measurement of $\text{Be}(\text{tfa})_2$ peaks could be improved by operating the GC column at 95 °C to separate the interference peak when both were present at nearly equal detector response concentrations.

To determine if less severe chelation conditions could be found which would still allow quantitative formation of $\text{Be}(\text{tfa})_2$ without excessive formation of the interfering peak, several chelations were performed on samples (2–10 micrograms) of both low-fired and high-fired ^{70}BeO in ampoules. The time of heating, the temperature of heating, the concentration of H(tfa), and total amount of H(tfa) were varied. Although it was possible to observe 50%–90% chelation of the low-fired ^{70}BeO with temperatures as low as 135 °C and times as short as 3 hours using neat H(tfa) or concentrations as low as 25% H(tfa) in benzene, the recoveries were irreproducible and the interference peak was significant. It was not possible to remove or inhibit the formation of this interference to levels below which it would not affect the measurement of trace (10^{-6} – 10^{-9} gram) levels of either form of the oxide. Therefore, it be-

Table III. Recovery of Low-Fired ⁷BeO Suspension in Dog Blood

Sample No.	$\mu\text{g } ^7\text{BeO per ml benzene extract}$		% Recovery GC vs. R	% Recovery of method ^d
	R ^b	GC ^c		
1 ^a				
A	3.69	4.11	111	113
B	3.61	4.26	118	117
C	3.69	3.92	106	108
2				
A	6.18	6.66	106	108
B	6.41	6.45	101	107
C	6.20	6.50	105	107
3				
A	2.24	2.31	103	110
B	2.11	2.32	110	110
C	2.15	2.41	112	114
4				
A	9.97	10.05	101	103
B	9.81	10.52	107	108
C	9.91	10.17	103	104
5				
A	8.52	9.05	106	108
B	8.57	8.87	104	106
C	8.42	7.95	94	95
		Mean	105.8	107.9
		SD ^e	5.6	5.1

^a A, B, and C are 5-ml aliquots of the same suspension of BeO. ^b Radiochemical value. ^c Gas chromatographic value. ^d Based on radiochemical measurement of the prepared oxide suspension vs. the gas chromatographic measurement of the analyzed sample. ^e Standard deviation.

came necessary to consider preparatory dissolution of the oxide so that the milder chelation conditions could be employed.

Base Dissolution of BeO in Blood and Tissue Media. Eisenbraut *et al.* (13) have described a procedure for the chelation-gas chromatography of rocket exhaust product (essentially high-fired BeO). This employed dissolution of the oxide in boiling 75% NaOH, and proved to be effective for ~30 and ~2500-ppm levels of the oxide dispersed in soil. It was decided to apply a very similar procedure (as outlined in the Experimental section) as the first step in the determination of either high-fired or low-fired BeO in blood and tissue. Whole blood and rat liver homogenates were spiked with suspensions of both high-fired and low-fired ⁷BeO at levels of about 1 mg/ml. Such large quantities of the oxide allowed the radiochemical measurement of the amounts of ⁷Be present in various fractions and aliquots of the successive reaction steps. The final benzene extracts that were analyzed for beryllium by gas chromatography contained levels of 1–15 $\mu\text{g } ^7\text{BeO/ml}$. Results are reported as the mean of at least three replicate injections of a sample referenced to the nearest injected standards. The standard deviation of replicate injections of the same sample at a given time was $\pm 5\%$. The results for the four combinations of the two types of ⁷BeO and two biological media tested are presented in Tables I–IV. In each series, five suspensions of differing ⁷BeO content were prepared, and the base dissolution procedure was applied. The efficiency of the dissolution step was greater than 95% in almost every case. Furthermore, in the majority of cases, the extraction step was greater than 98% complete.

The concentrations of Be(tfa)₂ in the benzene layer as determined by both radiochemistry and gas chromatography were compared on a double blind basis (columns two and three). The per cent recoveries of the gas chromatographic method were calculated relative to both the radiochemical measurement of the benzene extract (column

Table IV. Recovery of Low-Fired ⁷BeO Suspension in Rat Liver Homogenate

Sample No.	$\mu\text{g } ^7\text{BeO per ml benzene extract}$		% Recovery GC vs. R	% Recovery of method ^d
	R ^b	GC ^c		
1 ^a				
A	6.84	7.43	109	109
B	6.74	6.91	103	101
C	6.79	7.03	104	103
2				
A	7.24	7.67	106	104
B	7.34	7.67	105	104
C	7.34	7.65	104	104
3				
A	15.0	15.1	101	101
B	14.9	14.8	99	99
C	14.9	14.7	99	98
4				
A	5.02	5.30	106	114
B	5.22	5.41	104	116
C	4.83	5.00	104	107
5				
A	8.91	9.26	104	107
B	8.78	9.06	103	105
C	8.85	8.51	96	98
		Mean	103.1	104.7
		SD ^e	3.2	5.3

^a A, B, and C are 5-ml aliquots of the same suspension of BeO. ^b Radiochemical value. ^c Gas chromatographic value. ^d Based on radiochemical measurement of the prepared oxide suspension vs. the gas chromatographic measurement of the analyzed sample. ^e Standard deviation.

four) and the amount of oxide originally present in the suspensions (column five). The mean recoveries and standard deviations in each series do not differ significantly for either calculation. This implies that, within the precision of the overall method, the tendency for somewhat high mean recoveries is due to some small systematic error in the chelation-gas chromatography portion of the procedure. The source of this error is uncertain. An analysis of variance of these recovery data indicated that neither sample media nor firing mode of BeO had any significant effect (95% confidence level) on the relative error of the method within the range of concentrations studied. During the neutralization steps subsequent to the base dissolution, incompletely digested tissue matter and a precipitate identified as silicic acid (by emission spectrographic analysis detecting silicon as the major constituent) were present in the diluted solutions. At the BeO levels employed in this work, these constituted no interference.

None of the gas chromatograms showed evidence of any interfering peaks either from the base dissolution of the blood and tissue or from the chelation reaction performed on the products of the dissolution. Since every chromatogram in these series had an extremely clean base line, the analysis can be applied to much smaller quantities of BeO than were tested in these experiments (which were limited by ⁷BeO radioactivity levels). The completeness of the recovery of both high-fired and low-fired ⁷BeO from these representative biological fluids and tissues demonstrates that this procedure will detect and accurately measure the beryllium oxides (and presumably also any more soluble forms of beryllium) present in a biological sample. If an alternate chelation-gas chromatographic procedure (7, 9, 11), which does not employ preparatory dissolution steps sufficiently severe to solubilize BeO, is used to determine the amount of soluble beryllium present in the same sample, it would be possible to measure BeO as the difference between the two values.

ACKNOWLEDGMENT

The authors gratefully acknowledge the assistance of Kent J. Eisentraut for providing additional details and advice concerning the base dissolution of BeO and of Michael L. Taylor for advice on the construction of the Sephadex-base column for removing H(tfa).

Received for review July 20, 1973. Accepted November 12, 1973. The research reported in this paper was conducted in part by personnel of the Aerospace Medical Research Laboratory, Aerospace Medical Division, Air Force Sys-

tems Command, Wright-Patterson Air Force Base, Ohio, and in part by personnel of Monsanto Research Corporation, Dayton, Ohio, under Contract No. F33615-71-C-1794. This work was supported in part by the National Institute of Occupational Safety and Health, Division of Toxicology and Pathology, Cincinnati, Ohio. The experiments reported herein were conducted according to the "Guide for the Care and Use of Laboratory Animals," DHEW 73-23. This is the same material as in AMRL-TR-72-72. Further reproduction is authorized to satisfy the needs of the U.S. Government.

High Pressure Liquid Chromatographic Determination of Tetracyclines

Kiyoshi Tsuji, J. H. Robertson, and W. F. Beyer

Control Analytical Research and Development, The Upjohn Company, Kalamazoo, Mich. 49001

A high pressure liquid chromatographic method for the determination of tetracycline is described. The method requires no derivatization or gradient elution, and it can separate tetracycline (TC), anhydrotetracycline (ATC), 4-*epi*-tetracycline (ETC), 4-*epi*-anhydrotetracycline (EATC), chlorotetracycline (CTC), and doxycycline in less than 30 minutes. A 1-meter column packed with ZIPAX, HCP was used with a mobile phase of 13% methanol in 0.02M sodium phosphate, dibasic and 0.01M phosphoric acid at pH 2.5 at a flow rate of 0.85 ml/min (1,000 psi). The relative standard deviation of the method is 1.02% and the method is sensitive to approximately 10 nanograms TC per sample injected.

Many analytical methodologies have been reported for the determination of tetracycline (1-12), the latest being the gas liquid chromatographic (GLC) method of Tsuji and Robertson (13). The GLC method, however, requires derivatization of tetracyclines with trimethylsilyl reagents and the derivatization process, under certain conditions, forms degradation compounds of TC. The sensitivity for ATC, ETC, and EATC by the thin-layer chromatographic

method is low (1), and the diatomaceous earth column "classical" liquid chromatographic method (DECLC) is time consuming (12). The application of high-pressure liquid chromatography (HPLC) to the analysis of TC is preferred over other analytical methods because of its high speed and superior sensitivity.

EXPERIMENTAL

Apparatus. A Laboratory Data Control (LDC, Riviera Beach, Fla.) modular liquid chromatograph equipped with a 280-nm UV monitor (Model 1285), a Milton Roy Minipump (LDC), and a pulse dampener (Model 709) was used.

An empty duPont stainless steel column, 2.1×1000 mm, was treated as follows. The column was first rinsed with tetrahydrofuran followed by vigorous scraping of the inside of the tubing with a cotton string pre-soaked with tetrahydrofuran to remove loose metal particles. Chloroform was then drawn through the column by vacuum and the column was dried by a stream of dry nitrogen. The column was then conditioned by soaking overnight in 0.1M ethylenediaminetetraacetic acid (EDTA) solution. The column was rinsed with double-distilled water followed by absolute methanol and dried. Stainless steel frits of 2- and 10- μ m pore size were degassed by vacuum and soaked in 0.1M EDTA overnight.

The 10- μ m frit thus treated was fitted into the inlet end of the column, and a hex nut (duPont, No. 820349) with stainless steel front and back lock ferrules and cap (duPont, No. 201724) was attached to the column. Zipax-hydrocarbon polymer (HCP, duPont) was dry packed into the open end of the column by adding a small amount of HCP at a time and lightly tapping on the floor. After the column was tightly packed, an EDTA pre-treated 2- μ m pore size frit was inserted into the outlet end of the column.

The column thus packed was attached to a duPont injector port and to the 280-nm UV monitor. The column was then conditioned by first pumping 0.1M EDTA solution for approximately 4 hours prior to the mobile phase.

The theoretical plates of the column thus prepared were 900 per meter for the TC peak.

Reagents. Mobile Phase. A 13% Methanol and 0.001M EDTA in 0.01M phosphoric acid and 0.02M dibasic sodium phosphate at pH 2.5 or B. 3% Acetonitrile in 0.001M EDTA and 0.01M phosphoric acid and 0.02M dibasic sodium phosphate at pH 2.5 were used. Depending upon the performance of the column, either A or B mobile phase may be used to obtain the maximum separation of tetracyclines.

Internal Standard Solution. Approximately 70 ml of anhy-

- (1) P. P. Ascione, J. B. Zagar, and G. P. Chrekian, *J. Pharm. Sci.*, **56**, 1393 (1967).
- (2) I. C. Kiykhuis and M. R. Brommet, *J. Pharm. Sci.*, **59**, 558 (1970).
- (3) A. A. Fernandez, V. T. Noceda, and E. S. Carrera, *J. Pharm. Sci.*, **58**, 443 (1969).
- (4) P. B. Lloyd and C. C. Cornford, *J. Chromatogr.*, **53**, 403 (1970).
- (5) Y. Nishimoto, E. Tsuchida, and S. Toyoshima, *J. Pharm. Soc. (Jap.)*, **87**, 516 (1967).
- (6) D. L. Simmons, R. J. Ranz, H. S. L. Woo, and P. Picotte, *J. Chromatogr.*, **43**, 141 (1969).
- (7) A. Sina, M. K. Youssef, A. A. Kassem, and I. A. Attia, *J. Pharm. Sci.*, **60**, 1544 (1971).
- (8) B. W. Griffiths, R. Brunet, and L. Greenberg, *Can. J. Pharm. Sci.*, **5**, 101 (1970).
- (9) P. P. Ascione and G. P. Chrekian, *J. Pharm. Sci.*, **59**, 1480 (1970).
- (10) P. P. Ascione, J. B. Zagar, and G. P. Chrekian, *J. Pharm. Sci.*, **56**, 1396 (1967).
- (11) W. W. Fike and N. W. Brake, *J. Pharm. Sci.*, **61**, 615 (1972).
- (12) B. G. Kelly, *J. Pharm. Sci.*, **53**, 1551 (1964).
- (13) K. Tsuji and J. H. Robertson, *Anal. Chem.*, **45**, 2136 (1973).

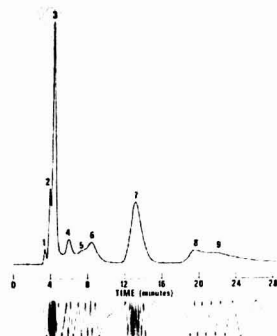


Figure 1. High-pressure liquid chromatography of tetracyclines using a 1-meter HCP column at 0.45 ml/min (500 psi) at room temperature. Mobile phase: 13% methanol and 0.001M EDTA in 0.02M phosphoric acid and 0.02M dibasic sodium phosphate, pH 2.5

(1) Injection, (2) 4-epi-tetracycline, (3) tetracycline, (4) chlorotetracycline, (5) impurity in doxycycline, (6) doxycycline, (7) internal standard (prednisolone), (8) 4-epi-anhydrotetracycline, (9) anhydrotetracycline

drous methanol was added to a 250-ml graduated cylinder containing a) 250 mg prednisolone, or b) 125 mg of 4-(*N*-butylamino)-benzoic acid (Aldrich Chemical Co., Milwaukee, Wis.), stoppered and shaken to dissolve. The mobile phase was then added to the volume. The internal standard solution (a) was used with mobile phase A and (b) for B.

Preparation of TC Standard. Tetracycline hydrochloride U.S.P. Reference Standard, Issue H was dried at 60 °C under <5 mm Hg vacuum for three hours. After drying, approximately 4 mg of the reference standard was accurately weighed using a Cahn Electrobalance, Model G (Cahn Instrument Corp., Paramount, Calif.) and placed in a 10-ml volumetric flask.

Procedure. Preparation of Sample. Approximately 4 mg of TC sample was accurately weighed into a 10-ml volumetric flask.

Just prior to the analysis, each standard and sample was diluted to volume with the internal standard solution. Since the epimerization of TC takes place in solution, each sample was dissolved just prior to analysis.

After injection of approximately 1.5 μ l of the TC sample into the column, the syringe was cleaned by first rinsing in 0.1M EDTA solution, followed by rinses with water, 95% methanol, and finally acetone. The syringe was then dried under vacuum. New syringes prior to use should be treated in 0.1M EDTA solution for approximately one hour followed by rinsing in water, methanol, and acetone.

Chromatographic Conditions. Mobile phase flow rate, 0.85 ml/min; column pressure, about 1000 psi; column temperature, about 25 °C; chart speed, 0.25 inch/min with Ball and Disc integrator attachment.

Calculations. Measure the area under the peaks of TC, ATC, ETC, and EATC. The biological equivalence of tetracycline content in μ g per mg sample is calculated using the formula:

$$[Ra/Rs] \times [Ws/Wt] \times F$$

where $Ra = \{[(\text{Area of TC}) + 0.27 (\text{Area of ETC}) + 0.43 (\text{Area of ATC}) + 0.18 (\text{Area of EATC})] \text{ of sample} / [\text{Area of internal standard}]$; $R_s = \text{Area of the standard TC peak} / \text{area of internal standard}$; $W_s = \text{Weight of reference standard in mg}$; $W_t = \text{Weight of sample powder in mg}$; and $F = \text{Assigned value of TC reference standard in } \mu\text{g/mg}$.

RESULTS AND DISCUSSION

Since TC readily forms a complex with metals (14), treatment of the stainless steel column and the sample injection syringe with an EDTA solution is essential to minimize tailing of the TC peak. The incorporation of 0.001M EDTA in the mobile phase after the EDTA column treat-

(14) E. D. Weinberg, *J. Inf. Dis.*, **95**, 291 (1954).

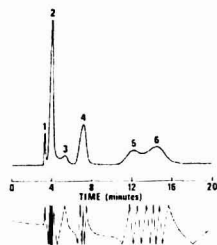


Figure 2. High-pressure liquid chromatography of tetracyclines using a 1-meter HCP column at 0.80 ml/min (1000 psi) at room temperature. Mobile phase: 3% acetonitrile and 0.001M EDTA in pH 4.5, 0.05M phosphate buffer.

(1) Injection, (2) 4-epi-tetracycline and tetracycline, (3) chlorotetracycline, (4) internal standard (4-*N*-butylamino-benzoic acid), (5) 4-epi-anhydrotetracycline, (6) anhydrotetracycline

ment did not affect the TC peak shape; however, this reagent in the mobile phase minimized tailing of some of the TC samples with high mineral content. Concentrations higher than 0.001M EDTA in the mobile phase interfered with the analysis due to the high UV absorption of this solution.

Prednisolone, selected as the internal standard, did not interfere with the tetracycline peaks (Figure 1). Prednisolone elutes after the doxycycline but before the EATC peaks. However, 4-(*N*-butylamino)-benzoic acid is less satisfactory as an internal standard because of its interference with the CTC peak.

Separation of Tetracyclines. As may be seen in Figure 1, TC, CTC, and doxycycline peaks are well separated without the use of a gradient elution; however, the separation of ETC from TC and ATC from EATC was less satisfactory. Demethylchlortetracycline eluted right after the TC peak and pyrrolidinomethyl tetracycline eluted after demethylchlortetracycline but before the CTC peak.

The retention time of TC peaks is a function of the methanol concentration in the mobile phase. The retention time of the TC peak, for example, is 9.7 minutes with a mobile phase containing 4% methanol, 6.2 minutes with 10% methanol, and 5.1 minutes with 13% methanol at a constant flow of 0.45 ml/min.

The OTC and ETC peaks may not be effectively separated by a mobile phase containing 13% methanol. When separation of OTC from ETC is of primary concern, the separation may be accomplished by a mobile phase containing less than 2% methanol. Under such conditions, however, a gradient elution with gradual increase in methanol concentration is required to satisfactorily elute ATC and EATC.

A ZIPAX ODS and a C_{18} Corasil column were also examined; however, no separation of TC from ETC nor ATC from EATC was obtained.

The pH of the mobile phase significantly affects separation of ETC from TC. Although ETC was separated from TC with the pH 2.5 mobile phase (Figure 1), no separation of ETC from TC by a HCP column was obtained when a 13% methanol-containing phosphate buffer of pH 4.5 or above was used as the mobile phase. A mobile phase containing 3% acetonitrile and 0.001M EDTA in 0.05M phosphate buffer of pH 4.5 was examined. As may be seen in Figure 2, ATC and EATC were separated in 16 minutes; however, ETC was not separated from TC. Use of pH 2.5 phosphoric acid buffer with acetonitrile helped to separate ETC from TC. The HCP column deteriorated significantly when acetonitrile was used as the mobile

Table I. Composition of the U.S.P. TC Reference Standard

	Percentage of			
	TC	ETC	ATC	EATC
HPLC ^a	99.8	0.2	<0.05	<0.05
DECLC ^b	97.2	2.8	<0.5	<0.5
GLC ^c	95.8	3.0	1.2	<0.5

^a High Pressure Liquid Chromatography. ^b Diatomaceous Earth Column "Classical" Liquid Chromatography. ^c Gas Liquid Chromatography.

Table II. Epimerization of Tetracycline in the Internal Standard Solution, pH 2.5

Time, hr	Percentage of	
	TC	ETC
0	99.8	0.2
0.33	99.3	0.7
2	98.3	1.7
3.6	97.5	2.5
26	82.3	7.7
48	75.2	24.8
54	73.2	26.8

$$y = -0.003x + 1.996$$

phase. However, when the column was rinsed with the mobile phase A and kept in the solution when not in use, the column life was significantly improved.

Separation and Quantitation of ETC and ATC in TC. As may be seen in Table I, the analysis of the U.S.P. TC reference standard, Issue H, by high-pressure liquid chromatography (HPLC) showed only 0.2% ETC and 99.8% TC with no detectable quantity (less than 0.05%) of ATC, EATC, or CTC. On the other hand, analyses by the diatomaceous earth column "classical" liquid chromatography (DECLC) (10) and by the GLC method showed that the TC sample contained 2.8% and 3.0% ETC, respectively. Fike and Brake (11) detected 1.9, 0.1, and 0.03% of ETC, ATC, and EATC, respectively, in the U.S.P. TC Reference Standard using a modified DECLC method.

To elucidate the cause of the discrepancy, the U.S.P. TC Reference Standard containing 0, 5, 10, 20, and 100% of the ammonium salt of 4-*epi*-tetracycline monohydrate 5897-WM-66 (80% pure with 5.5% TC) were prepared and analyzed. The HPLC results showed good linearity with a correlation coefficient of 0.9996 between the amount of ETC added and the ETC recovered with a linear equation of $y = 1.05x - 0.869$. The minimum detection of the HPLC method for ETC is calculated at 0.83%, an x value at $y = 0$. Therefore, it appears that the discrepancy of the ETC value in the U.S.P. TC Reference Standard is not due to the insensitivity of the HPLC method, but rather to the epimerization of TC by the DECLC and the GLC methods.

The epimerization of TC in the internal standard solution was also examined. The U.S.P. TC Reference Standard was dissolved in the internal standard solution and was analyzed after 0, 0.33, 2, 5, 24, and 48 hours (Table II). When the logarithm of TC concentration remaining was plotted against time, a straight line ($y = 0.003x + 1.996$) was obtained. Chromatography of TC by the DECLC method required approximately three hours, but only about six minutes by the HPLC method. From the data obtained, only 0.06% ETC would form during the six minutes required for the chromatography; this concentration is below the calculated detection limit of the method. Epimerization of TC was reported to occur in a variety of

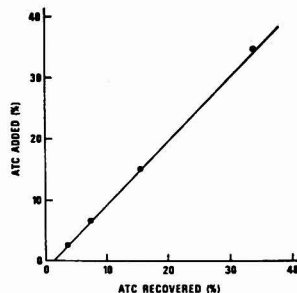


Figure 3. Correlation between the ATC added and the ATC recovered by high-pressure liquid chromatography

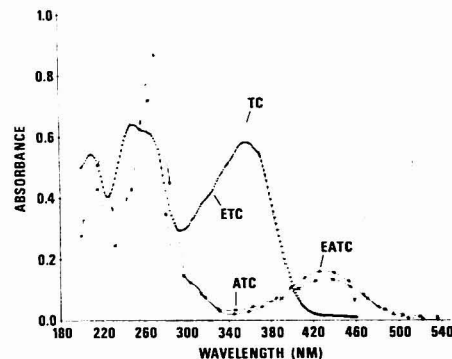


Figure 4. Computer plotted absorption spectra of tetracycline, 4-*epi*-tetracycline, anhydrotetracycline, and 4-*epi*-anhydrotetracycline

solvent systems within the pH range of two to six, and the rate is increased by the presence of certain anions, e.g., phosphate (15). Since the epimerization of TC does take place in the internal standard solution, it is imperative that the TC sample be dissolved just prior to the analysis.

Since ATC takes a long time to elute and would, therefore, be the most difficult to detect and quantitate by HPLC, ATC was added to the U.S.P. TC reference standard at 5, 10, and 20%. For comparative purposes, samples of TC containing 20, 40, and 60% ATC were prepared and analyzed by the DECLC and GLC methods. Results of the analysis indicate (Figure 3) that the HPLC showed good linearity for the detection of ATC (correlation coefficient 0.992) with a linear equation of $y = 1.00x - 0.88$, while $y = 1.04x - 2.71$ and $y = 1.10x - 0.69$ were obtained by the GLC and DECLC methods. Statistical analysis of the slopes of the three methods showed no significant difference, although the DECLC method showed a slight positive bias for ATC. The calculated intercept value for ATC, (x value at $y = 0$) by the HPLC (0.88) and DECLC (0.63) showed no significant difference. However, the calculated intercept by the GLC method (2.61) was significantly higher than that obtained by HPLC or DECLC, suggesting degradation of TC.

- (15) J. R. D. McCormick, S. M. Fox, L. L. Smith, B. A. Bitler, J. Reichenthal, V. E. Origeni, W. H. Muller, R. Winterbottom, and A. P. Doerschuk, *J. Amer. Chem. Soc.* **79**, 2849 (1957).

Table III. Precision of the Tetracycline Determination by High-Pressure Liquid Chromatography

Weight of tetracycline, mg/ml	Area of		Area weight ratio
	Tetracycline	Internal standard	
0.4117	208.7	236.6	0.2143
0.4025	203.1	234.7	0.2150
0.3974	203.0	237.5	0.2151
0.3926	191.7	225.5	0.2165
0.3912	202.0	233.2	0.2214
0.4008	206.5	237.5	0.2169
0.3984	200.0	236.1	0.2126
0.3988	203.5	235.0	0.2171
		Rel stand dev	1.02%

For the determination of TC and its degradation compounds by HPLC, a 280-nm monitor was used. As shown in a computer plotted absorption spectrum (Figure 4), the maximum UV absorption of ATC and EATC was closer to 280 nm than the more commonly available 254-nm UV monitor. No correction with the molar extinction coefficients of TC, ETC, ATC, and EATC was necessary for their quantitation.

Quantitative Determination of Tetracycline. Various amounts of the U.S.P. TC reference standard, ranging from 0.099 mg/ml to 0.90 mg/ml, were prepared. The calibration curve was linear (correlation coefficient 0.995) to 0.90 mg/ml, the highest TC concentration, with a linear

regression of $y = 3.33x - 0.036$. A 0.40 mg/ml level was used for the quantitation of TC samples so as not to overload the column. To determine ATC and EATC in a TC sample, the range setting was changed from 0.16 to 0.01 after the elution of the internal standard peak and prior to EATC and ATC peaks. The HPLC method is sensitive to approximately 10 nanograms of TC per sample injected. Therefore, the method may be of value for the analysis of clinical samples.

The precision of the HPLC method was determined by comparing eight replicate preparations of the U.S.P. TC reference standard. Table III indicates that the relative standard deviation of the tetracycline determination was 1.02%.

Eleven current TC lots from various commercial suppliers were analyzed (Table IV). The potency was calculated using the U.S.P. TC Reference Standard at 1000 µg/mg and ETC, ATC, and EATC to have anti-microbial activities of 27, 43, and 18% of TC against *Bacillus subtilis* (16). The potencies thus calculated were compared to those of the microbiological cylinder cup agar diffusion assay method using *Bacillus cereus* ATCC 11778 as the assay microorganism. The calculated potencies agreed well with those of the microbioassay method. In all samples examined, the percentage of ETC was less than 2.5%; ATC, 0.95%; and EATC, 0.07%. No detectable amount

(16) A. F. Zak, T. I. Navolotskaya, G. I. Loseva, N. I. Shukailo, O. B. Ermalova, and L. M. Yacobson, *Antibiotiki (Moscow)*, 18, 324 (1973).

Table IV. Tetracycline Hydrochloride Powder from Various Suppliers

Supplier	Lot No.	Potency, µg/mg		Percentage of				
		Microbioassay	HPLC	TC	ETC	ATC	EATC	CTC
A	1	967	996	98.1	1.5	0.42	<0.05	<0.05
	2	936	970	97.3	2.1	0.64	<0.05	<0.05
	3	980	988	96.9	2.0	0.95	0.07	<0.05
B	1	952	998	94.8	2.5	0.16	<0.05	<0.05
	2	920	968	97.4	1.9	0.64	0.07	<0.05
C	1	995	966	97.0	2.4	0.53	0.07	<0.05
	2	998	991	98.2	1.6	0.20	<0.05	<0.05
D	1	995	995	97.2	2.0	0.80	<0.05	<0.05
	2	968	980	97.4	1.9	0.66	<0.05	<0.05
E	1	984	979	97.5	2.5	<0.05	<0.05	<0.05
	1	962	991	97.2	1.9	0.87	<0.05	<0.05
			Average	97.4	2.0	0.59	0.02	<0.05

Table V. Tetracycline Powder Aged at Room Temperature

Length of storage	Potency, µg/mg		Percentage of				
	Microbioassay	HPLC	TC	ETC	ATC	EATC	CTC
Tetracycline hydrochloride							
8.0 yr	986	966	98.5	1.2	0.34	<0.05	<0.05
7.0 yr	990	980	96.9	1.9	1.2	<0.05	<0.05
6.5 yr	944	991	97.0	2.4	0.52	<0.05	<0.05
6.5 yr	964	985	97.2	1.2	1.6	<0.05	<0.05
6.2 yr	956	983	96.8	1.0	2.2	<0.05	<0.05
6.1 yr	965	980	98.1	1.2	0.67	<0.05	<0.05
Tetracycline base							
9.0 yr	931	893	97.0	2.25	0.59	<0.05	0.21
7.0 yr	923	919	97.7	2.0	0.22	<0.05	0.07
Tetracycline phosphate							
8.0 yr	701	684	72.4	15.8	11.5	0.33	<0.05
4.0 yr	638	601	71.3	17.0	11.4	0.35	<0.05
9 mo	732	680	85.5	9.6	4.6	0.29	<0.05
1 mo	766	726	93.0	4.7	2.2	0.14	<0.05

(above 0.05%) of CTC was found. From the results obtained above, the limit of ATC (0.5%) established by the British Pharmacopoeia (17) seems unrealistic.

Stored TC samples were then analyzed by the HPLC method (Table V). No significant increase in ETC nor ATC was observed in TC-HCl and TC base samples beyond 8 or 9 years storage in an airtight container at room temperature. However, TC phosphate samples were less stable and a significant increase in ETC and ATC was detected in samples stored for four years at room temperature.

The TC potencies calculated by the HPLC method agreed well with those of the microbiology assay. However, the calculated potencies of TC phosphate samples were consistently lower than those of the microbiology assay. Thus, it may be possible that the ETC, ATC, and EATC may have higher antimicrobial activities against *B. cereus* than *B. subtilis*. There is also evidence (16) that the antimicrobial activity of ETC, ATC, and EATC may differ from microbial species to species, as was demonstrated in Neomycins B and C (18) and in Erythromycins A, B, and C (19). Therefore, a study is being planned to determine the

(17) "British Pharmacopoeia," 1973, p. 468.

(18) J. H. Robertson, R. Baas, R. L. Yeager, and K. Tsuji, *Appl. Microbiol.*, 22, 1164 (1971).

(19) K. Tsuji and J. H. Robertson, *Anal. Chem.*, 43, 818 (1971).

microbiological response of ETC, ATC, and EATC using *Bacillus cereus* ATCC 11778 and *Staphylococcus aureus* ATCC 6538P, two officially accepted assay microorganisms (20).

After submission of our paper, we received a pamphlet, "Application Highlights" from Waters Associates, Inc., Framingham, Mass. and a paper by Butterfield *et al.* (21), both with a qualitative description of a HPLC separation for TC.

ACKNOWLEDGMENT

Bristol Laboratories and Charles Pfizer and Company are acknowledged for the supply of doxycycline hyclate, oxytetracycline, chlorotetracycline, 4-*epi*-tetracycline, anhydrotetracycline, and 4-*epi*-anhydrotetracycline. W. Morozowich is greatly acknowledged for the supply of the ammonium salt of 4-*epi*-tetracycline monohydrate. A. R. Lewis for the statistical analysis and computer print-out of the absorbance spectrum, and M. J. Kriekard for technical assistance.

Received for review August 8, 1973. Accepted October 19, 1973.

(20) Code of Federal Regulations, Title 21 Food and Drugs (1972).

(21) A. G. Butterfield, D. W. Hughes, N. J. Pound, and W. L. Wilson, *Antimicrob. Ag. Chemother.*, 4, 11 (1973).

Wide-Band, Precision, DC-Coupled Lock-In Detector and Gated Integrator for Electrochemical Measurements

A. J. Bentz, J. R. Sandifer, and R. P. Buck¹

The William R. Kenan, Jr., Laboratories of Chemistry, University of North Carolina, Chapel Hill, N.C. 27514

A low-cost, wide-band, dc-coupled lock-in detector and gated integrator have been developed for measurement of electrical responses of electrochemical systems. This simple instrument measures ac cell admittance from 0.005 Hz to 10 KHz over an impedance range from 10^2 ohms to 10^{11} ohms with 1% absolute accuracy (3% above 10^8 ohms) and better than one part in 10^4 resolution. Wide-band impedance measurements on a Beckman E-2 glass electrode were found to be in agreement with limited results obtained previously using bridge methods. The reaction rate of the ethanol-acetyl chloride esterification was followed by monitoring conductivity. The rate constants and activation energy (13.85 Kcal/mole) determined in this study are in excellent agreement with results obtained by other researchers.

The important role of the ac bridge in electrical measurements is common knowledge among those who investigate the properties of electrochemical systems. One theory and application of bridge techniques are reviewed extensively in a classic work by Hague (1). One serious limitation of the bridge method is that obtaining a true null is a time-consuming and tedious task, making measurements at low frequencies and measurements of rapid-

ly changing systems impractical or impossible. The problem of bridge balancing may be completely removed while retaining much of the high accuracy and precision of the bridge by using current feedback as shown in Figure 1.

This circuit is an analog of the conventional impedance bridge where two arms have been replaced by active elements: one, a signal generator, and the other, the output of an operational amplifier (Keithley 301K). The cell and R_m comprise the other two arms as in the conventional impedance bridge. The differential input of the operational amplifier (OA) serves as a null detector and keeps the bridge in continuous balance even as cell impedance changes with frequency or chemical composition. Since the bridge is continuously in balance and the OA output is the direct analog of the series RC arm in the conventional impedance bridge, one need only resolve the output of the OA into in-phase and quadrature components (with respect to the signal generator) to obtain the current voltage phase relationship in the cell. This is conveniently accomplished by cross-correlating the response with the excitation at zero time delay as suggested by Smith (2). When the output is correlated with a square wave in phase with the excitation, the result is proportional to the real component of the impedance. When the output is correlated with a square wave 90° out of phase with the signal generator, the result is proportional to the quadrature component. This method is essentially identical to

¹ To whom correspondence should be addressed.

(1) B. Hague, "Alternating Current Bridge Methods," Pitman, London, 1946.

(2) D. E. Smith, *Anal. Chem.*, 35, 1811 (1963).

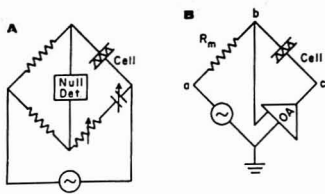


Figure 1. A. Conventional impedance bridge. B. Operational amplifier equivalent of (A)

lock-in or phase detection. If the positions of R_m and the cell are interchanged, the resulting circuit is the well known current transducer. The analysis is the same except that the result of cross-correlation is proportional to admittance rather than impedance. All work reported in this paper was done in the admittance mode.

It should be noted that use of a low-impedance signal generator and the low output impedance of the OA eliminate the problem of capacitance between points a and earth and c and earth. Since point b is virtually at ground potential (provided loop gain is high), the effective capacitance between b and ground is greatly reduced. The effect of stray capacitance across R_m and non-ideal behavior of the OA with emphasis on parameters affecting the signal-to-noise ratio have been reviewed in an excellent paper by Cath and Peabody (3). The measuring resistors used in this instrument are compensated for reactive behavior. Johnson, shot, and amplifier input noise including the $1/f$ component are taken into account in the design.

EXPERIMENTAL

A basic diagram of the complete instrument is shown in Figure 2. The signal generator (Hewlett-Packard 203A) drives OA-1 which lowers the driving impedance to the cell and provides dc offset. OA-2 (Keithley 301K) is an "electrometer" input (low noise MOS FET) current transducer which performs the functions outlined in the preceding paragraphs. OA-3 is a low-noise FET input amplifier with gain adjustable from 1 to 21. OA-4 and OA-5 comprise a simple lock-in detector or zero time delay cross-correlator which multiplies the square wave output of the HP 203A and the signal from OA-3. For all frequencies above 10 Hz, the ac component of the lock-in detector output is removed by a single section passive RC filter with a time constant of 1 second. Below 10 Hz, an integrator gated over one complete cycle is employed.

A diagram of the timing board is shown in Figure 3. The analog gates of the lock-in detector are driven in synchronization with the signal generator by flip-flop FF-4. The integrator input gate is controlled by toggled FF-1. This gate is open only during the first cycle after reset. The integrator reset gate controlled by FF-2 is closed upon reset command, opened at the beginning of the next cycle, and remains open until another reset command is given. FF-3 closes the gate (2N1305) connecting the integrator gating flip-flops to the synchronizing flip-flop (FF-4) after one cycle so the integral over that cycle is held until the reset command is given. This sequence is summarized in Table I. The flip-flop circuits used here are similar to a circuit described by Schwartz (4). These circuits change state upon application of a positive pulse of at least 3-volts magnitude and 1- μ sec duration. A positive pulse applied to R makes the output of Q_1 -10 volts and Q_2 zero volts. FF-1 was made to toggle by placing 3.3K resistors between the anode of the steering diodes and the collector of the respective transistors.

Finally, the cell admittance is related to the excitation and output of the instrument by the following easily derived equations.

Table I. Switching Sequence of Timer

Time	FF No.	Q_1 , volts	Q_2 , volts
Start-Reset to t_1	1	0	-10
	2	0	-10
	3	0	-10
t_1 to t_2	1	-10	0
	2	-10	0
	3	0	-10
t_2 to t_3	1	-10	0
	2	-10	0
	3	0	-10
t_3 to Start-Reset	1	0	-10
	2	-10	0
	3	-10	0

For frequencies above 10 Hz where passive integration is employed:

$$Y = E_{out} \left(\frac{1}{E_{ex} A R_m} \right) \quad (1)$$

For frequencies below 10 Hz where a gated analog integrator is employed:

$$Y = -E_{out} \left(\frac{RCf}{E_{ex} A R_m} \right) \quad (2)$$

where Y = cell admittance, E_{out} = output of instrument in volts (average), $(0.637/2)E_{peak}$ to peak, E_{ex} = excitation voltage to cell (average), A = gain of OA-3, R_m = measuring resistor in ohms, f = excitation frequency in Hz, and RC = integration constant of gated analog integrator.

The frequency response of the present instrument is limited primarily by the uncompensated shunt capacitance across R_m , the roll off of the Keithley 301K operational amplifier, and the switching speed of the FETs in the lock-in detector. Below 10 Hz, the open loop gain of the 301K is not frequency-dependent and the time response at low frequencies (10^{10} ohm-Hz) is limited by shunt capacitance across R_m . The dc gain of the 301K is greater than 5×10^4 , its input impedance in excess of 10^{12} ohms, and its bias current less than 10^{-14} A; therefore, the amplifier can be used with values of R_m approaching 10^{14} ohms at 1%. Since the tolerance of the high megohm measuring resistors (Keithley Model R20) used in this instrument is $\pm 3\%$ from 10^8 to 10^{11} ohms, the absolute accuracy in this range is $\pm 3\%$. At frequencies above 10 Hz, the open loop gain rolls off, limiting the useful high frequency range to 10 KHz or lower, depending on the magnitude of the quadrature admittance. Low impedance conductivity measurements were made using a type 741 integrated circuit operational amplifier in place of the 301K. In this case, the switching speed of the FETs in the lock-in detector limits the maximum usable frequency to 20 KHz.

Resolving capability is demonstrated by measurements on a dummy cell consisting of a two-megohm metal film resistor shunted by a 1000-pf ceramic capacitor. Using a one-megohm R_m and 50-mV peak-to-peak excitation, the resolution is better than one part in 10^4 from 0.00563 to 100 Hz. This corresponds to resolving the quadrature admittance to 1% when it is 100 times smaller than the real admittance. Resolving ability is further demonstrated by measurements on a glass electrode.

RESULTS AND DISCUSSION

Bipolar pulse techniques have recently been described (5, 6) which extend the range of conductance instrumentation to include rapid high- and low-resistance (100Ω - $1M\Omega$) measurements. These instruments rely on the rapid application of voltage (5) or current (6) pulses of alternating sign. The resulting signal is analyzed to determine the parameter of interest (conductance). The conductance cell model used to interpret the results is shown in Figure 4. It has been generally accepted that ac bridge measurements would not be applicable for these purposes because of lim-

(3) P. G. Cath and A. M. Peabody, *Anal. Chem.*, **43**(11), 91A (1971).
(4) S. Schwartz, "Selected Semiconductor Circuits Handbook," Circuit G-1, Wiley and Sons, Inc., New York, N.Y., 1961.

(5) D. E. Johnson and C. G. Enke, *Anal. Chem.*, **42**, 329 (1970).
(6) P. H. Daum and D. F. Nelson, *Anal. Chem.*, **45**, 463 (1973).

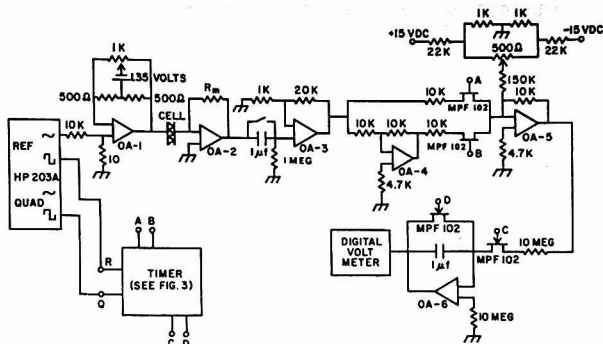


Figure 2. Instrument schematic

Table II. Reaction Rate Studies^a

Temperature, °C	<i>k</i>	No. of runs	<i>s</i>
0.0	0.0196	5	0.0004
9.0	0.0441	5	0.0005
15.0	0.0722	4	0.0008
19.8	0.1098	5	0.0008
25.0	0.165	6	0.001
35.0	0.355	3	0.002

^a $E_A = 13.85$ Kcal/mole, $s = 0.06$.

itations in the rate of bridge balancing and in dynamic range. We have found, however, that application of the principles of phase-lock detection results in instrumentation which also overcomes these limitations as demonstrated by the results reported below.

An analysis of the circuit shown in Figure 4 for ac measurements results in the following equations:

$$Y_R = \frac{\omega^2 R C_s^2}{1 + \omega^2 R^2 C_s^2} \quad (3)$$

$$Y_Q = \omega C_p + \frac{\omega C_s}{1 + \omega^2 R^2 C_s^2} \quad (4)$$

where Y_R and Y_Q are the in- and out-of-phase admittances, respectively, and ω is the angular frequency ($2\pi f$). At high frequency ($\omega^2 R^2 C_s^2 \gg 1$), $Y_R = G$, the conductance, which equals $1/R$. Use of the instrument described above for conductance measurements simply requires that the frequency employed be high enough so that Y_R is independent of frequency. This would require frequencies on the order of 1000 Hz.

Following the examples of Johnson and Enke (5) and of Daum and Nelson (6), we have chosen to demonstrate the rapid response of our instrument by studying the ethanolysis of acetyl chloride. For this purpose, ethanol was dried by the method of Lund and Bjerrum (7) and found to contain about 0.02% water (by weight) by Karl Fischer titration. Reagent grade acetyl chloride was used after one distillation. The electrodes used were unplanitized platinum electrodes, 20 mm² in area, placed 5 mm apart. The frequency was set at 1000 Hz where the in-phase response was not a function of frequency.

Approximately 3-μl samples of acetyl chloride were injected into rapidly stirred, thermostated, 125-ml samples



Figure 3. Timing circuit

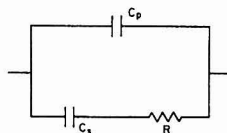


Figure 4. Equivalent circuit for conductance cell. C_p is usually considered the "geometrical" capacitance, C_s is the double layer capacitance, and $1/R$ is the conductance of the cell

of ethanol. The instrumental response was then recorded on a Hewlett-Packard (7004A) X-Y recorder for subsequent manual interpretation. The same ethanol sample could be used for several runs by use of an off-set control without loss of sensitivity. Rate constants for each run were determined by plotting $\ln(G_\infty - G)$ vs. time where G is the conductivity. The negative slopes of the straight lines resultant from these plots equal k , the rate constant. Rate constants were determined at each of seven temperatures, and this collection of data was used to determine the activation energy from an Arrhenius plot. A linear least-squares routine was used to determine the activation energy. The results are shown in Table II while Figure 5 is the Arrhenius plot. Except for the activation energy calculation, all calculations were done to slide rule accuracy. A computer was used to calculate the activation energy.

A comparison of our results with those obtained by other workers (5, 6, 8) is shown in Table III. Our value for

(7) H. Lund and J. Bjerrum, *Ber.*, **B64**, 210 (1931).

(8) E. Euranto and R. Leimu, *Acta Chem. Scand.*, **20**, 2029 (1966).

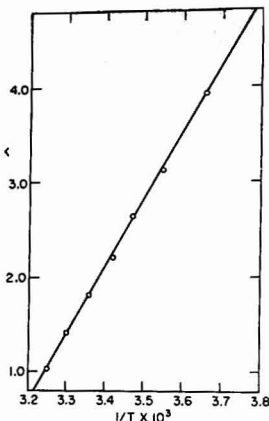


Figure 5. Arrhenius plot of conductance data for the ethanolysis of acetyl chloride

Table III. Comparison of Results

Workers	Activation energy
Euranto and Leimu (8)	13.23
Johnson and Enke (5)	12.93
Daum and Nelson (6)	13.95
This Work	13.85

the activation energy agrees well with that obtained by Daum and Nelson while the results of Johnson and Enke agree more closely with those of Euranto and Leimu. A *t*-test on data obtained by each group at 15 °C (corrected in each case by the appropriate activation energy) reveals that the results do not belong to the same data set. We can find no good reason for this discrepancy except that our ethanol was slightly wetter than that used by Euranto and Leimu. Compare 0.02% water to 0.014%. Neither Johnson and Enke nor Daum and Nelson reported % water content.

Our ability to measure the out-of-phase component resulted in the observation that this component was never greater than 3% of the in-phase component and was at its maximum when pure ethanol was used. After the first injection of acetyl chloride, the out-of-phase component dropped to insignificance. This indicates that a simple 1000-Hz oscillator would have sufficed for this experiment without recourse to the sophisticated instrumentation used by Johnson and Enke, Daum and Nelson, or ourselves. This is a reasonably good test of instrumental response but does not demonstrate resolving capability.

Glass Electrode Admittance. An important difference between our instrument and available commercial phase-lock detectors is the fact that it may be dc coupled. AC coupling was used for the conductivity measurements, but dc coupling is mandatory for glass electrode admittance measurements since much lower frequencies must be employed (9, 10). We feel that interpretation of glass electrode data is more convenient if the data are in the admittance form.

Figures 6 and 7 show the kind of results possible with this instrument. The admittance of a Beckman E-2

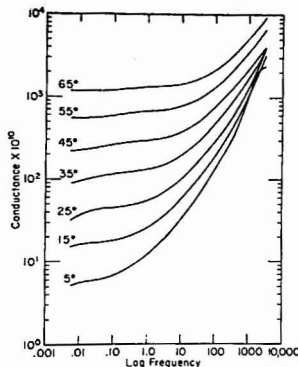


Figure 6. In-phase E-2 glass data expressed as conductance, *G*. Data points are spaced at quarter decade intervals. *G* = real admittance

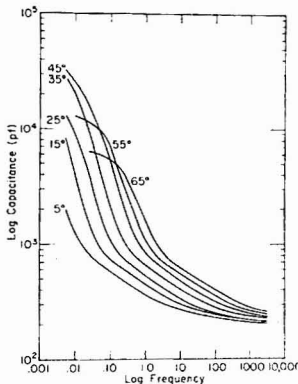


Figure 7. Out-of-phase E-2 glass data expressed as capacitance, *C*. Data points are spaced at quarter decade intervals. *C* = out-of-phase admittance/2 π f

(39004) glass electrode was measured at several temperatures. A Beckman SCE was used as reference for these measurements. The excitation was typically 50 mV peak-to-peak. Tenth normal KCl solutions were used. Notice that phenomena of interest are occurring at quite low frequencies (0.01 Hz). The interpretation of these results will be published elsewhere. They are, however, in excellent agreement with Buck and Krull (9).

Although low-frequency data have been reported by others (10) using nulling techniques or Lissajous figures, higher excitation (1 volt) had to be used, and the systems studied typically had phase angles of 10° to 30° at these frequencies. Noise would have been a limiting factor in these measurements if lower (50 mV) excitations had been used or if it had been necessary to measure smaller phase angles. It was necessary for us to resolve the phase angle down to less than 0.5° to obtain the data shown in Figures 5 and 6.

CONCLUSIONS

The dc-coupled cross-correlation technique has significant advantages over other detection systems (e.g. Lissajous figures). The real and quadrature admittance can be

(9) R. P. Buck and I. Krull, *J. Electroanal. Chem.*, **18**, 387 (1968).

(10) M. J. D. Brand and G. A. Rechnitz, *Anal. Chem.*, **41**, 1788 (1969).

read directly. More significant is the fact that information theory predicts that cross-correlation enhances the signal-to-noise ratio (11, 12). This allows greater resolution than could be obtained via Lissajous figures.

The instrument described above has been demonstrated to be well suited to its primary task of measuring high impedance systems at low frequencies using minimal excitation. However, the potential of the correlation method for use in systems where conductivity is a dynamic parameter

(11) G. M. Heitje, *Anal. Chem.*, **44**(6), 81A (1972).

(12) G. M. Heitje, *Anal. Chem.*, **44**(7), 69A (1972).

should not be underestimated, particularly since the necessary equipment is available commercially or may be constructed in the laboratory at low cost. The instrument may be easily modified to function in either the impedance or the admittance mode. In addition, the nature of the instrumental response makes it applicable to a wide variety of problems.

Received for review August 24, 1973. Accepted November 28, 1973. This work was supported by National Science Foundation Grant GP-20524.

Electroanalytical Studies of Methylmercury in Aqueous Solution

R. C. Heaton¹ and H. A. Laitinen

School of Chemical Sciences, University of Illinois at Urbana-Champaign, Urbana, Ill. 61801

The electrochemical reduction of monomethylmercury compounds in aqueous solution has been studied through the use of pulse polarography, cyclic voltammetry, and related techniques. Reduction of these compounds at a mercury electrode occurs in two one-electron steps, the first of which results in the formation of a methylmercuric radical on the electrode surface. This step is reversible under polarographic conditions, but the polarographic wave is distorted because of the involvement of the methylmercuric radical in subsequent chemical reactions. Addition of the second electron results in reduction of the methylmercuric compound to elemental mercury and methane, and gives rise to the second polarographic wave. This reduction is irreversible and the wave is also distorted. The first pulse polarographic wave has analytical utility arising from a linear peak current vs. concentration curve between concentrations of 10^{-7} and $10^{-4}M$. The analytical implications of the reduction mechanism are discussed, with particular attention given to effects of coordinating agents and to detection limits.

Electrochemical reduction of methylmercury was first observed by Kraus (1) in 1913. While other investigators (2-4) repeated Kraus's experiments and verified his results, little new insight into the reduction mechanism was gained until 1948, when Costa (5) published his studies of the reduction of ethylmercury by electrochemical means. Since that time, mechanistic studies of a variety of organomercury compounds have been reported (6-15),

the works of Benesch and Benesch being most often quoted. It is generally agreed that the polarographic reduction proceeds in two one-electron steps, the first yielding an organomercury radical, the second giving elemental mercury and, in the case of alkylmercury compounds, the alkane. Beyond this point, authors disagree as to the nature of the reduction process. Some investigators (5, 7, 8, 11) regard the first wave as irreversible, while others (6, 12-15) consider it to be reversible. Vojir (6) suggested the irreversible dimerization of the organomercury radical might take place following the electroreduction, giving rise to an insoluble film on the electrode surface. Although most workers since that time have included some sort of dimerization or disproportionation reaction in their formulations, little has been done to detail the fate of the organomercury radical, or to determine the nature of any intermediates which may be involved. Several authors have noted that the polarographic waves exhibit irregularities (6, 7, 8, 14) and that prewaves often occur (7-9, 12-14), but interpretations of these phenomena vary.

The finer details of the reduction mechanism may well depend on the particular organomercury compound in question, the solvent, and the experimental conditions employed. The purpose of this investigation is to determine the details of the electrochemical reduction of methylmercury in aqueous solution, and to assess the feasibility of using electrochemical techniques to determine methylmercury and to study its coordination chemistry.

EXPERIMENTAL

Instrumentation. Polarograms were recorded using a Heath polarography module, model EUA-19-2, connected to our own operational amplifier system. Recordings were made using either a Moseley model 7001AM x-y recorder or a Heath model EUW-20A variable speed servo recorder. Potential scales were calibrated with a Leeds and Northrup volt potentiometer, catalog number 8687. Drop times used in constructing electrocapillary curves were

¹ Present address, Hercules Research Center, Wilmington, Del.

(1) C. A. Kraus, *J. Amer. Chem. Soc.*, **35**, 1732 (1913).

(2) B. G. Gowenlock and J. Trotman, *J. Chem. Soc.*, **1957**, 2114.

(3) B. G. Gowenlock, P. P. Jones, and D. W. Ovenall, *J. Chem. Soc.*, **1958**, 535.

(4) J. L. Maynard and J. C. Howard Jr., *J. Chem. Soc.*, **1923**, 960.

(5) G. Costa, *Ann. Chim. (Rome)*, **38**, 655 (1948).

(6) V. Vojir, *Collect. Czech. Chem. Commun.*, **16**, 489 (1951).

(7) R. Benesch and R. E. Benesch, *J. Amer. Chem. Soc.*, **73**, 3391 (1951).

(8) R. Benesch and R. E. Benesch, *J. Phys. Chem.*, **56**, 648 (1952).

(9) R. F. Broman and R. W. Murray, *Anal. Chem.*, **37**, 1408 (1965).

(10) K. P. Butin, I. P. Beletskaya, A. N. Ryabtsev, and O. A. Reutov, *Elektrokhimiya*, **3**, 1318 (1967).

(11) V. G. Toropova, M. K. Saikina, and M. G. Khakimov, *Zh. Obshch. Khim.*, **37**, 47 (1967).

(12) C. Degrand and E. Laviron, *Bull. Soc. Chim. Fr.*, **5**, 2233 (1968).

(13) C. Degrand and E. Laviron, *Bull. Soc. Chim. Fr.*, **5**, 2228 (1968).

(14) B. Fleet and R. D. Jee, *J. Electroanal. Chem.*, **25**, 397 (1970).

(15) N. S. Hush and K. B. Oldham, *J. Electroanal. Chem.*, **6**, 35 (1963).

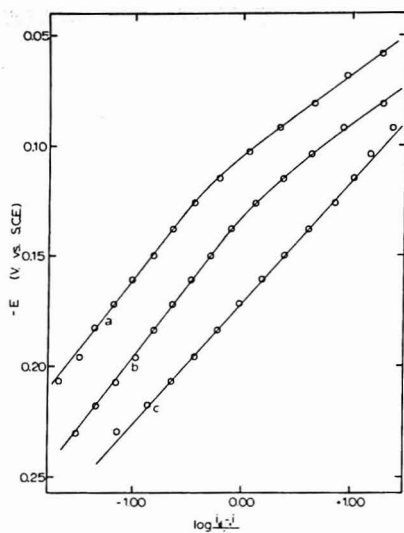


Figure 1. Dependence of E on $\log (i_d - i)/i$ for the first wave in 0.1M HClO_4 solution under normal pulse polarographic conditions

a) $9.76 \times 10^{-5} \text{M CH}_3\text{Hg}^+$; b) $4.88 \times 10^{-5} \text{M CH}_3\text{Hg}^+$; c) $2.44 \times 10^{-5} \text{M CH}_3\text{Hg}^+$

measured by allowing the falling mercury drops to interrupt a light beam and electronically timing the interval between two such events.

Cyclic voltammograms were obtained by the use of a Wenking potentiostat built by G. Bank Elektronik, No. 7163-61RS. The current was determined by measuring the voltage drop across a resistor in series with the counter electrode. Current-voltage curves were recorded using a Tektronix model 503 x-y oscilloscope equipped with a Tektronix model C-12 camera. Triangular voltage functions were generated by a function generator built in this laboratory.

A Princeton Applied Research model 174 Polarographic Analyzer was used to obtain normal pulse and differential pulse polarograms. The Heath servo recorder was used to record the results.

All electrochemical experiments were performed in completely enclosed, all-glass cells. Dropping mercury electrodes were of standard construction, using soft glass marine barometer tubing for the capillary. For a hanging mercury drop electrode, a micrometer electrode, obtained from Princeton Applied Research, catalog No. 9302, was used. Potentials were measured relative to a saturated calomel electrode.

Reagents and Solutions. With the exception of the methylmercury salts, all reagents were reagent grade, used without further purification. Methylmercuric hydroxide obtained from Alfa Inorganics was recrystallized from pyridine, yielding white crystals, melting range 92–102°C. In view of the fact that this melting range is significantly lower than that of the oxide (110–137°C) and considerably higher than that of the hydroxide (62–68°C), it seems likely that the sample is a mixture of the hydroxide and the oxide. This is of little consequence since the oxide is immediately converted to the hydroxide upon dissolution in water. Titration of the sample with perchloric acid in the presence of potassium iodide indicates that it is more than 95% pure as monomethylmercury. The equivalent weight determined by the titration was used to calculate solution concentrations.

Mercury was scrubbed successively with nitric acid and potassium hydroxide solutions, and then vacuum distilled. Glassware was cleaned with aqua regia and thoroughly washed with double distilled water immediately before use.

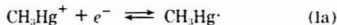
Millimolar solutions of methylmercuric hydroxide were prepared by introducing weighed amounts of the sample into volu-

metric flasks and then filling the flasks to the marks with the appropriate supporting electrolytes. More dilute solutions were prepared by dilution of the 1mM solution.

RESULTS AND DISCUSSION

Reduction of the methylmercuric cation in 0.1M perchloric acid solution or of methylmercuric hydroxide in 0.1M sodium hydroxide solution yields two well defined polarographic waves of nearly equal height. Both waves are diffusion controlled as the dependence of the limiting current on the concentration of the electroactive species is linear. In addition, the variation of the limiting current with the square root of the corrected mercury column height is also linear. The polarographic diffusion coefficients, calculated from either standard polarographic data or pulse polarographic data are $1.08 \pm 0.02 \times 10^{-5} \text{ cm}^2/\text{sec}$ in 0.1M HClO_4 solution, and $1.11 \pm 0.08 \times 10^{-5} \text{ cm}^2/\text{sec}$ in 0.1M NaOH solution.

The first wave is asymmetric, being more steep at the foot of the wave than at the head of the wave. This asymmetry is reflected in the standard polarographic log plot [E vs. $\log (i_d - i)/i$] which exhibits a change of slope near the half-wave potential. This distortion can be adequately explained by postulating the occurrence of a chemical reaction following the electrochemical reduction. The following reactions are proposed:



Because reaction 2 effectively lowers the activity of the methylmercury radical, $\text{CH}_3\text{Hg} \cdot$, the electrochemical process, 1, should be facilitated, increasing the slope of the polarographic wave and shifting the half-wave potential anodically. Also, because reaction 2 is second order in $\text{CH}_3\text{Hg} \cdot$, it should exert less influence on the electrochemical process as the concentration is lowered. Careful perusal of Figure 1 shows that all of these trends do in fact occur.

Bonnaterre and Cauquis (16) have developed a unified mathematical treatment of the polarographic wave observed in the general case of electroreduction followed by a chemical dimerization. While the equations were derived with a rotating disk electrode in mind, they can be made to apply to a dropping mercury electrode by writing the diffusion layer thickness in terms of the capillary characteristics and the drop time. Two cases have relevance to this investigation—that of a reversible electrochemical reduction followed by an irreversible dimerization, and that of a reversible electrochemical reduction followed by a fast reversible dimerization. For the former case the equations obtained are identical to those derived by Hanus (17), Hanus and Koutecky (18), and Mairanovskii (19, 20).

$$E = E^{0'} - \frac{RT}{nF} \ln \frac{i_d}{10^{-3} n F q D^{1/2} k_2^{1/2} C} - \frac{RT}{nF} \ln \frac{i^{2/3}}{i_d - i} \quad (A)$$

$$E_{1/2} = E^{0'} + \frac{RT}{3nF} \ln \frac{k_d C}{4} \quad (B)$$

(16) R. Bonnaterre and G. Cauquis, *J. Electroanal. Chem.*, **32**, 199 (1971).

(17) V. Hanus, *Chem. Zvesti.*, **8**, 702 (1954).

(18) J. Koutecky and V. Hanus, *Collect. Czech. Chem. Commun.*, **20**, 124 (1955).

(19) S. G. Mairanovskii, *Dokl. Akad. Nauk SSSR*, **110**, 593 (1956).

(20) S. G. Mairanovskii, *Izv. Akad. Nauk SSSR, Otd. Khim. Nauk*, **12**, 2140 (1961).

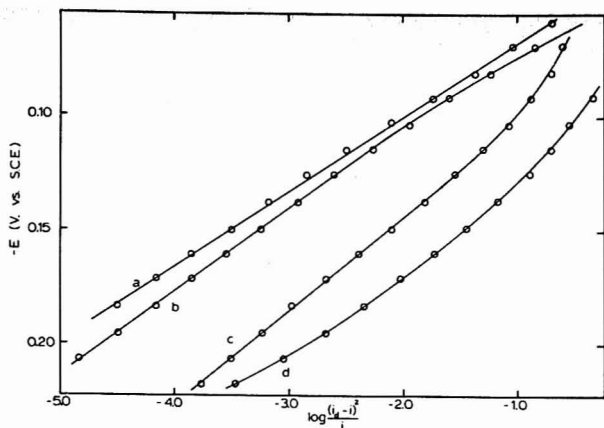


Figure 2. Dependence of E on $\log [(i_d - i)^2 / i]$ for the first wave in 0.1M HClO_4 solution under normal pulse polarographic conditions

a) $9.76 \times 10^{-5} \text{M CH}_3\text{Hg}^+$; b) $4.88 \times 10^{-5} \text{M CH}_3\text{Hg}^+$; c) $9.76 \times 10^{-6} \text{M CH}_3\text{Hg}^+$; d) $2.44 \times 10^{-6} \text{M CH}_3\text{Hg}^+$.

In these equations, q is the average area of the drop, t is the drop time, k_d is the chemical dimerization rate constant, and C is the bulk concentration of the electroactive species. The remaining variables have their usual significance. It is clear that a plot of E vs. $\log [(i_d - i)^2 / i]$ should yield a straight line whose slope is -59 mV for each decade increase in depolarizer concentration. It is, in principle, possible to calculate the dimerization rate constant if the formal potential is known.

If the chemical dimerization is fast and reversible, and if the equilibrium position strongly favors the dimer, then the following equations apply:

$$E = E^{\circ'} - \frac{RT}{nF} \ln \frac{1}{2} \sqrt{\frac{7}{3}} F D^{1/2} t^{-1/2} K + \frac{RT}{2F} \ln \frac{(i_d - i)^2}{i} \quad (\text{C})$$

$$E_{1/2} = E^{\circ'} + \frac{RT}{2F} \ln \frac{C}{K} \quad (\text{D})$$

K is the dissociation constant for the dimer. It is assumed that n is equal to unity. A plot of E vs. $\log [(i_d - i)^2 / i]$ should give a straight line with a slope of 30 mV . In addition, the half-wave potential shifts 30 mV in the positive direction for each decade increase in depolarizer concentration. The dissociation constant for the dimer may be calculated if $E^{\circ'}$ is known. Equations C and D represent a situation in which the diffusion of the reduced species away from the electrode exerts an insignificant effect on the observed polarographic current. Consequently, these equations apply equally well to systems involving either homogeneous or heterogeneous chemical reactions.

Figure 2 shows the pulse polarographic data for methylmercuric cations in 0.1M perchloric acid solution plotted according to Equation C. Similar results were observed for the standard polarographic data. At higher concentrations, the curves are linear between 10 and 90% of the wave height, suggesting that Equation C adequately describes the situation. As the concentration is lowered, the wave shifts cathodically and the curves begin to deviate from linearity. This behavior complements that shown by the curves in Figure 1. The standard log plots are nonlinear at high concentrations but become linear for concen-

trations of methylmercury less than $2.5 \times 10^{-6} \text{M}$ in 0.1M perchloric acid solution. This linear behavior at low concentrations is expected when the electrochemical reduction is followed by chemical reactions of orders greater than unity, because the equilibrium position of the chemical reaction favors the monomer more as the concentration is lowered. At very low concentrations, the chemical reaction may be ignored altogether.

Data for polarographic reductions of organomercury compounds have been plotted according to Equation A by previous authors (10, 11) and the resulting plots have been presented as evidence supporting the hypothesis that reaction 2 is irreversible. Plots of data according to Equation A made during this investigation were always nonlinear when plotted between 10 and 90% of the polarographic wave height. Consequently, it is suggested that the chemical dimerization is better described as a fast and reversible process than as an irreversible process.

The half-wave potential for the first wave shifts in the negative direction as the concentration decreases. However, at very low concentrations ($4 \times 10^{-6} \text{M}$ in perchloric acid solution), the half-wave potential becomes independent of concentration. Because this potential at very low concentrations is not influenced by the following chemical reaction, it should be closely related to the formal potential for the electrochemical process. If it is assumed that the ratio of the diffusion coefficients for the oxidized and reduced species is unity, then the formal potential for this reduction in 0.1M perchloric acid solution is $-0.143 \text{ volts vs. SCE}$. Knowledge of this value permits the calculation of the dissociation constant for the dimer by the use of Equation D. The value so obtained is $10^{-5.7}$. This must be regarded as an approximation because the kinetic scheme described thus far is not complete.

The second polarographic wave is distorted, having a long drawn out appearance. In addition, significant changes in shape are observed when the supporting electrolyte is changed from perchloric acid to sodium hydroxide. Although the drawn out appearance of this wave makes it appear to be irreversible under polarographic conditions, the electron transfer appears to be fairly fast, as it gives a well defined cyclic voltammetric peak even at sweep rates of 100 volts per second. The irreversible ap-

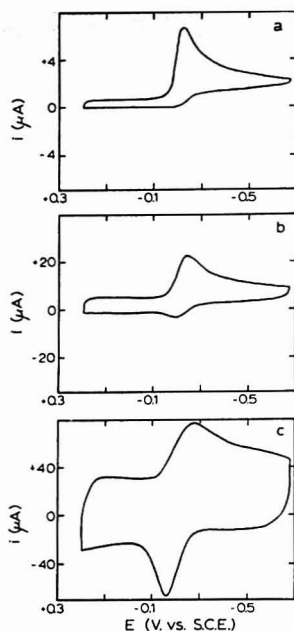


Figure 3. Cyclic voltammograms of $4.49 \times 10^{-4} M$ CH_3Hg^+ in $0.1 M$ $HClO_4$ with $1.2 \times 10^{-3} \%$ Triton X-100

a) Sweep rate = $0.50 V/sec$; b) Sweep rate = $5.0 V/sec$; c) Sweep rate = $50 V/sec$

pearance of the wave under polarographic conditions can be attributed to two factors. First, the reaction is chemically irreversible, meaning that the forward reaction is very fast, but that the reverse rate is negligible. This is due to the fact that the reduction product, methane, is inert under the conditions employed. The second factor affecting the wave shape is the fact that the electrochemical reduction is competing with the chemical dimerization of the radical, giving the wave a drawn out appearance.

The half-wave potential was observed to be independent of the supporting electrolyte and the types of buffers used, so that one may conclude that coordination is not a factor in the second reduction. However, the dependence of the half-wave potential on pH is interesting. At high pH values, the wave is independent of pH, but at pH values less than 5, the half-wave potential shifts 13 mV in the positive direction for each unit decrease in pH. This behavior may be interpreted in the following way. At high pH, where hydrogen ions are scarce, the organomercury radicals may be reduced to elemental mercury and a carbanion. The carbanion may then abstract a proton from a water molecule to give methane and a hydroxyl ion. The wave is thus unaffected by the hydrogen ion activity and, because the chemical reaction is irreversible, it is not affected by the hydroxyl ion activity either. At low pH, the reduction of the radical may be assisted by attack of a proton at the back side of the methyl group. This should aid the reduction, shifting the half-wave potential to more positive values and should also lead to inversion of the methyl group, which is without observable consequences. As this explanation essentially involves a change in the reduction mechanism with pH, differences in the wave

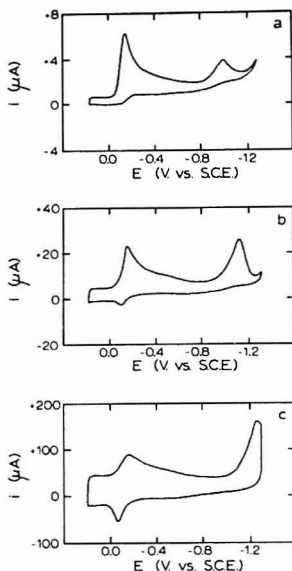
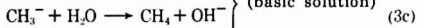
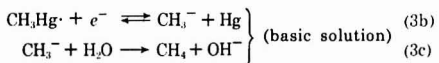
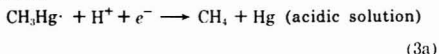


Figure 4. Cyclic voltammograms of $4.49 \times 10^{-4} M$ CH_3Hg^+ in $0.1 M$ $HClO_4$ with $1.2 \times 10^{-3} \%$ Triton X-100

a) Sweep rate = $0.50 V/sec$; b) Sweep rate = $5.0 V/sec$; c) Sweep rate = $50 V/sec$

shapes obtained in acidic and basic solutions are expected. The reactions for the second wave may be written as follows:



Cyclic voltammograms of the methylmercuric cation in $0.1 M$ perchloric acid solution are shown in Figure 3. Two characteristics of these curves are of major importance in the postulation of a reduction mechanism. The first is the shape of the anodic peak and the second is the ratio of the anodic peak current and the cathodic peak current.

It is clear that the amplitude of the anodic peak is dependent on the sweep rate. It is virtually nonexistent at slow sweep rates, but increases as the sweep rate increases. It is also apparent that the anodic peak does not show behavior typical of a diffusion controlled wave, although the cathodic peak does. The anodic peak shape is typical of a stripping peak—a peak resulting from the destruction of an adsorbed or insoluble film. The implications of this will be discussed shortly.

Similar behavior is exhibited by the second cathodic wave (Figure 4). While this wave never entirely disappears, its amplitude is small at slow sweep rates, and it increases as the sweep rate increases. In addition, the peak shape is again typical of a stripping process.

The situation is even better described in Figure 5, which shows the peak currents as functions of the sweep rate. The anodic peak current is less than the cathodic peak current at slow sweep rates, but greater than the ca-

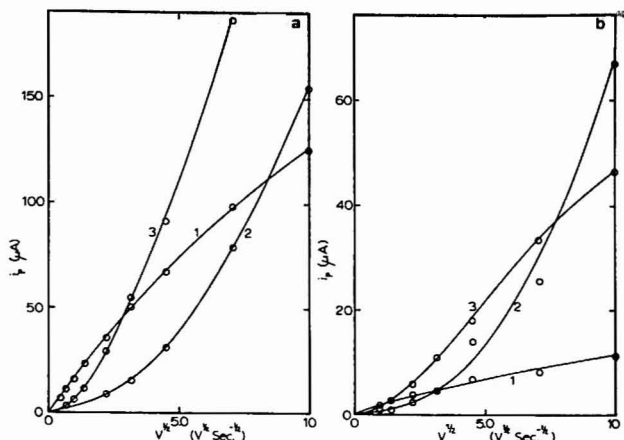


Figure 5. Cyclic voltammograms peak currents as functions of sweep rate in 0.1M HClO₄ solutions

a) $8.98 \times 10^{-4} M CH_3Hg^+ + 0.1M HClO_4 + 1.2 \times 10^{-2} \% Triton X-100$. 1. first cathodic peak; 2. anodic peak; 3. second cathodic peak. b) $1.08 \times 10^{-4} M CH_3Hg^+ + 0.1M HClO_4 + 1.2 \times 10^{-2} \% Triton X-100$. 1. first cathodic peak; 2. anodic peak; 3. second cathodic peak

thodic peak currents at fast sweep rates. Note that there is nothing wrong with having the anodic peak current larger than the cathodic peak current, since the anodic peak is taller, but narrower, than the diffusion-controlled cathodic peak. As the concentration is reduced, the anodic peak current increases relative to the cathodic peak current. This behavior is typical of a second-order process following the electrochemical reduction.

Because the second cathodic process corresponds to the reduction of the methylmercury radical, $CH_3Hg\cdot$, while the anodic wave results from the oxidation of the same radical, the peaks corresponding to these processes should behave very much alike. It can be seen that they do. Small quantitative differences are observed because the waves occur at different potentials.

The fact that the anodic peak is small or nonexistent at slow sweep rates but large and well defined at fast sweep rates, strongly suggests the occurrence of a slow chemical reaction following the electrochemical reduction. The evidence also suggests that the reaction is second order. This results in a dilemma, since the polarographic experiments seemed to indicate that the electrochemical reduction was followed by a fast chemical reaction. This dilemma can be resolved by rewriting reaction 2 in the following way:



Reactions 2a and 2b may be used to explain the cyclic voltammetry data in the following way. At very fast sweep rates, reaction 2b may not take place to a significant degree during the course of the experiment, so that the cyclic voltammogram looks like that expected for a mechanism including only steps 1 and 2a. However, at slow sweep rates reaction 2b may approach equilibrium. If the equilibrium of 2b favors the product, then the transformation of dimethylmercury to dimethyldimethylmercury should be much slower than even the forward reaction. Thus, reaction 2b should appear to be nearly irreversible. Consequently the dimer may be effectively transformed to an

inactive species at slow sweep rates, so that the anodic peak may be very small, or nearly non-existent.

Under polarographic conditions, in which the radical, $CH_3Hg\cdot$, is continually being generated by electrolysis, the system behaves much as if reactions 1 and 2a were the only things happening. The effect of reaction 2b is to cause some leakage of the dimethyldimethylmercury from the system, resulting in a larger apparent formation constant for the dimer.

The behaviors of the anodic and second cathodic peaks observed during the cyclic voltammetry experiments suggest that the reactions 2a and 2b may be heterogeneous. Further evidence to support this conclusion is the fact that the electrocapillary curve is slightly depressed in the potential interval between the two polarographic waves (Figure 6). That suppression of the interfacial tension only occurs negative of the electrocapillary maximum suggests that the adsorbed species is oriented in such a way as to resemble a dipole with its positive end toward the electrode.

The exchange of labeled elemental mercury with organic mercury compounds has been studied in some detail (21-27) and is directly relevant to this investigation. Of particular interest is the study of Butin *et al.* (27). It was proposed that the exchange occurs through the following steps. First, the diorganomercurial is adsorbed onto the mercury surface. This adsorption is a function of the structure and concentration of the organomercurial and the nature of the solvent. The second step involves an electron transfer from the diorganomercurial to the mercury metal. This may occur by the formation of a four-centered cyclic intermediate consisting of two mercury atoms in the electrode surface bridged by the two organic groups, and is believed by Butin and coworkers to be the rate-determining step. The third step involves separation of the intermediate into two adsorbed organomercurial radicals. Retention of configuration is retained as the radicals are strongly inserted into the mercury surface.

The series of steps just described is clearly the reverse of reactions 2a and 2b. The evidence obtained in this study requires that the transition between the adsorbed

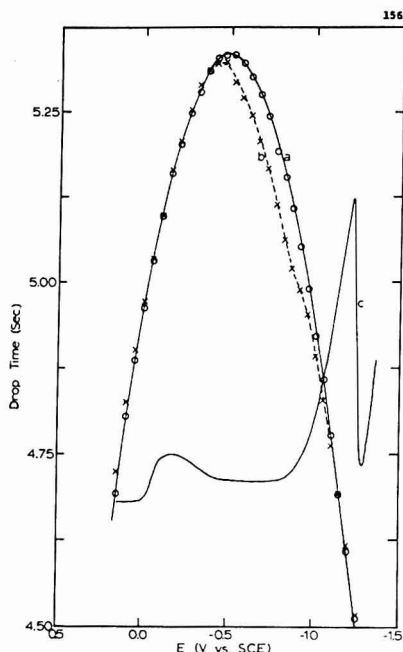
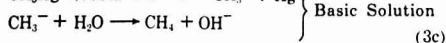
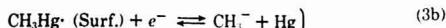
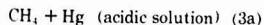
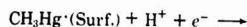
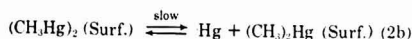
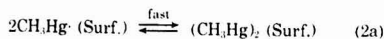
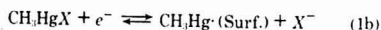


Figure 6. Electrocapillary curve for CH_3Hg^+ in 0.1M HClO_4 solution

a) 0.1M HClO_4 ; b) 9.59×10^{-4} M CH_3Hg^+ + 0.1M HClO_4 ; c) Polarogram of solution b

radicals and the intermediate dimer be fast and reversible, and that formation of the dimer be strongly preferred over the radical. The assertion by Butin and coworkers that the rate determining step is the electron transfer step is in perfect agreement with the results of this study. Some care is indicated here, as the electron transfer step in this case involves the chemical oxidation-reduction between elemental mercury and the diorganomercury compound to give the diorganodimercury compound, and is distinct from the electrochemical reduction of the organomercury cation.

To briefly summarize, the proposed reduction mechanism embodies the following reactions:



Basic Solution

Fleet and Jee (14) have explained the anodic cyclic voltammetric peak behavior for a number of organic mercury compounds in terms of the stability of the adsorbed radical. They go on to assume that the unadsorbed radical undergoes rapid dimerization and that the concentration dependence of the anodic to cathodic peak current ratio is due to a variation in the proportion of the radical adsorbed. While the first part of this explanation is essentially in agreement with that offered here (except that the present work details the subsequent fate of the radical), the second assumption is at variance with the observation of a number of investigators (21-27) that the exchange reactions between elemental mercury and organic mercury are heterogeneous, and involve adsorbed dimeric intermediates. In addition, it has been shown above that the concentration dependence of the anodic to cathodic peak current ratio can be adequately explained by the occurrence of reactions 2a and 2b.

In contrast to previously published work on a number of other organic mercury compounds, no prewaves were observed in this study of methylmercury, nor were irregularities observed in the current-time behavior at the foot of the first polarographic wave. Polarographic maxima of the first kind often occur at the head of the first wave, while the maximum at the head of the second wave satisfies Frumkin's criteria for maxima of the third kind. All of the irregularities observed can be suppressed by the addition of suitable surfactants to the system, and thus constitute no particular obstacle to the analytical chemist.

ANALYTICAL IMPLICATIONS OF THE REDUCTION MECHANISM

A number of reports have been made of the use of polarographic half-wave potentials to evaluate complex equilibrium constants for organomercury compounds (5, 7, 10, 11, 14, 15, 28). Of these studies, the ones by Costa (5), Benesch and Benesch (7), and Toropova *et al.* (11) deal primarily with the effects of pH on the half-wave potential. In several cases, difficulties in achieving consistent results were encountered. Although the fact that the methylmercuric cation forms stable complexes with most commonly used buffer anions and with most halide ions (28-31) would explain most of the difficulties by itself, other factors may also influence the potential of the polarographic wave.

The chemical reactions 2a and 2b, cause a positive shift in the half-wave potential which depends on the concentration. While the magnitude of the shift is predictable and reproducible if the solution conditions are maintained constant, it may change with the solution composition. In any pH study or any study involving different concentra-

- (21) O. A. Reutov and G. M. Ostapchuk, *Dokl. Akad. Nauk SSSR*, **117**, 826 (1957).
- (22) D. R. Pollard and J. V. Westwood, *J. Amer. Chem. Soc.*, **87**, 2809 (1965).
- (23) D. R. Pollard and J. V. Westwood, *J. Amer. Chem. Soc.*, **88**, 1404 (1966).
- (24) M. M. Kreevoy and E. A. Walters, *J. Amer. Chem. Soc.*, **89**, 2986 (1967).
- (25) R. A. G. Marshall and D. R. Pollard, *J. Amer. Chem. Soc.*, **92**, 6723 (1970).
- (26) R. A. G. Marshall and D. R. Pollard, *J. Organometal. Chem.*, **27**, 149 (1971).
- (27) K. P. Butin, A. N. Kashin, A. B. Ershler, V. V. Strelets, I. P. Beletskaya, and O. A. Reutov, *J. Organometal. Chem.*, **39**, 39 (1972).
- (28) R. B. Simpson, *J. Amer. Chem. Soc.*, **83**, 4711 (1961).
- (29) T. D. Waugh, H. F. Walton, and J. A. Laswick, *J. Phys. Chem.*, **59**, 395 (1955).
- (30) G. Schwarzenbach and M. Schellenberg, *Helv. Chim. Acta*, **48**, 28 (1965).
- (31) P. Zanella, G. Plazzogna, and G. Tagliavini, *Inorg. Chim. Acta*, **2**, 340 (1968).

tions of complexing agents, the solution conditions are not constant, so that the chemical reaction, whose rate may depend on the structure of the electrode-solution interface, may cause different potential shifts at different concentrations of complexing agents. Consequently, the results of such studies should be treated with some caution. It is possible to obtain unambiguous results by using concentrations low enough so that the chemical reaction does not exert a significant effect on the half-wave potential. This requires concentrations of $10^{-6}M$ or less, so that differential pulse polarography must be used. It is important to demonstrate that the half-wave (or peak) potential is independent of the concentration in order to be certain that the chemical reactions do not cause changes in the potential of the wave.

The second major factor in the determination of the half-wave potential, that of coordination with the buffer anions as well as hydroxide ions, is entirely predictable (14). Assume that there are three ions in the solution which form stable complexes with the electroactive species. If the three ions are represented by X , Y , and Z and the respective formation constants by K_X , K_Y , and K_Z , then the half-wave potential may be written as follows:

$$E = E^{\circ} - \frac{RT}{nF} \ln(K_X[X] + K_Y[Y] + K_Z[Z]) \quad (E)$$

It is assumed that the diffusion coefficients for the oxidized, reduced, and complexed species are equal, and that the activity coefficients are constant. In addition, the concentrations of the complexing agents must be at least 100 times larger than the concentrations of methylmercury in order to minimize changes in concentration at the electrode surface during electrolysis. In a real experiment, X ,

Y , and Z might represent the two buffer anions and the hydroxyl ion. Use of a supporting electrolyte with coordinating tendencies toward methylmercury would add a fourth variable to the equation. It is clear that the coordinating properties of all the ions in the solution must be considered when evaluating the significance of the half-wave potential. The fact that methylmercury forms complexes with most common buffer anions to about the same degree as hydroxide (23-31) attests to the futility of attempting pH studies without accounting for this behavior.

The differential pulse polarographic peak current vs. concentration curve for the first wave is linear from 10^{-7} to $10^{-4}M$ methylmercury. The extreme length of this linear range suggests that this technique may have analytical utility. Two improvements over previous procedures may be realized by this technique. First, sensitivities of $10^{-7}M$ or $20 \mu g/l.$ in the solution polarographed can be achieved. If a small degree of concentration can be effected during the required extraction procedures, it should be possible to accurately measure methylmercury concentrations less than $1 \mu g/l.$ in the original sample. Second, one may construct synthetic systems and study coordination chemistry at concentrations less than $10^{-6}M$. It is not possible to do this type of study with most of the normally used techniques. The main drawback to the use of polarographic means for measuring methylmercury concentrations is that the peak potential is dependent upon the solution conditions. However, this problem can be eliminated if sufficient care is taken to devise extraction procedures which yield reproducible solution conditions in the final solution.

Received for review June 6, 1973. Accepted November 29, 1973.

Mixed-Potential Mechanism for the Potentiometric Response of the Sodium Tungsten Bronze Electrode to Dissolved Oxygen and in Chelometric Titrations

P. B. Hahn,¹ D. C. Johnson, M. A. Wechter,² and A. F. Voigt

Department of Chemistry and the Ames Laboratory—USAEC, Iowa State University, Ames, Iowa 50010

Evidence is presented showing that an adsorption mechanism which was proposed in earlier work to explain the potentiometric response of the Na_xWO_3 electrode in alkaline solution is not correct. The potential response to dissolved oxygen in alkaline solution and the potential shift observed at the equivalence point in titrations of metal ions in ammoniacal solution with EDTA are explained by a mixed-potential mechanism. The potential is established as a result of the spontaneous oxidation of the Na_xWO_3 electrode by dissolved oxygen. These responses were found to be unique to the cubic Na_xWO_3 among all the highly conducting alkali metal tungsten bronzes.

Sodium tungsten bronzes, highly conducting nonstoichiometric compounds of formula Na_xWO_3 ($0.5 < x < 0.9$), have recently been demonstrated to be useful as po-

tentiometric indicating electrodes in alkaline solution for the determination of dissolved oxygen and for indicating the equivalence point in chelometric titrations of many metals with EDTA (1-3). The response to dissolved oxygen in the 0.2-8 ppm concentration range in 0.1M KOH-1mM EDTA was determined to be a linear function of the log of O_2 concentration with an unexpected large slope of approximately 120 mV/decade. For chelometric titrations in ammoniacal solution, negative potential shifts of 50-

¹ Present address, Radiation Management Corp., Philadelphia, Pa. 19104.

² Present address, Southeastern Massachusetts University, North Dartmouth, Mass. 02747.

(1) P. B. Hahn, M. A. Wechter, D. C. Johnson, and A. F. Voigt, *Anal. Chem.*, **45**, 1016 (1973).

(2) M. A. Wechter, P. B. Hahn, G. M. Ebert, P. R. Montoya, and A. F. Voigt, *Anal. Chem.*, **45**, 1267 (1973).

(3) P. B. Hahn, Ph.D. Thesis, Iowa State University, Ames, Iowa, 1973.

150 mV were observed at the equivalence point when 0.01–2.5 millimoles of metal ion were titrated with EDTA in the presence of dissolved oxygen. Moreover, substantial potential shifts were obtained in the titration of such electroinactive species as calcium(II), magnesium(II), and zinc(II) without the presence of an electroactive metal cation. Additional details concerning the response of the tungsten bronze electrodes may be found in References 1–3.

These observations cannot be explained in terms of simple oxidation-reduction reactions. The Nernst equation predicts either a 15 or 30 mV/decade response for the reduction of oxygen to water or to hydrogen peroxide, much less than the 120 mV/decade response experimentally observed. The apparent response to electroinactive species in the chelometric titrations also cannot be explained on the basis of simple redox reactions.

Very early in the course of these investigations, a correlation was made between the unique behavior of the Na_2WO_3 electrode and the presence of hydroxyl ion. The electrode potential is a function of hydroxyl ions exhibiting a negative shift with increasing concentration. At low pH, there is negligible potentiometric response to oxygen and to reducible metals (1, 2).

A mechanism was proposed for the response of the Na_2WO_3 electrode on the basis of adsorption of the negatively charged hydroxyl ion (1, 2). Numerous examples of adsorption mechanisms can be cited for the response of ion-selective potentiometric electrodes developed in recent years (4, 5). A similar mechanism would explain the response of the Na_2WO_3 electrode if uncharged oxygen molecules are strongly adsorbed at the electrode displacing hydroxyl ions and causing a positive potential shift. The success of EDTA titrations could be similarly explained only if the metal cations titrated are adsorbed displacing hydroxyl ions.

Observations from subsequent experiments, including voltammetric studies of the Na_2WO_3 and other alkali-metal tungsten bronze electrodes in alkaline solution, place serious doubt on the adsorption mechanism. Spontaneous oxidation of the Na_2WO_3 electrode and reduction of dissolved oxygen was demonstrated at potentials in the same potential region as the potentiometric response. These observations are consistent with those of Straumanis (6, 7) who demonstrated the oxidation of Na_2WO_3 to WO_4^{2-} (tungstate ion) during prolonged contact with alkaline solutions of oxidizing agents such as oxygen, sodium peroxide, and silver(I). The potential of the Na_2WO_3 electrode is now concluded to be a mixed potential resulting from the spontaneous reaction of the electrode with the oxidizing agents in the solution.

Mixed potential phenomena have been discussed by various authors (8–12) and are considered to arise when a nonequilibrium state exists involving two or more electrode processes. Such a state is associated with a spontaneous change at the electrode surface where simultaneous oxidation and reduction occur. The algebraic sum of the

partial currents at the electrode, $i_{\text{cathodic}} + i_{\text{anodic}}$, must be equal to zero and, since the partial currents are related to electrode potential, the mixed potential satisfying the condition of zero net current is established. If the voltammetric polarization curves of the cathodic and anodic processes can be individually determined, the value of the mixed potential can be calculated graphically by the method of Wagner and Traud (8) or mathematically if representative equations can be written for the rates of the partial cathodic and anodic processes (10, 11).

EXPERIMENTAL

Materials and Apparatus. The tungsten bronze crystals used for electrodes were cubic sodium tungsten bronze, Na_2WO_3 ($x \approx 0.65$ and 0.79); cubic lithium tungsten bronze, Li_2WO_3 ($x \approx 0.35$); tetragonal potassium tungsten bronze, K_2WO_3 ($x \approx 0.5$); and hexagonal potassium, rubidium, and cesium tungsten bronzes ($x \approx 0.3$). Details of the bronze preparation (13) and electrode fabrication (14) are presented elsewhere.

All solutions were prepared from reagent grade chemicals and deionized water. Gases used to establish a given oxygen concentration in solution were dry 99.995% nitrogen, 99.6% oxygen, Matheson "Zero" grade air, and specific oxygen-nitrogen mixtures (10.12, 3.27, 0.99, 0.35, and 0.10% O_2 by volume) prepared and analyzed ($\pm 2\%$ relative) by Matheson Gas Products.

Potential measurements were made with a Beckman Zeromatic SS-3 pH meter using a saturated calomel electrode as reference electrode. Voltammetric measurements were made with a Leeds and Northrup Electro-Chemograph Model E polarograph using a large area saturated calomel reference electrode (15).

Procedure. The response to metal ions in the 10^{-6} to $10^{-2} M$ concentration range was performed in 0.1M NH_4OH by diluting 5- μl to 10-ml aliquots of the appropriate 0.1M or 0.01M metal solution to 100–200 ml. The titration of 1 millimole of calcium(II) with 0.1M disodium ethylenediamine tetracetate (EDTA) and 0.3 millimole of EDTA with 0.1M CaCl_2 was also performed in 1M NH_4OH . The response to dissolved oxygen was determined in 0.1M KOH–1mM EDTA by equilibrating the solution with air or one of the five pre-mixed gases and measuring the potential of the bronze electrode vs. a SCE electrode after the potential reached a steady-state value (approximately 10 min). The temperature of the solution was maintained at $25 \pm 1^\circ\text{C}$ using a constant temperature bath. Solutions were stirred magnetically for all potentiometric measurements.

Voltammetric studies were performed with rotating bronze electrodes at 300 rpm. Voltage scans were from positive to negative at 0.200 V/min. The concentrations of dissolved oxygen were established as described for potentiometric measurements using the appropriate gas mixture.

RESULTS AND DISCUSSION

Figure 1 illustrates the potentiometric response of several alkali-metal tungsten bronze electrodes to dissolved oxygen in 0.1M KOH–1mM EDTA solution. The cubic $\text{Na}_{0.65}\text{WO}_3$ electrode exhibited the greatest response (~ 120 mV/decade) and a linear potential-log(O_2) relationship. The hexagonal $\text{Rb}_{0.3}\text{WO}_3$ and $\text{K}_{0.3}\text{WO}_3$ electrodes showed virtually no response and the cubic $\text{Li}_{0.35}\text{WO}_3$ exhibited a marginal 30 mV/decade response to dissolved oxygen. Significant response (60–80 mV/decade) was observed for the hexagonal $\text{Cs}_{0.3}\text{WO}_3$ and tetragonal $\text{K}_{0.5}\text{WO}_3$ electrodes but these electrodes responded much more slowly and much less reproducibly than the $\text{Na}_{0.65}\text{WO}_3$ electrode.

The potentiometric response of the $\text{Na}_{0.65}\text{WO}_3$ electrode to a number of metals in 1M NH_4OH is presented in Figure 2. Response was found to be limited to those species which are easily reduced in aqueous solution. Response to calcium(II) and other electroinactive species was extremely small while the responses to silver(I) (80–150

- (4) "Glass Electrodes for Hydrogen and Other Cations," G. Eisenman, Ed., Marcel Dekker, New York, N.Y., 1967.
- (5) "Ion-Selective Electrodes," R. A. Durst, Ed., National Bureau of Standards Special Publication 314, U.S. Government Printing Office, Washington, D.C., 1969.
- (6) M. E. Straumanis, *J. Amer. Chem. Soc.*, **71**, 679 (1949).
- (7) M. E. Straumanis and S. S. Hsu, *J. Amer. Chem. Soc.*, **72**, 4027 (1950).
- (8) C. Wagner and W. Traud, *Z. Electrochem.*, **44**, 391 (1938).
- (9) J. Koryta, J. Dvorak, and V. Bockackova, "Electrochemistry," Methuen and Co. Ltd., London, England, 1970, pp. 318–21.
- (10) D. Gray and A. Cahill, *J. Electrochem. Soc.*, **116**, 443 (1969).
- (11) J. M. Herbelin, T. N. Anderson, and H. Eyring, *Electrochim. Acta*, **15**, 1455 (1970).
- (12) J. O'M. Bockris and A. K. N. Reddy, "Modern Electro-Chemistry," Vol. 2, Plenum Press, New York, N.Y., 1970.

- (13) H. R. Shanks, *J. Crystal Growth*, **13**, 14, 433 (1972).
- (14) M. A. Wechter, H. R. Shanks, G. Carter, G. M. Ebert, R. Guglielmino, and A. F. Voigt, *Anal. Chem.*, **44**, 850 (1972).
- (15) A. I. Vogel, "Quantitative Inorganic Analysis," John Wiley and Sons, New York, N.Y., 1961.

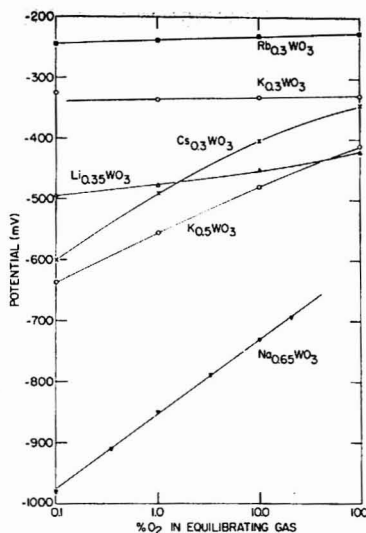


Figure 1. Oxygen response of hexagonal $\text{Rb}_{0.3}\text{WO}_3$, $\text{K}_{0.3}\text{WO}_3$, and $\text{Cs}_{0.3}\text{WO}_3$ electrodes, and cubic $\text{Li}_{0.35}\text{WO}_3$, tetragonal $\text{K}_{0.5}\text{WO}_3$ and cubic $\text{Na}_{0.65}\text{WO}_3$ electrodes in 0.1M KOH-1mM EDTA

mV/decade), ferricyanide (180-300 mV/decade), and copper(II) (~125 mV/decade) were very large, paralleling that for oxygen in alkaline solution. The responses of other alkali-metal tungsten bronzes to oxidizing agents in 1M NH_4OH were less than for Na_xWO_3 . The responses to copper(II) were 30-40 mV/decade.

Serious doubt was placed on the adsorption mechanism proposed in earlier work following the observations that the sodium tungsten bronze electrode responded only to oxidizing agents. The absence of response to calcium(II) and other electroinactive species was not consistent with the proposal that these species were causing the desorption of hydroxyl ion at the electrode surface and the observed potential shift at the equivalence point of chelometric titrations.

Current-potential (I - E) curves obtained at a $\text{Na}_{0.65}\text{WO}_3$ electrode in 0.1M KOH-1mM EDTA for several oxygen concentrations are presented in Figure 3. The curves were recorded scanning E from -0.4 to -1.5 V vs. SCE. The I - E curve exhibits the expected cathodic wave for the reduction of H_2O to H_2 at approximately -1.5 V vs. SCE. Also observed is an anodic wave beginning at -1.0 to -1.2 V vs. SCE, becoming extremely large at potentials more positive than -0.5 to -0.6 V vs. SCE. The anodic wave is attributed to the oxidation of the $\text{Na}_{0.65}\text{WO}_3$ electrode to tungstate ion (WO_4^{2-}). When oxygen was present, a cathodic wave was observed with a half-wave potential in the same potential range (-0.6 to -1.0 V) where the $\text{Na}_{0.65}\text{WO}_3$ oxidation takes place. Similar voltammetric curves were observed for a $\text{Na}_{0.79}\text{WO}_3$ electrode.

The existence of the anodic (Na_xWO_3 oxidation) wave in oxygen-free solutions at potentials more negative than the cathodic (O_2 reduction) wave provides strong evidence that spontaneous oxidation of the Na_xWO_3 electrode is occurring in the presence of oxygen in alkaline solution

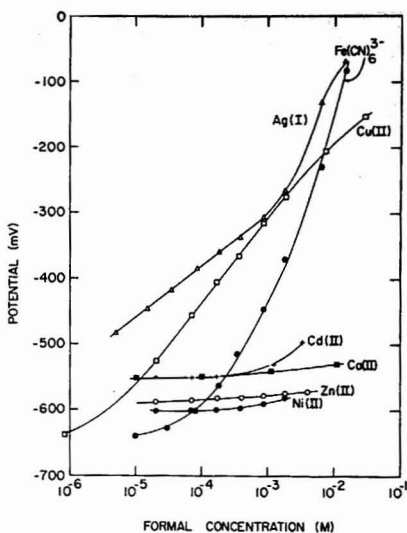


Figure 2. Potentiometric response of the $\text{Na}_{0.65}\text{WO}_3$ electrode to several species in 1M NH_4OH

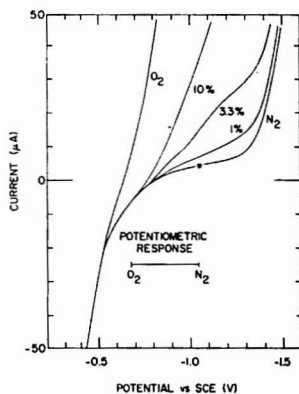


Figure 3. Voltammetric curves of $\text{Na}_{0.65}\text{WO}_3$ electrode in 0.1M KOH-1mM EDTA as a function of oxygen concentration. \star = open circuit potential in a nitrogen-saturated solution

and that the potential established at the electrode is a mixed potential.

The effect of varying the concentration of dissolved oxygen on the mixed potential is schematically illustrated in Figure 4. Represented in this figure are the anodic wave for the oxidation of the Na_xWO_3 electrode in 0.1M KOH-1mM EDTA and a series of cathodic waves for the reduction of oxygen at various concentrations ($C_1 < C_2 < C_3 < C_4$). The anodic wave is that obtained in a nitrogen-saturated solution while the cathodic oxygen waves were estimated by subtracting the anodic wave from the net I - E curves obtained in the presence of oxygen (Figure 3). The condition of equal and opposite anodic and cathodic currents (zero net electrode current) to establish the mixed

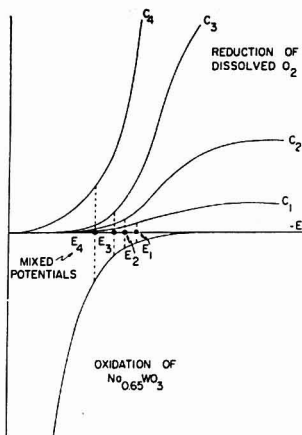


Figure 4. Schematic diagram illustrating the establishment of the mixed potential as a function of oxygen concentration

Per cent O_2 in gas mixture: C_1 , 1%; C_2 , 3.3%; C_3 , 10%; and C_4 , 100%

potentials is represented by the vertical dashed lines for the various concentrations of dissolved oxygen. The shift of the mixed potential toward positive values with increasing dissolved oxygen concentration is clearly illustrated.

Assuming the back reactions are negligible for the anodization of the tungsten bronze electrode and the reduction of dissolved oxygen, the net electrical current is given by Equation 1.

$$i_{\text{net}} = i_{\text{cathodic}} + i_{\text{anodic}} \\ = n_c F A k_c C_{O_2} \exp \left\{ \frac{-\alpha_c n_c F}{RT} E \right\} \\ - n_a F A k_a \exp \left\{ \frac{\beta_a n_a F}{RT} E \right\} \quad (1)$$

In Equation 1, the subscripts c and a denote that the designated quantities apply to the cathodic and anodic half-reactions, respectively, and α_c and β_a are empirical coefficients. The surface concentration of dissolved oxygen is C_{O_2} . At $i_{\text{net}} = 0$, $E = E_m$ and

$$n_c k_c C_{O_2} \exp \left\{ \frac{-\alpha_c n_c F}{RT} E_m \right\} = \\ n_a k_a \exp \left\{ \frac{\beta_a n_a F}{RT} E_m \right\} \quad (2)$$

Solving Equation 2 for E_m ,

$$E_m = \frac{2.3RT}{pF} \log \left\{ \frac{n_c k_c}{n_a k_a} \right\} + \frac{2.3RT}{pF} \log [C_{O_2}] \quad (3)$$

where

$$p = \beta_a n_a + \alpha_c n_c \quad (4)$$

Equation 3 is of the Nernstian form and at 25 °C

$$E_m = E_c + \frac{0.0591}{p} \log [C_{O_2}] \quad (5)$$

If the cathodic partial current is negligible in comparison to the limiting current for the reduction of dissolved oxygen, C_{O_2} equals the bulk concentration of oxygen, $C_{O_2}^b$. A

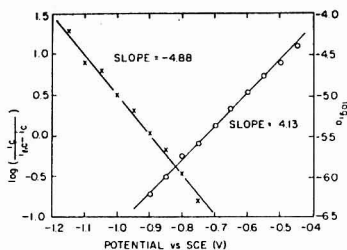


Figure 5. Results of wave analyses for anodic and cathodic partial currents illustrated in Figure 4

x = cathodic wave for solution equilibrated with 3.3% O_2 -96.7% N_2 mixture; o = anodic wave

plot of E_m vs. $\log[C_{O_2}^b]$ is expected to be linear with a slope of $0.0591/p$ mV/decade.

Analyses of the anodic wave for the electrode in oxygen-free solution and the cathodic wave for dissolved oxygen, corrected for charging current, are shown in Figure 5. A plot of $\log i_a$ vs. E for the anodic reaction is linear with a slope $\beta_a n_a / 0.0591$ at 25 °C. A plot of $\log i_c / (i_{l,c} - i_c)$ vs. E for the cathodic reaction, where $i_{l,c}$ is the limiting cathodic current, is linear with slope $-\alpha_c n_c / 0.0591$ at 25 °C. From the measured slopes, 4.13 and -4.88, $\beta_a n_a$ is 0.244 and $\alpha_c n_c$ is 0.289. The value of p in Equation 3 is 0.533 and the coefficient to $\log[C_{O_2}]$ in Equation 4 is 111 mV/decade. This is in excellent agreement with experimentally observed responses.

The large potentiometric response observed in the determination of oxygen, copper(II), and ferricyanide is consistent with other results reported in the chemical literature. Herbelin *et al.* (11) encountered similarly large potentiometric responses (125-250 mV/decade) for cerium(IV) and iron(III) when studying a mixed potential system involving the cerium(IV)/cerium(III) and iron(III)/iron(II) redox couples.

Responses larger than observed in this study could be obtained under unique conditions. If the cathodic current for the reduction of dissolved oxygen were diffusion limited, it would be directly proportional to the concentration of oxygen and independent of the electrode potential. A tenfold increase in the oxidant concentration would result in a tenfold increase in the cathodic partial current which in turn would require a tenfold increase in the anodic partial current to satisfy the condition of zero net current. It is evident from the wave analysis for the anodic wave (Figure 5) that this increase in anodic current would require a 250-mV shift in the mixed potential of the electrode.

The mixed-potential mechanism also provides excellent explanations for several secondary observations associated with the oxygen response of the Na_2WO_3 electrode (3). Any factor influencing either the rate of Na_2WO_3 oxidation or the rate of oxygen reduction will subsequently alter the mixed-potential response of the electrode. An enhanced response in the presence of trace silver(I) is explained in terms of trace silver depositing on the electrode and catalyzing the oxygen reduction. The poor oxygen response of Na_2WO_3 electrodes with low x value in LiOH is thought to be due to an adsorbed Li_2WO_3 layer inhibiting the bronze oxidation reaction. The day-to-day variations in electrode response to dissolved oxygen and the dependence of the potential on stirring rate can also be understood in terms of the mixed-potential mechanism. Changes in electrode surface characteristics may result

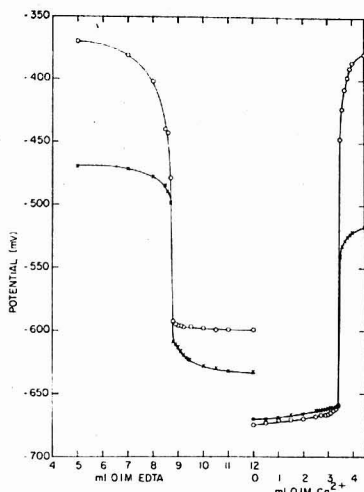


Figure 6. Titration of 1.0 millimole Ca^{2+} with 0.1M EDTA and 0.3 millimole EDTA with 0.1M Ca^{2+} with zero (x) and $5 \times 10^{-5}\text{M}$ (O) added Cu(II)

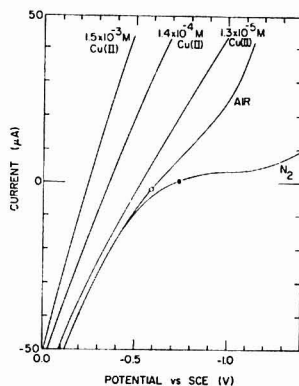


Figure 7. Voltammetric curves of $\text{Na}_{0.65}\text{WO}_3$ electrodes in 1M NH_4OH as a function of Cu(II) concentration

O, ★ = open circuit potentials

from the slow dissolution of Na_2WO_3 and possibly cause alterations of the anodic and cathodic reaction rates and the oxygen response. The shift in potential toward more negative values at slow stirring speeds is a result of a decrease in the rate of mass transfer of the electroactive species and the consequential decrease of the cathodic partial currents.

The substantial positive shift in the potential of the Na_2WO_3 electrode at the equivalence point in EDTA titrations of electroinactive species can also be explained by the mixed-potential mechanism. Evidence was found that trace copper(II) or some other oxidizing agent with a large formation constant for its EDTA complex would indeed act as a potentiometric indicator in these titrations. The addition of $1.3 \times 10^{-5}\text{M}$ copper(II) resulted in significantly larger potential breaks in both the titration of calci-

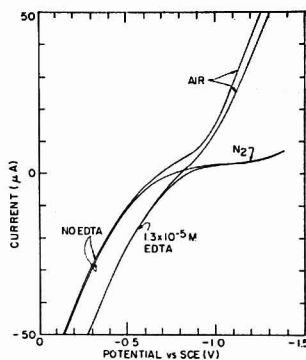


Figure 8. Voltammetric curves for the $\text{Na}_{0.65}\text{WO}_3$ electrode in 1M NH_4OH showing effect of added EDTA

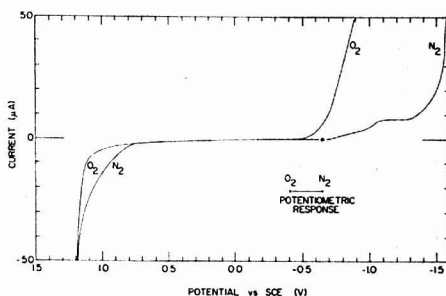


Figure 9. Voltammetric curves of cubic $\text{Li}_{0.35}\text{WO}_3$ electrode in oxygen and nitrogen-saturated 0.1M KOH -1mM EDTA solutions

★ = open circuit potential in nitrogen-saturated solution

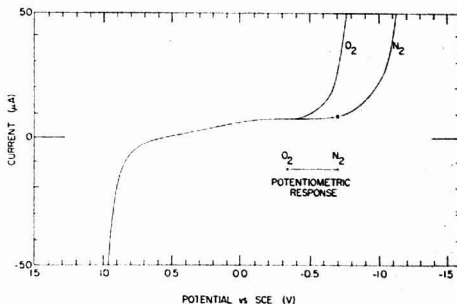


Figure 10. Voltammetric curves of hexagonal $\text{Cs}_{0.3}\text{WO}_3$ electrode in oxygen and nitrogen-saturated 0.1M KOH -1mM EDTA solutions

★ = open circuit potential in nitrogen-saturated solution

um(II) with EDTA and the titration of EDTA with CaCl_2 (Figure 6). Voltammetric curves of the $\text{Na}_{0.65}\text{WO}_3$ electrode in 1M NH_4OH at several copper(II) concentrations are presented in Figure 7. A positive shift in the mixed potential ($i_{\text{net}} = 0$) with increasing copper(II) concentration is demonstrated. In the complexometric titrations of calcium(II), copper(II) and other oxidizing agents were absent. The shift in the mixed potential at the equiva-

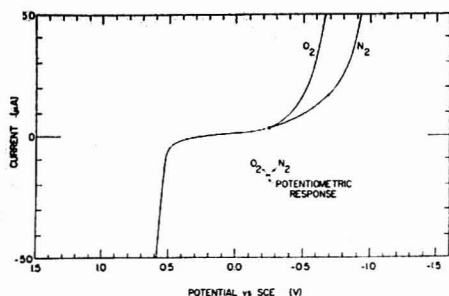


Figure 11. Voltammetric curves of hexagonal $\text{Rb}_{0.3}\text{WO}_3$ electrode in oxygen and nitrogen-saturated 0.1M KOH-1mM EDTA solution

★ = open circuit potential in nitrogen-saturated solution

lence point is actually due to the presence of EDTA. Figure 8 presents voltammetric curves for the $\text{Na}_{0.65}\text{WO}_3$ electrode in nitrogen and air-saturated 1M NH_4OH showing the effect of EDTA at a concentration of $1.3 \times 10^{-5}\text{M}$. The presence of trace EDTA shifts the anodic polarization wave for the oxidation of the $\text{Na}_{0.65}\text{WO}_3$ electrode to more negative potentials by 120-140 mV. This shift in the anodic wave results in a similar shift in the mixed potential established from the spontaneous oxygen reduction- Na_xWO_3 oxidation reactions and explains the potential break observed at the equivalence point in the chelometric titrations.

Both the large oxygen response and the large potential break in EDTA titrations are unique to the cubic sodium tungsten bronze electrodes. Voltammetric curves for several other highly conducting alkali metal tungsten bronze electrodes in 0.1M KOH-1mM EDTA are presented in Figures 9-12. Immediately apparent is the absence of any bronze oxidation wave at potentials between -0.5 and -1.0 V vs. SCE in oxygen-free solutions. The stability of these bronzes toward oxidation by dissolved oxygen is consistent with their poor performance in responding to dissolved oxygen and in detecting the end point in chelometric titrations.

The observations that cubic $\text{Li}_{0.35}\text{WO}_3$ and hexagonal $\text{Cs}_{0.3}\text{WO}_3$ exhibit some response and hexagonal $\text{K}_{0.3}\text{WO}_3$

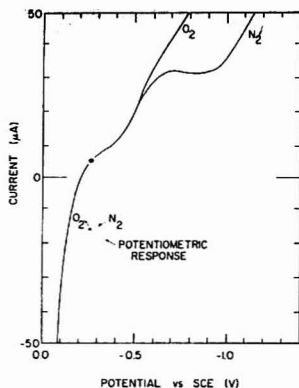


Figure 12. Voltammetric curves of hexagonal $\text{K}_{0.3}\text{WO}_3$ electrode in oxygen and nitrogen-saturated 0.1M KOH-1mM EDTA solutions

★ = open circuit potential in nitrogen-saturated solutions

and $\text{Rb}_{0.3}\text{WO}_3$ exhibit essentially no response to dissolved oxygen can be rationalized from their voltammetric waves and the mixed-potential mechanism. For both the $\text{Li}_{0.35}\text{WO}_3$ and $\text{Cs}_{0.3}\text{WO}_3$ electrodes, the cathodic oxygen wave begins at more positive potential than the open circuit potential in oxygen-free solution as required for response. However, the anodic wave is not in the region of the mixed potential. For the hexagonal $\text{K}_{0.3}\text{WO}_3$ and $\text{Rb}_{0.3}\text{WO}_3$ electrodes, the oxygen waves begin at more negative values of potential than the open circuit potential in oxygen-free solution. In these instances, dissolved oxygen is not a sufficiently strong oxidizing agent to participate in establishing a mixed potential and no response is noted.

ACKNOWLEDGMENT

The authors thank Howard Shanks of the Ames Laboratory for providing the tungsten bronze crystals used for construction of electrodes in this study.

Received for review August 20, 1973. Accepted November 14, 1973.

Mechanistic Studies Using Double Potential Step Chronoamperometry The EC, ECE, and Second-Order Dimerization Mechanisms

R. Joe Lawson¹ and J. T. Maloy

Department of Chemistry, West Virginia University, Morgantown, W. V. 26506

Chronoamperometry, the study of the current semintegral $m(t)$ in the potential step experiment, is suggested as a method for investigating the rates and mechanisms of chemical reactions following electrode reactions. Working curves obtained through exact methods and through digital simulation are presented to assist in the determination of reaction mechanisms and in the evaluation of rate constants for the EC, ECE, and second-order dimerization mechanisms. Because of the constancy (or near-constancy) of $m(t)$ at all points in the double potential step experiment, the uncertainty in the determination of $m(t)$ is shown to be small with respect to that associated with the determination of either the current or the charge; thus, chronoamperometry is proposed to be superior to either chronoamperometry or chronocoulometry in the study of subtle variations necessary for the elucidation of reaction mechanisms.

Semiintegration of current-time data in potential step and potential sweep experiments has been proposed as an analytical method because the current semintegral may be proportional to the concentration of the electroactive species present (1). More importantly, the current semintegral has been shown to achieve a constant value independent of the way the potential is changed from its initial value, so long as the concentration of electroactive species is virtually zero at the electrode surface (2). If a reactant R is oxidized or reduced to a product P in the electrode reaction



at a potential at which the concentration of R at the electrode surface is zero, the current semintegral $m(t)$ at any time t is given by

$$m(t) = nFACD^{1/2} \quad (2)$$

where n is the number of moles of electrons transferred per mole of R, F is Faraday's constant, A is the electrode area, C is the bulk concentration of R, and D is the diffusion coefficient of species R (2, 3). The invariability of $m(t)$ renders it particularly inviting to those engaged in the study of the kinetics of homogeneous reactions following an electrode reaction; variations in current, $i(t)$, or charge, $Q(t)$, during a short time experiment limit the effectiveness of these parameters in the study of the rates and mechanisms of following reactions. Thus, double potential step chronoamperometry, the study of $m(t)$ in a double potential step experiment, may offer important advantages over conventional chronoamperometric and chronocoulometric techniques in these mechanistic stud-

ies. Contained herein are working curves obtained from the semiintegration of digitally simulated double potential step current-time curves; these working curves illustrate the utility of the current semintegral in kinetic studies and serve as a theoretical basis for this novel use of the semintegral in mechanistic studies.

THEORY

The current semintegral has been defined (3, 4) as

$$m(t) = \frac{1}{\pi^{1/2}} \int_0^t \frac{i(\lambda) d\lambda}{\sqrt{t-\lambda}} \quad (3)$$

and may be regarded as that operation which, when performed twice on the function $i(t)$, results in $Q(t)$; hence, performing the operation once, as in Equation 3, results in semiintegration. In the double potential step experiment at a planar electrode when the potential is stepped from an initial potential E_0 , where no faradaic process takes place, to a potential E_1 , where the electrolysis of R takes place at a diffusion-limited rate for the time interval t_1 , and then stepped back to the potential E_2 , where the electrolysis of P occurs under diffusion-limited conditions, the current in the absence of kinetic complications is given (5) by

$$i(t) = \frac{nFACD^{1/2}}{\pi^{1/2}} \left[\frac{1}{t^{1/2}} - \frac{S_{t_1}(t)}{(t-t_1)^{1/2}} \right] \quad (4)$$

In this equation, $S_{t_1}(t)$ is the unit step function which is defined

$$\begin{aligned} S_{t_1}(t) &= 0 & \text{For } t \leq t_1 \\ S_{t_1}(t) &= 1 & \text{For } t > t_1 \end{aligned}$$

Substitution of Equation 4 into Equation 3 yields

$$\frac{m(t)}{nFACD^{1/2}} = \frac{1}{\pi} \int_0^t \frac{d\lambda}{\sqrt{\lambda(t-\lambda)}} = 1 \quad \text{For } 0 < t \leq t_1 \quad (5)$$

a result identical to Equation 2, and

$$\frac{m(t)}{nFACD^{1/2}} = 1 - \frac{1}{\pi} \int_{t_1}^t \frac{d\lambda}{\sqrt{(\lambda-t_1)(t-\lambda)}} = 0 \quad \text{For } t > t_1 \quad (6)$$

Thus, in kinetically uncomplicated double potential step chronoamperometry, the disappearance of the semintegral is observed at all times after the second potential step.

If the product of the initial electrode reaction is depleted so rapidly by the following chemical reaction that there is no current after the second potential step, the semintegral may be written

$$\frac{m(t)}{nFACD^{1/2}} = \frac{1}{\pi} \int_0^{t_1} \frac{d\lambda}{\sqrt{\lambda(t-\lambda)}} = \frac{2}{\pi} \sin^{-1} \sqrt{\frac{t_1}{t}} \quad \text{For } t > t_1 \quad (7)$$

¹ Present address, School of Chemical Sciences, University of Illinois at Urbana-Champaign, Urbana, Ill. 61801.

(1) K. B. Oldham, *Anal. Chem.*, **44**, 196 (1972).

(2) M. Grenness and K. B. Oldham, *Anal. Chem.*, **44**, 1121 (1972).

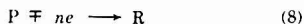
(3) P. E. Whiston, H. W. VandenBorn, and D. H. Evans, *Anal. Chem.*, **45**, 1298 (1973).

(4) K. B. Oldham and J. Spanier, *J. Electroanal. Chem. Interfacial Electrochem.*, **28**, 331 (1970).

(5) T. Kambara, *Bull. Chem. Soc. Jap.*, **27**, 523 (1954).

so that in the limit of very fast following reaction, $m(2t_f)$ is equal to one half $m(t_f)$.

Equations 6 and 7, then, represent the extreme conditions in the semiintegration of $i(t)$ in the double potential step experiment. To investigate the effects of kinetic complications at intermediate times, digital simulation was performed to obtain kinetically perturbed $i(t)$ curves for semiintegral transformation. In each of the mechanisms considered, the reaction given by Equation 1 was assumed at E_1 while its reverse



was assumed at E_2 , both occurring under diffusion-limited conditions. The effects of three different kinetic complications were simulated; these mechanisms are similar to three of those considered by Imbeaux and Saveant (6) in their recent development of convolutive potential sweep voltammetry. In each case the kinetic perturbation leads to the electroinactive entity X:

Mechanism EC₁ (first-order ec)—in this case, the kinetic complication was



where k_1 is a first-order rate constant.

Mechanism EC₁E (first-order ecc)—where the kinetic complication was



with P' subsequently electroactive at E_1



Mechanism EC₂ (second-order dimerization)—with the kinetic complication



where k_2 is a second-order rate constant.

After the effect of one of these kinetic perturbations upon $i(t)$ had been determined for a particular value of the dimensionless rate constant $k_1 t_f C^{1/2}$ (where j is the order of reaction in the rate determining step), the simulated current-time curve was semiintegrated at selected points along the curve.

For the EC₁E mechanism the current on the forward step has been shown (7) to be

$$i(t) = (nFACD^{1/2}/\sqrt{\pi t})(2 - e^{-k_1 t}) \quad (13)$$

for $t \leq t_f$. This may be substituted into Equation 3 in an attempt to obtain an analytical solution for the kinetically perturbed semiintegral

$$\frac{m(t)}{nFACD^{1/2}} = \frac{1}{\pi} \int_0^t \frac{(2 - e^{-k_1 \lambda}) d\lambda}{\sqrt{\lambda(t - \lambda)}} \quad (14)$$

Although this integral resists evaluation with elementary functions, it may be expressed

$$\frac{m(t)}{nFACD^{1/2}} = 2 - e^{-k_1 t/2} I_0(k_1 t/2) \quad (15)$$

where $I_0(k_1 t/2)$ is the zero order modified Bessel function of the first kind. This modified Bessel function may be computed through the expansion (8)

$$I_0(x) = 1 + \frac{x^2/4}{(1!)^2} + \frac{(x^2/4)^2}{(2!)^2} + \frac{(x^2/4)^3}{(3!)^2} + \dots \quad (16)$$

to obtain a numerical solution for $m(t)$ at any value of $k_1 t \leq k_1 t_f$. The numerical evaluation of $m(t)$ may be compared with that obtained through digital simulation to test the validity of the simulated curve.

DIGITAL SIMULATION

The digital simulation procedures for obtaining modified current-time curves have been described previously (9) and copies of the Fortran program used are available upon request. In these simulations, t_f was represented by L iterations so that Δt , the duration of a single iteration, was given by

$$\Delta t = t_f/L \quad (17)$$

The diffusion coefficients of all species were taken to be equal. During each iteration, the dimensionless current was calculated as the quantity $Z(t)$ where

$$Z(t) = \frac{i(t)t_f^{1/2}}{nFACD^{1/2}} \quad (18)$$

The value of $k_1 t_f C^{1/2}$ was defined as an input parameter at the outset of an individual simulation, and $Z(t)$ was obtained at Δt intervals for all t in the range $0 < t \leq 2t_f$. The resulting current-time curve was numerically semiintegrated and integrated to obtain dimensionless representations of both $m(t)$ and $Q(t)$. A new value of $k_1 t_f C^{1/2}$ was then selected, and the entire process was repeated.

The numerical semiintegration of $Z(t)$ was obtained through the series equivalent of Equation 3

$$m(k\Delta t) = \frac{1}{\pi^{1/2}} \sum_{j=1}^{k-1} \frac{i(j\Delta t)\Delta t}{\sqrt{k\Delta t - j\Delta t + \frac{1}{2}\Delta t}} \quad (19)$$

where $t = k\Delta t$ and $\lambda = j\Delta t$. The term $\frac{1}{2}\Delta t$ was included in the denominator of the sum because $Z(t)$, and hence $i(t)$, was calculated at the mid-point of each Δt interval; thus, each current term in the sum was divided by the square root of its distance from the upper limit of integration. Combination of Equations 17, 18, and 19 results in the form used to semiintegrate $Z(t)$

$$\frac{m(k\Delta t)}{nFACD^{1/2}} = (\pi L)^{-1/2} \sum_{j=1}^{k-1} \frac{Z(j\Delta t)}{\sqrt{k - j + \frac{1}{2}}} \quad (20)$$

RESULTS AND DISCUSSION

The semiintegrated results of several simulations are shown in Figure 1. That there is good agreement between the simulated results and Equations 5, 6, and 7 is shown by curves *a* and *c*. The rounded portion of curve *a* does not agree with Equation 6, but this is to be expected within a few iterations of the switching point.

There are two possible sources for this deviation between Equation 6 and curve *a* in the vicinity of the switching point: the digital simulation of the current-time behavior or the numerical semiintegration of the simulated $i(t)$ curve. Since numerical semiintegration of the exact $i(t)$ behavior (Equation 4) results in a nearly identical $m(t)$ curve, one may conclude that this discrepancy is due primarily to the method selected to semiintegrate the simulated $i(t)$ curve rather than an error in the simulation itself. The method employed herein has been found to give slightly better results than one employed previously (2) in those cases where exact solutions exist for comparison; thus, it seems reasonable to assume that the good-

(6) J. C. Imbeaux and J. M. Saveant, *J. Electroanal. Chem. Interfacial Electrochem.*, **44**, 169 (1973).

(7) G. S. Alberts and I. Shain, *Anal. Chem.*, **35**, 1859 (1963).

(8) M. Abramowitz and I. A. Stegun, "Handbook of Mathematical Functions, Applied Mathematics Series No. 55," National Bureau of Standards, U.S. Government Printing Office, Washington, D.C., 1965, p. 375.

(9) W. V. Childs, J. T. Maloy, C. P. Keszthelyi, and A. J. Bard, *J. Electrochem. Soc.*, **118**, 874 (1971).

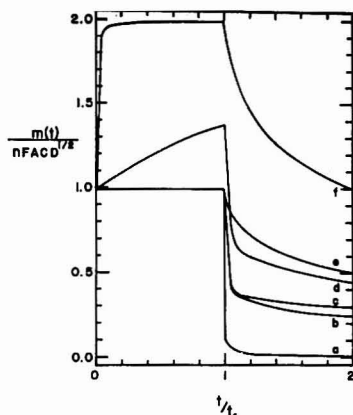


Figure 1. Simulated results of double potential step chronoamperometry under the influence of kinetic complications

All curves are the results of simulations with $L = 1000$. Curve a: Mechanism EC_1 , EC_2 , and EC_3 with $k_1 t_f C^{-1} = 0.001$. Curve b: Mechanism EC_2 with $k_2 t_f C = 1.0$. Curve c: Mechanism EC_1 with $k_1 t_f = 1.0$. Curve d: Mechanism EC_2 with $k_2 t_f = 1.0$. Curve e: Mechanisms EC_1 and EC_2 in the limit of large $k_1 t_f C^{-1}$. Curve f: Mechanism EC_1 in the limit of large $k_1 t_f$.

ness-of-fit in the vicinity of the switching point may be improved only by increasing the number of points sampled in this region. This was not deemed necessary, however; as t approaches $2t_f$ and the number of iterations becomes large (~ 2000), both curves a and e approach the values predicted by Equations 6 and 7. This indicates that the numerical semiintegration is most reliable when the number of iterations is large. For this reason, points were selected for the working curves presented below so as to avoid time intervals represented by a small number of iterations.

Curves b , c , and d show the effect of intermediate kinetic perturbations upon $m(t)$. Each curve was simulated with $k_1 t_f C^{-1}$ set equal to unity. It may be noted that $m(t)$ is neither zero nor constant after the switching point if there are kinetic complications; however, the slope of $m(t)$ after the switching point is small enough (maximum relative slope at $t = 2t_f$ is ~ 0.3) that its value can be determined at any point with a high degree of certainty.

Curves a , d , and f of Figure 1 show typical results expected with a system governed by the EC_1E mechanism. Here, $m(t)$ is not constant after the first potential step because the second electrode reaction contributes to the current. Since n is the same in both reactions, $m(t)$ doubles in the limit of large $k_1 t$. The simulated variation of $m(t)$ with $k_1 t$ is shown as the working curve in Figure 2. Superimposed on this working curve are several points evaluated through Equations 15 and 16; the agreement between the simulated working curve and that obtained through the modified Bessel function is within the uncertainty of electrochemical measurement. This working curve is similar to another previously published for this mechanism (10); however, the working curve in Figure 2 shows the variation of $m(t)$ rather than the variation of $i(t)t^{1/2}$. Since analog instrumentation is presently available to obtain $m(t)$ directly (11), this working curve en-

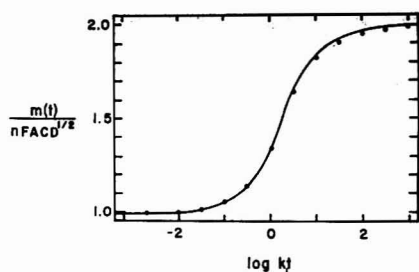


Figure 2. The chronoamperometric working curve for the single potential step study of the EC_1E mechanism. The curve is the result of the digital simulation and the points represent the exact solution (Equation 15)

Table I. Numerical Working Curves $m(2t_f)/m(t_f)$ vs. $k_1 t_f C^{-1}$ for Chronoamperometric Studies of Reaction Mechanisms^a

$k_1 t_f C^{-1}$	Mechanism EC_1	Mechanism EC_1E	Mechanism EC_2
0.001	0.008	0.009	0.008
0.01	0.013	0.015	0.013
0.10	0.055	0.071	0.055
0.40	0.167	0.200	0.148
1.0	0.301	0.326	0.245
3.0	0.440	0.434	0.354
10.	0.489	0.478	0.431
100.	0.502	0.500	0.487
∞	0.503	0.502	0.498

^aIn each simulation, $L = 1000$. ^bFor EC_1 and EC_1E , $k_1 t_f = 1000$; for EC_2 , $k_2 t_f C = 500$.

ables one to study the EC_1E mechanism through comparison with directly obtainable experimental data, thereby eliminating the need for tedious data treatment.

While single potential step methods are sufficient for the EC_1E mechanism, double potential step techniques must be employed for the other mechanisms treated because $m(t)$ is constant before the second potential step in each of these reaction schemes. One acceptable working curve for these mechanisms is the quantity $m(2t_f)/m(t_f)$ as a function of $k_1 t_f C^{-1}$, and this is given for each mechanism in Table I. The working curves presented in this table and Figure 2 enable one to distinguish between these mechanisms and to determine the rate constants for the homogeneous reactions through double potential step chronoamperometry.

These working curves are shown graphically in the upper three panels of Figure 3. For the sake of comparison, the quantities $i(2t_f)/i(t_f)$ and $Q(2t_f)/Q(t_f)$ for each of the mechanisms are also shown. While times other than t_f and $2t_f$ could have been selected for these working curves, measurements at these particular times are obtained easily experimentally, and both the simulation and numerical semiintegration are reliable at these points. If these times are used, it may be seen that the $m(t)$ ratio undergoes a greater change with variations in $k_1 t_f C^{-1}$ than the $i(t)$ ratio; in fact, the ratio for $m(t)$ almost shows as much variation as the ratio for $Q(t)$. This observation is important in mechanistic studies because it is often only through slight variations in curvature that one mechanism can be distinguished from another, and the greater the relative change in the measured parameter, the more reliably the curvature can be determined.

The chief advantage of double potential step chrono-

(10) M. D. Hawley and S. W. Feldberg, *J. Phys. Chem.*, **70**, 3459 (1966).

(11) K. B. Oldham, *Anal. Chem.*, **45**, 39 (1973).

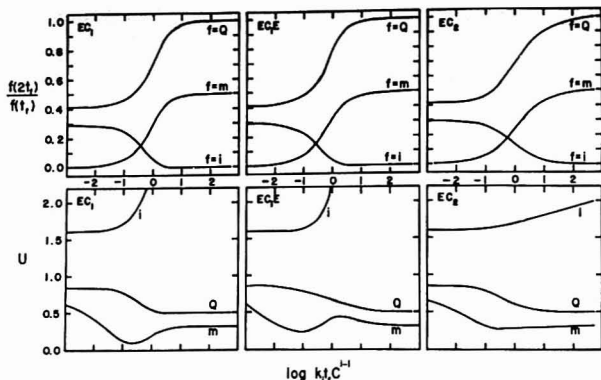


Figure 3. Working curves and uncertainties for the double potential step study of reaction mechanism

pometry in mechanistic studies, however, is the constancy (or near constancy) of $m(t)$. Even though $m(t)$ is not a constant after the second potential step for any mechanism, the variation of $m(t)$ is less than the variation of $i(t)$ or $Q(t)$ for all times during which the homogeneous chemical reaction influences these parameters. To illustrate this point, a quantity proportional to the relative uncertainty in the measurement of the value of the time-variant parameter at t_f and $2t_f$ was calculated for each $f(t)$ [either $i(t)$, $Q(t)$, or $m(t)$] at several values of $k_1 t_f C^{-1}$. This was determined by numerically evaluating the derivative of each $f(t)$ to obtain the relative slope $[f'(t)/f(t)]$ at t_f and $2t_f$. The absolute values of these quantities were then added to obtain U , a quantity proportional to the relative uncertainty in the determination of the ratio $f(2t_f)/f(t_f)$:

$$U = \left| \frac{f'(t_f)}{f(t_f)} \right| + \left| \frac{f'(2t_f)}{f(2t_f)} \right| \quad (21)$$

The variation of U with $k_1 t_f C^{-1}$ for each of the mechanisms is shown in the lower three panels of Figure 3. From these graphs, it is clear that if U is a valid measure of total relative uncertainty, $m(2t_f)/m(t_f)$ may be determined with a greater degree of relative certainty than either $i(2t_f)/i(t_f)$ or $Q(2t_f)/Q(t_f)$ for any of these mechanisms regardless of t_f . This direct result of the invariance of $m(t)$ suggests that double potential step chronoamperometry offers a more reliable way to compare experimental kinetic data with theory than either chronoamperometry or chronocoulometry.

The actual experimental uncertainty in the $f(2t_f)/f(t_f)$ ratio, of course, is not represented by U . Multiplication of U by dt , the experimental uncertainty in the recording of time, would yield relative uncertainty in the ratio determination. Further multiplication by the ratio itself would yield the absolute uncertainty in the measurement. Even if U is multiplied by $f(2t_f)/f(t_f)$ to obtain a quantity proportional to the absolute uncertainty in the ratio determination, this quantity is significantly less for $m(t)$ over most of the range in which kinetic complications cause a ratio varia-

tion with variations in t_f . (Obviously, since $i(2t_f)/i(t_f)$ under the influence of kinetic perturbation approaches zero in the limit of long t_f while $m(2t_f)/m(t_f)$ approaches zero as t_f approaches zero, the absolute uncertainties in each of these ratios approach zero in the same limits.) In addition, this development completely ignores the problem of charging currents which also contribute to the overall experimental uncertainty. Indeed, these may even be a more serious cause for experimental uncertainty in the determination of $f(2t_f)/f(t_f)$ than those discussed above. However, any discussion of the utility of the current semiintegral in the determination of charging effects is beyond the scope and intent of this communication. The alteration of chronoamperometric data by these effects is presently being investigated and it is anticipated that the results of these investigations will be the subject of a future publication.

CONCLUSIONS

Chronoamperometry has been shown to offer some important advantages over conventional chronoamperometry and chronocoulometry in the study of reaction mechanisms. In the study of the EC_1E mechanism, variation of $m(t)$ may be used directly to elucidate the mechanism and determine the rate constant. In double potential step studies of any of the mechanisms treated herein, chronoamperometry has been shown to lead to more reliable results because the semiintegral is either constant or varies slowly with time. The working curves presented above serve as a theoretical basis for mechanistic studies presently under way.

ACKNOWLEDGMENT

The authors wish to thank Keith B. Oldham and John Gruninger for their helpful discussions.

Received for review August 6, 1973. Accepted November 13, 1973. Research supported by the donors of the Petroleum Research Fund administered by the American Chemical Society.

Recording Polarization of Fluorescence Spectrometer—A Unique Application of Piezoelectric Birefringence Modulation

John E. Wampler and Richard J. DeSa

Department of Biochemistry, University of Georgia, Athens, Ga. 30602

This paper describes the action and application of an optical train which can be used to obtain a continuous measure of polarization of fluorescence when incorporated into a fluorimeter. The optical train consists of a piezoelectric birefringence modulator (variable retardance waveplate) and an analyzing polarizer. Theoretical analysis using Mueller calculus of the action of this optical train on partially polarized fluorescence shows that the intensity is modulated in time as the cosine of a sine function and that subsequent components (e.g., the detector) see a light flux of varying intensity but fixed polarization. The optical train has been incorporated into a complete on-line computer-controlled instrument system, which has been programmed to obtain polarization of fluorescence excitation spectra or polarization dependence on the temperature-to-viscosity ratio. The computer allows automated control, such as wavelength stepping, scan averaging, comparison among spectra, etc. Each spectrum is represented by up to 500 data points. The effective fluorescence bandwidth is greater than 25 nm over a range of 380–700 nm. Circuitry suitable for analog signal processing is described and details of hardware and computer software are presented with examples of the performance of the whole system.

Fluorescence measurements have become increasingly useful in chemical and biochemical research because of their sensitivity, selectivity, and precision. One very useful analytical fluorescence parameter is emission polarization which aids in the analysis of electronic structure and the molecular movements of biomolecules. However, polarization excitation fluorimetry has been exploited by only a few investigators, presumably because of the requirement for specialized instrumentation. In this paper, we describe a simple instrument capable of collecting high precision polarization of fluorescence spectra. Our instrument uses a piezo-optical birefringence modulator in an arrangement not previously described; no moving or rotating parts are used and only one photomultiplier is required. Significantly, the sample cell is bracketed by fixed excitation and emission polarizers making the polarization sensitivity of other components (e.g., monochromators, filters, photomultiplier, etc.) irrelevant. The optical components of the system could readily be adapted to most scanning fluorimeters without in any way altering their normal function. We have used an on-line digital computer system (1, 2) to control the instrument described here, but we also present analog circuitry suitable for processing the signal from the fluorimeter to give a direct readout of polarization.

THEORETICAL

Polarization of fluorescence emission can be measured by analyzing the vertical and horizontal components of emission caused by excitation with polarized light. One simple way to do this is to place a linear polarizer on the optical axis between the detector and the emission source (usually the emission is viewed at 90° to the axis of excitation). Under steady illumination, the analyzer is alternately set vertical or horizontal to obtain readings for the two components of the emission intensity. The polarization, P , is defined by Equation 1 as

$$P = \frac{I_v - I_h}{I_v + I_h} \quad (1)$$

where I_v is the vertical intensity component and I_h is the horizontal intensity component. Determining the polarization of fluorescence in this way, however, is not readily compatible with continuous measurement of a spectrum since the polarizer must be turned from vertical to horizontal at each wavelength at which P is to be determined. Mechanical rotation of the polarizer could be used to automate these measurements, a procedure employed by some workers (3, 4). The main limitations of this technique are limited time resolution and dependence upon the polarization sensitivities of analyzing components. Another approach to measuring P is to use two photomultipliers (4–8), one analyzing the vertical and one the horizontal component of the fluorescence. This technique requires careful matching of the photomultipliers and the precision of the results can be dependent upon the polarization sensitivity of other components of the optical system. In addition, such instruments are generally limited to making polarization measurements. Another possible method to measure P would be to fix the analyzer in the horizontal position and periodically interpose a half-wave plate between the fluorescent sample and the analyzer. Since a half wave plate in effect rotates the plane of polarization 90°, I_h would be measured without the plate in place and I_v with it. This method would be impractical because of the wavelength dependence of half-wave plates; also, it would require mechanical components if spectra were to be automatically scanned. The following theoretical analysis will demonstrate that the unique method employed in our instrument is somewhat analogous to this hypothetical half-wave plate method, but results in an instrument with no moving parts and with simple, electronic compensation for wavelength dependence. When a fluorescent sample is excited with vertically polarized light, the emission is depolarized because of Brownian rotation of the emitter, the degree of anisotropy of the emitting transition and other factors (9). The emission can be rep-

- (1) J. E. Wampler and R. J. DeSa, *Appl. Spectrosc.*, **25**, 623 (1971).
- (2) R. J. DeSa, in "Computers in Chemical and Biochemical Research," Vol. 1, C. Klotz and C. Wilkins, Eds., Academic Press, New York, N.Y., 1972.
- (3) J. Lavoncel, C. Vernotte, B. Arrio, and F. Rocher, *Biochimie*, **54**, 161 (1972).

- (4) R. H. McKay, *Arch. Biochem. Biophys.*, **16**, 438 (1969).
- (5) D. A. Deranleau, *Anal. Biochem.*, **16**, 438 (1966).
- (6) G. Weber and B. Bublousian, *J. Biol. Chem.*, **241**, 2558 (1966).
- (7) S. Ainsworth and E. Winter, *Appl. Opt.*, **3**, 371 (1964).
- (8) B. Wittholt and L. Brand, *Rev. Sci. Instrum.*, **39**, 1271 (1968).
- (9) P. P. Feofilov, "The Physical Basis of Polarized Emission," Consultants Bureau, New York, N.Y., 1961.

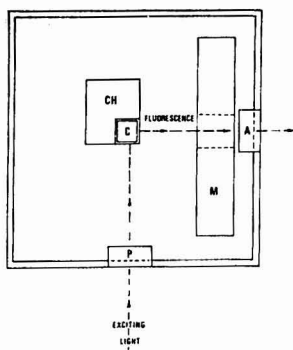


Figure 1. Complete polarization module of the polarization of fluorescence spectrometer

A, Analyzer; C, sample cuvette; CH, thermostated cuvette holder, M, piezoelectric birefringence modulator; P, polarizer

represented by the combination of a polarized and a depolarized component; thus, the Stokes vector for a fluorescence intensity, I_F , is $[I_F, -PI_F, 0, 0]$ where the brackets indicate a column vector and P is the polarization. In our system, this emission is passed through an "analyzing train" and the resultant light is detected by a photomultiplier (Figure 1). The analyzing train consists of a piezo-electric modulator and an analyzing polarizer. The modulator acts as a rapidly varying (50 KHZ) variable wave plate; the retardance, δ , produced by it is proportional to the voltage driving it and varies sinusoidally according to the following equation.

$$\delta = \delta_0 \sin(\omega t) \quad (2)$$

For a given applied voltage, the maximum retardance, δ_0 , is proportional to the ratio of this voltage to the wavelength of light being modulated. [See Kemp (10) for a full discussion of this device.]

The action of the modulator on the fluorescence emission can be analyzed rigorously using Mueller calculus as described by Shurcliff (11). Thus the effect of both modulator and polarizer on the fluorescent emission can be expressed in terms of a matrix which is the product of the matrices for each of the two devices. This matrix, MT, has the form shown where δ varies with time as indicated by Equation 2 above.

$$MT = \frac{1}{2} \begin{bmatrix} 1 & 1 & 0 & 0 \\ 1 & 1 & 0 & 0 \\ 0 & 0 & 0 & 0 \\ 0 & 0 & 0 & 0 \end{bmatrix} \begin{bmatrix} 1 & 0 & 0 & 0 \\ 0 & \cos \delta & 0 & \sin \delta \\ 0 & 0 & 1 & 0 \\ 0 & -\sin \delta & 0 & \cos \delta \end{bmatrix} = \begin{bmatrix} 1 & \cos \delta & 0 & \sin \delta \\ 1 & \cos \delta & 0 & \sin \delta \\ 0 & 0 & 0 & 0 \\ 0 & 0 & 0 & 0 \end{bmatrix} \quad (3)$$

polarizer modulator

The light beam which is seen by the detector is, then, the product of the matrix of this train and the Stokes vec-

(10) J. C. Kemp, *J. Opt. Soc. Amer.*, **59**, 950 (1969).

(11) N. A. Shurcliff, "Polarized Light," Harvard University Press, Cambridge, Mass., 1966.

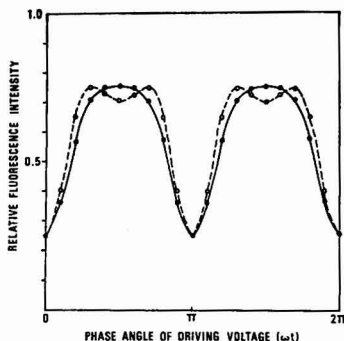


Figure 2. Variation of fluorescence intensity with time calculated from Equation 5

The piezoelectric modulator is operated at 50 KHZ. The solid line is for a maximum retardance, δ_0 , of π radians while the dashed line is for $\delta_0 = 1.22\pi$. This latter value gives the largest value for the integrated area under the curve

tor of the incident light and is characterized by a time dependent product vector:

$$MT[I_F, -PI_F, 0, 0] = \frac{1}{2} \begin{bmatrix} I_F - \cos(\delta) I_F P + 0 + 0 \\ I_F - \cos(\delta) I_F P + 0 + 0 \\ 0 + 0 + 0 + 0 \\ 0 + 0 + 0 + 0 \end{bmatrix} \quad (4)$$

The detector sees only a time variant plane polarized light beam with an intensity, I_d , given by Equation 4.

$$I_d = 0.5I_F - 0.5I_F P \cos[\delta_0 \sin(\omega t)] \quad (5)$$

The amplitude variation expressed by Equation 5 is shown in Figure 2 for a polarization value, P , of 0.5 and for maximum retardance values, δ_0 , of π and 1.22π . The peaks and troughs (for $\delta_0 = \pi$) represent I_v and I_h , respectively, and their values could be used in Equation 1 to calculate polarization. Obviously, any conventional analog demodulation circuit (e.g., a lock-in amplifier) used to process this waveform would need to take account of its marked asymmetry; a simpler analysis can be employed, however.

By using a photocurrent-to-voltage transducer at the photomultiplier anode, a time dependent voltage, V , is obtained. V is determined by the gain of the transducer, k , and the sensitivity of the photomultiplier, S ; thus the working form of Equation 5 is given by Equation 6.

$$V = kSI_d = 0.5kSI_F - 0.5kSI_F P \cos[\delta_0 \sin(\omega t)] \quad (6)$$

A mean voltage, V_m , defined as the average of V when it is examined for a time much longer than the cycle time of the modulator, is given by Equation 7,

$$V_m = \frac{\int V dt}{\int dt} = 0.5kSI_F - 0.5kSI_F P \frac{\int \cos[\delta_0 \sin(\omega t)] dt}{\int dt} \quad (7)$$

The integral in Equation 7 can be solved by numerical integration to give a constant mean value, C . Figure 3 shows C as a function of δ_0 .

If the modulator is switched off, the quartz becomes isotropic and the detector sees only the component of the

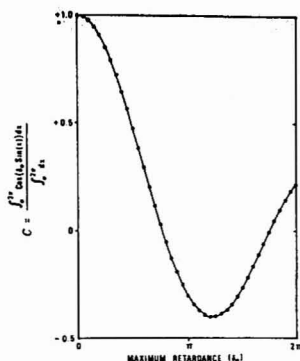


Figure 3. The mean value of $\cos[\delta_0 \sin(\omega t)]$ as a function of δ_0 . This value, C , goes to a minimum at 1.22π retardance corresponding to the maximum difference between the modulated and unmodulated signals.

incident light beam which can pass through the horizontal polarizer, the I_0 component, which gives a voltage, V_0 ,

$$V_0 = 0.5kSI_F - 0.5kSI_F P \quad (8)$$

It can readily be seen that if the ratio V_m/V_0 is taken, the gain, sensitivity, and intensity components of Equations 7 and 8 cancel and the working equation becomes

$$\frac{V_m}{V_0} = \frac{1 - CP}{1 - P} \quad (9)$$

When rearranged to give polarization, Equation 9 becomes

$$P = \frac{V_m - V_0}{V_0 - CV_0} \quad (10)$$

V_m can most readily be obtained by simply using a long time constant in the feedback circuit of the photocurrent-to-voltage transducer and V_0 is obtained when the driving voltage to the modulator is turned off.

The data of Figure 3 show that the optimum value of δ_0 for this analysis is 1.22π , corresponding to a C value of -0.402 . This value of δ_0 gives the largest absolute difference between V_m and V_0 , and the widest bandwidth in terms of the wavelength dependence of δ_0 (Figure 4). Figure 4 shows the control voltage required to give 1.22π maximum retardance from our modulator. The dashed lines of either side of this curve show the envelope of wavelengths of light which correspond to values of C (from Figure 3) which gave an error in the calculated polarization of 1% or less. From curves of this type, the bandwidth for a particular wavelength and a given acceptable error can be determined (Figure 4 inset). An examination of these data clearly indicates that the bandwidth for $<1\%$ error is wider than most fluorescence emissions and that the use of wideband filters or monochromators in the instrument could not deteriorate performance.

INSTRUMENTATION

The analyzing train of modulator and polarizer (Figure 1) is, of course, the heart of this instrument. The exciting light is vertically plane polarized, impinging upon the sample to excite partially depolarized fluorescence. The fluorescence is subjected to the retardance of the modulator (set at -45° to the vertical) and then passed through the horizontal analyzing polarizer. Figure 2 shows the time-dependent plane polarized intensity (expressed by

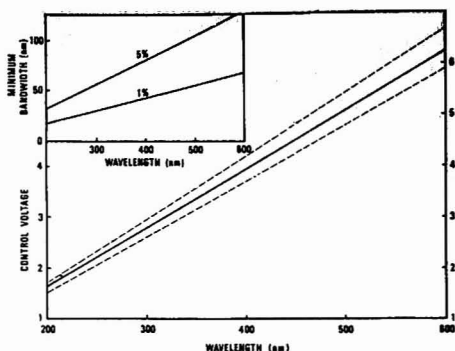


Figure 4. The required control voltage necessary to maintain 1.22π retardance as a function of wavelength (solid line). Since the calculation of polarization involves a retardance dependent term, C , the bandwidth of the calculation is limited. The dashed lines show the bandwidth allowed for a maximum calculation error of 1%. The inset shows this bandwidth as a function of wavelength for 1% and 5% maximum calculation error.

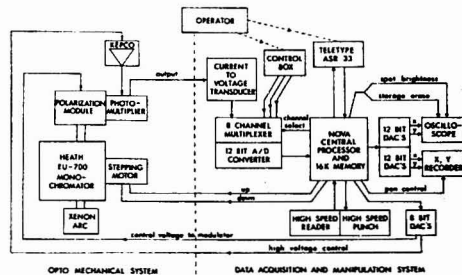


Figure 5. A diagram of the on-line recording polarization of fluorescence spectrometer which shows its organization into two major sections. This figure should be compared with Figure 1, ref. (1), and Figure 1, ref. (13).

Equation 5) seen by subsequent components. Almost any combination of filter or monochromator and photomultiplier could then be used to analyze this light beam. In fact, the moderate size of the modulator and polarizers and their fixed mounting position should allow conversion of many fluorimeters to measure polarization; since the sample cell and the modulator are between fixed polarizers, the polarizing characteristics of the remainder of the instrument will in no way affect the precision of the polarization measurements.

We constructed a complete instrument using this optical train, and the on-line computer system previously described (1, 2). Figure 5 is a block diagram of our complete fluorimeter. The light source is a 150-watt xenon arc powered by a current stabilized power supply (12). The excitation monochromator is a Heath EU-700 (Heath, Benton Harbor, Mich.) to which we have fitted a 200 step/revolution stepping motor (Model 23H-02A, Computer Devices, Inc., Santa Fe Springs, Calif.). The motor is coupled to the wavelength drive of the monochromator with appropriate gears so that 1 step of the motor produces a $1\text{-}\text{\AA}$

(12) R. J. DeSa, *Anal. Biochem.*, **35**, 293 (1970).

(13) R. J. DeSa and J. E. Wampler, *Applied Spectrosc.*, **27**, 279 (1973).

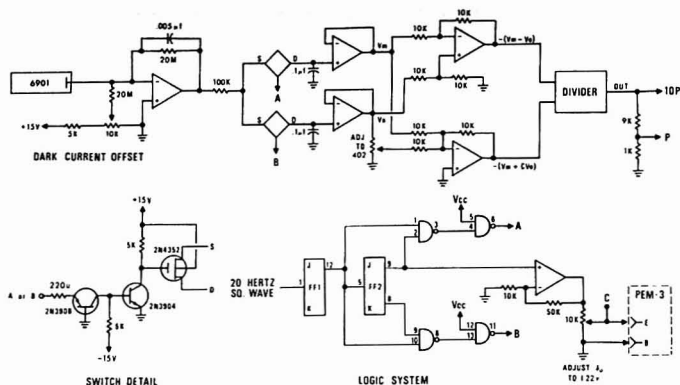


Figure 6. Complete analog circuit suitable for obtaining polarization of fluorescence spectra

All amplifiers are Analog Devices, Inc., Model 118. The divider is an Analog Device 432J. The flip flops (SN7473) and gates (SN7400) were obtained from Texas Instruments, Inc. The 20-hertz square wave can be obtained from any convenient source. The logic is designed to switch the photomultiplier in synchrony with the switching of the piezoelectric modulator.

change in wavelength. Light from the exit slit is vertically polarized by a Glan-Thompson prism (10-mm aperture, Karl Lambrecht, Chicago, Ill.) and impinges upon a 1-cm cuvette mounted in a thermostated holder (see Figure 1). The birefringence modulator is a commercial quartz unit with a 20-mm aperture and a 50-KHz resonant frequency (Model PEM-3, Morvue Electronics, Tigard, Ore.). The polarizer supplied with the modulator is placed immediately behind it, and is followed by an appropriate interference filter (Ditric Optics, Inc., Marlboro, Mass.). The detector is an EMI 9601 end window photomultiplier connected to an operational amplifier current-to-voltage transducer (shown in Figure 6). High voltage for the PM is supplied by a Kepco Model ABC 1500 power supply.

The computer program which directs data collection and controls other functions of the fluorimeter is a simple adaptation of existing software (1, 13). The necessary changes were easily implemented because of the modular form of our software package and the similarities between this instrument and the others we have described (1, 2, 13). For instance, stepping motor control (including "manual" wavelength scanning), scope display, and plotter functions are essentially identical to the other programs. Only the actual data acquisition and manipulation routines were rewritten. Figure 7 gives a simplified flow chart for the progress of a representative experiment. For details of the various program subroutines, the reader is referred to references 1 and 13.

Prior to collection of a polarization spectrum, a filter appropriate to the fluorescence being measured must, of course, be chosen and placed before the photomultiplier. The computer is then informed of the wavelength range to be scanned, the stepping rate to be employed, etc. via input from the teletype. Initial control functions are next performed by the computer: the programming voltage to the Morvue control unit is set by the computer via an 8-bit digital-to-analog converter (DAC) to that value which will maximize the difference between V_m and V_0 ; that is, the retardance, δ_0 , is set to 1.22π . The high voltage to the photomultiplier is also adjusted via an 8-bit DAC and finally the dark current (D) from the photomultiplier is evaluated (with the slits of the monochromator closed). The monochromator is then stepped to the starting wavelength and the polarization of the fluorescence spectrum

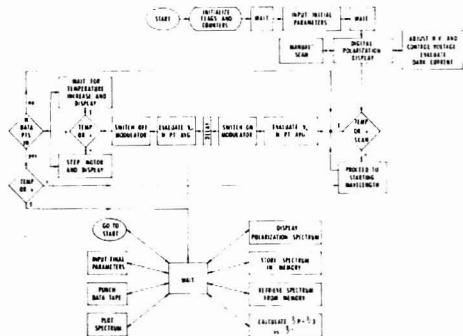


Figure 7. A simplified flow diagram representing the progress of a typical experiment

The solid arrows outline an obligatory sequence of events with the exception of those events selected by the control section (WAIT signifies a control section of the program where execution is suspended until the operator selects a routine from the teletype keyboard) of the program. The dashed arrows represent transfers in the progress of the experiment which are achieved when the operator interrupts the current routine from the teletype keyboard. The DELAY subroutine is needed because of the slow switching time of the piezoelectric modulator.

is obtained in the following manner. The control voltage to the Morvue control unit is set to zero, turning off the modulator; V_0 is measured by averaging 1000 analog-to-digital converter (ADC) samples of the photomultiplier output. The control voltage to the modulator is then set to that value determined to give 1.22π retardance and the computer collects a 1000-sample average of V_m . P is then calculated according to Equation 10:

$$P = \frac{V_m - V_0}{V_m + 0.402V_0 - 1.402D} \quad (10)$$

The P value at wavelength λ is stored in memory. The modulator is again switched off; the wavelength is stepped to the next appropriate value; and the data collection process is repeated. When a complete spectrum has been collected (usually 500 points), it is retained in memory to

Table I. Instrument Specifications and Performance

General specifications:

Light source: 150-W xenon arc (Osram)
 Excitation optical train: Heath EU-700 monochromator with 10-mm aperture Glan-Thompson prism (Lambert)
 Emission optical train: Morvue Model PEM-3 modulator and polarizer; Ditrac Optics interference filters
 Detector: EMI 9601B photomultiplier
 Slits: Variable to 2 mm
 Excitation bandwidth: variable to 4 nm
 Emission bandwidth: 6–10 nm
 Drive motor: Rapid-syn Model 23H-02A stepping motor
 Scan speed: 0.2 sec per data point (limited by modulator switching time)

Performance:

Fluorescein in glycerol:
 when $C \rightarrow 0$, $T/\eta \rightarrow 0$, then $P_0 = 0.452 \pm 0.002$
 Rhodamine B in glycerol:
 when $C \rightarrow 0$, $T/\eta \rightarrow 0$, then $P_0 = 0.463 \pm 0.005$
 Wavelength resettability: $\pm 1 \text{ \AA}$
 Data presentation scales: arbitrary
 Dark current: numerically corrected

become part of a running sum if scan averaging is desired (to further improve the signal-to-noise ratio) or the spectrum can be displayed and/or plotted.

The procedures involved in determining a polarization *vs.* temperature-viscosity profile are very similar to those for excitation spectra just outlined, except that the wavelength of exciting light is not altered. In order to collect this profile, the sample is precooled and then allowed to spontaneously warm to room temperature. The increase in temperature is monitored by the computer *via* the output of a Yellow Springs Model 42 SC telethermometer with a Model 423 probe. The probe must be painted flat black in order to minimize the reflection of fluorescence from its surfaces. Data are collected, as above, but at predetermined temperature intervals. Since the solvent viscosity varies nonlinearly with temperature, as does the temperature response of the thermistor probe, the computer is programmed to interpolate standard experimental curves for these two parameters. The data are displayed as the familiar $(1/P-1/3)$ *vs.* T/η plot for subsequent analysis (14).

The preceding discussion describes the operation of the fluorimeter when it is under direct computer control. Analog methods can also be used if the computer facilities are not available. The circuit shown in Figure 6 gives polarization directly so that spectra can be determined using a strip chart recorder, and the original stepping drive of the Heath monochromator.

The circuit is designed to switch the modulator on and off at a 5-Hertz rate, to sample the photomultiplier output during the on (V_m) and off (V_0) periods, and to com-

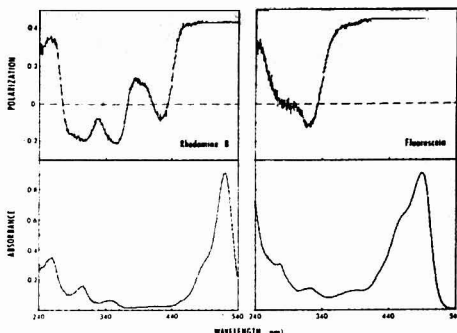


Figure 8. Polarization of fluorescence excitation spectra of Fluorescein and Rhodamine B in 98% glycerol at 20 °C

The lower portion of this figure shows the absorption spectrum of stock solutions. The polarization data were obtained using $10^{-6}M$ solutions. 520 nm and 580 nm emission filters, respectively, and a single scan

pute P from these signals. The sampling of the signal is delayed for 100 milliseconds after switching to allow for the slow response of the modulator to changes in the control voltage. Further details of the circuit are given in the legend to the figure.

PERFORMANCE

Performance specifications for the polarization of the fluorescence spectrometer are presented in Table I. Figure 8 shows some examples of spectra collected with the complete on-line instrument. These spectra are single scans of $10^{-6}M$ solutions in glycerol at 20 °C. Note that the expected fine structure is easily resolved. Scan averaging could, of course, be used to further improve the signal-to-noise ratio. Polarization values are routinely reproducible with a precision of greater than 1%.

The flexibility of the on-line instrument in collecting spectra or automatically collecting and displaying polarization *vs.* temperature-viscosity profiles emphasizes the advantages of computer controlled instruments. Data collection can be more extensive and more accurate, and the repetition and critical evaluation of experimental results is much easier. Since the program which controls this instrument shares data storage and format with the programs used to collect and manipulate fluorescence (1) and absorption (13) spectra, it is possible to compare data collected with one instrument with those collected with the others, to plot them together as in Figure 8, or to manipulate them in a variety of ways (1, 13).

Received for review September 5, 1973. Accepted November 20, 1973. Supported in part by Grants GM-16834-04 and 5 S05 RR07025-08 from the United States Public Health Service.

(14) G. Weber, *Biochem. J.*, **51**, 145 (1952).

Novel Mass Spectrometric Sampling Device—Hollow Fiber Probe

L. B. Westover, J. C. Tou, and J. H. Mark

Analytical Laboratories, Dow Chemical U.S.A., Midland, Mich. 48640

Hollow fiber probes, constructed of different permeable materials, were designed and evaluated as a mass spectrometric sampling device. A silicone rubber hollow fiber probe was found to be the most useful because of its unique properties of rapid preferential permeability as applied to direct monitoring, qualitatively and quantitatively, of the ppm level of volatile organic compounds in aqueous solution and in air. The molar enrichment factors of chloroform and methanol on passage through the silicone rubber hollow fiber of the probe were measured to be 1.1×10^4 and 8.3 in aqueous solution, and 53 and 23 in nitrogen atmosphere, respectively. Strong hydrogen bonding in aqueous solution is believed to be the most important reason leading to the higher detection limit for methanol, ~ 1 ppm, than for chloroform, ~ 10 ppb. Because of its speed and extremely high sensitivity, the technique is being used to analyze for trace volatile contaminants in aqueous solution and in air. This type of analysis would be very difficult, if not possible, by other methods.

To meet the low pressure ($<10^{-6}$ Torr) requirement inherent in the operation of a mass spectrometer, techniques involving restricted gas flow and temperature controlled evaporation are used in the design of the conventional mass spectrometric sampling devices (1). Recent advances in gas chromatograph-mass spectrometer (GC-MS) interfaces provide scientists with an extremely useful inlet for the analysis of complex mixtures (2). Most of the sampling devices that have been designed involve a batchwise sample introduction, which at times makes the study of a kinetic system rather difficult. Except for GC-MS sampling systems, other types of inlets lead to either low sensitivity of detection (reservoir inlet) or lack of quantitation (direct probe inlet).

In recent years, and also in the future, the detection and quantitative measurement of organic contaminants in water and air has become and will continue to be a matter of major concern in regard to the environment. As concern for the quality of these two life-giving elements of our biosphere grows, and the realization matures that some materials even at very low concentrations in the environment are harmful, the development of rapid and sensitive analytical techniques becomes a necessity. The mass spectrometric technique is one of the well-known techniques with high sensitivity and specificity. However, in solving the above analytical problems, the present inlet systems, including GC-MS, usually require considerable sample preparation, such as extraction, separation, etc. Following the fast change in composition of a chemical system is extremely difficult, if not impossible, with these inlet devices.

Employing the principle of the permeation of organic components across polymer membranes, hollow fiber probes, constructed of different permeable materials, have been designed and evaluated as mass spectrometric sampling devices. Reported here are descriptions of their construction, permeation characteristics, and some of the applications of the device. As revealed in the data presented, the device can be used to solve very difficult problems involving trace analysis for organic contaminants.

EXPERIMENTAL

Construction of the Hollow Fiber Probe. The majority of the hollow fibers used in the work were spun at Western Division Research of The Dow Chemical Co., Walnut Creek, Calif. The normal size of fibers used was 150–200 μ o.d. with a 25- μ wall thickness. Hollow fibers investigated included Dow Corning silicone rubber (DCSR), polyethylene (PE), regenerated cellulose (CEL), General Electric Co's Lexan MEM-213, polyethylene vinyl acetate copolymer (PE + VA), and polypropylene (PP).

Hollow fiber probes were constructed of both single and multiple fibers. A $\frac{1}{2}$ -in. length of hollow fiber was inserted approximately $\frac{1}{4}$ -in. into the end of a No. 23 hypodermic needle. The open end of the fiber and the space between the inserted fiber and needle wall were sealed with Dow Corning Silastic RTV-731. An 1–3-in. length of $\frac{1}{4}$ -in. stainless steel tubing was machined to insert into the hub end of the needle and soldered into place. Multiple hollow fiber probes were constructed in the same manner using a No. 13 hypodermic needle with the point removed. The number of fibers used ranged from 3 to 15. It was found necessary to pot each fiber carefully with silastic to obtain a satisfactory seal in multiple hollow fiber probes. A 10-element hollow fiber probe is shown in Figure 1. Attachment to a mass spectrometer direct inlet was achieved through the use of a Cajon Ultra-Torr fitting.

Chemicals. Chemicals used in the study were purchased technical grade materials. No attempt was made to purify any of the materials further.

Qualitative Characterization. Single hollow fiber probes constructed with different materials were used in the qualitative study of the permeation of organic compounds present in air and in water. Data obtained showed that the permeation of air and of water containing trace levels of the organic compounds tested was low enough that the normal operating pressure of 10^{-6} Torr could be maintained in the spectrometer source. Three types of mass spectrometers were used in the study: a Bendix Time-of-Flight Model 101 mass spectrometer, a Dow-built cycloidal mass spectrometer, and a DuPont 21-491 mass spectrometer.

Quantitative Characterization. A 10-element probe made with Dow Corning silicone rubber fiber was coupled directly to a Varian-MAT CH4B mass spectrometer equipped with an EFO4B source. The source temperature was regulated at 250 $^{\circ}$ C and the pressure was monitored to be 10^{-6} Torr with a Penning gauge. The multiplier voltage was kept at 1.6 kV with a 50-M Ω and 33-pF input to the amplifier.

In order to ensure that the solutes dispersed in water immediately upon mixing, standard solutions were prepared in methanol at the 0.01, 0.1, and 10% levels. A 30-cm³ bottle was filled with deionized water and closed tightly with a cap using a Teflon (DuPont)-lined silicone rubber septum leaving no head space. The fiber probe was passed through the cap and immersed in the water. Selective amounts of the prepared standard solutions were successively injected, using a micro syringe, into the water through the septum to prepare different concentrations. The solution was stirred magnetically and constantly. Recording of mass

(1) J. H. Beynon, "Mass Spectrometry and Its Applications to Organic Chemistry," Elsevier Publishing Co., New York, N.Y., 1960, Chapter 5.

(2) G. A. Junk, *Int. J. Mass Spectrom. Ion Phys.*, **8**, 1 (1972).

Table I. Qualitative Screening of the Probe Materials for Permeation of Compounds in Vapor Phase^a

Compound	DCSR ^b	PE ^b	CEL ^b	MEM-213 ^b	PE + VA ^b	pp ^b
Benzene	+	+	-	+	+	+
Toluene	+	+	-	+	+	+
Ethylbenzene	+	+	-	+	+	+
Styrene	+	+	-	+	+	+
Methylene Chloride	+	+	-	+	+	+
Carbon tetrachloride	+	+	-	+	+	+
<i>o</i> -Dichlorobenzene	+	+	-	+	+	+
Bromobenzene	+	+	-	+	+	+
Methanol	+	-	-	+	-	-
<i>sec</i> -Butanol	+	-	-	+	-	-
Decanol	+	-	-	+	-	-
Phenol	+	-	-	+	-	-
<i>o</i> -Chlorophenol	+	+	-	+	-	-
1-Methoxy-2-propanol	+	-	-	+	-	-
<i>n</i> -Hexane	+	+	-	+	+	+
<i>n</i> -Decane	+	-	-	+	+	+
Diethyl ether	+	+	-	+	+	+
Diphenyl oxide	+	-	-	+	+	+
Tetrahydrofuran	+	-	-	+	+	+
Aniline	+	-	-	+	+	+
Nitrobenzene	+	+	-	+	+	+
Pyridine	+	+	-	+	+	-
Acetone	+	+	-	+	+	+
Formaldehyde	+	-	-	+	+	+
Benzaldehyde	+	+	-	+	+	+

^a The permeation of compounds through the Silastic seal was found to be insignificant. ^b See the Experimental Section.

Table II. Comparison of Permeation Times of Two Hollow Fiber Probes

Fiber	Compound	Approx. time from immersion to detection	
		Vapor	100 ppm in H ₂ O
Silicone	Acetone	1-2 sec	19 sec
	Ethanol	1-2 sec	Not observed
	Hexane	<1 sec	<1 sec
	Benzene	<1 sec	<1 sec
	Methylene chloride	<1 sec	1-2 sec
	Isobutyl alcohol	3 sec	Not observed
	Methoxyflurane	<1 sec	1 sec
	CH ₃ OCF ₂ CHCl ₂		
Polyethylene	2,4-Dichlorotoluene	3 sec	Not run
	Acetone	17 sec	
	Ethanol	25 sec	
	Hexane	6 sec	
	Benzene	4-5 sec	
	Methylene chloride	3-4 sec	
	Isobutyl alcohol	2 min	

spectra was delayed approximately 2-3 minutes after each injection to allow the solution to become homogeneous. The responses of the ion peaks of interest were recorded in arbitrary units.

In the study of gas phase contaminants, a 2800 ppm by volume standard mixture of chloroform or methanol in nitrogen was prepared in a 5-l. Saran (The Dow Chemical Co.) bag purchased from Ansapac, Ann Arbor, Mich. The 10-element fiber probe used in the previous study was inserted into a 12-l. Saran bag filled with 10 l. of nitrogen and connected to the mass spectrometer with use of a Cajon Ultra-Torr fitting. The portion of the hollow fiber probe in the bag was protected from possible damage with a slit plastic sleeve during the kneading of the bag, as required for thorough mixing. Selective amounts of the standard mixture were injected successively into the 12-l. bag with a gas syringe to prepare different concentrations. A piece of Scotch tape was placed on the bag where the injection was to take place in order to strengthen the bag wall. The hole made by the syringe needle was immediately sealed with a second piece of Scotch tape. Mixing was achieved by kneading the bag. Mass spectra were taken ap-



Figure 1. A 10-element hollow fiber probe

proximately 2-3 minutes after each injection. Responses of ion peaks of interest were recorded.

RESULTS AND DISCUSSION

Qualitative Characterization. The initial effort was concentrated on the qualitative screening of the different probe materials. Thirty different organic compounds were selected as being representative of various classes of compounds in the screening experiments. The probe was immersed at ambient temperature in the vapor of each compound above its liquid in a bottle open to the air. The data are shown in Table I. The plus sign or minus sign indicates that the mass spectrum of the compound was or was not observed, respectively. The absence of either sign indicates the material was not examined. The time to detection after immersion in the compound vapor differed widely over the range of compounds tested. This is shown in Table II for two probes, silicone rubber and polyethylene, both in the compound's vapor and its aqueous solutions at a concentration of 100 ppm. The difference in detection times suggests that the transfer of the solute from water to the fiber is dependent on the degree of hydrogen bonding of the solute with water. As shown later, the levels of detection in water were found to vary in the same direction as the detection times. As indicated in Tables I and II, the hollow fiber probe made of silicone rubber was found to have superior performance over probes made of other materials.

In an attempt to show the usefulness of the probe inlet in cases other than the well-controlled system, a single element silicone rubber hollow fiber probe was used to monitor concentrations of methoxyflurane (CH₃OCF₂CHCl₂) an anesthetic, in blood. The probe was embedded in the venous blood stream of a rat after the animal had been anesthetized with a suitable non-mass spectrometric interfering second anesthetic. The animal was then exposed to methoxyflurane for a short period following which the source of the second anesthetic was removed. The mass spectrometric response to the most intense peak, *m/e* = 81, in the mass spectrum of methoxyflurane, as shown in Figure 2, was rapid, being observed approximately 0.5 min after the start of the exposure and rising to a maximum in 1.5 min. Following removal of the source of the anesthetic, the level of methoxyflurane in the blood stream dropped to less than one-tenth the maximum level in one minute.

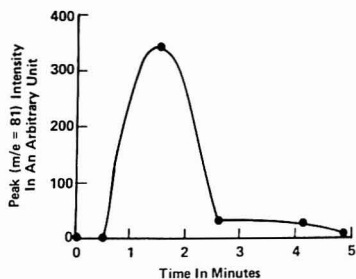


Figure 2. Mass spectrometric response to methoxyflurane in venous blood stream of a rat

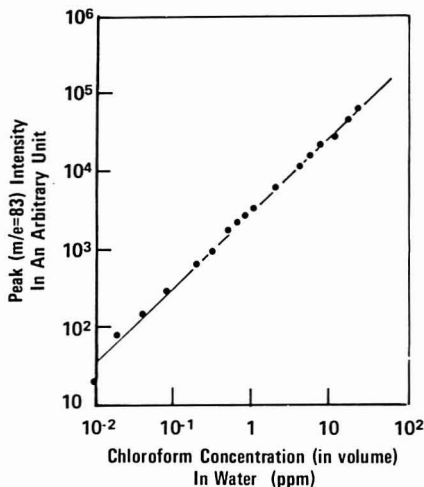


Figure 3. Response curve for chloroform in water

Such a rapid analysis would be extremely difficult, if not impossible, by other methods.

As with any other method, the hollow fiber probe technique faces its own limitations. The volatility of a compound at ambient temperature is anticipated to be the most limiting factor. Strong interaction between solute and water and low permeability through the polymer membrane are also expected to affect the sensitivity of the probe. For example, the silicone rubber hollow fiber probe was found to be a very effective device for determining the sub-ppm level of dimethylmercury in water. However, efforts to observe methylmercury chloride in water were unsuccessful, apparently due to the ionic character of the chloride in aqueous solution.

Quantitative Characterization. The hollow fiber probe made of silicone rubber was further investigated for quantitative characteristics. The mass spectrometric responses of chloroform and methanol in both water and nitrogen at different volume concentrations are shown in Figures 3 to 5. The linear relationships between responses and concentrations over several orders of magnitude are clearly shown in the figures and this indicates the usefulness of the probe for quantitative analysis. Generally speaking, the data points are more scattered in the case of measure-

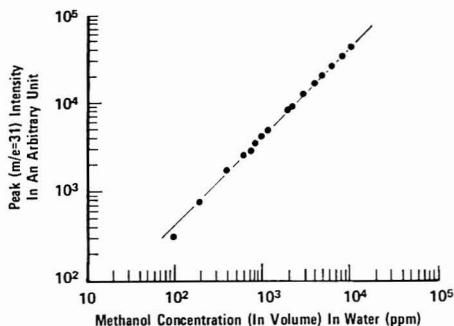


Figure 4. Response curve for methanol in water

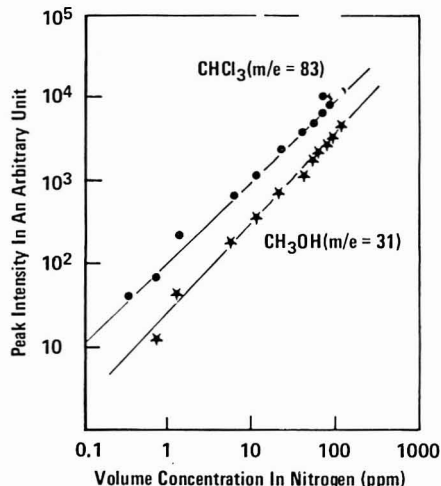


Figure 5. Response curves for chloroform and methanol in nitrogen

ments of compounds in the gas phase than in the aqueous phase. This is believed to be caused by insufficient mixing in the gas phase in the kneading operation.

When comparing Figures 3, 4, and 5, the responses of chloroform and methanol are quite different in aqueous solution but, on the other hand, exhibit similar magnitude in the gas phase. The detection limit for chloroform in water under conditions examined is estimated to be 10 ppb as compared to ~1 ppm in the other cases studied. The problem can be analyzed in the following way.

An enrichment factor, E , is defined as

$$E = \frac{\text{mole fraction observed in a mass spectrometer } (X')}{\text{mole fraction prepared in aqueous solution or nitrogen } (X)} \quad (1)$$

The quantity, X' , can be determined by

$$X' = K_a I_a / K_b I_b \quad (2)$$

with

$$K_a = S_a/S_c \text{ and } K_b = S_b/S_c$$

In this expression, S_a , S_b , and S_c are the mass spectro-

Table III. Enrichment Factors Determined with Use of a Silicone Rubber Hollow Fiber Probe

Compounds	Media	
	Aqueous solution	Nitrogen atmosphere
CHCl ₃	1.1×10^4	53
CH ₃ OH	8.3	23

metric mole sensitivity factors (scale divisions/micron) predetermined for the compound, water (or nitrogen), and *n*-butane which was chosen for standardization of the instrument used. These three quantities were calculated based on the intensities of the peaks at masses *a*, *b*, and *c* (*m/e* = 58), respectively. Quantities, *I_a* and *I_b*, are the intensities of the corresponding peaks measured. For a first approximation, the quantities *K_a* and *K_b* will not be instrument-dependent. Substituting Equation 2 into Equation 1, we obtain

$$E = \frac{K_a I_a / X}{K_b I_b} \quad (3)$$

The following data were determined at ambient temperature with use of a DuPont 21-104 mass spectrometer,

$$K_{\text{CHCl}_3}, m/e \ 83 = 0.21$$

$$K_{\text{CH}_3\text{OH}}, m/e \ 31 = 0.22$$

$$K_{\text{H}_2\text{O}}, m/e \ 18 = 0.21$$

$$K_{\text{N}_2}, m/e \ 28 = 0.15$$

The quantities, *I_b* and *I_a*/*X*, were measured from the corresponding spectrum and the slope of the linear response curve, respectively, after converting the volume concentrations to the mole ratios. The calculated enrichment factors are shown in Table III.

The drastic difference in the enrichment is clearly demonstrated. In the gas phase, the interaction between molecules is very minor. Therefore, the measured enrichment factors of chloroform and methanol reflect the difference in their permeabilities through the silicone rubber fiber. On the other hand, in aqueous phase, the enrichment is dependent not only on the permeability which is the prod-

uct of solubility and diffusivity of the compound but also on the interaction between molecules of solvent and solute. Strong hydrogen bonding between molecules of water and methanol and weak interaction between molecules of water and chloroform are believed to be the most important reason leading to the drastic difference in the measured enrichment factors of the two compounds.

CONCLUSION

The construction of the hollow fiber probe as a mass spectrometric sampling device was described. Among probes made of different materials, the silicone rubber probe was found to be the most useful because of its unique properties of rapid preferential permeability for volatile organic compounds. The probe serves as a means not only of pressure reduction, but also for the enrichment of volatile organic components in aqueous solution and in air. This leads to its great usefulness in direct monitoring, qualitatively and quantitatively, of the ppm level of volatile organic compounds in aqueous solution and in air. The sensitivity of the probe for measurements in aqueous solution varies widely according to the degree of hydrogen bonding between water and solute. The detection limit in the case examined is estimated to be 10 ppb for chloroform, where there is no significant hydrogen bonding, as contrasted to 1 ppm for methanol, where strong hydrogen bonding occurs. Generally speaking, the sensitivity is dependent on both the permeability of the organics across the polymer membrane and the matrix effects like hydrogen bonding.

Because of its fast response to the volatile organics, the probe technique has also been used successfully in the studies of many kinetic systems (3, 4).

ACKNOWLEDGMENT

The authors express their thanks to T. Ts'o, M. Chenoweth, J. Davis, and G. Kallos for valuable discussions and experimental assistance.

Received for review August 20, 1973. Accepted November 26, 1973.

- (3) J. C. Tou, L. B. Westover, and L. F. Sonnbend, 167th National Meeting, ACS, Div. of Anal. Chem., Los Angeles, Calif., April 1974.
- (4) J. C. Tou and G. J. Kallos, 167th National Meeting, ACS, Div. of Environ. Chem., Los Angeles, Calif., April 1974.

Quantitative Dye Laser Amplified Absorption Spectrometry

Robert C. Spiker, Jr.,¹ and James S. Shirk

Department of Chemistry, Illinois Institute of Technology, Chicago, Ill. 60616

If the sample is included inside the optical cavity of a broad band organic dye laser, it is possible to use weak absorptions for quantitative analysis. For Ho^{3+} and Pr^{3+} solutions in the range 5×10^{-3} to 10^{-4} M with optical densities in the range ~ 0.005 to ~ 0.0001 , the laser intensity is related empirically to the sample concentration. The method can be used for gases and for atomic absorptions as well as for solutions. The sensitivity of the technique may be increased several orders of magnitude.

Dye laser technology has progressed rapidly. There are now commercially available flashlamp pumped dye lasers covering the wavelength range 3500 Å into the near infrared. A variety of spectroscopic and analytical uses have been devised for these lasers. Recently we, and others, have reported a laser technique for detecting very weak absorptions (1-4). In this technique, an organic dye laser that is operating with a broad band (10-20 nm bandwidth) output is used. The sample is placed within the optical cavity of the laser. When an absorber is placed in the laser cavity, the laser action is substantially decreased or completely quenched at the absorbed wavelengths. The wavelength dependent losses introduced by even a very weak absorber decrease the laser output intensity selectively. By directing the output into a monochromator or a spectrograph, it is possible to use a dye laser to detect weak absorptions. Sample absorptions with optical densities ($\log I_0/I$) equal to 5×10^{-5} or smaller have been detected by this method (1). This technique has been used on gaseous and solution samples. It has also been used to detect atomic absorptions in flames and free radicals produced by flash photolysis. It is clear that this technique can be used to increase the sensitivity of an absorption measurement by two to three orders of magnitude beyond conventional methods, with the possibility of an even greater enhancement.

Earlier work demonstrated that this technique can be used for qualitative detection of species with very weak absorptions. For an analytical chemist, there remained the question as to whether the technique could be used for quantitative analysis of molecules with weak absorptions. In this paper, we give results which show that, with the proper calibration, the technique can be used for quantitative analysis. Reliable calibration graphs of laser intensity vs. concentration of some rare earth ion (Ho^{3+} , Pr^{3+}) solutions are constructed. Rare earth ion solutions were used for two reasons. The half width of the absorption bands is about 1 nm; thus, it is easy to ensure that the slit width of our monochromator is narrow with respect to the

absorption band width, and the absorption bands are sufficiently weak so that direct spectrophotometry is not applicable to dilute solutions.

THEORY

The origin of the sensitivity of the intracavity absorption technique can be understood simply. We define a quantity $G = \alpha/L$, where α is the unsaturated single pass gain in passing through the dye solution and L is the sum of the losses in the cavity, including the losses due to absorption by the sample. When $G \gg 1$, the gain is sufficient to overcome the losses and lasing will occur. In any laser, both G and, consequently, the laser intensity will be wavelength dependent. Figure 1 gives an idealized picture of G vs. wavelength for a broadband organic dye laser with a weak absorber inside the optical cavity. A small intracavity absorption increases the cavity losses and thus decreases G where the absorption occurs. This small change in G causes a dramatic change in the intensity of the laser output. By monitoring the wavelength dependence of the intensity of the laser output, it is possible to obtain a spectrum of a very weak absorber. For quantitative studies, it is expected that the intensity of the laser might be a rather complex function of G , and thus also of the losses due to the absorption by a sample inside the cavity.

The calculation of the intensity of a dye laser as a function of small additional losses in the cavity is difficult, and the result is not yet available in closed form for a satisfactory model. In this paper, we construct an empirical correlation between sample absorption and laser intensity that is useful for quantitative analysis. We report our data as plots of I_0/I vs. sample concentration, where I_0 is the laser intensity with no sample in the cavity and I is the laser intensity with a sample in the cavity. We also use plots of concentration vs. $\Delta I/I_0$ (5) where $\Delta I = I_0 - I$.

Theoretical treatments of dye laser quenching are available. Hänsch, Schawlow, and Toschek (4) gave a description of the quenching of a continuous dye laser by an intracavity absorber. However, they calculated only the ultimate sensitivity of the technique and not the functional form of the dependence of the laser intensity upon the extinction coefficient of the absorber. Keller, Zalewski, and Peterson (3) numerically solved a set of coupled differential equations for a model of a pulsed dye laser. Their results imply that a quantitative relationship between sample absorbance and laser intensity is possible for a particular laser; however, their results are not given in a useful closed form.

EXPERIMENTAL

Apparatus. Figure 2 shows a diagram of the experimental apparatus. A commercial (Chromabeam 1050, Synergetics Research Inc, Princeton, N.J.) dye laser was used. In order to obtain a broad band output, the intracavity grating was replaced with a 1.0-m radius of curvature mirror coated for maximum reflectivity in the range 450-650 nm. The dyes used were 7-diethylamino-4-methylcoumarin or Rhodamine 6G, both at 4×10^{-5} M in etha-

¹ Present address, NIAMD, National Institutes of Health, Bethesda, Md. 20014.

(1) R. J. Thrash, H. von Weysenhoff, and James S. Shirk, *J. Chem. Phys.*, **55**, 4659 (1971).

(2) N. C. Peterson, M. J. Kurylo, W. Braun, A. M. Bass, and R. A. Keller, *J. Opt. Soc. Amer.*, **61**, 746 (1971).

(3) R. A. Keller, E. F. Zalewski, and N. C. Peterson, *J. Opt. Soc. Amer.*, **62**, 319 (1972).

(4) T. W. Hänsch, A. L. Schawlow, and P. E. Toschek, *IEEE J. Quantum Electron.*, **10**, 802 (1972).

(5) T. P. Belikova, E. A. Sviridenkov, A. F. Suchkov, L. V. Titova, and S. S. Churilov, *Sov. Phys.-JETP*, **35**, 1076 (1972).

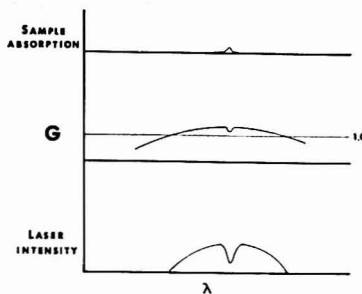


Figure 1. Effect of an intracavity absorber on a laser

A small absorption increases the losses and decreases the laser intensity dramatically

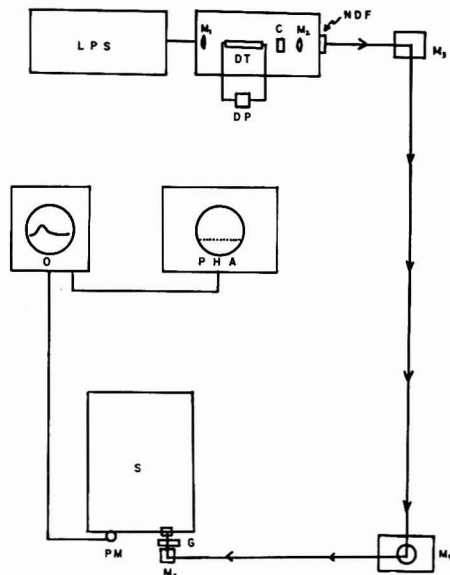


Figure 2. Experimental apparatus

Energy from the laser power supply (LPS) is discharged through a lamp coaxial with the dye tube (DT). A pump (DP) circulates the dye. Mirrors M_1 and M_2 form the optical cavity of the laser; the sample is contained in a cuvette (C). The laser output passes through a neutral density filter (NDF) and via mirrors M_3 - M_5 to a ground glass scatter plate (G) in front of the entrance slit to a monochromator (S). The output of a photomultiplier detector (PM) at the exit slit is fed to an oscilloscope (O) and a multichannel pulse height analyzer (PHA).

nol. The laser is pumped by a coaxial xenon flashlamp. The sample solutions were in a rectangular cuvette with a 1-cm light path. The cuvette was placed inside the laser cavity approximately equidistant between the dye cell and the output mirror. The laser output passed through an o.d. = 0.5 neutral density filter and onto a ground-glass scatter plate placed directly in front of the entrance slit to a monochromator. This arrangement reduced the laser intensity to prevent overloading the detector and removed the effect of any spatial inhomogeneities in the laser beam. The monochromator was a 0.3-m Hilger Engis Model 600. Slit widths were 5 or 10 μ m, ensuring that the slit width was less than the half width of the sample absorptions. The detector was a 1P28A

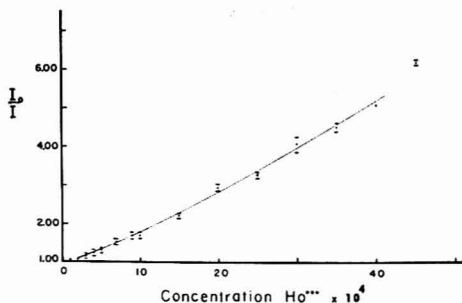


Figure 3. Laser intensity at 450.4 nm vs. Ho^{3+} concentration

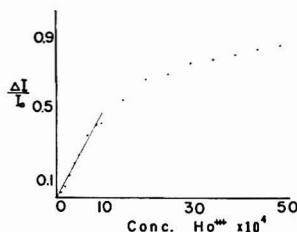


Figure 4. $\Delta I/I_0$ at 450.4 nm vs. Ho^{3+} concentration

photomultiplier. The detector output was fed to an oscilloscope for monitoring and to a 100-channel pulse height analyzer where the laser intensity was recorded.

Some quantitative studies were made using photographic recording of the laser output. In this case, the output of the laser was directed onto the slit of a 1.5-m Wadsworth spectrograph with a dispersion of 11 Å/mm. The spectra were recorded on Kodak SA-1 film. All the spectra of sample solutions, as well as exposures of the laser through neutral density filters for calibration of the film, were recorded and developed at the same time. Densitometry of the film was performed on a modified Hilger densitometer.

Reagents. Holmium chloride (99.9%, anhydrous, Research Organic/Inorganic Chemical Corp.) and praseodymium chloride (hydrated, 99.9%, Research Organic/Inorganic Chemical Corp.) were used without further purification. Samples of the rare earth chlorides (1×10^{-4} - 1×10^{-2} M in 0.1N HCl) were prepared from stock solutions.

Procedure. In a typical experiment, a sample or a blank (0.1N HCl) was placed in the laser cavity. The xenon flashlamp was discharged manually at a typical input energy of 61.5 J at 20 kV. This energy was well above the lasing threshold for either dye. Special care was taken to ensure a constant input energy to the flashlamp. The intensity of the laser at a particular wavelength was measured as the peak height of the resulting photomultiplier pulse. Prior to each experiment, the response of the photomultiplier and the electronics were checked for linearity by placing neutral density filters in the laser beam and ensuring that the measured pulse height was indeed proportional to laser intensity.

RESULTS AND DISCUSSION

Holmium Determination. Figure 3 shows a plot of I_0/I vs. concentration of holmium ions in a 0.1N HCl solution. As can be seen, the plot is nearly linear in the 3×10^{-4} to 4×10^{-3} M concentration range, but curves off at both high and low concentrations. Figure 4 shows a plot of $\Delta I/I_0$ for the same data. It is linear for low concentrations but falls off at high concentrations. The graph of I_0/I seems more satisfactory, so I_0/I is used to express our results in the rest of this paper. The error bars in these graphs are the standard errors ($= \sigma/\sqrt{n}$) for all the mea-

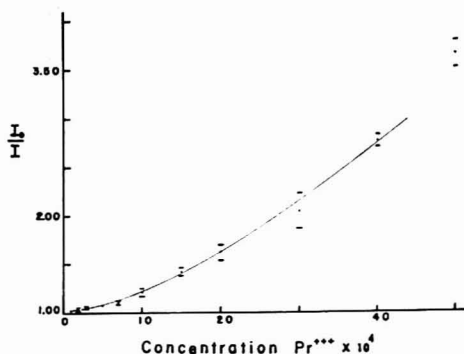


Figure 5. Laser intensity at 588.3 nm vs. Pr^{3+} concentration

measurements on the solutions. These results were reproducible from day to day. Each point represents measurements recorded on from 2 to 5 different days. The graph depicts an easily constructed calibration curve from which unknown concentrations of holmium ions in solution may be ascertained.

The calibration curve is, of course, sensitive to the laser parameters. Several important parameters were closely monitored to obtain the observed reproducibility. The spectral slit width was narrow compared to the bandwidth of the holmium absorption. The input energy to the laser was kept constant. The laser was operated well above the lasing threshold of each dye to minimize the effect of variations in the dye. We found that the coumarin dye decomposed slowly and we corrected for it. Finally, we were careful to ensure that we were operating in a linear region of the photomultiplier.

With these precautions, we found that for the fiftyfold change in concentration (16 solutions) studied, only two solutions showed relative standard errors of greater than 5%. Such reproducibility is an important factor in making the technique useful for quantitative analysis.

Praseodymium Determination. Figure 5 displays the calibration curve obtained for solutions of praseodymium chloride ranging in concentration from 1×10^{-4} to $5 \times 10^{-3}M$. The relatively weak 588.3-nm absorption band of praseodymium was used. Again the results were easily reproduced. Each point represents measurements from at least 3 different days. It should be observed that this curve is similar to the Ho^{3+} calibration curve. For both holmium and praseodymium solutions, concentrations of greater than $10^{-2}M$ quenched the lasing action enough so that detection of a signal above the noise level was not possible.

Photographic Technique. Preliminary to the use of the photomultiplier detector, we used photographic recording of the laser output with Ho^{3+} solutions inside the laser

cavity. Concentrations of holmium ions in the range 0.81 to 5.42 mg/ml were investigated using the coumarin dye. Densitometry of the film provided the data for a calibration curve. This calibration curve could then be used for the analysis of unknown concentrations of holmium ions. The limit of detectability using this technique was not as low as that for the electronic detection, and this technique proved to be more time consuming.

CONCLUSIONS

We have demonstrated that it is possible to use the intracavity absorption technique with a dye laser for quantitative analysis. Reliable calibration curves have been constructed for our laser for Ho^{3+} and Pr^{3+} solutions in the range 5×10^{-3} to $10^{-4}M$. This corresponds to holmium concentrations down to 27 $\mu\text{g/ml}$ (ppm) using the 450.4-nm Ho^{3+} absorption band. Thus, the intracavity absorption technique is ca. 2 orders of magnitude more sensitive than direct spectrophotometry of the solution. Our technique is not, however, as sensitive as atomic absorption or atomic emission methods (6).

Even though this technique is not yet the most sensitive technique available for the analysis of Ho^{3+} and Pr^{3+} ions, we have demonstrated that it is possible to extend the sensitivity of a particular technique (spectrophotometry of rare earth ion solutions) by two orders of magnitude. We expect that the sensitivity of the atomic absorption technique can be similarly extended by intracavity absorption. In fact, preliminary work in our laboratory with Sr and Na atomic absorptions indicates that this is readily accomplished. We did not choose atomic absorption for these studies because of the narrow slit width required for absorption studies with atomic lines. More sophisticated detection techniques are necessary in these cases.

In this study, the operating parameters of the laser were chosen to ensure reproducible results. Different lasers or changes in the operating characteristics of the same laser will give different calibration curves. It is, for example, possible to increase the sensitivity of the intracavity absorption technique by operating the laser nearer threshold. However, near threshold the laser will become more sensitive to small changes in operating characteristics. The ultimate limit on the sensitivity may arise from instabilities in the laser, although it should be possible to approach the gain of 10^7 in sensitivity that Henschel *et al.* (4) calculate for the intracavity absorption technique.

ACKNOWLEDGMENT

We thank Harley Borders for experimental assistance.

Received for review August 17, 1973. Accepted November 19, 1973. We thank the Research Corporation and the Illinois Institute of Technology for financial assistance.

(6) N. Omenetto, N. N. Hatch, L. M. Fraser, and J. D. Winefordner, *Anal. Chem.*, **45**, 195 (1973).

The Vidicon Tube as a Detector for Multielement Flame Spectrometric Analysis

K. W. Busch, N. G. Howell, and G. H. Morrison

Department of Chemistry, Cornell University, Ithaca, N.Y. 14850

An instrument for multielement flame emission analysis is described which consists of a 0.5-m Ebert monochromator, a silicon diode vidicon tube, and an optical multichannel analyzer. Optical and electronic considerations of the system are discussed. Using this system, a spectral "window" of 20 nm is monitored simultaneously and atomic lines 1.4 Å apart are resolvable. Detection limits, obtained under compromise flame conditions, are presented for Mo, Fe, Ca, Al, Ti, W, Mn, and K using spectral lines present in a single window. The multielement analysis of a geological standard rock sample for Fe, Ca, Al, and Ti is described, and the results are compared with the accepted values. Other potential windows for multielement analysis are presented.

In terms of the amount of information obtained in a given analysis, trace methods may be conveniently classified into single- and multielement methods. A single-element method is optimized to determine a given element with high accuracy and precision. Multielement methods are particularly valuable for survey analyses where simultaneous information on a large number of elements is desired. The need for simultaneous multielement methods of analysis is particularly acute for those situations where maximum information is required on a limited amount of sample or where time is limited. The potential of flame spectrometry for multielement analysis has recently been reviewed (1).

To perform multielement flame spectrometry, a device capable of measuring intensities at different wavelengths is necessary—i.e., a multichannel device is necessary. Two major classes of multichannel systems are temporal multichannel devices and spatial multichannel devices (1). Temporal multichannel devices employ a single detector, where each channel is separated from the previous one in time. Spatial multichannel devices employ multiple detectors, where each channel is separated in space. Temporal multichannel detection systems include scanning spectrometers (2-8), scanning detectors (9, 10), and rotating filter photometers (11-13). Spatial multichannel detection

systems include direct reading spectrometers (14, 15) and multichannel detectors. The advantages of multichannel detection include the measurement of intensities at closely spaced wavelengths—i.e., line and background—and a substantial increase in the number of wavelengths which can be monitored.

The first and perhaps most widely used multichannel detector has been the photographic plate. Among the potential multichannel detectors proposed as alternatives to photographic detection have been television camera tubes (16, 17) and mosaics of either photodiodes, phototransistors, or photoresistors (18, 19). This paper describes the application of a silicon diode vidicon tube as a detector in multielement flame emission spectrometry. This system, which is easily amenable to automation, has the potential for simple, rapid, inexpensive analyses of complex samples. Analytical development of such methods will find ready application to a variety of samples, including clinical, metallurgical, geological, agricultural, and environmental samples.

EXPERIMENTAL

Table I lists the experimental facilities used in this study.

Instrumental. Multichannel Detection System. The multichannel detection system (SSR Instruments Co.) used in this study consisted of a UV-sensitive vidicon tube and its associated detector housing, which contained the deflection coil system and a low-noise preamplifier, the electronic console, and a CRT display. The electronic console has two separate memories, which allow the storage of both a data spectrum and a blank spectrum; each memory contains 500 words with 5 BCD digits per word. The contents of a given channel are displayed digitally on the display panel of the console, and on the CRT as an intensified cursor spot. An arithmetic unit permits channel-by-channel subtraction of memory B from memory A. Signal averaging may be accomplished by accumulating a preset number of frame scans into either memory. In the real-time mode, the spectrum displayed on the CRT is the result of a single sweep. The integrated intensity of a line or band may be obtained by selecting the summation mode, moving the cursor over the given line or band, and reading the summation—i.e., integral, of the counts for each channel covered in the integration on the digital display panel.

Optical System. Figure 1 shows a photograph of the system which consists of a flame source, external optics, monochromator, vidicon tube, optical multichannel analyzer, and oscilloscope display. The vidicon was mounted on a 0.5-m Ebert monochromator. A plate was constructed to position the vidicon target in the vertical plane formerly occupied by the exit slit of the monochromator. In order to mount this plate to the monochromator, it was necessary to cut the standard slit housing in half to separate the entrance and exit portions. The entrance half of the slit housing was remounted on the entrance port of the monochromator and a new slit cover was constructed to fit the modified slit housing. The vidicon mounting plate was attached to the monochromator adjacent to the modified entrance slit housing so that the vidicon tube was positioned over the exit port of the monochromator.

- (1) K. W. Busch and G. H. Morrison, *Anal. Chem.*, **45**(8), 712A (1973).
- (2) A. M. Harris and J. H. Jackson, *J. Phys. E: Sci. Instrum.*, **3**, 374 (1970).
- (3) H. A. Kruegle and S. A. Dolin, *Appl. Opt.*, **8**, 2107 (1969).
- (4) G. H. Dieke and H. M. Crosswhite, *J. Opt. Soc. Amer.*, **35**, 471 (1945).
- (5) J. L. Dye and L. H. Feldman, *Rev. Sci. Instrum.*, **37**, 154 (1966).
- (6) R. K. Behrm and V. A. Fassel, *J. Opt. Soc. Amer.*, **43**, 886 (1953).
- (7) J. B. Dawson, D. J. Ellis, and R. Milner, *Spectrochim. Acta*, **23B**, 695 (1968).
- (8) H. V. Malmstadt and E. Cordos, *Amer. Lab.*, **4**, 35 (1972).
- (9) P. T. Farnsworth, *J. Franklin Inst.*, **218**, 411 (1934).
- (10) R. A. Harber and G. E. Sonnek, *Appl. Opt.*, **5**, 1039 (1966).
- (11) D. G. Mitchell and A. Johansson, *Spectrochim. Acta*, **25B**, 175 (1970).
- (12) R. M. Dagnall, G. F. Kirkbright, T. S. West, and R. Wood, *Analyst (London)*, **97**, 245 (1972).
- (13) R. M. Dagnall, G. F. Kirkbright, T. S. West, and R. Wood, *Anal. Chem.*, **43**, 1765 (1971).

- (14) B. L. Vallee and M. Margoshes, *Anal. Chem.*, **28**, 1975 (1956).
- (15) C. J. Pickford and G. Rossi, *Analyst (London)*, **98**, 329 (1973).
- (16) M. Margoshes, *Spectrochim. Acta*, **25B**, 113 (1970).
- (17) K. W. Jackson, K. M. Aldous, and D. G. Mitchell, *Spectrosc. Lett.*, **6**, 315 (1973).
- (18) P. W. J. M. Boumans and G. Brouwer, *Spectrochim. Acta*, **27B**, 247 (1972).
- (19) G. Horlick and E. G. Codding, *Anal. Chem.*, **45**, 1490 (1973).



Figure 1. Multielement flame spectrometer system

(1) flame source; (2) external optics; (3) monochromator; (4) vidicon tube; (5) optical multichannel analyzer; (6) oscilloscope display

Table I. Experimental Facilities

External optics	Five-cm diameter Supracil lens with 12.5-cm focal length. Lens stopped down to 2.6-cm diameter
Burner	Varian Techtron 5-cm slot burner for nitrous oxide-acetylene
Monochromator	Jarrell-Ash, Model 82000, 0.5-m Ebert mounting scanning monochromator with 1180 grooves/mm grating blazed for 3000 Å. Reciprocal linear dispersion 16 Å mm^{-1} in the first order
Entrance slit	Fixed slit, 25 μm wide, straight edged
Detector	UV sensitive silicon diode vidicon, Model 1205 F, SSR Instruments Co.
Optical multichannel analyzer	Model 1205A, SSR Instruments Co.
Readout	Techtronix oscilloscope, 604 Monitor and Moseley x-y recorder, Model Autograph 2D-2
Flow meters	Brooks Full-view Rotameters calibrated for nitrous oxide and acetylene, Brooks Instrument Division

The target of the RCA type 4532 vidicon used in the optical multichannel analyzer is 0.4 inch in height. The optical multichannel analyzer is designed electronically to subtract the signal originating from the upper 0.2-inch portion from that originating from the lower 0.2-inch portion. This allows dark current to be subtracted from each channel if the upper surface is not illuminated. Since an Ebert mounting is stigmatic, a point on the entrance slit is imaged as a point in the focal plane. In addition, an inverted image of the entrance slit is formed at the focal plane. Therefore, in order to prevent the spectrum from falling on the upper portion of the target, the lower portion of the entrance slit was masked by a triangular shaped sliding diaphragm. This diaphragm was adjusted until no light hit the upper half of the vidicon tube. This was determined by adjusting the diaphragm until the negative side bands adjacent to a given spectral line displayed on the oscilloscope just disappeared.

A 5-cm diameter Supracil lens with a 12.5-cm focal length was used to form a 1:1 image of the flame on the monochromator entrance slit. This lens was stopped down to a diameter of 2.6 cm to match—i.e., fill the solid angle of the monochromator collimator mirror. To obtain the maximum light throughput with a monochromator, the collimating mirror should be completely filled with radiation. Care must be taken, however, not to overfill the collimator with an Ebert mounting. In this case, light overfilling the collimating portion of the mirror spills over onto the camera portion of the mirror and is reflected onto the vidicon tube without ever hitting the grating. This results in a stray light signal which does not move across the vidicon tube as the grating position is changed.

While the method of dark current subtraction should also re-

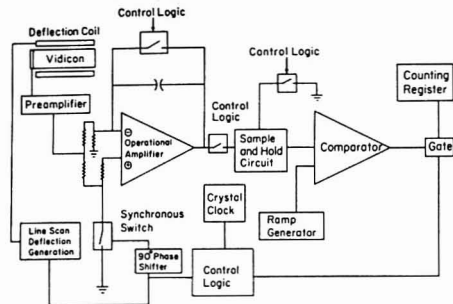


Figure 2. Optical multichannel analyzer electronics

duce the effect of scattered light, this is true only if the scattered light uniformly illuminates the upper and lower surfaces of the target. Therefore, to further restrict the viewing angle of the vidicon tube to the camera mirror and to prevent the zero order spectrum, which hits the side of the monochromator housing adjacent to the vidicon, from illuminating the vidicon surface, a blackened cardboard tube was installed. This tube was 4.5 inches long and 1.25 inches in diameter. A portion of the tube adjacent to the grating had to be cut to allow the grating to rotate to shorter wavelengths.

Samples and Standards. Samples of from 100 to 200 mg of the USGS standard rock sample BCR-1, which had previously been dried for 2 hours in a drying oven at 110°C and stored in a desiccator, were dissolved with a Teflon bomb technique using HF (20). The dissolution took approximately 1 hour. The advantages of this sample dissolution step over fusion techniques are the absence of contamination from crucible materials (we found sizable amounts of Mn contamination from Ni crucibles when carrying out sodium peroxide fusions) and the complete dissolution of the sample—i.e., silica is dissolved in HF. Furthermore, no additional salts are added to the matrix and losses of volatile elements are kept to a minimum. The dissolved sample from the bomb was diluted to 100 ml and a 25-ml aliquot was transferred to a 100-ml volumetric flask. Ten milliliters of 10,000 ppm Na solution was added to the flask as an ionization buffer, and the sample solution was diluted to volume.

Stock solutions were prepared from high purity metals or oxides (21). Multielement standards, containing all of the elements to be analyzed in the sample, were prepared from these stock solutions. Four multielement standards were used to prepare the analytical curves for the individual elements. Each successive multielement standard contained increasing amounts of each element. Sufficient 10,000 ppm Na solution was added as an ionization buffer to each multielement standard to produce a concentration of 1000 ppm Na in the final solutions.

Data Acquisition. The analytical curves for each element in the sample were prepared simultaneously by aspirating each multielement standard for 1000 accumulation cycles (32.7 sec) and storing the result in memory A. A blank solution of deionized distilled water was aspirated for an equivalent amount of time, and the result stored in memory B. The A-B mode was selected to display the channel-by-channel difference between the two memories; this difference spectrum was recorded with an x-y recorder. Peak heights of analytical lines were measured from the recorder tracing and plotted vs. concentration to give the analytical curves. Alternatively, the peak heights can be read directly from the digital display or peak areas can be readily obtained using the summation mode.

The sample spectrum was obtained in the same manner as described above for each multielement standard. The resulting peak heights of the analytical lines were obtained from the recorder tracing of the difference spectrum and compared with the analytical curves to obtain the concentrations in the sample.

(20) B. Bernas, *Anal. Chem.*, **40**, 1682 (1968).

(21) "Standard Solutions for Flame Spectrometry" by J. A. Dean and T. C. Rains in "Flame Emission and Atomic Absorption Spectrometry," Vol. 2, J. A. Dean and T. C. Rains, Eds., Marcel-Dekker, New York, N.Y., 1971, p. 327.

Table II. Effect of Frame Scan Voltage on Wavelength Range Covered with 0.5-m Monochromator

Frame scan voltage	Wavelength range, Å
4.1	132
5.0	152
7.1	200

RESULTS AND DISCUSSION

Electronic Considerations. The principle of operation of the silicon diode vidicon tube has recently been described (1). Figure 2 shows a block diagram of the optical multichannel analyzer (SSR Instruments Co.) used in this study. A sawtooth wave with a 32.768-msec period is applied to the horizontal deflection coils of the vidicon yoke to produce the frame scan. A square wave of 64- μ sec period is applied to the vertical deflection coils to produce the line scan. Thus, there are 512 periods of 64- μ sec duration during the frame scan time of 32.768 msec. Five hundred periods are used during the active scan time and twelve 64- μ sec periods are used for retrace.

The analog displacement current produced when the electron beam in the tube recharges the partially discharged "diode capacitors" of the target back down to the negative cathode potential is amplified by the current amplifying preamplifier. This analog signal is then fed to a gated inverting-noninverting operational amplifier integrator. This amplifier is gated synchronously with the line scan voltage so that the signal is integrated with one polarity when the electron beam is scanning the upper half of the vidicon target and with the opposite polarity when the electron beam is addressing the lower half of the target. The resulting integral from a complete line scan is therefore the difference of the integrals between the top and bottom halves of the vidicon target. A sample and hold circuit stores the result of a complete line scan. This voltage signal is applied to a comparator and compared with a voltage ramp. The comparator is used to gate pulses from a clock into a counter, the resulting digital signal being stored in memory.

The vidicon tube used in the optical multichannel analyzer is an RCA 4532 UV-sensitive silicon diode vidicon, with the diodes arranged in a rectangular array with 72 diodes per linear mm in both directions. This results in 900 vertical lines of diodes across the 12.5 mm width of the target.

It is apparent from the previous discussion that the 500 channels of the optical multichannel analyzer are electronic channels. If the frame scan voltage is adjusted to cover the full 12.5-mm width of the target, each channel is $\frac{1}{500}$ of 12.5 mm or 25 μ m in width. Table II shows the effect of frame scan voltage on the wavelength range covered with a 0.5-m Ebert monochromator. This monochromator has a reciprocal linear dispersion of 16 Å/mm in the first order. With the frame scan voltage adjusted to cover the full width of the target, the expected wavelength range of 200 Å with this monochromator results, giving a channel width of 25 μ m. Reducing the frame scan voltage to its lowest attainable value reduces the scan width to 8.25 mm as calculated from the wavelength range covered and the reciprocal linear dispersion. This gives a channel width of 16.5 μ m. With the frame scan voltage adjusted to cover the full target, the magnetic focus could be adjusted so that, using 25- μ m slits, the majority of the total signal for a spectral line in the center of the screen occurs in three channels.

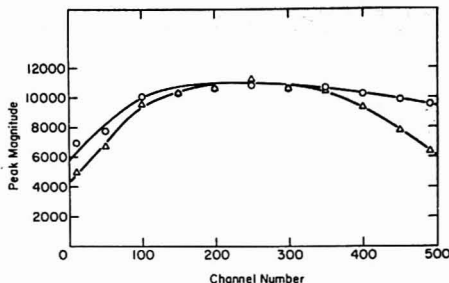


Figure 3. Channel response of vidicon target to Hg 4047-Å line

○ peak area; Δ peak height

Optical Considerations. Figure 3 shows the response of the overall system to the same spectral line set at different channel settings. These measurements were made using the Hg 4047-Å line emitted from a Hg pen lamp. A 1:1 image of the source was focused on the entrance slit of the monochromator. The grating was rotated over a range of 200 Å to move the spectral line to the different positions across the vidicon target.

The data using peak area most closely represent the intensity of the line. Compared with the data using peak area, the data obtained using peak height fall off faster at the extreme ends of the wavelength range. Since the vidicon target is flat and the focal plane of the monochromator is curved, a lack of focus at the ends of the wavelength range results. This lack of focus at either end causes the peak profile to broaden, reducing the peak height. This does not prevent the use of peak height as a measure of intensity in an analysis, since the orientation of the spectrum with respect to the channels does not change.

At least part of the reduction in sensitivity at either extremity of the target can be explained on the basis of optical considerations of the system. For uniform response across the target, a monochromator is not the ideal spectrometric system, primarily because it has been designed to measure one wavelength at a time. Light from the entrance slit strikes the collimating mirror, where it is collimated into a parallel beam which strikes the plane grating. This parallel beam, striking the plane grating, is diffracted into a family of parallel beams which diverge according to their wavelength. The camera mirror of a monochromator is designed so that it is filled by that particular parallel beam which corresponds to the wavelength to be passed by the exit slit of the monochromator. For a monochromator, a symmetrical design is commonly used, so that the collimating mirror and the camera mirror are the same size. Therefore, the camera mirror cannot accept the entire diverging family of parallel beams, which constitute any given range of wavelengths. This results in a loss of intensity at the extremities of the wavelength range as compared to the middle, because all of the light from the grating is not used in forming the image of the line at the focal plane.

The extent to which this effect should reduce the intensity at the extremities can be estimated by calculating the amount by which the parallel beams diffracted from the grating are shifted from that position that fills the camera mirror. The fraction of the parallel beam which strikes the mirror should indicate the fraction of the intensity transmitted. The dispersion of a plane grating is given by

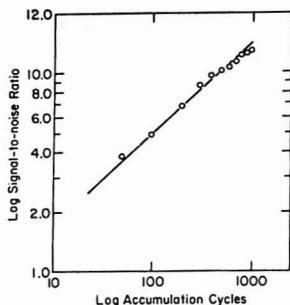


Figure 4. Signal-to-noise as a function of accumulation cycles for Hg 4047-Å line

$$\frac{d\phi}{d\lambda} = \frac{Nm}{A \cos \phi} \quad (1)$$

where ϕ is the angle of diffraction, m is the order, A is the linear aperture of the grating, and N is the number of grooves/mm and a linear aperture of 52 mm and assuming $\cos \phi \sim 1$, gives a change in the diffraction angle of 0.0236 radians or 1.35° for a 200-Å range in wavelengths. This results in a shift in the parallel beam of 9.9 mm over the distance from the grating to the mirror (420 mm). Thus each extremity would be expected to be reduced by about 5% (where the width of the camera mirror is 52 mm) or about 10%. The measured reduction at one end is 45% less than the peak value while the reduction at the other extreme is 15%. At this time, it is not known whether this additional reduction is due to other optical considerations or to the vidicon itself.

Signal Averaging. In the real time mode, each target element is addressed every 32.768 msec. The signal measured, therefore, results from the discharge of the diodes either from photon-induced hole collection or leakage during the period since the electron beam last addressed that particular target element—i.e., the signal is a time integrated signal with a period of 32.768 msec. In spite of this integration, the standard vidicon is considerably less sensitive in the real time mode than a multiplier phototube. Thus, in the real time mode, only high concentrations of analyte can be detected by flame emission. This limitation can be greatly improved, however, with signal averaging techniques. The optical multichannel analyzer has two separate memories which permit the storage of the signals from each of the 500 channels. By adding the results of successive frame scans to the respective channel locations in memory, the signal may be accumulated. Since the signal is directly proportional to the number of cycles accumulated, and the noise is proportional to the square root of the number of cycles accumulated, the signal-to-noise ratio increases proportionally to the square root of the number of accumulations. Figure 4 shows the increase in the signal-to-noise ratio with the number of accumulation cycles for the Hg 4047-Å line emitted by a Hg pen lamp. The rms value of the noise is most conveniently obtained by calculating the standard deviation of the digital counts in the adjacent channels. The resulting log-log plot is a straight line with a least-squares slope of 0.46, in good agreement with the expected slope of 0.5 for square root behavior.

In addition to improving the signal-to-noise ratio, the accumulation mode increases the dynamic range of the

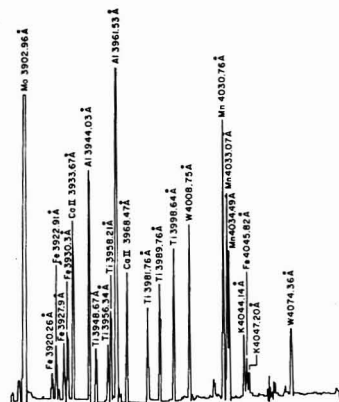


Figure 5. Multielement flame emission spectrum from 3886 to 4086 Å

system. In the real-time mode, the vidicon tube is limited to 750 counts in any given channel before overloading that channel. This active dynamic range is limited by the charge storage capacity of the target during a machine cycle as well as time restrictions imposed on the analog-to-digital conversion by the scanning rate of the electron beam. By using the accumulation mode, each channel is capable of accumulating 10^5 counts, thereby extending the dynamic range.

Simultaneous Multielement Flame Analysis. Monochromator Selection. Simultaneous multielement analysis using the vidicon as a detector is based on a "window" concept—i.e., the range of wavelengths simultaneously monitored by the target. Thus, the number of elements which can be determined simultaneously depends on the extent of the wavelength window and the number of spectral lines emitted by various elements in that particular wavelength region. This depends on the dispersion of the monochromator and the choice of the window—i.e., the particular portion of the UV-visible spectrum to be monitored.

An advantage to using flame emission for simultaneous multielement analysis is that one is not limited to using resonance lines. Thus, although resonance lines are usually stronger in emission than nonresonance lines, the concentration of the given element in the particular sample determines whether any given atomic line will emit useful intensity at the flame temperature. This is an advantage for a system utilizing a window concept since it allows more possible combinations of spectral lines of various elements within a given window than if one were limited strictly to resonance lines. This makes the system inherently versatile, in that a given element may be determined in combination with one set of elements in one window, while the same element may also be determined with an entirely different set of elements in a different window.

The choice of the focal length of the monochromator for the system is a compromise between window width and resolution. For a given grating, monochromators employing a shorter focal length have a lower dispersion and therefore compress a greater spectral range in a given width than a similar monochromator with a larger focal length. Thus, for a given grating, a shorter focal length monochromator covers a wider window, at the expense of

decreased resolution, than a longer focal length monochromator. The 0.5-m Ebert monochromator used in this study was arbitrarily chosen because it was available in our laboratory. Other shorter focal length monochromators are currently being investigated in this laboratory. The compromise between window width and resolution depends to a certain extent on the complexity of the sample if spectral overlap is to be avoided. For complex samples containing large amounts of transition metals, the analytical spectrum emitted from the flame can be surprisingly complex as shown in Figure 5, where a flame emission spectrum of a synthetic solution containing Mo, Fe, Ca, Al, Ti, W, Mn, and K is shown from 3886 Å to 4086 Å. With the 0.5-m monochromator, lines 1.4 Å apart are resolvable, as illustrated by the Mn triplet.

In addition to affecting the window width and resolution, the focal length of the monochromator indirectly influences the radiant flux F in ergs sec⁻¹ or watts through the monochromator because longer focal length instruments generally have higher numerical apertures. For a properly designed monochromator, all of the light collected from the fully illuminated collimator is transmitted through the system to the image. Therefore the radiant flux through the system depends on the characteristics of the collimator. For a source of a given radiance B in watts cm⁻² sr⁻¹ at the slit of a monochromator, the radiant flux in watts transmitted through the system is given by

$$F = B\omega = Ba \left(\frac{A}{X^2} \right) = \frac{1}{4} \pi Ba \left(\frac{d^2}{f^2} \right) = \frac{1}{4} \pi Ba \left(\frac{1}{f} \right)^2 \quad (2)$$

where a is the slit area, ω is the solid angle collected by the collimator, A is the area of the collimator, X is the distance from the slit to the collimator (which for a collimator is the focal length of the lens or mirror), d is the linear aperture of the lens or mirror, and f is the f /number (where the f /number is the ratio of the focal length to the linear aperture) of the monochromator. It can be seen that the radiant flux through the monochromator is inversely proportional to the square of the numerical aperture or f /number of the monochromator. For two monochromators, with the same source and slit width, the ratio of the radiant fluxes is given by,

$$\frac{F_1}{F_2} = \frac{(1/f_1)^2}{(1/f_2)^2} = (f_2/f_1)^2 \quad (3)$$

Thus the radiant flux through an $f/3.6$ (typical f /number for 0.25-m focal length) monochromator is increased by a factor of 5.7 over that transmitted through an $f/8.6$ (typical f /number for 0.5-m focal length) monochromator with the same source and slit width and with the collimators of both monochromators fully filled. Because the smaller focal length monochromator with the lower f /number transmits a greater radiant flux than the longer focal length system with the higher f /number, a smaller focal length monochromator should increase the sensitivity of the optical multichannel system for those situations where high resolution is unnecessary, and wide wavelength coverage desired.

To reduce the loss in sensitivity observed at the extremities of the wavelength range described earlier, an asymmetric Czerny-Turner spectrograph would be the best choice of polychromator mounting. With this mounting, the camera mirror is larger than the collimating mirror, and therefore collects the entire dispersed beam of the wavelength window from the grating.

Flame Selection. An ideal flame for simultaneous multielement flame emission spectrometry should 1) be capable of atomizing a wide variety of elements efficiently, 2) have a slow burning velocity to provide a long residence

Table III. Comparison of Peak Height and Peak Area for a Calibration Curve Using Ca (3933.67 Å)

Concentration, ppm	Average peak height	Average peak area	Peak area/peak height
500	56437	129460	2.29
100	32473	73407	2.26
50	22890	51973	2.27
10	7013	16149	2.30
5	3711	8643	2.33
1	800	1997	2.50

time for atoms in the optical path, 3) have a high temperature for good excitation efficiency, and 4) have a large variation in excitation conditions over a small flame region to allow simultaneous excitation and observation of many elements. Boumans (22) has studied this aspect of multielement flame emission and concluded that the shielded N₂O-C₂H₂ flame was a good choice on the basis of criterion 4). The fuel-rich oxyacetylene flame has also been suggested (1).

An unshielded nitrous oxide-acetylene flame was used in this study due to the previous unavailability of a shielded nitrous oxide burner in our laboratory, as well as a lack of a burner for the fuel-rich oxyacetylene flame. Other flames and burners are being investigated in our laboratory to determine the optimum excitation source for use with the vidicon system.

Measure of Intensity. Using the optical multichannel analyzer, both peak height and peak area are readily measurable. Table III shows the results of using both modes for a calibration curve for the Ca 3933.67-Å ion resonance line. This line undergoes self-absorption at higher concentrations, resulting in a curved calibration line for the extended range covered. Peak area was obtained digitally by using the summation mode. Both peak height and peak area were corrected for background. From the table, it can be seen that the ratio of peak area to peak height does not change significantly as the intensity varies. Therefore, analytical data may be acquired either as peak height or peak area. The use of peak height is justified as long as any single channel in the profile of the spectral line is registering less than about 750 counts in real time. At this point, an overload indicator is observed. In real time, the maximum count possible in a single channel is 840 counts. Intensities greater than this result in no further increase in peak height but merely result in appreciable broadening of the peaks into adjacent channels—i.e., formation of a plateau.

One source of error which affects the reproducibility of measuring peak height is due to the discrete nature of the 500 separate electronic channels. Although the n -type silicon wafer target in the vidicon is continuous and radiation striking any portion will result in the production of holes, the peak height of a spectral line depends on the relative alignment of the electronic channels with respect to those particular diodes which have collected the holes and are therefore partially discharged. Thus if an electronic channel is aligned coincident with the center of the optical image—i.e., coincident with the center of those diodes which have been most discharged by the light—the majority of the signal will appear in this channel, resulting in a triangularly profiled peak of a given peak height. If the position of the optical image is moved slightly by altering the grating position, those diodes which are most discharged by the light are shifted between two electronic channels. In the extreme case, both channels monitor the

(22) P. W. J. M. Boumans and F. J. DeBoer, *Spectrochim. Acta*, **27B**, 391 (1972).

Table IV. Detection Limits for Mo, Fe, Ca, Al, Ti, W, Mn, and K Using Spectral Lines in Region from 3886 to 4086 Å

Element	Spectral line, Å	Detection limit, $\mu\text{g/ml}$
Mo	3902.86	0.31
Fe	3930.3	19.3
Ca(II)	3933.67	0.009
Al	3961.53	0.14
Ti	3998.64	1.33
W	4008.75	25.9
Mn	4030.76	0.29
K	4044.12	140.0

signal equally, resulting in a peak which is flat on top—i.e., a box-shaped profile—and a concomitant decrease in peak height of about 8%.

A comparison of the precision of measuring peak height and peak area was made under typical operating conditions by aspirating a 10 ppm Ca solution into the nitrous oxide-acetylene flame and accumulating the isolated 3933-Å line for 1000 machine cycles. This produced a signal with a large signal-to-noise ratio. Both peak height and peak area were determined on each run. Under these conditions, the relative standard deviation in ten successive measurements of peak height was 4.5%. Using the same data, the relative standard deviation in the measurement of peak area was 1.5%. Since manually measuring peak area excessively prolongs the measurement step (particularly in multielement analysis), a complete study of the optimum data format was postponed until the interface of the optical multichannel analyzer to our PDP-11 computing system is completed.

Flame Optimization and Detection Limits. In single-element flame emission determinations, the operating conditions are optimized for the given element according to its spectrochemical properties. These spectrochemical properties include the excitation potential of the analytical line, the ionization potential of the element, and the tendency for the element to form compounds in the flame. This optimization is conventionally carried out by optimization of the flame zone sampled by the spectrometer—i.e., height—and by altering the chemical and physical environment by optimization of the fuel-to-oxidant ratio. For simultaneous multielement analysis, individual optimization is not possible and a compromise must be reached.

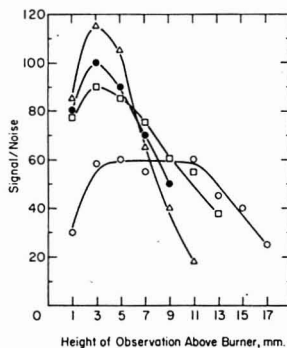


Figure 6. Nitrous oxide-acetylene flame profiles

Δ Ti; ● Mn × 10; ■ Mn × 10; □ Mo × 5; ○ Al

In this study, we arbitrarily chose to investigate the simultaneous multielement capabilities of our system with a 200-Å window centered on 3986 Å. Table IV lists selected spectral lines of Mo, Fe, Ca, Al, Ti, W, Mn, and K which occur in this window. Of these elements, Mo, Al, Ti, W, and Mn were selected to obtain the optimum flame conditions for simultaneous analysis of the entire group listed in Table IV. These elements were chosen because they are sensitive to changes in flame conditions. The behavior of Mo, Al, Ti, W, and Mn were investigated individually in the nitrous oxide-acetylene flame by making vertical flame profile measurements—i.e., signal-to-noise ratio as a function of burner height—for various acetylene flow rates at a constant nitrous oxide flow rate. From these measurements, the best acetylene flow rate was selected for each element. For the elements chosen in this optimization study, all of the elements showed the largest peak in the vertical flame profile at the same acetylene flow rate. Figure 6 shows the vertical flame profiles obtained with each element at an acetylene flow rate of 3700 $\text{cm}^3 \text{ min}^{-1}$ and a nitrous oxide flow rate of 4750 $\text{cm}^3 \text{ min}^{-1}$. This gave a fuel-rich nitrous oxide-acetylene flame with a red feather about 20 mm high. The red feather was on the verge of showing luminosity from carbon particles. From this figure, a height of observation above the burner of 3 mm was chosen, which caused the spectrometer to sample the portion of the red feather of the flame directly above the primary reaction zone.

Table IV shows the detection limits obtained using an accumulation time of 1000 cycles. These detection limits were obtained individually using the compromise conditions determined above. The detection limit was taken as that concentration which produced a signal-to-noise ratio of 2. This concentration was determined by extrapolating a plot of the signal-to-noise ratio vs. concentration (for solutions whose concentrations were close to the detection limit) down to a signal-to-noise ratio of 2. These detection limits can no doubt be improved by using a faster monochromator, a silicon intensifier vidicon (1), and a shielded nitrous oxide burner.

Analysis of Standard Rock Sample. Recognizing the potential application of this system to the analysis of complex geological and agricultural samples—i.e., the determination of multiple elements in soils and soil extracts, a well characterized geological standard (BCR-1) was simultaneously analyzed for Fe, Ca, Al, and Ti using the compromise flame conditions determined previously. Mo, W, and K were not present in sufficient concentrations to be determined using the atomic lines present in the given window. The Mn concentration was only slightly above the detection limit for the diluted sample (it could be easily determined in the undiluted sample solution) and could not be determined simultaneously with the other elements. The most intense peak in the spectrum—i.e., Al 3961.5 Å—was recorded from the same spectrum as the remaining elements, but with a vertical scale setting a factor of ten less. The calcium ion lines were strongly affected by the presence of easily ionized salts, but emitted analytically useful information in terms of precision and accuracy if the standards and sample were buffered using an ionization buffer.

Table V compares the results of the simultaneous multielement analysis of BCR-1 for Fe, Ca, Al, and Ti with the recommended published values (23) for this standard. It must be noted that the USGS does not certify standards, but only recommends values based on compilations of analyses reported in the literature. Along with the rec-

(23) F. J. Flanagan, *Geochim. Cosmochim. Acta*, **37**, 1189 (1973).

Table V. Analysis of USGS Standard Rock Sample, BCR-1

Element	Recommended concn, % ^a	Concn determined with vidicon, % ^b	Relative error, %
Al	7.20 (±0.24) ^c	7.47	3.7
Fe	9.37 (±0.21)	9.99	6.6
Ca	4.95 (±0.12)	4.93	0.40
Ti	1.32 (±0.19)	1.45	9.8

^a Reference (23). ^b Average of three runs. ^c Standard deviations estimated from data presented in Reference (24).

ommended values are estimates of the standard deviations of the reported values.

The sample was diluted so that the concentrations of Fe, Ca, Al, and Ti present in the sample that was aspirated into the flame were 31.7, 16.6, 24.1, and 4.5 ppm, respectively. The dilution was chosen to allow the simultaneous determination of all four elements in one aliquot.

The agreement of the determined values with the recommended ones varies from element to element. This is to be expected in simultaneous multielement analyses, since the favorability of the given analytical condition varies from element to element. Thus, the agreement for Ca and Al is excellent because they produce strong lines at the concentrations in which they occur in the sample. In the case of Fe and Ti, the agreement is not as good, because both elements are close to their detection limits for the lines used in the window, resulting in a proportionately larger effect of determinate errors in the estimate of the background.

It should be noted that a minimum of experimental investigation on the presence of interferences and other analytical considerations was carried out, since the purpose of the experiment was to demonstrate the feasibility of simultaneous multielement analyses of a complex geological sample using this system, not to present an analytical method for these samples.

Table VI lists some other possible windows of 200-Å width. The spectral lines used to compile these windows are those commonly used in flame analysis. A total of 36 elements are covered in nine windows. It should be stressed again, that many of the commonly determined elements emit more lines in the nitrous oxide flame than are normally used in flame analysis. Whether these lines appear in the spectrum depends on the flame temperature and the concentration of the given element. Their appearance in a given window may increase the number of elements determinable in that window or they may interfere with a line already present in the window and thereby reduce the number of elements determinable in that window. The ultimate goal is an automated system which can slew from window to window sequentially to provide max-

Table VI. Other Potential 200-Å Windows Using Spectral Lines Commonly Used in Flame Analysis

Window 1	
Zn 2138.6 Å, Pb 2170. Å, Sb 2175.8 Å, Bi 2230.6 Å, Sn 2246.0 Å, Cd 2288.0 Å, Ni 2320.0 Å	
Window 2	
Be 2348.6 Å, Co 2407.2 Å, Au 2428.0 Å, Fe 2483.3 Å, B 2496.8 Å, Si 2516.1 Å, Hg 2536.5 Å	
Window 3	
Ir 2639.7 Å, Ge 2651.2 Å, Au 2676.0 Å, Ti 2767.9 Å, Mn 2794.8 Å	
Window 4	
Pb 2833.1 Å, Sn 2840.0 Å, Mg 2852.1 Å, Ga 2874.2 Å	
Window 5	
In 3039.4 Å, Mo 3132.6 Å, V 3184.0 Å	
Window 6	
Cd 3261.1 Å, Cu 3274.0 Å, Ag 3280.7 Å, Ni 3414.8 Å, Co 3453.5 Å	
Window 7	
Cr 3578.7 Å, Zr 3601.2 Å, Y 3620.9 Å, Ti 3642.7 Å, Rh 3692.4 Å, Fe 3719.9 Å, Ru 3728.0 Å	
Window 8	
Mo 3902.9 Å, Fe 3930.3 Å, Ca 3933.7 Å, Al 3961.5 Å, Ti 3998.6 Å, W 4008.8 Å, Mn 4030.8 Å, K 4044.1 Å, Ho 4053.9 Å, Pb 4057.8 Å, Y 4077.4 Å	
Window 9	
Ca 4226.7 Å, Cr 4254.4 Å, V 4379.2 Å	

imum coverage. Each window must be investigated separately to determine its analytical potential and possible interferences.

The vidicon detector provides a unique means of simultaneous multichannel detection. Its use, however, is not confined only to flame emission but should prove useful for multielement atomic absorption and fluorescence as well. In addition to multielement quantitative analysis, the vidicon system should also prove useful in rapid qualitative survey analysis to determine what elements are present in a sample. In single element analysis, the vidicon permits the simultaneous measurement of an internal standard line for those situations which can benefit from this technique. The vidicon should also prove useful in investigating matrix effects on several elements in a sample simultaneously, as well as to monitor changes in background continuum radiation.

Received for review August 6, 1973. Accepted November 8, 1973. Financial support was provided by the National Institutes of Health under Grant No. GM-19905-01.

(24) F. J. Flanagan, *Geochim. Cosmochim. Acta*, **33**, 81 (1969).

Analysis of Twelve Amino Acids in Biological Fluids by Mass Fragmentography

R. E. Summons, W. E. Pereira, W. E. Reynolds, T. C. Rindfleisch, and A. M. Duffield

Genetics Department, Stanford University Medical Center, Stanford, Calif. 94305

A computerized method has been developed for the simultaneous quantitation of 12 amino acids in biological fluids using the technique of quadrupole mass fragmentography. The amino acids were determined as their *n*-butyl ester *N*-trifluoroacetyl derivatives and a commercially available mixture of deuterated amino acids was used as an internal standard. The combination of individual internal standards with the utilization of the mass spectrometer as a specific ion detector enabled several sources of error inherent in currently used chromatographic procedures to be eliminated. Furthermore, the use of a quadrupole mass spectrometer coupled with an on-line data system allowed the continuous and accurate monitoring of many ions (up to 25 in the present case) over the complete mass range (0 to 750) of the mass spectrometer. Reduction of stored data (establishment of background levels and peak location and calculation of results) was achieved by a totally operator-independent computer analysis program. Analysis on 50- μ l samples of plasma and urine were reproducible with a standard deviation of less than 10% over 5 determinations and this precision was obtained at a lower limit of quantitation of approximately 1 nanogram of an amino acid.

Mass fragmentography is rapidly gaining wide acceptance as an accurate and extremely sensitive technique for the simultaneous identification and quantitation of picogram levels of biologically important compounds. Most approaches (1-4) have involved the use of sector mass spectrometers as detectors and consequently are severely restricted in the range of the *m/e* continuum and in the number of different ions that can be successively monitored. Recent publications have reported the use of a quadrupole mass spectrometer as an analog signal detector (5, 6) with the significant advantage of a greatly increased range of mass values that can be repeatedly scanned.

The ease of application of on-line data systems to a quadrupole mass spectrometer (7) points to an obvious and important extension of this work. Initially, we reported (8) the computer controlled operation of the quadrupole mass filter for mass fragmentography and its application to the determination of phenylalanine in serum, and subsequently (9) to the simultaneous quantitation of

10 amino acids in soil extracts. We have now made substantial improvements to the method whereby a computer program completes the entire analysis of the data collected. As a demonstration of the utility of the method, we wish to report its application to the simultaneous determination of 12 amino acids in biological fluids.

EXPERIMENTAL

Reagents. A deuterated amino acid mixture was supplied by Merck Laboratory Chemicals, Rahway, N.J. The 1.25N HCl in *n*-butanol, 25% (v/v) trifluoroacetic anhydride in methylene chloride, and Talsorb column packing (EGA on chrom W) were obtained from Regis Chemical Co., Morton Grove, Ill. A standard amino acid solution was purchased from Pierce Chemical Co., Rockford, Ill.

Equipment. GLC separations were carried out using a 6-foot by 4-mm (i.d.) coiled glass column packed with Talsorb, and using helium as carrier gas (60 ml/min). The gas chromatograph, a Varian Model 1200, was coupled via an all-glass membrane separator to a Finnigan 1015 Quadrupole mass spectrometer which in turn was interfaced to the ACME computer system of the Stanford University Medical Center.

Interface hardware is that previously described (7). The data acquisition software assumes an operating cycle of: (a) Transmission of a control number, *N*, from the computer to the interface controller which sets the quadrupole mass analyzer to the specified point in the *m/e* continuum. (b) Integration of the ion signal for a pre-set period, *T*, (8 milliseconds in our work), and (c) Computer reading of the integrated ion signal with a 12 bit *A* \rightarrow *D* conversion. Characteristics of the IBM 360/50 to IBM 1800 data path of the ACME computer system dictate that data points be buffered into groups of 250 and, therefore, in our operation, ions are monitored in multiples of 25 with 10 data points or cycles per mass value. The first of the 10 cycles serves only to direct the quadrupole electronics to the approximate mass region of interest. The remaining nine cycles collect a series of ion current integrations 0.5 amu about the *m/e* being monitored. The nine points are then smoothed with a five-point quadratic function (10), and the highest is then selected as the intensity of the particular ion. This procedure allows for small drifts in instrument calibration to be corrected at each mass on every scan. A "spectrum" of precision intensities is collected and filed on disk at 2-second intervals and typically 750 such passes are made in the direction of each sample run. A sum of the precision intensities in each "spectrum" can be used to construct the total ion monitor shown in Figure 1.

Data Analysis Program. The mass fragmentogram data are reduced by a computer program requiring no operator intervention. The program has as its input the series of mass fragmentogram pairs illustrated in Figure 2. Each fragmentogram is represented as a series of 12-bit digital samples measuring the ion current at that mass as a function of time. The program locates candidate peaks in the various mass fragmentograms, selects those peak pairs corresponding to the deuterated and undeuterated analogs of each derivatized amino acid, and measures the area ratio for each pair to quantitate the test mixture for the various amino acids. A sample print-out of the results of this process is shown in Figure 3.

Background Removal. As illustrated in Figure 1, the gas chromatograph effluent has two components: 1) a gently rising background arising from column bleed and other continuously present materials and 2) the test sample and internal standard component peaks. One of the first steps in the data processing is to construct an approximation to this background component so that it can be removed. This is important both to facilitate the detection

- (1) C. G. Hammar, B. Holmstedt, and R. Ryhage, *Anal. Biochem.*, **25**, 523 (1968).
- (2) U. Axen, K. Green, D. Horlin, and B. Samuelsson, *Biochem. Biophys. Res. Commun.*, **45**, 519 (1971).
- (3) C. C. Sweeley, W. H. Elliott, I. Fries, and R. Ryhage, *Anal. Chem.*, **38**, 1549 (1966).
- (4) J. F. Holland, C. C. Sweeley, R. E. Thrush, R. E. Teets, and M. A. Bieber, *Anal. Chem.*, **45**, 308 (1973).
- (5) E. J. Bonelli, *Anal. Chem.*, **44**, 603 (1972).
- (6) J. M. Strong and A. J. Atkinson, Jr., *Anal. Chem.*, **44**, 2287 (1972).
- (7) W. E. Reynolds, V. A. Bacon, J. C. Bridges, T. C. Coburn, B. Halpern, J. Lederberg, E. C. Levinthal, E. Steed, and R. B. Tucker, *Anal. Chem.*, **42**, 1122 (1970).
- (8) W. E. Pereira, V. A. Bacon, Y. Hoyano, R. E. Summons, and A. M. Duffield, *Clin. Biochem.*, 1973 (in press).
- (9) W. E. Pereira, Y. Hoyano, W. E. Reynolds, R. E. Summons, and A. M. Duffield, *Anal. Biochem.*, **55**, 236 (1973).

- (10) A. Savitsky and M. J. E. Golay, *Anal. Chem.*, **36**, 1627 (1964).

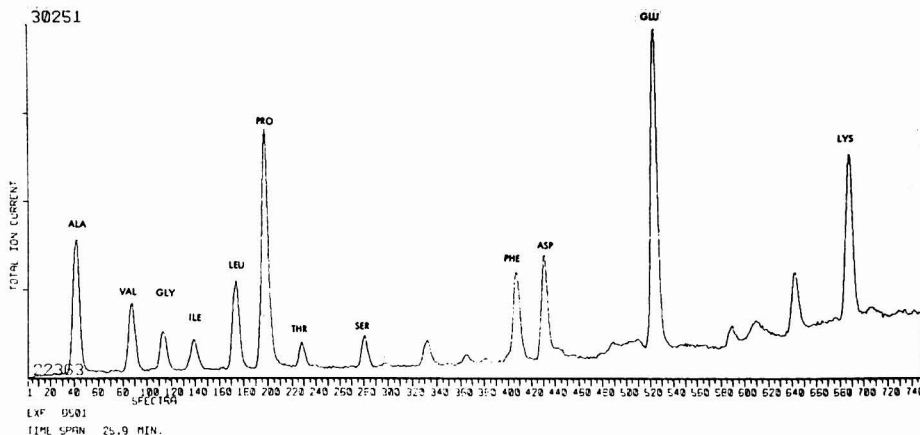


Figure 1. Total ion current from a normal plasma

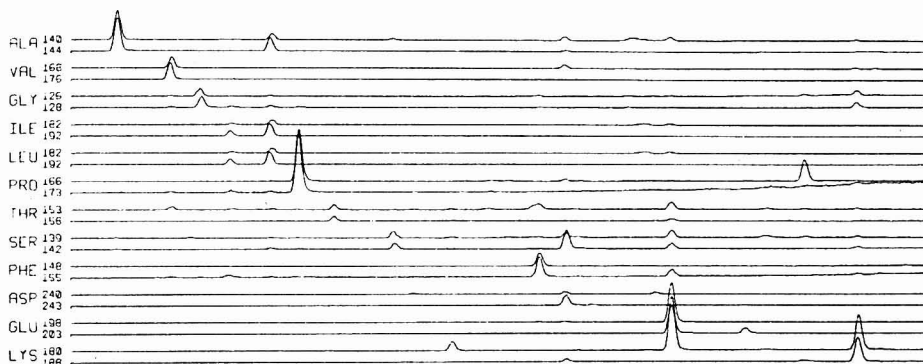


Figure 2. Individual ion chromatograms of monitored fragments

of sample peaks (this is easier in the presence of a flat background rather than a time-varying background) and to make the peak area measurements more accurate (areas of small peaks would be significantly influenced by a background component of comparable size). The plots in Figure 2 (particularly the fragmentograms for masses 166 and 173 used to measure proline and proline-d₂) illustrate the fact that this background varies with elution time. Thus the program approximates the background of each fragmentogram independently.

The local minima of each trace provide a basis for the approximation. For the most part, the sequence of local minima is representative of the background although points between unresolved peaks, for example, may give rise to local minima deviating significantly from the actual background curve. To eliminate the effects of such points, we construct the background approximation as a two-step process. First a "piece-wise least squares fit" through all of the relative minima is constructed [Figure 4(a)]. The minima whose signal amplitudes fall above this first approximation (such as between unresolved peaks) are then eliminated prior to a second pass. The piece-wise LS fit resulting from this second analysis is taken to represent the background portion of the signal [Figure 4(b)].

The "piece-wise LS fit" is a procedure used to develop a smooth approximation to the irregularly positioned signal minima and to provide an interpolation for points between successive minima. Rather than attempt to fit the entire background by a single polynomial or other function, we construct local least

squares fit polynomial approximations to successive small groups of points. These local solutions are then joined together in a way which guarantees continuity of the function and its first derivative. We consider sequences of N minima,

$$S_i = [(y_i, t_i), (y_{i+1}, t_{i+1}), \dots, (y_{i+N-1}, t_{i+N-1})]$$

where y_i is the signal amplitude at the local minimum at time t_i . Through the points in the sequence S_i , we least squares fit a polynomial, $P_i(t)$ (in our case we use a straight line approximation through 9 points). Successive polynomials, e.g., through S_i and S_{i+1} , are joined together so that at times between $t_{i+(N-1)/2}$ and $t_{i+(N+1)/2}$ (the midpoints of S_i and S_{i+1} respectively, assuming N is odd), the background, $B(t)$, is approximated by

$$B(t) = f(\epsilon)P_i(t) + [1 - f(\epsilon)]P_{i+1}(t)$$

where

$$f(\epsilon) = 1 - 3\epsilon^2 + 2\epsilon^3$$

and

$$\epsilon = \frac{t - t_{i+(N-1)/2}}{t_{i+(N+1)/2} - t_{i+(N-1)/2}}$$

The joining function, $f(\epsilon)$, ensures continuity through the first derivative. This procedure has produced reasonable background approximations, even to quite complex chromatograms.

Having constructed a background function, this component is removed so that the fragmentogram peaks ride on a "flat" back-

```

CRT display (Y or N) =?n
mass 140, amp 31.24
mass 144, amp 36.92
Amino Acid ALA Masses 140/144 Areas 8390.1/ 10036.3 RATIO = 0.8360 Location Error = 0
mass 168, amp 11.98
mass 176, amp 18.48
Amino Acid VAL Masses 168/176 Areas 3115.1/ 4672.0 RATIO = 0.6667 Location Error = 6
mass 126, amp 8.26
mass 128, amp 12.00
Amino Acid GLY Masses 126/128 Areas 2168.5/ 3357.7 RATIO = 0.6458 Location Error = 2
mass 182, amp 1.79
mass 192, amp 5.90
Amino Acid ILE Masses 182/192 Areas 456.2/ 1476.4 RATIO = 0.3090 Location Error = 1
mass 182, amp 5.47
mass 192, amp 14.02
Amino Acid LEU Masses 182/192 Areas 1360.7/ 3552.5 RATIO = 0.3830 Location Error = 5
mass 166, amp 50.99
mass 173, amp 65.63
Amino Acid PRO Masses 166/173 Areas 16074.4/ 18638.5 RATIO = 0.8624 Location Error = 1
mass 153, amp 5.33
mass 158, amp 5.19
Amino Acid THR Masses 153/158 Areas 1307.9/ 1204.6 RATIO = 1.0857 Location Error = 2
mass 139, amp 7.53
mass 142, amp 6.48
Amino Acid SER Masses 139/142 Areas 1870.4/ 1558.1 RATIO = 1.2062 Location Error = 1
mass 148, amp 14.68
mass 155, amp 22.44
Amino Acid PHE Masses 148/155 Areas 4221.4/ 6180.2 RATIO = 0.6830 Location Error = 4
mass 240, amp 2.86
mass 243, amp 11.00
Amino Acid ASP Masses 240/243 Areas 705.1/ 2936.8 RATIO = 0.2401 Location Error = 0
mass 198, amp 43.69
mass 203, amp 31.23
Amino Acid GLU Masses 198/203 Areas 12399.6/ 8524.1 RATIO = 1.4547 Location Error = 4
mass 180, amp 38.79
mass 188, amp 26.54
Amino Acid LYS Masses 180/188 Areas 11357.7/ 7587.3 RATIO = 1.4969 Location Error = 5
FINAL ANALYSIS (mg/100ml)
AMINO ACID FOUND
ALA 2.96
VAL 1.97
GLY 2.20
ILE 0.66
LEU 1.48
PRO 2.20
THR 1.94
SEP 3.17
PHE 1.55
ASP 1.09
GLU 4.73
LYS 2.06

```

Figure 3. Terminal output of calculations and results

ground which has a mean value slightly above zero [Figure 5(a)]. The new background is not precisely zero because the approximation to the original data background was fitted through the data MINIMA. Thus, since the background itself contains small fluctuations (caused by noise or very small effluent peaks), these will, in general, fall slightly above the new signal zero. This fact can be used to advantage to assist in setting a more adaptive threshold for peak detection which is the next step in the process.

Peak Detection. The signal peaks are separated from the flattened background by means of a threshold, above which a signal is considered to belong to a component peak and below which to the background. This threshold is set so as to exclude the majority of the background fluctuations while minimizing the truncation of the true peaks. Since background fluctuations will vary in amplitude from run to run (e.g., because of different instrument set-up gain), we have found it desirable to set this threshold based on actual data statistics. If one plots a histogram of the frequency of occurrence of each amplitude level in the flattened fragmentogram, one sees a peak just above zero where most of the new background values lie. Since the sample peaks are relatively few in number and are spread over higher amplitude values, they appear as a "tail" on the high side of the background histogram peak [see Figure 5(b)]. Thus, by detecting the mode of the background histogram peak and measuring its width (standard deviation), a data-adaptive threshold value can be set (threshold =

mode + 2.5 × standard deviation). The multiplier value of 2.5 is chosen based on an assumption of Gaussian background statistics and a 1% probability that a point above the threshold belongs to the background. This then serves to isolate candidate effluent peaks [Figure 5(c)].

These isolated peaks are further screened by a minimum width criterion to eliminate any wideband electronic noise which may be present (actual peaks tend to be at least 10 samples wide because of the way we have set up the data system sampling rate). The remaining peak candidates are then tested to make sure they contain only one maximum—i.e., that they are fully resolved peaks. If not, they are subdivided at successive minima into single peaks. This latter problem is rare in the present application. In more complex situations, more sophisticated peak-resolving algorithms can be utilized to get better area and location approximations.

After sorting out the various component peaks in each of the fragmentograms, the members of each fragmentogram pair are compared to each other and only peaks with an analog at the same time position are considered further. The locations of peaks are determined by fitting a parabola about the peak maximum and using the parabola maximum as the peak position. Analogous peaks must coincide in position to within 10 time units.

Peak Identification and Quantitation. Finally, given the set of coincident peaks between the two mass fragmentograms for an

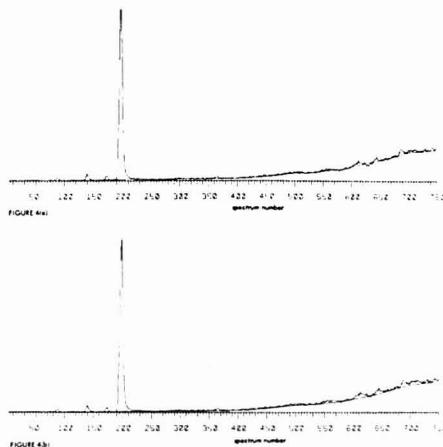


Figure 4. (a) First approximation to the fragmentogram background for m/e 173. (b) Second approximation to the fragmentogram background for m/e 173

amino acid, the appropriate peak pair is selected on the basis of position relative to those found previously. We know for the GC column and temperature profile approximately where each amino acid should be eluted in time. The time differences between successive amino acids were measured and stored as a table in the program as the result of a system calibration. For actual data runs, this table is consulted to determine where to search for each particular amino acid, having determined those preceding it in time. About each such projected location, a search is made (within 30 time units) for the largest candidate peak pair. This is assumed to represent the appropriate amino acid. If no peak pair is found within this search window, that amino acid is assumed to be undetectable in the test sample. If a particular amino acid is missing (or undetectable) in a run, its estimated location is used in projecting for the locations of the remaining acids.

Each of these displacements is relative to a previous peak position and thus, a start-up procedure is necessary. We use the fact that alanine comes off our column first and for at least the deuterated analog standard (mass 144), will be the largest peak within the first 100 time units. This algorithm has proved reliable in automatically starting the analysis procedure and accommodates a certain amount of fluctuation between when spectrum recording begins relative to column injection. Using the previous peak screening procedure, this algorithm would not work if alanine were undetectable in the test sample—in this case, the deuterated analog peak would be cast out for lack of a co-located sample peak. Thus, for this special case, we search for the location of the deuterated analog peak in the fragmentogram for mass 144 to locate the starting position and apply the previous screening procedure subsequently for quantitation.

This program is coded to run on the ACME 360/50 time-shared computer facility in the Stanford Medical Center using a PL/1-like programming language. The time to analyze a run varies depending on the loading of the computer facility and the 360/50 clock does not allow us to measure CPU time for this program alone. Using estimates of running times on a relatively unloaded system, several minutes (wall clock time) are required to analyze a run for the 12 amino acids currently being quantitated.

Procedure. Fifty microliters of body fluid (plasma, urine), 25 μ l of the deuterated standard amino acid solution (1 mg/ml) and 25 μ l of 0.1N HCl were mixed (plasma samples were treated with 1 ml of absolute ethanol, the precipitated protein removed by centrifugation and the supernatant liquid evaporated to dryness *in vacuo*) and made up to approximately 2 ml with water. This solution was passed through a 5-cm³ bed volume column of Bio-Rad AG-50W-X12 (50-100) cation exchange resin. After washing with 20 ml of water to remove neutral and acidic components, the amino acids were eluted with 20 ml of 3N ammonia solution. The eluate was evaporated to dryness *in vacuo* and the residue re-

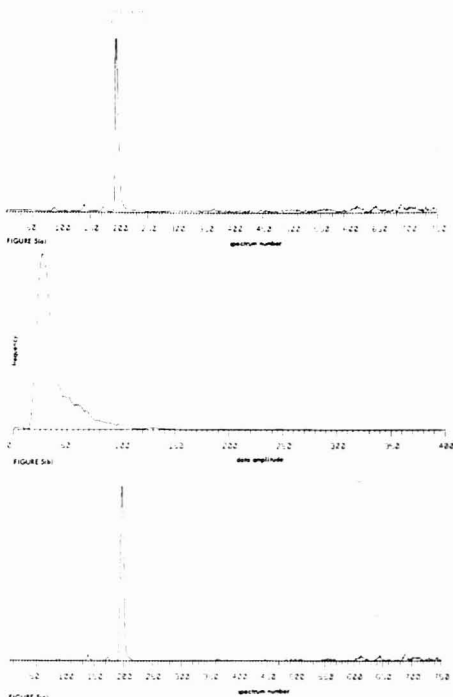


Figure 5. (a) Flattened fragmentogram for m/e 173, obtained by subtracting the background from 4b. (b) Histogram of flattened fragmentogram amplitudes. (c) Result of thresholding flattened fragmentogram with background found by histogram 5(b)

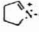
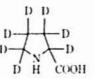
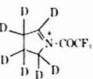
fluxed with 1.25N HCl in *n*-butanol for 15 min and evaporated to dryness. Trifluoroacetic anhydride in methylene chloride (1:1, 0.5 ml) was added to the residue and the solution heated in a sealed tube at 60 °C for 10 min. The solvent was removed under a stream of dry nitrogen and the residue taken up in 50 μ l of ethyl acetate. An aliquot (1-2 μ l) was injected into the injection port of the gas chromatograph (oven temperature 100 °C) and, after a 2-minute delay, the oven was programmed at 4 °C/min (to 220 °C). Data acquisition was commenced when the oven temperature reached 115 °C. The mass spectrometer was operated using an ionizing voltage of 70 eV and an ionizing current of 250 μ A.

Calibration of Internal Standards. Six aliquots (500 μ l) of normal plasma were each mixed with 250 μ l of the deuterated amino acid solution (1 mg/ml) and to 5 of these in turn were added aliquots (10, 20, 30, 40, and 50 μ l) of the Pierce standard amino acid solution (1.25 μ mole of each amino acid per ml of solution). The six solutions were deproteinized with absolute ethanol and the free amino acids recovered and derivatized as above. Each solution was processed in the GC-MS-computer system and the ratio of the areas of the selected fragment ion and its deuterated analog for each amino acid, plotted vs. the amount of that amino acid added. The slopes of each of the straight line graphs obtained were used to calculate a calibration factor for each of the amino acids in the deuterated mixture.

RESULTS AND DISCUSSION

Table I summarizes the structures and m/e values of the selected characteristic fragment ions of the normal and deuterated amino acid TAB derivatives. The combination of *O,N*-trifluoroacetyl,*n*-butyl ester derivatization with gas chromatography on EGA on Chrom W (Tabsoorb) was chosen because of the excellent separation and peak

Table I. Characteristic Fragment Ions Selected for Mass Fragmentography of Undeuterated and Deuterated *N*-TFA-*O*-*n*-Butyl Amino Acids

Amino acids	Fragment ion	Deuterated amino acids	Fragment ion
ALA	$\text{CH}_2\text{CH}=\text{NHCOCF}_3$ (<i>m/e</i> 140) ⁺	$\text{CD}_3\text{CD}(\text{NH}_2)\text{COOH}$	$\text{CD}_2\text{CD}=\text{NHCOCF}_3$ (<i>m/e</i> 144) ⁺
VAL	$i\text{-C}_3\text{H}_7\text{CH}=\text{NHCOCF}_3$ (<i>m/e</i> 168)	$i\text{-C}_3\text{D}_7\text{CD}(\text{NH}_2)\text{COOH}$	$i\text{-C}_3\text{D}_7\text{CD}=\text{NHCOCF}_3$ (<i>m/e</i> 176)
GLY	$\text{CH}_2=\text{NHCOCF}_3$ (<i>m/e</i> 126)	$\text{NH}_2\text{CD}_2\text{COOH}$	$\text{CD}_2=\text{NHCOCF}_3$ (<i>m/e</i> 128)
ILEU	$\text{C}_6\text{H}_5\text{CH}(\text{CH}_3)\text{CH}=\text{NHCOCF}_3$ (<i>m/e</i> 182)	$\text{C}_6\text{D}_5\text{CD}(\text{CD}_3)\text{CD}(\text{NH}_2)\text{COOH}$	$\text{C}_6\text{D}_5\text{CD}(\text{CD}_3)\text{CD}=\text{NHCOCF}_3$ (<i>m/e</i> 192)
LEU	$i\text{-C}_6\text{H}_5\text{CH}_2\text{CH}=\text{NHCOCF}_3$ (<i>m/e</i> 182)	$i\text{-C}_6\text{D}_5\text{CD}_2\text{CD}(\text{NH}_2)\text{COOH}$	$i\text{-C}_6\text{D}_5\text{CD}_2\text{CD}=\text{NHCOCF}_3$ (<i>m/e</i> 192)
PRO	 (<i>m/e</i> 166)		 (<i>m/e</i> 174)
THR	$\text{CH}_2\text{CH}=\text{CHNHCOCF}_3$ (<i>m/e</i> 153)	$\text{CD}_3\text{-CDOH-CD}(\text{NH}_2)\text{COOH}$	$\text{CD}_2\text{CD}=\text{CD-NHCOCF}_3$ (<i>m/e</i> 158)
SER	$\text{CH}_2=\text{CH-NHCOCF}_3$ (<i>m/e</i> 139)	$\text{CD}_2\text{OH-CD}(\text{NH}_2)\text{COOH}$	$\text{CD}_2=\text{CD-NHCOCF}_3$ (<i>m/e</i> 142)
PHE	$\text{C}_6\text{H}_5\text{CH}=\text{CHCOOH}]^+$ (<i>m/e</i> 148)	$\text{C}_6\text{D}_5\text{CD}_2\text{CD}(\text{NH}_2)\text{COOH}$	$\text{C}_6\text{D}_5\text{CD}=\text{CDCOOH}]^+$ (<i>m/e</i> 155)
ASP	$\text{BuOOCCH}_2\text{CH}=\text{NHCOCF}_3$ (<i>m/e</i> 240)	$\text{HOOCDD}_2\text{CD}(\text{NH}_2)\text{COOH}$	$\text{BuOOCDD}_2\text{CD}=\text{NHCOCF}_3$ (<i>m/e</i> 243)
GLU	$\text{HOOCCH}_2\text{CH}_2\text{CH}=\text{NHCOCF}_3$ (<i>m/e</i> 198)	$\text{HOOCDD}_2\text{CD}_2\text{CD}(\text{NH}_2)\text{COOH}$	$\text{HOOCDD}_2\text{CD}_2\text{CD}=\text{NHCOCF}_3$ (<i>m/e</i> 203)
LYS	$\text{CH}_2=\text{CHCH}_2\text{CH}_2\text{CH}=\text{NHCOCF}_3$ (<i>m/e</i> 180)	$\text{NH}_2(\text{CD}_2)_3\text{CD}(\text{NH}_2)\text{COOH}$	$\text{CD}_2=\text{CDCD}_2\text{CD}_2\text{CD}=\text{NHCOCF}_3$ (<i>m/e</i> 188)

shape characteristics obtained with this system (11). One serious disadvantage, however, is that the derivatives of arginine, cysteine, and histidine decompose under these chromatographic conditions. Although the problem has been under study by several groups (12, 13), there is at present no combination of derivatization procedure and conventional packed GC column conditions which can give rise to a complete peak separation of all protein amino acids on a single column. A complete separation of all the amino acids would be an ideal but not a necessary prerequisite for a quantitative amino acid analysis by mass fragmentography. Complete separations are only necessary for those amino acids for which it is difficult or impossible to select fragments with non-interfering *m/e* values. For example the TAB derivatives of alanine, serine, threonine, and valine all have the ion at *m/e* 126 in common and therefore must all be completely separated from TAB glycine where this is the only ion suitable for monitoring. Leucine and isoleucine, because of their isomerism, also have to be completely separated. With larger amino acids there is usually little problem in finding non-interfering ions since these show several prominent unambiguous fragments as compared with the one or two shown by the smaller compounds.

Table II shows the amino acid determinations for a normal plasma, plasma of a patient with Maple Syrup Urine Disease (14), and a normal urine. The results shown are the means and standard deviations obtained from five separate analyses and are expressed in mg/100 ml. Some amino acids analyzed consistently better than others (e.g., phenylalanine, alanine, valine, and lysine) but, in all

Table II. Amino Acid Determinations, mg/100 ml

	Normal plasma	MSUD plasma	Normal urine
Alanine	2.56 ± 0.12	8.58 ± 0.24	3.47 ± 0.04
Valine	1.82 ± 0.12	5.62 ± 0.23	0.56 ± 0.03
Glycine	1.82 ± 0.06	6.06 ± 0.04	13.89 ± 0.38
Isoleucine	0.68 ± 0.05	5.00 ± 0.45	0.42 ± 0.04
Leucine	1.40 ± 0.08	21.29 ± 1.09	1.02 ± 0.05
Proline	2.15 ± 0.09	8.49 ± 0.24	5.59 ± 0.26
Threonine	1.75 ± 0.16	8.13 ± 0.24	4.29 ± 0.17
Serine	2.05 ± 0.06	9.23 ± 0.30	5.37 ± 0.53
Phenylalanine	1.50 ± 0.06	5.74 ± 0.11	0.94 ± 0.03
Aspartic acid	1.10 ± 0.04	2.31 ± 0.14	3.28 ± 0.16
Glutamic acid + glutamine	4.32 ± 0.33	12.62 ± 0.27	3.72 ± 0.11
Lysine	1.98 ± 0.08	9.65 ± 0.14	10.08 ± 0.54

cases, the standard deviations were less than 10% of the mean. This compares favorably with other methods of amino acid analysis currently in general use (15). Replicate injections of the same solution gave results with a standard deviation of less than 4% of the mean over five determinations for each amino acid. Under routine operating conditions, 1 nanogram of an amino acid can be quantitated with this precision. Extension of the method to cover more than 12 amino acids is primarily dependent on obtaining appropriate deuterated standards. Sufficient amounts of arginine and histidine are present in the commercially available mixture used for the present work. Tyrosine-*d*₇ is also commercially available while other labeled amino acids would have to be chemically synthesized. As the internal standard is itself calibrated vs. a

(11) D. Roach and C. W. Gehrke, *J. Chromatogr.*, **43**, 303 (1969).

(12) C. W. Gehrke and H. Takeda, *J. Chromatogr.*, **76**, 63 (1973).

(13) J. P. Zanetta and G. Vincendon, *J. Chromatogr.*, **76**, 91 (1973).

(14) J. B. Stanbury, J. B. Wyngaarden, and D. S. Fredrickson, "The Metabolic Basis of Inherited Disease," 3rd ed., McGraw-Hill Book Co., New York, N.Y., 1972, p 426.

(15) E. D. Pellizzari, J. H. Brown, P. Talbot, R. W. Farmer, and L. F. Fabre, Jr., *J. Chromatogr.*, **55**, 281 (1971).

standard amino acid solution, it is not necessary to know either the degree of isotope incorporation or the amount of each deuterated compound in the standard solution.

The use of a separate deuterated internal standard for each amino acid being analyzed allows several errors inherent in commonly used methods of amino acid analysis to be eliminated. These include loss of material from non-quantitative transfer, derivatization and column (ion exchange and GLC) recovery; loss of the very volatile derivatives of alanine, valine, glycine, etc. during concentration of the derivatized sample prior to injection on the gas chromatograph (16); and loss of basic amino acids which are co-precipitated with protein during plasma work-up (17). Furthermore the chances of errors arising through co-elution of interfering compounds in the conventional GC or ion exchange methods of amino acid analysis are significantly reduced since the mass spectrometer detects only those ions known to be specific to the mass spectrum of the amino acid being analyzed.

The fact that the quantitative result obtained for the amino acid composition or soil samples compared very fa-

vorably with results obtained from an amino acid analyzer (9) suggests quadrupole mass fragmentography will find wide application for the analysis of amino acids in the future. It will be particularly useful for determinations on neonatal plasma and amniotic fluid samples where low sample size or low amino acid content dictates that optimum sensitivity is an important consideration.

The time taken for one complete analysis using this computer directed mass fragmentography system, exclusive of derivatization, is 40 minutes for data collection with an additional 10 minutes before the computer presents the final analytical result.

ACKNOWLEDGMENT

The authors are grateful to Neil Buist, Department of Pediatrics, University of Oregon, for a sample of plasma from a patient with Maple Syrup Urine disease.

Received for review June 11, 1973. Accepted November 12, 1973. This work was supported by the National Aeronautics and Space Administration (Grant No. NGR-05-020-004) and the National Institutes of Health (Grant No. RR00612).

(16) R. W. Zumwalt, K. Kuo, and C. W. Gehrke, *J. Chromatogr.*, **55**, 267 (1971).

(17) L. Z. Bito and J. Dawson, *Anal. Biochem.*, **28**, 95 (1969).

NOTES

Electrochemical Oxidation of Thin Palladium Films on Gold

Steven H. Cadle¹

Chemistry Department, Vassar College, Poughkeepsie, N. Y. 12601

The results obtained in studying the anodic behavior of thin palladium deposits on gold are reported. The purpose of this work was to develop a technique for the quantitative determination of submonolayer deposits of palladium on gold in sulfuric acid media. Furthermore, it was hoped that a comparison between the results of this work and the work of other authors on bulk palladium would help characterize the surface oxidation state of bulk palladium electrodes. A knowledge of the surface oxidation state of palladium is needed to provide an electrochemical means of determining its roughness factor.

The electrochemical behavior of palladium-gold alloys has been studied by Woods (1) and Rand and Woods (2). They found that palladium and gold form a homogeneous alloy. The nature of the chemisorption of hydrogen and oxygen on these alloys is a composite of the properties of the individual metals. The potential of the adsorption and desorption peaks of a cyclic voltammogram of the alloy differs significantly from the potential of the corresponding peaks for the separate metals.

The oxidation of palladium electrodes in aqueous acid media has been investigated by several workers. However, there is disagreement about the potential at which mono-

layer oxygen coverage of the electrode occurs. Rand and Woods (3) investigated palladium oxide formation in 1M H₂SO₄. A plot of the quantity of palladium oxide formed vs. electrode potential showed a step at -1.7 V vs. RHE. They concluded that a stoichiometry of 1 oxygen atom per surface palladium atom exists at this potential and that at more positive potentials, a phase oxide forms. Burshtein *et al.* (4) determined the surface area of palladium powders using the BET method. The surface area was then compared to the quantity of hydrogen and oxygen adsorbed on the electrode as a function of potential in 1N H₂SO₄. It was concluded that a monolayer of oxygen is adsorbed on the electrode at +1.2 V vs. RHE.

EXPERIMENTAL

Electrochemical Equipment. Electrochemical experiments were performed using a Beckman Electroscan 30. An external voltage source was used to step the electrode potential when required. An all-glass 500-ml electrochemical cell was used. A Luggin capillary was used between the reference electrode and the rotating disk electrode. The reference electrode was a Leeds and Northrup 1199-31 saturated calomel electrode. The auxiliary electrode was a coil of platinum wire separated from the working electrode compartment by a medium-porosity glass frit. A belt-driven electrode rotator capable of speeds of 20 to 100 (rpm)^{1/2} in intervals of 10 (rpm)^{1/2} was used. The rotating gold disk electrode and palladium disk electrode had an area of 0.457 cm² and 0.452

(3) D. A. J. Rand and R. Woods, *J. Electroanal. Chem.*, **31**, 29 (1971).

(4) R. Kh. Burshtein, M. R. Tarasevich, and V. S. Vilinskaya, *Electrokhimiya*, **3**, 349 (1967).

¹ Present address, Research Laboratories, G. M. Technical Center, Warren, Mich. 48090.

(1) R. Woods, *Electrochim. Acta*, **14**, 632 (1969).

(2) D. A. J. Rand and R. Woods, *J. Electroanal. Chem.*, **36**, 57 (1972).

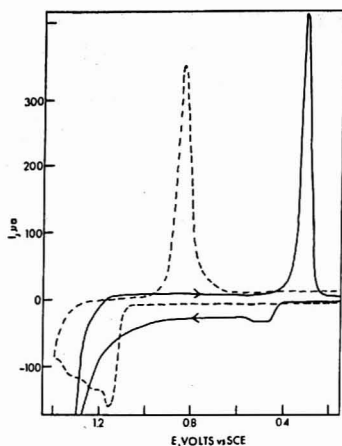


Figure 1. Current-potential curves at a palladium disk electrode (—) and a gold disk electrode (---); 0.2M H_2SO_4 , 2500 rpm, potential scan rate 100 mV/sec

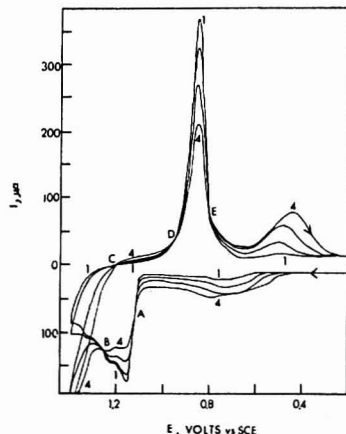


Figure 2. Current-potential curves at a gold electrode in 0.2M H_2SO_4 , $2.36 \times 10^{-6}\text{M}$ Pd(II) ; 2500 rpm, potential scan rate 100 mV/sec

Quantity of palladium deposited: Curve 1) 30 μC , Curve 2) 59 μC , Curve 3) 100 μC , Curve 4) 137 μC

cm^2 , respectively. All potentials are reported vs. the saturated calomel electrode (SCE).

Chemicals and Solutions. All solutions were prepared using triply distilled water. The 0.2M sulfuric acid supporting electrolyte was prepared from Fisher reagent grade sulfuric acid. Palladium does not dissolve in cold concentrated sulfuric acid. Therefore, a stock solution of $1.18 \times 10^{-3}\text{M}$ Pd(II) was prepared by anodizing a 1.2 cm^2 palladium electrode at a constant current of 3.00 mA in concentrated sulfuric acid. The concentration of the Pd(II) solution was calculated from the change in weight of the palladium electrode. Repetitive experiments showed that this process produced Pd(II) at $98.3 \pm 0.5\%$ current efficiency. All solutions were deoxygenated by passing nitrogen through and over the solution.

Electrode Pretreatment. In order to obtain reproducible current-potential curves in the supporting electrolyte, pretreatment

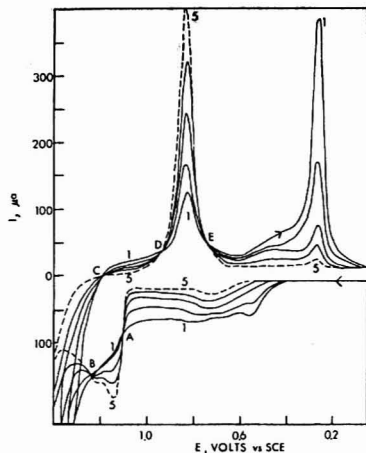


Figure 3. Current-potential curves at a gold electrode in 0.2M H_2SO_4 , $2.36 \times 10^{-5}\text{M}$ Pd(II)

Initial quantity of deposited palladium, 500 μC . Electrode potential cycled continuously. 2500 rpm, potential scan rate 100 mV/sec. Curve 1) 3rd cycle, Curve 2) 6th cycle, Curve 3) 10th cycle, Curve 4) 13th cycle, Curve 5) 16th cycle

of the gold electrode was required. First, the electrode was polished with Buehler 0.05- μ gamma micropolish. The electrode was then introduced into solution and oxidized at +1.6 V for 10 minutes, followed by reduction at -0.4 V for 5 minutes. The electrode was then scanned repeatedly between -0.3 V and +1.6 V until a reproducible current-potential curve was obtained. A similar pretreatment sequence was used for the palladium electrode.

Palladium Plating and Oxidation. Linear plots of $\omega^{1/2}$, the square root of the rotation speed vs. current were obtained at -0.1 and -0.2 V in a $2.36 \times 10^{-5}\text{M}$ Pd(II) , 0.2M H_2SO_4 solution. The convective-diffusion controlled limiting current for the reduction of Pd(II) at 2500 rpm was 13.8 μA at the rotating gold disk electrode. It was observed that the current decreased slowly with time ($\sim 3\%/min$ at 2500 rpm) but returned to its original value if the electrode was oxidized at ± 1.3 V. For this reason, all plating experiments were limited to a maximum of 1 minute. In the experiments described below, palladium was deposited from solutions of various Pd(II) concentration at 2500 rpm and -0.10 V. At the end of the plating time, the electrode potential was scanned at 100 mV/sec to more positive potentials. In the experiments which required integration of the current-potential curves, the electrode potential was stepped from -0.10 V to +0.40 V at the end of the plating time, and then scanned at 100 mV/sec to more positive potentials. The resulting current-potential curve was integrated in the potential region $+0.4 \text{ V} \leq E \leq +1.0 \text{ V}$. In this region, the current is due solely to the residual current and the oxidation of palladium. In calculating the current due to palladium oxidation, it was assumed that the deposition of small quantities of palladium on gold does not change the residual current.

RESULTS AND DISCUSSION

Current-Potential Curves of Palladium on Gold. Current-potential curves for bulk palladium and bulk gold electrodes are shown in Figure 1. This figure is presented to facilitate the comparison of the electrochemical processes occurring on the pure metals to those which occur on a gold electrode partially covered by palladium (Figures 2 and 3). Note that the reduction peak associated with oxidized gold, $E_D = +0.82 \text{ V}$, is well separated from the reduction peak associated with oxidized palladium, $E_D = +0.29 \text{ V}$. Also, the oxidation of palladium at $E_D \leq +1.0 \text{ V}$ occurs in a potential region in which no gold oxidation occurs.

Various amounts of palladium, Q_{Pd} , were plated on a gold disk electrode from a solution of known concentration and the current-potential curves were obtained by cycling the electrode potential between 0.0 and +1.4 V. Typical current-potential curves at low coverage, $Q_{Pd} < 150 \mu C$, are shown in Figure 2. Both the oxidation and reduction of palladium occur at more positive potentials than the corresponding processes at pure palladium electrodes (see Figure 1).

The high palladium coverage current-potential curves in Figure 3 were obtained in a different manner from those of Figure 2. Five hundred μC of palladium were deposited on the gold electrode from a $2.36 \times 10^{-3} M$ Pd(II) solution. Then the electrode potential was cycled continuously between 0.0 and +1.4 V. This process results in the dissolution of palladium (2), thereby decreasing the quantity of deposited palladium on each cycle. Under these conditions, a reduction peak occurs at approximately the same potential, +0.27 V, as the reduction peak of an oxidized bulk palladium electrode, +0.29 V (see Figure 1). Palladium reduction also occurs at more positive potentials. This suggests that both thin and thick deposits of palladium exist on the gold electrode under these conditions, and that the thick palladium deposits are electrochemically identical to pure palladium. The thin palladium deposits interact with the gold and, when oxidized, form an oxide layer which is more easily reduced than the oxide layer formed on the thick deposits.

Isopotential Points. Isopotential points (5) in Figure 2 are labeled A-E. The residual curve for the gold electrode passed through these points. Therefore, bulk gold must be one of the two independent areas, A_1 , on the electrode surface giving rise to these points. The other area, A_2 , must consist of the thin layer deposits of palladium on the gold electrode. At isopotential point A, (IP-A), and IP-B the faradaic processes are the oxidation of gold on A_1 and the oxidation of palladium on A_2 . IP-C occurs at $i = \sim 0.0$ and must be due to the sum of the faradaic and charging current densities on both electrode areas. IP-D and IP-E are caused by the reduction of gold at A_1 and the reduction of palladium at A_2 . IP-E is not as sharp as the other isopotential points.

The presence of these isopotential points is important since they indicate that the electrochemical behavior of the thin palladium deposits is independent of surface coverage at the potential of the IP's under these conditions. Therefore, they support the assumption that the average oxidation state of thin palladium deposits on gold at a given potential—i.e., +1.0 V—will be independent of surface coverage.

Isopotential points were also observed under conditions where both thin and thick layers of palladium were deposited on the gold electrode (Figure 3). These IP's occurred at the same potentials as those in Figure 2 and are therefore assumed to be due to the same processes. This is somewhat surprising, since it implies that the current density on thin and thick palladium deposits must be the same at the potential of the IP's. The presence of IP-E varied markedly with different surface coverages and frequently was not observed. Deviation from IP-B was observed at high coverage (Figure 3, curve 1) due to the oxidation of H_2O on palladium. At even higher coverage (not shown), the curves did not pass through IP-A and IP-D.

Average Oxidation State of Thin Palladium Layers. Various amounts of palladium, Q_{Pd} , were deposited on a gold disk electrode. Q_{Pd} was determined from the plating time and the Pd(II) convective-diffusion controlled cur-

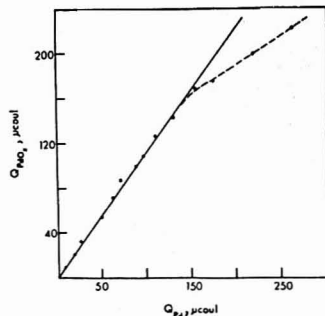


Figure 4. Relationship between the quantity of palladium, Q_{Pd} , deposited and the charge, $Q_{PdO(x)}$, required to oxidize the palladium at $E_D \leq +1.0$ V during a potential cycle of the electrode. Potential scan rate 100 mV/sec; electrode rotation speed, 0 rpm

rent. The charge required to oxidize the palladium at $E \leq +1.0$ V, $Q_{PdO(x)}$, during a potential scan at 100 mV/sec was calculated. The results are presented graphically in Figure 4. Each point is the average of at least three separate measurements. Each measurement was obtained in a fresh solution. The data are represented by $Q_{PdO(x)} = 1.10 Q_{Pd}$ where $0 \leq Q_{Pd} \leq 150 \mu C$ or $0 \leq Q_{PdO(x)} \leq 165 \mu C$.

Thus, the average oxidation state of palladium at +1.0 V is 2.20 under these conditions. It should be noted that this data includes the oxidation state (+2) of soluble palladium which forms during the potential scan. The deviation from linearity at $Q_{Pd} > 150 \mu C$ suggests that thicker, incompletely oxidized deposits are formed. These results can be used to quantitatively analyze for small quantities of palladium in 0.2M H_2SO_4 solution, and have been successfully used (6) to study the corrosion of palladium electrodes.

Determination of the Depth of Coverage. The depth of coverage was determined using the following argument. The deposition of palladium on gold inhibits the subsequent oxidation of the gold electrode (Figures 2 and 3). One palladium atom deposited on the gold electrode surface will inhibit the oxidation of one gold atom if it deposits in a Pd/Au ratio of 1:1 or 0.91 gold atom if it deposits in a close packed plane (7). If the palladium is deposited at depths greater than one monolayer, then less inhibition of the gold oxide will be observed—i.e., less than 0.91 gold atom inhibited.

Current-potential curves of a gold electrode partially covered by palladium, $Q_{Pd} < 150 \mu C$, were recorded. The surface area of the gold was calculated from the gold oxide reduction peak (8). The existence of IP's shows that it is valid to treat the oxidation of the gold as being independent of the palladium coverage. The quantity of palladium deposited on the electrode was calculated using the results of the previous section. The quantity of palladium must be determined on the first positive scan after the reduction of the gold oxide in order to minimize losses due to soluble palladium formation. The oxidation of 0.92 ± 0.05 gold atom was inhibited for every palladium atom deposited, indicating that monolayer formation does occur.

Comparison to Pure Palladium. Three points must be considered in the comparison of the average oxidation

(5) D. F. Untereker and S. Bruckenstein, *Anal. Chem.*, **44**, 1009 (1972).

(6) S. H. Cadle, *J. Electrochem. Soc.*, in press, 1974.

(7) B. J. Bowles, *Nature (London)*, **212**, 1458 (1966).

(8) S. H. Cadle and S. Bruckenstein, *Anal. Chem.*, **44**, 2225 (1972).

state of monolayer palladium on gold obtained from Figure 4 to literature values for the average oxidation state of bulk palladium. First, complete surface oxidation of bulk palladium electrodes at a given potential takes approximately 10 minutes. The data in Figure 4 were obtained from current-potential curves recorded at 100 mV/sec. Longer oxidation times of palladium on gold are not practical because of the significant dissolution of the monolayer palladium. Second, both oxidation and reduction of monolayer palladium occur at more positive potentials than the corresponding processes on bulk palladium (Figure 2). Third, dissolution of Pd(II) occurs during the potential cycle. Experiments showed that approximately 10% of the palladium deposit was dissolved during a potential cycle between 0.0 V and +1.0 V at 0 rpm. All of these considerations indicate that the average oxidation state of the monolayer palladium deposits on gold under these experimental conditions may be less than the average oxidation state of bulk palladium at +1.0 V.

To verify the above result, an experiment based on the following reasoning was performed. The deposition of copper at underpotential has been studied on platinum (9, 10) and gold (11, 12) electrodes. One monolayer of the metal is deposited at underpotential with a ratio of approximately one atom of copper per atom of platinum or

gold. A similar phenomenon is found for several other metals (13, 14). If copper plates at underpotential on palladium, it would be reasonable to expect that one monolayer of copper will be deposited. The charge required for this process can be compared to the charge required to oxidize the palladium electrode at various potentials. The potential at which the two charges are equal should correspond to the potential at which a monolayer of oxygen has been adsorbed—i.e., an average oxidation state of 2.0.

Copper was deposited on a palladium electrode from a $2 \times 10^{-2} M$ Cu(II), $0.2 M$ H₂SO₄ solution. Underpotential deposition of Cu(0) was observed. The maximum quantity of Cu(0) which could be deposited at underpotential was 290 μC at +0.04 V. Comparison of this value to the oxidation of the electrode indicated that monolayer oxygen formation occurred at +1.05 V. This result is in reasonable agreement with the above data on submonolayer palladium deposits on gold, although it does indicate a lower oxidation state than expected.

The results of this work support the data of Burshtein *et al.* (4) who found that the average oxidation state of palladium is 2.0 at +1.2 V vs. RHE in 1N H₂SO₄. It is suggested that Burshtein's results be used to estimate the roughness factor of palladium electrodes.

Received for review July 30, 1973. Accepted November 16, 1973.

- (9) S. H. Cadle and S. Bruckenstein, *Anal. Chem.*, **43**, 1858 (1971).
 (10) M. W. Breiter, *Trans. Faraday Soc.*, **65**, 2197 (1969).
 (11) E. Schmidt, P. Beutler, and W. J. Lorenz, *Ber. Bunsenges. Phys. Chem.*, **75**, 71 (1971).
 (12) W. J. Lorenz, I. Moutzies, and E. Schmidt, *Electroanal. Chem.*, **33**, 121 (1971).

- (13) S. H. Cadle and S. Bruckenstein, *J. Electrochem. Soc.*, **119**, 1166 (1972).
 (14) E. Schmidt and N. Weithuck, *J. Electroanal. Chem.*, **40**, 400 (1972).

New Methods for the Preparation of Perchlorate Ion-Selective Electrodes

T. J. Rohm and G. G. Guilbault

Department of Chemistry, Louisiana State University in New Orleans, New Orleans, La. 70122

The increased interest in ion-selective electrodes has led to the development of new sensor materials which show selectivity for a variety of anions and cations and new methods for the construction of electrodes from these materials. Recently, Davies, Moody, and Thomas incorporated a commercially available liquid ion exchanger in a poly(vinyl chloride) matrix to prepare a nitrate selective electrode (1).

Griffiths, Moody, and Thomas have prepared calcium-selective electrodes by mixing a liquid ion exchanger which is sensitive to calcium with poly(vinyl chloride) (2). A potassium-selective electrode was reported by Davies, Moody, Price, and Thomas based on the same principle (3). Kneebone and Freiser coated a platinum wire with a nitrate-selective liquid ion exchange in a poly(methyl methacrylate) and used the electrode to determine nitrogen oxides in ambient air (4). Ansaldi and Epstein prepared a calcium-selective electrode by coating a graphite rod with a calcium exchanger in poly(vinyl chloride) (5).

These innovations greatly reduce the cost of ion-selective electrodes and provide insight for the study of charge transport through the membrane. Furthermore, these "solid" electrodes are reported to have longer lifetimes than the liquid electrodes (1).

In this study, we have prepared perchlorate-selective electrodes by mixing a commercially available (Orion) exchanger for perchlorate in PVC and used the material to construct an electrode in which the membrane is used with a reference solution and internal reference electrode, and an electrode in which the exchanger is coated on a platinum wire. The performance of these electrodes is compared to the commercial perchlorate electrode.

EXPERIMENTAL

The commercial electrode was prepared according to the manufacturer's manual (Orion Perchlorate Ion Activity Electrode-92-81) (6). The PVC perchlorate material was prepared by mixing 360 mg (20 drops) of the commercial liquid ion exchanger with 170 mg of PVC (Breon 119) dissolved in 5 ml of THF. When mixed, the solution was poured into a glass ring (32-mm i.d.) resting on a glass plate. The ring was then covered with a piece of filter paper and a watch glass. After 24 hours, the glass ring and membrane were turned over to permit the solvent to evaporate from the underside of the membrane. Circles 1 mm in thickness

- (1) J. E. W. Davies, G. J. Moody, and J. D. R. Thomas, *Analyst (London)*, **97**, 87 (1972).
 (2) G. H. Griffiths, G. J. Moody, and J. D. R. Thomas, *Analyst (London)*, **97**, 420 (1972).
 (3) J. E. W. Davies, G. J. Moody, W. M. Price, and J. D. R. Thomas, *Lab. Pract.*, **22**, 20 (1973).
 (4) B. M. Kneebone and H. Freiser, *Anal. Chem.*, **45**, 449 (1973).
 (5) A. Ansaldi and S. I. Epstein, *Anal. Chem.*, **45**, 595 (1973).

- (6) Orion Research Instruction Manual 92-17/92-81, Cambridge, Mass. 02139.

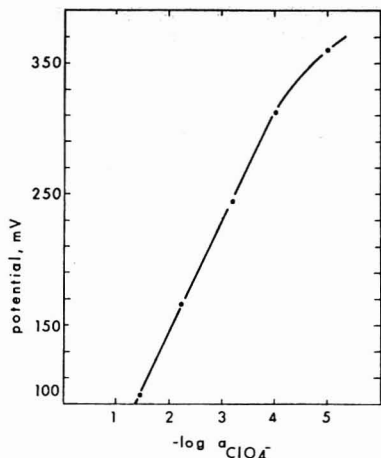


Figure 1. Calibration curve for the commercial perchlorate ion-selective electrode

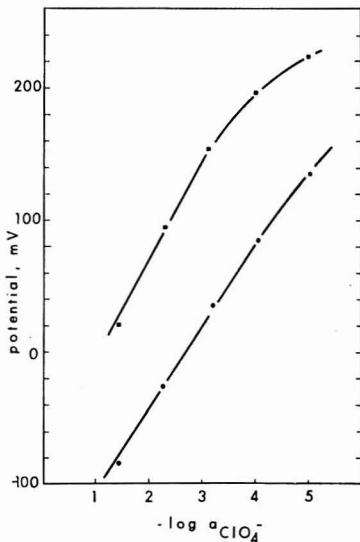


Figure 2. Calibration curves for PVC perchlorate ion-selective electrodes: ● PVC-disk, ■ PVC-wire

and 8 mm in diameter, were cut from the large membrane and glued to the ends of glass tubes (8-mm o.d.). The internal reference solution used with these electrodes was 0.05M ClO_4^- in 0.05M Cl^- . Sodium chloride was used as source of potassium perchlorate. A silver/silver chloride electrode was used as the internal reference.

Alternatively a platinum wire (0.32-mm diameter, 5-cm length), which had been heated until a small drop of platinum formed at the tip, was dipped into the PVC-exchanger mixture and let dry. The uncoated portion of the wire was coated with silicone rubber. Coaxial cables with the outer shield grounded, were used with both the PVC-disk electrode and PVC-wire electrode.

All potential measurements were made vs. a SCE using a Corning Digital 110 Expanded Scale pH meter.

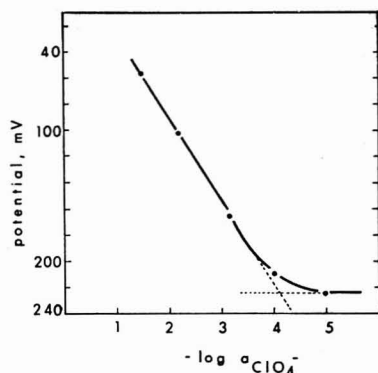


Figure 3. Selectivity coefficient evaluation of the commercial perchlorate ion-selective electrode in 0.1M NaOH

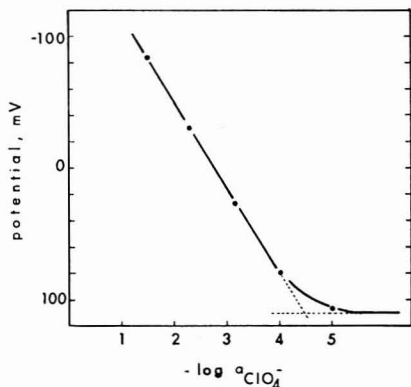


Figure 4. Selectivity coefficient evaluation of the PVC-disk ion-selective electrode in 0.1M NaOH

All chemicals were reagent grade and were used without further purification. Deionized water was used in the preparation of all solutions.

Perchlorate standards were prepared by serial borate buffer dilution of a 10^{-1}M NaClO_4 solution in 0.01M borate buffer.

Solutions used for the determination of selectivity coefficients (K_{ij}) by the two solution method, were prepared by dissolving the potassium salts of the various anions in borate buffer and diluting to volume with buffer.

Solutions used for the study of selectivity coefficients by the mixed solution method were prepared by diluting a 10^{-1}M ClO_4^- in 0.1M NaOH with 0.1M NaOH.

All perchlorate electrodes were soaked for 24 hours in 10^{-1}M ClO_4^- before use and were stored in this solution when not in use. Measurements were made in stirred solutions at ambient temperature (23°C).

RESULTS AND DISCUSSION

Results of measurements of the potential of perchlorate solutions with the commercial electrode assembly, PVC-disk, and PVC-wire electrodes are shown in Figures 1 and 2. The different internal references of each of the electrodes are responsible for the potential differences for a given perchlorate solution. The commercial electrode and the PVC-disk electrode show linear near-Nernstian response from 10^{-1} to 10^{-4}M solutions. The linear range of the PVC-wire electrode is smaller, but still near-Nern-

stian. The commercial electrode and the PVC-disk electrode gave stable responses for one month. The PVC-wire electrode could be used for a period of two weeks before it lost linear response.

Hydroxide ion is reported to interfere with the measurement of perchlorate (6). This interference is shown in Figures 3 and 4 by the mixed solution procedure in which the activity of the interfering ion is constant and the activity of the ion of interest is varied (7). The selectivity coefficients of these electrodes were calculated from

$$K_{ij} = \frac{a_i}{a_j} \quad (1)$$

where a_i and a_j are the activities of the perchlorate and the hydroxide ion, respectively. K_{ij} equals 1.2×10^{-3} for the commercial perchlorate electrode and 1.3×10^{-3} for the PVC-disk electrode in 0.1M NaOH solution.

Interference by iodide, bromide, and nitrate ions was determined by the separate solution method and calculated from,

$$-\left(\frac{E_2 - E_1}{2.303RT/zF}\right) = \log K_{ij} + \log a \quad (2)$$

The selectivity coefficients determined for these ions using the PVC-disk electrode are 5.0×10^{-3} ($10^{-1}M I^-$),

(7) G. J. Moody and J. D. R. Thomas, *Talanta*, **19**, 623 (1972).

1.0×10^{-6} ($10^{-2}M Br^-$) and 2.9×10^{-5} ($10^{-2}M NO_3^-$), respectively. The selectivity coefficients for the same ions are reported to be 1.2×10^{-2} for iodide, 5.6×10^{-4} for bromide, and 1.5×10^{-3} for nitrate, with the commercial liquid electrode (6).

The response times for measurements of the more concentrated solutions of perchlorate were of the order of 30 to 60 seconds. The response time for measurements of the $10^{-5}M$ solution was approximately 120 seconds.

CONCLUSION

Electrodes prepared by using liquid ion-exchangers in PVC show approximately the same characteristics as the commercially available electrode. The PVC-disk perchlorate electrode has the same linear range as the commercial electrode, but the PVC-wire perchlorate electrode had a shorter linear range. The selectivity of the electrode was improved by incorporating the exchanger in a PVC matrix.

ACKNOWLEDGMENT

The authors wish to thank J. D. R. Thomas for a generous supply of poly(vinyl chloride).

Received for review June 6, 1973. Accepted October 25, 1973. The financial assistance of the Environmental Protection Agency (Grant No. R-800359) is gratefully acknowledged.

Change in Potential of Reference Fluoride Electrode without Liquid Junction in Mixed Solvents

Kathleen M. Stelling¹ and Stanley E. Manahan²

Department of Chemistry, University of Missouri—Columbia, Columbia, Mo. 65201

A major problem in the determination of formation constants of metal-organic solvent complexes is liquid junction potentials in mixed solvent systems. This is particularly true in the determination of the formation constants of weak complexes where it is necessary to add organic solvent ligand to such an extent that an appreciable fraction of the solvent medium no longer is water. The fluoride electrode (1) used in cells without liquid junction provides some unique possibilities as a reference electrode. The electrode is quite stable; it has a low impedance; it is relatively interference-free; and, in many cases, the low concentrations of fluoride ion required to poise the potential of the electrode can be tolerated in a medium without detrimental effect upon the system. This paper describes the use of the fluoride electrode as a reference in a cell without liquid junction for the determination of silver-acetonitrile complexes. It shows that discrepancies in this system can be explained on the basis of altered solubility of lanthanum fluoride in a medium containing an appreciable mole fraction of solvent as acetonitrile.

¹ Present address, Department of Chemistry, California State University, Fresno, Calif. 93710.

² Author to whom inquiries should be addressed.

(1) Stanley E. Manahan, *Anal. Chem.*, **42**, 128 (1970).

EXPERIMENTAL

Apparatus. For the attempted determination of formation constants in a cell without liquid junction, a dual electrode system consisting of a solid-state silver/sulfide indicating electrode (Orion No. 94-16) and a solid-state fluoride electrode (Orion No. 94-09A) was used. The electrode system was contained in a jacketed glass cell regulated to $25.00 \pm 0.05^\circ C$ with a constant temperature bath. The solution in the cell was stirred magnetically during measurements. The silver/sulfide electrode was connected to the measuring side of a Corning Model 12 expanded scale pH meter and the fluoride electrode was connected directly to the reference input, a configuration permitted by the low impedance of the fluoride electrode. An electrode system with liquid junction consisted of a silver/sulfide electrode and a conventional aqueous calomel electrode with a 4.0N NaCl filling solution bridged with an agar bridge made up with 0.100M sodium perchlorate. For studies involving the glass sodium electrode (Beckman No. 39137), the glass electrode was connected to the high impedance terminal of the meter and the fluoride or calomel electrode to the low impedance terminal. Subsequent mention of "reference electrode" in this work does not imply the terminal to which the electrode was connected—e.g., the glass electrode used as a reference was actually connected to the measuring terminal.

Reagents. Acetonitrile, Eastman Chromatography Reagent Grade, was used without additional purification. Sodium perchlorate supporting electrolyte was prepared by neutralization of perchloric acid (Mallinckrodt AR Grade) with sodium hydroxide. Solutions were stored in polyethylene bottles.

Procedure. To solutions containing $1.00 \times 10^{-3}F$ Ag(I), $1.00 \times 10^{-4}F$ NaF, and 0.100M sodium perchlorate were added solutions consisting of the same constituents containing also 12N acetonitrile. Potential readings were taken in media ranging up to 4M in acetonitrile.

RESULTS AND DISCUSSION

The shift in potential upon addition of acetonitrile solution as a function of $\log[CH_3CN]$ is shown in Figure 1. The complex formation curve for the solution having a cell with liquid junction is of the normal shape expected for such a complexation system. Overall formation constants calculated from this curve are (2) $\beta_1 = 2.6$ and $\beta_2 = 6.0$ for the complex species $AgCH_3CN^+$ and $Ag(CH_3CN)_2^+$, respectively. In calculating these formation constants, correction was made for liquid junction potential changes at the reference electrode resulting from the addition of organic solvent. This was done by following the potential of the reference electrode vs. a glass sodium electrode as acetonitrile was added. Details of the correction are given in Reference 2. Basically, the assumption is made that the potential of a relatively nonhydrated glass electrode is essentially independent of the composition of a variety of water-organic solvent mixtures (3-5). The potential of the calomel electrode and the potential of the fluoride electrode, both vs. the glass sodium electrode, are shown in Figure 2 as a function of acetonitrile concentration. The potential of the fluoride electrode shifts -44 mV in going from aqueous solution to 4M acetonitrile.

Acetonitrile affects the silver/sulfide electrode potential by complexing with silver ion. That there is no effect of acetonitrile on the electrode *per se* is confirmed by identical results obtained with a silver metal electrode (2).

The plot obtained from the cell without liquid junction (Figure 1) deviates considerably from that taken in the cell with liquid junction. Furthermore, with increasing level of complexing agent, the negative shift in potential does not increase as would be expected. This discrepancy must be attributed to the reference electrode used. The deviation in potential cannot be explained upon the basis of a change in activity coefficient of fluoride ion. It can be estimated (2) from the Debye-Hückel theory, that the maximum change in activity coefficient of the fluoride ion in going from pure water to a medium 3.75M in acetonitrile would cause a potential change of only approximately 0.1 mV.

If the discrepancy is due to an asymmetry potential across the lanthanum fluoride membrane, this potential should be manifested as a difference in solubility of lanthanum fluoride in water as compared to a water-acetonitrile mixture. The solubility of lanthanum fluoride in water and in 4.0M acetonitrile can be evaluated by the titration of La^{3+} with F^- in water and in 4.0M acetonitrile. The titration curves are shown in Figure 3. The titration curve is sharper in 4.0M acetonitrile indicating a lower solubility product. Equivalence points, evaluated by the Gran method were used for calculation of K_s by the Nernst equation. The average value calculated for K_s of freshly precipitated lanthanum fluoride in aqueous solution at 0.100 molar ionic strength is $4.8 \pm 0.6 \times 10^{-18}$. This value compares favorably with the value of 1.2×10^{-18} at an ionic strength of 0.03M reported by Lingane (6). The average value calculated for K_s of LaF_3 in 4.0M

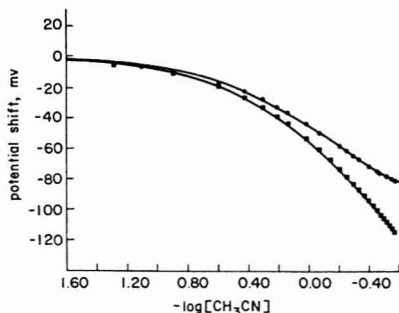


Figure 1. Potential of the silver/sulfide electrode vs. the calomel electrode (■) and vs. the fluoride electrode (●) in a medium $1.00 \times 10^{-3}F$ in Ag(I), $1.00 \times 10^{-4}F$ in NaF, and 0.100M in NaClO₄ upon addition of acetonitrile

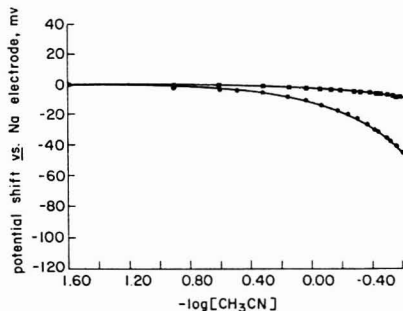


Figure 2. Potential of the calomel electrode (■) and fluoride electrode (●) vs. sodium glass electrode upon addition of acetonitrile

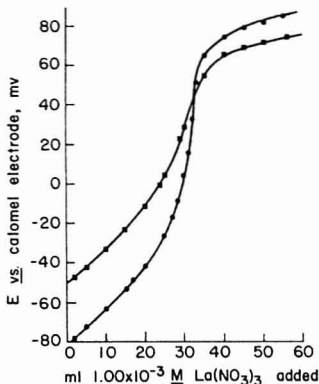


Figure 3. Titration of $3.00 \times 10^{-3}M$ NaF with $1.00 \times 10^{-3}M$ $La(NO_3)_3$ in water (■) and 4.0M acetonitrile (●). Both media are 0.100M in NaClO₄

(2) Kathleen Stelling, Ph.D. Thesis, University of Missouri—Columbia, 1973.

(3) G. Rechnitz and S. Zamochnick, *Talanta*, **11**, 979 (1964).

(4) R. Lanier, *J. Phys. Chem.*, **69**, 2697 (1965).

(5) *Advan. Anal. Chem. Instrum.*, **4**, 302 (1965).

(6) James J. Lingane, *Anal. Chem.*, **40**, 935 (1968).

acetonitrile under identical conditions is $4.3 \pm 0.5 \times 10^{-20}$. Thus lanthanum fluoride is appreciably less soluble in 4.0M acetonitrile than in water.

The difference in solubility product between the aqueous and partially organic media may be used to explain the shift in potential of the fluoride electrode when used as a reference. The equation for fluoride electrode response at 25 °C may be written as

$$E = E_a - 0.0592 \log a_{F^-} \quad (1)$$

where E is the potential in volts, E_a is a constant for a specific electrode system in a specific medium, and a_{F^-} is the activity of the fluoride ion. However, the electrode also responds to lanthanum ion, and the potential may be expressed as the following:

$$E = E_a^* + \frac{0.0592}{3} \log a_{La^{3+}} \quad (2)$$

Since $a_{La^{3+}}$ and a_{F^-} are related through the solubility product constant for lanthanum fluoride,

$$K_s = (a_{La^{3+}})(a_{F^-})^3 \quad (3)$$

the equation for electrode response may be expressed as follows:

$$E = E_a^* + \frac{0.0592}{3} \log \frac{K_s}{(a_{F^-})^3} \quad (4)$$

This equation separates the E_a term normally referred to in describing fluoride electrode response into a membrane solubility term (expressed as $0.0592/3 \log K_s$ and E_a^* , a term representing all other contributions to the "constant" term. In aqueous solution, the potential measured for a given fluoride concentration therefore can be given by

$$E_w = E_a^* - 0.0592 \log a_{F^-} + \frac{0.0592}{3} \log K_{s,w} \quad (5)$$

where $K_{s,w}$ is the solubility product constant for the lanthanum fluoride membrane in water. Likewise, potentials measured in a partially organic medium may be expressed as

$$E_o = E_a^* - 0.0592 \log a_{F^-} + \frac{0.0592}{3} \log K_{s,o} \quad (6)$$

where $K_{s,o}$ is the solubility product constant of the lanthanum fluoride membrane in the partially organic solvent mixture. Thus, the shift in potential, ΔE_{obs} , at a given, constant fluoride concentration on transfer from aqueous to partially nonaqueous solution is given by

$$\Delta E_{obs} = \frac{0.0592}{3} \log \frac{K_{s,o}}{K_{s,w}} \quad (7)$$

For 4.0M acetonitrile, potential changes resulting from changes in LaF_3 solubility were determined by substituting $K_{s,o} = 4.3 \times 10^{-20}$ and $K_{s,w} = 4.8 \times 10^{-18}$ into Equation 7. The potential shift predicted on the basis of solubility differences is -40.4 mV. The shift actually observed was -44 mV. Therefore, the shift observed at the fluoride electrode on addition of acetonitrile may be explained in terms of changes in the solubility of the LaF_3 membrane. Since the K_s values from which the potential shift was predicted are for freshly precipitated lanthanum fluoride rather than large, well-aged crystals, it is doubtful that any particular significance can be attached to differences of less than ± 5 mV.

The fluoride electrode in a cell without liquid junction has been found less suitable than the calomel electrode with liquid junction as a reference electrode for complexation studies in systems where addition of an organic ligand and appreciably alters the properties of the solvent. The relatively large negative shift in potential of the fluoride reference electrode in going from an aqueous medium 0.100M in acetonitrile to a similar medium 4.0M in acetonitrile can be explained entirely upon the basis of decreased solubility of the lanthanum fluoride electrode membrane in the partially organic medium.

Received for review August 20, 1973. Accepted November 7, 1973. This research was supported in part by the United States Department of the Interior Office of Water Resources Research Allotment Grant A-049-Mo. K. M. Steltling gratefully acknowledges support through N.D.E.A. Title IV Fellowship funds and an American Chemical Society Analytical Division Summer Fellowship sponsored by Carle Instruments, Inc.

Quantitative Spectrometric Determination Specific for Mannose

Ralph W. Scott and Jesse Green

Forest Products Laboratory, Forest Service, U.S. Department of Agriculture, Madison, Wis. 53705

Specific quantitative methods for single sugars in sugar mixtures generally require a preliminary separation of the sugars or the application of specific enzymes such as glucose oxidase for the measurement of glucose. Photometric methods are of interest because they are sensitive and simple, but their use is often limited by a lack of specificity. Maksimenko *et al.* (1) have recently described a method that deals with the specificity problem in mannose-glucose mixtures by using the different sensitivities of mannose and glucose in the phenol-sulfuric acid reaction.

(1) O. A. Maksimenko, L. A. Zyukova, N. S. Andreev, and R. M. Fedorovich, *Zh. Anal. Khim.*, **26**, 2467 (1971).

In the procedure described here, use is made both of the dehydration of sugars to furans in concentrated sulfuric acid and of a rather specific change in the dehydration of mannose caused by chloride and boric acid. This sensitivity to chloride and to boric acid permits the determination of mannose in plant materials without preliminary separations of sugars.

EXPERIMENTAL

Apparatus. Concentrated sulfuric acid and 72% sulfuric acid were dispensed by glass hand-pumped dispensers (5-ml Repipet, Labindustries, 1802 Second St., Berkeley, Calif. 94710) with caps to fit 9-lb sulfuric acid reagent bottles.

Test solutions were accurately sampled with a spring-loaded syringe set for 0.125 ml and fitted with a 0.74-mm Teflon needle (Hamilton Co., P.O. Box 307, Whittier, Calif. 90608). This modification of a 1-ml tuberculin syringe has been described (2).

Reaction tubes were 15 × 85-mm culture tubes covered with loose-fitting polypropylene bacteriological caps. The tubes closely fitted into an electrically heated aluminum block with 15 × 50-mm holes.

Absorbance was measured with a Beckman DU spectrophotometer.

Reagents. Technical grade concentrated sulfuric acid (about 96%) gave low absorbance blanks between 0.05–0.03 in the range 280 to 320 nm. If blanks are much higher, it is best to change to a better lot of acid. The only reagent in addition to the H_2SO_4 was a solution containing 12 grams of NaCl and 2 grams of H_3BO_3 in 100 ml of water.

Purchased sugars were D-forms except for L-arabinose. Only mannose was recrystallized to a white powder (3). 4-O-Methylglucuronic acid was recovered from hydrolyzates of hardwood xylan.

Procedure for Dissolving Water-Insoluble Polysaccharides. Most carbohydrate polymers dissolve in 72% H_2SO_4 at room temperature. The time for solution may be reduced by heating the sample at 50 °C for 10–15 min with some trituration.

A suggested procedure for plant cell walls is solution of about 20 mg of 40–80 mesh dry material in 2–5 ml of 72% H_2SO_4 at 50 °C followed by dilution with water to exactly 25 ml. The solution is then ready for the first step in the mannose analysis.

Lignin from plant material will remain mostly insoluble. It may be allowed to settle out in the 25-ml volume or it may be centrifuged down from a few milliliters of suspension. Amounts of lignin which do not greatly add to absorbance do not adversely affect the absorbance difference due to mannose.

Procedure for Mannose Analysis. Transfer 0.125 ml of sample solution into each of two reaction tubes. To one tube, add the same volume of water and to the other tube, add a like volume of the NaCl- H_3BO_3 solution. Add 2.0 ml of concentrated H_2SO_4 to each tube and mix briefly by alternately swirling and tilting the tube. Heat each tube in the heating block at 70 °C for 30 min; remove each tube and cool by swirling for 15 sec in water at room temperature. Read absorbances at 280 nm vs. a water reference. The difference between absorbances with and without NaCl- H_3BO_3 is directly proportional to mannose concentrations between zero and 250 $\mu g/ml$. A reliable standard value is obtained from standard mannose solutions containing 5–6 mg in 25 ml by averaging the results of three separate runs, each run having triplicate analyses.

Technique. It is advisable to keep tubes free of dust by using loose-fitting caps at all times, including a drying period in a clean oven after washing.

Sulfuric acid can be added to a series of samples at 20-sec intervals with tubes being removed from the heating block at the same intervals. The small amount of HCl released when H_2SO_4 is added to the NaCl solution is not a problem in a well-ventilated room.

The dehydration procedure has been described (4, 5).

Sampling. The amount of sample to be weighed depends upon the percentage of mannose and also upon which carbohydrate monomers are most prevalent in the mixture. It is desirable to maximize the absorbance difference due to mannose without exceeding readable total absorbances due to mannose and other sugars. Mixtures of mannose and glucose varying in mannose content from 2 to 20% require sample sizes varying from 26 to 17 mg. Corresponding amounts of mannose with xylose require sample sizes varying from 17 to 13 mg.

RESULTS AND DISCUSSION

The Dehydration Reaction. The usefulness of analytical procedures based upon carbohydrate dehydration in concentrated sulfuric acid is due to the simplicity of reac-

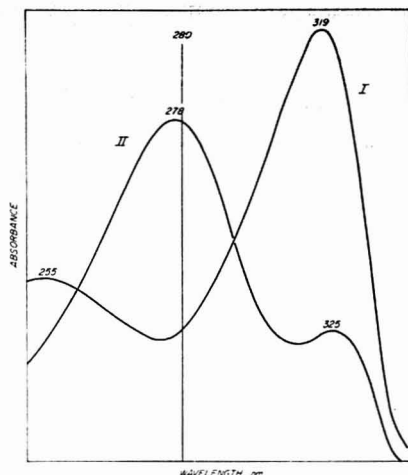


Figure 1. Absorption spectra after dehydration of mannose in 90% H_2SO_4 without NaCl- H_3BO_3 in solution (I) and with NaCl- H_3BO_3 in solution (II).

tion conditions, the applicability to soluble oligomers without prior complete hydrolysis, the quantitative formation of a few relatively stable furan products, and the characteristic and strong ultraviolet light absorption by these products. Although reagents such as phenol or anthrone may form analytically useful colored products with furans or with intermediates in the dehydration reactions, their use may be less precise, and sometimes even less specific, than a direct ultraviolet absorption measurement. Since the dehydration reaction is dependent upon sugar structure, time, temperature, concentration of sulfuric acid, and reagents such as chloride and boric acid, these factors can be used to steer the dehydration in favorable directions.

Major products of dehydration in sulfuric acid are 2-furancarboxaldehyde from pentoses, 5-(hydroxymethyl)-2-furancarboxaldehyde from hexoses, and 5-(formyl)-2-furancarboxylic acid from hexuronic acids. Although the amounts of these products are not in stoichiometric proportions with the starting sugars, the dehydrations are rapidly completed to give repeatable amounts of furans characteristic of the starting sugars.

In Figure 1, curve I is primarily the absorption spectrum of 5-(hydroxymethyl)-2-furancarboxaldehyde formed from mannose in the dehydration mixture without NaCl- H_3BO_3 . Curve II shows the altered absorption spectrum brought about by the dehydration of the same quantity of mannose in the presence of NaCl- H_3BO_3 . The chloride-boric acid reagent caused a decreased amount of 5-(hydroxymethyl)-2-furancarboxaldehyde and an increased amount of an unknown absorber with a maximum absorbance at 278 nm. Tests showed that the alteration in mannose dehydration was primarily due to the chloride; boric acid had a synergistic effect on this change.

The slight shift in the 319-nm peak to 325 nm in Figure 1 is most likely due to the conversion of 5-(hydroxymethyl)-2-furancarboxaldehyde to 5-(chloromethyl)-2-furancarboxaldehyde in the presence of chloride (6). A similar shift of absorbance from 322 nm to 325 nm occurs

(6) F. H. Newth, *Advan. Carbohydr. Chem.*, **6**, 87 (1951).

- (2) American Society for Testing and Materials, ASTM Designation D 1915-63 (Reapproved, 1970), 1916 Race Street, Philadelphia, Pa. 19103.
- (3) F. J. Bates, and Associates, "Polarimetry, Saccharimetry and the Sugars," *Nat. Bur. Stand. (U.S.) Circ.* **440**, 1942, p. 471.
- (4) R. W. Scott, and J. Green, *Tappi*, **55**, 1061 (1972).
- (5) R. W. Scott, W. E. Moore, M. J. Effland, and M. A. Millett, *Anal. Biochem.*, **21**, 68 (1967).

Table I. Interference by Some Sugars

Sugar	Relative absorbance difference at 280 nm (by weight; mannose = 1.00) ^a
Rhamnose	+0.58
Fucose	+0.42
Glucuronic acid	+0.41
Lyxose	+0.23
Ribose	-0.20
Galactose	+0.15
4-O-Methylglucuronic acid	-0.13
Fructose	+0.08
Galacturonic acid	-0.07
Glucose	-0.01
Xylose	-0.02
Arabinose	-0.01

^a A negative value results from a decrease in absorbance due to NaCl-H₂BO₃ and will cause a low mannose determination.

when NaCl is added to 5-(hydroxymethyl)-2-furancarboxaldehyde in 90% H₂SO₄. In this case, the peak height is not decreased.

Interference by Other Sugars. Some sugars which interfere with the determination are listed in Table I. The list indicates that cis hydroxyl groups (especially at carbon atoms 2 and 3) in neutral sugars may cause interference unless there happens to be an intersection of the two absorption spectral curves at about 280 nm as results from the dehydration of arabinose. Comparison of recorded absorption spectra with and without NaCl-H₂BO₃ permits the estimation of interference and perhaps the choice of a slightly better wavelength to decrease interference. Absorbance measurements at 280 nm are specified here primarily to decrease interference from glucose, xylose, and arabinose.

The interference by glucuronic acid is due to slow dehydration of glucuronolactone in 90% H₂SO₄ and to an increased dehydration rate in the presence of boric acid. It should be possible to greatly reduce interference from glucuronic acid by standardizing the procedure without boric acid because the increase in absorbance at 280 nm due to boric acid is not essential. Galacturonic acid and 4-O-methylglucuronic acid do not interfere because they do not form lactones that retard dehydration in 90% H₂SO₄.

Although glucose, xylose, and arabinose can be considered as noninterfering sugars, the absorbance which they produce limits the sample size at low percentages of mannose. Furthermore, when they are in high percentage they may cause small absorbance differences at 280 nm. These differences can be estimated from sugar blanks, but an accumulation of errors causes decreasing reliability below 5% mannose.

Since mannose dehydration is complete in 20 min and absorbance is then stable, it would be possible to remove tubes from the heating block as a group after a minimum of 20 min and to leave them at room temperature. However, the glucose dehydration rate is decreased by the NaCl-H₂BO₃ so that only at 30 min are the absorbances from glucose dehydration approximately equal for the two solutions. The heating period recommended here for the dehydration was chosen for samples high in glucose.

Measurement of Mannose in Sugar Mixtures. The absorbance difference at 280 nm had a linear response to mannose concentrations up to 250 µg/ml. Since the primary usefulness of this measurement is for mannose in sugar mixtures, a few mixtures were prepared and analyzed (Table II). Except for the increased relative errors in amounts of mannose below 5%, the averages of triplicate samples show satisfactory estimations for these simple mixtures.

The analysis was applied to the materials in Table III where results are compared to the mannose content mea-

Table II. Determination of Mannose in Mixtures with Glucose and Xylose (25-ml total volume)

Composition	Mixture No.					
	1	2	3	4	5	6
Mg Glucose	16.40	20.10	20.30	21.90	20.30	20.90
Mg Xylose	2.50	2.12	1.25	2.00	2.00	2.00
Mg Mannose	5.00	2.50	1.25	0.50	0.25	0.00
Mg Mannose found	5.13	2.52	1.21	0.40	0.44	0.00
Weight percentage mannose found	21.4	10.2	5.3	1.6	2.0	0.0
Error in weight percentage found	+0.5	+0.1	-0.2	-0.5	+0.9	

Table III. Analysis of Plant Material for Mannose

Source of material	Percentage of mannose anhydride ^a				By chromatography
	1	2	3	Average	
Douglas fir wood	13.6	14.6	13.2	13.8	13.0
Western hemlock wood	11.9	12.0	12.2	12.0	13.3
Ponderosa pine kraft pulp	6.2	5.7	5.8	5.9	5.7 ^b
Aspen wood	2.0	1.6	2.2	1.9	1.8 ^b
Southern pine kraft pulp	5.4				5.6 ^b
Glucomannan (pine)	60.0				61.5
Galactomannan (locust bean gum)	49.0				51.0 ^b

^a Each figure under 1, 2, 3 is an average of three determinations on a single solution. ^b Data calculated from mannose as percentage of total sugar and from a corrected total sugar analysis (4).

sured by paper chromatography (7) followed by elution and use of the Nelson procedure (8). The dehydration solutions from the galactomannan and from its mannose standard were read at 285 nm rather than at 280 nm to reduce the interference from galactose. From a reading at 280 nm, the apparent mannose content was 10% higher.

Application to Certain Total Sugar Analyses. A dehydration procedure can be used for total sugar analysis when one or two sugars dominate the carbohydrates in a mixture (4). An example is structural tissue of broadleaf plants where the predominating glucose and xylose contents can be measured by comparison to a single glucose standard. Significant amounts of mannose in coniferous wood cause low total sugar estimates (4), but the mannose measurement described here can give the necessary correction.

Precision. Average blank values from water and from NaCl-H₂BO₃ solutions were the same; thus blank determinations were unnecessary for the analysis. However,

(7) J. F. Saeman, W. E. Moore, R. L. Mitchell, and M. A. Millett, *Tappi*, **37** (8), 336 (1954).

(8) N. Nelson, *J. Biol. Chem.*, **153**, 375 (1944).

blanks contained much of the variability of the determination. A standard deviation of 0.012 was found for the absorbance difference between 18 pairs of blanks run during a month. Fifteen sets having three mannose samples in each set had an average standard deviation of absorbance of 0.010 within a set.

The first four lines in Table III show the variability between averages of three replicates per solution. These results also include variability in the initial step of dissolving samples in 72% H₂SO₄ and diluting. The relative standard deviations calculated from three averages are 4.5%, 1.3%, 5.2%, and 15.8%, respectively, for the first four lines in Table III. At the lowest concentration, 2% mannose, the basic variability of the method seen in blank runs becomes large compared to the mannose measurement itself.

Received for review August 20, 1973. Accepted October 12, 1973. The Forest Products Laboratory is maintained in cooperation with the University of Wisconsin. Mention of trade or proprietary names is for identification purposes only and does not imply endorsement of the product by the Forest Service, U.S. Department of Agriculture.

Application of the Carbon Rod Atomizer to the Determination of Mercury in the Gaseous Products of Oxygen Combustion of Solid Samples

Duane Siemer and Ray Woodruff

Department of Chemistry, Montana State University, Bozeman, Mont. 59715

The analysis of solid samples for fractional part per million levels of mercury is a common problem in analytical laboratories. Several excellent reviews containing the analytical methodology have been published recently (1-3). The most commonly utilized methods at present are neutron activation analysis or some form of atomic absorption preceded by wet ashing and/or extraction. The former technique is disadvantageous in many cases in that it is expensive and usually involves sending samples off to central laboratories equipped with high neutron flux sources. Atomic absorption, on the other hand, is relatively inexpensive and can be accomplished rapidly.

Atomic absorption analysis for mercury is usually accomplished by adding a reducing agent (usually stannous chloride) to a digestate and sweeping the evolved atomic mercury out of the solution into a cold vapor absorption tube or flame by means of a gas bubbled through the system. In order to increase the sensitivity and to reduce the error due to the molecular absorption often encountered, some workers have concentrated the elemental mercury in the gas streams onto gold surfaces and released the mercury suddenly (by heating the gold substrate) into the atomic absorption cell. Finally, in order to eliminate pre-ashing or extraction steps, some workers have applied the

above technique directly to the combustion gases of samples burned in oxygen (4). The approach used in this paper is to burn the samples completely in a modified combustion tube, to collect the evolved mercury on the inner surface of a porous, gold plated, carbon rod atomizer tube, and, finally, to measure the atomic absorption when the tube is heated in the normal fashion.

EXPERIMENTAL

Apparatus. Figure 1 depicts the combustion apparatus used for this research. The combustion tube consists of a U tube of about 4-cm radius made of 12-mm diameter Vycor tubing with a 15-cm long, 2.0-cm diameter combustion chamber sealed to it. There are oxygen inlets sealed both to the combustion chamber and the "afterburner." The combustion apparatus is wrapped with 20-gauge nichrome wire as indicated. The after burner section is loosely filled with a 50-50 vol/vol mixture of 8-mesh activated alumina and calcium oxide powder. Oxygen flow is controlled and measured by two Gilmont flow gauges and needle valves. The combustion boat is made of a short section of 10-mm diameter quartz tubing sealed to a length of 4-mm quartz rod inserted into a No. 2 rubber stopper. The combustion gases are passed through a water jacketed cold finger made of borosilicate glass to condense some of the water evolved if a large number of samples are burned in rapid succession.

The preparation of the gold plated atomizer tubes, a description of the filter adaptor and the details of the atomic absorption apparatus used have been described in the paper by Siemer, Lech, and Woodruff (5). In addition, a deuterium lamp powered by a Beckman power supply is utilized for measurement of non-

(1) H. R. Jones, "Mercury Pollution Control," Noyes Data Corp., Park Ridge, N.J., 1971.

(2) R. Hartung and B. D. Dinman, "Environmental Mercury Contamination," Ann Arbor Science Publishers, Ann Arbor, Mich., 1972.

(3) F. M. D'Itri, "The Environmental Mercury Problem," Chemical Rubber Co., Cleveland, Ohio, 1972.

(4) V. Liddums and U. Ulvarson, *Acta Chem. Scand.*, **22**, 2150 (1968).

(5) D. Siemer, J. Lech, and R. Woodruff, *Appl. Spectrosc.*, in press.

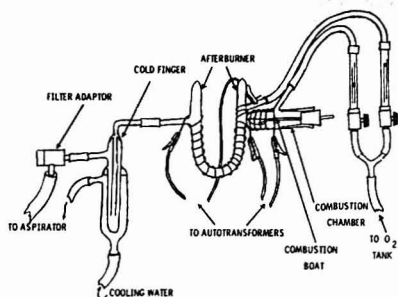


Figure 1. Combustion and filter apparatus

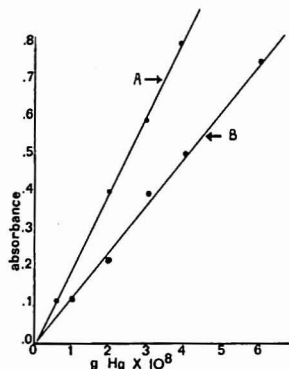


Figure 2. Standard curves for mercury

(A) 110-A atomization current, (B) 70-A atomization current

atomic interferences. A Nalgene aspirator is used to draw the gases from the combustion through the combustion train.

Reagents. The 1000 ppm stock mercury solution was made by dissolving $\text{Hg}(\text{NO}_3)_2 \cdot \text{H}_2\text{O}$ in 0.1N HNO_3 . This solution was stabilized by adding 0.01 gram/100 ml of $\text{K}_2\text{Cr}_2\text{O}_7$. The oxygen used was USP grade supplied by NCG. It proved to be free of mercury vapor and did not require any further purification.

Procedure. From 5 to 200 mg of sample is placed into the combustion boat. The current through the nichrome wire is adjusted to heat it to about 1100 °C as measured by an optical pyrometer. However, the temperature of the center of the tube is considerably lower than this. The O_2 flow rates are adjusted to 30 cm^3/min for the inlet situated directly over the boat and to about 150 cm^3/min for the inlet at the beginning of the "afterburner." A plated atomizer tube is placed into the filter adaptor and then the filled combustion boat is quickly inserted into the back of the combustion tube. The flow of water through the aspirator is adjusted until there is a net increase in oxygen flow. This ensures that a leak in the system will result in no loss of mercury. The sample is burned to completion (1 to 2 minutes) and then the system is allowed to flush for about 3 minutes more. Then the plated carbon tube is removed from the filter adaptor and is inserted into the carbon rod atomizer. Nitrogen gas at 500 ml/min flow rate is passed over the carbon rod to flush out oxygen, and then the atomizer power supply is adjusted to supply 110 A for about 3 seconds. An atomization setting of "3.5" for 2.5 seconds in the "step" mode is satisfactory if the Varian model 63 CRA is used. The mercury is driven off quickly before the tube reaches incandescence, resulting in an atomic absorbance spike proportional to the total mercury in the sample. These tubes may be

reused many times without loss of efficiency if they are not heated to more than 1000 °C during the atomization step.

RESULTS AND DISCUSSION

This method is calibrated by placing various volumes of 2 ppm mercury solution into the combustion boat and treating it exactly like a solid sample. In Figure 2 are standard curves for mercury achieved in this manner at two different atomization current values. The addition of ammonium sulfide in several thousand-fold excess of what is required to convert the mercury to the sulfide had no effect upon the oxidation of mercury. The relative standard deviation of a series of such runs with 2×10^{-8} gram of mercury is 4%.

Samples. Several different types of organic samples were analyzed by this technique. It was necessary to grind the sample to less than 100 mesh to get reproducible results with some samples. In all cases, standard additions of mercury solution to the samples gave analytical curves parallel to curves prepared with the solutions alone. When this was established, the samples were then run directly and the results calculated from the standard curve. The amount of sample was chosen to give on the order of 10 to 50 ng of mercury collected on the tube. Molecular absorption due to incomplete oxidation of tars was noted in preliminary work. However, filling the "afterburner" section with the mixture of alumina and calcium oxide and, if necessary, reducing the size of sample burned, eliminated this problem.

Ground orchard leaves (NBS No. 1571) were the only samples analyzed with a known mercury content. The results obtained with seven replicates of 50 mg of leaves burned each time, were a mean value of 0.16 ppm and a relative standard deviation of 7.8%. This agrees well with the accepted value of 0.16 ppm.

Coal samples were the primary reason for beginning research on a quick, reliable method for mercury. Recent development of low sulfur coal fields in eastern Montana has sparked considerable interest in possible trace metal contamination of the environment resulting from use of the coal. Mean values for a series of these coals ran from less than 0.1 ppm to about 0.3 ppm with relative standard deviations of about 7% for replicates on individual coals. Very finely ground samples were required for good reproducibility with coal samples.

Hair and toenail samples from a number of individuals were analyzed. Approximately 5 mg of sample is required for these tests. Values ranged from 0.8 ppm to 3.0 ppm for hair and somewhat less than this for the nail samples. Relative standard deviations for hair samples were 8%.

In conclusion, this technique of combining the sensitivity and ease of operation of the carbon rod type of atomizer with the straightforward combustion of organic samples has resulted in an analytical system which gives good results for mercury in a wide range of organic matrices. It is possible to burn a series of samples and standards at one time, store the tubes in a desiccator, and analyze them whenever the carbon rod atomizer is not being used for other work. The sensitivity of the technique is 2.0×10^{-10} gram (1% absorption) and the detection limit (2 s of blank) is about 1×10^{-10} gram. This sensitivity compares favorably with that of neutron activation and is better than that of most AA techniques reported in the literature.

Received for review July 16, 1973. Accepted November 12, 1973.

Graphite Braid Atomizer for Atomic Absorption and Atomic Fluorescence Spectrometry

Akbar Montaser, S. R. Goode,¹ and S. R. Crouch²

Department of Chemistry, Michigan State University, East Lansing, Mich. 48824

Non-flame atomizers for atomic absorption (AA) and/or atomic fluorescence (AF) spectrometry have become increasingly useful in recent years. A wide variety of non-flame atomizers have been proposed. The most common of these are "thermal" atomizers, which are heated by dissipating electrical energy in the atomization element. Thermal atomizers include furnace types (1-3), rods (4, 5), and metal strips or filaments (6-9). The atomizers made from carbon or graphite appear to be highly applicable because of the high operating temperatures (2500-3000 °C) which can be achieved.

The real and potential advantages of non-flame atomizers have been summarized recently by Kirkbright (10). Despite the many attractive features of non-flame atomization, some of the previously described atomizers have several practical limitations. Graphite or carbon tubes and furnaces, for example, may require several kilowatts of power to achieve atomization temperatures in the range of 2500 to 3000 °C (2, 5). Even smaller carbon rods and filaments may require 1 kilowatt of power to achieve similar temperatures (5). Since the transfer of electrical energy into thermal energy is not perfectly efficient, a fraction of the electrical energy will be dissipated as electromagnetic radiation. Extensive shielding and/or careful circuit design must be employed to minimize these electromagnetic interferences. The sheer bulk of a system which requires kilowatts of power also prevents its application as a portable field analyzer.

In this communication, a new filament-type non-flame atomizer, the graphite braid atomizer (GBA), is described and characterized. The electrically heated GBA is capable of providing temperatures similar to other carbon or graphite atomizers, but with lower applied powers. The graphite braid has been used in the AA and AF determination of several elements and shows good sensitivity and linearity. A procedure for the direct analysis of copper in a serum matrix is presented to illustrate the application of the GBA to biological samples. Only a dilution of the serum sample is required prior to the analysis step.

EXPERIMENTAL

Graphite Braid Atomizer. The graphite braid (Union Carbide Corp., Parma, Ohio) contains high strength, flexible, continuous

filaments of graphite which are woven to form a braid of 1.5- to 2-mm diameter. The total impurity content of braids is reported to be less than 150 ppm (11). Braids used in this work were out-gassed by resistive heating to about 2500 °C for a period of 2-3 sec. The cleaning procedure was repeated until the AA or AF base line was constant. This usually required two or three repetitions of the cleaning cycle.

Apparatus. Graphite braids 3 cm in length were mounted below the optical path of an AA/AF spectrometer by an arrangement similar to that described previously (8). The spectrometer consisted of a grating monochromator (EU-700, Heath Co., Benton Harbor, Mich.), a photomultiplier module (EU-701-30, Heath Co.), radiation sources to be described below, a current-to-voltage converter (Model 427, Keithley Instruments, Inc., Cleveland, Ohio) and a PDP Lab 8/e computer (Digital Equipment Corp., Maynard, Mass.). Details of the computer-controlled non-flame spectrometer have been described (12). Computer integration of the peak-shaped signals was used in all cases. In addition, background correction, conversion of transmittance to absorbance, and other calculations were performed by the computer, and the analytical results were printed on a teletype.

Cadmium and zinc metal discharge lamps (George W. Gates & Co., Inc., Franklin Square, N.Y.) were used as AF excitation sources, while a lead hollow cathode lamp (WL 22927, Westinghouse Electric Corp., Electronic Tube Division, Elmira, N.Y.) and a Cu-Zn-Pb-Ag multielement hollow cathode lamp (JA 45448, Fisher Scientific, Waltham, Mass.) were used as AA sources.

Samples were dispensed onto the graphite braid atomizer by either a pneumatically operated automatic sampler (8), or a 5-μl syringe (Unimetrics Universal Corp., Anaheim, Calif.).

The GBA current was controlled by a programmable, current-regulated power supply (12). A three-stage current program for desolvation, ashing, and atomization was used for biological samples. For aqueous solutions, only the desolvation and atomization steps were utilized. The GBA was shielded by two concentric sheaths of argon gas. Unless otherwise stated, the parameters given in Table I were used throughout this study. Measurements of the atomizer temperature were made with an optical pyrometer (Catalog No. 8622-C, Leeds & Northrup Co., Philadelphia, Pa.). All temperature measurements had an uncertainty of approximately ±50 °C.

Reagents. All stock solutions were prepared from the pure metal dissolved in a minimum amount of hydrochloric or nitric acid. Aqueous standards were prepared by dilution of the stock solution with distilled water which had been purified by an Osmonics Inc. "Ultrapur Water System" (Osmonics, Inc., Hopkins, Minn.). For the blood serum analysis, the serum matrix (Monitrol I, Scientific Products, Inc., Detroit, Mich.) was diluted tenfold and then spiked with standard solutions of copper.

Procedure. When aqueous solutions were analyzed, 2-μl samples were placed on the graphite braid, and the integrated absorption or fluorescence was measured under the conditions shown in Table I. The GBA was allowed to cool for 10 seconds between analyses. For the analysis of copper in serum, the sample was dried for 10 seconds at 100 °C, ashed for 30 seconds at 500 °C, and atomized for 3 seconds at 1900 °C.

RESULTS AND DISCUSSION

To evaluate the graphite braid atomizer for AA and AF spectrometry, several tests were performed. First, the

¹ Present address, Department of Chemistry, University of South Carolina, Columbia, S.C. 29208.

² Author to whom reprint requests should be addressed.

- (1) H. Massmann, *Spectrochim. Acta*, **23B**, 215 (1968).
- (2) R. Woodruff, R. W. Stone, and A. M. Held, *Appl. Spectrosc.*, **22**, 408 (1968).
- (3) M. S. Black, T. H. Glenn, M. P. Bratzel, and J. D. Winefordner, *Anal. Chem.*, **43**, 1769 (1971).
- (4) T. S. West and X. K. Williams, *Anal. Chim. Acta*, **45**, 27 (1969).
- (5) M. D. Amos, P. A. Bennett, K. G. Brodie, P. W. Y. Lung, and J. P. Matousek, *Anal. Chem.*, **43**, 211 (1971).
- (6) M. P. Bratzel, R. M. Dagnall, and J. D. Winefordner, *Anal. Chim. Acta*, **48**, 197 (1969).
- (7) M. P. Bratzel, R. M. Dagnall, and J. D. Winefordner, *Appl. Spectrosc.*, **24**, 518 (1970).
- (8) S. R. Goode, Akbar Montaser, and S. R. Crouch, *Appl. Spectrosc.*, **27**, 355 (1973).
- (9) H. M. Donega and T. E. Burgess, *Anal. Chem.*, **42**, 1521 (1970).
- (10) G. F. Kirkbright, *Analyst (London)*, **96**, 609 (1971).

(11) D. J. Page, Union Carbide Corp., Parma, Ohio, personal correspondence, 1973.

(12) Akbar Montaser and S. R. Crouch, The Pittsburgh Conference on Analytical Chemistry and Applied Spectroscopy, Cleveland, Ohio, March 1973, Paper 119.

Table I. Experimental Parameters* Selected in the Study of Graphite Braid Atomizer

Method	Element	Analysis wavelength, nm	Monochromator slit, width, mm	Sheath gas flow rate, l./min	Atomization power, W	Atomization temperature, °C
AF	Cadmium	228.8	1.5	1	95	1485
	Zinc	213.86	1.5	1	95	1485
	Lead	283.31	0.2	2	165	1900
AA	Copper	324.75	0.2	2	165	1900

* The following parameters were the same for all elements: PMT supply voltage, 800 V; drying time, 11 sec; drying power, 3 W; atomization time, 3 sec; and sample size, 2 μ l.

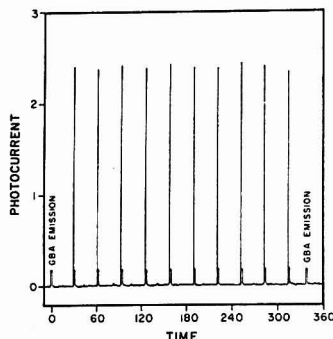


Figure 1. Fluorescence peaks for 150-pg Cd samples. Vertical scale, 10^{-7} A/div; horizontal scale, 60 sec/div; relative standard deviation, 4%.

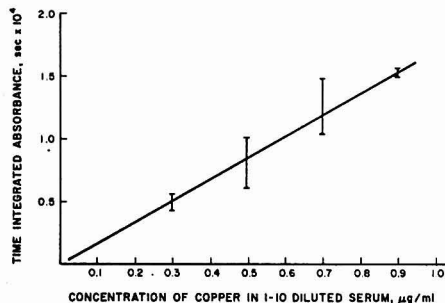


Figure 2. Standard addition analytical curve for copper added to tenfold diluted serum.

temperature vs. applied power relationship was established. Studies were made to determine typical braid lifetimes under a variety of operating conditions. The general characteristics of AA and AF signals with graphite braid atomization were studied, and the atomizer was used for the analysis of copper in serum to illustrate its potential application for biological samples.

Braid Temperature. The temperature of the atomizer was found to be variable up to 2600 °C. The temperature dependence on power for a GBA 3 cm long, was approximately linear over the range 1000 to 2500 °C and had a slope of ≈ 5 °C/W in this range, with only 350 W needed to heat the atomizer to 2500 °C. When the length of the braid is shortened, the required power needed to reach a

given temperature is considerably less than the power needed for the longer braid. In contrast to carbon rods or graphite furnaces, no cooling system for the atomizer holders was required with the GBA.

Braid Lifetime. The lifetime of any non-flame atomizer depends on a variety of parameters such as sample size, matrix, gas flow, and applied power. Although no extensive study was made of the effects of all these parameters, the results of four different sets of AF experiments on aqueous samples containing 100 pg of Cd, performed under the selected conditions shown in Table I, gave an average of 228 determinations before the braid deteriorated. This decreased to about 60 determinations at 2000 °C before the braid was weakened significantly. Deterioration of the braid can be seen as a hot spot develops at a point which is usually located between the inner and outer gas flow. The braid separates if heating is continued after a hot spot has developed.

AA and AF Signal Characteristics. During the atomization step, the atomic vapor above the atomizer gives rise to an AA or AF signal with a time duration which depends on a variety of factors such as the sample size, matrix, and atomization temperature. Typical signals were approximately Gaussian in shape with half-widths on the order of 0.5 sec. Integration of the absorption and fluorescence peaks was used to improve the accuracy and to extend the linearity of the working curves. The photometric signal was integrated for the duration of the atomization step.

After an aqueous sample is placed on top of the braid, it soaks down between the graphite fibers. Heating the fibers produces a furnace-like environment. The heating processes are very efficient because a high surface area is kept in contact with the sample. The possibility of sample explosion is minimized, again due to the furnace-type environment around the sample. An explosion and a concurrent loss of sample could be observed if the sample were too viscous to soak into the braid and the desolvation temperature were set well above the boiling point of the solvent.

The effects of varying the length of time which the sample remained on the atomizer prior to desolvation were studied. For soaking times of up to 20 seconds, the mean AF signal for a 1 μ g/ml aqueous zinc solution remained constant, within a 95% confidence interval. The standard deviation of replicate trials was also unaffected by the soaking time, probably because the entire length of the braid is heated to a uniform temperature. Soaking of the sample into the braid may be a problem with different sample matrices, however.

Analytical Results. Analytical data were obtained for four different elements in aqueous solutions. Analyses were performed for cadmium and zinc by atomic fluorescence, and the experimental detection limits ($S/N = 2$) were approximately 10^{-11} gram for both elements, which corresponds to concentrations of about 5 ng/ml in both

cases. Copper and lead were analyzed by atomic absorption, and detection limits of approximately 2×10^{-11} gram were obtained. All of the analytical curves showed good linearity over two to three orders of magnitude in concentration. The relative standard deviation was usually between 4-7% at concentrations one order of magnitude greater than the detection limit. In Figure 1, typical recorder tracings of AF signals from 10 consecutive samples of 150 pg of Cd are shown. The relative standard deviation of the peak areas of these signals is 4%. These data were obtained without optimization of instrumental parameters. The detection limits and the dynamic range can probably be improved substantially if the system is optimized (8).

The ability of a non-flame atomizer to utilize samples in complex matrices is one of its greatest assets. Because of its clinical significance, copper (13) in a serum matrix was chosen as a good test of the GBA in a practical analysis. When copper is analyzed by flame spectrometry, the serum matrix affects the results, probably because of changes in the transport parameters. The transport is nearly 100% efficient in the non-flame atomizers, and matrix effects are minimized when appropriate temperatures are used to desolvate, ash, and atomize the sample. Different amounts of aqueous copper were added to the tenfold diluted serum samples, and the standard addition analytical curve shown in Figure 2 was obtained by AA.

(13) Norbert W. Tietz, "Fundamentals of Clinical Chemistry," W. B. Saunders Co., Philadelphia, Pa., 1970, p. 663.

Only a rough optimization for the ashing step was performed to obtain these data. Figure 2 demonstrates the excellent linearity in a complex matrix without any difficult sample preparation steps. The relative standard deviations ranged from 4 to 16% with a sample population of 3. Since sample volumes are often limited in clinical situations, the automated sampler, with a dead volume of 150 μ l, could not be used. A syringe was used to transport the sample, and the high relative standard deviation of individual points can be attributed to the difficulty of placing samples on the atomizer in a reproducible manner.

CONCLUSIONS

The graphite braid non-flame atomizer has been shown to be a medium power alternative to the more commonly used graphite rods and furnaces. In addition to the high operating temperature and other advantages of non-flame atomizers which are preserved, the graphite braid provides a furnace-type environment with uniform temperature throughout the GBA. The atomizer requires relatively low power and no cooling system is necessary. The good detection limits and precision suggest that the GBA should have widespread application in AA and AF spectrometry. Further investigations of the GBA and its applications are being carried out in these laboratories.

Received for review August 13, 1973. Accepted November 16, 1973.

Double Modulation Atomic Fluorescence Flame Spectrometry

W. K. Fowler, D. O. Knapp, and J. D. Winefordner¹

Department of Chemistry, University of Florida, Gainesville, Fla. 32601

A continuum source and double modulation—i.e., modulation of the source radiation and modulation of the spectral image over a small wavelength range—has been used previously in atomic absorption flame spectrometry by Elser and Winefordner (1). Some of the advantages presented for such a system are applicable to atomic fluorescence flame spectrometry (AFFS). For example, emission radiation from the flame cell and incident radiation scattering can be minimized in AFFS by such a system. Modulation of the source radiation compensates for thermal emission from the flame cell, and wavelength modulation, which results in a derivative of the signal with respect to the wavelength, compensates for scattering from particles in the flame. A continuum source offers several advantages distinct from line sources among which are a savings in analysis time and cost of many sources and the convenience of having one source for all elements. Continuum sources unfortunately have rather low spectral radiance over an absorption line compared to the spectral radiance of intense line sources—e.g., thermostated electrodeless discharge lamps (EDL) (2).

¹ Author to whom reprint requests should be sent.

- (1) R. C. Elser and J. D. Winefordner, *Anal. Chem.*, **44**, 698 (1972).
- (2) R. F. Browner, B. M. Patel, T. H. Glenn, M. E. Rietta, and J. D. Winefordner, *Spectrosc. Lett.*, **5**, 311 (1971).

In this work, the limits of detection of nine elements in an air-acetylene flame and three elements in a nitrous oxide-acetylene flame using a 900-watt xenon arc are measured by double modulated atomic fluorescence flame spectrometry (DMAFFS). Specifically, the spectral radiation from a 900-W xenon arc (XBO, 900 W/P, Osram, Berlin, Germany) enclosed in a suitable housing (LH 151 N, Schoeffel Instrument Co., Westwood, N.J.) and powered by a regulated dc supply (Sola Electric Co., Elk Grove Village, Ill.) was modulated at 666 Hz by a mechanical chopper (Model 125, Princeton Applied Research, Princeton, N.J.) and focused on the center of the flame cell. The burner system, which utilized capillaries, has been described elsewhere (3). Gas flow rates of 14.3 and 2.6 l. min⁻¹ and 12.0 and 6.4 l. min⁻¹ were used with air/C₂H₂ and N₂O/C₂H₂ flames, respectively. All measurements were made approximately 2 cm above the burner top. The monochromator, refractor plate for wavelength modulation, and associated electrical components have been described previously (1) except that in the present case a low noise preamplifier (PAR, Model CR-4) and lock-in amplifier (PAR, Model JB4) were utilized. All aqueous solutions were prepared from reagent-grade chemicals.

- (3) L. M. Fraser and J. D. Winefordner, *Anal. Chem.*, **43**, 1693 (1971).

Table I. Limits of Detection of Several Elements by Double Modulation Atomic Fluorescence Flame Spectrometry (DMAFFS)

Element	Wavelength, nm	Flame ^a	DMAFFS ^b	Limits of detection, $\mu\text{g/ml}$	
				Previous work, ^c continuum	Previous work, line
Ag	328.1	A/A	0.03	0.001 (4) ^d	0.0001 (5)
Al	396.2	A/N	0.8	...	0.1 (6)
Ca	422.7	A/A	0.3	0.02 (7) ^d	0.02 (5) ^d
Cr	357.9	A/A	0.6	...	0.005 (8)
Cu	324.8	A/A	0.05	0.2 (9) ^d	0.0005 (10) ^d
Mg	285.2	A/A	0.03	0.002 (11) ^d	0.0001 (12)
Mn	279.8	A/A	0.09	0.003 (11) ^d	0.001 (13)
Mo	313.3	A/N	1.	...	0.5 (6)
Ni	232.0	A/A	4.	1. (7) ^d	0.003 (14) ^d
Pb	405.8	A/A	5.	0.2 (15) ^d	0.02 (16) ^d
Tl	377.6	A/A	0.6	0.07 (7) ^d	0.008 (5) ^d
V	318.4	A/N	6.	...	0.07 (6)

^a A/A = acetylene/air flame, A/N = acetylene/nitrous oxide flame. ^b Source was 900-W CW xenon arc. ^c Only references to non-laser line sources are given. ^d Flame used was 11/entrained air or H₂/argon/entrained air.

The limits of detection (LOD) defined as that concentration giving a signal to (rms) noise ratio equal to two are given in Table I for twelve elements and compared with other limits of detection for both continuum sources and line sources. A 1000 $\mu\text{g ml}^{-1}$ zirconium solution was indis-

tinguishable from the blank signal in all cases. Although the present detection limits are inferior to those obtained in AFS with line sources, the double modulated continuum source AFS system compensates for scattering which is difficult to correct for in resonance fluorescence with line sources and allows the determination of several elements with only one source.

- (4) D. W. Ellis and D. R. Demers, *Anal. Chem.*, **38**, 1943 (1966).
- (5) K. F. Zacha, M. P. Bratzel, J. M. Mansfield, and J. D. Winefordner, *Anal. Chem.*, **40**, 1733 (1968).
- (6) R. M. Dagnall, G. F. Kirkbright, T. S. West, and R. Wood, *Anal. Chem.*, **42**, 1029 (1970).
- (7) D. W. Ellis and D. R. Demers, "Atomic Fluorescence Flame Spectrometry," Chapter in "Trace Inorganics in Water," H. A. Beller, Ed., *Advan. Chem. Ser. No. 73*, Government Printing Office, Washington, D.C., 1968.
- (8) J. D. Norris and T. S. West, *Anal. Chim. Acta*, **59**, 355 (1972).
- (9) M. P. Bratzel, R. M. Dagnall, and J. D. Winefordner, *Anal. Chim. Acta*, **52**, 157 (1970).
- (10) H. G. C. Human, *Spectrochim. Acta*, **27B**, 301 (1972).

Received for review July 30, 1973. Accepted November 21, 1973. Research supported by AF-AFOSR-70-1880I.

- (11) A. Heli and S. Ricchio, Talk given at Pittsburgh Conference on Analytical Chemistry and Applied Spectroscopy, Cleveland, Ohio, 1970.
- (12) P. L. Larkins, *Spectrochim. Acta*, **26B**, 477 (1971).
- (13) L. Ebdon, G. F. Kirkbright, and T. S. West, *Talanta*, **17**, 965 (1970).
- (14) J. Matousek and V. Sycha, *Anal. Chem.*, **41**, 518 (1969).
- (15) R. Smith, C. M. Stafford, and J. D. Winefordner, *Can. Spectrosc.*, **14**, 2 (1969).
- (16) V. Sycha and J. Matousek, *Talanta*, **17**, 363 (1970).

Direct Mass Spectrometric Analysis of High Pressure Gasoline Streams Containing Light Ends

Dirk V. Rasmussen

Gulf Oil Canada Limited, Research and Development Department, Sheridan Park, Ontario, Canada

Hydrocarbon process streams boiling up to 200 °C and containing light ends (C₁-C₅ hydrocarbons) are often sampled at pressures up to 500 psi. Conventional mass spectrometric techniques require the venting of the sample cylinder, transfer of the liquid to a glass bottle, depentanization (1), and analysis of the depentanized fraction (2, 3). Depentanization is required because of calibration limitations, but it also introduces errors and much additional work.

This paper describes a high pressure liquid introduction system for mass spectrometers and a method of analysis in which depentanization is eliminated. Constant volumes

of gasoline type samples containing large amounts of C₁-C₅ hydrocarbons at pressures up to 500 psi are introduced by means of a four-port slide valve. The high ionizing voltage mass spectrum is mathematically depentanized (4) using the gas chromatographic light ends analysis (5) of the sample.

EXPERIMENTAL

Instrumental. Spectra were obtained on a Consolidated Electrodynamics Corporation Model 21-103C mass spectrometer, modified by the addition of a Bendix Greenbrier four-port slide valve. The valve has a sample volume of 1 μl and is actuated by 40 psi nitrogen and a four-way Skinner solenoid valve. A high pressure helium supply was installed so that sample cylinders could be pressurized at the mass spectrometer. The configuration of the modification is shown in Figure 1.

- (1) American Society for Testing Materials, "Standards on Petroleum Products and Lubricants," Vol. 17, 712 (1970).
- (2) American Society for Testing Materials, "Standards on Petroleum Products and Lubricants," Vol. 17, 1103 (1970).
- (3) American Society for Testing Materials, "Standards on Petroleum Products and Lubricants," Vol. 17, 589 (1970).

- (4) H. E. Howard and W. C. Ferguson, *Anal. Chem.*, **31**, 1048 (1959).
- (5) R. D. Beckham and R. J. Libers, *J. Gas Chromatogr.*, **6**, 188 (1968).

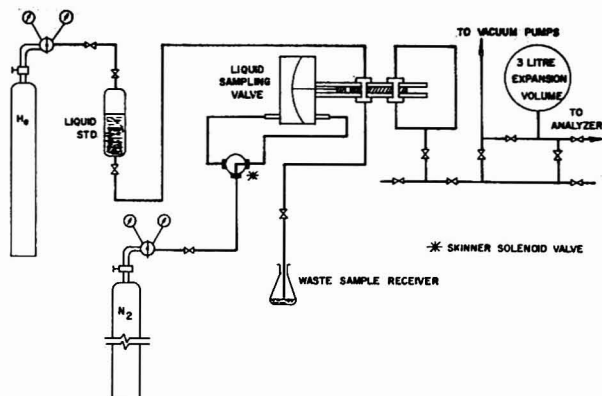


Figure 1. High pressure liquid sampling system

Table I. Mass Spectrometric Calibration for Paraffinic Light Ends

<i>m/e</i>	Constant volume sensitivities (peak height/injection)				
	<i>i</i> -C ₄ H ₁₀	<i>i</i> -C ₅ H ₁₂	<i>n</i> -C ₅ H ₁₂	<i>i</i> -C ₆ H ₁₄	<i>n</i> -C ₆ H ₁₄
41	549	2047	1331	1949	1856
43	897	4899	4187	2685	4250
55		26	52	161	151
57		149	109	1554	558
67				1	2
68					
69				1	1
71				50	22

Procedure. High pressure gasoline range process streams are normally sampled in stainless steel cylinders. The sample pressure is measured and a constant volume (1 μ l) is injected into the mass spectrometer by means of the Bendix slide valve. The 70-eV mass spectrum is obtained.

A stainless steel cylinder, containing a benzene standard, is pressurized with helium to a value equivalent to the sample pressure. The benzene is injected by the slide valve, and from the mass spectrum, the constant volume benzene sensitivity associated with the sample is obtained.

When a series of samples is analyzed, the pressures are generally similar and only a small number of benzene standards is required.

The C₁-C₅ hydrocarbons present in the sample are determined by the conventional gas chromatographic procedure (5).

Calibration. Calibration requirements for this method consist of the constant liquid volume sensitivities of each C₃-C₅ hydrocarbon of interest at each of the matrix peaks. The peak heights at *m/e* 41, 43, 55, 57, 67, 68, 69, 71 due to fixed volumes of propane, isobutane, *n*-butane, isopentane, and *n*-pentane are required.

Each standard is run as a liquid by means of the liquid sampling valve. The gaseous standards, obtained in lecture bottles, are further pressurized to 300 psi with helium. The liquid standards (*n*-pentane, benzene) are placed in 300-ml stainless steel cylinders and are similarly pressurized to 300 psi. Benzene is used to supply a reference sensitivity. The contribution of each hydrocarbon standard to each matrix peak is expressed in "peak height per unit volume" at a benzene parent peak sensitivity of 7000. A typical light ends calibration is shown in Table I.

Previously published calibration data are used for the hydrocarbon type analysis of the C₆+ hydrocarbons.

Calculations. The contributions of the C₃-C₅ hydrocarbons at *m/e* 41, 43, 55, 57, 67, 68, 69, 71 are calculated from the gas chromatographic light ends analysis and the mass spectrometric calibration data (Table I). The sum of the contributions at each mass number is removed from the respective "full range" peak,

Table II. Analytical Results of Reformer Reactor Product

	High pressure full range analysis	Corrected, ASTM D 2789	Conventional, ASTM D 2789
Light ends	(16.4)	(16.4)	(16.4)
Methane	0.5	0.5	0.5
Ethane	2.3	2.3	2.3
Propane	3.8	3.8	3.8
Isobutane	1.6	1.6	1.6
<i>n</i> -Butane	2.8	2.8	2.8
Isopentane	3.0	3.0	3.0
<i>n</i> -Pentane	2.4	2.4	2.4
Paraffins	35.5	35.8	36.5
Monocycloparaffins	5.6	5.7	5.6
Dicycloparaffins	0.3	0.2	0.2
Alkylbenzenes	(42.2)	(41.9)	(41.3)
Benzene	0.9	0.8	0.8
Toluene	5.7	5.6	5.5
C ₈	15.5	15.6	15.4
C ₉	15.6	15.6	15.4
C ₁₀	4.2	4.0	3.9
C ₁₁	0.3	0.3	0.3
Total liquid vol. %	100.0	100.0	100.0

resulting in the light ends corrected mass spectrum. The latter is subjected to matrix analysis for paraffins, cycloparaffins, and dicycloparaffins and direct volume calculations for alkylbenzenes. The results are combined with the GC light ends to complete the analysis.

The calculations are easily computerized and in this laboratory, an on-line IBM 1800 computer system performs all the required GC and MS computations.

RESULTS AND DISCUSSION

The liquid sampling valve was extensively evaluated. The repeatability of sample volumes was 0.2% at the 95% confidence level and proved to be considerably better than the repeatability obtained by a constant volume capillary dipper. Sample volumes were found to be somewhat dependent on sample pressure. This was attributed to the dilation of the Teflon sample cavity and not the isothermal compressibility of the liquid. The pressure dependence amounted to 0.01% per psi and, though not desirable, did not present a problem since the benzene standard was run at the same pressure as the sample.

The procedure described is used extensively in this laboratory. Samples of reformer reactor products and straight

run naphthas are routinely analyzed using this technique. A typical analysis is shown in Table II and is compared to the results of the conventional procedure. A comparison is also made with the results of the conventional method after correction for errors introduced by the depentanization. These errors include approximately 1.5% light ends that are habitually left in the depentanized fraction and approximately 3.5% C₆ components that are often cut out of it. The corrections are based solely on the gas chromatographic analyses of the overhead and bottoms of the depentanizations. The analytical results of the new technique are in good agreement with those of the corrected conventional method, but differ significantly from the uncorrected one.

The repeatability of the new method was determined to be 0.6% at the 95% confidence level and compares favorably to the 2.4% obtained for the conventional procedure. The analytical technique presented here is therefore more accurate and precise than the conventional mass spectrometric method of analysis. Furthermore, the lengthy depentanization procedure is no longer required and high pressure process streams may be analyzed at their sampling pressures.

To date, the technique has been applied solely to low-olefinic stocks. It should also be applicable to olefinic streams.

Received for review August 21, 1973. Accepted November 5, 1973.

Semimicro Procedure for the Determination of Hydrocarbon Types in Shale-Oil Distillates

Larry P. Jackson,¹ Charles S. Allbright,² and Howard B. Jensen

U.S. Department of the Interior, Bureau of Mines, Laramie Energy Research Center, Laramie, Wyo. 82070

The characterization and analysis of crude shale oils and their various distillate fractions have been objectives of the work carried out at the Laramie Energy Research Center. Analysis of the crudes usually involves the quantitative determination of five general compound types: tar acids, tar bases, saturates, olefins, and aromatics. For the purposes of this paper, tar acids and tar bases are referred to as polars; saturates, olefins, and aromatics are hydrocarbons. The limited quantities of sample frequently encountered in research and development make it very difficult to apply, with accuracy, standard methods of analysis such as acid absorption (1), bromine number (2), and silica gel chromatography (3) because of the subjective judgments that must be made in each test. This paper describes an analytical procedure based on a new application of the reaction of olefins with diborane in the quantitative determination of saturates, olefins, and aromatics in shale oil.

Two major sources of difficulty in the analysis of shale-oil distillates are the high concentrations of nitrogen compounds and olefins. In the procedure reported here, the first of these problems is circumvented by the removal of the nitrogen compounds and the other polars from the hydrocarbons by column chromatography on Florisil (4). For the purposes of this study, no further characterization was done on the polars. Because of the high concentration of olefins in the hydrocarbon fraction, accurate analysis by

fractionation on silica gel is difficult, especially on small samples (5). In the present analytical scheme, the well-known reaction between olefins and diborane is used as the key step in the selective, destructive removal of olefins from the hydrocarbon fraction (6). The reaction is carried out on a sample consisting of a 1:1 mixture of the hydrocarbons from a shale-oil distillate fraction and a suitable internal standard made up of *n*-alkanes and *n*-alkylcyclohexanes whose boiling points are at least 25 °C removed from that of the hydrocarbon fraction. Gas chromatography (GC) is used as the data readout to determine the ratios of sample to internal standard before and after treatment to remove the olefins. The difference in the two ratios is a measure of the olefin content. The percentage of saturates is determined on another portion of the same sample solution by selective removal of both the olefins and aromatics with a modification of the H₂SO₄-P₂O₅ acid absorption procedure (1). The resulting raffinate is analyzed by the same gas chromatographic technique. The value obtained for saturates is combined with the olefin value and the result is used to calculate the percentage of aromatics in the sample.

The procedure which we propose uses modern GC techniques for which the precision of any given quantitative measurement is about ±1%. This degree of precision is seldom attainable in classical methods of analysis where a subjective judgment often has to be made in tests that give no clearly defined end points or separations and where competing chemical reactions give erroneous results. Specifically, acid absorption end points are frequently diffuse when samples are rich in aromatics and olefins; bromine number values are affected by nitrogen compounds and alpha olefins, both of which occur in high concentrations in shale oil; silica gel chromatography yields high values for aromatics when nitrogen com-

¹ Present address, Department of Biochemistry, University of Wyoming, Laramie, Wyo. 82070.

² Correspondence should be addressed to this author at the Laramie Energy Research Center.

(1) "ASTM Book of Standards, 1971," Part 17, Method D 1019-68, "Olefinic and Aromatic Hydrocarbons in Petroleum Distillates," pp 342-51.

(2) Ref. 1, Method D 1159-66, "Bromine Number of Petroleum Distillates and Commercial Aliphatic Olefins by Electrometric Titration," pp 378-89.

(3) Ref. 1, Method D 1319-70, "Hydrocarbon Types in Liquid Petroleum Products by Fluorescent Indicator Adsorption," pp 474-79.

(4) G. U. Dinneen, J. R. Smith, R. A. Van Meter, C. S. Allbright, and W. R. Anthony, *Anal. Chem.*, **27**, 185 (1955).

(5) D. F. Fink, R. W. Lewis, and F. T. Weiss, *Anal. Chem.*, **22**, 858 (1950).

(6) H. C. Brown, "Hydroboration," W. A. Benjamin, Inc., New York, N.Y., 1962, Chapter 1.

pounds are present and vague boundaries when olefin concentrations are high. The removal of olefins by hydroboration and removal of both olefins and aromatics by acid absorption with subsequent GC analysis of the raffinates avoid the need for operator judgment and permit accurate hydrocarbon-type analysis of semimicro samples as small as 50 milligrams. The separation procedure is outlined in Figure 1.

EXPERIMENTAL

Apparatus. A Beckman GC-4 gas chromatograph with a hydrogen flame ionization detector was used as previously described by Poulson and Jensen (7). The inlet was a 12.7-cm section of 0.46-cm i.d. tubing packed with 100-120 mesh silanized borosilicate glass beads with a small plug of glass wool to keep the beads in place. Syringe sample injections were made with the inlet at 200 °C to minimize fractionation and with the inlet rapidly heated to 375 °C over a period of about 10 minutes to minimize peak distortions in the resulting chromatogram. The chromatographic column used was 45.7 cm \times 0.46-cm i.d. Initial loading of liquid phase before conditioning was 5% Dexsil on 70-80 mesh acid-washed HMDS-treated Chromosorb W. The column was operated with a helium carrier gas flow of 90 ml/min and with linear temperature programming from 50-350 °C at 10 °C/min. The hydrogen flame ionization detector was operated with a total flow of 120 ml/min helium. Hydrogen flow was adjusted to provide maximum response at this helium flow. Air flow was 400 ml/min. A laboratory potentiometric recorder with a disc integrator was used to collect the data output.

Reagents. Cyclohexane, tetrahydrofuran, and hexane were reagent grade from commercial sources and were used directly from the bottle without further purification. The normal paraffins and *n*-alkylcyclohexanes used as internal standards and the model compounds obtained for the test blends were purchased from commercial sources in the highest purity available and used as received. The internal standard that was used with the blends of saturate, olefin, and aromatic model compounds was prepared by mixing equal parts of *n*-C₂₂H₄₆, *n*-C₂₃H₄₈, *n*-C₂₄H₅₀, pentadecylcyclohexane, heptadecylcyclohexane, and nonadecylcyclohexane. The internal standard for the analyses of the shale-oil distillates consisted of a mixture of *n*-nonane, 3-methylnonane, cyclooctane, *n*-decane, and *sec*-butylcyclohexane. The alumina was Alcoa F-20, 100-120 mesh, dried at 400 °C for 24 hours, cooled to room temperature, and partially deactivated by the addition of 3.8 wt % water to the alumina in a closed container. After 24 hours for gel-water equilibration, the alumina was ready for use. Snyder (8) has described the principles involved in adsorbent deactivation. Florisil was 30-60 mesh and was used as received from the supplier.

A 1-molar diborane solution was prepared by the method of Brown and Tierney (9) with one modification. As the diborane was generated, it was swept from the reaction flask with a stream of nitrogen into a flask containing cyclohexane with 2 molar equivalents of tetrahydrofuran and cooled to 0 °C. The resulting solution was stored at 0 °C and used as needed.

Sample Preparation. Three hydrocarbon samples in the light distillate range (200-325 °C) and one from heavy distillate (325-500 °C) were isolated from shale-oil fractions by elution with hexane through a column of Florisil (4). The volume of eluent collected was sufficient to remove the aromatics from the column. The hexane was removed on a rotary evaporator using a slight negative pressure and a warm water bath. A portion of each hydrocarbon sample was then combined with an equal volume of an internal standard made up of *n*-alkanes and *n*-alkylcyclohexanes whose boiling points were all at least 25 °C outside the boiling range of the hydrocarbons.

Procedure. For the determination of total olefins, 0.1 ml of hydrocarbon-internal standard solution was charged into a glass ampoule made from 12-mm standard wall glass tubing with a neck suitable for sealing made from 6-mm tubing. The total capacity of the ampoule was about 8 ml. The sample was frozen in Dry Ice, 1.0 ml of the stock diborane solution was added, and the ampoule was sealed with a torch. The sealed ampoule was al-

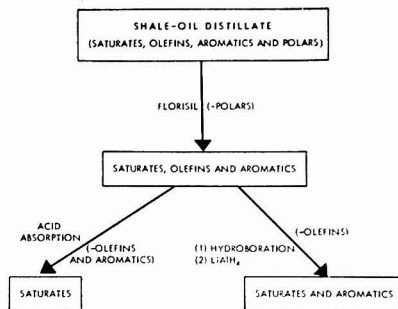


Figure 1. General separation scheme for saturates, olefins, and aromatics from shale-oil distillates

Saturates = sample - (olefins and aromatics); acid absorption. Olefins = sample - (saturates and aromatics); hydroboration. Aromatics = sample - saturates - olefins; subtraction

lowed to come to room temperature, shaken vigorously to ensure proper mixing, heated at 80 °C for 4 hours in an oven, removed, again frozen in Dry Ice, opened, and allowed to thaw. The oxidation of the alkylboranes was carried out by the careful addition of 1 ml of 3*N* sodium hydroxide followed by 1 ml of 30% hydrogen peroxide, resealing of the ampoules, and heating in a 45 to 50 °C oven for 1 hour (see Precautions). For high boiling samples such as middle distillates and heavier, heating in the open tube in a 45 to 50 °C water bath for an hour is satisfactory. After the oxidation period, the sealed samples were cooled in liquid nitrogen to reduce the pressure and opened. Four milliliters of water was added to the liquid reaction mixture and mixed by vigorous shaking. After the hydrocarbon layer had separated, it was drawn off and added to a vial containing a small quantity of LiAlH₄ to convert the alcohols to insoluble salts. When the effervescence had subsided, salts were removed by filtration through a 6-mm glass column plugged with glass wool and containing about 2.5 cm of alumina deactivated with 3.8% water. After the sample had passed through the tube, the filter was washed with enough hexane to bring the total volume to about 2 ml. In cases where the excess tetrahydrofuran had not been completely removed from the solution by the water wash, the LiAlH₄ which remained dissolved in the tetrahydrofuran reacted with the water in the alumina causing the column to fracture, but this did not appear to affect the results. Integrated GC patterns were next obtained on the dilute solution—now containing the hydrocarbons minus the olefins—and on the original sample solution. The ratio of sample pattern area to internal standard pattern area was calculated for each solution; the difference between the two ratios represented the amount of olefins in the sample.

For the determination of total saturates, all olefins and aromatics were removed by acid absorption (1). In a typical run, 200 μ l of a 10% solution of the hydrocarbons plus internal standard in cyclohexane was shaken with 5 ml of the H₂SO₄-P₂O₅ acid mixture in a precision sulfonation flask using the manual procedure described in the ASTM method. After the addition of H₂SO₄ and centrifugation, a sample was withdrawn from the hydrocarbon layer and analyzed by GC. As with the olefins, calculations of the pattern areas for sample solution before and after chemical treatment gave the amount of saturates.

The aromatic content of the sample was calculated by subtraction of the per cent saturates value and the per cent olefins value from 100.

Precautions. The release of oxygen during the oxidation step will generate some internal pressure in sealed ampoules and cer-

Table I. Olefins Tested in the Hydroboration Reaction

1-Tridecene	1,2-Dimethylcyclopentene
2,4,4-Trimethyl-2-pentene	Indene
2,2,5,5-Tetramethyl-3-hexene	2,5-Dimethyl-2,4-hexadiene
<i>trans</i> -1-Phenyl-2-butene	1-Allylcyclohexene
<i>trans</i> -5-Decene	Bicyclo[4.4.0]deca-1(6),3-diene
<i>trans</i> -3-Dodecene	

(7) R. E. Poulson and H. B. Jensen, *J. Chromatogr. Sci.*, **9**, 300 (1971).

(8) L. R. Snyder, "Principles of Adsorption Chromatography," Marcel Dekker, Inc., New York, N.Y., 1968, p 129.

(9) H. C. Brown and P. A. Tierney, *J. Amer. Chem. Soc.*, **80**, 1552 (1958).

Table II. Saturate and Aromatic Hydrocarbon Blends

Blend I, n-Paraffins	Blend II, n-Paraffins + cycloparaffins	Blend III, n-Paraffins + branched paraffins	Blend IV, n-Paraffins + aromatics
n-Heptane	n-C ₇ through n-C ₁₃	n-C ₇ through n-C ₁₃	n-C ₇ through n-C ₁₃
n-Octane	Ethylcyclohexane	Ethylhexane	Ethylbenzene
n-Nonane	n-Propylcyclohexane	2-Methylheptane	o-Xylene
n-Decane	Isopropylcyclohexane	3-Ethylheptane	1,2,4-Trimethylbenzene
n-Undecane	Methylcyclohexane	2,2-Dimethylheptane	1-Methyl-4-ethylbenzene
n-Dodecane	c,c,c-1,2,3-Trimethylcyclohexane	2-Methylundecane	Isopropylbenzene
n-Tridecane	1,1,3,5-Tetramethylcyclohexane	Internal standard	n-Pentylbenzene
Internal standard	n-Hexylcyclohexane		Internal standard
	Internal standard		

Table III. Hydroboration Determination of Olefins in Hydrocarbon Samples

Sample	Volume % olefins			
	Run 1	Run 2	Run 3	Average
I	9.0	8.8	6.8	8.1
II	14.8	14.4	15.7	15.0
III	27.3	27.8	27.5	27.5
IV	32.3	33.9	33.4	33.2

Table IV. Acid Absorption Determination of Saturates in Hydrocarbon Samples

Sample	Volume % saturates		
	Run 1	Run 2	Average
I	73.0	72.7	72.9
II	8.2	7.6	7.9
III	45.3	46.4	45.9
IV	42.7	42.8	42.8

Table V. Composition of Hydrocarbon Samples

Sample	Volume % hydrocarbon types		
	Saturates	Olefins	Aromatics
I	72.9	8.1	19.0
II	7.9	15.0	77.1
III	45.9	27.5	26.6
IV	42.8	33.2	24.0

tain precautions are advisable to minimize the danger of breakage. Make certain that the ampoules are free of defects and are sealed carefully. Carry out the oxidation in an oven, with the ampoules isolated from one another. If the hydroboration procedure is scaled up to a larger quantity of sample and more H₂O₂ is used, choose a larger capacity tube whose volume will accommodate the pressure buildup. After the oxidation period, cool the ampoule in liquid nitrogen to reduce the pressure before opening.

RESULTS AND DISCUSSION

To test the reactivity of olefins to diborane, a synthetic blend of 11 olefins representing many of the types believed to be present in shale oil was made up and subjected to the hydroboration reaction. The olefins chosen are listed in Table I. Although there are no tetrasubstituted ethylenes on the list, tetrasubstitution is represented by the cyclic monoolefin, 1,2-dimethylcyclopentene. Two of the compounds—*trans*-1-phenyl-2-butene and indene—are generally known as aromatics even though they possess both olefinic and aromatic character. These two olefinic aromatics were included in the tests of olefins as a class for their reactivity with diborane, and results showed that both did indeed react quantitatively as olefins. The sole

exception among the compounds was 2,5-dimethyl-2,4-hexadiene, which was incompletely removed. It appears from this somewhat abbreviated study that hindered conjugated dienes may be resistant to this treatment, but it is believed that their concentration is negligible in shale oil and they may therefore be disregarded.

Saturates and aromatics are generally believed to be inert toward reaction with diborane, but with the complexity of shale oils, it was deemed necessary to run a few controls to confirm this belief. Four synthetic blends of known composition were made up and subjected to hydroboration. The compounds chosen were believed to be representative of components of shale-oil distillate fractions; the compounds contained in each blend are listed in Table II. GC analysis of the reaction products after work-up in the usual manner showed that each of the model compounds was inert to the diborane under the reaction conditions.

Each of the four shale-oil derived samples was subjected to hydroboration in triplicate. The results of all determinations are listed in Table III; each reported value is the average of repeated GC analyses. For the range of determined olefin contents, 7 to 34%, the hydroboration results from replicate tests deviated from the average values by 1.3% or less.

Table IV gives the percentage of saturates in each sample as determined by duplicate acid absorption. These values agree well within the $\pm 1\%$ guidelines determined by the reliability of the integral readout from the GC, deviating 0.6% or less from average. When the dilute solutions resulting from the hydroboration reaction were subjected to the acid absorption procedure, the same values were obtained for saturates as were previously obtained on the hydrocarbon samples. By combining the results given in Tables III and IV, it was possible to arrive at the value for the aromatic content of each sample. These results are summarized in Table V.

The method offers another advantage which makes it useful in the analysis of petroleum and shale-oil samples. Saturates and aromatics are unaffected by the hydroboration reaction so that olefin-free samples are obtained which may be efficiently separated into saturated and aromatic fractions by silica gel chromatography or GC techniques.

Two primary sources of error of minor concern are the presence of unreactive olefins in the sample which will not be removed by hydroboration and will therefore be reported as aromatics when they are removed by acid absorption and the presence of sulfur and nitrogen compounds which are not removed by the Florisil treatment. These two heteroatoms—sulfur and nitrogen—both react with diborane and will therefore be removed during the reaction and reported as olefins, giving a value on the high side for the olefin content. In addition, olefinic aromatics such as indene will be reported as olefins.

CONCLUSIONS

Destructive removal of olefins offers several advantages over existing techniques for the quantification of the hydrocarbon types in shale-oil distillate fractions. Handling and manipulation of the sample is minimal; an elution chromatography is the only preparation prior to analysis. The method avoids the problems associated with chemical and physical procedures normally used to quantify the three functional types; the specificity of compound-type removal, coupled with the accuracy of the GC readout, gives improved results for complex mixtures containing a significant concentration of olefinic material. The technique is amenable to batch analysis of a large number of samples, and automated GC makes the data readout step

a simple operation not requiring extensive operator time. An accurate analysis can be performed on samples as small as 50 milligrams, and the sample may be in the form of a dilute solution.

Received for review May 29, 1973. Accepted October 29, 1973. The work upon which this report is based was done under a cooperative agreement between the Bureau of Mines, U.S. Department of the Interior, and the University of Wyoming. Reference to specific equipment or trade names does not imply endorsement by the Bureau of Mines. Larry P. Jackson was a National Research Council-U.S. Bureau of Mines Post-Doctoral Research Associate, 1971-73.

Improved Ion-Exchange Technique for the Concentration of Manganese from Sea Water

Ralph G. Smith, Jr.

Skidaway Institute of Oceanography, P.O. Box 13687, Savannah, Ga. 31406

Because manganese occurs at $\mu\text{g/l.}$ and sub $\mu\text{g/l.}$ levels in sea water, its direct determination is difficult. The sensitivity of 0.002 ppm by direct determination with atomic absorption claimed by some workers (1) should be questioned, since it is approximately an order of magnitude greater than has been reported by others (2, 3). Photometric techniques involving leuco base (4) and leuco crystal violet (5) have been described; however, samples of varying ionic strengths require special calibration.

Most workers concentrate manganese from sea water either by co-precipitation (6, 7) and/or extraction techniques (6, 8). Riley and Taylor (9) have shown that a chelating ion-exchange resin can be used for this purpose. The resin, Chelex-100, undergoes swelling and contraction as its counter-ion is changed, causing difficulty in maintaining a constant flow rate through exchange columns. The difficulty increases with decreasing resin particle size, making it desirable to use the largest particle size available (50-100 mesh). Bio-Rad Laboratories, the only commercial source of Chelex-100, recently discontinued manufacture of the 50-100 mesh size, and attempts to substitute the 100-200 mesh resin using the column technique result in the difficulties described above. This paper describes a quantitative batch technique which uses the small particle size resin and is free of the difficulties of the column method.

EXPERIMENTAL

Chelex-100 resin is converted to the hydrogen form by washing a suitable quantity three times with an excess of 2N HNO_3 . Approximately 10 ml of wet resin are required per sample, and an acid:resin ratio of 1:1 provides the necessary excess. The resin is washed with redistilled water and converted to the ammonium form by washing three times with 2N NH_4OH . A final washing with redistilled water removes excess base. All preparation steps are carried out in Vycor or polypropylene flasks.

Ten ml of the ammonium form of the resin is added to 500 ml of sea water having an adjusted pH of 9.0 in a 1-l. polypropylene flask. The sample is equilibrated for 16 hr on a mechanical shaker, after which time the solution is decanted through an ion-exchange column allowing the resin particles to pour off last. The flask is washed with redistilled water which is then passed through the column. The sample flask is washed with 30 ml of 2N HNO_3 to remove manganese adsorbed on the flask. The resin is then eluted with the acid wash. Ten ml of redistilled water are added to the column to completely flush the resin. The eluate is collected in a Vycor flask and evaporated to dryness at low temperature. Prolonged heat after dryness should be avoided since this tends to make the residue difficult to redissolve.

At this point, the residue is redissolved with 1 ml of 2N HCl and diluted to a 5.0-ml volume with redistilled water in preparation for analysis by atomic absorption spectrophotometry. Acetone or other organic solvents have been used in the diluent by other workers (9) to enhance sensitivity. This, in some cases, leads to the formation of precipitates which clog the aspiration assembly of the atomic absorption system. Standards for atomic absorption analysis may be prepared by spiking previously stripped sea water with incremental amounts of manganese and treating the spiked sample as described in the procedure above.

RESULTS AND DISCUSSION

The most critical factor in the above described procedure was to establish the time required for equilibration of the resin with the water sample. To investigate the resin uptake efficiency as a function of time, 500-ml aliquots of sea water were spiked with $10 \mu\text{Ci}$ of carrier-free ^{54}Mn . The samples were equilibrated for varying lengths of time and eluted according to the described procedure. Aliquots of the eluate and sample solution were then counted in a sodium iodide well detector connected to an

- (1) B. P. Fabricand, R. R. Sawyer, S. G. Ungar, and S. Adler, *Geochim. Cosmochim. Acta*, **26**, 1023 (1962).
- (2) E. E. Angino and G. K. Billings, "Atomic Absorption Spectrophotometry in Geology," Elsevier Publishers, Amsterdam, 1967, p 12.
- (3) Perkin-Elmer Corp., "Analytical Methods for Atomic Absorption Spectrophotometry," Norwalk, Conn., (1971).
- (4) J. D. H. Strickland and T. R. Parsons, "A Practical Handbook of Sea Water Analysis," 3rd ed., Fisheries Research Board of Canada, Ottawa, Canada, 1968, p 109.
- (5) M. A. Kessick, J. A. Vuceta, and J. J. Morgan, *Environ. Sci. Technol.*, **6**, 642 (1972).
- (6) B. A. Loveridge, G. W. C. Milner, G. A. Barnett, A. Thomas, and W. M. Henry, *At. Energy Res. Estab. Rept. R. 3323*, 36 pp.
- (7) D. C. Burrell, *Anal. Chim. Acta*, **38**, 447 (1967).
- (8) Elizabeth Rona, D. W. Hood, Lowell Muse, and Benjamin Buglio, *Limnol. Oceanogr.*, **7**, 201 (1962).
- (9) J. P. Riley and D. Taylor, *Deep-Sea Res.*, **15**, 629 (1968).

Table I. Recovery of Added ^{54}Mn from Sea Water

Equilibration time, hr	Recovery, %		
	Effluent	Sample solution	Resin
2	93	6.8	0.1
4	94	6.0	0.2
6	95	5.2	0.2
8	96	4.8	0.2
16	99	1.0	0.2
16	99	1.0	0.2
16	98	1.0	0.2
16	99	1.0	0.1
16	99	1.0	0.1

Ortec single channel analyzer. Results shown in Table I indicate quantitative recovery in 16 hours with less than 1% of the manganese remaining in the water and less than 0.2% remaining on the resin. The recovery efficiency for five samples, each with $10\ \mu\text{Ci}$ of ^{54}Mn and each equilibrated for 16 hours, had a coefficient of variation of

$\pm 0.6\%$. The actual analysis of the samples by atomic absorption was not necessary since previous studies have proved its utility (9).

Results in Table I indicate that optimum recovery may conveniently be achieved by equilibrating the samples overnight and eluting them the following morning. This batch-wise method extends the analytical use of Chelex-100 to the smaller resin sizes and should be suitable for the concentration of other metals (10).

ACKNOWLEDGMENT

The author wishes to thank Robert Rahn and Elizabeth Waiters for their assistance in this work. My special thanks to Herbert Windom for making this work possible and for his review of the manuscript.

Received for review June 11, 1973. Accepted November 26, 1973. This work was partially supported by EPA Grant (R-800372).

(10) J. P. Riley and D. Taylor, *Anal. Chim. Acta*, **40**, 479 (1968).

Separation of the Trivalent Actinides from the Lanthanides by Extraction Chromatography

Terry D. Filer

Health Services Laboratory, U.S. Atomic Energy Commission, Idaho Falls, Idaho 83401

One of the more difficult problems in actinide chemistry is the separation of the trivalent actinides from the trivalent lanthanides. The solution of this problem is necessary in the analysis of greater than gram quantities of soil because of the presence of milligram quantities of the rare earths. Since even microgram quantities of the rare earths have been shown to produce serious losses in the electrodeposition of the trivalent actinides (1), a separation procedure with high decontamination factors is needed. Single-step liquid-liquid extraction procedures did not provide sufficiently large decontamination factors. Anion exchange involving ammonium thiocyanate (2) and cation exchange involving hydrochloric acid-ethanol (3) provide excellent decontamination factors but are cumbersome and time-consuming. Extraction chromatography provides an attractive means of separating metal ions of close chemical similarity because it combines the multistage process of ion exchange without sacrificing to a great extent the simplicity, selectivity, and speed of liquid-liquid extraction.

Bis(2-ethylhexyl)orthophosphoric acid (HDEHP) is an excellent reagent for intragroup separations of the trivalent lanthanide or actinide ions (4, 5) because separation factors are higher than those observed in ion exchange methods. Also, the high reaction rate of HDEHP with these ions permits relatively high flow rates. Extraction

chromatographic methods based on HDEHP for the separation of lanthanides in mineral acid systems have been reviewed (6). Kooi and coworkers used the HDEHP-hydrochloric acid system for the chromatographic separation of several transplutonium elements (7, 8). Moore and Juriaanse (9) extended the use of HDEHP in extraction chromatography to nitric acid systems, utilizing Teflon (Du Pont) powder as an inert support. All of these procedures, however, are based on the extraction of lanthanides and trivalent actinides by HDEHP from mineral acid solutions. The distribution coefficients of the two groups of elements overlap, with americium behaving most like cerium or praseodymium. Therefore, the separation of lanthanides from trivalent actinides is not clean even with the use of a multistage process such as extraction chromatography.

Weaver and Kappelmann (10) showed that the substitution of carboxylic acids for mineral acids shifts the americium distribution coefficients downward slightly relative to the lanthanides. In addition, the presence of strongly complexing aminopolyacetic acids causes a much larger shift. Percival and Martin (11) showed that the light trivalent lanthanides and actinium could be separated from americium by extraction in HDEHP from an aqueous solution containing diethylenetriaminepentaacetate.

- (6) E. Cerrai, *Chromatogr. Rev.*, **6**, 129 (1964).
- (7) J. Kooi, B. Boden, and J. Wijkstra, *J. Inorg. Nucl. Chem.*, **26**, 2300 (1964).
- (8) J. Kooi and B. Boden, *Radiochim. Acta*, **3**, 226 (1964).
- (9) F. L. Moore and A. Juriaanse, *Anal. Chem.*, **39**, 733 (1967).
- (10) B. Weaver and F. A. Kappelmann, *J. Inorg. Nucl. Chem.*, **30**, 263 (1967).
- (11) D. R. Percival and D. B. Martin, "Sequential Determination of Radium-226, Radium-228, Actinium-227, and Thorium Isotopes in Environmental and Process Waste Samples," U.S. Atomic Energy Commission, Idaho Falls, Idaho, in preparation.

- (1) K. W. Puphal and D. R. Olsen, *Anal. Chem.*, **44**, 284 (1972).
- (2) J. S. Coleman, L. B. Asprey, and R. C. Chisholm, *J. Inorg. Nucl. Chem.*, **31**, 1167 (1969).
- (3) K. Street, Jr., and G. T. Seaborg, *J. Amer. Chem. Soc.*, **72**, 2790 (1950).
- (4) D. F. Peppard, G. W. Mason, J. L. Maier, and W. J. Driscoll, *J. Inorg. Nucl. Chem.*, **4**, 334 (1957).
- (5) D. F. Peppard, G. W. Mason, W. J. Driscoll, and R. Sironen, *J. Inorg. Nucl. Chem.*, **7**, 276 (1958).

tic acid (DTPA) in a chloroacetic acid buffer at pH 3. In the present work, the use of HDEHP in extraction chromatography was extended to include the chloroacetic acid system containing the ammonium salt of DTPA, utilizing Teflon powder as an inert support. The new system provides excellent separation of the trivalent actinides from the trivalent lanthanides in a relatively pure actinide-lanthanide fraction at room temperature with relatively high flow rates.

EXPERIMENTAL

Apparatus. A 2½-inch hemispherical gas flow proportional counter using methane counting gas was used for alpha counting.

A NaI well-type scintillation counter with a 2- by 2½-inch well in a 3- by 3-inch crystal was used for gamma counting.

A 65-cm³ germanium detector coupled to a multichannel analyzer was used for gamma spectrometry.

A Beckman liquid scintillation spectrometer (Model LS 200), which features automatic standardization by channel ratio and ambient temperature operation, was used for beta counting.

An ion exchange column, 1-cm inside diameter, with a small glass wool plug at the bottom was used for the column.

Reagents. HDEHP, 0.45M. Dilute 150 ml of HDEHP (V-C Chemical Company, Richmond, Va.) to 1 liter with *n*-heptane and transfer to a 2-liter separatory funnel. Wash twice with 200-ml portions of 1:1 2M diammonium citrate and concentrated ammonium hydroxide, twice with 200-ml portions of 4M nitric acid, and twice with 500-ml portions of water. Use mixing times of one minute (11).

Eluting Solution. DTPA, 0.025M; 1M Monochloroacetic Acid. Dissolve 10 grams of DTPA in 100 ml of water containing 30 ml of concentrated ammonium hydroxide. Add 100 grams of chloroacetic acid and dilute to 900 ml. Adjust the pH to 3.0 with 5 to 10 ml of concentrated ammonium hydroxide. Dilute to 1 liter.

Procedures. Column Preparation. Add 45 ml of 0.45M HDEHP to 25 grams of Tee Six, polytetrafluoroethylene powder, 70 to 80 mesh (Analabs, Inc., Hamden, Conn.) in a 4-oz glass bottle. Cap the bottle and shake vigorously for 5 minutes. Filter the slurry through a double glass filter paper in a small Buchner funnel. Allow the powder to air dry at room temperature. Add 5.0 grams of the dry powder to the column (column of Tee Six is 10 cm high) and wash three times with 25-ml portions of water. Condition the column by passing three 10-ml portions of the eluting solution through it. The flow rate should be adjusted to 10 to 12 drops per minute.

Separation of the Trivalent Actinides from the Lanthanides. The procedure given below for the separation of the trivalent actinides from the trivalent lanthanides is that used in the development of the procedure with pure solutions containing only the actinide and 2 mg of the traced lanthanide and is to be followed on actual samples such as soil only after total decomposition of the sample and isolation of the actinide-lanthanide fraction from the sample. Add 1 ml of a 10% sodium hydrogen sulfate solution and 2 to 3 drops of concentrated sulfuric acid to the sample solution in a 30-ml beaker. Evaporate the solution to dryness on an asbestos-covered hot plate until evolution of sulfuric acid fumes has ceased. Cool the residue, add 5 ml of the eluting solution, and heat to boiling to dissolve the residue. Cool and add the solution to the conditioned column. Wash the beaker with 3- and 2-ml portions of the eluting solution and add to the column. Load the column with the 10 ml of solution at a rate of 10 to 12 drops per minute. Continue the elution with an additional 30 ml of eluting solution at a rate of 10 to 12 drops per minute to recover the transplutonium elements. Wash the column with 50 ml of 6M hydrochloric acid to remove the lanthanides. Wash the column with 50 ml of water prior to the next separation. The columns have been used for as many as ten runs with no loss of efficiency; however, cross contamination must be considered.

RESULTS AND DISCUSSION

Teflon powder was selected as the inert support because of its exceptional stability to chemical reagents and its strongly hydrophobic tendencies. The advantages of Teflon powder over various other supports in extraction chromatography have been discussed by Moore and Jurriaanse (9).

Preliminary experiments were performed to evaluate

Table I. Recovery and Decontamination of Trivalent Actinides as a Function of Eluate Volume

Eluate, ml	Found in actinide fraction, %			
	Actinides		Lanthanides	
20	²⁴¹ Am	99.0	¹⁴⁰ La	0.10
	²⁴¹ Cm	96.0	¹⁴⁴ Ce	0.20
	²⁴⁹ Cf	83.3	¹⁴⁷ Pm	1.3
			¹⁵² Eu- ¹⁵⁴ Eu	1.4
40			¹⁷⁰ Tm	0.03
	²⁴¹ Am	100.2	¹⁷¹ Lu	0.06
	²⁴¹ Cm	100.0	¹⁴⁰ La	0.10
	²⁴⁹ Cf	96.5	¹⁴⁴ Ce	0.20
			¹⁴⁷ Pm	8.9
			¹⁵² Eu- ¹⁵⁴ Eu	2.2
			¹⁷⁰ Tm	0.08
			¹⁷¹ Lu	0.07

the pertinent variables in the Teflon-HDEHP system. Americium-241 and cerium-144 were used to check the effectiveness of the separation because immediate results could be obtained by gamma-counting each fraction. With 0.45M HDEHP as the stationary phase, DTPA concentrations were varied from 0.050M to 0.0025M. The optimum concentration range of DTPA for maximum separation of americium from cerium was 0.013M to 0.025M. Lower concentrations of HDEHP also gave excellent separation but the columns might become overloaded when separating milligram quantities of lanthanides from the actinides.

Several experiments were performed in which the height of the column was varied from 40 mm to 100 mm. Column lengths of 60 mm gave quantitative separation of trivalent cerium from americium, but were inadequate to separate other transplutonium elements with less favorable distribution coefficients from cerium. A column length of 100 mm was necessary to adequately separate all of the trivalent actinides from the lanthanides.

The normal flow rate used with the standard 10- by 100-mm column was 10 to 12 drops per minute. Such a relatively fast flow rate is of practical importance because it allows the complete separation of actinides from lanthanides in about 80 minutes. Flow rates of 1 to 2 drops per minute showed negligible improvement in separations while flow rates as fast as 30 drops per minute have acceptable separations; for example, 1% of the cerium was found in the americium fraction.

On the basis of these studies, the following conditions were selected for the separation of the trivalent lanthanides from the trivalent actinides: 10- by 100-mm column of 70- to 80-mesh Tee-Six powder containing 0.45M HDEHP-heptane as the stationary phase, 0.025M DTPA in 1M monochloroacetic acid adjusted to a pH of 3.0 with ammonium hydroxide as eluant, and a flow rate of 10 to 12 drops per minute.

To determine the precision obtained using the above conditions, six samples containing americium-241 and six samples containing cerium-144 with 2 mg of cerium carrier present in each were carried through the separation starting with the evaporation of the solutions to dryness in the presence of sulfuric acid. In each case, fresh columns were prepared before the solutions were passed through the columns. The mean for the americium-241 recovery was 98% with a standard deviation of an individual about the mean of 1%. The mean for the cerium-144 recovery was 0.2% with a standard deviation of an individual about the mean of 0.2%.

The above conditions were selected on the basis of studies with trivalent americium and cerium. The procedure

Table II. Recovery of Americium and Decontamination from Cerium in Soil

Sample	Recovery, %		Lanthanide fraction	
	Actinide fraction			
	²⁴¹ Am	¹⁴⁴ Ce	²⁴¹ Am	¹⁴⁴ Ce
1	99.1	<0.05	0.9	100.0
2	99.6	0.2	0.4	99.8
3	99.2	<0.05	0.8	100.0

was extended to include curium and californium; lanthanum and cerium, representing the lightest and most abundant rare earths; promethium and europium, representing the mid-range rare earths; and thulium and lutetium, represent the heaviest rare earths. The results of the separations are shown in Table I.

Weaver and Kappelmann studied the distribution coefficients for each of the trivalent actinides and lanthanides under conditions similar to those used in the present study (10). They showed that as the atomic number increased for the transplutonium elements, the distribution coefficients also increased. Therefore, californium should be more difficult than curium and curium more difficult than americium to remove from the column, which is shown to be true in Table I. In the case of the lanthanides, Weaver and Kappelmann showed a general decrease in distribution coefficients with increasing atomic number through europium. Beyond europium, the distribution coefficients increased rapidly. Therefore, the middle rare earths with the lowest distribution coefficients should be more readily eluted from the column. Again, the data of Table I show this to be the case.

The greatest advantage of the present method over other lanthanide-actinide separations is speed. Cation exchange involving hydrochloric acid-ethanol as the eluant provided good decontamination factors. Americium-241 recovery was 98% with only 1.2% recovery of cerium-144. However, an extremely slow flow rate of 1 drop per minute and 90 ml of eluant were required which resulted in an elution time of 24 hours. Anion exchange involving ammonium thiocyanate was better. Americium-241 recovery

was 99% with only 1.2% recovery of cerium-144. However, a flow rate of 3 drops per minute and an eluant volume of 100 ml required 8 hours for the separation. In contrast, the present method has an americium-241 recovery of 98% with only 0.2% recovery of cerium-144. The rapid flow rate of 10 to 12 drops per minute and the small volume of 20 ml of eluant enable the separation to be accomplished in 40 minutes.

APPLICATIONS

The main objective in this work was to develop a practical method for the separation of the trivalent actinides from the lanthanides, particularly lanthanum and cerium, in 10-gram soil samples. Several soil samples were spiked with americium-241 and cerium-144 tracers, totally decomposed by potassium fluoride and pyrosulfate fusions, and carried through separations to isolate trivalent actinides and lanthanides (12). The actinide-lanthanide fractions were passed through the columns described above. The chloroacetic acid-DTPA fraction and the hydrochloric acid fractions were analyzed by gamma spectrometry. The per cent recoveries of americium-241 and cerium-144 were based upon the amount added to the column and do not reflect any chemical losses that may have taken place during the decomposition and separations involved in the procedure. The results shown in Table II illustrate the excellent rare earth decontamination of the transplutonium element fraction after separation of the actinide-lanthanide fraction from a complex matrix such as soil.

ACKNOWLEDGMENT

The author acknowledges the assistance of his associates during many helpful discussions. Special thanks are due to G. J. McNabb and K. W. Puphal for their assistance with the electrodeposition of the actinides.

Received for review June 28, 1973. Accepted October 15, 1973.

- (12) C. W. Sill, K. W. Puphal, and F. D. Hindman, "Simultaneous Determination of Alpha-Emitting Nuclides of Radium through Californium in Soil," U.S. Atomic Energy Commission, Idaho Falls, Idaho, in preparation.

Gas Chromatographic Separation of Water from Cryogenically Collected Air Samples—Enhanced Concentration of Trace Organic Volatiles Prior to GC-MS Analyses

Bennett J. Tyson and Glenn C. Carle

Ames Research Center, NASA, Moffett Field, Calif. 94035

The analysis of volatile trace compounds in a gaseous diluent requires a preconcentration to separate the diluent from the compounds of interest. Sample preconcentration is necessary when using a gas chromatograph-mass spectrometer (GC-MS) to analyze air pollutants, head space gases, and food aromas because these samples contain compounds that may be present only at the sub-ppb level.

There is generally a significant amount of water concurrently collected when the volatile organic compounds are preconcentrated from air. Cryogenic preconcentration eliminates most of the nitrogen and oxygen but condenses water, which then becomes the diluent. Since this secondary dilution can still be as much as 10^{-6} , a large sample would be required for GC-MS analysis. The analysis of

large water samples containing trace organic constituents by GC-MS is a particularly difficult problem that has been treated by several authors (1, 2).

Desiccants and porous polymers have been used for excluding water during the concentration of the volatile trace compounds in air. The porous polymers, Porapak Q and Chromosorb 102, have been used in packed beds for this purpose (1, 3). Concentration on porous polymer beds is possible because of the low retention volume of water relative to the volatile compounds of interest; however, some compounds have retention volumes less than the collection volume and would be vented (4). In addition, these polymers contain unreacted vinyl groups which may be responsible for the tailing of some polar compounds (5) that would make them difficult to elute quantitatively. Several desiccant beds have been evaluated for their ability to pass the compound of interest while retaining water (1, 2). The best desiccant for this purpose was found to be potassium carbonate which would not retain all the water without retaining some organic volatiles.

Preconcentration of volatile trace compounds in air by cryogenic methods has been demonstrated to be efficient and nonselective (6). Since all water vapor is trapped coincidentally with all the volatile compounds, the advantages of cryogenic preconcentration can be exploited only if these compounds can be further separated from the water.

The purpose of this study was to develop a cryogenic preconcentration method that would totally separate water from the trace organic compounds volatilized from plants, prior to GC-MS analysis. The method can also be used to separate water from a variety of organic compounds in any cryogenically collected air sample.

EXPERIMENTAL

Apparatus. The preconcentration and analytical system was constructed by interconnecting three basic subsystems: the first subsystem was a cryogenic preconcentration device, the second subsystem was a preparative gas chromatograph with associated transfer valves and collection traps, and the third subsystem was a GC-MS. Figure 1 is a schematic of the complete system.

The cryogenic trapping device or first-stage trap was a 6-inch \times 3/8-inch o.d. electropolished (summa process) stainless steel tube packed with 60/80 mesh glass beads. Temperatures above ambient were obtained with heating tape controlled by a variable transformer, and cryogenic temperatures were obtained with liquid nitrogen. Air or the gas to be sampled was drawn through the trap with a Model 941-6001 Varian "Vac Sorb" pump, which was cooled with liquid nitrogen. The flow path through the first-stage trap was controlled by Whitey on-off toggle valves, V_1 , V_2 , V_3 , and V_4 . The flow rate during preconcentration was controlled by a gas regulator and a Nupro metering valve, V_5 , at flow rates up to 2200 scc air/min. The flow rate was monitored with a model LF-5K Hastings mass flow meter. The helium flow rate during purging and transfer of sample was controlled by C_1 , a Model 8744 Brooks flow controller.

The preparative gas chromatograph was a Model 200 Varian Aerograph, equipped with a thermal conductivity detector that was operated at 200 mA and at a temperature of 140 °C. This gas chromatograph was fitted with a 1/4-inch o.d. \times 0.035-inch wall \times 6-foot stainless steel column packed with 15% Sorbitol and 5% Igepal on 60/80 mesh HMDS-treated Chromosorb P. The column oven was operated isothermally at 105 °C. Helium carrier gas flow

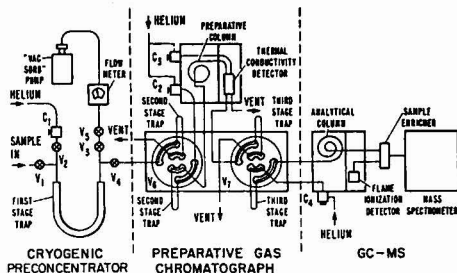


Figure 1. Schematic of the preconcentration and analytical system.

was maintained at 10 cm³/min with Model 8744 Brooks flow controllers.

The preparative gas chromatograph was fitted with an external valve oven maintained at 140 °C. This oven housed two Model 2014 Carle microvolume gas sampling valves, V_6 and V_7 . These valves were fitted with the second- and third-stage traps, respectively. The second-stage traps were open tubes constructed from 1/8-inch o.d. \times 0.010-inch wall \times 4-foot long stainless steel tubing and had a volume of 1 cm³. The third-stage traps were constructed from 1/8-inch o.d. \times 0.010-inch wall \times 2 1/2-inch long stainless steel tubing packed with 60/80 mesh glass beads, leaving a void volume of approximately 20 μ l. The traps extended outside the external oven to allow rapid heating and cooling. Cooling was attained by immersion in a Dewar filled with the appropriate cryogen while heating was accomplished with a stream of air from a 500 °F heat gun. V_6 was interconnected to the first-stage trap with a 1/8-inch o.d. \times 0.010-inch wall \times 2-foot stainless steel tube to allow transfer of the preconcentrated sample from the first-stage trap to the second-stage trap. V_6 was also interconnected to allow volatilization of the contents of the second-stage trap directly onto the sorbitol column. V_7 was connected to the outlet of the thermal conductivity detector to allow cryogenic collection of effluents of the sorbitol column in the third-stage trap. V_7 was also interconnected to allow volatilization of the contents of the third-stage trap directly onto the analytical column of the GC-MS.

The gas chromatograph mass spectrometer consisted of a Model 1522B Varian Aerograph gas chromatograph and a Model 491 DuPont mass spectrometer. The gas chromatograph was equipped with a flame ionization detector (FID), a temperature programmer, and Model 8744 Brooks flow controllers. Both detector oven and injection port temperatures were maintained at 150 °C. Depending on the type of analysis, the gas chromatograph was fitted with either SCOT or capillary columns. Helium from the injection port of this gas chromatograph alternately flowed through one of the third-stage traps and back to the inlet of the analytical column through 1/8-inch o.d. \times 0.007-inch i.d. \times 2-foot long stainless steel tubes. These tubes were heated to 150 °C.

The outlet of the analytical column was connected to a silicone membrane enricher (7) with a 1/8-inch o.d. \times 0.007-inch i.d. \times 2-foot long stainless steel tube. The low-pressure outlet of the enricher fed directly into the ion source of the mass spectrometer and the high-pressure outlet vented through a 1/8-inch o.d. \times 0.007-inch i.d. \times 2-foot long stainless steel tube to the flame ionization detector of the gas chromatograph. The enricher and the interconnecting lines were heated to 150 °C.

Ultra high purity grade helium (99.999%) was used in all flow systems.

Procedure. Before an air sample could be processed, the cryogenic traps were heated and purged with helium to remove any residual volatile materials. The first- and second-stage traps were purged by opening V_2 and V_4 and closing V_1 and V_3 and providing a helium flow of 15 scc/min which was controlled by C_1 . The first-stage trap was heated for 10 min at 140 °C and then allowed to cool to ambient before heating the second-stage trap. The second- and third-stage traps were then heated for 2 min. The purge gas for the third-stage trap was supplied by the outlet gas flow of the preparative gas chromatograph.

(7) D. R. Black, R. A. Flath, and R. Teranishi, *J. Chromatogr. Sci.*, **7**, 284 (1969).

- (1) T. H. Schultz, R. A. Flath, and R. T. Mon, *J. Agr. Food Chem.*, **19**, 1060 (1971).
- (2) D. A. Heathcote, R. E. Wrostad, and L. M. Libbey, *J. Agr. Food Chem.*, **19**, 1069 (1971).
- (3) A. Dravnieks, B. K. Krotoszyński, J. Whitfield, A. O'Donnell, and T. Burgwald, *Environ. Sci. Technol.*, **5**, 1220 (1971).
- (4) W. G. Jennings, R. Wohleb, and M. J. Lewis, *J. Food Sci.*, **37**, 69 (1972).
- (5) W. Herli and M. G. Neumann, *J. Chromatogr.*, **60**, 319 (1971).
- (6) R. A. Rasmussen, *Amer. Lab.*, **4** (7), 19-27 (1972).

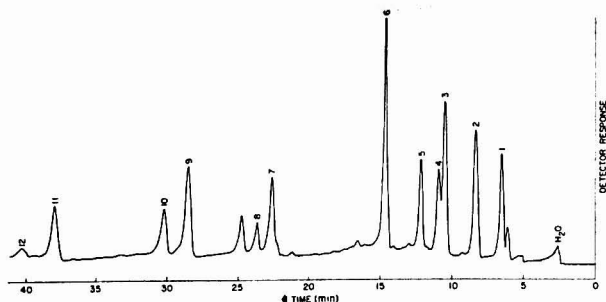


Figure 2. Typical beam monitor trace of test mixture containing terpenes processed through the entire system

Column: convalux 10 (polyphenyl ether) on 0.020-inch i.d. X 200-foot capillary, 80 °C for 10 min, programmed to 120 °C at 2°/min

Table I. System Recovery Efficiency for Selected Terpenes

Peak	Component	Peak height.		Recovery, %
		Direct injection ^a	Processed sample ^a	
1	α -Pinene	101	99	98
2	Camphene	121	133	110
3	β -Pinene	114	95	83
4	Myrcene	42	40	95
5	Δ -3-Carene	50	46	92
6	Limonene	90	84	93
7	Linalool	37	33	89
8	Thujone	27	16	60
9	Menthone	36	41	114
10	Isomenthone	51	30	59
11	Estragol	47	41	87
12	Bornyl acetate	34	10	30

^a Average of four analyses.

An air sample was preconcentrated by cooling the first-stage trap, and the "vac sorb" pump to -196 °C and opening V_1 and V_3 and closing V_2 and V_4 . The air flow rate was adjusted to 1 liter/min with V_5 . After the desired volume of air had been drawn through the first-stage trap, the second-stage trap was cooled to -75 °C in an alcohol-Dry Ice bath. V_1 and V_3 were then closed and V_2 and V_4 opened, sweeping purge gas through the first- and second-stage traps at 15 scc/min. The first-stage trap was then heated at 50 °C/min to 140 °C while its contents were transferred to the second-stage trap. The transfer process required 7 min. The third-stage trap was then cooled to -196 °C and V_6 was switched, placing the second-stage trap in the carrier gas stream of the preparative gas chromatograph. The second-stage trap was then heated, releasing the sample onto the sorbitol column. The effluents of the sorbitol column were monitored with the thermal conductivity detector and collected in the third-stage trap until just prior to the emergence of water. Just before water began to elute, V_7 was switched to vent water and place the third-stage trap in the carrier gas stream of the GC-MS. The trap was then heated, releasing the sample onto the analytical column of the GC-MS for analysis.

RESULTS AND DISCUSSION

Figure 2 shows a typical beam monitor recording of the GC-MS analysis of a test mixture containing terpenes. The test mixture was prepared by adding 0.1 μ l (10⁻⁴ gram) of a sample containing 6 oxygenated and 6 hydrocarbon terpenes to 200 mg of water. This amount of water is equivalent to that which would be collected from 20 liters of air if the air had a relative humidity of 50%. The

test mixture was injected into the inlet air stream of the first-stage trap where it was preconcentrated. This mixture was then separated from water and analyzed using the method described. The beam monitor recording clearly indicates that the water present in the test mixture was eliminated completely, and only that water collected from the helium carrier reached the analytical system.

A study was made to determine the overall efficiency of the system: 0.1 μ l of the terpene sample was injected directly onto the analytical column of the Varian 1522B and analyzed using the FID and bypassing the mass spectrometer. These results were compared to those obtained when the test mixture was processed through the entire system. A summary of the results is shown in Table I. The recovery of the hydrocarbon terpenes was greater than 83% in all cases. The recovery of the oxygenated terpenes was generally lower, but still good, with the exception of bornyl acetate. Bornyl acetate eluted just prior to water on the sorbitol column and was partially lost when water was vented.

With this high efficiency of recovery, trace organic components in air can easily be identified after their preconcentration and separation from water. The GC-MS system described requires an on-column injection of about 20 nanograms to obtain a good mass spectrum. Based on this sensitivity limit, a compound present in air at a concentration as low as 0.2 ppb could be identified when preconcentrated from 20 liters of air if the efficiency of recovery was 100%.

The terpenes used to determine the efficiency of this system are representative of several classes of volatile organic compounds and comprise acyclic, monocyclic, bicyclic, and aromatic hydrocarbons, which contain varying degrees of unsaturation, in addition to their oxygenated counterparts: the alcohols, ketones, ethers, and acetates. The efficiencies of recovery for other volatile compounds belonging to the same classes as those tested should be the same as indicated in Table I, provided these compounds have shorter retention times than water on the preparative sorbitol column.

The usefulness of sorbitol was demonstrated in a study of retention characteristics in which 259 of 316 organic compounds were found to elute prior to water (8). These compounds included aldehydes, pyrans, furans, and oxides in addition to the classes of compounds represented in Table I. We also have used sorbitol to separate water

(8) W. O. McReynolds, "Gas Chromatographic Retention Data," Preston Technical Abstracts Co., Evanston, Ill., 1966, p 152.

from 1,1,2-trichloroethane, furfural, butyl mercaptan, and pyridine. The separation of water from the several classes of organic compounds represented by the terpenes together with the compounds mentioned above illustrate the utility of the method described for the analysis of a wide variety of organic compounds.

If the compounds of interest in a sample cannot be separated from water using sorbitol, then another preparative

column can be used such as purified apiezon L on which water elutes prior to most organic compounds. In general, any preparative column that would provide a significant difference in retention characteristics for a diluent and those compounds of interest may be used with the system.

Received for review October 11, 1973. Accepted November 19, 1973.

Pyrolysis Esterification of Phosphorous-Containing Acids for Gas-Liquid Chromatographic Analysis

William L. Clapp,¹ Robert J. Valis, Stanley R. Kramer, and John W. Mercer

Process Technology Branch, Chemical and Plants Division, Manufacturing Technology Directorate, Edgewood Arsenal, Md. 21010

Conventional methods of analysis of dilute aqueous solutions of phosphorous acids have centered chiefly around their determination by means of the molybdovanadophosphoric acid complex (1, 2). The problems associated with analysis of organophosphorous acids are even more complicated in that they necessitate the conversion of such compounds into inorganic phosphates prior to analysis (3).

In recent years, a technique has been described whereby carboxylic acids are converted into their methyl esters by injection port pyrolysis of their tetramethylammonium salts. Robb and Westbrook (4) found that the methyl esters of saturated fatty acids could be formed by direct injection of methanolic solutions of their tetramethylammonium salts into a heated injection port of a gas chromatograph. However, the yields were variable with different acids and poor with small sample sizes. Downing (5, 6) modified the injection procedure and obtained more reproducible results, not only with saturated fatty acids but with mixtures of fatty acids containing unsaturated components as well. This procedure, with some additional modifications, has been applied to the pyrolysis esterification of organophosphorous acids.

EXPERIMENTAL

Apparatus. An F&M Scientific Corporation Model 720 gas chromatograph with a thermal conductivity detector was used with a 6-ft \times 1/8-in. o.d. stainless steel column packed with 5% Carbowax 20 M on 60/80 mesh Chromasorb W. The carrier gas was helium at a flow rate of 25 cm³/min. The injection port temperature was 190 °C while the detector temperature was 260 °C. The column was programmed from 125 °C to 200 °C at 7.5 °C/min.

An F&M Scientific Corporation Model 80 pyrolysis unit equipped with a standard M-type probe was used without modification for pyrolysis of samples. This unit and probe have been adequately described by Brodasky (7). A temperature calibration curve for each probe was supplied by the manufacturer.

¹ Present address, R. J. Reynolds Tobacco Company, Research Department, 115 Chestnut Street, S.E., Winston-Salem, N.C. 27102.

- (1) E. J. Griffith, *Anal. Chem.*, **28**, 525 (1956).
- (2) R. E. Kitson and M. G. Mellon, *Anal. Chem.*, **16**, 379 (1944).
- (3) S. G. Jankovic, D. T. Mitchell, and J. C. Buzzell, Jr., *Water Sewage Works*, **114**, 471 (1967).
- (4) E. W. Robb and J. J. Westbrook III, *Anal. Chem.*, **35**, 1644 (1963).
- (5) D. T. Downing, *Anal. Chem.*, **39**, 218 (1967).
- (6) D. T. Downing and R. S. Greene, *Anal. Chem.*, **40**, 827 (1968).
- (7) T. F. Brodasky, *J. Gas Chromatogr.*, **5**, 311 (1967).

Reagents. Methylphosphonic acid and methylfluorophosphonic acid were prepared and purified in this laboratory. Structures and purity were confirmed by infrared, nuclear magnetic resonance, and mass spectral analysis.

Procedure. A 0.500-gram sample of each acid was dissolved in 4 ml of distilled water in a 10-ml volumetric flask which was immersed in an ice bath. Tetramethylammonium hydroxide (Eastman, 25% in water) was added dropwise to a phenolphthalein end point, followed by dilution to the mark with distilled water. A 2- μ l aliquot of the sample was placed on the probe tip and allowed to evaporate to dryness at room temperature. (Additional sample could be added as necessary.) The probe was then attached to the injection port of the chromatograph and pyrolyzed for 15 seconds.

A typical chromatogram for the methyl esters of methylphosphonic acid and methylfluorophosphonic acid prepared by this technique is shown in Figure 1. The principal pyrolysis degradation product was determined to be trimethylamine, by combined gas chromatography-mass spectral analysis.

Reference samples of the methyl esters were prepared and purified by conventional techniques. Standard solutions of the esters in methanol were chromatographed and plots of peak area vs. concentration were obtained. Area measurements were made with an Infotronics Model CRS-108 digital integrator. The quantity of methyl ester formed through pyrolysis was then determined from standard curves.

RESULTS AND DISCUSSION

Several parameters which would be expected to have an effect on the yield of the pyrolysis methylation procedure were studied.

Effect of Pyrolysis Temperature. To determine the effect of this variable, aliquots of a standard solution of the tetramethylammonium salt of methylphosphonic acid were pyrolyzed at various temperatures. A mesa-like curve resulted (Figure 2). Incomplete conversion below 325 °C appears likely, with sample decomposition beyond 925 °C. The broad optimum range of pyrolysis temperatures permitted excellent control and reproduction of the pyrolysis phase; the standard deviation of the technique was typically $\pm 1.5\%$. All subsequent sample pyrolyses were made at 500 °C.

Effect of Sample Size. The relationship between the yield of the pyrolysis step and the sample size was also evaluated for samples containing 10–100 μ g of acid. Excellent results were obtained with methylfluorophosphonic acid (Table I) over the entire range studied. However, the ester yield with methylphosphonic acid (Table II) decreased significantly when the quantity of acid pyrolyzed

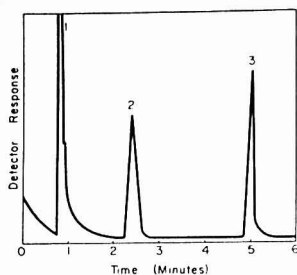


Figure 1. Chromatogram of a mixture of (1) pyrolysis degradation products, (2) methyl methylfluorophosphinate, and (3) dimethyl methylphosphonate

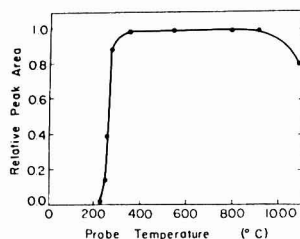


Figure 2. Yield of dimethyl methylphosphonate as a function of pyrolysis probe temperature

Table I. Effect of Sample Size on Yield of Methyl Methylfluorophosphinate

Sample size, μg	Yield, ^a %
100	99 \pm 1
75	99 \pm 1
37.5	98 \pm 2
11.3	97 \pm 3

^a Each analysis is the average of three chromatograms.

Table II. Effect of Sample Size on Yield of Dimethyl Methylphosphonate

Sample size, μg	Yield, ^a %
100	99 \pm 1
50	99 \pm 1
30	52 \pm 2
10	10 \pm 5

^a Each analysis is the average of three chromatograms.

was less than 50 μg . When the tetramethylammonium salts of both methylfluorophosphinic acid and methylphosphonic acid were pyrolyzed simultaneously, esterification was quantitative for both acids over the entire concentration range.

An attempt was made to esterify phosphoric acid under these same conditions but low, erratic yields were obtained, probably because of an inability to neutralize the third acid group.

Pyrolysis Probe. The nature of the pyrolysis unit was the key to the study. By producing a rapid, yet well-defined, probe temperature, reproducible injection port esterification was possible. In an earlier study, similar re-

sults were obtained with the use of this apparatus in the esterification of fatty acids (8).

The application of this type of unit for pyrolysis esterification offers several advantages over those cited earlier. First, the unit is commercially available and easily adapted to many types of chromatographs. Second, the configuration of the probe is such that, if necessary, repetitive additions to the probe tip of sample aliquots are easily accomplished prior to pyrolysis with a delay only for the solvent to evaporate. Since no degradation of the dry salts of these acids was observed on the probe, as many aliquots as were necessary could have been added, thus reducing the need to concentrate samples.

CONCLUSIONS

While most workers have focused their work with this technique on the determination of carboxylic acids, the data suggest that the technique can be applied to phosphorus-containing acids. The method appears ideally suited to the analysis of moderately dilute aqueous solutions of these acids where the approach is to conduct the analysis through gas chromatography of their methyl esters.

Received for review August 22, 1973. Accepted October 26, 1973.

(8) P. H. Latimer and W. L. Clapp, R. J. Reynolds Tobacco Company, unpublished work, 1968.

CORRECTION

Resolution by Gas-Liquid Chromatography of Diastereomers of Five Nonprotein Amino Acids Known to Occur in the Murchison Meteorite

In this article by G. E. Pollock, *Anal. Chem.*, 44, 2368 (1972), an error in nomenclature was made. The (+)-2-alkanols have an *S*(+) configuration in the Cahn-Ingold system, not *R*(+) as written in this paper. The following changes should be made:

p 2368, column 2, lines 11 and 12 ... the *N*-trifluoroacetyl-(*SR*)-amino acid (*S*)-2-butyl esters ...

p 2369, column 1 under Reagents, line 4, ..., optically active *S*-(+)-2-alkanols ...

p 2371, Tables III and IV, bottom of table

Peak 1—*RS* for *N*-methylalanine, β -amino-*n*-butyric,

Peak 2—*SS* and pipecolic acids.

Peak 1—*SS* for isovaline and β -aminoisobutyric acid

Peak 2—*RS*

p 2372, column 1, lines 9–15, *i.e.*, the *RS* peak elutes first and the *SS* peak second. Isovaline and β -aminoisobutyric acid, however, show a reversal of elution pattern, the *SS* peak elutes first and the *RS* peak second. Up to this time, only one case of reversal of elution order has been reported. Charles-Sigler and coworkers (10, 13) report that *N*-TFA-(*RS*)-phenylglycine-(*S*)(+)-2-octanol ester has a reversed elution order while the *S*(+)-2-butanol ester is normal.

I wish to thank Dr. E. Gil-Av for calling to my attention this error in nomenclature.

Sensitivities for Photon Activation Analysis with Thick-Target, 110-MeV Electron Bremsstrahlung

Enzo Ricci

Analytical Chemistry Division, Oak Ridge National Laboratory, Oak Ridge, Tenn. 37830

Recent reviews (1, 2) have described active progress in photon activation analysis (PAA). In particular, during the past few years, several authors have developed useful specific methods and determined elemental sensitivities, for a variety of bremsstrahlung production conditions (3-8). Yet, most of this work involved the use of relatively thin electron targets (2-6 mm thick) and electron energies below 40 MeV. Only two groups reported photon-activation yield determinations with bremsstrahlung from 70-72 MeV electrons (7, 8), and none beyond this electron energy.

The Oak Ridge Electron Linear Accelerator (ORELA) was designed with the main purpose of producing neutrons; these are used to determine cross sections of interest to the Liquid Metal Fast Breeder Reactor and other programs. The ORELA can accelerate electrons up to energies of 150-160 MeV, but normal operation—particularly during our experiments—has been at or near 110 MeV. Because of ORELA's main application, the electrons—whose energy is seldom lowered below 100 MeV—are made to impinge on a massive (3.03-cm thick) tantalum target. The beam power can easily be raised to a maximum of 50 kW—approximately equivalent to a 350 μ A current—but a beam of 30 kW or less is frequently used, as was the case in our work. The beam is pulsed, and to reach a 30- to 50-kW power at 100-140 MeV, typical conditions are 800 pulses per second of 20- to 50-nsec duration and 10- to 15-A peak intensity.

These somewhat rigid operation conditions—quite different from those characterizing most PAA experiments to date—govern bombardments at the ORELA. Also, economic efficiency reasons call for simultaneous use of the accelerator for both PAA and neutron physics experiments. Consequently, two important tasks became clear early in our work. First, to design a pneumatic system that would convey the sample—with the accelerator on, and while being used for other experiments—to a position where it could be cooled and bombarded homogeneously with ORELA's bremsstrahlung. Second, to determine experimentally PAA sensitivities and interferences for ORELA's conditions, and to put them in perspective with values from other authors (3-8), in light of differences between the bremsstrahlung photon-energy distributions involved. For the first task, we designed an original system (9), which we describe in detail and assess elsewhere (10). This paper concerns experiments and discussions relative to the second task.

BREMSSTRAHLUNG PHOTON ENERGY DISTRIBUTION

The uncommon characteristics of bremsstrahlung production at the ORELA pose two important questions at the theoretical or semi-empirical level. The first one refers to the influence of photon angular distribution—for both intensity and energy—on bombardment homogeneity; this has been studied in detail in another publication (10). The second question involves the influence of the bremsstrahlung energy spectrum on PAA sensitivities and interferences; we will attempt to answer it, in light of the scarce theoretical and experimental data available for ORELA's operating conditions.

Briefly, our PAA pneumatic transfer system (9, 10) consists of a spherical aluminum rabbit (5.1-cm diameter) that carries four 2-cm³ sample capsules to a bremsstrahlung photon irradiation chamber. The gamma radiation is originated by ORELA's intense electron bombardment of a 3.03-cm thick tantalum target consisting of ten parallel, vigorously water-cooled tantalum plates of 1.8- to 6.8-mm thickness. When the sphere arrives at the irradiation chamber, it floats there, on an air upstream, at 15.0 cm past the center of the tantalum target in the direction of the electron beam; the air also provides cooling and induces spinning, thus facilitating homogeneous bombardment of the samples.

When a sample is irradiated with bremsstrahlung—from a beam of electrons of energy E_0 impinging on a heavy-element target—it is exposed to a photon spectrum which includes all gamma-ray energies k up to E_0 . If a nuclear reaction is induced in one of the sample elements by this radiation, at each photon energy k the reaction yield is proportional to the cross section $\sigma(k)$, given in cm². The total yield in reactions per second is, then (11, 12),

$$Y(E_0) = n \int_0^{E_0} N(E_0, k) \sigma(k) dk \quad (1)$$

where n is the number of atoms of reacting element per cm² of sample seen by the bremsstrahlung, and $N(E_0, k)$ is the spectrum function—i.e., the number of photons of energy k , per unit energy k , which enter the sample per second. This function can thus be explicitly written as

$$N(E_0, k) = F(E_0, k) I(E_0, k) / k \quad (2)$$

where the function $I(E_0, k)/k$ is proportional to the bremsstrahlung photon energy distribution; $F(E_0, k)$ is a normalizing-correcting factor related to the converter and sample thickness.

The bremsstrahlung spectrum $I(E_0, k)/k$ vs. k , integrated over all photon angles for a very thin (1 μ m or less) platinum radiator can be calculated from tables (11) for electron energies E_0 from 1 to 960 MeV. We have thus plotted spectra for seven E_0 values (19 to 160 MeV) in

- (1) W. S. Lyon, E. Ricci, and H. H. Ross, *Anal. Chem.*, **44**, 438R (1972).
- (2) G. J. Lutz, *Anal. Chem.*, **43**, 93 (1971).
- (3) Y. Oka, T. Kato, K. Nomura, and T. Saito, *Bull. Chem. Soc. Jap.*, **40**, 575 (1967).
- (4) G. J. Lutz, *Anal. Chem.*, **41**, 424 (1969).
- (5) J. L. Lebrun and P. Albert, *Bull. Soc. Chim. Fr.*, **3**, 1020 (1969).
- (6) C. Engelmann, *French Rept., CEA-R-4072* (1970).
- (7) T. Kato and A. F. Voigt, *J. Radioanal. Chem.*, **4**, 325 (1970).
- (8) T. Kato and Y. Oka, *Talanta*, **19**, 515 (1972).
- (9) E. Ricci, T. H. Handley, and M. G. Willey, "Fluid Supported Sample Holder for Homogeneously Irradiated Samples," U.S. Patent No. 3,549,492 (Dec. 22, 1970).
- (10) E. Ricci, *Nucl. Instrum. Methods*, in press.

- (11) A. S. Penfold and J. E. Leiss, "Analysis of Photo Cross Sections," Rept. Physics Research Lab., U. Illinois (May 1958).
- (12) B. I. Goryachev, *At. Energy Rev.*, **2**, (3), 71 (1964).

Table I. Interference-Free PAA Sensitivities at ORELA's Analytical Facility

Element (target)	Reaction ^a	Half-life	Gamma-ray measured, ^b MeV	Sensitivity or specific absolute activity, dpm/ μ g element ^c	Average electron beam energy, E_0 , MeV
Be	⁹ Be(γ ,2n) ⁷ Be	53.6 d	0.477	0.813	110
B	¹⁰ B(γ ,p2n) ⁸ Be	53.6 d	0.477	0.138	110
C(graphite)	¹³ C(γ ,n) ¹⁴ C	20.34 m	0.511	3,996	105
N(NaNO ₂)	¹⁴ N(γ ,n) ¹⁵ N	9.96 m	0.511	3,878	110
O(PbO)	¹⁶ O(γ ,n) ¹⁷ O	2.07 m	0.511	4,750	140
F(NaBF ₄ OH)	¹⁹ F(γ ,n) ¹⁸ F	109.7 m	0.511	25,930	105
Na(NaNO ₂)	²³ Na(n, γ) ²⁴ Na	14.96 h	1.369 or 2.754	13.6*	110
	²³ Na(γ ,n) ²² Na	2.62 y	0.511	0.755	110
Mg	²⁴ Mg(γ ,p) ²³ Na	14.96 h	1.369 or 2.754	161	105
Al	²⁷ Al(n,p) ²⁶ Mg	9.46 m	0.84 or 1.013	49.1*	110
	²⁷ Al(n, α) ²⁴ Na	14.96 h	1.369 or 2.754	17.0*	110
P(red)	³¹ P(γ ,n) ³⁰ P	2.50 m	0.511	8,246	105
	³¹ P(γ ,2p) ²⁹ Al	6.6 m	1.28	137	105
	³¹ P(n, α) ²⁸ Al	2.31 m	1.780	171*	105
V(V ₂ O ₅)	⁵¹ V(n, γ) ⁵² V	3.75 m	1.434	2,521	110
	⁵¹ V(γ , α) ⁴⁷ Sc	3.43 d	0.160	4.15	110
	⁵⁰ V(γ ,2n) ⁴⁸ V	16.0 d	0.511	0.461	110
Ni	⁵⁸ Ni(γ ,n) ⁵⁹ Ni	36.0 h	0.511 or 1.37	455	115
Cd	¹¹² Cd(γ ,n) ^{113m} Cd	48.6 m	0.150 + 0.247	1,715	115
	¹⁰⁶ Cd(γ ,n) ¹⁰⁷ Cd	55.0 m	0.511	161	115
	¹¹⁴ Cd(γ ,n) ¹¹⁵ Cd \rightarrow ^{115m} In	53.5 h (eq.)	0.335	119	115
	¹¹⁴ Cd(γ ,p) ¹¹³ Ag	3.14 hr	0.617	68.3	115
Sn	¹¹⁶ Sn(γ ,p) ¹¹⁵ In	45.0 m	0.158	1,144	110
	¹¹⁷ Sn(γ ,p) ^{116m} In	54.0 m	1.09 + 1.293	50.7	110
	¹¹⁷ Sn(γ ,p) ¹¹⁷ In	2.81 d	0.247	8.08	110
Ta	¹⁸¹ Ta(γ ,p) ^{180m} Hf	5.5 h	0.215 + 0.333 + 0.444	72.2	105
Pb(PbO)	²⁰⁴ Pb(γ ,n) ²⁰⁵ Pb	52.1 h	0.279 + 0.401	777	140
	²⁰⁴ Pb(γ , γ) ^{204m} Pb	66.9 m	0.912 + 0.899	37.5	140

^a Only most probable reactions listed. ^b " γ " or " α " between energies means both γ -rays used to calculate independent, agreeing sensitivity values; "+" means all photopeak areas added together to obtain sensitivity. ^c At end of bombardment for one half-life (maximum 2 h) with bremsstrahlung from a 30-kW electron beam. Errors not listed because results are averages for two or four irradiation capsules (see Ref. 10). Asterisk stresses neutron reactions.

Figure 1. Though ORELA's thick tantalum radiator provides clearly different conditions, it is known (11) that a small difference in target atomic number (⁷³Ta to ⁷⁸Pt) does not result in significant change of the bremsstrahlung spectrum, and that only the shape of its high-energy tip is affected by radiator thickness. The histogram of Figure 1—calculated from data (13) for a thick Ta target (1.912 cm)—tends to prove this. It results from a rather accurate Montecarlo calculation and shows reasonable agreement, at low photon energies, with the thin-platinum bremsstrahlung spectrum curve corresponding to the same electron energy, $E_0 = 100$ MeV.

(13) R. G. Alsmiller and H. S. Moran, *Nucl. Instrum. Methods*, **48**, 109 (1967).

Moreover, Figure 1 shows that at low photon energies ($k \leq 20$ MeV), bremsstrahlung spectra from electrons of E_0 from 27 to 160 MeV do not differ by more than a factor of 1.5. This includes bremsstrahlung from a thick target also, as the histogram shows, at least up to 10 MeV; in fact, though the latter is for $E_0 = 100$ MeV, it approaches the low- E_0 , thin-target spectra, because of attenuation of high energy photons in the tantalum converter.

These facts are very important, in view of the behavior of the excitation function $\sigma(k)$ of Equation 1 for $k \leq 30$ MeV. It is well known that this function displays a so-called "giant resonance" for most photonuclear reactions (2). The giant resonance energy for the common reactions —i.e., (γ ,n), (γ ,2n), (γ ,p)—varies only from 20 to 13 MeV

Table II. Comparison of Sensitivities^a

Element (product)	A, this work, ^a $E_0 = 105$ to 115 MeV, dpm/ μ g	$E_0 = 25$ MeV		$E_0 = 30$ MeV		$E_0 = 40$ MeV	
		B, sensitivity, dpm/ μ g	B/A	C, sensitivity, dpm/ μ g	C/A	D, sensitivity, D/A dpm/ μ g	
C(¹⁴ C)	3,996	1,000	0.25	7,143	1.8	40,000	10
N(¹⁴ N)	3,878	1,205	0.31	3,571	0.92	12,500	3.2
O(¹⁶ O)	4,750	1,000	0.21	5,263	1.1	27,780	5.9
F(¹⁹ F)	25,930	7,692	0.30	15,390	0.59	45,460	1.8
Na(²³ Na)	0.755					7.11	9.5
Mg(²⁴ Na)	151						
P(³⁰ P)	8,246						
Ni(⁵⁹ Ni)	455	275	0.61	642	1.4	1,679	3.7
Cd(¹⁰⁶ Cd)	161	313	1.9	769	4.8	2,564	16
Cd(¹¹⁴ Ag)	68.3						
Pb(²⁰⁵ Pb)	777	65.7	0.085	144	0.19	525	0.68
Average ratio			0.52 \pm 0.63		1.5 \pm 1.5		6.3 \pm 5.2

^a All values normalized to end of bombardment for one half-life (maximum 2 h). ^b Bremsstrahlung from 30 kW (~ 210 μ A) electron beam on 30.33-mm thick

(light to heavy elements), while the width at half maximum of the resonance peak fluctuates between 3.8 and 10 MeV, with smaller values for magic-number nuclei (12, 14). Now, because $\sigma(h)$ has significant values only within the range of the giant resonance, just the low-energy part of the bremsstrahlung spectrum ($h \approx 10$ to 30 MeV) contributes to the photon activation yield in Equation 1. This, in addition to the observed similarity (Figure 1) of bremsstrahlung spectral shapes within approximately the same energy range, suggests that ORELA's PAA sensitivities should be similar to those obtained by other authors with E_0 below 30 or 40 MeV, and with thin converters.

EXPERIMENTAL

To determine interference-free sensitivities for 16 elements, we bombarded pure substances in our new facility. As bombardment is not perfectly homogeneous in the sphere-rabbit (10), to obtain average results we placed these substances either in each of the four sample capsules, or in two of them, oppositely located in the sphere; 1-cm² polyethylene inserts were used to hold loose powders. Irradiations ranged from 30 sec to 30 min—depending on the half-life of the product—at electron beam powers from 9.3 to 29.0 kW.

We counted the radioactivity of the products with a conventional gamma-ray spectrometer, consisting of an RCL 400-channel analyzer with paper tape readout and a 7.62 cm \times 7.62 cm NaI(Tl) detector; the latter was preferred to a Ge(Li) detector, to facilitate absolute counting. We sandwiched all positron emitters between sufficient thicknesses of Lucite, to count the annihilation radiation, and measured all samples through a 1.24-cm thick Lucite beta absorber.

We tried to identify—and follow the radioactive decay of—all the products induced in each of the elements irradiated that gave significant gamma photopeaks. Least-squares decay curve analysis (15) was applied to the results so obtained.

RESULTS AND DISCUSSION

Table I summarizes our results. The best sensitivities are for carbon, nitrogen, oxygen, and, particularly, fluorine—elements difficult or impossible to determine by neutron activation analysis—in agreement with other authors (3–7). Because ³⁰P is also induced significantly in sulfur—which often accompanies phosphorus—the highly sensitive (γ, n) reaction on the latter cannot be considered as useful. But heavier elements, such as nickel, cadmium,

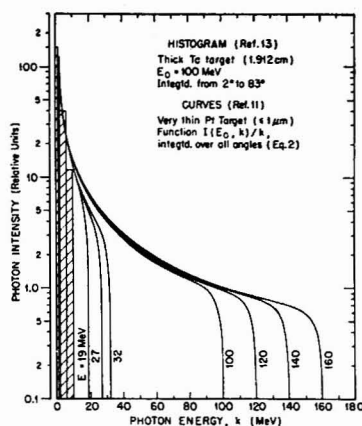


Figure 1. Integrated-over-angle bremsstrahlung spectra for electron beams of $E_0 = 19$ to 160 MeV impinging on thin (curves) and thick (histogram) converters

and lead—with poor neutron-activation sensitivities but great environmental significance—show encouraging results at the ORELA. We have stressed results from neutron reactions with an asterisk; they are characteristic of ORELA's design and not reported by most other laboratories. Note that the vanadium (n, γ) sensitivity is among the six highest in Table I. On the other hand, results for some reactions are low, but they are useful to estimate potential interferences in PAA.

We chose 11 elements—from light to heavy in the periodic table—among our 16 sensitivity determinations, to compare our results with those obtained by other authors for $E_0 \leq 40$ MeV, and thus test our theoretical expectations of agreement. Table II establishes this comparison and shows that, indeed, our results generally agree with experimental (6) and calculated (2, 4) ones, and fall between sensitivities for electron beam energies E_0 of 25 and 30 MeV. Sensitivity ratios bear out this agreement with standard deviations ranging from 53 to 121%. This variation is small, considering that it amounts to a factor of 2.2, while the sensitivity data range from 0.755 to 25,930 dpm/ μ g—thus implying a factor of 34,000. Furthermore, analogous ratios between sensitivities reported by the two

- (14) B. L. Berman, "Atlas of Photoneutron Cross Sections Obtained with Monoenergetic Photons," U.S. At. Energy Comm. Rept. UCRL-74622 (1973).
(15) J. B. Cumming, in "Applications of Computers to Nuclear and Radiochemistry," G. D. O'Kelley, Ed., Rept. NAS-NS 3107 Chemistry (1963), p. 25.

Lutz (calculated; Ref. 2, 4) ^d					
$E_0 = 25$ MeV		$E_0 = 30$ MeV		$E_0 = 35$ MeV	
E, sensitivity, dpm/ μ g	E/A	F, sensitivity, dpm/ μ g	F/A	G, sensitivity, dpm/ μ g	G/A
1,800	0.45	6,000	1.5	15,000	3.8
3,000	0.77	12,000	3.1	24,000	6.2
3,000	0.63	9,000	1.9	18,000	3.8
1,600	0.062	2,500	0.096	4,900	0.19
0.6	0.80	1.5	2.0	2.7	3.6
90.0	0.60	270	1.8	600	4.0
3,000	0.36	12,000	1.5	18,000	2.2
210	0.47	600	1.3	900	2.0
36.4	0.53	144	2.1	216	3.2
60.0	0.077	120	0.15	180	0.23
	0.47 \pm 0.25		1.5 \pm 0.9		2.9 \pm 1.8

Ta target. ^c 100 μ A electron beam on 2 mm Pt. ^d 100 μ A electron beam on 6 mm W.

other authors (Table II), yield standard deviations of a similar magnitude—e.g., ratio $E/B = 1.53 \pm 1.15$ (75%), $F/C = 1.31 \pm 1.12$ (85%), $G/D = 0.72 \pm 0.67$ (93%).

We should not assign great significance *a priori* to the fact that our sensitivities are between others' values for $E_0 = 25$ MeV and $E_0 = 30$ MeV. Our distance sample-converter is greater (15 cm), and our electron beam intensity double (~ 210 μ A) theirs. However, these features result in opposite effects. Moreover, the general agreement of sensitivity ratios is quite important, because it implies activation trends for our system, parallel with those of thin-target, low- E_0 facilities, for the whole range of giant resonance energies ($k \approx 10$ to 30 MeV). That is, it suggests reasonably similar bremsstrahlung spectrum shapes—within said range—for the ORELA and conventional facilities (2, 4, 6), as we had expected from Figure 1.

Table II shows, finally, that our sensitivities agree best

with Lutz's results. The latter were obtained from a comprehensive table (2, 4) which lists calculated sensitivities for 76 photon reactions on 59 elements for electron beam energies $E_0 = 25, 30$, and 35 MeV. With reasonable approximation, the average ratios of Table II can be used to estimate sensitivities for our PAA system, from Lutz's table, for elements and reactions not included in our work.

ACKNOWLEDGMENT

We thank J. A. Harvey and H. A. Todd for their continuous interest in our work, and ORELA's operators for smooth scheduling and conduction of our bombardments.

Received for review September 12, 1973. Accepted November 12, 1973. Oak Ridge National Laboratory is operated by the Union Carbide Corporation for the U.S. Atomic Energy Commission.

Determination of Lead in Paint with Fast Neutrons from a Californium-252 Source

George J. Lutz

Activation Analysis Section, Analytical Chemistry Division, National Bureau of Standards, Washington, D.C. 20234

Several decades ago in the United States, it was common practice to paint the interior walls and woodwork of dwellings with a formulation of paint containing large amounts of lead. This has created a tragic health problem, particularly in some of the larger cities, causing lead poisoning of children in certain susceptible age groups who have ingested this lead-bearing paint which has peeled or chipped off from the walls. The detection and alleviation of this hazard depends upon reliable chemical determinations of lead in suspected areas.

Currently, screening of suspected paints is oriented to the detection of those containing greater than $\sim 0.5\%$ of lead. The accurate determination of lead at this level is not particularly difficult by a variety of methods, but they usually require time consuming manipulations such as dissolution prior to measurement, although Rasberry (1) has studied portable X-ray fluorescence analyzers developed specifically for use in screening, *in situ*, wall paint for lead.

A purely instrumental activation analysis, particularly if it could be accomplished with a relatively inexpensive irradiation source would appear to have merit. It would dispense with lengthy chemical treatments and would have the potential for largely automating the determination. This paper describes the evaluation of a small ^{252}Cf source for this determination.

The element californium was first synthesized by Thompson *et al.* (2) in 1950. Californium-252 is currently manufactured by irradiating plutonium targets in a nuclear reactor. Starting with ^{239}Pu , the heaviest isotope available in large quantities, the production of ^{252}Cf requires a series of 13 neutron captures. Current production is about 1 gram per year. The isotope has a half-life of 2.65 years. It decays both by α particle emission and by spontaneous

fission. The neutron output from spontaneous fission of 1 gram of ^{252}Cf is 2.34×10^{12} per second. The unmoderated neutron spectrum of ^{252}Cf is roughly the same as that of ^{235}U . Relative to (α, n) isotopic neutron sources, ^{252}Cf sources have smaller dimensions and less radioactive material. They require less space for decay helium and, for practical purposes, rarely require cooling. They are also competitive on a cost per neutron basis with other radioisotope neutron sources (3). Ricci and Handley (4) aptly considered their system utilizing this isotope for laboratory activation analysis a "portable, maintenance-free, quasi-reactor."

EXPERIMENTAL

The NBS ^{252}Cf facility consists of 8 sources of 75 μg each at the time of these experiments. The sources are mounted in a $90 \times 90 \times 210$ -cm high aluminum tank filled with demineralized water. The source configuration is shown in Figure 1. The purpose of the octagonal source array is to produce a neutron flux as homogeneous as practical at the sample irradiation position. Since the stable isotopes of lead do not undergo nuclear reactions with thermal neutrons useful for analytical purposes, the sources are moved as close as possible to the central pneumatic tube to enhance fast neutron reactions. The fast neutron flux is approximately 5×10^7 n/cm²-sec.

Samples are packaged in a polyethylene snap cap vial of 1-cm diameter and 2.5-cm length. This is placed in a larger polyethylene vial with spacers to ensure that the sample is in the position of maximum neutron flux. A compressed air pneumatic transfer system transfers the samples to the irradiation position and return.

Preliminary experiments involved irradiating and counting a few grams of lead for various lengths of time. Three nuclear reactions were detected. These are shown in Table I. The threshold of the reaction $^{207}\text{Pb}(n, 2n)^{206}\text{Pb}$ is about 7.3 MeV and the yield even with long irradiation times is inadequate for analytical purposes. The inelastic scattering reactions, however, yielded sufficient activity to warrant further investigation although, because

(1) S. D. Rasberry, *Appl. Spectrosc.*, **27**, 102 (1973).

(2) S. G. Thompson, K. Street, Jr., A. Ghiorso, and G. T. Seaborg, *Phys. Rev.*, **78**, 298 (1950).

(3) J. L. Crandall, *Isotop. Radiat. Technol.*, **70**, 306 (1970).

(4) E. Ricci and T. H. Handley, *Anal. Chem.*, **42**, 378 (1970).

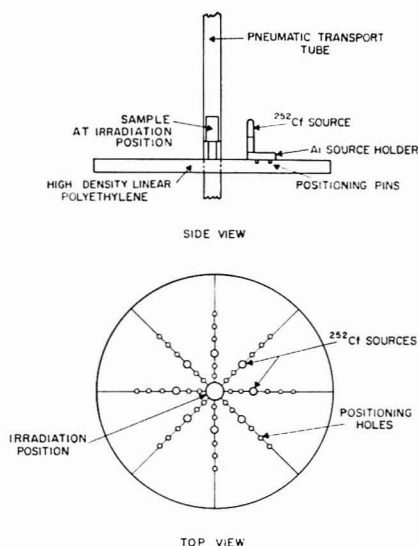


Figure 1. ^{252}Cf source configuration

of the difficulty of precisely timing the transit time to the detector for the short-lived ^{207}Pb , this reaction received only a cursory study.

Work was concentrated on three paint samples. Two of them were the "coarse" and "fine" fractions of a paint which had been scraped off the window sash of a home undergoing renovation. The sample had been crushed with a mortar and pestle. Material passing through a No. 40 mesh sieve and retained on a No. 100 mesh sieve was designated "coarse," material passing through the No. 100 mesh sieve was denoted "fine." The third sample was a mixture of paints from various sources which was carefully ground and homogenized. This material has had its lead content certified by the National Bureau of Standards and the material is available as Standard Reference Material 1579 (5). It is referred to in this paper as "SRM paint."

The reaction $^{204}\text{Pb}(n,n')^{204\text{m}}\text{Pb}$ was studied first. Samples of paint weighing approximately 1.7 grams were encapsulated in the

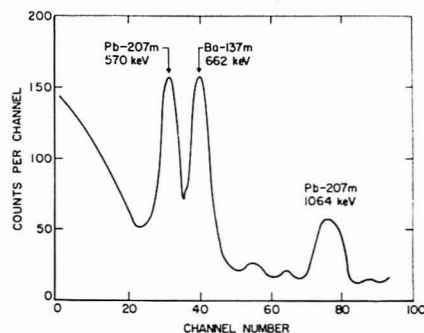


Figure 2. NaI(Tl) spectrum of paint sample irradiated for 3 seconds, counted for 6 seconds—recycled 20 times

small polyethylene vials. Cadmium sheet of about 1-mm thickness was wrapped around the vials to minimize thermal neutron reactions, and these were packaged in the larger vials with polyethylene spacers. Standards of lead salts were similarly packaged. Because of the intrinsic stability of the isotope source, flux monitors were not necessary.

Samples were irradiated for 1-2 hours and, after transfer to a clean counting vial, were examined with a NaI(Tl) detector and a multichannel analyzer. Only a few experiments were required to show that (n,p) reactions on stable titanium isotopes yielding scandium radionuclides had sufficiently high yields that the photopeaks of the lead isotopes could not be resolved with the NaI detector. With a Ge(Li) detector, however, all three gamma-ray lines of $^{204\text{m}}\text{Pb}$ could be adequately resolved. The elements titanium, iron, barium, calcium, magnesium, copper, silicon, strontium, and zinc, possible major and minor constituents in a paint sample, were irradiated and counted under the same conditions as the paint samples, and it was determined that they would not interfere with the lead activity measurement.

The $^{207}\text{Pb}(n,n')^{207\text{m}}\text{Pb}$ reaction was examined by irradiating the paint samples for about 3 seconds and, after allowing for about 2 seconds return, counting for 6 seconds with two 4-inch \times 4-inch NaI(Tl) detectors. Because the transit time of the samples from irradiation source to detectors exceeded two half-lives of the isotope produced, it was necessary to recycle the sample a number of times to build up adequate counting statistics. The precision of timing of sample return for this short-lived isotope was marginal and results are not as reliable as with the $^{204\text{m}}\text{Pb}$ isotope. A NaI spectrum of the SRM paint cycled 20 times is shown in Figure 2.

RESULTS AND DISCUSSION

Results on the determination of lead in the three paints are shown in Table II. Samples "coarse" and "fine" were also analyzed by nondestructive photon activation analysis.

- (5) B. Greifer, E. J. Maienthal, T. C. Rains, and S. D. Rasberry, "Development of NBS Standard Reference Material No. 1579, Powdered Lead-Based Paint," *Nat. Bur. Stand. (U.S.) Spec. Publ.* **260-45**, March 1973. Available from Superintendent of Documents, U.S. Government Printing Office, Washington, D.C. 20402.

Table I. Nuclear Reactions of Lead Observed with Unmoderated Neutrons of ^{252}Cf

Reaction	Product half-life	Prominent product gamma-rays MeV
$^{204}\text{Pb}(n,2n)^{203}\text{Pb}$	52 hr	0.279, 0.401
$^{204}\text{Pb}(n,n')^{204\text{m}}\text{Pb}$	67 min	0.375, 0.899, 0.912
$^{207}\text{Pb}(n,n')^{207\text{m}}\text{Pb}$	0.8 sec	0.570, 1.064

Table II. Comparison of ^{252}Cf Neutron Activation Analysis with Other Methods in the Determination of Lead in Paint

Paint sample	^{252}Cf Activation	
	$^{204}\text{Pb}(n,n')^{204\text{m}}\text{Pb}$, results, %	$^{207}\text{Pb}(n,n')^{207\text{m}}\text{Pb}$, results, %
"Coarse"	3.8, 3.5, 3.7	~3
"Fine"	7.2, 7.4	~8
SRM Paint	10.7, 10.6, 11.7, 11.4	
		Other methods and results, %
		Photon activation, 3.3, 3.5
		Photon activation, 7.6, 7.3, 7.2
		Polarography and atomic absorption, 11.87 (5)

sis. SRM paint was analyzed by polarography and atomic absorption. The reasonably good agreement between ^{252}Cf activation analysis and the other methods demonstrates the reliability and utility of the isotope source technique for this determination.

Irradiation for 2 hours with the 600- μg ^{252}Cf source followed by 100 minutes of counting with a 60-cm 3 Ge(Li) detector yields about 7 counts of the ^{204}mPb isotope per milligram of lead. For a paint sample weighing 1.5 grams, the lower limit of determination would be of the order of 1%.

As noted, analysis of the Ge(Li) spectrum of those elements likely to be major or minor constituents of paint indicates that they will not interfere in the quantitation of the gamma ray lines of ^{204}mPb . Self-shielding effects due to the matrix are expected to be negligible since the nuclear reaction involves fast neutrons and a paint sample is

unlikely to contain appreciable amounts of neutron moderating elements.

The results presented here indicate that with a ^{252}Cf source of several tens of milligrams and the 60-cm 3 Ge(Li) detector, the determination of ~1% of lead in a sample of 1-2 grams of paint could be accomplished with a 15-minute irradiation and 15-minute counting. The potential exists for largely automating the irradiation and counting of a large number of samples. Hence, it would appear possible that although the initial cost of equipment for this determination would be greater than for alternate methods, the speed and adequate reliability of the isotope source method would make it economically competitive.

Received for review August 23, 1973. Accepted November 13, 1973.

Colorimetric Determination of *N*-Arylhydroxylamines with 9-Chloroacridine

Richard E. Gammans, James T. Stewart, and Larry A. Sternson¹

The Bioanalytical Laboratory, Department of Medicinal Chemistry, School of Pharmacy, The University of Georgia, Athens, Ga. 30602

During the metabolic conversion of certain aromatic amines to excretable conjugates in the endoplasmic reticulum of liver cells, *N*-arylhydroxylamines are formed (1) which have been implicated in the chemical carcinogenesis (2) displayed by such compounds. Few analytical procedures are available for the rapid detection and assay of such aromatic hydroxylamines. Boyland and Nery (3) detected 1-3 $\mu\text{g}/\text{ml}$ of *N*-phenylhydroxylamine colorimetrically by complex formation with either salicylidenearylamine *N*-oxides and ferrocyanide or pentacyano-amine ferroate in aqueous solutions. Qualitative identification of arylhydroxylamines by thin-layer chromatography with the use of various spray reagents has also been described (4). In addition, some gas chromatographic determinations of arylhydroxylamines have been reported (5, 6).

The interaction of *N*-arylhydroxylamines with 9-chloroacridine to give highly-colored solutions has been observed in our laboratory. In this paper, we describe a new colorimetric method for determining microgram quantities of arylhydroxylamines with 9-chloroacridine.

EXPERIMENTAL

Apparatus. Spectra and absorbance measurements were made with a Perkin-Elmer Spectrophotometer, Model 202, and a Bausch and Lomb Spectronic 20 colorimeter.

Reagents. 9-Chloroacridine was obtained from Eastman Organic Chemicals. *N*-Phenylhydroxylamine, *p*-chlorophenylhydroxylamine, and *p*-tolylhydroxylamine were synthesized by the method reported by Smissman and Corbett (7). Cyclohexylhydroxylamine was prepared by reduction of cyclohexanone oxime

(8) by the procedure of Feuer *et al.* (9). The melting points of the synthesized compounds were in agreement with literature values (10, 11). All other chemicals were commercially available and were utilized as received.

Fresh solutions of arylhydroxylamines were prepared daily by dissolving weighed amounts in 95% ethanol. Solutions of 9-chloroacridine were prepared immediately before use by dissolving weighed amounts in ethanol and were kept refrigerated.

Procedure. A quantity of an ethanolic solution of arylhydroxylamine was placed in an appropriate volumetric flask. An ethanolic solution containing an approximate 10-fold excess of 9-chloroacridine was added to the flask. The solution was acidified with 10% v/v aqueous hydrochloric acid, shaken briefly, and allowed to stand at room temperature for 5 minutes. Ethanol was added to volume so that the final concentration of arylhydroxylamine in the flask was equal to or greater than $1 \times 10^{-5} \text{M}$. The absorbance was measured at 450 nm and the measurements were corrected for reagent blanks in the procedure.

RESULTS AND DISCUSSION

9-Chloroacridine interacts with an arylhydroxylamine in the analytical procedure to yield a highly-colored yellow-orange solution. The absorption curve in the visible spectrum for an analytical solution of *N*-phenylhydroxylamine shows an absorption maximum at 450 nm. Preliminary data have revealed that the reaction yields a nucleophilic addition product similar to the one reported for primary aromatic amines (12). Further work on the identification of the compound formed between arylhydroxylamines and 9-chloroacridine is under way in our laboratory.

In comparing absorption curves of the colored solutions obtained with equimolar concentrations of the various arylhydroxylamines, it was noted that *p*-chlorophenylhydroxylamine was prepared by reduction of cyclohexanone oxime

¹ Author to whom correspondence should be directed.

(1) C. C. Irving, *J. Biol. Chem.*, **239**, 1589 (1964).

(2) J. A. Miller, J. W. Cramer, and E. C. Miller, *Cancer Res.*, **20**, 950 (1960).

(3) E. Boyland and R. Nery, *Analyst (London)*, **89**, 95 (1964).

(4) J. Booth and E. Boyland, *Biochem. J.*, **91**, 362 (1964).

(5) H. B. Hucker, *Drug Metab. Disposition*, **1**, 322 (1973).

(6) A. H. Beckett and S. Al-Sarraj, *J. Pharm. Pharmacol.*, **24**, 916 (1972).

(7) E. E. Smissman and M. D. Corbett, *J. Org. Chem.*, **37**, 1847 (1972).

(8) A. I. Vogel, "A Textbook of Practical Organic Chemistry," 3rd ed., John Wiley, New York, N. Y., 1956, p 344.

(9) H. Feuer, B. F. Vincent, and R. S. Bartlett, *J. Org. Chem.*, **30**, 2877 (1965).

(10) A. Lapworth and L. Pearson, *J. Chem. Soc.*, **119**, 765 (1921).

(11) R. D. Haworth and A. Lapworth, *J. Chem. Soc.*, **119**, 768 (1921).

(12) J. T. Stewart, T. D. Shaw, and A. B. Ray, *Anal. Chem.*, **41**, 360 (1969).

Table I. Calibration Data for Various Arylhydroxylamines

Compound	Final concn, $M \times 10^{-4}$	Absorbance ^a
<i>N</i> -Phenylhydroxylamine	1.5	0.163 ± 0.019^a
	3.0	0.320 ± 0.011
	6.0	0.605 ± 0.008
<i>p</i> -Chlorophenylhydroxylamine	1.5	0.096 ± 0.014
	3.0	0.196 ± 0.008
	6.0	0.403 ± 0.008
<i>p</i> -Tolylhydroxylamine	1.5	0.096 ± 0.014
	3.0	0.196 ± 0.008
	6.0	0.396 ± 0.002

^a Measured at 450 nm and based upon 5 replicate determinations of each solution. ^b Confidence limits at $p = 0.05$

droxylamine and *p*-tolylhydroxylamine produce color which absorbs at the same wavelength maximum as *N*-phenylhydroxylamine but with diminished intensity. The absorbance data are shown in Table I. The reduced absorption for the substituted derivatives of phenylhydroxylamine may be the result of a less-than-quantitative yield of the colored product under the conditions of the analytical determination.

It was suggested that heating the hydroxylamine and acridine on a steam bath might ensure a more complete reaction. However, maximum color development could be obtained upon shaking the solution and allowing it to stand at room temperature for 5 minutes. Repeated readings on a series of different samples indicated good color stability for periods up to 24 hr. Although stability of the 9-chloroacridine reagent solution has been discussed previously (12, 13), our present work has further revealed that refrigeration of the acridine solution after preparation allows use of the solution for approximately 8 hours before decomposition occurs.

The analysis method is a micro procedure, and sensitivity is in the 0.8–3 $\mu\text{g/ml}$ range ($10^{-5}M$) of arylhydroxylamine. Reagent preparation is simple and rapid since 9-chloroacridine is commercially available and can be used without further purification or modification procedures. The time involved in the actual analysis procedure is less than 30 minutes compared to the colorimetric method by complex formation which takes from 2 to 14 hours depending upon the reagent used (3).

Standard curves can be prepared by plotting absorbance readings vs. the volumes taken of equimolar concentrations of various arylhydroxylamines. In all cases, Beer's law holds for this system.

Data from several systems shown in Table II indicate that this procedure permits the determination of arylhydroxylamines in the presence of primary aromatic amines (whose colorimetric determination with 9-chloroacridine has been previously reported, *vide infra*), primary aliphatic amines, phenols, aromatic nitro compounds, aliphatic and aromatic amides, and aliphatic hydroxylamines. It has been shown previously that secondary and tertiary aromatic, heterocyclic, and aliphatic amines and carbonyl-containing compounds did not interfere with colorimetric determinations utilizing 9-chloroacridine. Although one cannot exclude the possibility that these other functional

(13) J. T. Stewart, A. B. Ray, and W. B. Fackler, *J. Pharm. Sci.*, **58**, 1261 (1969).

Table II. Analysis of Known Arylhydroxylamine Mixtures for Arylhydroxylamine

Mix- ture	Components ^b	Arylhydroxylamine ^a	
		Found, $M \times 10^{-4}$	% of Theory
1	<i>N</i> -Phenylhydroxylamine Aniline	1.496	99.75 ± 3.62^c
2	<i>N</i> -Phenylhydroxylamine Phenol Acetamide <i>n</i> -Butylamine	1.489	99.27 ± 1.59
3	<i>N</i> -Phenylhydroxylamine Nitrobenzene Acetanilid	1.485	98.97 ± 2.50
4	<i>N</i> -Phenylhydroxylamine Cyclohexylhydroxylamine	1.514	100.90 ± 1.81

^a Based upon 3 replicate determinations of each solution. ^b Final concentration of phenylhydroxylamine and all other components in mixtures was $1.500 \times 10^{-4}M$; except aniline which was present in a final concentration of $1.500 \times 10^{-5}M$. ^c Confidence limits at $p = 0.05$.

groups react with 9-chloroacridine in typical nucleophilic displacement reactions, only primary arylamines produce any colored product under the conditions of the analytical reaction. Measurements reveal that arylhydroxylamines can be quantitated in the presence of a hundredfold excess of primary aromatic amine. Specificity permitting the determination of arylhydroxylamines with 9-chloroacridine in the presence of primary arylamines is obtained by measuring absorbance at 450 nm, where the absorption characteristics of any 9-chloroacridine-arylamine adduct show minimal interference.

Received for review September 10, 1973. Accepted November 20, 1973. This investigation was supported in part by NIH Grant CA-14158-01 from the National Cancer Institute.

CORRECTION

Application of a Piezoelectric Quartz Crystal as a Partition Detector. Development of a Digital Sensor

In a paper by Morteza Janghorbani and Harry Freund, *Anal. Chem.*, **45**, 325 (1973), piezoelectric crystals for assay of SO_2 in air were described using carbowax as coating.

This paper did not refer to the previously described, successful, studies on piezoelectric crystals for SO_2 , by G. G. Guilbault "Use of Tetrachloromercurate as a Coating for SO_2 ," *Environ. Lett.*, **2**, 35 (1971), and the "Use of Piezoelectric Crystals as Sensitive and Specific Detectors for SO_2 ," *Anal. Lett.*, **5**, 255 (1972). The latter paper describes the use of carbowax as a coating for SO_2 , the same as discussed by Janghorbani and Freund.

AIDS FOR ANALYTICAL CHEMISTS

On the Use of a Power Divider for Thermostated Electrodeless Discharge Lamps in Atomic Fluorescence Spectrometry

D. O. Knapp, C. J. Molnar, and J. D. Winefordner¹

Department of Chemistry, University of Florida, Gainesville, Fla. 32611

In recent years, electrodeless discharge lamps (EDLs) have been put forth as intense sources for atomic spectrometry. However, it has not been until recently that work involving temperature-controlled (thermostated) EDLs has resulted in stable, intense, reliable EDL sources for atomic spectrometry. It has previously been demonstrated that single- and multielement EDLs are very sensitive to temperature changes when operated with a thermostated antenna (1, 2). The insensitivity of spectral output of EDLs operated with the thermostated "A"-antenna to changes in microwave power has been discussed previously (1-3). Some of the reasons given for using thermostated EDLs have been: microwave generators are difficult to stabilize adequately, whereas air temperatures can be regulated with good precision; and changes in the coupling efficiency between the microwave field and the EDL discharge can, in the absence of temperature control, lead to drastic changes in lamp spectral output. Until recently (4), one microwave generator per antenna had been used when operating EDLs. This is readily understood when one considers the myriad of papers on EDLs and the art and skill needed to utilize EDLs for analytical studies. However, with the insensitivity of thermostated EDLs to changes in microwave power, it is readily conceivable that more than one thermostated EDL could be operated simultaneously from one microwave generator utilizing a microwave power divider and that such a system would be very advantageous for multielement analysis. Norris and West (4) have reported the use of a two-port power divider for two dual-element EDLs and mentioned that it was an economical means of illuminating a flame cell with radiation from more than one EDL simultaneously.

In this study, thermostated EDLs operated at their optimal temperatures and powered by one microwave generator using a power divider are evaluated. Detection limits for atomic fluorescence spectrometric measurement of several elements with these EDLs were obtained and compared with other published results.

EXPERIMENTAL

A block diagram of the optical system is shown in Figure 1. The microwave power from a 200-W, 2450-MHz generator with a separate reflected power meter (Electromedical Supplies Ltd., Wantage, Berkshire, U.K.) was divided (D2-2TN, 2-Port-3 db Power Divider, Microlab/FXR, Livingston, N.J.) and used to power two "A" antennas (Model 2254-5002G1; the Raytheon Co., Microwave

Devices, Farmington, Conn.). The EDL temperature control assemblies used have been described before (1). The spectral radiation from the sources was mechanically modulated with a laboratory-constructed mechanical chopper operating at 248 Hz and focused onto an air/hydrogen flame used with a pre-mix laminar flow burner chamber (Model 303-0110; Perkin-Elmer Corp., Norwalk, Conn.) and a capillary burner (5). Atomic fluorescence measurements were performed with a 0.5-m Ebert monochromator (Type 82-000 with grating blazed at 3000 Å and 1180 grooves/mm; Jarrell-Ash Corp., 590 Lincoln St., Waltham, Mass.), and R.C.A. 1P28A photomultiplier and a lock-in amplifier (Model 353, Ithaco, Inc., Ithaca, N.Y.). A potentiometric recorder (Sargent Model SR, Sargent-Welch Scientific Co., Birmingham, Ala.) was used to record data. Optical grade biconvex quartz lenses (S1-UV, Esco Products, Oak Ridge, N.J.) were utilized throughout for focusing. The single element Ag, Mg, Pb, Sb, Sn, Te, and Ti EDLs contained the iodide form of each element, and the Cu, Cr, and Ni EDLs, the chloride; while the metals were used for the Hg and Cd, Zn, and Se EDLs.

RESULTS AND DISCUSSION

Thirteen elements were evaluated and detection limits, defined as the concentration resulting in a signal-to-rms noise ratio equal to 2, are given in Table I and are compared to other reported best detection limits.

The optimum temperature reported for each element in a particular EDL was, in general, reproducible from day to day. There were, however, several notable exceptions—i.e., for two Mg single element EDLs, the optimum temperature increased from 340 °C in initial work to 400 °C in later work with a loss in radiant output of 15% for one EDL, whereas for the other Mg EDL actually used for the Mg AF measurements, the optimum temperature was a reproducible 470 °C. Three Cd/Zn EDLs were evaluated; two dual-element EDLs contained just Zn and Cd metal had optimum temperatures of 280 and 250 °C, respectively, while for a third tube containing Cd, Zn, and Se as metals, the optimum temperatures were 400 and 420 °C for Zn and Cd, respectively. There was no observable Se emission from this (which was also the case with other Cd/Zn/Se EDLs) EDL. It was previously assumed that the temperature dependence of the radiant output for

¹ Author to whom reprint requests should be sent.

- (1) R. F. Browner, B. M. Patel, T. H. Glenn, M. E. Rietta, and J. D. Winefordner, *Spectrosc. Lett.*, **5**, 311 (1972).
- (2) B. M. Patel, R. F. Browner, and J. D. Winefordner, *Anal. Chem.*, **44**, 2272 (1972).
- (3) R. F. Browner and J. D. Winefordner, *Spectrochim. Acta*, **28B**, 263 (1973).
- (4) J. D. Norris and T. S. West, *Anal. Chem.*, **45**, 226 (1973).

- (5) L. M. Fraser and J. D. Winefordner, *Anal. Chem.*, **43**, 1693 (1971).
- (6) K. E. Zacha, M. P. Bratzel, J. M. Mansfield, and J. D. Winefordner, *Anal. Chem.*, **40**, 1733 (1968).
- (7) J. D. Norris and T. S. West, *Anal. Chim. Acta*, **59**, 355 (1972).
- (8) H. G. C. Human, *Spectrochim. Acta*, **27B**, 301 (1972).
- (9) P. L. Larkins, *Spectrochim. Acta*, **26B**, 477 (1971).
- (10) J. Matousek and V. Sychra, *Anal. Chem.*, **41**, 518 (1969).
- (11) D. L. Manning and P. Heneage, *At. Absorp. Newsl.*, **6**, 124 (1967).
- (12) R. M. Dagnall, K. C. Thompson, and T. S. West, *Talanta*, **14**, 1151 (1967).
- (13) R. F. Browner, R. M. Dagnall, and T. S. West, *Anal. Chim. Acta*, **46**, 207 (1969).
- (14) A. Hell and S. Ricchio, Pittsburgh Conference on Analytical Chemistry and Applied Spectroscopy, Cleveland, Ohio, 1970.
- (15) M. P. Bratzel and J. D. Winefordner, *Anal. Lett.*, **1**, 43 (1967).

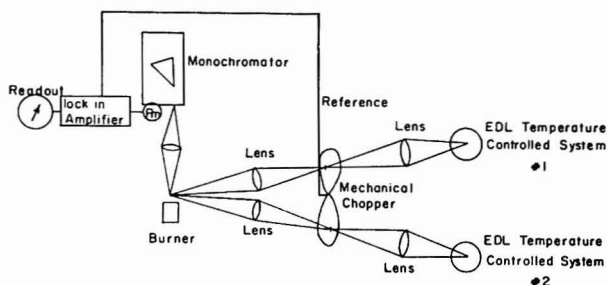


Figure 1. Block diagram of optical system containing power divider for thermostated electrodeless discharge lamps in atomic fluorescence spectrometry

Table I. Detection Limits of Several Elements in Atomic Fluorescence Flame (Air/H₂) Spectrometry Using Electrodeless Discharge Lamps Operated with Two "A" Antennas Joined via Two-Port Power Divider

Element	Wavelength, nm	EDL Temperature, °C*	Detection limits, µg/ml	
			This study	Best reported (Reference)
Ag	328.1	580	0.0008	0.0001 (6)
Cd	228.8	420	0.001	0.000001 (6)
Cr	357.9	475	0.01	0.005 (7)
Cu	324.8	430	0.002	0.0005 (8)
Hg	253.7	50	0.01	0.02 (2)
Mg	285.2	470	0.00005	0.00015 (9)
Ni	232.0	65	0.07	0.003 (10)
Pb	405.7	255	0.03	0.02 (11)
Sb	231.1	150	0.01	0.05 (12)
Sn	303.4	110	0.5	0.1 (13)
Te	214.3	410	0.07	0.006 (14)
Tl	377.6	310	0.002	0.008 (6)
Zn	213.8	400	0.005	0.00004 (15)

* All EDLs except for Hg and Pb were operated at 120-W microwave power or 60 W per EDL because of use of the power divider. The Hg and Pb EDLs were operated at 80 W or 40 W per EDL.

each element (or compound) present in a lamp is largely uninfluenced by the presence of other elements (2). The Tl and the multielement Cd/Zn/Se EDL were operated simultaneously with the power divider; switching the two lamps in the thermostated systems resulted in similar atomic fluorescence signals for a solution containing 1 µg/ml of each element (signals within 8% for Cd, Zn, and Tl resulted for the two orientations). The Pb and Hg EDL were operated simultaneously at 40-W incident microwave power under both thermostated and nonthermostated conditions. Without thermostating, because of the low radiant output from the Pb EDL, there was no observable AF signal, while for a 100 µg/ml solution of Hg, without thermostating, there was a decrease of 10× in AF signal. There were not any noticeable problems or difficulties associated with using two thermostated EDLs with the power divider and a single microwave generator. The most obvious advantage with the use of thermostated EDLs is the ease with which maximum spectral output from an EDL can be obtained via variation of the EDL temperature. Future work is planned for the use of a multipoint power divider and a 800-W microwave power supply for the simultaneous use of several thermostated EDLs.

Received for review August 22, 1973. Accepted November 19, 1973. The research was supported by AF-AFOSR-1880-701.

High Pressure Gradient Chamber for Liquid Chromatography

E. H. Pfadenhauer, T. E. Lynes, and T. V. Updyke

Newport Pharmaceuticals International, Inc., 1590 Monrovia Boulevard, Newport Beach, Calif. 92660

Gradient elution is a useful technique in many applications of chromatography, and is especially important to high pressure liquid chromatography where speed and resolution of analysis are major factors in justifying the expense of the necessary equipment. In our work, we were interested in doing rapid, high resolution determinations of oxypurines in blood plasma, and wished to explore the possibility of using gradient elution in high pressure liquid chromatography. In cases where the gradient can be made up at atmospheric pressure, the problem is trivial. However, if a screw-driven syringe type high pressure pump is used, the gradient must necessarily be made at high pressures.

Commercial gradient accessories include a second high pressure pump (Nester-Faust 1200, Varian Aerograph 4200) or a complex arrangement of 5 high pressure valves, a holding coil, and a mixing chamber (DuPont 820). The device described here suffers from the limitation of being able to deliver only a single convex gradient shape which is not usually the most desirable chromatographically, but is considerably less expensive than a second pump, entailing approximately only one-tenth the cost. The DuPont arrangement is not available as a separate unit.

As seen in Figures 1a and 1b, the gradient device consists of a removable mixing chamber, and a cap through which is drilled an inlet from the high pressure pump and



Figure 1a. Assembled and disassembled views of the gradient chamber

Top: Assembled as viewed from the underside. Bottom: (lower left to right) Retainer; mixing chamber with "O" ring; cap

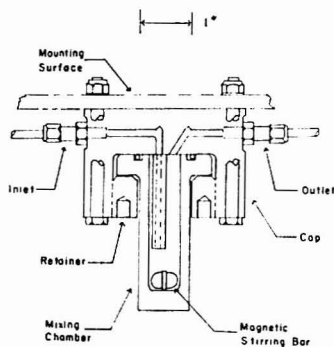


Figure 1b. Cutaway schematic of assembled gradient chamber

an outflow to the column. Stainless steel, type 303, was used throughout for corrosion resistance and relatively easy machineability. Tube fittings were 316 stainless steel and were purchased from Parker-Hannifin Company. "O" rings (Parker Seal Company) were selected for solvent resistance. Polysulfide was found to be an excellent material for "O" rings, showing stability against diethylether, alcohols, water, and dilute acetic acid. Unfortunately, polysulfide is a rather soft material and not resistant to mechanical abrasion. Teflon-covered silicone "O" rings would give a wider range of chemical resistance if desired.

The overall seal design gave excellent performance, and ether was held under 5000 psi with no apparent leakage. The size of the holes in the outlet part of the cap, as well

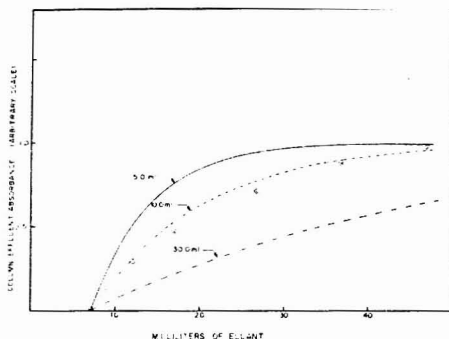


Figure 2. Gradient shapes calculated for chamber size of 5, 10, and 30 ml with a column dead volume of 7 ml

Circled points are of the observed gradient for a 10-ml chamber volume as described in text

as the associated tubing connections, should be as small as possible to minimize dead volume.

In actual operation, the chamber is filled with the starting eluant, and a solvent of higher elution power is pumped in at high pressure at the desired flow rate. Mixing is accomplished with a small Teflon-coated magnetic stirring bar placed in the bottom of the chamber. Most stainless steels are nonmagnetic and there is no difficulty with the stirring operation. During routine use of the system, retention times of compounds after repetitive injections were found to remain stable, indicating satisfactory mixing in the chamber.

The actual size of the chamber is dictated by the shape of the gradient desired. A larger chamber will give a less steep gradient and vice versa. The size illustrated here has a 10-ml capacity, and the theoretically calculated and actual gradient delivered by the device are illustrated in Figure 2. The observed points were obtained by using a solvent in the high pressure pump of higher UV absorbance than the initial eluant in the gradient chamber, and monitoring UV absorbance of a column effluent.

The device has also been found useful in "slurry packing" small diameter packing materials into columns. With this method, the packing material is added to a carrier solvent in the desired slurry consistency and then poured into the mixing chamber. The empty column is attached to the outlet of the cap, the magnetic stirrer turned on, and the slurry pumped through at high pressure.

ACKNOWLEDGMENT

The authors wish to acknowledge the help of R. F. Updyke of Engineering Specialists, Canoga Park, Calif., in the design of this instrument.

Received for review August 6, 1973. Accepted October 3, 1973.

INDEX TO ADVERTISERS IN THIS ISSUE

*Alconox, Inc.	443A	Infrared Industries, Inc.	428A	*Union Carbide, Linde Division	414A
Alden Advertising Agency, Inc.		*International Crystal Labs	472A	Y & R Enterprises Inc.	
Alpha Analytical Laboratories	468A	Tek-Mark, Inc.			
Don Wise & Company, Inc.		*ISCO	422A	*Varian	459A, 461A, 463A, 464A
*American Instrument Co., Div. of		Graham Printing & Advertising		Ahern Advertising Agency	
Travenol Laboratories, Inc.				Varian MAT	397A
383A, 467A, 478A					
Industrial Advertising Assoc.		*Kevex Corporation	408A		
Applied Materials, Inc.	392A	Fred Schott & Assoc.			
Hall Butler Blatherwick, Inc.		Kontes Glass Company	395A		
		Aitkin-Kynett Co., Inc.			
*J. T. Baker Chemical Company	430A-431A	*Labindustries	452A	LABORATORY SUPPLY CENTER	480A
deMartin Marona & Assoc.		Fred Schott Assoc.		Austin Science Assoc., Inc.	
*Barnes Engineering Company	472A	*Leco Corporation	468A	Bio-Rad Laboratories	
Albert A. Kohler Company, Inc.		Juhl Advertising Agency, Inc.		Eastern Chemical Div. of Guardian	
*Bausch & Lomb, Analytical Systems		Leeds & Northrup Company	410A-411A	Chemical Corporation	
Div.	381A	Schaefer Advertising Inc.		Ernest F. Fullam, Inc.	
Wolf Associates, Inc.		Los Alamos Scientific Laboratory	468A	Gollob Analytical Service Corp.	
*Beckman Instrument, Inc.	445A	Toppino-Golden Agency		Polymeric Enzymes Inc.	
Lescaurboura Advertising Inc.		*Lumicon Inc., Div. of International	474A	Regis Chemical Company	
Behlchem Apparatus Co., Inc.	474A	Crystal Labs		Southwestern Analytical Chemicals	
Beaumont, Heller & Sperling, Inc.		Tek-Mark, Inc.			
Bio-Rad Laboratories	476A			Advertising Management for the	
Fred Schott & Assoc.				American Chemical Society Publications	
Brinkman Instruments, Inc.	436A	*Mallinckrodt Chemical Works	457A	CENTCOM, LTD.	
Blatt Advertising, Inc.		Batz, Hodgson, Neuwochner, Inc.		Thomas N. J. Koerwer, President; Clay S.	
Buchler Instruments Div. of Searle		McKee-Pedersen Instruments	479A	Holden, Vice President; Benjamin W. Jones,	
Analytic		*Mettler Instrument Corporation	475A	Vice President; Robert L. Voepel, Vice	
Jud Jaffe Advertising		386A, 387A, 447A, 471A, 473A		President; C. Douglas Wallach, Vice President;	
		Harris D. McKinney Inc.		142 East Avenue, Norwalk, Connecticut	
Cajon Company	432A	*MFE Corporation	462A	06851 (Area Code 203) 853-4488	
Falls Advertising Company		The Brightman Company, Inc.			
*Carle Instruments, Inc.	435A	MISCO	467A	ADVERTISING SALES MANAGER	
Cochrane Chase & Co., Inc.		C-C Advertising, Inc.		Thomas N. J. Koerwer	
Diano Corporation	476A	Nicolet Instrument Corporation	396A	SALES REPRESENTATIVES	
Design Associates		Hagen Advertising Inc.		Chicago . . . Eugene Eldridge, CENTCOM,	
*Dimco-Gray Company	482A	Nissei Sangyo Instrument, Inc.	445A	LTD., 540 Frontage Rd., Northfield, Ill.	
Weber, Guiger & Kalat, Inc.		Kaneko-Murakami Advertising		60093. 312-441-6383.	
*Dohrmann Div. of Envirotech	420A			Cleveland . . . Michael Hayes, CENTCOM,	
Fred Schott & Assoc.				LTD., 20340 Center Ridge Rd., Rocky	
*Du Pont Instruments	426A	*Orion Research Inc.	385A	River, Ohio 44116. 216-331-2324.	
N. W. Ayer & Son, Inc.		Orice Incorporated	394A	Houston . . . Michael Hayes, CENTCOM,	
		Thomas R. Sundheim Inc.		LTD., 216-331-2324	
*Eastman Kodak Company	413A			Denver . . . Clay S. Holden, CENTCOM,	
Rumrill-Hoyt, Inc.		Parr Instrument Company	482A	LTD., 213-776-0552.	
*EM Laboratories, Inc.	444A-445A	F. Willard Hills Advertising Service		Los Angeles 90045 . . . Clay S. Holden,	
Kenyon Hoag Associates		*The Perkin-Elmer Corporation	418A-419A, 421A, 423A, 425A, 467A, 48C	CENTCOM, LTD., Airport Arcade	
Carlo Erba S.p.A.	440A	Gaynor & Ducis Advertising		Bldg., 8820 S. Sepulveda Blvd., Suite	
Publicitas S.p.A.		*Pharmacia Fine Chemicals Inc.	478A	215, 213-776-0552	
Finnigan Corporation	401A, 450A	Cummins, MacFail & Nutry, Inc.		New York 10017 . . . Richard L. Going,	
Bachrach Advertising		Philips Electronic Instruments	390A, 439A	CENTCOM LTD., 60 East 42nd St.,	
*Fisher Scientific Company	455A	J & M Condon Inc.		212-972-9660	
Tech-Ad Associates		*Princeton Applied Research Corp.	470A	Norwalk 06851 . . . Don Davis, CENTCOM,	
*Forma Scientific Inc.	412A	The Message Center, Inc.		LTD., 142 East Avenue, 203-853-4488.	
E-Lee Advertising Agency		*Pyre Unicam Ltd.	FI-F2	Philadelphia . . . Robert E. Moran, Eastern	
*GCA McPherson Instrument	449A			Regional Sales Manager, CENTCOM	
Culver Advertising Inc.		*H. Reeve Angel & Company, Inc.	477A	LTD., 535 Pennsylvania Avenue, Fort	
*GCA Precision Scientific	478A	Arthur Falconer Associates Corp.		Washington, Pa., 19034. 215-643-2586.	
Tri-State Advertising				San Francisco . . . Clay S. Holden, CENT-	
*Gifford Instrument Laboratories	429A	Schoeffel Instrument Corporation	470A	COM, LTD, 213-776-0552	
Bayless-Kerr Company Advertising		Tek-Mark, Inc.			
*Hach Chemical Company	475A	SGA Scientific Inc.	378A	Great Britain and Western Europe . . . Mal-	
Wesley Day & Co., Inc.		Lakewood Advertising Agency		colm Thiele, Technomedia Ltd., Wood	
*Hamilton Company	427A	Siemens AG	446A	Cottage, Beenhams Heath, Shurlock Row,	
Mealer & Emerson Inc.		Linder Presse Union GMBH		Reading RG10 0QE, Berkshire, England.	
*W. A. Hammond Drierite Company	467A	Spex Industries Inc.	382A, 465A	Japan . . . Haruo Moribayashi, International	
Harleco Div. American Hospital		Seymour Nussenbaum Commercial		Media Representatives, Ltd., 1 Shiba-	
Supply Corporation	388A	Art Service		Kotohiracho, Minato-Ku, Tokyo, Tele-	
Graphic Productions		Spectra Physics, Autolab Division	409A	phone 502-0656.	
*Heath Schlumberger Instruments	384A	Regis McKenna Inc.			
Advance Advertising Service				PRODUCTION DEPARTMENT	
*Helm International, Inc.	443A	*Arthur H. Thomas Company	437A-438A	Production Director	
Miller Advertising Agency, Inc.		Harris D. McKinney, Inc.		Joseph P. Stenza	
*Hewlett Packard, San Diego Division	377A	*Tracor Analytical Instruments	424A	Advertising Production Assistant	
Phillips Ramsey Advertising		Aim Advertising Agency		Donna C. Bifano	

*See ad in ACS Laboratory Guide

**Company so marked has advertisement in the foreign regional edition only.

GRAY LAB micro timer stop clocks

meet all timing needs exactly



Split-second measure of elapsed time for lab tests, production work, micro-motion study, instrument calibration, etc. Synchronous motor-driven. Large 8" dial. Two models: 1/10 second or 1/1000 minute dial divisions. Start-stop from switch on timer or remote control cord (included). Quick manual reset. Portable model \$50. Write for new catalog.

DIMCO-GRAY COMPANY

207 East Sixth Street, Dayton, Ohio 45402

CIRCLE 61 ON READER SERVICE CARD



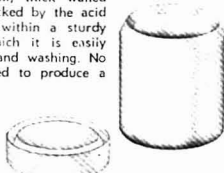
THE PARR® ACID DIGESTION BOMB

The rapid and safe way to dissolve inorganic samples in HF, HCl or HNO₃, or to digest organic materials in strong alkalis or oxidizing acids with complete sample recovery.

Samples are held in a 25 ml, thick walled Teflon® cup which is not attacked by the acid charge. This cup is confined within a sturdy stainless steel bomb from which it is easily removed for sample recovery and washing. No wrenches or clamps are needed to produce a tight seal.

Ask for PARR Bulletin 4745 describing this rapid method for dissolving difficult samples.

*duPont TFE fluorocarbon resin.



PARR INSTRUMENT COMPANY

211 Fifty-Third St.

Moline, Ill. 61265

(309) 762-7716

CIRCLE 192 ON READER SERVICE CARD

Future Articles

Separation of Trace Amounts of Uranium and Thorium and Their Determination by Mass Spectrometric Isotope Dilution

J. W. Arden and N. H. Gale

Luminescence Properties of Sulfonamide Drugs

J. W. Bridges, L. A. Fittford, W. P. Hayes, J. N. Miller, and D. Thorburn Burns

Automatic Digital System for Quantitative Kinetic Analysis—Application to Catalytic Determination of Thyroid

Gunter Knapp and Hans Leopold

Structural Interpretation of Proton Magnetic Resonance Spectra by Computer: First-Order Spectra

Graham Beech, Roger T. Jones, and Keith Miller

Simple Apparatus for On-Site Continuous Liquid-Liquid Extraction of Organic Compounds from Natural Waters

Martin Ahnoff and Bjorn Josefsson

Role of Nitric Oxide in Positive Reactant Ions in Plasma Chromatography

Francis W. Karasek and Donald W. Denney

Photoinduced Luminescence of 9,10-Anthraquinone—Secondary Photolysis Products

David M. Hercules and Steven A. Carlson

Applications of Fourier Transform Techniques to Steric-Exclusion Chromatography

T. A. Maldacker, J. E. Davis, and L. B. Rogers

Subpicogram Detection System for Gas Phase Ionization (API) Mass Spectrometry

D. I. Carroll, I. Dzidic, R. N. Stillwell, M. G. Horning, and E. C. Horning

Determination of Iron in Glass and Cobalt via Charged Particle Activation Analysis

Dale L. Swindle, Leo R. Novak, and Emile A. Schweikert

Present Status of the N-Silicon/Stainless Steel Combination Electrode for Acid Determinations

J. P. McKaveney and M. D. Buck

Easily Operated Direct Current Argon Plasma Arc for Atomic Spectrometric Analysis

D. A. Mordick, Jr., and E. H. Piepmeier

Direct Current, Alternating Current, Pulse, and Anodic Stripping Voltammetric Methods with Glassy Electrodes in Hydrofluoric Acid

A. M. Bond, T. A. O'Donnell and R. J. Taylor

On the Instability of Current Followers in Potentiostat Circuits

J. E. Davis and E. Clifford Toren, Jr.

New Spectrophotometric Reagent for the Determination of Osmium—2,3-Quinoxalinedithiol

Harvey F. Janota and Sabrina B. Choy

Photographic Quantitation in Spark Source Mass Spectrography Using an On-Line Densitometer and Ion Intensity Areas

R. A. Burdo, J. R. Roth, and G. H. Morrison

Polarographic Microdetermination of Cobalt, Nickel, and Antimony in Organic Compounds

S. W. Bishara, Y. A. Gawargious, and B. N. Faltaoos

Polarographic Method for the Determination of Hexafluorosilicate

Indira Rajagopalan and S. R. Rajagopalan